Appendix B

Topical Reports

Foreword

The intention in presenting the topical reports in this appendix is to describe the broad basis for the scoring by the experts. The audience for these topical reports includes technical peers, corporate level engineers and regulators. The depth of knowledge (including plant experience and laboratory data) differs immensely among the topics, and the nature of the topical reports reflects this. The reports are not consensus documents, but have each been reviewed by one or more of the technical experts. Differing opinions and additional factors that enter into each expert's scoring/judgments are addressed in the individual comments put in the spreadsheet used for scoring each sub-group of components. The topical reports also rely on Appendix A, which provides an overview of all environmental degradation phenomena.

Contents

B.1 SCC of Sensitized and Non-sensitized Austenitic Stainless Steels and Weldments

This topical paper provides a foundation for understanding the proactive materials degradation concerns for stress corrosion cracking (SCC) of ***wrought, unirradiated austenitic stainless steels in both boiling water reactor (BWR) and pressurized water reactor (PWR) environments, including weldments***. There are separate topical papers for irradiated assisted SCC of stainless steels, for SCC of cast stainless steels, and for lower temperature, mostly-chloride-related pitting and SCC of stainless steels. There are also topical papers related to BWR and PWR water chemistry, evolving operational practice, start-up and shutdown, and other considerations that influence SCC.

There is a long history of SCC in stainless steels exposed to high temperature water [1-4], and extensive research work designed to understand the dependencies and underlying causes [1-8]. While the mechanical behavior of stainless steels is not dramatically different at 300 °C than at room temperature, many aspects of corrosion and SCC are quite different. All structural materials (e.g., iron and nickel base alloys) are suitable for service in water environments because they form a protective passive film on the surface. When the film is broken (e.g., by scratching or plastic straining), the "bare surface" corrosion rates are *very high*, decaying in a logarithmic fashion over time as the protective oxide film reforms. Even after long time, the corrosion rate does not decrease to zero, but is sustained at a low, "passive" current density.

The nature of the oxide film on stainless steel is quite different in high temperature water (in this context, defined to be above about 150 °C). Near room temperature, the films on stainless steel are very thin (nanometers) and very protective (in terms of passive corrosion current). However, the films on standard "18Cr-8Ni" stainless steels are not that protective in terms of their resistance to aggressive species like chlorides, and even this limited resistance decreases as temperature increases [9,10]. The breakdown of the film can lead to pitting corrosion, crevice corrosion, stress corrosion cracking, etc., with the primary aggravants being increased chloride (halide), H^+ (lower pH), temperature, and oxidant concentration.

Above ≈ 150 °C, the oxides become much thicker (hundreds or even thousands of nanometers) and somewhat less protective (both in terms of passive current density and tolerance for breakdown from, e.g., chloride) [11]. The composition of the films is not uniform, either through thickness or from environment to environment [11]. For example, in oxidizing (e.g., traditional BWR) environments, Cr is oxidized from Cr^{3+} (e.g., Cr_2O_3) to Cr^{6+} (e.g., $CrO_4^{=}$), which is soluble in water (Figure B.1.1). Thus, these films have an inner layer, which is Cr-rich and an outer layer low in Cr. In deaerated water, the addition of H_2 reduces the corrosion potential (lowering line (a) in Figure B.1.1, which is the H_2/H_2O reaction), which results in an increase in the solubility of Fe^{2+} (more in pure water than in PWR primary water, whose pH_T is ≈ 1.5 units higher). Note that oxidants like O_2 are consumed in cracks and crevices, so those films are somewhat different than exterior films (in oxidizing environments). Both films form oxide crystallites on the surface by re-precipitation, which are typically 0.1 – 10 micrometers in size. The films that form in the presence of oxidants are somewhat more protective (i.e., lower passive current density) [11,12].

While there is not complete concurrence on the mechanism(s) of SCC of stainless steels in hot water, the consensus opinion is that SCC growth occurs by a process involving localized deformation (e.g., at the crack tip), which is a shear process that "breaks" or damages the inner protective oxide and produces an accelerated oxidation process as the film repairs. This was originally conceived as "slip – film rupture – dissolution", but there is in fact no requirement for an aqueous electrolyte since steam, air or other gaseous environments produce oxidation, which meets the requirement for the underlying mechanism. Thus, many people refer to the mechanism as "slip – oxidation". An important element of this mechanism is that it is not fundamentally related to (local) stress per se, but to (local) dynamic strain that damages the protective film. Dynamic strain at constant load (e.g., when cracks grow primarily from weld residual stresses) is sustained because the stress / strain field at the crack tip is redistributed as the crack advances, and this requires local strain. Thus, there is an inherent inter-dependency between dynamic strain that produces crack advance, which in turn sustains the dynamic strain. The slow repassivation process in hot water, long term thermal creep, the interaction among crack advance in adjacent grains, irradiation creep, operating fluctuations (e.g., in temperature or pressure), start-up and shut-down, etc. also help sustain crack advance.

Factors such as simplistic or flawed experiments and extrapolation of room temperature data led to the early presumption that SCC would not occur in non-sensitized, unirradiated stainless steel; or in high purity water; or without oxidants in the water, etc. However, it is now recognized that SCC can occur in essentially any environment-material combination in high temperature water, although the ease of initiation and rate of SCC growth can vary markedly. Thus, the concepts of *thresholds* (e.g., in sensitization, water purity, oxidant level, radiation dose/fluence, etc.) that produce immunity to SCC have given way to an understanding of an inherent susceptibility to SCC that varies markedly with material, environment and stress. However, pragmatically, in many cases there conditions of use that lead to very long lives.

The traditional view of SCC is reflected in Figure B.1.2, which expresses the need for a confluence of stress, environment and metallurgical parameters to exist for SCC to occur. (Drawn today, the central over-lapping region of SCC susceptibility would be much larger). The various parameters that control the initiation or growth rate do not operate independently but rather inter-dependently; thus, some factors (e.g., 10 – 30 ppb sulfate) can have a huge influence under some conditions (e.g., in oxidizing water), but not under other conditions (e.g., deaerated / hydrogenated water). Many such inter-dependencies exist in SCC; indeed, to some extent the effect of essentially all factors are influenced by all other factors. Thus, focusing on the engineering factors that influence SCC can produce a confusing variety of observations, and successful understanding and prediction of SCC must be built on an accurate image of the "crack tip system".

The primary factors that control SCC of stainless steels in hot water are:

- Degree of sensitization. Sensitization results from Cr carbides that form during thermal exposure (from heat treatment or welding) in the range of 550 – 750 °C, although Cr carbide nucleation can occur below 400 °C in cold worked stainless steels, and growth of existing Cr carbides can occur below 300 °C. The fundamental phenomenon relates to the formation of Cr carbides (usually $Cr_{23}C_6$ in stainless steels), which nucleate preferentially in the grain boundaries. Because C diffuses much faster than Cr, a Cr depletion profile is created adjacent to the grain boundary (the diffusivity of Cr within the grain boundary is much higher than within the grain, so the Cr concentration is reasonably constant along the grain boundary). At higher temperature, the Cr profile is deeper and wider. When the carbon is consumed, the carbide stops growing, and the Cr depletion profile eventually vanishes. This is difficult to accomplish in stainless steels, but such "healed" microstructures can be fairly readily produced in nickel-base alloys.

The effect of Cr depletion is most evident in oxidizing and/or pH-shifted water chemistries (oxidizing environments create a pH shift in cracks and crevices). In oxidizing (e.g., traditional BWR) environments with impurities (e.g., 50 – 100 ppb sulfate), the presence of sensitization can produce a > 20X increase in crack growth rates, and a similar acceleration in crack initiation. However, in deaerated, near-neutral pH water, Cr depletion plays a much lesser role; indeed, the presence of carbides in the grain boundary reduces SCC susceptibility, apparently by making deformation in the grain boundaries more difficult.

Nucleation of Cr carbides is greatly delayed in time, e.g., by reducing the C content (L-grade stainless steels) and adding Mo (type 316 stainless steels). Thus, modern stainless steel components are either not welded or are fabricated from L-grade stainless steels.

Cr depletion also develops during irradiation due to *radiation-induced segregation*. The Cr profiles are much narrower, and the minimum Cr level is generally higher – usually in the range of 12 – 14% Cr for stainless steels containing ≈ 18% Cr. The report on irradiation assisted SCC goes into this phenomenon in more detail.

- Oxidants and Corrosion Potential. The presence of oxidants like dissolved O_2, H_2O_2, and Cu ion can increase SCC and corrosion fatigue (CF) growth rates markedly. Oxidants react on metal surfaces and elevate the corrosion potential. As oxidants diffuse into cracks and crevices, they are consumed (electrochemically balanced by reaction with H_2 or metal corrosion). Thus, the interior of cracks and crevices are at low corrosion potential, and the difference in corrosion potential drives migration of anions (like chloride) into the cracks, and cations (like H^+ and Na^+) out of the cracks. The effect on SCC and CF of a complex mix of oxidants (and reductants) is fully captured by their effect on corrosion potential. The corrosion potential is not linear with oxidant concentration, and small (ppb) levels of oxidants can produce large (> 300 mV) change in corrosion potential.

  Figure B.1.3 shows an example of the effect corrosion potential of SCC. While its effect is very strong on sensitized stainless steels, it also affects non-sensitized stainless steel (and nickel-base alloys, and carbon and low alloy steels). However, SCC growth occurs at moderate rates in deaerated water (and without any prior exposure to water containing oxidants) and so is also a potential concern in PWRs if cracks can initiate.

- Water Purity and pH. Water purity has a profound effect on SCC and CF, and in oxidizing water there is sensitivity to ≈ 10 ppb levels of impurities. The most damaging impurities are chloride and sulfate, but most impurities are damaging. In oxidizing environments, even buffering chemistries (e.g., the B/Li chemistries used in PWRs) produce accelerated growth rates (compared to pure water) in oxidizing environments. Because the oxidizing conditions produce a pH-shifted chemistry in cracks and crevices, there is somewhat less sensitivity to bulk pH (for crack growth – crack initiation is more directly dependent on the bulk chemistry).

In deaerated water (where essentially no difference in corrosion potential occurs in cracks), the sensitivity to impurities is low, although levels > 1 ppm can accelerate SCC. The relatively minor shifts in pH associated with pure (deaerated) water ($pH_{300C} \approx 5.63$) and various standard levels of B (as H_3BO_3) and Li (as LiOH) ($pH_{300C} \approx 6.8 – 7.4$) have a relatively minor effect on SCC growth rates.

The addition of H_2 to deaerated water produces a small decrease in corrosion potential (59.3 mV per 10X change in H_2 at 325 °C). This is very important for nickel-base alloys, because it can produce a transition across the Ni/NiO phase stability. However, there is pragmatically no way to cross the Fe/Fe_3O_4 phase boundary by adding H_2. There is evidence that increasing H_2 produces somewhat enhanced SCC susceptibility, but this has been observed in slow strain rate tests on smooth specimens, and may be associated with accelerated initiation under these conditions – a broadly parallel observation to enhanced corrosion fatigue initiation in stainless steels at low potential vs. high potential.

- Yield Strength / Cold Work / Weld Shrinkage Strain. There are multiple factors that can increase the yield strength in materials, including cold work, irradiation, precipitation hardening, etc. It appears that all have a similar effect on SCC growth rate. For stainless steels, the primary factors are cold work and irradiation, and irradiation is covered in a separate report on irradiation assisted SCC. Cold work occurs as bulk cold work; surface cold work from machining, rolling, grinding, etc.; and weld shrinkage strain in the heat-affected zone adjacent to welds. The latter factor has only recently been recognized and quantified, and equivalent room temperature strains of >20% are often observed near the fusion line. This explains the shift in location of most cracks from ≈ 6 – 8 mm (depending on wall thickness) from the fusion line in sensitized piping compared to ≈ 1 – 3 mm for unsensitized piping observed in BWRs.

  As materials are cold (or warm) worked, the effect of yield strength increases, and its effect on SCC growth rates appear to be captured by yield strength. The presence or absence of martensite in the deformed structure is small, at least for crack growth in high temperature water; martensite might affect crack initiation and lower temperature SCC response (e.g., < 150 °C). Figure B.1.3c shows the effect of cold work. Figure B.1.4 shows that the increase in growth rate is not linear with yield strength, and that yield strength affects SCC in a similar fashion at low and high corrosion potential.

- Temperature. In the range of 250 – 350 °C, increasing temperature increases SCC growth rates. Equally importantly, it appears to help sustain SCC growth. At lower temperature – all things being equal – the growth rates may continue to decrease; but “all things” are never equal. In particular, the corrosion potential changes with temperature;

this is especially pronounced and important in the presence of oxidants (Figure B.1.5). Pragmatically, as components cool down, many are exposed to unusual loading and/or water chemistry. BWR components vary only between 274 and 288 °C, where the difference in growth rates is limited. In PWRs, the temperature ranges from 286 °C (core inlet) to 323 °C (core outlet) to 343 °C (pressurizer), and the crack growth rate varies more significantly.

- Stress and Stress Intensity Factor. Stress and stress intensity factor obviously play a large role in SCC initiation and growth. In general, few components are designed for use above a nominal stress ≈ 80% of the yield strength. The effect of stress intensity factor on crack growth rate appears to vary with water chemistry, and tends to be in the range of K^2 to K^3 (Figure B.1.6). Many cracks grow adjacent to welds, where the weld residual stress profile must be accounted for along with operating stresses. The weld residual stress profile combined with the inherent effect of crack length, a, on stress intensity factor ($K \propto \sqrt{a}$), causes a large variation in K vs. crack length – sometimes resulting in an increase in K, and sometimes in a K that rises, then drops to zero.

- Low frequency vibratory loading, high frequency "ripple" loading, and even occasional load perturbations can significantly accelerate SCC growth rates. The distinction between SCC and corrosion fatigue (CF) is poorly demarcated, and with good reason: in most if not all cases, SCC and CF represent a continuum in the *environmentally assisted cracking* spectrum, with increasing strain rate causing higher propagation rates but a lower factor of improvement for SCC mitigation approaches such as water chemistry or material modifications (Figure B.1.7).

  K_{ISCC} was once considered to be an invariant material property. However, there is extensive evidence that "K_{ISCC}" depends on many parameters – indeed, the evidence of "K_{ISCC}" has been based on non-optimal experiments (e.g., use of transgranular fatigue pre-cracked specimens as a basis for growth or non-growth of intergranular stress corrosion cracks). Other tests were performed under decreasing stress intensity factor conditions where the change in K was large and/or the increment of growth small (e.g., compared to the size of the plastic zone). More recent data has shown well-behaved crack growth rates as low at 5.5 MPa√m. It is impossible to prove that a K_{ISCC} *doesn't exist*, because one can always choose an incrementally smaller K, and the growth rates become too small to study in a realistic time frame, e.g., below 3 MPa√m.

Predictability of SCC of Stainless Steels

A strong qualitative understanding and good quantitative predictive capability exists for SCC of stainless steels, esp. for BWR water chemistries and temperatures where extensive SCC has occurred, initially in sensitized pipe weld heat affected zones, and later in unsensitized vessel internal components (while there is a well-behaved continuum between unirradiated and irradiated stainless steels, SCC has occurred in stainless steel components that receive essentially no radiation damage (e.g., <0.01 dpa, such as the core spray lines).

The distinction between BWR and PWR primary operating conditions is not nearly as great as once thought, esp. as BWRs shift toward low corrosion potential operating by adding H_2 and, far more effectively, introducing NobleChem™ (which creates a sub-monolayer of Pt or Pt/Rh on all wetted surfaces [13-15]. Under such conditions, the primary differences between BWR and PWR primary water chemistry are: coolant additives (typically H_3BO_3 and LiOH) that shift the pH at temperature from 5.6 to ≈7.2; H_2 fugacity (≈50 vs. 3000 ppb H_2); and temperature (274 – 288 °C vs. 286 – 343 °C). Of these, temperature may be the most important factor for stainless steels; for nickel alloys (where the Ni/NiO transition can be traversed) both temperature and H_2 fugacity are important [4-8].

Examples of crack growth predictive capability are shown in Figures B.1.3, 4, 6 and 7 for sensitized and cold worked stainless steel [6,16-19]. Cold work is a particular concern – not only are some components used in a cold worked state (such as PWR baffle bolts), but most fabricated components have a surface layer of deformed, hardened material. Shrinkage strain during welding also produces a residual strain profile in the heat-affected zone (and the weld metal) in addition to the more-thoroughly studied residual stress profile [6,16-19]. These strains usually peak at the weld fusion line, generally at an equivalent room temperature cold work level of 15 – 20% (but sometimes higher) (Figure B.1.8).

Quantifying and understanding SCC in most systems relies predominantly on high quality, reproducible, consistent SCC data [20,21]. This has proven difficult enough in crack growth rate measurements, but is generally more difficult in crack initiation experiments as well as evaluation of plant data.

It is important to understand that the effect of individual changes (such as corrosion potential, water purity, temperature, cold work, stress intensity factor, irradiation, etc.) on SCC cannot be viewed in isolation in most experiments, and rarely if ever in plant components. For example, the effect of BWR water purity is dramatically different at moderate to high corrosion potential than at low corrosion potential (as indicated by the predicted curves in Figure B.1.3). Similarly, the factor of improvement observed for various mitigation techniques varies with loading and water chemistry conditions (Figure B.1.7).

It must also be recognized that there is a time-based evolution (e.g., related to plant operating conditions, or to radiation damage – as addressed in the IASCC topical report) and a crack-depth based evolution (e.g., in residual stress, stress intensity, cold work, sensitization, microstructure…), and these produce complex changes in predicted and observed response. Figure B.1.9 shows an example of this interaction in terms of the predicted difference in crack growth trajectory vs. time in different welds. Figure B.1.10 shows an example of crack length vs. time observations and predictions for sensitized type 304 stainless steel pipes.

SCC Mitigation

There are many approaches that have been pursued and adopted to mitigation SCC in stainless steels. In BWRs, eliminating sensitization (grain boundary Cr depletion) was a primary focus in the 1970s, and most BWRs replaced all recirculation piping with grades of stainless steel that resisted weld sensitization (by lowering C, adding Mo, using lower heat input, etc.). Efforts were also made to reduce weld residual stress by last-pass heat sink welding, induction heating, and mechanical stress improvements. Some BWRs operated with high aqueous impurity levels (esp. chloride and sulfate), and major efforts were undertaken to improve water purity.

The most effective mitigation strategy for existing plant components is to reduce the corrosion potential (Figure B.1.3), and the most effective way to accomplish this is using electrocatalysis. The techniques to make surfaces electrocatalytic are numerous, but the most effective and economical approach is NobleChem™ [13-15], which involves the injection of ionic forms or Pt (or Pt and Rh), which electrolessly reduce and deposit on the surfaces of all wetted parts in BWRs. Applications have been performed on about 30 BWRs, and a new on-line application technique will be performed at a lead plant in 2005.

There is a possibility of attaining further SCC mitigation by adding Zn [22,23]. This is applicable to both BWRs and PWRs, and because Zn is a cation, it is most effective if the corrosion potential is low (i.e., BWRs operating with NobleChem™). Accurate quantification of the benefit of various Zn levels must still be performed and validated. Other approaches are more achievable only in new plants or if components are replaced. For example, the presence of grain boundary carbides or other particles impedes crack advance provided that they are not accompanied by Cr depletion [16,17].

SCC of Stainless Steels – Concerns and Emerging Issues

A number of ambiguities and emerging concerns exist in the area of SCC of stainless steels. Despite some improvements, the quality of experimental crack growth rate data is still a large factor in the observed scatter and disagreements over the quantitative effect of specific parameters. Even more problematical is the lack of statistical confidence and even qualitative insight into the controlling factors for crack initiation, although in general the same factors that enhance the crack growth rate also accelerate crack initiation.

Among the emerging concerns is that role of increasing stress intensity factor (K) as the crack grows (dK/da) [24. There is usually a large positive dK/da early in the crack growth process because $K \propto \sigma\sqrt{a}$ (stress times the square root of crack depth), and the integrated effect of the weld residual stress profile produces an increasing stress at the crack as the crack grows. There continues to be a change in K as the crack grows longer, but the magnitude of the +dK/da or –dK/da is smaller (Figure B.1.11). Unfortunately, the few studies that have evaluated dynamic changes in K have been performed using a fixed change in load (dP/dt) or displacement vs. time (similar to dK/dt). However, this is expected and observed to yield non-conservative response because it does not produce the accelerating effect of *positive feedback* as the crack begins to growth faster, causing K to increase faster, causing the crack to grow faster… (Figure B.1.11) Conversely, with decreasing dK/da, as the crack slows, the rate of change of K slows, causing further slowing in the crack growth rate… At plant-relevant values of –dK/da, stable, well-behaved SCC can be sustained from 30 MPa√m to below 12 MPa√m [16,17,25]. Using –dK/dt (or –dP/dt) fails to provide the important feedback between the rate of change of K and the rate of crack growth, and tends to produce crack arrest.

Another concern is the role of Si, which has been shown to cause elevated crack growth rates and a limited effect of stress intensity factor or corrosion potential (Figure B.1.12) [16,17,25]. While this may be a particular concern for irradiated materials, many stainless steels have a nominal Si content of 0.7 – 1.0%, which may be sufficient to cause elevated growth rates. Si readily oxidizes and is quite soluble in high temperature water – indeed, it is typically present in BWR (and probably PWR) water at levels about 100X higher than other impurities (typically 100 – 1000 ppb). It does not affect conductivity because is dissolves primarily in non-ionic form. A more speculative concern is the role of Mo, esp. in type 316 stainless steels, which have 2 – 3% Mo. Mo does not impart large improvements in corrosion or stress corrosion resistant in high temperature water (as it does below ≈ 100 °C), and it does readily oxidize and become soluble. Importantly, many type 316 stainless steels show very high Mo segregation at the grain boundary (10 – 20% Mo), the extent of which peaks at certain cooling rates following annealing [26]. This could have a significant effect on SCC response, although no studies have yet been performed to confirm it.

A final concern relates to the role of environment in fracture toughness data. Essentially all of the fracture toughness data obtained above 200 °C were obtained in air. It is well established that high crack propagation rates under constant load – and reduced toughness in J-R tests – are observed in the range of about 75 – 140 °C for precipitation hardened Ni alloys [27-29], and it is reasonable to suspect that this might occur in stainless steels and Ni alloys like alloys 600 and 690 (esp. if their yield strength is elevated from cold worked, weld shrinkage strain or irradiation). Very preliminary data at 288 °C on cold worked stainless steel showed that the specimen unexpectedly failed as the K was allowed to increase to about 88 MPa√m at the end of a test. The load was accurately known, as was the crack depth from post-test fractography at the point sudden failure occurred [17].

References

[1] R.L. Cowan and G.M Gordon, "Intergranular Stress Corrosion Cracking and Grain Boundary Composition of Fe-Ni-Cr Alloys", Stress Corrosion Cracking and Hydrogen Embrittlement of Iron-Base Alloys, Eds. R.W. Staehle, J. Hochmann, R.D. McCright and J.E. Slatern, NACE, Houston, 1977, p.1063-1065.
[2] Proc., Fundamental Aspects of Stress Corrosion Cracking, Eds. RW Staehle, AJ Forty and D van Rooyen, NACE, 1969.
[3] Proc. 1st – 11th Int. Symp. on Environmental Degradation of Materials in Nuclear Power Systems – Water Reactors, NACE / ANS / TMS, 1983 – 2003.
[4] F.P. Ford and P.L. Andresen, "Corrosion in Nuclear Systems: Environmentally Assisted Cracking in Light Water Reactors", in "Corrosion Mechanisms", Ed. P. Marcus and J. Ouder, Marcel Dekker, p.501-546, 1994.
[5] P.L. Andresen and F.P. Ford, "Life Prediction by Mechanistic Modelling and System Monitoring of Environmental Cracking of Fe and Ni Alloys in Aqueous Systems", Materials Science and Engineering, A103, p.167-183, 1988.
[6] P.L. Andresen, "Perspective and Direction of Stress Corrosion Cracking in Hot Water", Proc. Tenth Int. Symp. on Env. Degradation of Materials in Nuclear Power Systems – Water Reactors, NACE, Houston, 2001.
[7] P.L. Andresen, T.M. Angeliu and L.M. Young, "Immunity, Thresholds, and Other SCC Fiction", Proc. Staehle Symp. on Chemistry and Electrochemistry of Corrosion and SCC, TMS, Feb. 2001.
[8] P.L. Andresen, "Conceptual Similarities and Common Predictive Approaches for SCC in High Temperature Water Systems", Paper 96258, Corrosion/96, NACE, 1996.
[9] P.L. Andresen and D.J. Duquette, "The Effect of Chloride Ion Concentration and Applied Potential on the SCC Behavior of Type 304 Stainless Steel in Deaerated, High Temperature Water", Corrosion, Vol. 36, No. 2, p. 85 (1980).
[10] P.M. Manning and D.J. Duquette, Corrosion Science 20, p.597-610, 1980. See also P. E. Manning, "The Effect of Environmental Variables on the Pitting Corrosion Behavior of Single and Duplex Phase 304L Stainless Steel", Ph.D. Thesis, Rensselaer Polytechnic Institute, December 1978.
[11] Y.J. Kim, "Analysis of the Oxide Film Formed on 304 SS in 288C Water Containing O_2, H_2 and H_2O_2", Corrosion 55, p.81, 1999.
[12] Y.J. Kim and P.L. Andresen, "Data Quality, Issues and Guidelines for ECP Measurements in High Temperature Water", Corrosion 59, 7, p.584-596, 2003.
[13] P.L. Andresen, "Application of Noble Metal Technology for Mitigation of Stress Corrosion Cracking in BWRs", Proc. Seventh International Symposium on Environmental Degradation of Materials in Nuclear Power Systems – Water Reactors, NACE, p.563-578, 1995.
[14] S. Hettiarachchi, G.P. Wozadlo, T.P. Diaz, P.L. Andresen and R.L Cowan, "The Concept of Noble Metal Addition Technology for IGSCC Mitigation of Nuclear Materials", Proc. Seventh Int. Symp. on Environmental Degradation of Materials in Nuclear Power Systems – Water Reactors, NACE, p.735-746, 1995.
[15] P.L. Andresen, T.P. Diaz and S. Hettiarachchi, "Effect on Stress Corrosion Cracking of Electrocatalysis and Its Distribution Within Cracks", Proc. of 11th Int. Symp. on Environmental Degradation of Materials in Nuclear Power Systems – Water Reactors, ANS, 2003.

[16] P.L. Andresen, P.W. Emigh, M.M. Morra and R.M. Horn, “Effects of Yield Strength, Corrosion Potential, Stress Intensity Factor, Silicon and Grain Boundary Character on the SCC of Stainless Steels”, Proc. of 11th Int. Symp. on Environmental Degradation of Materials in Nuclear Power Systems – Water Reactors, ANS, 2003.

[17] P.L. Andresen, P.E. Emigh and L.M. Young, “Mechanistic and Kinetic Role of Yield Strength / Cold Work / Martensite, H_2, Temperature, and Composition on SCC of Stainless Steels”, Proc. Int. Symp. on Mechanisms of Material Degradation in Non-Destructive Evaluation in Light Water Reactors, Osaka, Japan, May 2002, published by Inst. of Nuclear Safety System, Japan, 2002.

[18] T.M. Angeliu, P.L. Andresen, J.A. Sutliff and R.M. Horn, “Intergranular Stress Corrosion Cracking of Unsensitized Stainless Steels in BWR Environments”, Proc. Ninth Int. Symp. on Environmental Degradation of Materials in Nuclear Power Systems – Water Reactors, AIME, 1999.

[19] P.L. Andresen, L.M. Young, W.R. Catlin and R.M. Horn, “Stress Corrosion Crack Growth Rate Behavior of Various Grades of Cold Worked Stainless Steel in High Temperature Water”, Corrosion/02, Paper 02511, NACE, 2002.

[20] P.L. Andresen, “SCC Testing and Data Quality Consideration”, Proc. Ninth Int. Symp. on Environmental Degradation of Materials in Nuclear Power Systems – Water Reactors, AIME, 1999.

[21] P.L. Andresen, K. Gott and J.L. Nelson, “Stress Corrosion Cracking of Sensitized Type 304 Stainless Steel in 288C Water: A Five Laboratory Round Robin”, Proc. Ninth Int. Symp. on Environmental Degradation of Materials in Nuclear Power Systems – Water Reactors, AIME, 1999.

[22] P.L. Andresen and Thomas P. Diaz, “Effects of Zinc Additions on the Crack Growth Rate of Sensitized Stainless Steel and Alloys 600 and 182 in 288C Water”, Bournemouth Conference, BNES, England, October 1993.

[23] P.L. Andresen and T.M. Angeliu, “Effects of Zinc Additions on the Stress Corrosion Crack Growth Rate of Sensitized Stainless Steel, Alloy 600, and Alloy 182 Weld Metal in 288C Water”, Corrosion/95, Paper #95409, T-2A Symposium, NACE, 1995.

[24] P.L. Andresen and M.M. Morra, “Effect of Rising and Falling K Profiles on SCC Growth Rates in High Temperature Water”, Paper 71643, ASME PVP 2005, Denver, 2005.

[25] P.L. Andresen and M.M. Morra, “Effects of Si on SCC of Irradiated and Unirradiated Stainless Steel and Ni Alloys”, Paper 05591, Corrosion/05, NACE, Houston, 2005.

[26] J. T. Busby, G. S. Was, S. M. Bruemmer, D. Edwards and E. A. Kenik, “Influence of the Initial Grain Boundary Composition on the Evolution of Radiation-Induced Segregation Profiles,” Proc. Mater. Res. Soc., MRS, vol. 540, 1999, pp. 451-456. See also E. P. Simonen and S. M. Bruemmer, “Thermally Induced Grain Boundary Composition and Effects on Radiation-Induced Segregation,” Proc. 8th International Symposium on Environmental Degradation of Materials in Nuclear Power Systems–Water Reactors, ANS, 1997, p. 751.

[27] C.A. Grove and L.D. Petzold, “Mechanism of SCC of Alloy X750 in High Purity Water”, J. of Materials for Energy Systems, Vol. 7, No. 2, p.147-162, Sept 1985. See also, L.D. Petzold and C.A. Grove, “Mechanism of SCC of Alloy X750 in High Purity Water”, Proc. Corrosion of Nickel Alloys, Ed. R.C. Scarberry, ASM, 1985, p.165.

[28] G.A. Young, N. Lewis, M. Hanson, W. Matuszyk, B. Wiersma, S.C. Gonzalez, “Microstructural and Microchemical Characterization of Dual Step Aged alloy X-750 and its Relationship to Environmentally Assisted Cracking”, Proc., Tenth International Conference on Environmental Degradation of Materials in Nuclear Power Systems – Water Reactors, NACE, 2002.
[29] Mills, W. J., Brown, C. M. and Burke, M. G., “Effect of Microstructure on Low Temperature Cracking Behavior of EN82H Welds,” Tenth International Conference on Environmental Degradation in Nuclear Power Systems – Water Reactors, NACE, 2002(a). See also C. M. Brown and W. J. Mills, “Effect of Water on Mechanical Properties and Stress Corrosion Behavior of Alloy 600, Alloy 690, EN82H Welds, and EN52 Welds”, Corrosion, Vol. 55, 1999, p. 173.
[30] C.M. Chen, K. Aral and G.J. Theus, “Computer Calculated Potential pH Diagrams to 300 °C,” EPRI NP-3137 Vol.2 (1167-2), June 1983.
[31] M.E. Indig and A.R. McIlree, “High Temperature Electrochemical Studies of the Stress Corrosion of Type 304 Stainless Steel”, Corrosion 35, p.288, 1979.

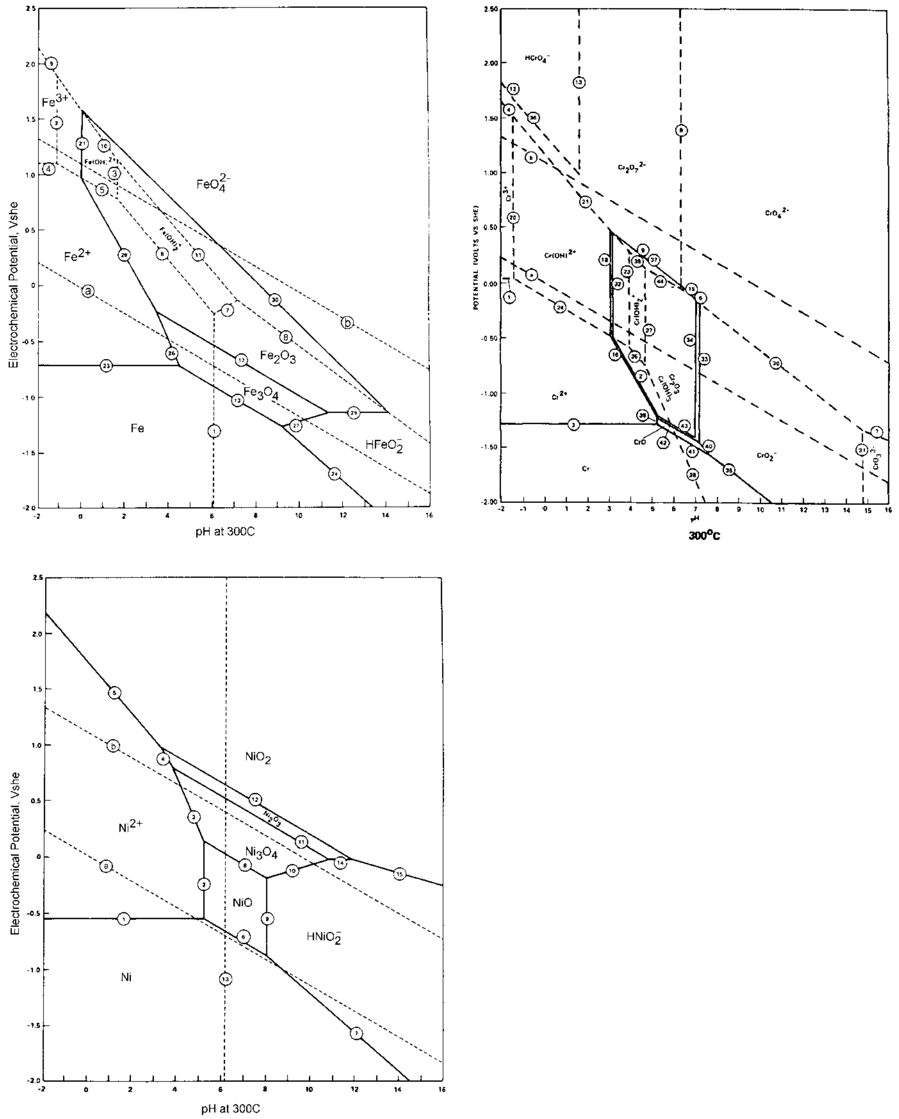

Figure B.1.1 Pourbaix diagrams for Cr, Fe and Ni in 300 °C water [30].

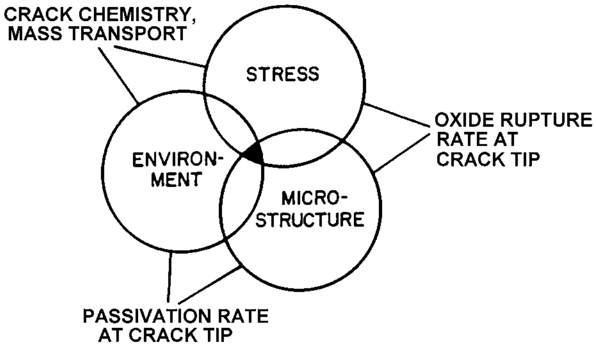

Crack depth vs. time = f (Material, Stress, Environment)

Chromium	Primary	Corrosion Potential
% Cold Work	Static	Oxidizing Species
Neutron Fluence	Dynamic	Anionic Species
Silicon	Residual	Type
Nickel	Crack Depth	Activity
Sulfur	Neutron Fluence	Temperature
Phosphorus	Relaxation	Flow Rate
Carbon	Thermal	Neutron flux
Weld heat input	Radiation	Crack Depth

Figure B.1.2 The complexity of SCC is reflected in the large number of influential variables and the associated requirement that all 20 to 40 in a given system be adequately controlled [4,5].

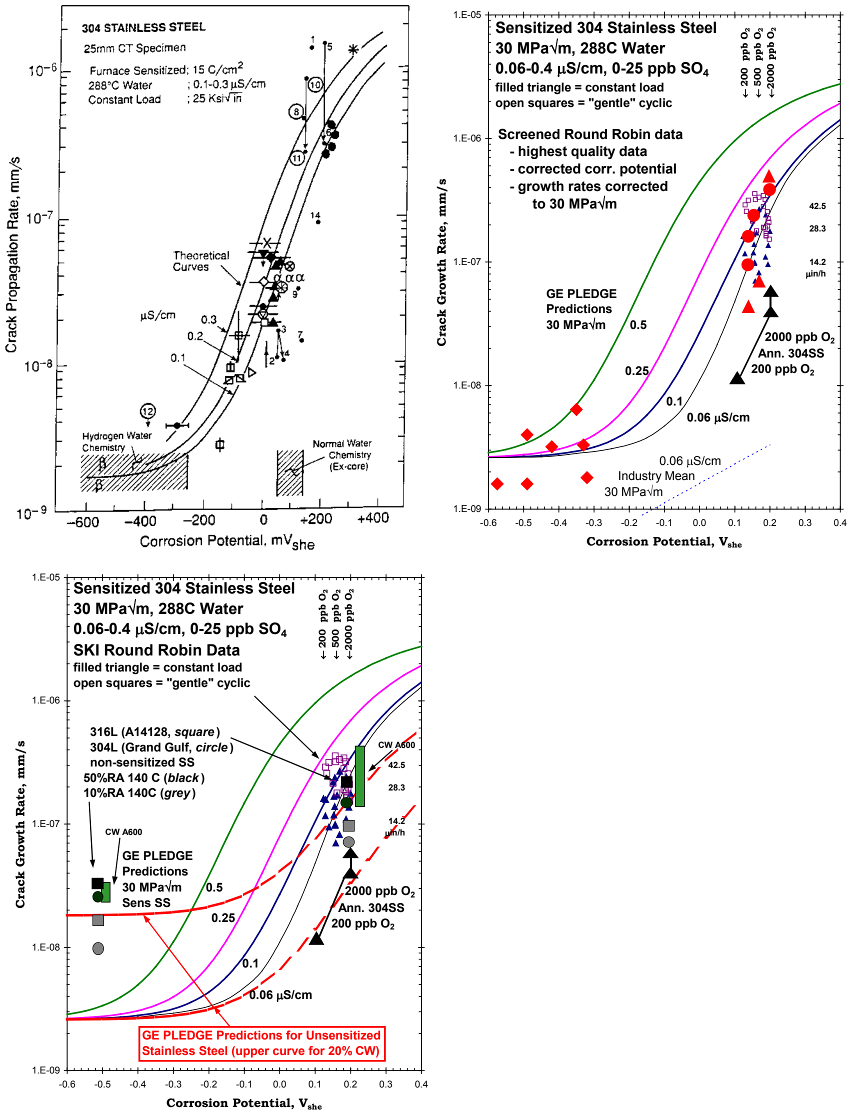

(a) (b) (c)

Figure B.1.3 SCC growth rate vs. corrosion potential for stainless steels tested in 288 °C high purity water containing 2000 ppb O_2 and 95 – 3000 ppb H_2 [4,5,16,17].

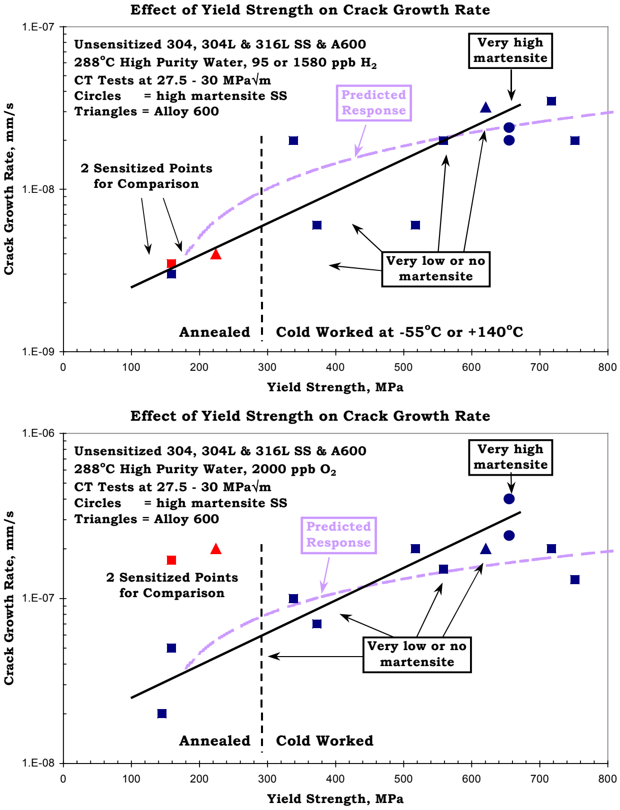

(a) (b)

Figure B.1.4 Effect of yield strength and martensite on the stress corrosion crack growth rate on stainless steel and alloy 600 in 288 °C, high purity water (<0.10 μS/cm outlet) at (a) low and (b) high potential [16,17].

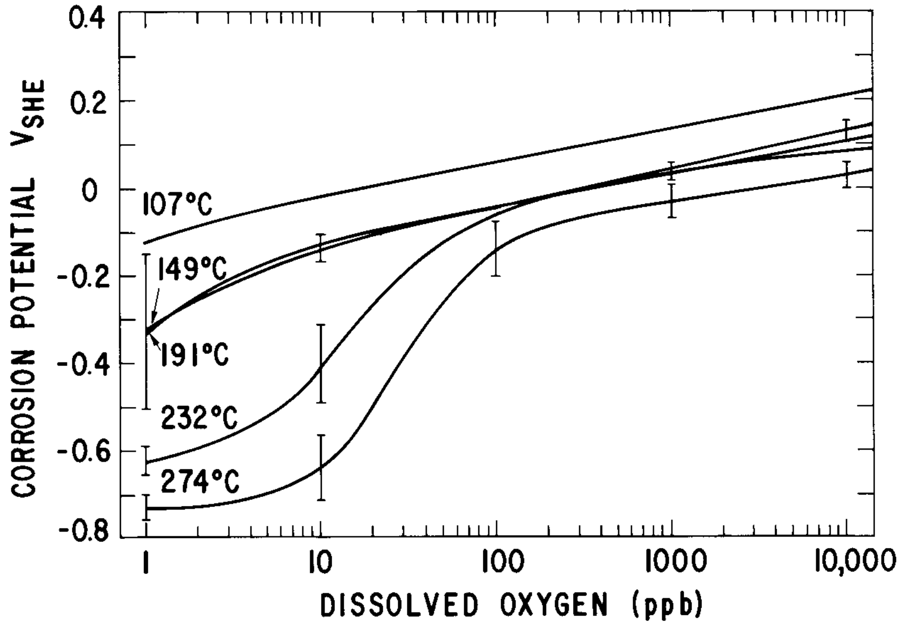

Figure B.1.5 Corrosion potential vs. dissolved O_2 and temperatures for stainless steels in pure water [31].

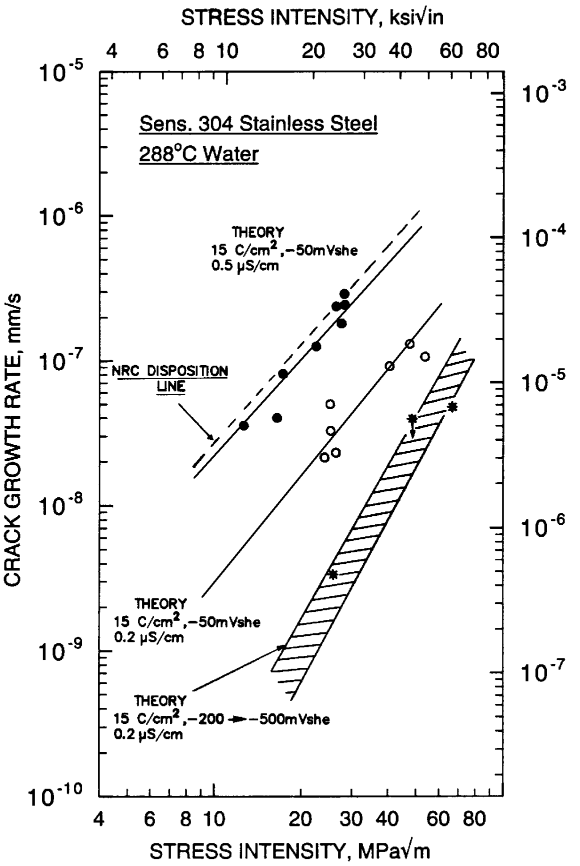

Figure B.1.6 Effect of stress intensity factor on the SCC growth rate of sensitized type 304 stainless steel in high temperature water [4,5].

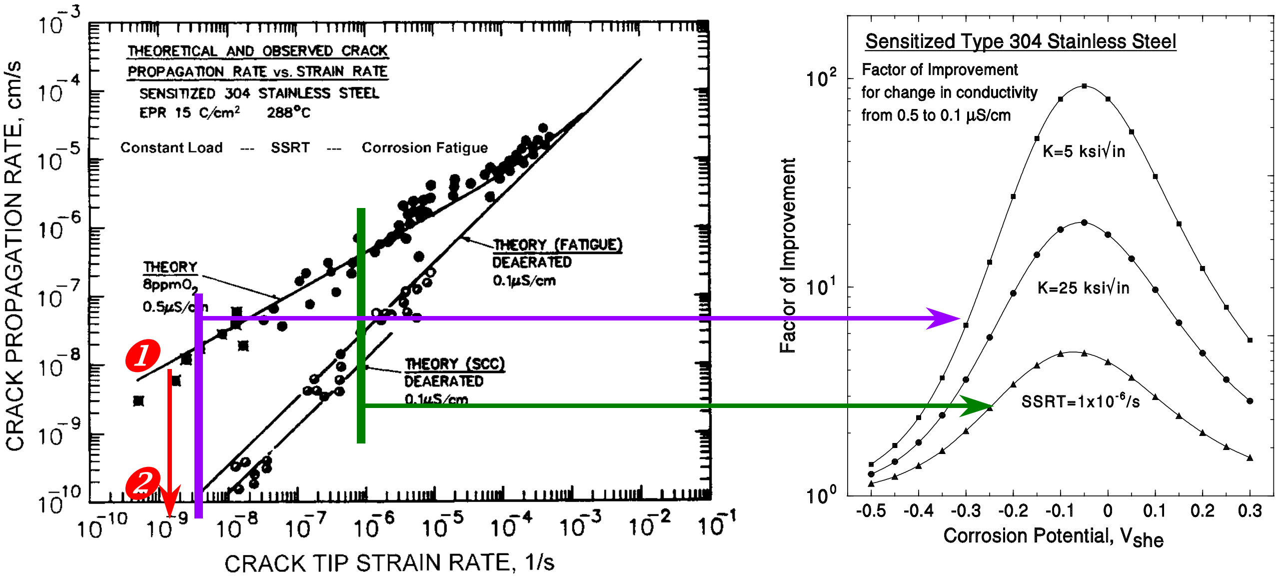

Figure B.1.7 Crack growth rate vs. crack tip strain rate showing the ability to predict environmental cracking across a range of constant load/K, slow strain rate and corrosion fatigue response. When water chemistry or the material is changed, the resultant curves are not parallel, but diverge at lower crack tip strain rate. Thus, the benefit observed in a laboratory test or component will depend on the testing condition, both loading and water chemistry [4-6].

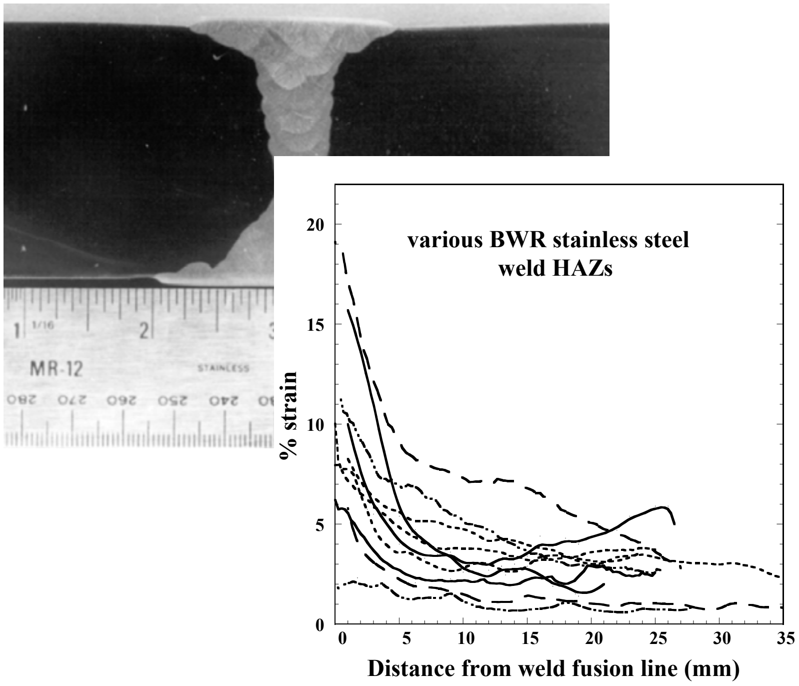

Figure B.1.8 Weld residual strain vs. distance from the weld fusion line for stainless steel welds. If the number of welding passes is limited, the peak residual strain can be below 10% equivalent room temperature tensile strain. However, most pipe welds that have been analyzed show residual strains in the range of 15 – 20%, with some slightly above 25%. The residual strain is also highest near the root of the weld [18].

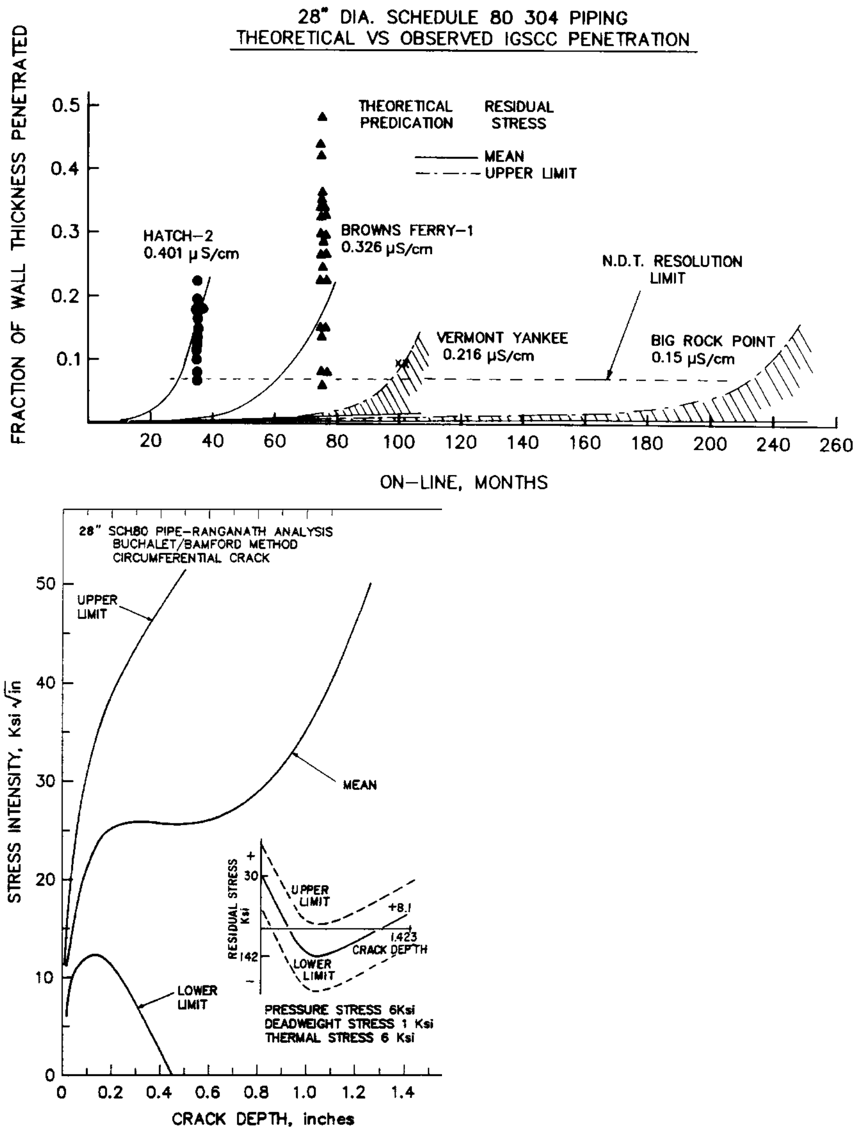

Figure B.1.9 (a) Crack length vs. time for pipe welds in various BWRs whose water purity varied markedly during their first years of operation. (b) Stress intensity factor vs. crack depth for pipe welds. The complex changes in residual stress, stress intensity factor and crack length vs. time that results in plant components. Irradiation makes the situation much more complex (see IASCC topical paper).

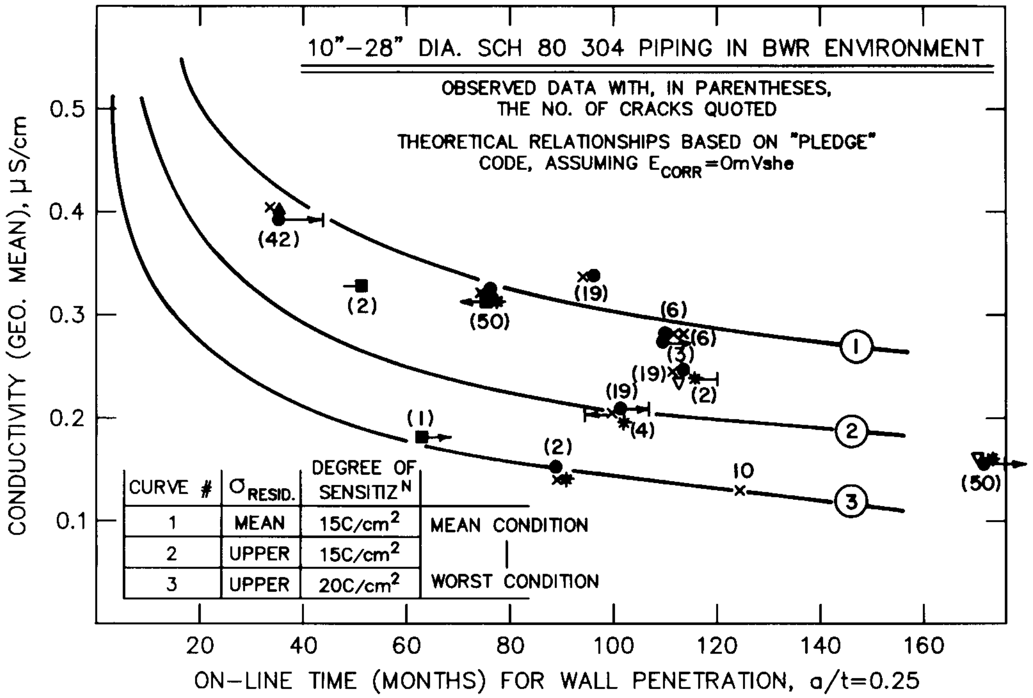

Figure B.1.10 The effect of conductivity on on-line months to achieve a crack depth of 25% of through-wall [4,5].

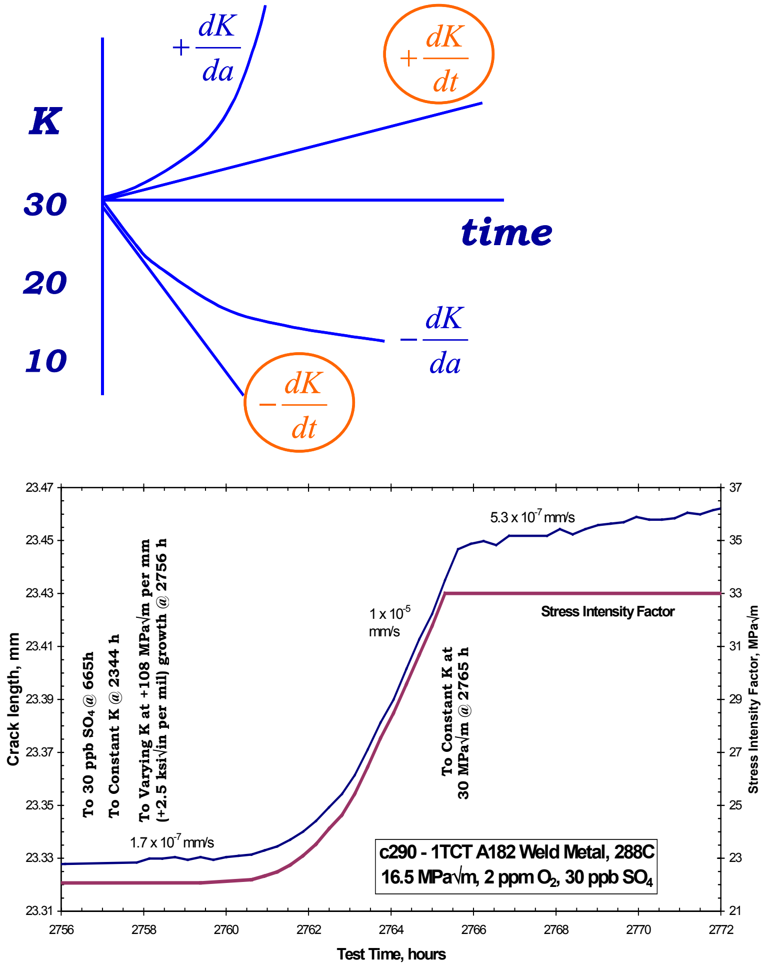

Figure B.1.11 Schematic and example crack length vs. time data showing the important role of +dK/da on crack growth rate, and the important difference between dK/da and dK/dt testing. In general, dK/dt always leads to non-conservative growth rates. +dK/da provide a positive feedback that often leads to dramatic increases in crack growth rate, while –dK/da represents negative feedback that slows the change in K as the crack slows down [24].

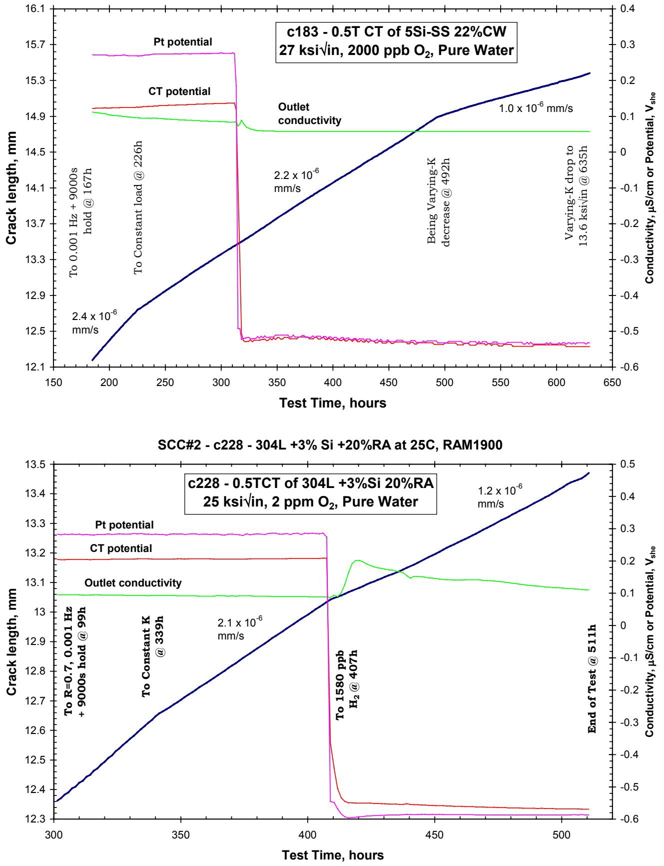

Figure B.1.12 Effect of Si on the crack growth rate of "stainless steels" whose bulk composition was designed to simulate an irradiated grain boundary. Reasonable questions can be raised about how realistic it is to create bulk alloys that represent the composition of a few nm region, but the qualitative observations remain important – i.e., that there is little effect of corrosion potential or stress intensity factor on crack growth rate [16,17,25].

B.2 IASCC of Stainless Steels and Other Irradiation Induced Phenomena

This topical paper provides a foundation for understanding the proactive materials degradation concerns originating from irradiation effects. The emphasis is on irradiation assisted stress corrosion cracking (IASCC) of ***wrought, austenitic stainless steels*** in BWR and PWR environments. Other radiation induced phenomena that are discussed include radiation creep relaxation, swelling and microstructural evolution. There are separate topical papers for SCC in unirradiated stainless steels, in cast stainless steels, and for lower temperature, mostly-chloride-related pitting and SCC of stainless steels. There are also separate topical papers related to BWR and PWR water chemistry, evolving operational practice, start-up and shut-down, and other factors that influence SCC.

The topical paper on SCC of unirradiated stainless steels provides an introduction to the mechanisms, processes and dependencies in high temperature water. The primary factors that control SCC of stainless steels in hot water [1-8] – many of which are affected by radiation – include:

- Degree of sensitization, i.e., Cr depletion along the grain boundaries.
- Oxidants and corrosion potential, which affect the crack chemistry as well as the nature of the oxide films on the free surfaces.
- Water purity and pH, which primarily affects the crack chemistry.
- Yield strength, which produces an increase in crack growth rate. There are many ways by which yield strength is increased, including bulk or surface cold work, weld residual strain, precipitation hardening, etc., but not usually to the same degree as is caused by irradiation.
- Temperature.
- Stress and Stress Intensity Factor.

It is widely accepted that irradiation assisted SCC (IASCC) is literally that: an *irradiation assisted* process [2,9-19]. When viewed in a given time frame in plant components (Figure B.2.1a) or in accelerated laboratory tests, there can appear to be a threshold fluence for IASCC, but in fact SCC is observed in unirradiated stainless steels [2-5,9,15,16,20-22]. Irradiation is known to affect primarily the grain boundary chemistry (i.e., degree of sensitization), the oxidants and corrosion potential, the yield strength and the stress (via irradiation creep relaxation) components in this list of factors. In sufficiently careful and sensitive laboratory tests (e.g., crack growth rate tests), all grades of austenitic stainless steel have been shown to have inherent susceptibility to SCC. However, the numerous factors that promote SCC give rise to orders of magnitude difference in susceptibility – i.e., the incidence of cracking. Importantly, the effects of most parameters, such as corrosion potential, water impurities, stress, stress intensity factor, temperature, etc. are known to have a similar effect on both irradiated and unirradiated stainless steels.

The effect of corrosion potential (Figure B.2.1b) and water purity (Figure B.2.2) is similar for unirradiated and irradiated stainless steels exposed in BWR environments, which supports the concept that the underlying mechanisms and dependencies are similar. While the term "threshold fluence" appears in the literature, it should be recognized that unirradiated (and unsensitized, un-cold-worked) materials have some small susceptibility to SCC, and an apparent "threshold fluence" depends strongly on the details of other controlling parameters, such as the environment, loading, cold work, temperature, etc. Thus, a "threshold fluence" has relevance primarily from an engineering perspective within a specific context of environment, loading, etc. [5,9,11]

Figure B.2.1 shows the increasing SCC incidence with increasing fast neutron fluence in BWR crevice control blade sheath and in laboratory slow strain rate tests. While small amounts of intergranular cracking have been observed in tests in inert environments on irradiated stainless steels, there is an incontestable and dominant aqueous environmental effect. Thus, the concerns for cracking in irradiated components are appropriately characterized as IASCC, not as a simple effect on mechanical properties [2,9-19].

The radiation dose achieved in various components and the onset of various radiation effects is shown in Figure B.2.3 [11]. Most aspects of IASCC are well understood qualitatively, and a good quantitative description seems to exist in BWR water chemistry and temperature regime, but it is not completely clear that all of the aggravating effects of radiation on SCC are identified or qualified for all light water reactor conditions, esp. at the higher temperatures and fluences in PWRs. For all systems, the following factors are known to be important (Figure B.2 .4):

I. **Radiation hardening** (RH), in which the radiation generated defects produce an increase in yield strength (and a localization of deformation to "channels" in the material). Figure B.2.5 shows the increase in yield strength of a variety of austenitic stainless steels vs. irradiation dose. An increase in the yield strength from 150 – 200 MPa up to 750 – 1000 MPa is commonly observed, with a saturation after several dpa. Cold worked materials have a higher initial yield strength, but follow a broadly similar trajectory vs. dose, achieving a similar yield strength at saturation. Much of the microstructural evidence of the initial cold worked microstructure has vanished after about 5 dpa.

   The increase in yield strength results primarily from the formation of vacancy and interstitial loops (Figure B.2.6). Source hardening and dispersed barrier hardening models provide reasonable correlations between hardening and the dislocation loop microstructure, with the increase in yield strength (or hardness) proportional to $(N_{loop} \times d_{loop})^{0.5}$, where N_{loop} is the loop number density and d_{loop} is the loop diameter.

   The effect of yield strength on SCC growth rates is discussed in the topical paper on unirradiated austenitic stainless steels, and appears to be a common effect among many materials and many mechanisms of yield strength enhancement (cold work, martensite formation, irradiation, precipitation hardening, etc.). Growth rates are increased in both BWR and PWR chemistries.

   The homogeneous nature of deformation at low dose is replaced by heterogeneous deformation at higher doses as the defect microstructure impedes the motion of dislocations. Initial dislocations clear defects along narrow channels, and plasticity becomes highly localized. The channels are very narrow (< 10 nm) and closely spaced (<1 mm) and typically run the full length of a grain, terminating at the grain boundaries. Dislocation channeling results in intense shear bands that can cause localized necking and a sharp reduction in uniform elongation, but the reduction in area generally remains very high. Dislocation channeling may also be an important in IASCC [11,19].

II. **Radiation induced segregation** (RIS), in which the migration of radiation generated defects (vacancies and interstitials) to sinks (esp. grain boundaries), alters the local chemistry within the material. Figure B.2.7 shows two examples of the grain boundary composition of high purity and commercial purity heats of stainless steel. The enrichment or depletion of major alloying elements and impurity elements can be significant [2,9-19], with depletion of Cr of >5% and enrichment of Si by >5-10X often observed [2,9-22].

RIS is driven by the flux of radiation-produced defects to sinks, and is therefore fundamentally different from thermal segregation or elemental depletion from grain boundary precipitation processes (e.g., sensitization from Cr carbide or boride formation and growth). In simple terms, radiation displaces an atom from its lattice site, and it comes to rest in a relatively distant location in an interstitial site. In fact, this primary displaced atom itself interacts with other atoms along its path, producing a cascade of damage as it loses energy and comes to rest. The resultant vacancies and interstitials can reach concentrations that are orders of magnitude greater than the thermal equilibrium concentrations. They migrate and are absorbed at sinks, creating profiles in concentrations of the constituent elements near grain boundaries. The species that diffuse more slowly by the vacancy diffusion mechanism are enriched at the grain boundary and the faster diffusers become depleted. Enrichment and depletion can also occur by association of the solute with the interstitial flux. In this case, the undersized species will enrich and the oversized species will deplete.

Even though the depletion and enrichment profiles are very narrow compared to those that form from, e.g., Cr carbide formation during welding or heat treatment, the effect on SCC remains very pronounced. For example, very narrow Cr depletion profiles can be generated during complex, multi-step heat treatments, and for a given level of Cr depletion, they have as strong an effect on SCC in high temperature water as much wider Cr depletion profiles.

Si enrichment is potentially of great concern because many stainless steels containing 0.5 – 1% Si can enrich to >5% at the grain boundary. Indeed, since the measurements are generally made by analytical electron microscopy, which has a 1 – 2 nm beam size, the actual Si concentration at the grain boundary can approach 50 atomic percent. Crack growth rate measurements on stainless steels with elevated Si levels (e.g., 1.5 – 5% Si) show high growth rates and limited or no effect of stress intensity factor and corrosion potential (Figure B.2.8) [20-22]. This may help explain the loss of the benefit of lowering the corrosion potential at high fluence in some stainless steels, esp. since Si enrichment appears to continue after Cr depletion saturates.

III. **Radiation creep relaxation**, in which the migration of radiation generated defects under stress produces an accelerated creep rate (e.g., at constant load) and/or stress relaxation (e.g., at constant displacement, as for weld residual stresses, bolts and springs). Figures B.2.9 and 10 show two examples of radiation creep relaxation, which produces a large reduction in stress after a dose of several dpa. The radiation creep rate is proportional to the dose rate (flux) and stress.

Radiation creep relaxation is a mixed benefit. For welds, the weld residual stress is significantly relaxed in the same range of fluence where radiation hardening and segregation occur, and the net effect is generally beneficial. However, in many bolting application, the loss of stress over time can cause other problems related, e.g., to inadequate clamping forces that allow leakage that can produce erosion or fatigue.
Because radiation creep inherently represents deformation, it can also promote SCC nucleation and help sustain crack growth. The radiation creep rates are very small compared to other sources (e.g., cyclic loading, slow strain rate testing, and strain redistribution at the tips of SCC cracks), so there is no evidence or expectation that growth rates will be elevated. However, the low rates of continuous deformation resulting from radiation creep may promote crack nucleation and help sustain crack advance.

Radiation creep provides a good example of a complicating factor in understanding the effects of radiation. Because radiation affects grain boundary chemistry and increases yield strength while it simultaneously reduces the stress near welds and in bolts, understanding and deconvoluting the effects of radiation on SCC is very difficult to do from field data. Add to this the effects of plant operating conditions (such as having high impurity levels early in BWR life), and it becomes very difficult to use plant data as a basis for understanding the real affects of various parameters on SCC, or to anticipate the response of one component (e.g., with constant displacement stresses) with others (e.g., with active pressurization stress). This is an example of the importance of developing a fundamental framework from which hypotheses can be formulated and tested. Such an approach has been undertaken, and even twenty years after the original hypotheses, this framework still represents the basis for current understand of irradiation effects on SCC. While some improvements in quantifying some aspects of irradiation effects on yield strength, corrosion potential, radiation induced segregation and radiation creep relaxation could undoubtedly be made, there is a strong basis for both understanding and predicting radiation effects on SCC.

IV. **Radiolysis**, in which H_2O is broken into various constituent elements, including H_2O_2 and H_2 (the longer lived species) as well as radicals (e.g., e_{aq}^-, H, OH, HO_2). While stoichiometric quantities of oxidizing and reducing species are formed, the corrosion potential inevitably increases, sometimes dramatically. Radiolysis is suppressed at coolant H_2 levels above about 500 ppb (5.6 cc/kg), so there is little concern for radiolysis in PWRs (whose coolant H_2 level is typically 25 – 35 cc/kg).

In BWRs, the primary radiolytic species of interest are H_2 and H_2O_2. H_2 preferentially partitions to the steam phase, while H_2O_2 remains in the recirculating water, creating a net oxidizing environment. The effect of these (and other) species on SCC is accurately characterized by their effect on corrosion potential. The corrosion potential on most structural materials is similar in deaerated water, and drops by about 57 mV per 10X increase in H_2 and 114 mV per unit increase in pH at 300 °C. As soon as even very small amounts of oxidants are present (e.g., ppb levels), the corrosion potential can rise dramatically, generally increasing by 500 mV or more at >10 ppb of oxidant. Most importantly, when oxidants change the corrosion potential, a differential aeration cell forms, which produces an altered crack chemistry – this does not occur if only H_2 is present because it is not consumed in cracks (as is H_2O_2 and O_2).

Concerns have been expressed that radiolysis could produce oxidizing conditions within cracks, and thereby alter the corrosion potential, mass transport processes, and SCC. However, an evaluation of the corrosion potential in a tight crevice under highly irradiated conditions showed no consequential elevation in corrosion potential (e.g., < 25 mV).

V. **Radiation induced swelling**, in which voids form within the material that produce a change in material density and dimensions. This can produce distortion and warping, which can in turn produce elevation in stresses, e.g., in bolted structures. The occurrence of swelling in austenitic stainless steels is very rare and/or limited below 310 °C, even at high fluence (>30 dpa). Gamma heating of thick components can produce perhaps a 40 – 50 °C elevation in internal temperature, and at such temperatures swelling is more likely at moderate to high fluence.

One possible area of significance for void swelling is in PWR baffle plates and bolts. Because the bolts are fabricated from cold worked stainless steel, swelling is delayed compared to the adjacent annealed plates. Radiation creep relaxation will reduce the stress applied by the bolts, but differential swelling of the plates relative to the bolts will cause re-loading of the bolts, which achieves some dynamic equilibrium (between re-loading from differential swelling and on-going radiation creep relaxation). This is difficult to quantify precisely at this time.

VI. **Gamma heating** has already been mentioned in relation to swelling. Another possible consequence of gamma heating is superheating of crevices in PWRs above the temperature of the pressurizer (for example crevices between the shanks of baffle bolts and baffle plates). Thus local boiling with consequent changes in environmental chemistry can occur. Although there is no hard evidence that this has caused any environmentally induced cracking, the phenomenon cannot be ignored when searching for contributing factors in service failures.

VII. **Fracture toughness** is reduced substantially in irradiated stainless steels. There is substantial scatter in the available data, but many stainless steels drop by a factor of five or more from 250 – 300 MPa√m to 50 MPa√m or even slightly lower (Figure B.2.11). These are also data obtained in air, and there may be further environmental degradation in fracture toughness in the environment, both at 288 – 323 °C and in the 75 – 140 °C regime [23].

Predictability of IASCC

A solid qualitative understanding and at least semi-quantitative predictive capability exists for IASCC, esp. for BWR water chemistries and temperatures (there may be additional aggravating effects of radiation that become important at the higher temperatures and fluences in PWRs).

The crack growth predictive capability is built on the basis of irradiation *assisted* SCC – that is, the understanding and predictive framework used for unirradiated stainless steels can be extended to radiation effects by defining key characteristics of SCC and quantifying those effects. This has been done for the four primary radiation induced phenomena: segregation, hardening, radiolysis and relaxation (Figure B.2.4) [2,9,15,17,18]. Figure B.2.12 shows the crack growth response at high and high corrosion potential of irradiated stainless steel and of sensitized stainless steel exposed to high and flow neutron fluxes. These (and other) data are replotted in Figure B.2 13 to show crack velocity vs. corrosion potential. Other examples of predictive capability are shown in Figure B.2.14, which shows the response of neutron irradiated stainless steel in slow strain rate and constant load tests in 288 °C water. As in many SCC systems, obtaining high quality, reproducible, consistent SCC data experimentally is often a limiting factor in quantifying and validating predictive models.

The effect of individual changes (such as flux, fluence, temperature, radiolysis, segregation, hardening, relaxation, etc.) cannot be viewed in isolation in most experiments, and rarely if ever in plant components. For example, the temperature of irradiation, the presence of stress, the radiation dose rate (flux), etc. can all affect the result at a given dose / fluence. It must also be recognized that there is a time-based evolution in radiation damage (Figure B.2.15), and these produce complex changes in predicted and observed response. In most components that undergo IASCC, there are damaging elements of radiation exposure (e.g., hardening and segregation) and beneficial elements (radiation creep relaxation of constant displacement stresses). There are then further complications when considering plant operation and the evolution of cracks. For example, if the water chemistry in BWRs is good, so that cracks don't nucleate (or remain vanishingly small) by a dose of 1 – 3 x 10^{21} n/cm^2, then the weld residual stresses will have markedly decreased and the likelihood that SCC will occur also decreases markedly. Figure B.2.15 shows an example of this interaction in terms of the predicted difference in crack growth trajectory vs. time for different water purities in a BWR core shroud. Figure B.2.16 shows an example of crack length vs. time predictions for a type 304 stainless steel BWR core shroud with multiple inspections and multiple cracks, and a comparison of observed and predicted crack depth for a number of BWR core shrouds.

IASCC in baffle bolts has also been evaluated and some controlling factors identified [24], although the state of knowledge does not yet permit prediction.

IASCC Mitigation

There are a variety of approaches for mitigating SCC in light water reactors, and they fall into categories of water chemistry, operating guidelines, new alloys, stress mitigation and design issues. Since most components in light water reactors are not intended to be replaceable (and are therefore very expensive to replace), water chemistry is the most attractive mitigation strategy, with operating guidelines and perhaps stress mitigation providing more limited opportunities. While the focus of this paper is on IASCC, the most mitigation approaches (esp. water chemistry) are applicable to both irradiated and unirradiated components.

Water chemistry mitigation approaches are the easiest to implement, and can often provide mitigation to many areas and components in the plant. In BWRs, the focus is primarily on lowering the corrosion potential, which can be done with H_2 injection, but is more effectively achieved using NobleChem™ [25-27]. In both BWRs and PWRs, the addition of Zn appears to provide some crack growth rate benefit for stainless steels, although more work is needed. Similarly, improvements in surface finish, stresses, etc. are effective in both reactor types.

Alloying with oversized elements reduces the extent of radiation-induced segregation (esp. Cr depletion) [19], but it's not clear that it will reduce Si enrichment. Cr depletion is less important in BWRs at low potential and in PWR primary water, but low potentials cannot be achieved in all locations in a BWR (it requires stoichiometric excess H_2 in the water, which doesn't exist in areas where boiling occurs). Radiation hardening differs somewhat among stainless steel types and heats, but it's not clear that it can be changed sufficiently to make an adequate difference in SCC response. Slip localization may aggravate SCC, and there are alloying approaches for altering stacking fault energy which influences slip localization [19]. Operationally, it is always wise to avoid higher stresses, vibration, start up and shutdown, fatigue (e.g., from mixing of cold and hot water, which has increased in low leakage core configurations in PWRs), etc. The timing of H_2O_2 injection during PWR cooling and deaeration and H_2 injection during PWR heat up may be important. In BWRs, the early injection of H_2 during start up, and maintaining H_2 injection close to 100% of the time during operation should reduce SCC.

IASCC – Concerns and Emerging Issues

There remains a number of uncertainties and emerging concerns in the area of IASCC. The uncertainties arise in part from the huge scatter in data that has been obtained on irradiated stainless steel, much of which is caused by weaknesses in the experimental techniques. While factors such as good control and monitoring of water chemistry, transitioning from transgranular fatigue to intergranular SCC morphology, and similar concerns exist, perhaps the biggest issue is associated with K-size validity for crack growth specimens of irradiated materials [16,28]. There remain some concerns for the prospect of additional radiation related degradation (such as precipitation of new phases, high He and void swelling) at higher temperatures and fluences associated with PWR components. As in all materials / systems, the understanding and prediction of crack nucleation is much weaker than for crack growth.

Among the emerging concerns is the role of Si, which appears to continue to segregate under irradiation at fluences where Cr depletion has effectively saturated. This may occur because Si undergoes radiation-induced segregation by a different (or an additional) mechanism than does Cr. Evidence of highly elevated (> 3%) Si levels in irradiated stainless steels and very pronounced effects of Si on crack growth rate are a significant concern, esp. since many stainless steels have a nominal Si level of 0.6 – 1%. Crack growth rate studies show elevated growth rates and a limited effect of stress intensity factor or corrosion potential (Figure B.2.8) [20-22]. Si readily oxidizes and is quite soluble in high temperature water – indeed, it is typically present in BWR (and probably PWR) water at levels about 100X higher than other impurities (typically 100 – 1000 ppb). It does not affect conductivity because is dissolves primarily in non-ionic form.

Another concern is that role of increasing stress intensity factor (K) as the crack grows (dK/da) [29]. Because $K \propto \sigma\sqrt{a}$ (stress times the square root of crack depth), and because the weld residual stress profile changes vs. crack depth, there is usually a large positive dK/da early in the crack growth process. K also changes when the crack is longer, but the magnitude of the +dK/da or –dK/da is smaller. Unfortunately, most studies have been performed using a fixed change in load or displacement vs. time (similar to dK/dt), but this yields non-conservative response since it does not produce the accelerating effect of *positive feedback* as the crack begins to growth faster, causing K to increase faster, causing the crack to grow faster… Conversely, with decreasing dK/da, as the crack slows, the rate of change of K slows, causing further slowing in the crack growth rate… dK/dt fails to provide the important feedback between the rate of change of K and the rate of crack growth, and tends to produce crack arrest. Examples of this are shown in the topical paper on SCC unirradiated stainless steel and in reference [29].

Finally, fracture toughness data obtained in-situ (after prolonged exposure to high temperature water) [21] might be substantially lower than the vast majority of available data, all obtained in air. The reduction in toughness from irradiation might be broadly representative of cold worked stainless steel (Figure B.2.11), and both may show significant effect of the environment, both in 288 C and ~100 °C tests, and in tearing resistance (e.g., J-R tests) and impact loading (e.g., Charpy or K_{IC}).

References

[1] R.L. Cowan and G.M Gordon, "Intergranular Stress Corrosion Cracking and Grain Boundary Composition of Fe-Ni-Cr Alloys", Stress Corrosion Cracking and Hydrogen Embrittlement of Iron-Base Alloys, Eds. R.W. Staehle, J. Hochmann, R.D. McCright and J.E. Slatern, NACE, Houston, 1977, p.1063-1065.

[2] F.P. Ford and P.L. Andresen, "Corrosion in Nuclear Systems: Environmentally Assisted Cracking in Light Water Reactors", in "Corrosion Mechanisms", Ed. P. Marcus and J. Ouder, Marcel Dekker, p.501-546, 1994.

[3] P.L. Andresen and F.P. Ford, "Life Prediction by Mechanistic Modelling and System Monitoring of Environmental Cracking of Fe and Ni Alloys in Aqueous Systems", Materials Science and Engineering, A103, p.167-183, 1988.

[4] P.L. Andresen, "Perspective and Direction of Stress Corrosion Cracking in Hot Water", Proc. Tenth Int. Symp. on Env. Degradation of Materials in Nuclear Power Systems – Water Reactors, NACE, Houston, 2001.

[5] P.L. Andresen, T.M. Angeliu and L.M. Young, "Immunity, Thresholds, and Other SCC Fiction", Proc. Staehle Symp. on Chemistry and Electrochemistry of Corrosion and SCC, TMS, Feb. 2001.

[6] P.L. Andresen, "Conceptual Similarities and Common Predictive Approaches for SCC in High Temperature Water Systems", Paper 96258, Corrosion/96, NACE, 1996.

[7] Proc., Fundamental Aspects of Stress Corrosion Cracking, Eds. RW Staehle, AJ Forty and D van Rooyen, NACE, 1969.

[8] Proc. 1st – 11th Int. Symp. on Environmental Degradation of Materials in Nuclear Power Systems – Water Reactors, NACE / ANS / TMS, 1983 – 2003.

[9] P.L. Andresen, F.P. Ford, S.M. Murphy and J.M. Perks, Proc. Fourth International Symposium on Environmental Degradation of Materials in Nuclear Power Systems – Water Reactors, D. Cubicciotti and G.J. Theus, Eds., NACE, Houston, 1990, p. 1-83.

[10] A.J. Jacobs and G.P. Wozadlo, "Irradiation Assisted Stress Corrosion Cracking As a Factor in Nuclear Power Plant Aging", Proc. Int. Conf. on Nuclear Power Plant Aging, Availability Factor and Reliability Analysis, San Diego, CA, ASM, p.173, 1985. See also, A.J. Jacobs, Letter Report and Literature Search, GE Nuclear Energy, San Jose, CA, May 1979.

[11] S.M. Bruemmer, E.P. Simonen, P.M. Scott, P.L. Andresen, G.S. Was and J.L. Nelson, J. Nucl. Mater., Vol 274, 1999, p 299-314.

[12] G.S. Was and P.L. Andresen, J. Metals Vol. 44 (No. 4), 1992, p. 8.

[13] P.M. Scott, J. Nucl. Mat., Vol 211, 1994, p. 101.

[14] J.L. Nelson and P.L. Andresen, "Review of Current Research and Understanding of Irradiation-Assisted Stress Corrosion Cracking," Proc. Fifth International Symposium on Environmental Degradation of Materials in Nuclear Power Systems – Water Reactors, D. Cubicciotti, E.P. Simonen and R.E. Gold, Eds, American Nuclear Society, La Grange Park, IL, 1992, p 10.

[15] P.L. Andresen and F.P. Ford, "Modeling and Prediction of Irradiation Assisted Stress Corrosion Cracking", Proc. Seventh International Symposium on Environmental Degradation of Materials in Nuclear Power Systems – Water Reactors, NACE, Houston, p.893-908, 1995.

[16] P.L. Andresen, "Similarity of Cold Work and Radiation Hardening in Enhancing Yield Strength and SCC Growth of Stainless Steel in Hot Water", Corrosion/02, Paper 02509, NACE, 2002.

[17] I. Suzuki, N. Maeda, A. Yamaguchi, J. Sanoh, J.P. Higgins, M.L. Herrera, P.L. Andresen, H. Mimaki, T.R. Mager, M. Akiyama, T. Okubo, Y. Mishima, "Perspective on PLEX Program at JAPEIC", Int. Conf. on Nuclear Plant Life Management and Extension, ANS, Nice, France, Nov 27-30, 1995.

[18] P.L. Andresen, F.P. Ford, J.P. Higgins, I. Suzuki, M. Koyama, M. Akiyama, T. Okubo, Y. Mishima, S. Hattori, H. Anzai, H. Chujo, Y. Kanazawa, "Life Prediction Of Boiling Water Reactor Internals", Proc., ICONE-4 Conference, ASME, 1996.

[19] G.S. Was and P.L. Andresen, "SCC Behavior of Alloys in Aggressive Nuclear Reactor Core Environments", Topical Research Symposium on Corrosion in Aggressive Environments, Corrosion/05, NACE, Houston, 2005.

[20] P.L. Andresen, P.W. Emigh, M.M. Morra and R.M. Horn, "Effects of Yield Strength, Corrosion Potential, Stress Intensity Factor, Silicon and Grain Boundary Character on the SCC of Stainless Steels", Proc. of 11th Int. Symp. on Environmental Degradation of Materials in Nuclear Power Systems – Water Reactors, ANS, 2003.

[21] P.L. Andresen, P.E. Emigh and L.M. Young, "Mechanistic and Kinetic Role of Yield Strength / Cold Work / Martensite, H_2, Temperature, and Composition on SCC of Stainless Steels", Proc. 10th Anniversary INSS Symp. on SCC in Nuclear Power Systems, Osaka, Japan, May 2002, published 2003.

[22] P.L. Andresen and M.M. Morra, "Effects of Si on SCC of Irradiated and Unirradiated Stainless Steel and Ni Alloys", Paper 05591, Corrosion/05, NACE, Houston, 2005.

[23] J.C. Van Duysen, P. Todeschini and G. Zacharie, "Effects of Neutron Irradiations at Temperatures below 550 °C on the Properties of Cold Worked 361 Stainless Steels: A Review", Effects of Radiation on Materials: 16th Int. Symposium, STP1175, ASTM, p.747-776, 1993.

[24] P. M. Scott, M-C. Meunier, D. Deydier S. Silvestre, A. Trenty, “An Analysis of Baffle/Former Bolt Cracking in French PWRs,” Environmentally Assisted Cracking: Predictive Methods for Risk Assessment and Evaluation of Materials, Equipment and Structures, ASTM 1401, R. D. Kane, Ed., American Society for Testing and Materials, West Conshohocken, PA, 2000.

[25] P.L. Andresen, “Application of Noble Metal Technology for Mitigation of Stress Corrosion Cracking in BWRs”, Proc. Seventh International Symposium on Environmental Degradation of Materials in Nuclear Power Systems – Water Reactors, NACE, p.563-578, 1995.

[26] S. Hettiarachchi, G.P. Wozadlo, T.P. Diaz, P.L. Andresen and R.L Cowan, “The Concept of Noble Metal Addition Technology for IGSCC Mitigation of Nuclear Materials”, Proc. Seventh Int. Symp. on Environmental Degradation of Materials in Nuclear Power Systems – Water Reactors, NACE, p.735-746, 1995.

[27] P.L. Andresen, T.P. Diaz and S. Hettiarachchi, “Effect on Stress Corrosion Cracking of Electrocatalysis and Its Distribution Within Cracks”, Proc. of 11th Int. Symp. on Environmental Degradation of Materials in Nuclear Power Systems – Water Reactors, ANS, 2003.

[28] P.L. Andresen, “K / Size Effects on SCC in Irradiated, Cold Worked and Unirradiated Stainless Steel”, Proc. of 11th Int. Symp. on Environmental Degradation of Materials in Nuclear Power Systems – Water Reactors, ANS, 2003.

[29] P.L. Andresen and M.M. Morra, “Effect of Rising and Falling K Profiles on SCC Growth Rates in High Temperature Water”, Paper 71643, ASME PVP 2005, Denver, 2005. See also P.L. Andresen and M.M. Morra, “Effects of Increasing and Decreasing Stress Intensity Factor on SCC in Hot Water”, Paper 05469, Corrosion/05, NACE, Houston, 2005.

[30] G. Odette, P. Maziasz and J. Spitznagel, J. Nuclear Mat’ls, 85/86, p.1289, 1979.

[31] P. Maziasz, “Effects of Helium on Microstructural Development in Type 316 Stainless Steel Under Neutron Irradiation”, ORNL-6121, 1985.

[32] A. Jenssen and L.G. Ljungberg, “Irradiation Assisted Stress Corrosion Cracking – Post Irradiation CERT Tests of Stainless Steels in a BWR Test Loop”, Proc. 7th Int. Symp. on Env. Degr. Of Materials in Nuclear Power Systems – Water Reactors, NACE, 1995, p.1043-1054.

[33] A.J. Jacobs and G.P. Wozadlo, “Stress Corrosion Testing of Irradiated Type 304 Stainless Steel Under Constant Load”, Paper #41, Corrosion/91, NACE, 1991. See also Corrosion 49, p.145, 1993.

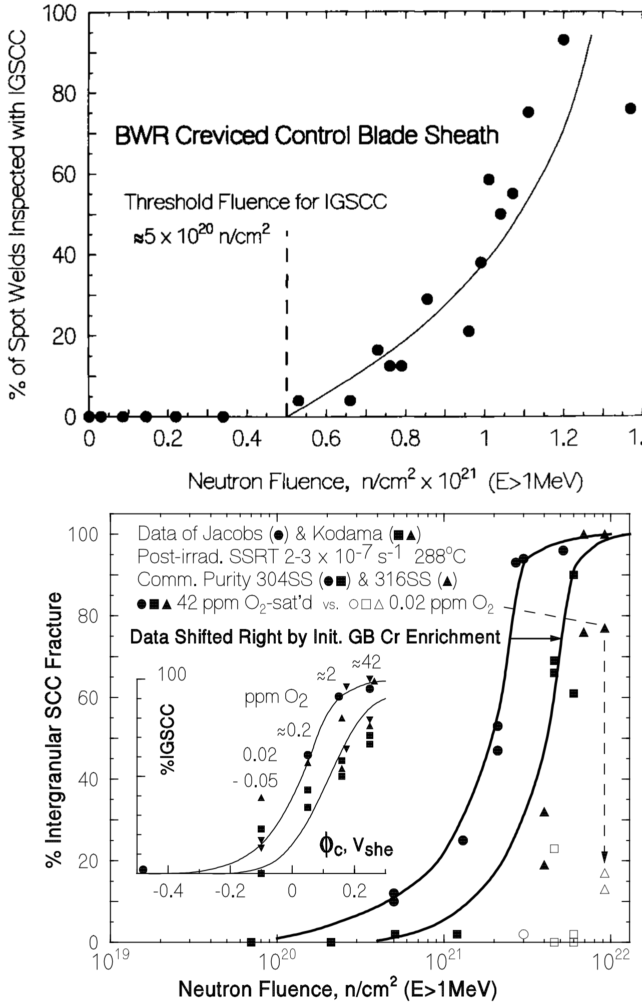

Figure B.2.1 Dependence of IASCC on fast neutron fluence for (a) creviced control blade sheath in high conductivity BWRs and (b) as measured in slow strain tests at 3.7 x 10^7 s^{-1} on pre-irradiated type 304 stainless steel in 288C water. The effect of corrosion potential via changes in dissolved oxygen is shown at a fluence of ≈ 2 x 10^{21} n/cm^2. The effect of corrosion potential on unirradiated and irradiated materials is similar under BWR conditions [2,9,15].

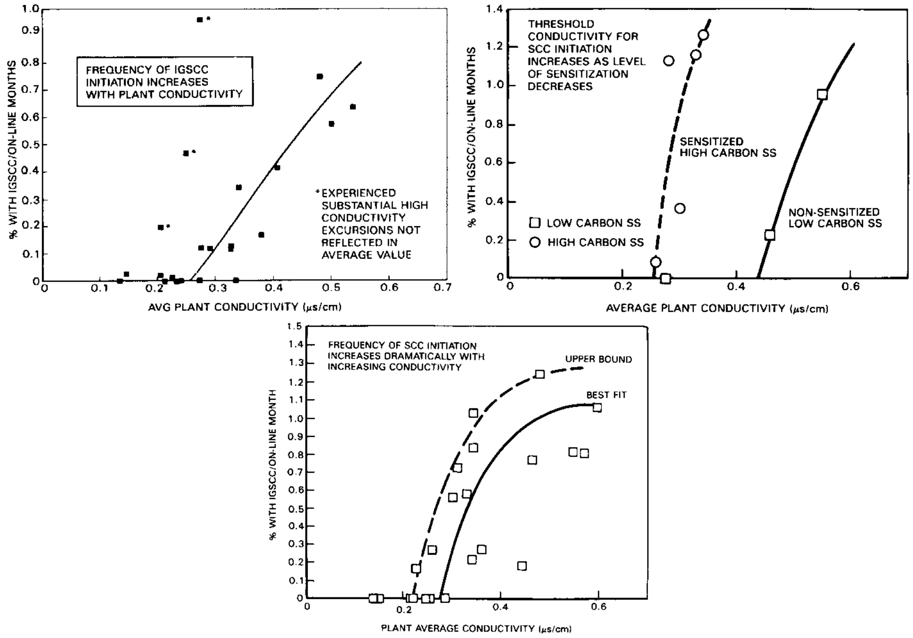

Figure B.2.2 The effects of average plant water purity are shown in field correlations of the core component cracking behavior for (a) stainless steel IRM/SRM instrumentation dry tubes, (b) creviced stainless steel safe ends, and (c) creviced Inconel 600 shroud head bolts, which also shows the predicted response vs. conductivity. The effect of conductivity on unirradiated and irradiated materials is similar under BWR conditions [2,9,15].

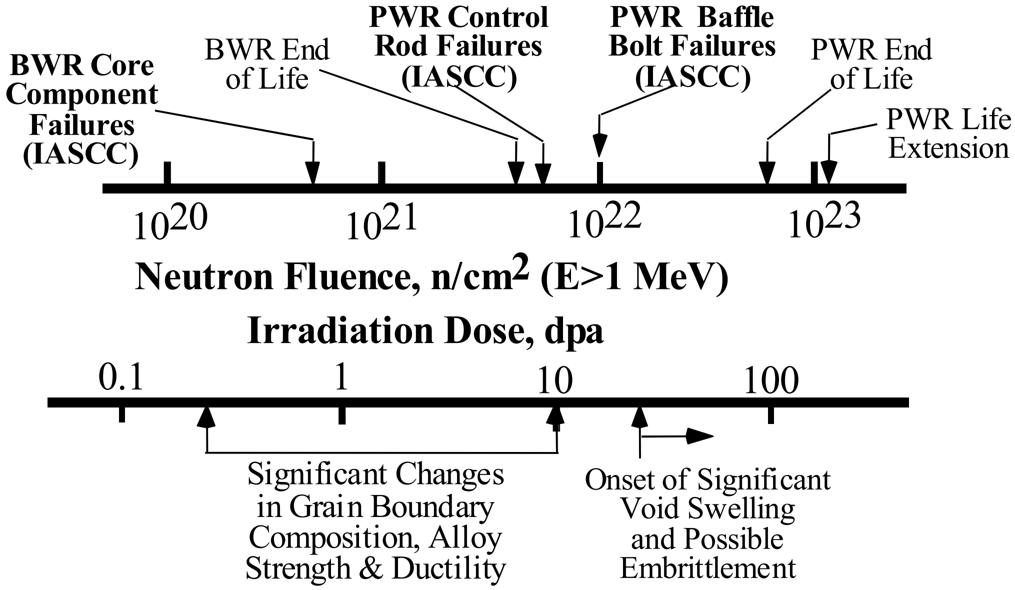

Figure B.2.3 Neutron fluence effects on irradiation-assisted stress corrosion cracking susceptibility of type 304SS in BWR environments [11].

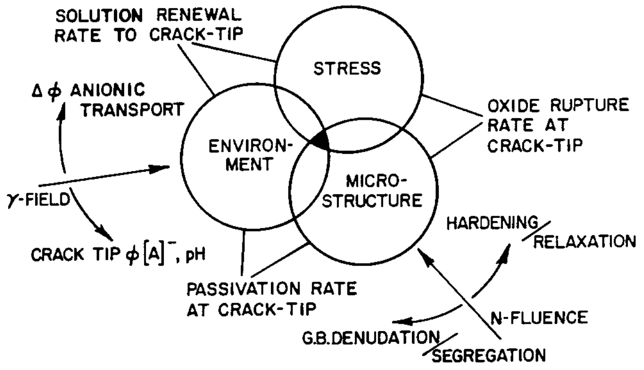

Crack depth vs. time = f (Material, Stress, Environment)

Chromium	Primary	Corrosion Potential
% Cold Work	Static	Oxidizing Species
Neutron Fluence	Dynamic	Anionic Species
Silicon	Residual	Type
Nickel	Crack Depth	Activity
Sulfur	Neutron Fluence	Temperature
Phosphorus	Relaxation	Flow Rate
Carbon	Thermal	Neutron flux
Weld heat input	Radiation	Crack Depth

Figure B.2.4 Schematic diagram of the engineering parameters (stress, environment and microstructure), underlying scientific processes (mass transport, oxide rupture, and repassivation rates) and effects of radiation. The complexity of SCC is reflected in the large number of influential variables and the associated requirement that all 20 to 40 in a given system be adequately controlled, all of which are inter-dependently affect SCC [2,9,15].

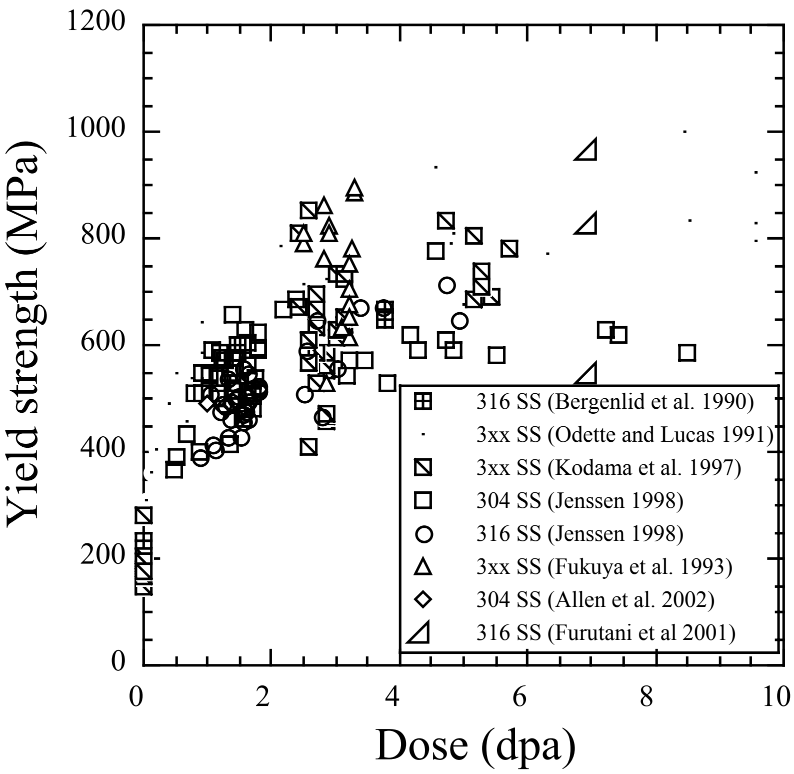

Figure B.2.5 Irradiation dose effects on measured tensile yield strength for several 300-series stainless steels, irradiated and tested at a temperature of about 300°C [11,19].

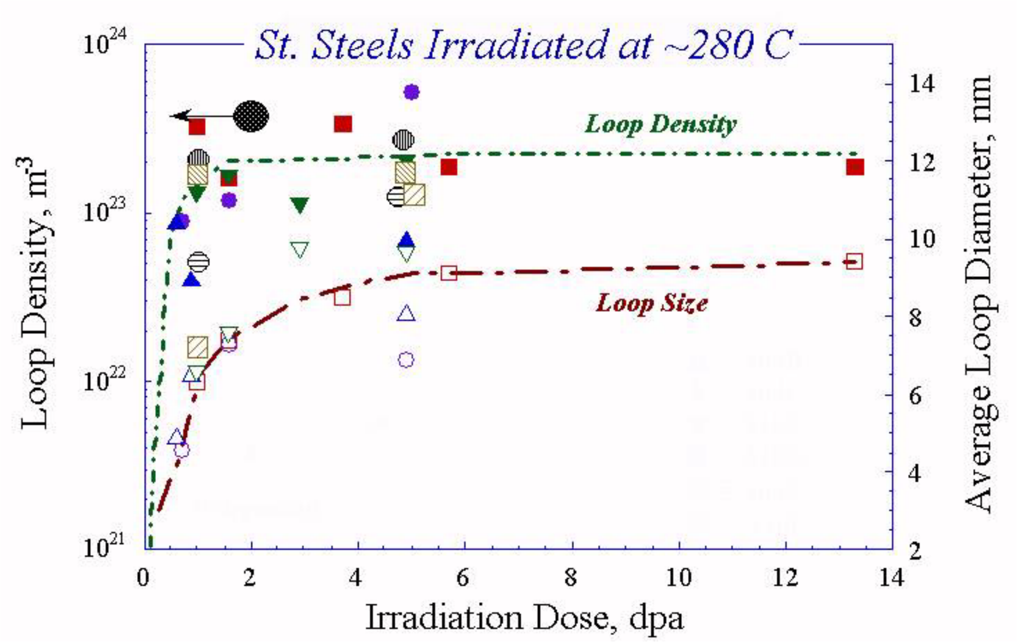

Figure B.2.6 Irradiation dose effects on the measured loop diameter and density for austenitic stainless steels at 280°C [11,19].

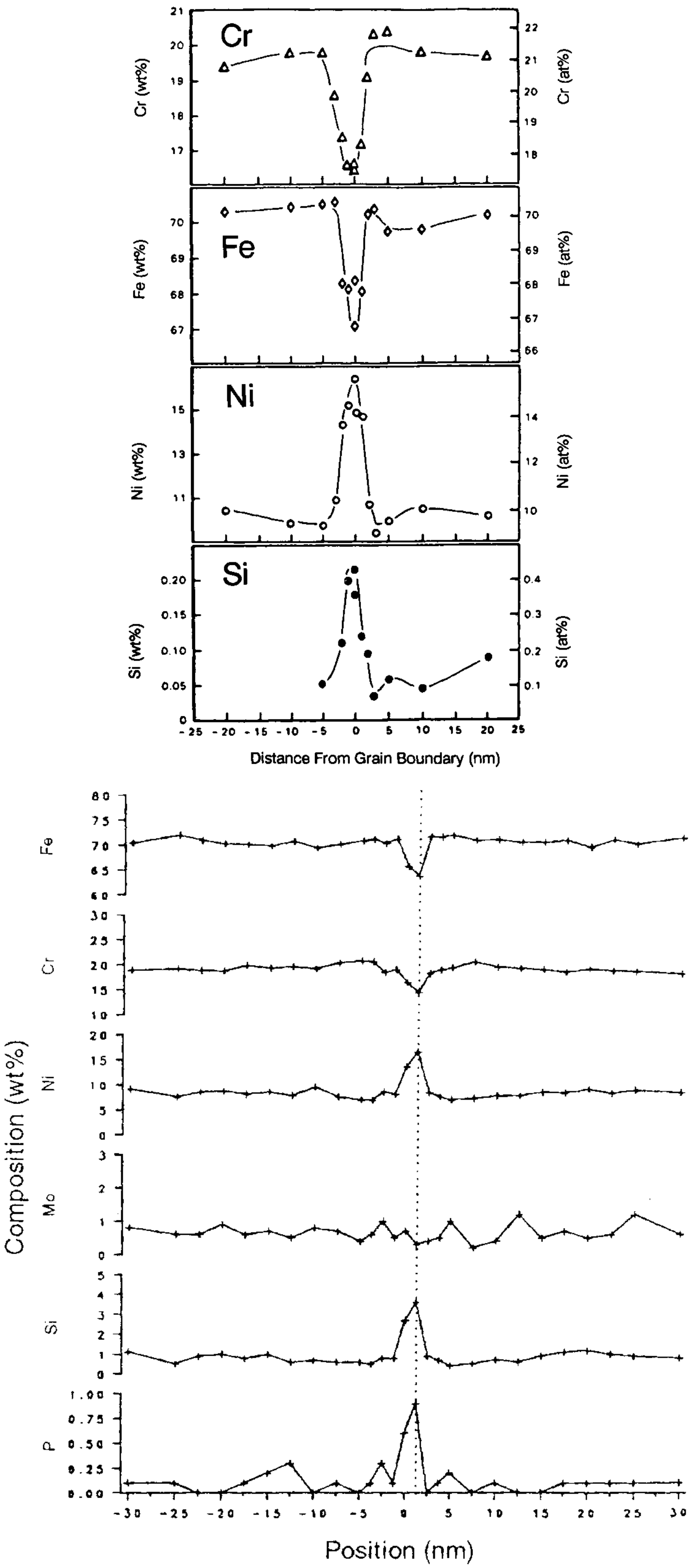

Figure B.2.7 Radiation induced segregation (RIS) of (a) high purity (including low Si) and (b) commercial purity stainless steel [9].

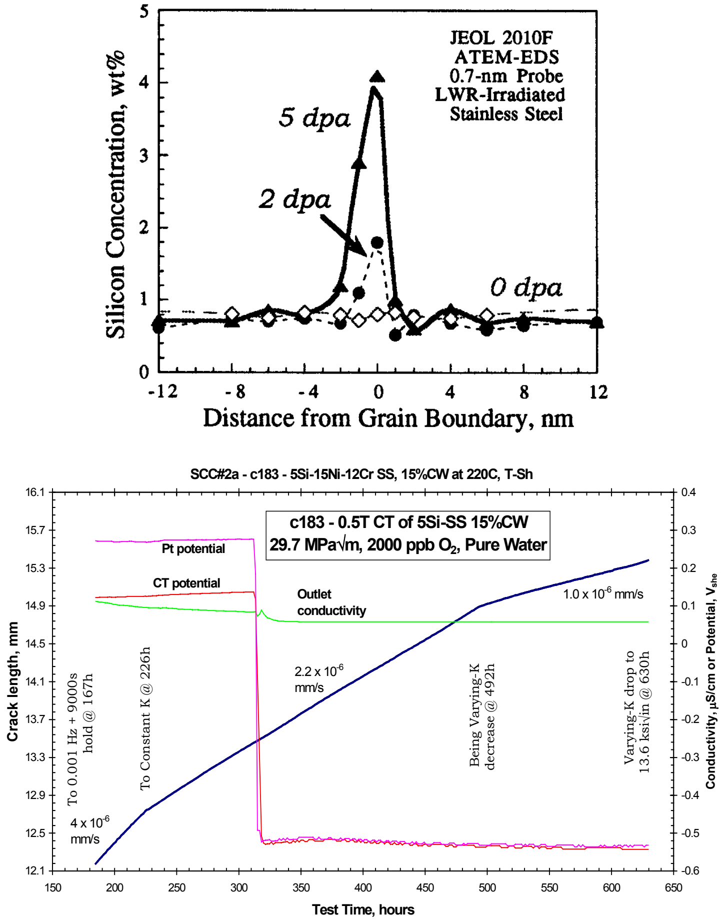

Figure B.2.8 (a) Grain boundary Si concentration in irradiated stainless steel. (b) Crack length vs. time for a 5% Si "stainless steel" whose composition simulates that in an irradiated grain boundary. No effect of corrosion potential and or stress intensity was observed. [20-22]

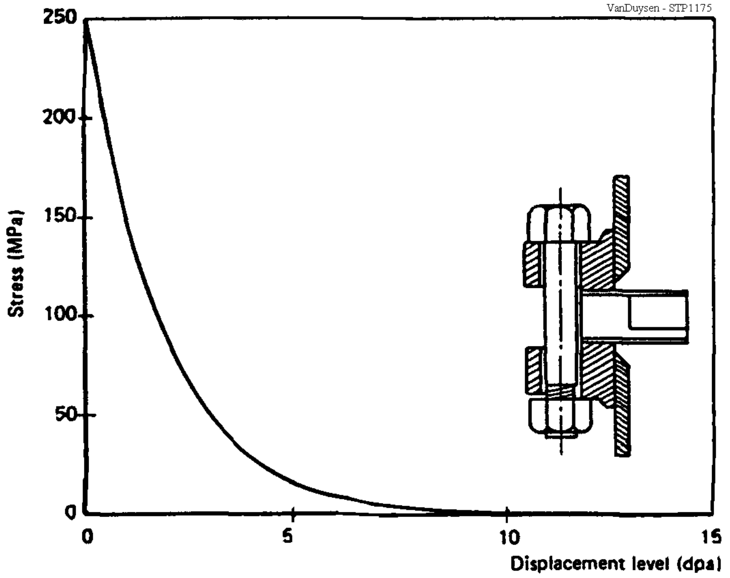

Figure B.2.9 The effects of radiation-induced creep on load relaxation of stainless steel in a constant displacement (bolt) condition [23].

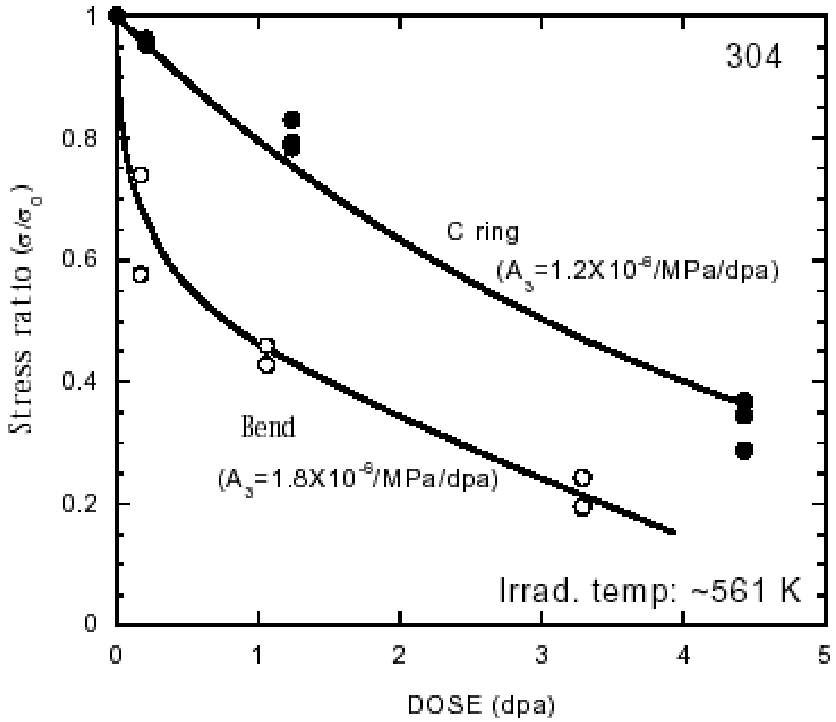

Figure B.2.10 Stress relaxation of bent beam and C-ring specimens of 304 SS in JMTR during irradiation at 288°C [23].

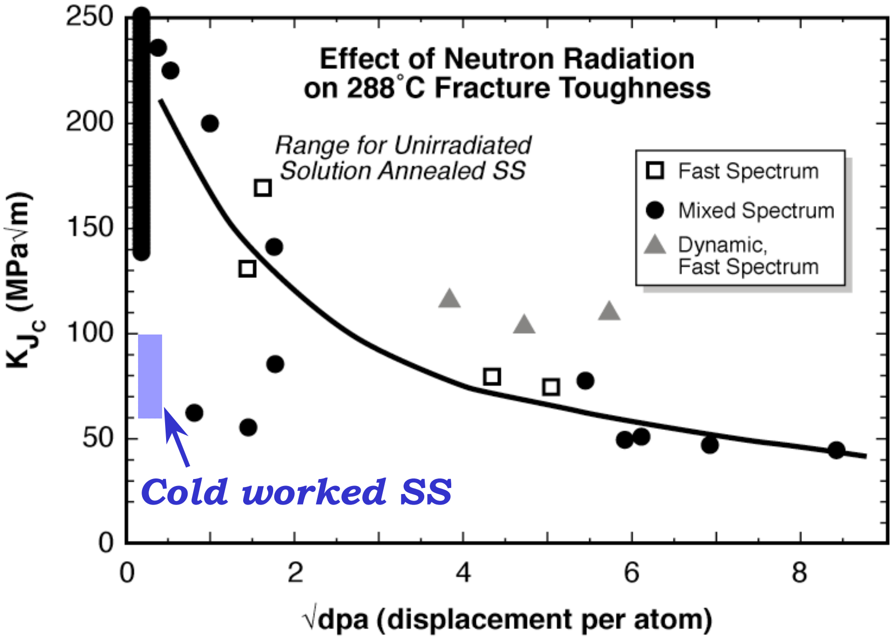

Figure B.2.11 The effect of fast neutron fluence under LWR conditions on fracture toughness of types 304 and 304L stainless steel at 288 °C [9,30,31]. A preliminary band based on the fracture toughness response of a few tests on unirradiated, cold worked stainless steel tested in-situ in 288 °C pure water is also shown [21].

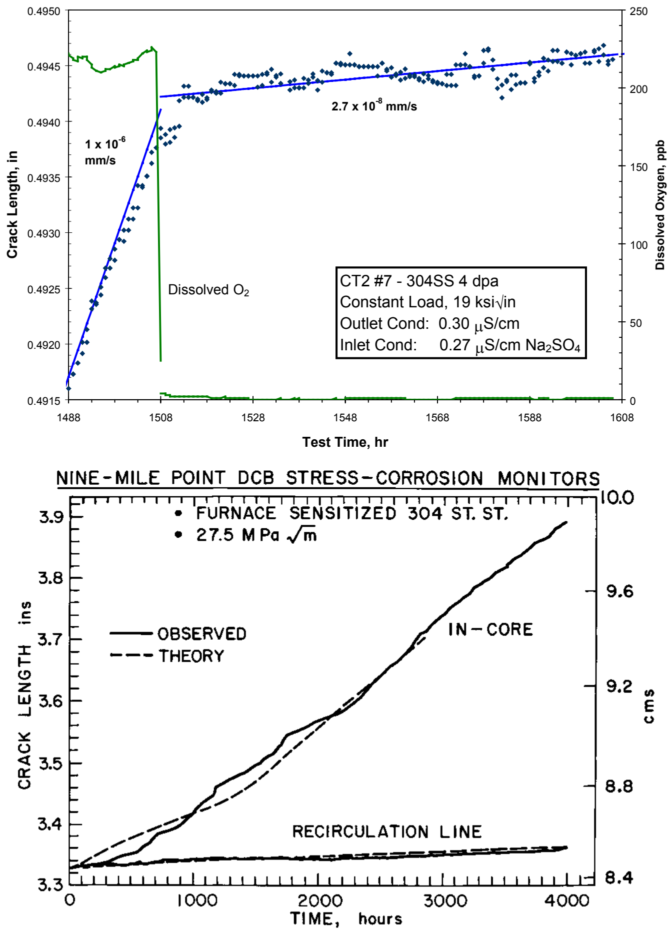

Figure B.2.12 Crack length vs. time for: (a) a CT specimen of irradiated type 304 stainless steel tested at constant load in 288 °C water at both high and low corrosion potential at 19 ksi√in. (b) DCB specimens of sensitized type 304 stainless steel exposed in core (high corrosion potential from radiolysis) and in the recirculation system [2,9,15-19].

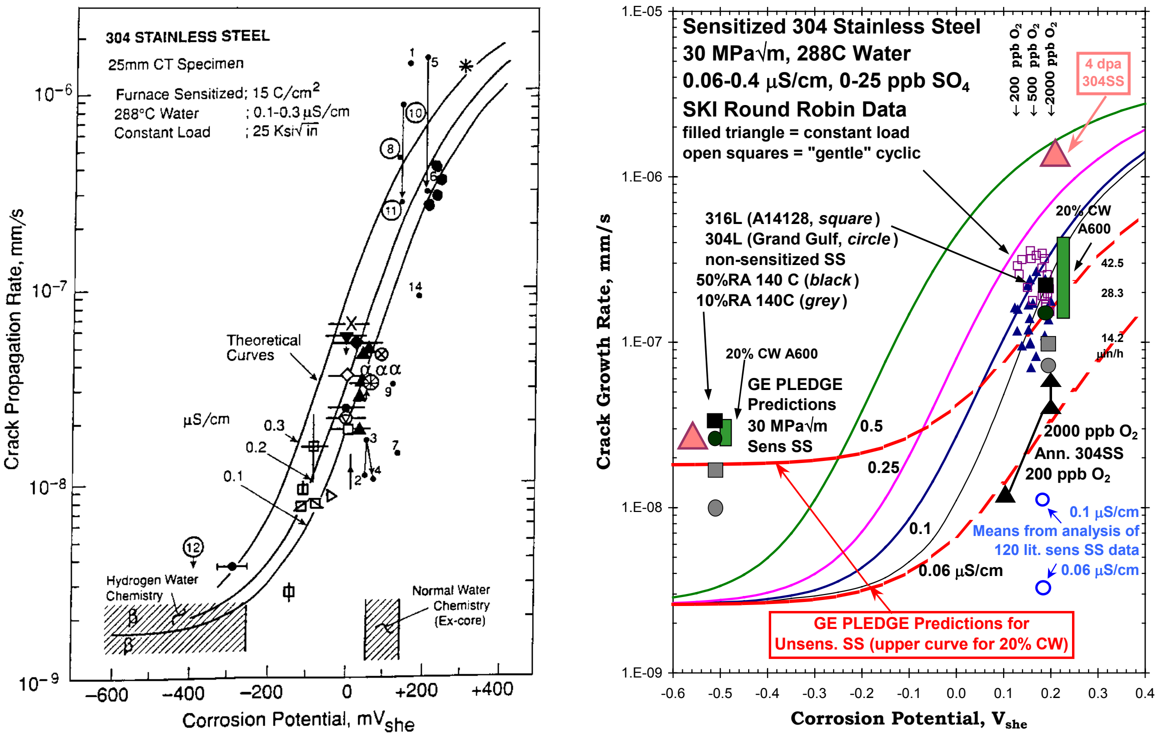

Figure B.2.13 SCC growth rate vs. corrosion potential for sensitized (left graph) and for cold worked, sensitized and irradiated (right graph) SS in 288 °C water. Unirradiated and irradiated (pink triangles) materials of similar yield strength show similar SCC response at low corrosion potential. At high potential, the combined effect of radiation hardening and radiation segregation produces a higher growth rate than either factor alone (i.e., in the unirradiated data that is either cold worked or sensitized). [2,9,15-19]

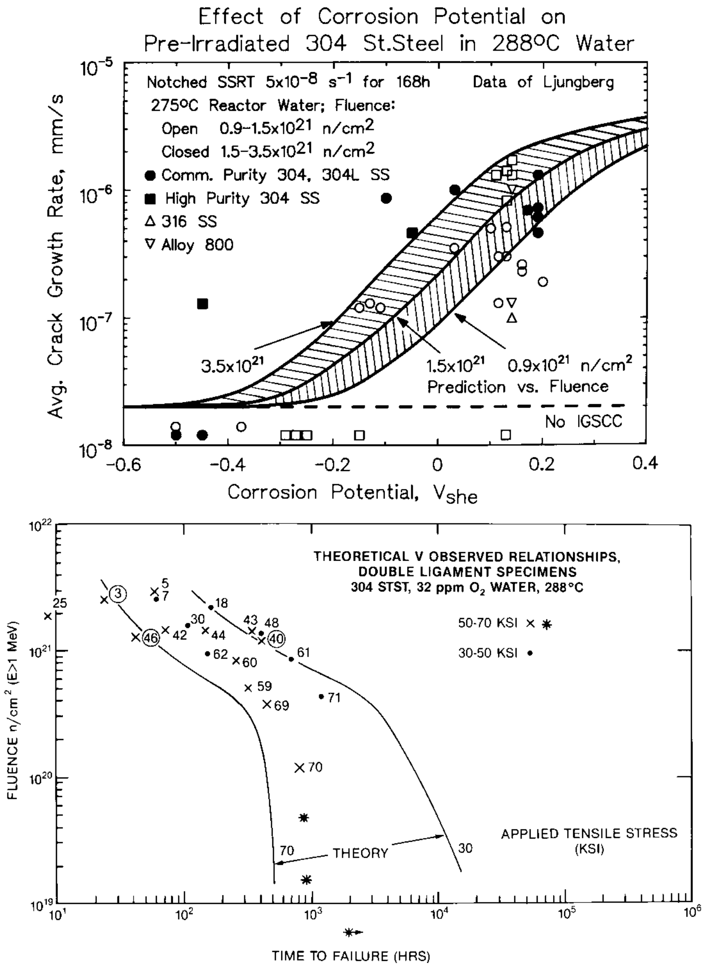

Figure B.2.14 Comparison of predicted and observed crack growth rates for stainless steels irradiated in a BWR at 288C to various fluences [2,9,15-19]. (a) Notched tensile specimens were tested by Ljungberg [32] at a slow strain rate in 288C pure water and interrupted after a given strain / time. (b) time-to-failure for the effect of fast neutron fluence on pre-irradiated type 304 stainless steel tested at constant load in the laboratory in oxygen saturated, 288 °C water [31].

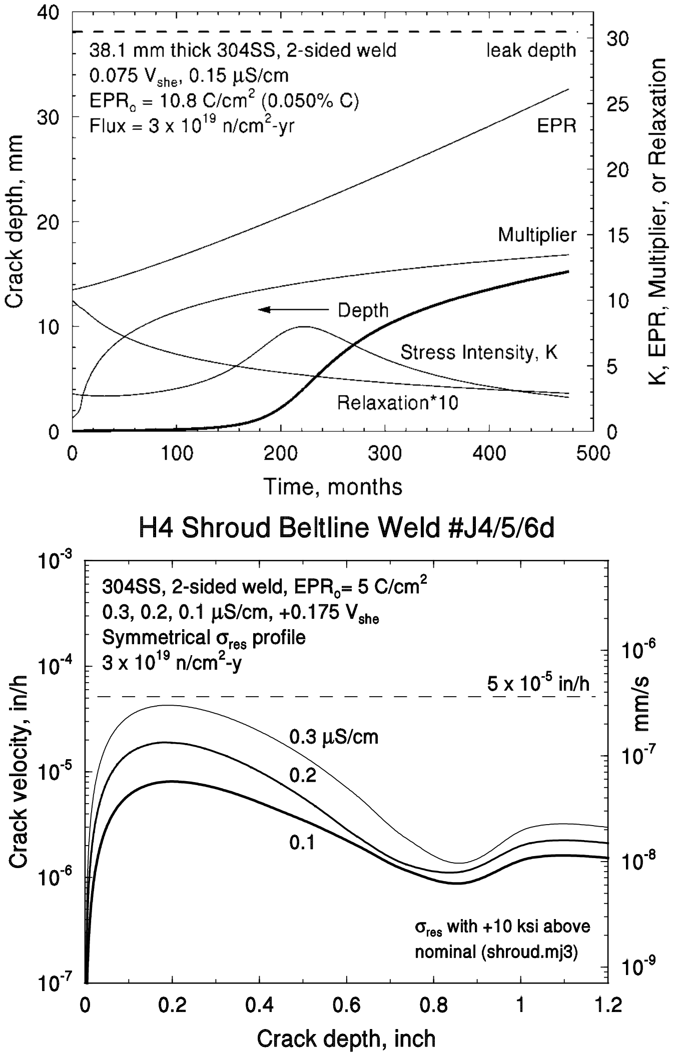

Figure B.2.15 Examples of IASCC predictions illustrating the interactions among radiation "damage" (segregation and hardening) and radiation creep relaxation (reduction in weld residual stress) for a BWR core shroud. (a) crack depth vs. time with individual curves for the increase in EPR (Cr depletion), stress relaxation, and "multiplier" (radiation hardening). The stress intensity factor is also shown, which goes through a peak due to the nature of the residual stress profile as well as radiation relaxation. (b) crack velocity vs. depth illustrating that at high coolant conductivity (0.3 μS/cm), cracks nucleate and grow earlier in life when the weld residual stresses are higher, resulting in higher growth rates and a shorter time to achieve a given crack depth [9,15].

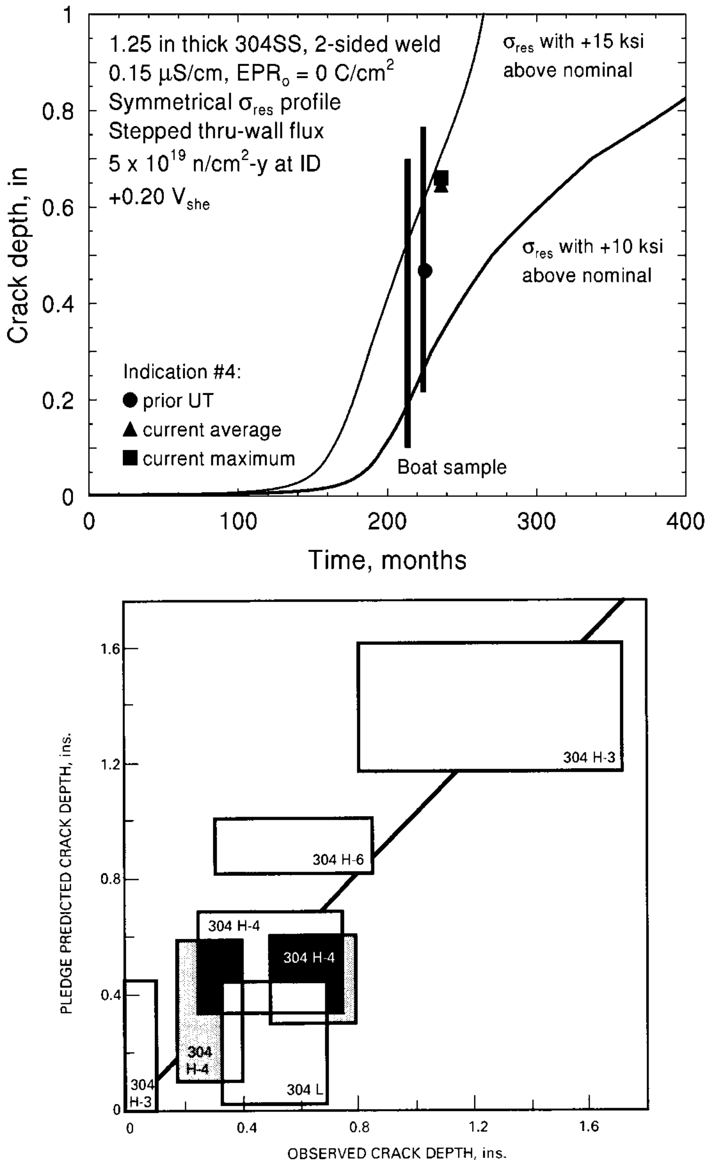

Figure B.2.16 (a) Crack length vs. time predictions and observations for a type 304 stainless steel BWR core shroud with multiple inspections and multiple cracks. (b) Comparison of observed and predicted crack depth for a number of BWR core shrouds. [9,15]

B. 3 Stress Corrosion Cracking and Pitting: Contaminating External Environments

Background

Since commercial nuclear power began, extensive research has been concerned with corrosion processes inside the piping and components. Most of this project is concerned with the results of this research including mitigations and improved procedures for operation. This chapter is concerned with corrosion in environments that are *outside* the piping and components. While the environments inside the boundaries of nuclear plants are reasonably well defined and monitored, there is a class of environments that occurs outside these pipes and components. Such environments are miscellaneous and result from impurities carried in the air, adventitious leaks, and animals including bacteria and fungi.

Many commonly-used metallic materials are susceptible to localized and general corrosion when exposed to ambient, or external, conditions. Typically such corrosion occurs only when the external surface of the material or component is cool enough that ambient moisture, or in unusual circumstances, potentially corrosive non-aqueous vapors, can condense on the surface. For nuclear power plants the ambient external environment is assumed to be air, occasionally moist or wet and periodically contaminated with potentially corrosive species. The most important, and common, of these contaminants is the chloride ion, present either as salts from the local environment (sea air, for instance) or as a contaminant leached from the immediate environment, such as insulation. Sometimes contaminants arrive via animal wastes and at other infrequent times bacteria and fungi produce corrosive metabolic products.

In nuclear power plants, the most likely materials to be exposed to contaminated external environments are stainless steels (SS), usually austenitic stainless steels such as types 304 and 316, and carbon steels. The austenitic stainless steels are susceptible to stress corrosion cracking (SCC and pitting in chloride-contaminated aqueous solutions. Carbon steels may sustain [RT: a quirk of mine to avoid human emotions to describe physical processes; do as you wish] pitting in such environments. This Technical Supplement outlines the rationale behind judgments of susceptibility of nuclear power plant materials to contaminated external environments, predicted future behaviour of these materials, and mitigation and life management strategies to avoid significant degradation or failures.

Factors Influencing Material Susceptibility in External Environments

This discussion emphasizes the corrosion behavior (susceptibility factors) for austenitic stainless steels and carbon steels in nuclear power plant systems where components fabricated from these materials present their outside surfaces to environments that may cause external damage. The knowledge bases underlying these susceptibility factors are discussed in the following sections. Note that for austenitic alloys, and ferritic stainless steels also, containing more than about 20% Cr, the susceptibilities to such degradation is considerably less than that of the “18-8” Cr-Ni stainless steels, and commonly-used nickel-base alloys such as Incoloy 800 or 825. Thus a possible materials solution to under-deposit or marine corrosion could be selection of materials such as type 310 or 321 SS, or use of "superalloys such as AL-6X, or a Hastelloy. However this is usually not a cost-effective solution for most nuclear applications, other than for steam condensers exposed to seawater or brackish water.

In the discussion that follows the modes of pitting and stress corrosion cracking are emphasized. These modes are the most likely to lead to damage especially as pitting might also initiate SCC or corrosion fatigue.

There are several different environments that can produce pitting and SCC. These include deposits that accumulate and crevices that form and contacts between metals or metals and non-metals. In addition bacteria and fungi can accumulate and through their metabolic processes can produce local corrosive conditions. The action of these microbes is favored by moisture and oxygen as well as nutrients. Finally, galvanic cells such as those as might occur with juxtaposed carbon and stainless steels. While the three sometimes lead to the terms "crevice corrosion, microbiological corrosion (MIC), and galvanic corrosion, these terms are really incorrect and are simply different environmental configurations where pitting and SCC both can occur.

With the configurations of crevices, MIC and galvanic juxtaposition, the chemistries that produce corrosion are acidic impurities in the atmosphere, salts such as chlorides from the ocean waters, the various chemistries of animal wastes, and acids from the metabolism of microbes. Also, corrosive chemicals are sometimes leached from insulation, polymers, paints, and floor dirt

Stress Corrosion Cracking:

SCC of austenitic SS occurs in low temperature environments only if the material is subject to high stress, the surface is abused by grinding or by poor machining practice, is exposed to a corrosive environment, and if the material is sensitized, for instance by heat treatment such as that which occurs on welding. Welding-induced residual stress is the most likely source of the high stresses necessary to initiate SCC, although fit-up stresses and other fabrication-related cold work (cold bending, for example) are other examples. Thus welds and bends are locations most likely to be susceptible to SCC. In the presence of chloride contamination (see below), the cracking usually takes the form of transgranular SCC (TGSCC).

The corrosive environment responsible for most external ambient temperature is oxygenated water contaminated with chloride ions. The usual temperature range of concern is from about 50°C (120°F) to about 100°C (212°F). The upper temperature depends on the dew point of the environment; typically the surface must be wet at least part of the time for SCC to occur. The source of the chloride is usually either ambient air or adjacent materials. Marine coastal environments are those most commonly chloride-contaminated, but nearby industrial sources may also occur if the power plant is situated near a large industrial complex that can emit chloride- or chlorine-contaminated air. Note that external pipe surfaces routinely exposed to rain, or frequently washed down, are at little risk of TGSCC or pitting, even in marine environments, since the rain and washing will remove the soluble chlorides.

Pipe insulation or polymeric materials such as tape are often contaminated with chloride, although the insulation sometimes contains a chemical inhibitor to reduce corrosion. For SCC to occur under insulation, or some other chloride-containing material, the material surface must be wet and in intimate contact with the insulation. Wet insulation is the worst case, since the insulation provides a crevice environment as well as a chloride-contamination source, resulting in an increase in chloride concentration in the crevice with time. As noted above, a crevice environment can build up with time, so SCC conditions may not develop for several years.

SCC of carbon steels is unlikely to occur under these conditions but can possibly occur in the range of 100C if sufficient water and stress are available.

<u>Pitting</u>

Pitting of stainless steels occurs under the same conditions as noted above for SCC, with the important exception that pitting does not require high stresses or sensitized material. Thus pitting can develop anywhere on a stainless steel component exposed to chloride contamination in a crevice environment. Austenitic SS with molybdenum additions (type 316SS, for example) are more resistant to pitting than non-Mo stainless steels such as type 304SS.

Pitting of carbon steels also can occur in external environments, although typically such pitting usually is associated with deposits or other crevices. Otherwise, carbon steels usually exhibit general or uniform corrosion in the presence of wet chloride-contaminated external environments.

Typical Occurrences of (TG) SCC and Pitting in Power Plants

The most common occurrences of TGSCC or pitting of austenitic SS (primarily types 304 and 316) are under wet insulation or where piping is exposed to marine air and deposits can build up. Insulation can become wetted by water leakage from adjacent components, by washing or by soaking as a result of fire sprinkler action. Chlorides in the insulation leach out and deposit on the piping, eventually reaching concentrations sufficient to cause SCC (highly stressed areas, typically near joints/welds or at bends) or pitting. Examples of this are SCC of instrument lines and other small diameter lines.

Inspection and Remediation Strategies

Inspection strategies require an assessment of which sections of piping are exposed to conditions which can promote SCC or pitting. These locations are those which can be wetted and which are in contact with chloride-contaminated insulation or coatings/adhesives/tapes, or where deposits can build up and chloride contamination is also present. Typical areas at risk are in the temperature range 60°C to about 100°C. Visual inspection for water drips, wet areas on the pipe, deposits and rust stains are a first step required to focus any further inspection. Where insulation or other coverings are present, these may need to be removed to allow an effective visual inspection. If any welds, bends or other stressed areas show any visual evidence for possible corrosive conditions, non-destructive examinations (NDE) should be carried out. Surface eddy current, ultrasonic inspection, magnetic particle, radiography or equivalent alternative and qualified procedures may be used for these inspections.

Mitigation strategies center around preventing wetting of the pipe surface or any surrounding materials that might contain chlorides. Most insulations contain corrosion inhibitors that are designed to prevent corrosion of adjacent contacted surfaces, but this needs to be verified for specific plants. Much of the insulation in power plants is covered with metallic water-resistant jackets, and this is a good mitigation strategy, although it does interfere with any subsequent inspections. For piping exposed to outdoor environments, the mitigation strategy is to keep the piping clean and free of deposits. This is of most concern in marine environments, or areas where chloride-contaminated deposits may build up. Washing down such piping periodically is a good counter-measure. For piping that does not see high temperature internal fluids, coatings are a good corrosion prevention approach.

As noted earlier, a possible remediation strategy is to use highly corrosion-resistant materials for components exposed to potentially corrosive external environments, rather than 18-8 stainless steels or carbon steels, but this is not normally a cost-effective solution compared to good maintenance practices.

Life Management Issues

Current industrial practice should include routine visual inspections for wetted, rust stained, or fouled areas of low temperature piping. This would be an effective mitigation strategy for the longer term if accompanied by cleaning/washing and/or NDE as appropriate. It is not clear if visual inspections are a routine practice at nuclear power plants; many incidents of TGSCC of low temperature piping are managed by repair following detection of a leak. This is feasible because the low temperature piping sections or systems may be isolated and repaired on-line.

References

[1] *Uhlig's Corrosion Handbook*, Ed. R. Winston Revie, Second Edition, The Electrochemical Society, John Wiley & Sons, New York, 2000.

[2] *Corrosion*, Volumes 1 and 2, Ed. L. L. Shreir, Second Edition, Newnes-Butterworths, Boston, 1976.

[3] *Atmospheric Corrosion*, W. H. Ailor, The Electrochemical Society, John Wiley and Sons, 1982.

[4] *Metals Handbook, Volume 13, Corrosion*, Ninth Edition (or latest), ASM International, Metals Park, Ohio, 1987

[5] *Stress-Corrosion Cracking*, Ed. R. H. Jones, ASM International, Materials Park, Ohio, 1992.

[6] *Pitting Corrosion of Metals*, Z. Szklarska-Smialowska, Natonal Association of Corrosion Engineers, Houston, Texas, 1986.

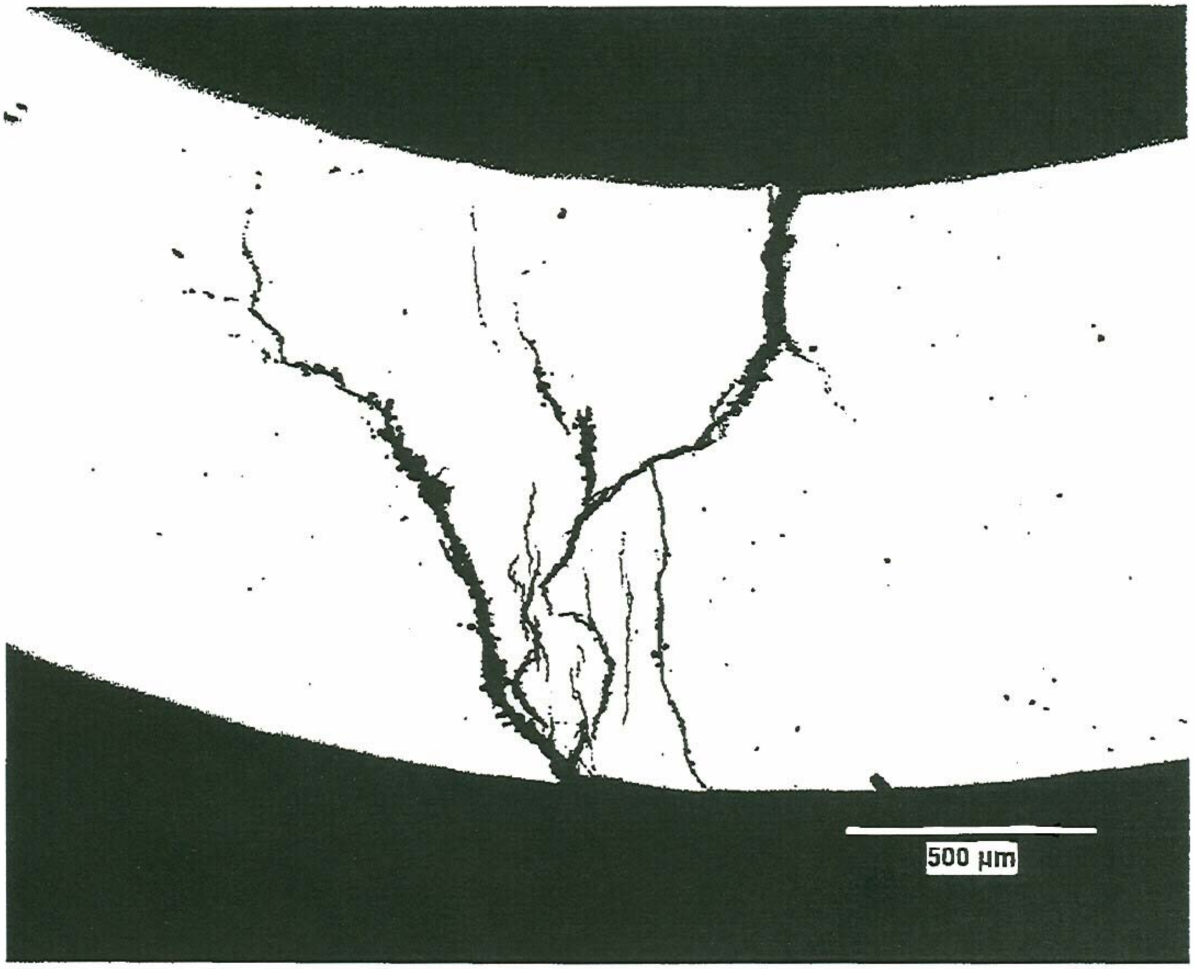

Figure B.3.1: Cross-Section of OD-initiated transgranular cracking in a cold-worked stainless steel line.

B.4 Thermal Aging and Embrittlement of Cast Stainless Steels

Introduction

Cast stainless steels (CASS) are used for many components in Light Water Reactors including piping, elbows and T's, and particularly those components with complex shapes such as pump and valve bodies. They are not normally subject to high neutron fluxes although some CASS components on the edges of PWR cores may reach fast neutron fluences on the order of 10^{20} n/cm^2 at end of life (for 40 years initial licensing period).

The most commonly used CASS materials are SA-351 grades CF-3, CF-3A, CF-8, CF-8A and CF-8M, the specifications of which are shown in Table B.4.1. They have a duplex (γ) austenite / δ ferrite microstructure and are susceptible to thermal aging embrittlement of the δ ferrite phase at typical PWR and BWR operating temperatures. The volume fraction of ferrite is typically 10 to 20% but may attain 25%; only the lower limit is imposed by the ASME code. Stainless steel weld deposits, typically Type 308 and 309, have a similar duplex microstructure but with a lower volume fraction of ferrite typically in the range 5 to 10% and notably lower Cr contents.

Embrittlement of the δ ferrite phase results in an increase in hardness and loss of ductility and of fracture toughness. The mechanisms of thermal aging have been extensively studied from the point of view of microstructural changes resulting in the formation of nanometer-scale embrittling phases. Predictive, albeit empirical, equations have been developed for the purpose of forecasting the deterioration in mechanical properties over typical reactor lifetimes.

The purpose of this appendix is to provide a summary of current understanding of the thermal aging mechanism of CASS and the application of that knowledge currently proposed in the United States for predicting changes in mechanical properties and loss of fracture toughness in PWR and BWR components [1,2,3]. There are no known published studies of the stress corrosion resistance of these materials in the aged and embrittled condition when exposed to PWR or BWR primary coolants although there are some instances of stress corrosion cracks propagating into stainless steel weld metals in BWRs, apparently along the δ ferrite, after long periods of service. There are also no known published studies of the influence of these aqueous environments compared to air on fracture resistance.

Mechanism of thermal aging

Thermal aging embrittlement of CASS at temperatures below about 400°C arises primarily as a consequence of a thermally activated separation of chromium by diffusion in the Fe-Cr solid solution of the δ ferrite phase resulting in the formation of an iron rich α phase and a chromium rich α' phase. This process is called 'spinodal decomposition' and occurs mainly at the higher chromium contents greater than ~23% in the δ ferrite (for temperatures <400°C). The α' phase may also form by precipitate germination and growth, particularly at temperatures >400°C, but can also contribute at lower temperatures depending on the precise combination of chromium content and temperature e.g. <~26%Cr at 400°C and <~23%Cr at 300°C. The austenite phase of CASS is unaffected by thermal aging in the same temperature range.

The formation of α' during thermal aging can affect all Fe-Cr solid solutions with Cr contents in solution >10%. An "oscillation" in the resulting Cr distribution is observed by high resolution microscopic techniques with both "amplitude" and "wavelength" (measured in nanometers) increasing with aging time and temperature. The effect increases notably with the Cr and Mo content of the ferrite phase and consequently CF-8M is less resistant to aging than CF-8 or CF-3 without Mo. The formation of embrittling α' phase from δ ferrite is enhanced by other alloying elements such as silicon which together with Cr and Mo can be represented by the chrome equivalent. The presence of the adjacent austenite phase in CASS appears to exert a detrimental influence relative to purely ferritic alloys of similar composition.

Other precipitation phenomena occur in the δ ferrite phase and at the ferrite-austenite interfaces above about 350°C, particularly the formation of the fcc Ni,Si,Mo rich G phase which can reach up to 12% by volume in Mo containing CASS. Carbon also enhances G phase precipitation. Nevertheless, G phase does not appear to contribute significantly to hardening and loss of toughness. At higher temperatures between 400 and 500°C other intermetallic phases precipitate but to a much lesser extent than G phase. However, extensive carbide (and sometimes nitride) precipitation, particularly at austenite-ferrite interfaces, occurs in the Mo-free CASS.

Although the microstructural evolution of CASS during thermal aging is fundamentally driven by solid-state diffusion processes, the complexity and changing nature of the phenomena with temperature is such that extrapolation over large temperature ranges using Arrhenius type relations is very difficult. Accelerated thermal aging for PWR and BWR applications is generally only carried out up to 400°C where hardening of the δ ferrite by α' formation is the predominant aging process. Even with this restriction, the apparent activation energy observed for changes in mechanical properties such as hardness and toughness (see next section) can be very variable and sometimes significantly below the activation energies of 210 to 260 kJ/mole associated with diffusion of metallic species, particularly Cr, in ferrite.

Mechanical properties of thermally aged CASS

The complexity of the microstructural changes associated with thermal aging of CASS gives rise to very strong material and heat dependencies for the extent and kinetics of evolution of mechanical properties. Consequently, very careful studies have been necessary to determine the range of temperature, composition etc for which mechanical properties data obtained from accelerated aging tests can be applied to service conditions.

The overall degree of embrittlement depends strongly on the amount, composition and distribution of the ferrite phase. The increase in hardness and decrease of ductility of the ferrite phase due to thermal aging promotes premature cleavage in this phase that can extend preferentially through it if there is a continuous ferrite network. Even if the fracture path intersects the austenite, deformation induced martensitic transformation can allow the brittle fracture to extend beyond the embrittled ferrite.

The main parameter used for characterizing the evolution of mechanical properties due to thermal aging has been the Charpy impact energy. Measurements of tensile properties, hardness, microhardness of the ferrite phase and J-R fracture resistance curves have also been made.

Thermal aging of CASS at BWR and PWR operating temperatures is characterized by an increase in hardness and tensile strength and a decrease in ductility, impact strength and toughness. In addition, the "brittle-ductile" transition temperature increases and the upper shelf decreases. Examples of Charpy impact energy measurements at room temperature on many heats of CASS are shown in Figure B.4.1. Although the dispersion in the results is large, all heats show a saturation of the aging effect (minimum plateau value of Charpy impact energy) that is independent of aging temperature, at least up to 400°C. The main trends in the data are with chemical composition, the plateau Charpy impact energy decreasing with increasing ferrite and chrome equivalent.

The procedure adopted in the United States for estimating the toughness of CASS components in service is based on empirical equations relating Charpy impact energy to the chemical composition, notably Cr, Mo, Si and C (i.e. Cr_{eq}), and time and temperature, including accelerated aging data at temperatures up to 400°C. The kinetics of aging are based on Arrhenius type correlations in which the apparent activation energy also depends on the concentrations of the aforementioned elements. The toughness ($J_{0.2}$) and J-R curve are then estimated from empirically established correlations with the Charpy impact energy. Lower bound estimates of end-of-life toughness are made based only on the chemical composition and lower bound correlations if no further details of the microstructure are available. The procedure can be refined if the initial Charpy impact energy and/or ferrite content are known, for example by classifying the material into three groups defined for <10%, 10 to 15%, and >15% ferrite.

The method proposed in the United States for screening CASS components for their potential susceptibility to thermal aging embrittlement is to divide all such components into six categories as shown in Table B.4.2. The indicated ferrite levels may be calculated or measured. All components identified as having a potentially significant reduction in fracture toughness due to thermal aging are then placed in an aging management program. A corollary of this classification is that no significant thermal aging is anticipated for stainless steel weld deposits. However, studies of the fracture properties of weld heat affected zones in aged CASS do not appear to have been published.

It is important to note that there is significant variability internationally in approaches used to estimate the degradation in CASS toughness that can lead to differing judgments of the significance and extent of thermal aging embrittlement. In particular, the US approach eliminates from consideration all heats known or believed to contain niobium on the grounds that these are out of specification in the USA. The counter argument is that niobium precipitates as niobium carbide very quickly and in any case has no significant effect on toughness in either the as-received or thermally aged condition. An even greater dispersion in possible toughness levels and a significantly reduced lower bound compared to that adopted in the US have been measured [1,4], i.e., significantly lower than the saturation room temperature impact energy of ~25 J/cm^2 seen in Figure B.4.1. It is acknowledged, however, that the very low toughness heats in the international population of CASS heats is strongly influenced by heats from a particular foundry that has not supplied the US market. Nevertheless, the range of ferrite contents and chrome equivalents are not considered to be unrepresentative of the range encountered in CASS used in US plants.

Other possible degradation phenomena

It is well known that fracture resistance can be affected by the environment in which the fracture events occur. For example, the fracture resistance of nickel base weld metals appears to be significantly reduced in a PWR primary water environment compared to air at temperatures below about 150°C, probably due to hydrogen embrittlement (See Topical Report N° 13). Given the nature of the embrittlement of the ferrite phase in CASS, it is reasonable to suppose that some effects of hydrogen embrittlement may also combine with thermal aging embrittlement in this case. However, there are no known published studies of the effects of aqueous environments on fracture resistance of CASS although certain electrochemical non-destructive tests proposed for the detection of thermal aging embrittlement of CASS depend on different dissolution response between aged and non-aged material. In oxidizing environments such as BWR normal (oxygenated) water chemistry, this could result in preferential dissolution/oxidation at the γ-ferrite interface. Such differences would be less likely hydrogenated BWR hydrogen water chemistry or PWR primary water chemistry.

An ancillary question to the one posed above concerns the stress corrosion / hydrogen embrittlement behavior of thermally aged CASS but again there are no known published studies other than the (unexpected) observations of stress corrosion cracks propagating into stainless steel weld metals mentioned in the Introduction.

Some effort has been devoted to examining fatigue and corrosion fatigue S-N and fatigue crack propagation behavior of CASS. The corrosion fatigue data for de-oxygenated PWR environments appear to present similar environmental effects as wrought stainless steels. Given the unresolved controversy regarding how to incorporate such environmental effects in fatigue evaluations no further discussion is given here. The extent to which these corrosion fatigue studies extend to thermally aged material is not known.

References

[1] M. Guttmann, "Intermediate temperature aging of duplex stainless steels. A review", pp 79- 92, proceedings of "Duplex Stainless Steels '91", October 28-30, 1991, Beaune, France. Ed J. Charles & S. Bernhardsson.

[2] O. K. Chopra, "Estimation of fracture toughness of cast stainless steels during thermal aging in LWR systems – Revision 1", NUREG Report CR-4513-Rev1, August 1994.

[3] License Renewal Issue No. 98-0030, "Thermal aging embrittlement of cast austenitic stainless steel components", NRC, May 19, 2000.

[4] A. Bache, M. Akamatsu, P. Ould, P. Thibaut, H. Churier-Bossenec, G. Bezdikian, "Contribution de l'expertise des coudes déposés lors de RGV à la validation des méthodes de caractérisation et la justification de la tenue en service des produits moulés" (Translated: "Contribution of experimental investigations on cast elbows removed from service during steam generator replacement and validation of the methods used for characterizing and justifying the in-service behavior of CASS"), pp 967-976, Proceedings of International Symposium Fontevraud V, 23-27 September 2002.

Table B.4.1 ASME Specifications for CASS Grades Commonly Used in PWR and BWR

	CF-3	**CF-3A**	**CF-8**	**CF-8A**	**CF-8M**
Carbon %max	0.03	0.03	0.08	0.08	0.08
Manganese %max	1.50	1.50	1.50	1.50	1.50
Silicon %max	2.00	2.00	2.00	2.00	1.50
Sulfur %max	0.040	0.040	0.040	0.040	0.040
Phosphorus %max	0.040	0.040	0.040	0.040	0.040
Chromium	17.0-21.0	17.0-21.0	18.0-21.0	18.0-21.0	18.0-21.0
Nickel	8.0-12.0	8.0-12.0	8.0-11.0	8.0-11.0	9.0-12.0
Molybdenum %max	0.50	0.50	0.50	0.50	2.0-3.0
Tensile strength Min Ksi (MPa)	70 (485)	77 (530)	70 (485)	77 (530)	70 (485)
Yield strength Min Ksi (MPa)	30 (205)	35 (240)	30 (205)	35 (240)	30 (205)
Elongation Min %	35.0	35.0	35.0	35.0	30.0

Table B.4.2 Proposed Thermal Aging Screening Criteria in EPRI TR 106092

Mo Content (Wt. %)	**Casting Method**	**Ferrite Content**	**Significance of Thermal Aging**
High (2.0 – 3.0	Static	All	Potentially significant
	Centrifugal	>20%	Potentially significant
		œ 20%	Non-significant
Low (0.50 max.)	Static	> 20%	Potentially significant
		œ20%	Non-significant
	Centrifugal	All	Non-significant

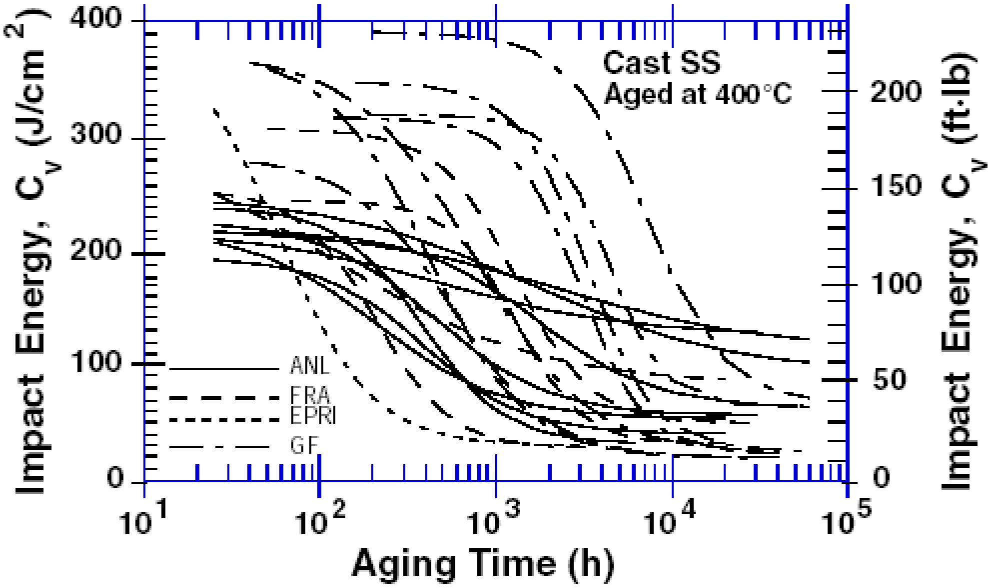

Figure B.4.1 Decrease in Charpy impact energy for various heats of cast stainless steels aged at 400°C (2).

B.4 SCC of Alloy 600 and Alloy 182, 132, 82 Weldments in BWR Water

[To be done later]

B. 6 SCC of Alloys 600, 690, 182, 82, 152 and 52 in PWR Primary Water

Introduction

Nickel base alloys are attractive for PWR primary circuit components because of the close similarity of their coefficients of thermal expansion to that of the low alloy steels used to fabricate the reactor pressure vessel, pressurizer and steam generator shells, as well as their low general corrosion and corrosion product release rates in PWR primary and secondary water. A list of PWR components where Alloys 600 and 690 and their compatible weld metals are used in PWRs is given in Table B.6.1. Typical compositions are shown in Table B.6.2.

Table B.6.1 PWR Components Fabricated from Nickel Base Alloys

PWR components	Nickel base alloy grades used
Steam generator tubes	Alloys 600 MA & TT, 690TT (& 800)
Steam generator divider plates	Alloys 600 & 690
Upper head penetrations	Alloys 600 & 690
Lower head penetrations	Alloy 600
Core supports	Alloy 600
Pressurizer nozzles	Alloys 600 & 690
Safe ends	Alloy 600
Weld metal deposits	Alloys 82, 182, 52 & 152

The susceptibility of Alloy 600 to Intergranular Stress Corrosion Cracking (IGSCC) in high temperature water was first revealed in laboratory testing in 1959 and then in operational service in PWR primary water from the early 1970s. IGSCC following exposure to the primary side environment is today commonly referred to in the industry as Primary Water Stress Corrosion Cracking (PWSCC).[1,2] Initially, highly cold worked components were affected such as tight U-bends in steam generator tubes and rolled or explosively expanded, cold-worked transitions in diameter of the tubes within the tube sheet [3]. This then became a major cause of steam generator tube cracking in the 1980s, and later, premature steam generator retirement and replacement. PWSCC of pressurizer nozzles and control rod drive mechanism (CRDM) nozzles in the upper heads of PWR reactor pressure vessels followed in the late 1980's and has continued for over a decade [4,5]. CRDM nozzle cracking appeared first in French PWRs in 1991 but was not widely observed elsewhere until the last five years or so.

Apparently interdendritic, but in fact intergranular, stress corrosion cracking (along dendrite "packet" boundaries) of the weld metals Alloys 182 and 82, the former having a composition similar to Alloy 600 (Table B.6.2), has also been observed in recent years in major primary circuit welds of several plants, often after very long periods in service ranging between 17 and 27 years [4,5].

A more detailed description of PWSCC observed in each type of nickel alloy PWR component and the phenomenology of PWSCC in various nickel base alloys is summarized below. A brief description of the methodologies developed to predict and mitigate cracking until, as is often the case, replacement becomes unavoidable, is also given. When Alloy 600 components are replaced, it is usually by Alloy 690 and its compatible weld metals, Alloys 152 and 52, which have so far proved resistant to PWSCC both in severe laboratory tests and, to date, after up to 16 years in service. Alloy 800 steam generator tubes have also proved resistant to PWSCC without any known cracking in primary water service.

Table B.6.2 Some Composition Specifications for Nickel Base Alloys Used in PWRs

	Alloy 600	Alloy 182	Alloy 82	Alloy 690	Alloy 152	Alloy 52
Nickel	>72.0	Bal.	Bal.	>58.0	Bal.	Bal.
Chromium	14-17	13-17	18-22	28-31	28-31.5	28-31.5
Iron	6-10	≤10.0	≤3.00	7-11	8-12	8-12
Titanium		≤1.0	≤0.75		≤0.50	≤1.0
Aluminum						≤1.10
Niobium plus Tantalum		1.0-2.5	2.0-3.0		1.2-2.2	≤0.10
Molybdenum					≤0.50	≤0.05
Carbon	≤0.05	≤0.10	≤0.10	≤0.04	≤0.045	≤0.040
Manganese	≤1.0	5.0-9.5	2.5-3.5	≤0.50	≤5.0	≤1.0
Sulfur	≤0.015	≤0.015	≤0.015	≤0.015	≤0.008	≤0.008
Phosphorus		≤0.030	≤0.030		≤0.020	≤0.020
Silicon	≤0.5	≤1.0	≤0.50	≤0.50	≤0.65	≤0.50
Copper	≤0.5	≤0.50	≤0.50	≤0.5	≤0.50	≤0.30
Cobalt	≤0.10	≤0.12	≤0.10	≤0.10	≤0.020	≤0.020

Alloy 600 steam generator tubes

Most PWR steam generators are of the ‘recirculating’ type although some are ‘once-through’ where all the secondary water entering the steam generator is transformed into steam. Most in-service PWSCC has occurred in recirculating steam generators. An important difference between the two from the point of view of PWSCC is that the once-through steam generators were subjected to a pre-service stress relief of the whole steam generator at a temperature of about 610 °C (1130 °F). In addition to provoking grain boundary carbide precipitation in Alloy 600, some grain boundary chromium depletion (sensitization) also occurred. The lower strength and grain boundary carbide precipitation in once-through steam generators tubes has proved to be advantageous for resistance to PWSCC on the primary side, despite the sensitization, although even these steam generators are now being steadily replaced after typically 20 to 25 years service [6]. In one case, however, an accidental ingress of thiosulfate into the once-through steam generators led (predictably) to extensive intergranular attack (IGA) of the sensitized tubes.

PWSCC of Alloy 600 steam generator tubing in the mill annealed (MA) condition became a major degradation mechanism from the 1970s onwards for recirculating steam generators [7]. In 1971, the first confirmed primary side cracking of mill annealed Alloy 600 tubes of recirculating steam generators occurred when leakage at U-bends was experienced in the Obrigheim steam generators after only 2 years of operation [2]. Cracking occurred both in the tight U-bends, mainly on the inner two rows at the apex and at the tangent points as well as in the tube sheet at the transition expansion or roll expansion regions of the tubes. The latter has been responsible for premature steam generator replacement at a number of plants.

The first roll transitions experiencing PWSCC were located on the hot leg side where the temperature is typically around 320 °C (610 °F) and is 30 to 40 °C (55 to 70 °F) hotter than the cold leg inlet at 280 °C (535 °F). Thus, it was clear that temperature had a significant influence on PWSCC, indicating a strongly thermally activated process. The apparent activation energy from fitting the temperature dependence to the Arrhenius equation is rather high (~ 180 kJ/mole) so that a typical temperature difference of 30 °C (55 °F) between hot and cold legs could easily account for a factor of four to five increase in the time to the onset of detectable cracking. Thus, reduction of hot leg temperature has been one possible mitigating action that has been used. Hot leg temperature reductions from 4 to even 10 °C have been applied.

The magnitude of the tensile stresses, particularly residual stress from fabrication, has also had a major impact on the time for detectable PWSCC to develop; only the most highly strained regions of steam generator tubing (that is, row-one and two U-bends, roll transition regions, expanded regions, and dented areas) have exhibited PWSCC. Consequently, several stress mitigation techniques have been evolved such as local stress relief of first and second row U-bends by resistance or induction heating, and shot peening or rotopeening to induce compressive stresses on the internal surface of roll transitions [8,9]. While peening helps to prevent initiation of new cracks, it cannot prevent the growth of existing cracks whose depth is greater than that of the induced compressive layer, typically 100 to 200 μm. Thus, peening has been most effective when most tubes have either no cracks or only very small ones, i.e. when practiced before service or very early in life [9,10].

Material susceptibility, in combination with the factors mentioned above, is also a major factor affecting the occurrence of PWSCC in service. Most PWSCC has occurred in mill annealed tubing. However, it is important to emphasize that there is not a single product called "mill-annealed" Alloy 600 tubing since each tubing manufacturer has employed different production processes. Whereas some mill-annealed tubing has not experienced any PWSCC over extended periods of operation, in other cases it has occurred after only 1 to 2 years of service, particularly at roll transitions. This variability of PWSCC susceptibility is even seen between heats from the same manufacturer in the same steam generator [11]. The variation in susceptibility to PWSCC of the heats of Alloy 600 typically fits approximately a lognormal distribution so that a rather small fraction of Alloy 600 heats may be responsible for a disproportionately high number of tubes affected by primary side PWSCC. The reasons for such variability are only partly understood.

This microstructural aspect of susceptibility to PWSCC has been observed to be strongly affected by the final mill-annealing temperature, which determines whether carbide precipitation occurs predominantly on grain boundaries or intragranularly. The most susceptible microstructures are those produced by low mill-annealing temperatures, typically around 980 °C (1800 °F) that develop fine grain sizes (ASTM 9 to 11), copious quantities of intragranular carbides, and, usually, few if any intergranular carbides [12,13]. Higher mill annealing temperatures in the range of 1040 to 1070 °C (1900 to 1960 °F) avoid undue grain growth and leave enough dissolved carbon so that intergranular carbide precipitation occurs more readily during cooling.

A further development to exploit the apparent advantages of grain boundary carbides for PWSCC resistance was to thermally treat the tubing for ~15 h at 705 °C (1300 °F) after mill annealing. This both increases the density of intergranular carbides in the grain boundary and provides enough time so that most of the carbon in solution is consumed, and the chromium can diffuse to eliminate its depletion profile and thus avoid sensitization [13]. The beneficial influence of grain boundary chromium carbides on primary side PWSCC resistance has been extensively evaluated in laboratory studies and suggests an improvement in life of thermally treated tubing of between 2 and 5 times relative to the mill annealed condition. In fact, primary side PWSCC resistance is improved with or without grain boundary chromium depletion, as also deduced from the generally much better operating experience of Alloy 600 tubing of once-through steam generators [6,12,13]. However, even thermally treated Alloy 600 tubing has cracked in service, although much less frequently than mill annealed Alloy 600. This has usually been attributed to a failure of the thermal treatment to produce the desired intergranular carbide microstructure either due to insufficient carbon or factors such as tube straightening prior to thermal treatment, which has favored carbide precipitation on dislocations instead of grain boundaries.

Steam generator tubes with PWSCC detectable by non-destructive testing have usually been preventively plugged either to avoid leakage or before the crack length reaches some pre-defined conservative fraction of the critical size for ductile rupture. Sleeving has sometimes been deployed as a repair method in operating PWRs to avoid plugging and maintain the affected tubes in service. The sleeves bridge the damaged area and are attached to sound material beyond the damage. The ends of the sleeves may be expanded hydraulically or explosively and are in most cases sealed by rolling, welding, or brazing [3].

Modern (usually replacement) steam generators have been fabricated using Alloy 690 tubes thermally treated for 5 hours at 715 °C. As well as being highly resistant in severe laboratory tests to PWSCC in PWR primary water compared to either mill annealed or thermally treated Alloy 600, the lead steam generators with thermally treated Alloy 690 tube bundles have, to date, about 16 years of service with no known tube failures.

Thick section Alloy 600 components

Thick section, forged, Alloy 600 components started to crack in the mid 1980's starting with the hottest components, pressurizer nozzles [11,14]. In France, for example, all pressurizer nozzles were replaced with stainless steel. In 1991, the first cracking of Alloy 600 upper head Control Rod Drive Mechanism (CRDM) nozzles occurred at the Bugey 3 plant in France. At first, it was thought that this could be a special case because of the combination of a stress concentration due to a counter bore in the nozzles just below the level of the J-groove seal weld with the upper head, as well as a relatively high operating temperature that was believed to be closer to that of the hot leg in this first generation French plant. However, the problem spread during the 1990's to CRDM nozzles in other plants with no counter bore, nor with a tapered lower section to the CRDM nozzle, and in upper heads where the temperature was the same as the inlet cold leg temperature [15,16].

Three common features of the cracking of upper head CRDM nozzles were the presence of a significant cold worked layer due to machining or grinding on the internal bore, some distortion or ovalization induced by the fabrication of the J-groove seal welds, and a tendency to occur much more frequently in the outer set-up circles where the angles between the vertical CRDM nozzle and the domed upper head were greatest. The combination of these three features plus the fact that the upper head is stress relieved before the CRDM nozzles are welded in place pointed to high residual stresses being responsible for these premature failures.

Although the generic problem of Alloy 600 CRDM nozzle cracking first appeared in France, only sporadic instances of similar cracking were observed in other countries until the beginning of the 21st century, since when numerous other incidents have been reported. In some cases, where cracking was allowed to develop to the point of leaking primary water into the crevice between the CRDM nozzle and the upper head, circumferential cracks initiated on the outer surface of the CRDM nozzle at the root of the J-groove seal weld [17]. This latter observation had also been made in 1991 at Bugey 3 but only to a minor extent. No further leaks of primary water due to CRDM nozzle cracking have occurred in France because of an inspection regime adopted to avoid them and a decision taken to replace all upper heads using thermally treated Alloy 690 CRDM nozzles [15,16]. The same strategy has often been adopted elsewhere as more economic than the cost of repairs and repeat inspections. The dangers of allowing primary water leaks to continue over several years so that extensive boric acid deposits accumulated was amply demonstrated by the discovery of very severe corrosion (wastage) of the low alloy steel of the upper head at the Davis Besse plant in 2002 [5,17].

Nickel base weld metals

The history of PWSCC in Alloy 600 and similar nickel base alloys has continued in recent years with the discovery of cracked Alloy 182 welds in several PWRs around the world [17,18]. This has occurred on the primary water side of the J-groove welds that seal the CRDM nozzles in the upper head and also in a few cases in the safe end welds of the reactor pressure vessel or pressurizer. One case has also occurred in the J-weld of a lower head instrumentation penetration [19]. Cracking seems to be significantly exacerbated by the presence of weld defects and of weld repairs made during fabrication, usually to eliminate indications due to hot cracking, or slag inclusions, thus again implicating high residual stress in the failures observed to date. The cracking has often been described as interdendritic but recent work shows that it is in fact intergranular [20]. Incubation periods before detectable cracking seem to be very long, of the order of twenty years.

It should be noted that all the nickel base weld metal cracking observed to date has concerned welds that have not experienced the stress relief given to adjacent low alloy steel pressure vessel components [18]. Although the stress relief temperature is clearly not optimized for nickel base alloys (or stainless steels), it has been shown on mockups that the surface residual stress of the welds is very significantly reduced and doubtless imparts greater resistance to PWSCC in PWR primary water.

Life prediction

In spite of the improvements available for new plants or for replacement components equipped with Alloy 690 and welded with Alloys 52 or 152, many Alloy 600 components, either mill annealed, thermally treated or forged remain in service. While most show no sign of cracking in service, it is important to assess component life and endeavor to predict when replacement may become necessary. Prediction methodologies were first developed for steam generator tubes and later extended to pressurizers and upper head CRDM penetrations. Both deterministic and probabilistic methods have been developed [21,22].

Modeling of Alloy 600 component life is often based on the assumption that the time to detectable cracking varies as the inverse fourth power of the stress (including residual stress) above a threshold stress of ~250 MPa with a temperature dependency approximated by the Arrhenius equation. Despite the scatter observed in determinations of apparent activation energy, there is a reasonable consensus that a value of 180 kJ/mole (44 kcal/mole) is adequate for component life estimations. Some approaches to modeling also attempt to include material variability in susceptibility to PWSCC [22,23,24,25]. However, in the case of classification of the susceptibility of CRDM nozzle cracking in US PWRs this aspect has not been taken into account [17]. Nevertheless, as can be seen in Figure B.6.1, the plants most at risk from PWSCC of Alloy 600 CRDM nozzles have been correctly identified.

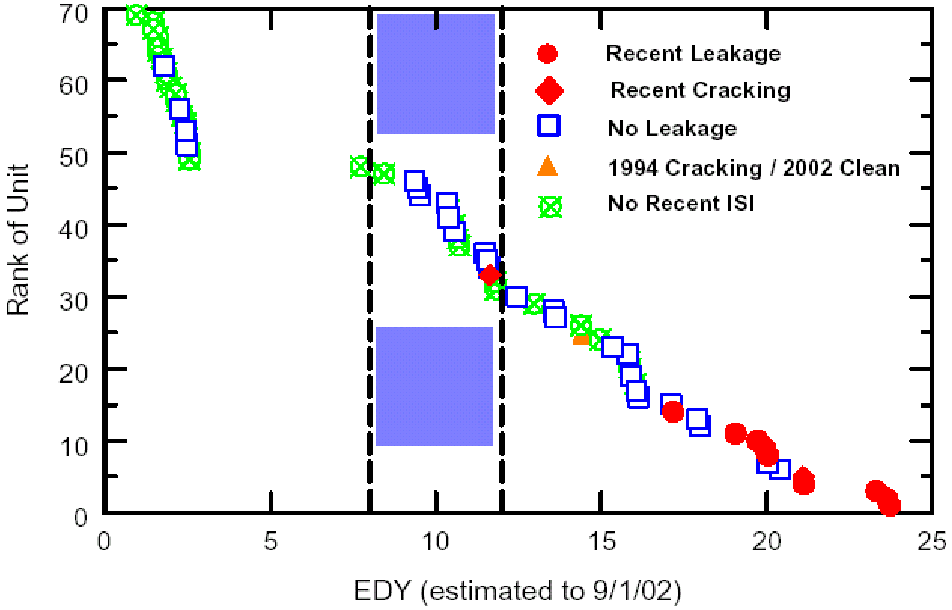

Figure B.6.1 Equivalent damage years for the upper head CRDM nozzles of US PWRs in September 2002 [17]

Application of the Weibull distribution to quantify the dispersion in stress corrosion data is well established and has been successfully applied to PWSCC in Alloy 600 steam generator tubes and upper head penetrations [21,22]. The dispersion in times to observe detectable cracks arises from the inherent variability in susceptibility of materials to stress corrosion cracking and, in the case of plant components, to uncertainty in the stress and temperature. The Weibull distribution can be fitted to the early observations of PWSCC as a function of operating time and provides a very effective tool for predicting the future development of cracking so that informed inspection and repair plans can be formulated [21]. An alternative Monte Carlo simulation approach to improving the stochastic prediction of PWSCC has also been developed in the context of upper head penetration cracking taking into account the inherent dispersion in the input parameters of stress, temperature, activation energy and material susceptibility [22,23,24,25].

Another parameter that can have a dramatic influence on component susceptibility to cracking in service is the quality of the surface finish due to machining, grinding etc. Based on careful characterizations of the thicknesses of cold worked layers and residual stresses left by different machining techniques, a quantitative framework for assessing their impact on component resistance to PWSCC has been developed [14,23,24,25].

Once a stress corrosion crack has been detected by non-destructive examination in a PWR primary circuit component, an essential step in the justification of structural integrity and further operation without repair or replacement of the affected component is an assessment of crack growth during the next few operating cycles. Practical approaches to assessing crack growth by PWSCC in Alloy 600 components have relied on empirical measurements of crack growth rates as a function of crack tip stress intensity, K_I, , as follows [26,27]:

$$\frac{da}{dt} = C.(K_I - 9)^n \qquad \left(K_I\ in\ MPa\sqrt{m}\right)$$

The values of the coefficients C and n vary for given practical circumstances, but there is a reasonable consensus that the apparent activation energy to be used for adjusting the coefficient C for temperature is ~130 kJ/mole, which is somewhat lower than the value quoted above for overall life prediction, where time to crack initiation usually dominates.

Other variables that are known to influence the rate of crack growth in Alloy 600 are cold work, hydrogen overpressure and possibly pH or lithium hydroxide concentration. Cold work can easily affect the value of the coefficient C by as much as an order of magnitude. Hydrogen overpressure effects are also potentially significant [28]. However, the effect has not been explicitly included in crack growth assessment equations to date, probably because the hydrogen concentration in PWR primary water is controlled within a relatively narrow range. Concerning the possible influence of pH or lithium concentration in PWR primary water on crack growth kinetics, the effect is, at most, small within the range of pH or lithium concentrations permitted by the PWR primary water specification [11,22]. More recent work suggests that the effect of lithium within this range is virtually non-existent [29].

Summary of laboratory investigations

As early as 1957, laboratory studies of cracking of high-nickel alloys in high-purity water at 350 °C (660 °F) were reported [1,5] although at that time the importance of the corrosion potential as fixed by the hydrogen partial pressure was not understood. During the following years, numerous laboratory tests were performed in different environments to duplicate and explain these observations. Nevertheless, despite considerable experimental efforts, no consensus exists as to the nature of the cracking mechanism [29] and, as noted above, both remedial measures and life modeling have relied on empirical, phenomenological correlations. The essential phenomenological features of primary water PWSCC of Alloy 600 have, nevertheless, been very well characterized, as follows:

- a profound influence of hydrogen partial pressure (or corrosion potential) and observation of maximum susceptibility centered on corrosion potentials near the Ni/NiO stability equilibrium;
- an apparently continuous mechanism of failure between 300°C sub-cooled water and 400°C superheated steam;
- a high and variable apparent activation energy typically 180 kJ/mole for initiation but with a scatter band of 80 to 220 kJ/mole;
- a strong influence of carbon content and microstructure, particularly a favorable influence of grain boundary carbides and an undesirable effect of cold work;

- a high stress exponent of ≈ 4 for lifetime to failure.

It can be noted that despite differing opinions about the mechanism of PWSCC of Alloy 600, most recent models incorporate the idea that solid state grain boundary diffusion is rate controlling [30]. Such models provide physically based support for the empirical value of the activation energy, which is typical of solid-state grain boundary diffusion in nickel. Physical support for the fourth power dependency on applied stress comes mainly from studies of grain boundary sliding (itself dependent on grain boundary diffusion) observed during primary creep in Alloy 600 at temperatures between 325 and 360°C [23,31]. Grain boundary sliding rates are also observed to depend on grain boundary carbide coverage, greater coverage being associated with slower grain boundary sliding rates and higher resistance to PWSCC. However, although grain boundary carbide morphology is a major reason for heat-to-heat variability in susceptibility to PWSCC of Alloy 600 in PWR primary water, it is clear that other metallurgical parameters, albeit poorly characterized or unidentified, must be involved.

Research into PWSCC, particularly of thick-walled components made of Alloy 600 and its weld metals, is ongoing throughout the world and significant progress, both in practical assessment of service life and mitigation measures, as well as in more fundamental understanding, is anticipated within the next few years.

Alloy 690 has been extensively tested in the laboratory in order to quantify its resistance to PWSCC and to estimate the advantage gained relative to Alloy 600 (32). The improvement factor for thermally treated Alloy 690 relative to mill annealed Alloy 600 has been determined to be greater than 26, and greater than 13 relative to thermally treated Alloy 600. These factors have been judged to be sufficient to conclude that failure is unlikely in 60+ years. The corresponding weld metals, Alloys 152 and 52, have also been tested although to a lesser extent than the base material but nevertheless appear to have similar resistance to Alloy 690.

Some knowledge gaps have been identified apart from an insufficient data base for Alloy 152 and 52 weld metals mentioned above (32). One important gap concerns possible effects of product form and subtle changes of composition and mechanical processing effects on PWSCC resistance since it has proved possible to produce structures that can crack under extremely severe test conditions. A potential concern for susceptibility of weld heat affected zones has also been identified by analogy with known data for Alloy 600 and this could also be extended to the mixing zones with stainless and low alloy steels in bimetallic welds. Little information is available on corrosion fatigue properties of Alloy 690 although these are expected to be similar to those of Alloy 600. Possible low temperature crack propagation during transient conditions encountered during plant cooldown has also been identified as requiring some study.

References

[1] J. Blanchet, H. Coriou, L. Grall, C. Mahieu, C. Otter, G. Turluer, "Historical review of the principal research concerning the phenomena of cracking of nickel base austenitic alloys", Proceedings of NACE-5 'Stress Corrosion Cracking and Hydrogen Embrittlement of Iron Base Alloys', National Association of Corrosion Engineers 1977, pp 1149-1160.

[2] H.J. Schenk, "Investigation of tube failures in Inconel 600 steam generator tubing at KWO Obrigheim", Materials Performance, Vol 15 (3), 1976, pp 25–33.

[3] S. J. Green, "Steam generator failure or degradation", Corrosion in the Nuclear Power Industry, ASM Handbook, Volume 13, "Corrosion", 1987, pp 937-945.

[4] W. Bamford, J. Hall, "A review of Alloy 600 cracking in operating nuclear plants: historical experience and future trends", Proceedings of 11th Int. Conference on Environmental Degradation of Materials in Nuclear Power Systems - Water Reactors, Stevenson, American Nuclear Society 2003, pp 1071-1079.

[5] W. H. Cullen, Jr., T. S. Mintz, "A survey of worldwide experience with the cracking susceptibility of alloy 600 and associated welds", Office of Nuclear Regulatory Research, US Nuclear Regulatory Commission, Washington, DC 20555.

[6] P. A. Sherburne, "OTSG materials performance – 25 years later", Proceedings of the Fontevraud IV International Symposium, SFEN 1998, pp 529-540.

[7] D. R. Diercks, W. J. Shack and J. Muscara, "Overview of steam generator tube degradation and integrity issues", Nuclear Engineering and Design, Vol 194, 1999, pp 19-30.

[8] G. Frederick and P. Hernalsteen, "Generic Preventive Actions for Mitigating MA Inconel 600 Susceptibility to Pure Water Stress Corrosion Cracking," Paper presented at The Specialist Meeting on Steam Generators, Stockholm, Sweden, NEA/CSNI-UNIPEDE, Oct 1984.

[9] P. Saint-Paul, G. Slama, "Steam generator materials degradation", Proceedings of 5th Int. Symposium on Environmental Degradation of Materials in Nuclear Power Systems - Water Reactors, Monterey, American Nuclear Society 1992, pp 39-49.

[10] P. Pitner, T. Riffard, "Statistical evaluation of the effects of shot-peening on stress corrosion of Alloy 600 in PWR steam generators", Proceedings of 6th Int. Symposium on Environmental Degradation of Materials in Nuclear Power Systems - Water Reactors, The Metallurgical Society 1993, pp 707-712.

[11] P. M. Scott, "Stress corrosion cracking in Pressurized Water Reactors - Interpretation, modeling and remedies", Corrosion, Vol 56(8), 2000, pp 771-782.

[12] G. P. Airey, "The stress corrosion cracking (SCC) performance of Inconel Alloy 600 in pure and primary water environments", Proceedings of 1st International Symposium on Environmental Degradation of Materials in Nuclear Power Systems-Water Reactors, National Association of Corrosion Engineers, 1984, pp 462-476.

[13] A.A. Stein, A. R. McIlree, "Relationship of annealing temperature and microstructure to primary side cracking of Alloy 600 steam generator tubing and the prediction of stress corrosion cracking in primary water", Proceedings of 2nd International Symposium on Environmental Degradation of Materials in Nuclear Power Systems-Water Reactors, Monterey, CA, American Nuclear Society 1986, pp 47-51.

[14] Ph. Berge, "Importance of surface preparation for corrosion control in nuclear power stations", Materials Performance Vol 36 (11), 1997, p 56.

[15] F. Champigny, F. Chapelier, C. Amzallag, "Maintenance strategy of Inconel components in PWR primary systems in France", Proceedings of Conference on Vessel Penetration Inspection, Cracking and Repairs, Gaithersburg, MD, September 29-October 2, 2003.

[16] P. Chartier, D. Edmond, G. Turluer, "The French regulatory experience and views on nickel-base alloy PWSCC prevention", Proceedings of Conference on Vessel Penetration Inspection, Cracking and Repairs, Gaithersburg, MD, September 29-October 2, 2003.

[17] A. Hiser, "US regulatory experience and prognosis with RPV head degradation and VHP nozzle cracking", Proceedings of Conference on Vessel Penetration Inspection, Cracking and Repairs, Gaithersburg, MD, September 29-October 2, 2003.

[18] C. Amzallag, J-M Boursier, C. Pagès, C. Gimond, "Stress corrosion life assessment of 182 and 82 welds used in PWR components", Proceedings of the 10th International Conference on Environmental Degradation of Materials in Nuclear Power Systems – Water Reactors, August 3 to 9, 2001, Lake Tahoe, CA, NACE International 2001.

[19] S. Thomas, "Bottom mounted instrumentation penetration condition resolution", Proceedings of Conference on Vessel Penetration Inspection, Cracking and Repairs, Gaithersburg, MD, September 29-October 2, 2003.

[20] L. E. Thomas, J. S. Vetrano, S. M. Bruemmer, P. Efsing, B. Forssgren, G. Embring, K. Gott, "High resolution analytical electron microscopy characterization of environmentally assisted cracks in Alloy 182 weldments", Proceedings of 11th International Conference on Environmental Degradation of Materials in Nuclear Power Systems – Water Reactors, Stevenson, Washington, American Nuclear Society 2003, pp 1212-1224.

[21] R.W. Staehle, J. A. Gorman, K. D. Stavropoulos and C. S. Welty, "Application of statistical distributions to characterizing and predicting corrosion of tubing in steam generators of Pressurized Water Reactors", Proceedings of Life Prediction of Corrodible Structures, ed. R. N. Parkins, (Houston, TX: NACE International, 1994), pp 1374-1439.

[22] P. Scott and C. Benhamou, "An overview of recent observations and interpretation of PWSCC in nickel bas alloys in PWR primary water", Proceedings of 10th Int. Symposium on Environmental Degradation of Materials in Nuclear Power Systems - Water Reactors, Lake Tahoe, NACE International 2001.

[23] S. LeHong, C. Amzallag, A. Gelpi, "Modeling of stress corrosion crack initiation on Alloy 600 in primary water of PWRs", Proceedings of 9th International Symposium on Environmental Degradation of Materials in Nuclear Power Systems – Water Reactors, Newport Beach, CA, The Metallurgical Society 1999, pp 115-122.

[24] C. Amzallag, S. Le Hong, C. Pagès, A. Gelpi, "Stress corrosion life assessment of Alloy 600 components", Proceedings of 9th International Symposium on Environmental Degradation of Materials in Nuclear Power Systems – Water Reactors, Newport Beach, CA, The Metallurgical Society 1999, pp 243-250.

[25] C. Amzallag, S. LeHong, C. Benhamou, A. Gelpi, "Methodology used to rank the stress corrosion susceptibility of Alloy 600 PWR components", Pressure Vessel and Piping Conference, (Seattle: ASME, 2000).

[26] C. Amzallag, F. Vaillant, "Stress corrosion crack propagation rates in reactor vessel head penetrations in Alloy 600", Proceedings of 9th International Symposium on Environmental Degradation of Materials in Nuclear Power Systems – Water Reactors, Newport Beach, CA, The Metallurgical Society 1999, pp 235-241.

[27] G. A. White, J. Hickling, L. K. Mathews, "Crack growth rates for evaluating PWSCC of thick-walled Alloy 600 material", Proceedings of 11th International Conference on Environmental Degradation of Materials in Nuclear Power Systems – Water Reactors, Stevenson, Washington, American Nuclear Society 2003, pp 166-179

[28] S. A. Attanasio, J. S. Morton, "Measurements of nickel/nickel oxide transition in Ni-Cr-Fe alloys and updated data and correlations to quantify the effect of aqueous hydrogen on primary water SCC", Proceedings of 11th International Conference on

Environmental Degradation of Materials in Nuclear Power Systems – Water Reactors, Stevenson, Washington, American Nuclear Society 2003, pp 143-154.

[29] P. M. Scott, P. Combrade, "On the mechanism of stress corrosion crack initiation and growth in Alloy 600 exposed to PWR primary water", Proceedings of 11th International Conference on Environmental Degradation of Materials in Nuclear Power Systems – Water Reactors, Stevenson, Washington, American Nuclear Society 2003, pp 29-35.

[30] F. Vaillant, J-D Mithieux, O. de Bouvier, D. Vançon, G. Zacharie, Y. Brechet, F. Louchet, "Influence of chromium content and microstructure on creep and PWSCC resistance of nickel base alloys", Proceedings of 9th International Symposium on Environmental Degradation of Materials in Nuclear Power Systems – Water Reactors, Newport Beach, CA, The Metallurgical Society 1999), pp 251-258.

B.7 Corrosion of Steam Generator Tubes

1.0 Introduction

The objective of this topical report is to describe the corrosion of tubing materials used in PWR steam generators of LWRs. This tubing includes Alloys 600MA, 600TT, 690TT and 800. The corrosion behavior of these materials has been discussed comprehensively by Staehle and Gorman.[1] This present report emphasizes mainly the initiation stage of SCC since SG tubes are relatively thin compared to thicker sections in pipes and various instrument and control rod housings. Some information on SCC propagation is included.

This discussion considers the development and application of Alloy 600MA, Alloy 600TT, Alloy 690TT and Alloy 800, together with the modes of corrosion they sustain and some of the principal dependencies of these modes of corrosion.

The terminology of MA (mill-annealed) and TT (thermal treatment) is used in this discussion. MA for Alloy 600 is heat treated at about 1000˚C and for Alloy 690 at about 1070˚C. TT for Alloy 600 is heat treated at 700˚C for 15 hours and for Alloy 690 at 716˚C for 10 hours. A slight variation for MA is given by LTMA (low temperature mill-annealed) and HTMA (high temperature mill-annealed). LTMA is heat treated at 985˚C and HTMA at 1010˚C.

The earliest tubing used in steam generators was the Type 304 stainless steel in the Shippingport plant[2] and noted in Scharfstein et al.[3,4] However, even with the horizontal steam generators used in this application, chlorides and caustic were concentrated at the tube supports and tubesheets thereby producing SCC. In 1962 the Navy program decided to use Alloy 600MA in steam generators, and the subsequent evolution of the use of alloys in LWRs is shown in Figure B.7.1.[1] The Russian designed VVERs followed a different path, continuing to use horizontal austenitic stainless steel tubes terminating at vertical cylindrical collectors. On the whole, these have been reliable in service.

The alloys used for steam generator tubing are nominally single phase with a face centered cubic structure, usually called an "austenitic structure," as shown in the ternary diagram of Figure B.7.2.[5] Chemical compositions of the alloys for SG tubing and for tube supports are given in Table B.7.1.

The choice of the high nickel alloys for replacing the stainless steels for SG tubing was based essentially on the work of Copson and Cheng,[6] who had studied the effect of nickel on the SCC of Fe-Cr-Ni alloys in boiling $MgCl_2$ solutions as shown in Figure B.7.3a. This work showed that the alloys with nickel concentration exceeding about 40w/o would resist

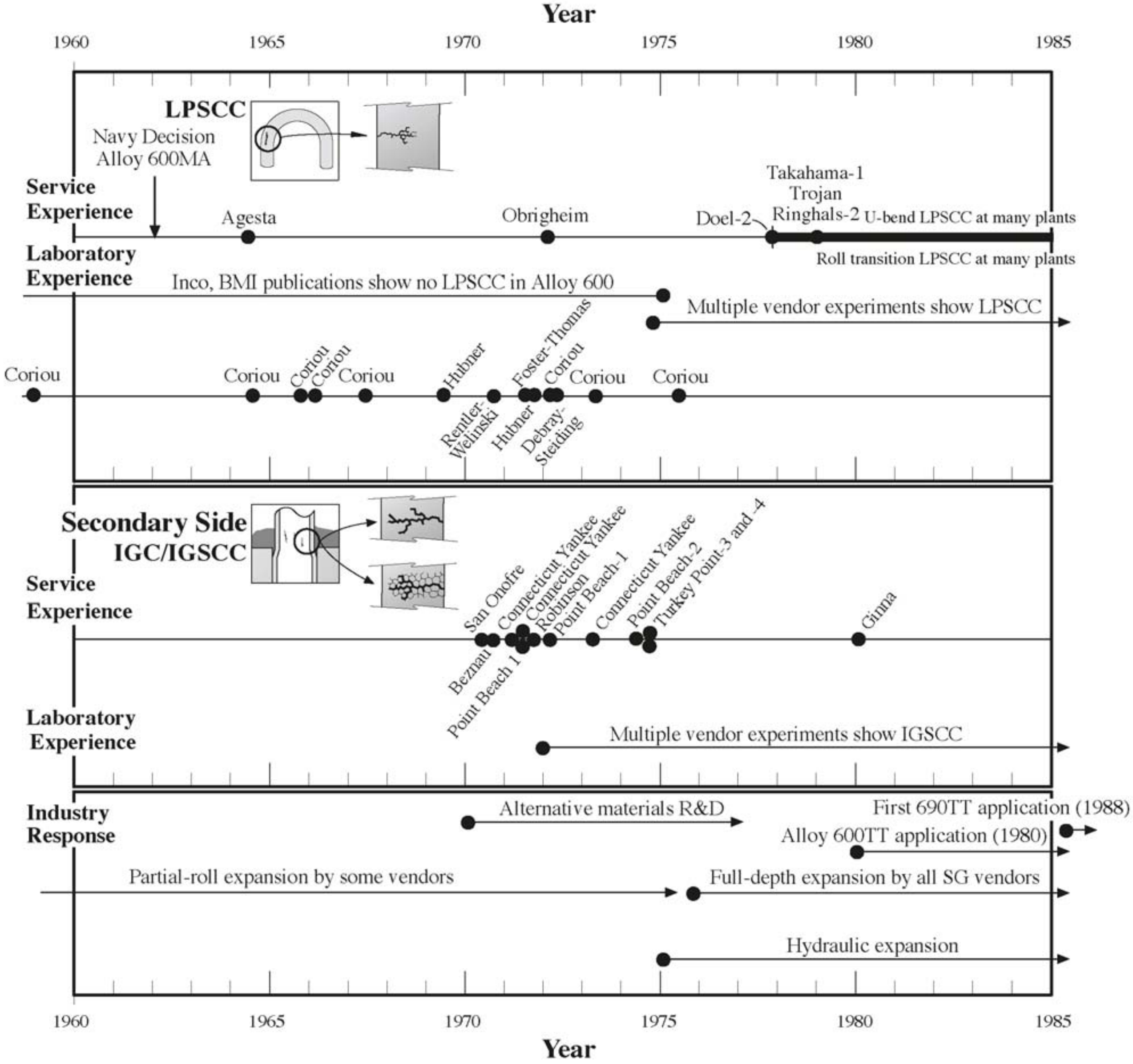

Figure B.7.1 Service and laboratory experience with LPSCC and IGSCC vs. time. Industry response to these experiences vs. time. From Staehle and Gorman.[1]

SCC in the concentrated $MgCl_2$ solutions. By implication, and assuming that the boiling $MgCl_2$ solutions represented characteristically aggressive solutions generated from seawater or estuarine water ingress at leaking condensers, these results suggested that the high nickel alloys would resist a broad range of stress corrosion cracking. Figure B.7.3b from Berge and Donati[7] shows results from SCC testing of Alloy 600MA in a boric acid solution containing chloride at 100°C; the extensive transgranular SCC in Alloy 600 shows that the assumption of aggressiveness of the $MgCl_2$ solutions was not correct.

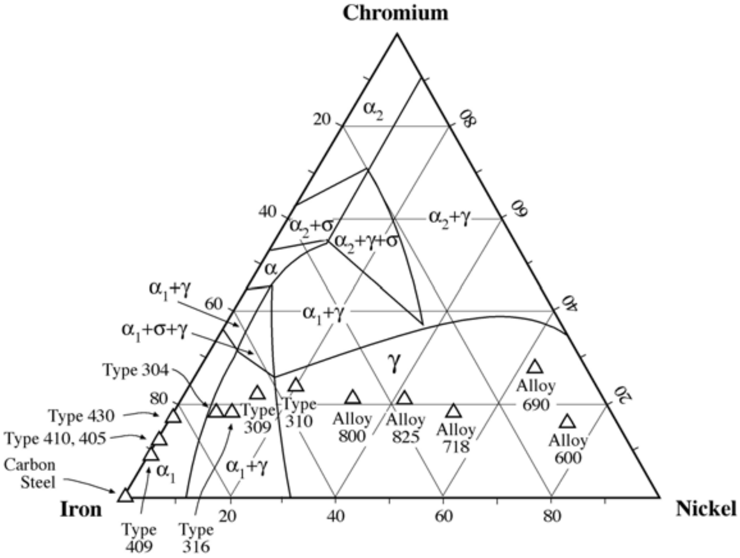

Figure B.7.2 Alloys of interest to steam generators superimposed on an Fe-Cr-Ni ternary diagram for 400°C. Fe-Cr-Ni diagram from Pugh and Nisbet.[5]

Table B.7.1
Composition of Alloys Used in Tubing and Tube Supports
(maximum w/o, except where noted.)

Elem.	**Type 304**[A]	**Type 316**[A]	**Alloy 600 EPRI Guidelines** [B]	**Alloy 690 EPRI Guidelines** [C]	**Alloy 800 Nuclear Grade**[D]	**Carbon Steel ASTM A285 Gr C**[A]	**Type 405 ASME SA479**[A]	**Type 409**[A]	**Type 410 ASME SA479**[A]
C	0.08	0.08	0.025-0.05	0.015-0.025	0.03	0.28	0.15	0.08	0.15
Mn	2.00	2.00	1.00 max.	0.50	0.4-1.0	0.90	1.00	1.00	1.00
P	0.045	0.045	0.015	0.015	0.020	0.035	0.040	0.045	0.040
S	0.03	0.03	0.010 max.	0.003	0.015	0.035	0.030	0.045	0.030
Si	1.00	1.00	0.50 max.	0.50	0.3-0.7	-	0.50	1.00	1.00
Cr	18-20	16-18	15.0-17.0	28.5-31.0	20-23	-	11.5-13.0	10.5-11.75	11.5-13.5
Ni	8.0-10.5	10-14	>72	Bal. (>58)	32-35	-	-	0.50	-
Mo	-	2.0-3.0	-	0.2	-	-	-	-	-
Fe	Bal.	Bal.	6.0-10.0	9.0-11.0	Bal.	-	Bal.	Bal.	Bal.
Cu	-	-	0.50 max.	0.10	0.75	-	-	-	-
Co	-	-	0.015 ave.	0.014	0.10	-	-	-	-
Al	-	-	-	0.40	0.15-0.45	-	-	-	-
Ti	-	-	-	0.40	0.60	-	-	6xC-0.75	-
Other	-	-	-	N = 0.050 B = 0.005 Nb = 0.1	Ti/C≥12 Ti/(C+N)≥8 N≥0.03	-	-	-	-

[A] From ASM Handbook.[8]
[B] From EPRI.[9]
[C] From Gorman.[10]
[D] From Stellwag et al.[11]

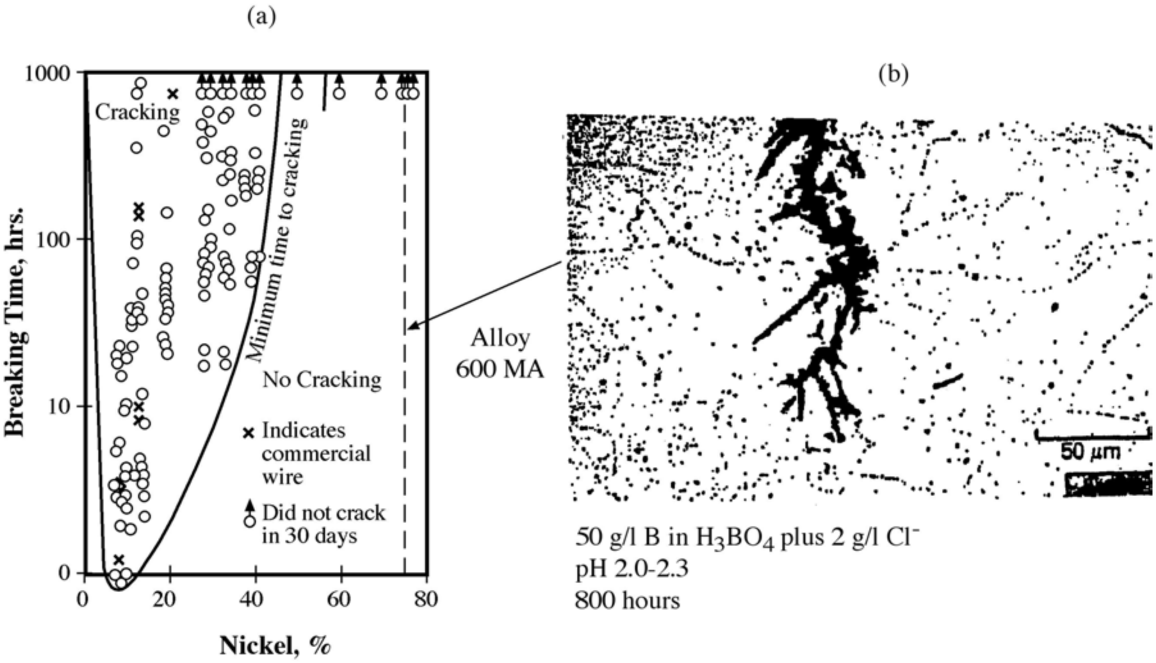

Figure B.7.3 (a) Breaking time vs. Ni in w/o for Fe-20Cr-Ni alloys exposed to 42% boiling $MgCl_2$. pH of solution is about 4.1. From Copson and Cheng.[6] (b) Photomicrograph of Alloy 600MA exposed at 100°C in a solution containing 50 g/l boron as boric acid and 2 g/l Cl^-. pH of solution is 2.0 to 2.3. U-bend specimen examined after 800h. From Berge and Donati.[7]

At about the same time as Copson and Cheng had published the work in Figure B.7.3a, Coriou at al. published their work on the SCC of high nickel alloys which were exposed to 100˚C pure water.[12] This 1959 paper, together with subsequent ones, showed conclusively that Alloy 600 would sustain SCC in pure deaerated water. Coriou et al.[13] then published a schematic view shown in Figure B.7.4 indicating that the SCC in pure deaerated water was most aggressive in high nickel alloys while the SCC in chloride solutions was most aggressive in low nickel alloys following Figure B.7.3 from Copson and Cheng. This figure indicated that an optimum material would be in the mid-range of nickel concentration. This observation was the basis for choosing Alloy 800 for some SG tubing as well as indicating that the Alloy 690 composition, to be developed later, would be attractive.

In summary, the chronology of corrosion of tubing in PWR steam generators has been dominated by extensive SCC on both the inside and outside of the Alloy 600 tubes. The application of improved alloys has responded to this corrosion first with Alloy 600TT and then with Alloy 690TT as shown in Figure B.7.5. Today, Alloy 690TT is increasingly used for replacement steam generators because of its improved corrosion resistance; although it should be noted, as shown in Section 4.0, that Alloy 690TT is not immune to SCC. In addition, Alloy 800 has given excellent service as predicted by Coriou et al.[13] in Figure B.7.4, in SGs designed by AECL, Sandvik and Siemens.

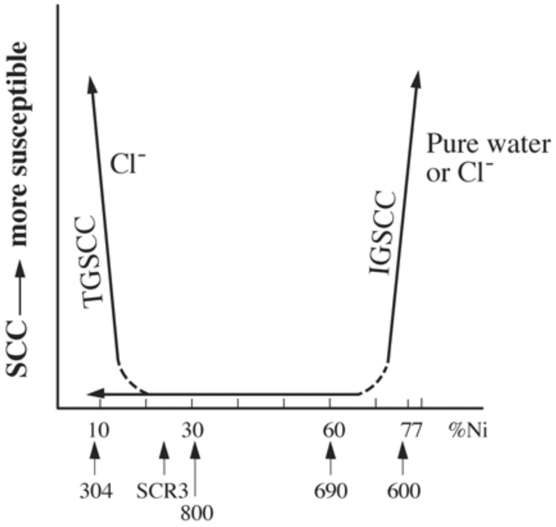

Figure B.7.4 Schematic view of SCC intensity vs. Ni concentration for Fe-Cr-Ni alloys in high temperature water for pure deaerated water and chloride-containing water. Important commercial alloys noted. From Coriou et al.[13]

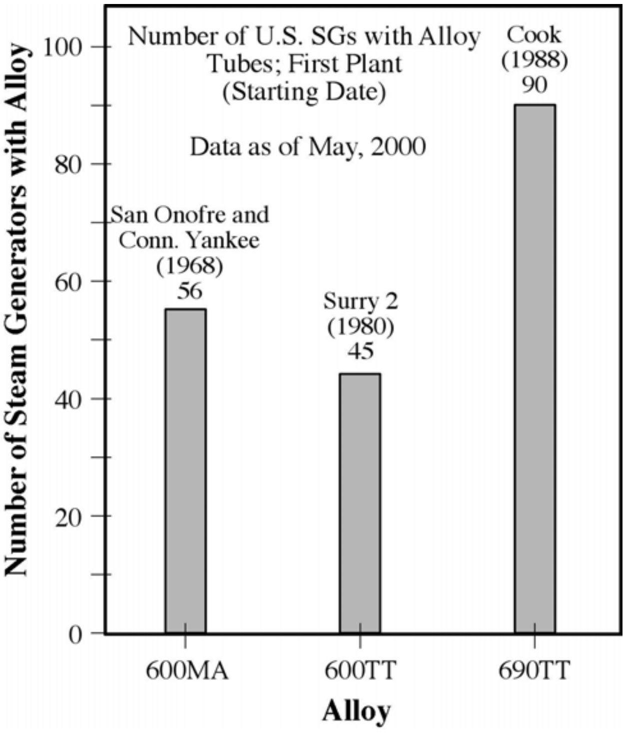

Figure B.7.5 Number of U.S. steam generators with various alloy tubing as of May 2000. First plant to use the alloy and start dates noted. Private communication from P. Scott, Framatome and Al McIlree, EPRI. Note that Alloy 800 continues to exhibit excellent performance in international applications.

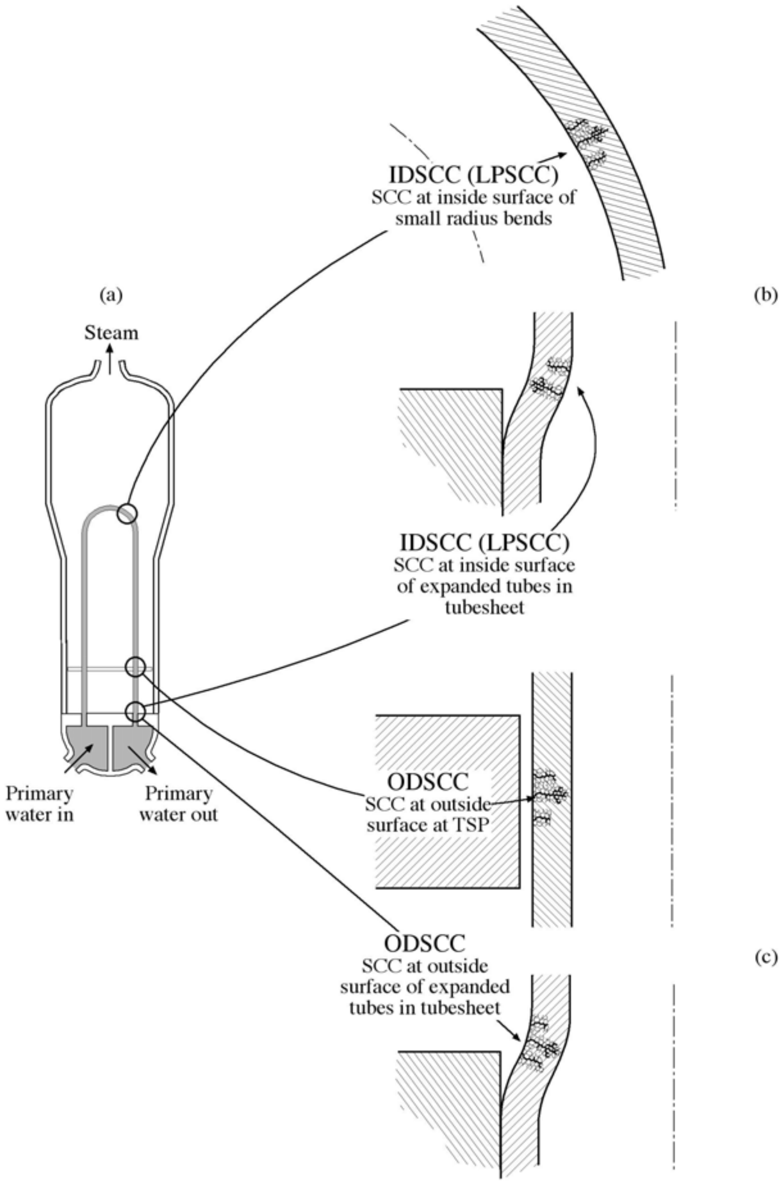

Figure B.7.6 Schematic view of principal location of SCC damage. SCC from the primary side is mostly stress-related and from the secondary side is mostly chemistry related.

Corrosion of Alloy 600 steam generator tubes has occurred both on the inside surface (IDSCC) as well as the outside surface (ODSCC) as shown in Figure B.7.6. On the inside primary surfaces, SCC has occurred mainly at locations of relatively high stresses and high temperatures. These high stresses occur at the tubesheet where the tubes are expanded and at the U-bends, especially the inner U-bends where the radii of curvature are the smallest. SCC on the primary side also occurred during the slow straining associated with "denting." On the outside surfaces, SCC has occurred mainly on surfaces inside heat transfer crevices both at the top of the tubesheet and at tube supports. This corrosion has occurred again mainly at the hottest locations along the tubes; although the stresses at these locations, except at the top of the tubesheet, were nominal being associated with pressure forces and residual stresses due to fabrication of the tubes.

Much of the corrosion that has occurred in the Alloy 600 tubing of SGs has resulted from erroneous assumptions:

- Assumption that Copson and Cheng's data, Figure B.7.3, were correct as were the implications for adequate performance in other environments.
- Assumption that the Coriou et al. data were not applicable and erroneous.
- Assumption that water chemistry that worked in fossil systems would work on the secondary side of PWR SGs.
- Assumption that significant fouling and hence corrosive concentrations would not occur in drilled hole heat transfer crevices.
- Assumption that residual stresses in expanded regions and in straight tubes were not sufficient to produce SCC.

Figure B.7.7 shows the chronology for the replacement of SGs. These replacements resulted from the corrosion failures associated with these erroneous assumptions.

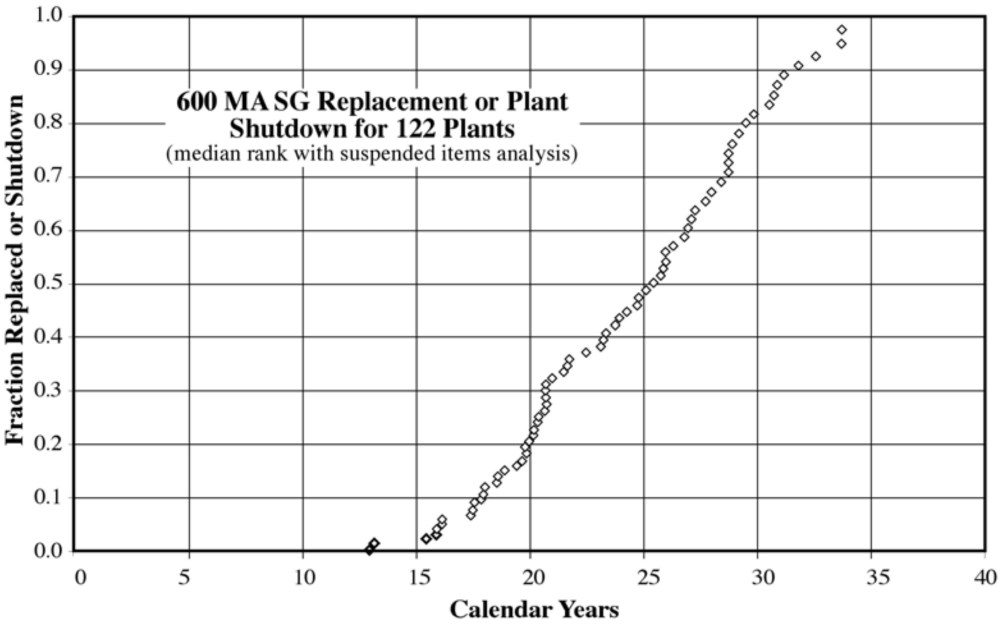

Figure B.7.7 Fraction of replaced or shutdown steam generators vs. calendar years for 600MA plants in the world. Data from Steam Generator Progress Report.[14]

Failures involving multiple modes of corrosion and multiple locations occurred with the combination of Alloy 600MA, as it was exposed on both primary and secondary sides, and with drilled holes on the secondary side. The multiple mode-location cases of failures with Alloy

600MA are summarized in Figure B.7.8.[1] Here, there are 25 mode-location cases of corrosion failures associated with the use of Alloy 600MA.

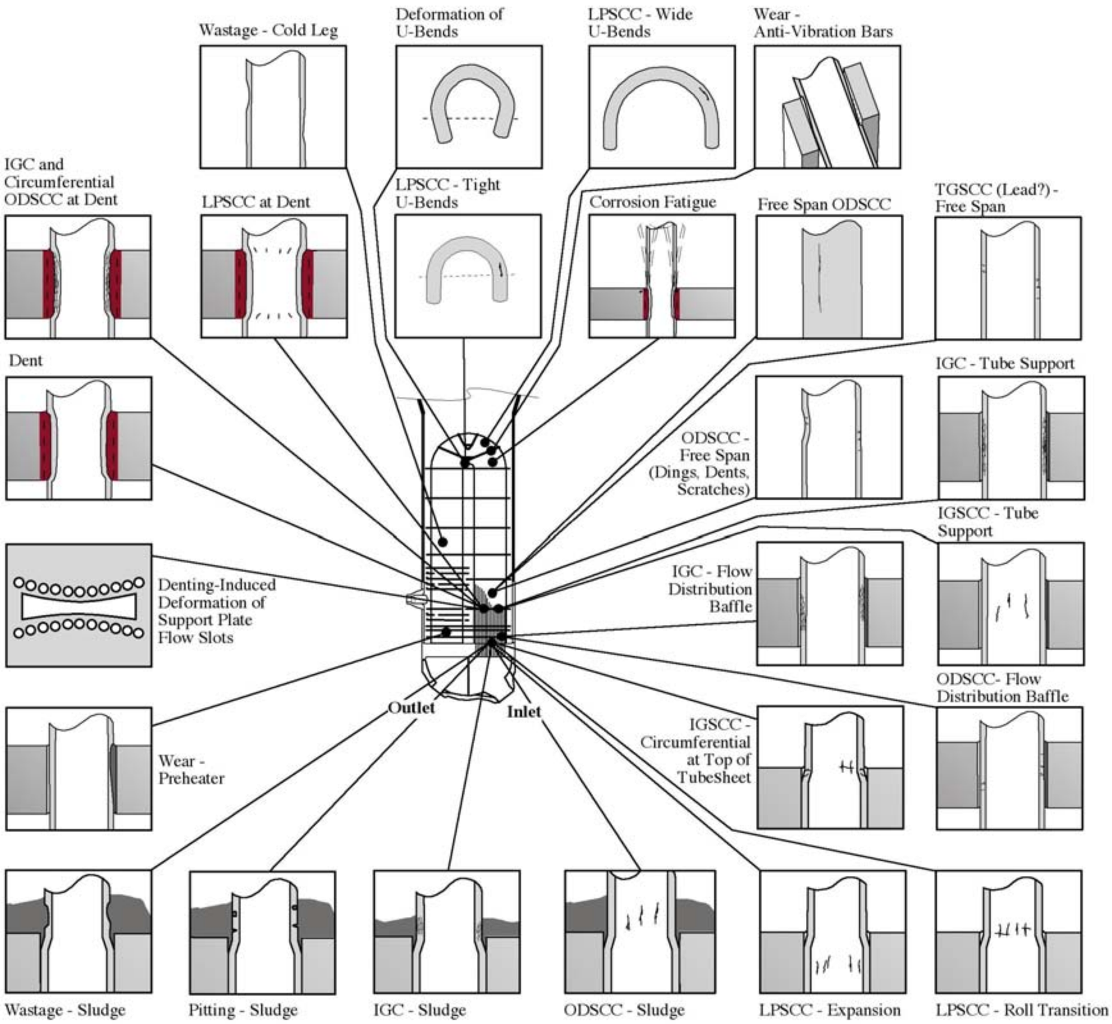

Figure B.7.8 Array of modes of failure at various locations (mode-location cases) that have occurred in recirculating steam generators using Alloy 600MA at drilled hole tube supports. From Staehle and Gorman.[1]

As these failures, which are shown in Figure B.7.8, evolved, extensive corrosion studies were undertaken both in the laboratory and of failed tubes. These experiments included studies of SCC on the primary side, where there were no crevices, and the secondary side, where there were extensive heat transfer crevices. SCC was identified in regions that were not so surprising based on the past history of SCC in steels and stainless steels. Figure B.7.9 shows the locations of the occurrence of SCC in the framework of the electrochemical variables of pH and potential. The occurrence of such SCC in the acidic, alkaline, low potential and high potential regions corresponds generally with regions where protective films are transiently unstable when broken. The bases for the diagram shown in Figure B.7.9a are described by Staehle and Gorman.[1] In addition to the diagram in Figure B.7.9a that shows the "primary" submodes of SCC, Figure B.7.9b shows the general locations of other submodes of SCC. Again, this diagram has been extensively described by Staehle and co-workers. Also, a similar diagram has been published by Combrade et al.[15,16,17] The term, "submode," refers to the corrosion mode of SCC, but differentiates occurrences of unique dependencies on the primary variable of pH, potential, species, alloy composition, alloy structure, temperature, and stress (e.g. each submode consists of a different set of dependencies).

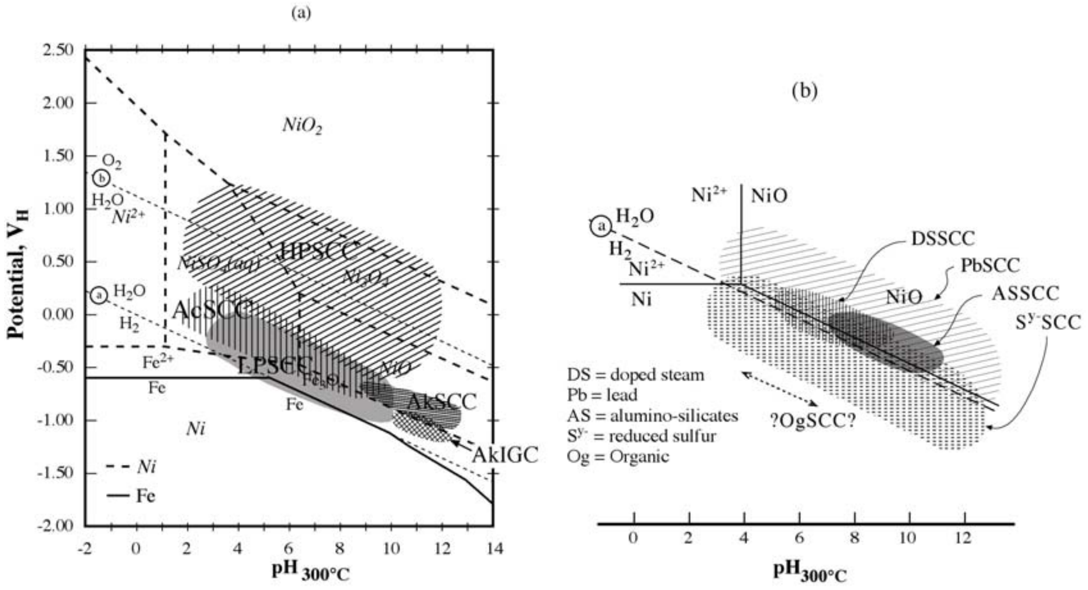

Figure B.7.9 (a) Major submodes of SCC plotted with respect to coordinates of potential and pH for significant SCC occurrences at 300°C. Extent of the submodes based on experience from laboratories and reasonable interpolations and extrapolations. Submodes applicable to Alloy 600MA in the range of 300 to 350°C. (b) Minor submodes of SCC for Alloy 600MA plotted with respect mainly to the NiO/Ni half cell equilibrium at 300°C. From Staehle and Gorman.[1]

The mode diagram of Figure B.7.9 has been verified also by systematic experimental and review work of Ohsaki et al.[18] and by Tsujikawa and Yashima[19] as shown in Figure B.7.10; and they have extended the framework to Alloys 600TT and 690TT. These alloys are discussed in Sections 3.0 and 4.0, respectively. It should be noted that in some cases the regions of SCC in Figure B.7.10 are not complete, as shown by Staehle and Gorman.[1]

This early evolution of SCC associated with Alloy 600 has been eventually mitigated as shown in Figures B.7.11[1] and 12[1] where the various mitigations in alloy, water chemistry, and design are summarized: Alloy 600MA was replaced by Alloys 600TT and 690TT; the water became more pure and certain inimical species, such as copper, were eliminated; the drilled hole tube support was eliminated in favor of the line contacts; and residual fabrication stresses were lowered.

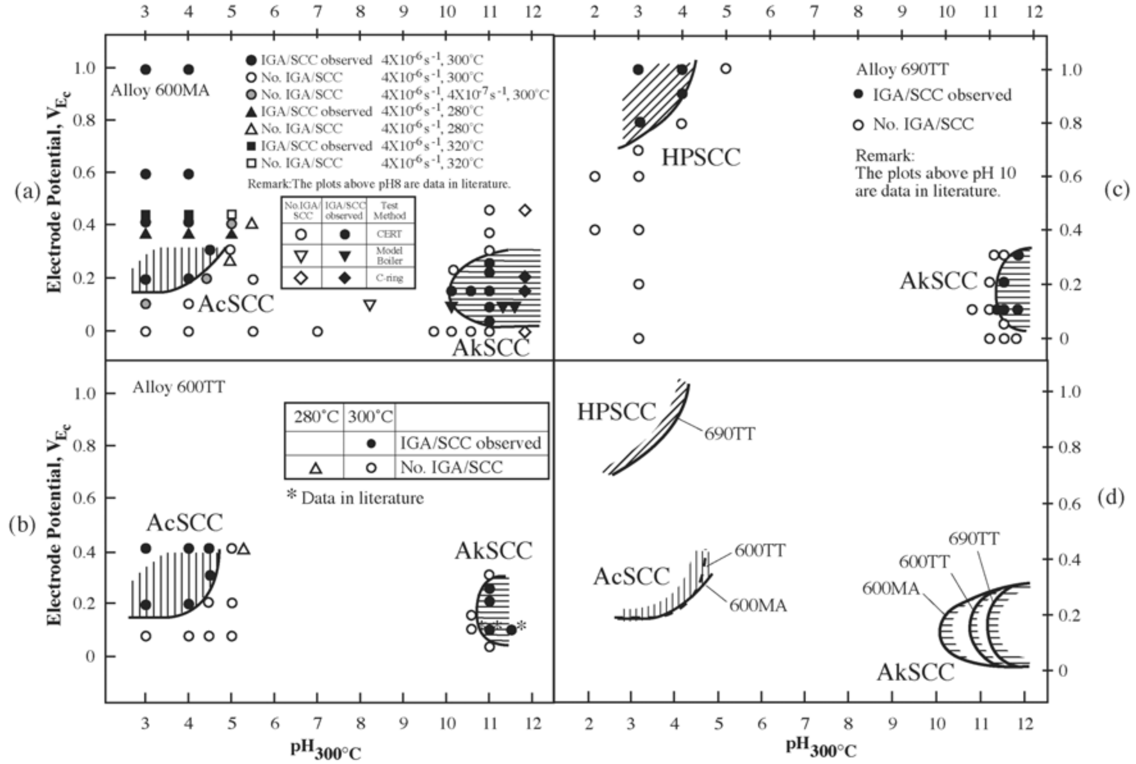

Figure B.7.10 IGA/SCC tests results in the range of 180 to 320°C range as a function of electrode potential and pH taken at 300°C for (a) Alloy 600MA, (b) Alloy 600TT, (c) Alloy 690TT. From Ohsaki et al.[18] (d) Comparison of IGA susceptibility among Alloy 600MA, Alloy 600TT, and Alloy 690TT in the range of 280 to 320°C as a function of electrode potential and pH taken at 300°C. From Tsujikawa and Yashima.[19]

Section 1.0 has provided an overview of corrosion, the alloys, and mitigations. Sections 2.0, 3.0, 4.0, and 5.0 consider some important aspects of the corrosion of the Alloys 600MA, 600TT, 690TT, and 800.

2.0 Alloy 600MA

2.1 Introduction

Alloy 600MA was the alloy used widely for tubing in SGs of PWRs from 1962 through the mid-1980s in France, Japan, Spain, Sweden and the US. The corrosion that occurred with the use of Alloy 600MA required replacement of the steam generators as shown in Figure B.7.7. Replaced SGs have been tubed with Alloys 600TT or 690TT with the latter being preferred as indicated in Figure B.7.5. Also, Alloy 800 as used in some German and Canadian steam generators, has given excellent service as discussed in Section 5.0.

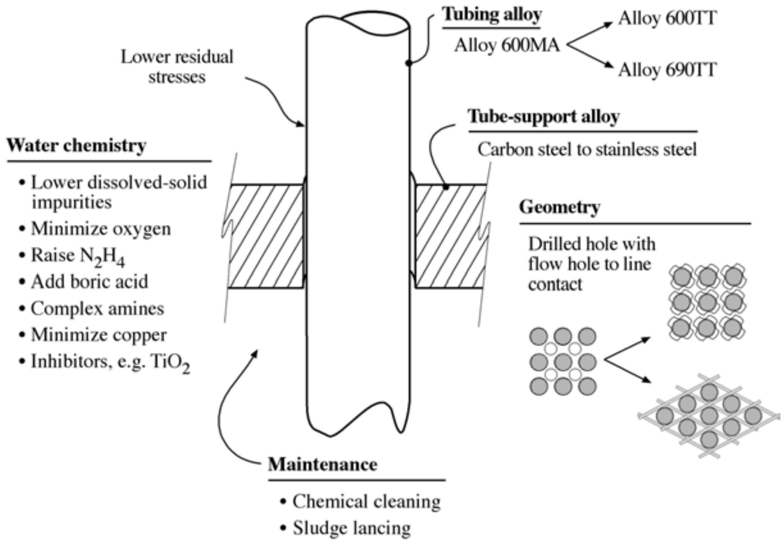

Figure B.7.11 Schematic view of changes in maintenance, materials, designs, and water in order to minimize the corrosion of the tubing. From Staehle and Gorman.[1]

During the Alloy 600MA period, corrosion was dominated by two general patterns, mainly of SCC. One was SCC from the ID of the tubes, which was exposed to high purity primary water containing the standard chemical additions of hydrogen, boric acid and lithium hydroxide. The other was SCC and some corrosion from the OD, which was associated mainly with impurity chemicals that were concentrated in the superheated crevices of tube supports and at the top of tubesheets. Figure B.7.6 shows these essential locations, which are discussed here in Sections 2.2 and 2.3, respectively.

The overall chronology of modes of corrosion of Alloy 600 has been described in two different figures as shown in Figure B.7.13.[20] These figures both show the same trends. An early mode of failure was general corrosion associated with phosphate water chemistry in those plants that adopted this secondary water treatment. Following this, IGSCC occurred, which was mainly due to concentrations of alkaline impurities. Next was denting involving the corrosion products from corroding carbon steel tube supports pressing on the tubes to constrict the diameter. Next was an increase in IGSCC on the primary side followed by more IGSCC on the secondary side. These patterns involve mainly the occurrence of corrosion in Alloy 600MA.

Essentially, the evolution of corrosion concerning Alloy 600MA involved mitigating one mode only to find the intensification of another; such was the sensitivity of this alloy to corrosion in contrast to the prediction of Copson and Cheng as shown in Figure B.7.3.

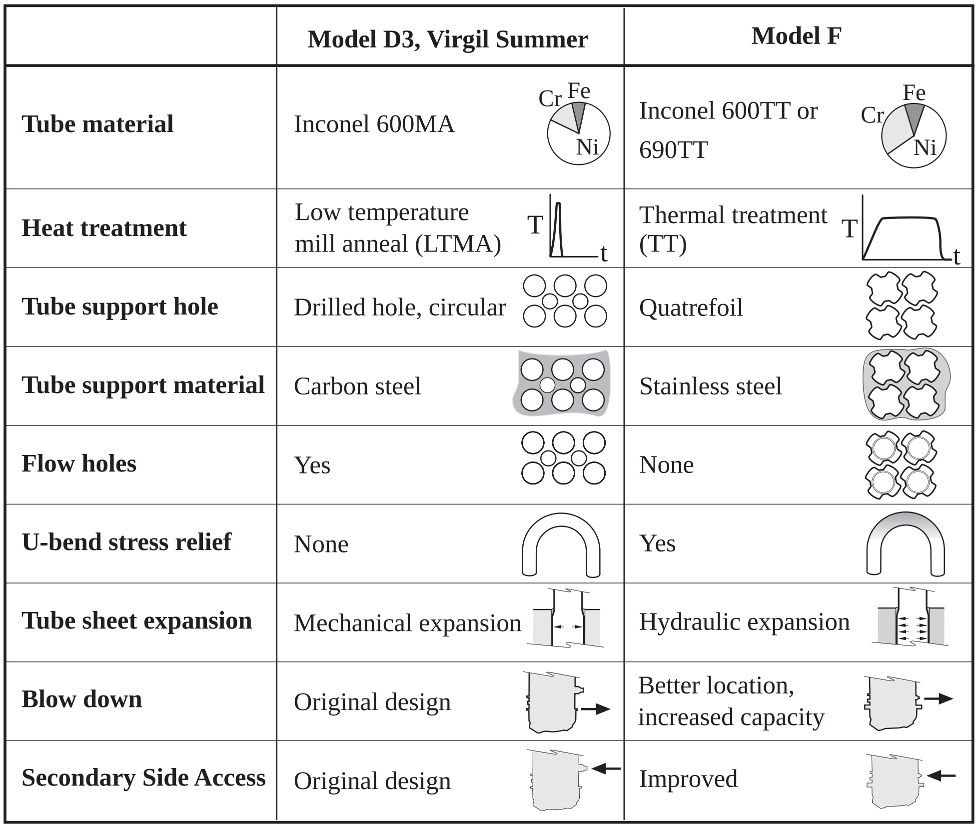

	Model D3, Virgil Summer	Model F
Tube material	Inconel 600MA	Inconel 600TT or 690TT
Heat treatment	Low temperature mill anneal (LTMA)	Thermal treatment (TT)
Tube support hole	Drilled hole, circular	Quatrefoil
Tube support material	Carbon steel	Stainless steel
Flow holes	Yes	None
U-bend stress relief	None	Yes
Tube sheet expansion	Mechanical expansion	Hydraulic expansion
Blow down	Original design	Better location, increased capacity
Secondary Side Access	Original design	Improved

Figure B.7.12 Comparison of Models D3 and F from Westinghouse design plants where changes are intended to minimize corrosion of the tubing. From Staehle and Gorman.[1]

2.2 SCC of Alloy 600MA on the ID

SCC on the ID (primary) surfaces of SG tubes is mainly associated with Alloy 600MA, and such SCC has contributed substantially to the failure and widespread replacement of steam generators shown in Figure B.7.7. This section summarizes the main dependencies of SCC on the ID of Alloy 600MA tubes.

Since the SCC on the inside of Alloy 600MA tubes has been associated with the primary side or inside of the tubes, it was initially called “PWSCC” or “Primary Water SCC.” This is also interpreted by some as “Pure Water SCC.” Both terms however are misleading as they imply that this SCC can occur only on the primary side. A better terminology is “Low Potential SCC (LPSCC),” since this SCC is principally characterized by its occurrence at low electrochemical potentials, as shown in Figure B.7.9, just as some SCC occurs exclusively in the alkaline region and is called AkSCC. Incidentally, as a supporting note here, efforts to reproduce the early work of Coriou failed to identify this SCC, most likely due to the lack of sufficient deaeration of the tests.

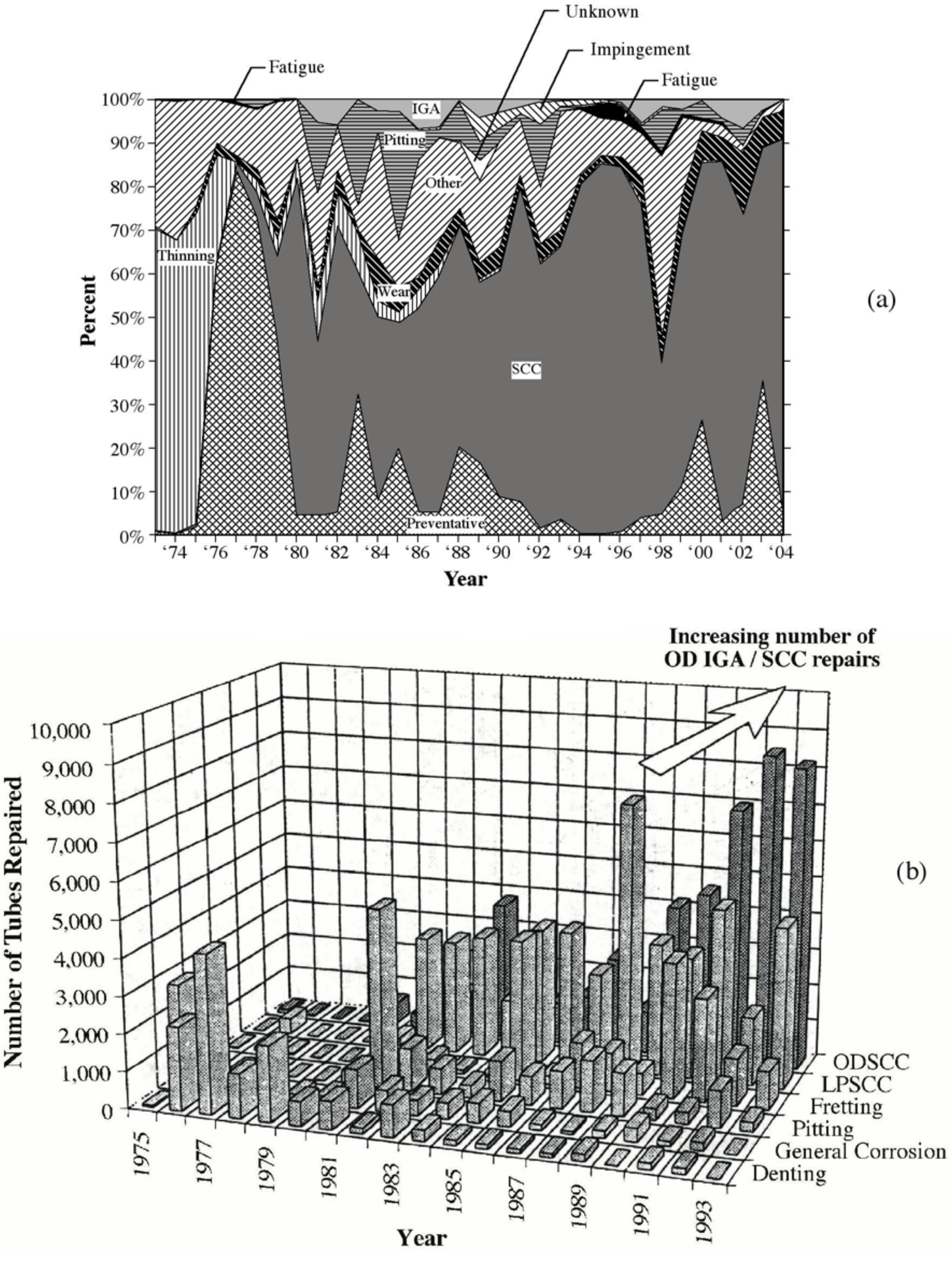

Figure B.7.13 Chronology of modes of corrosion vs. time mainly for Alloy 600 in drilled hole tube supports. (a) Two dimensional. From EPRI. (b) Three dimensional. From Varrin, Jr.[20]

Principal characteristics of LPSCC in Alloy 600MA are the following according to the seven primary variables that affect aqueous corrosion:

1. pH

LPSCC is generally independent of pH over a range from about pH 3 to pH 9 as summarized by Staehle and Gorman.[1]

2. Potential

A central feature of LPSCC has been its confinement to low potentials in the general range of the H_2O/H_2 and NiO/Ni equilibria. There seems to be a tendency for LPSCC to be maximum, both in initiation and propagation, at the NiO/Ni equilibrium, as shown in Figure B.7.14.[15,21,22] In each figure the location of the NiO/Ni equilibrium potential is noted; this is an invariant and thermodynamically defined line, not depending on concentration of species in solution. Figure 14a is based on testing of initially smooth specimens; and Figure 14b is based on initially precracked specimens. Thus, the former relates to conditions of initiation and the latter relates to propagation.

3. Species

LPSCC has been investigated with respect to concentrations of boric acid and lithium hydroxide as summarized by Staehle and Gorman.[1] Effects of these species are not significant. However, there has been little investigation of effects of chloride, sulfate, or other species over significant ranges of concentration; this lack of breadth impedes connecting LPSCC to domains of chemistry that might be important to the secondary side.

4. Alloy composition

Another defining characteristic of LPSCC is its dependence upon alloy composition. With respect to the concentration of chromium, the data from two different investigations in Figure B.7.15[23,24] show that increasing chromium decreases sensitivity to LPSCC. It is noteworthy that Fe-Ni alloys sustain rapid LPSCC and that LPSCC is negligible above 20% Cr, which is relevant to the compositions of Alloy 690 with a Cr content around 30% and Alloy 800.

5. Alloy structure

LPSCC is generally influenced by the distribution of carbides. As carbides accumulate at grain boundaries, LPSCC is minimized. Figure B.7.16 shows this effect from work by Norring et al.[25] and Cattant et al.[26] A further important result was published by Blanchet et al.[32] where they showed that sensitization greatly reduced the sensitivity to LPSCC as shown in Table B.7.2.

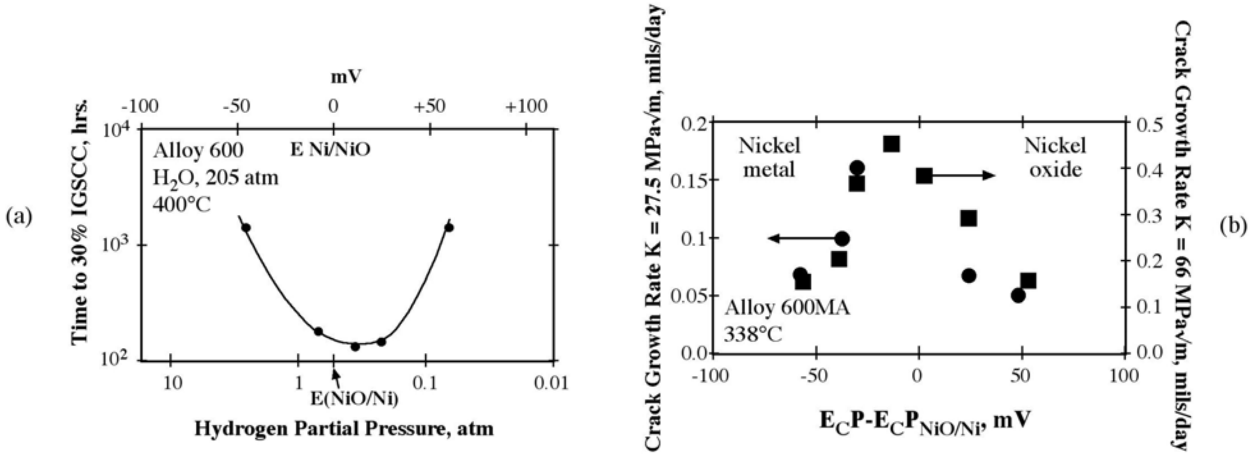

Figure B.7.14 (a) Time to 30% IGSCC vs. hydrogen pressure and potential reference to NiO/Ni equilibrium. Experiments at 400°C and 205 atm pressure of steam. Original data from Economy et al.[21] Dependencies recalculated by Scott and Combrade.[15] (b) Crack growth rate at two stress intensities vs. potential (E_CP=electrochemical potential) relative to the NiO/Ni equilibrium potential for Alloy 600MA at 338°C. From Morton et al.[22]

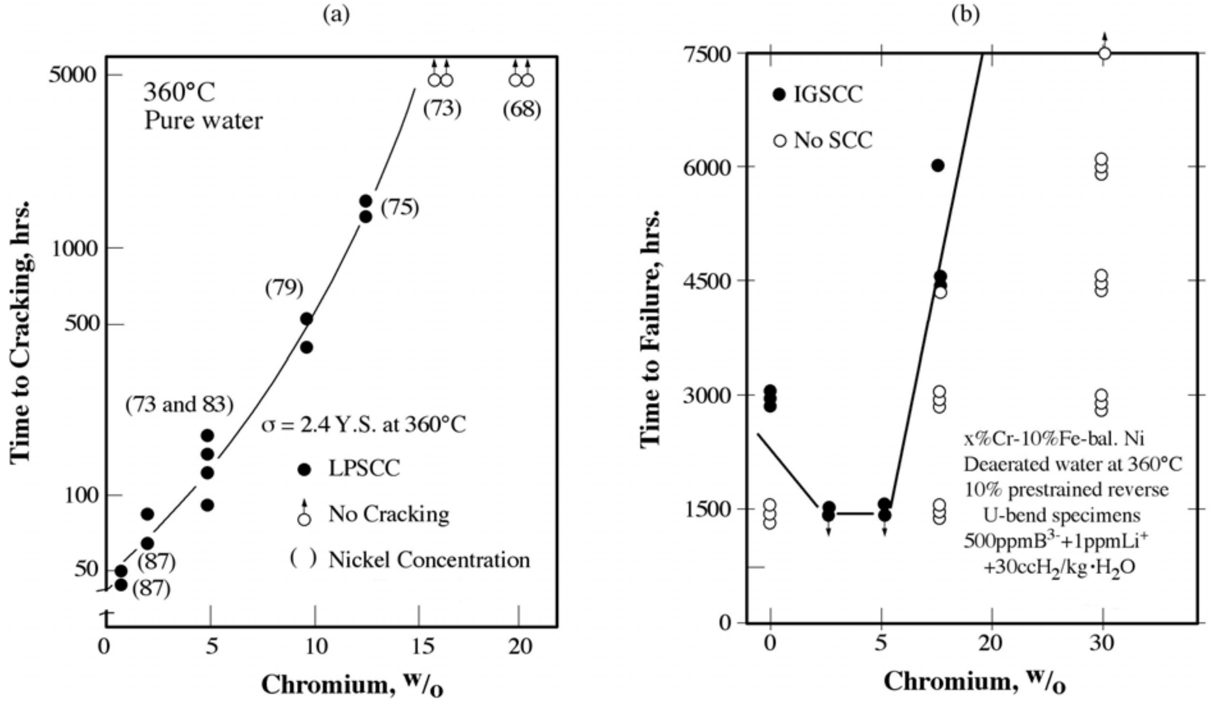

Figure B.7.15 (a) Time-to-cracking vs. concentration of Cr for Ni-Cr-Fe alloys exposed in pure water at 2.4 Y.S. at 360°C. From Yonezawa and Onimura.[23] and (b) Time-to-failure as concentration of Cr for Fe-Cr-Ni alloys with 10w/o Fe. From Nagano and Kajimura.[24]

6. Temperature

The temperature dependence of LPSCC has been extensively studied, and this work is reviewed by Staehle and Gorman.[1] The most reliable values of the activation energy for initiation seems to be about 40-55 Kcal/mol and for propagation about 30-35 Kcal/mol.

Figure B.7.17 shows some typical data for initiation and propagation from the work of Webb[27] (Figure B.7.17a) and the review by Cassagne et al.[28] (Figure B.7.17b).

7. Stress

The dependence of LPSCC on stress for Alloy 600MA has also been extensively investigated. Figure B.7.18 shows results from studies of the effects of stress on initiation and propagation, respectively, from Bandy and van Rooyen[33] and Scott.[34] In general, for initiation from smooth specimens the stress required is in the range of the annealed yield stress, with a stress exponent of about 4 as shown in Figure B.7.18a. For propagation, the correlation by Scott has been the most widely used and is shown in Figure B.7.18b.

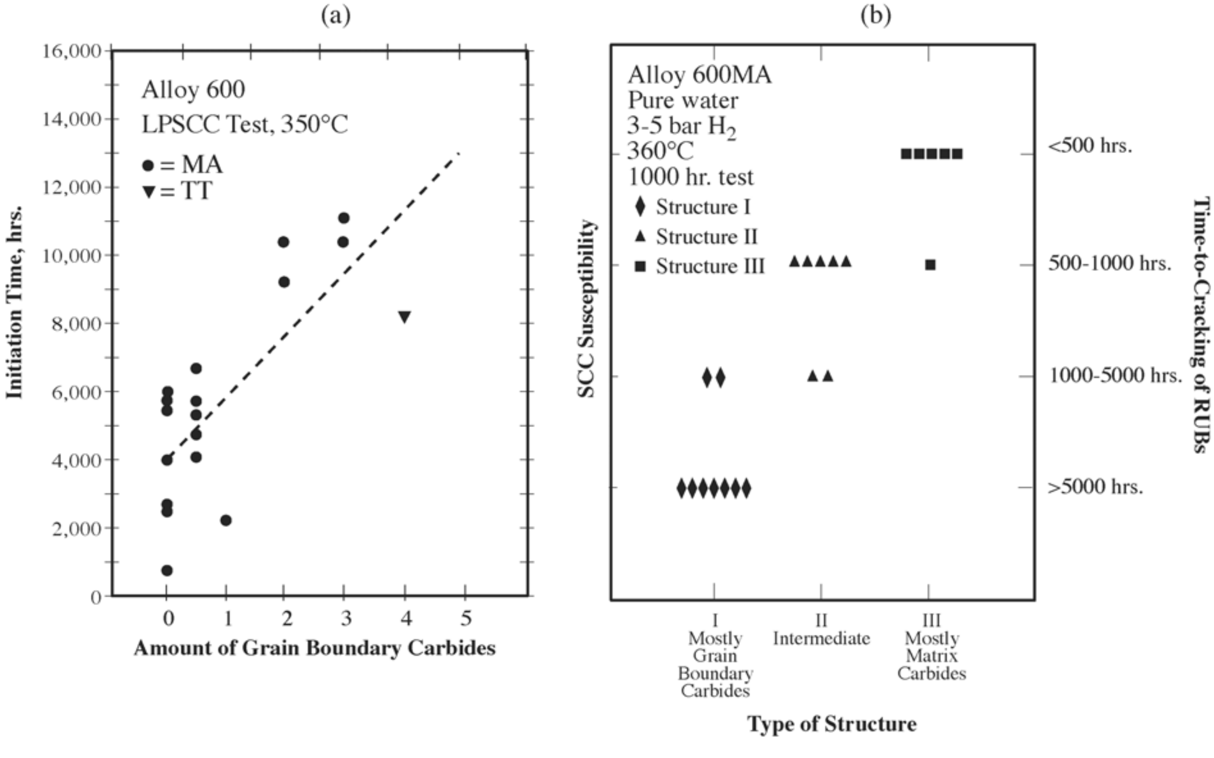

Figure B.7.16 (a) Time-for-initiation vs. extent of grain boundary carbides. From Norring et al.[25] (b) Relationship between structure and SCC susceptibility. From Gras[29]; Cattant et al.[26]; Saint-Paul et al.[30]; and Garriga Majo et al.[31]

Table B.7.2[32]

Effect of Heat Treatment and Fabrication on Failure at 350°C in Demineralized and Deoxygenated Water. From Blanchet et al.

Metallurgical Condition	Alloy A Alloy 600, C = 0.063 $^{w}/_{o}$			Alloy B Alloy 600, C = 0.040 $^{w}/_{o}$			Alloy C Cr 17%, Ni 77%, C = 0.002 $^{w}/_{o}$	
	As-Received	As-Quenched	Sensitized	As-Received	As-Quenched	Sensitized	As-Received	Sensitized
Determination σ_{max} at the outer fiber at 20°C (kg/mm^2) (± 15%)	72	36	72	43	29	43	41	41
Samples cracked after:								
750 hours	0/6	0/3	0/3	0/3	0/2	0/2	6/7	0/5
1500 hours	6/6	0/3	0/3	0/3	0/2	0/2	7/7	3/5
2250 hours	-	0/3	0/3	1/3	0/2	0/2	-	5/5
3000 hours	-	0/3	0/3	2/3	0/2	0/2	-	-
4500 hours	-	1/3	0/3	2/3	0/2	0/2	-	-
8250 hours	-	1/3	0/3	3/3	0/2	0/2	-	-
10000 hours	-	2/3	0/3	-	1/2	0/2	-	-

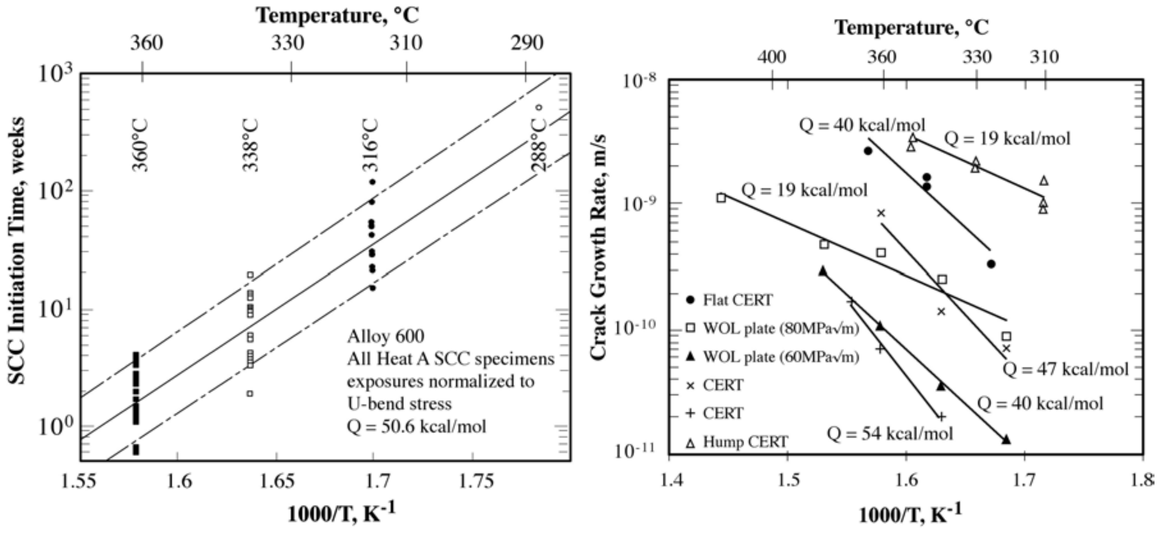

(a)

(b)

Figure B.7.17 (a) SCC initiation time vs. 1000/T for Alloy 600 using U-bend specimens in pure water. From Webb.[27] (b) Crack growth rate vs. 1000/T for Alloy 600MA from six authors using CERT and WOL type specimens. From Cassagne et al.[28]

2.3 SCC of Alloy 600MA on the OD

1. Geometry, phases, and chemistry

SCC on the OD of SG tubes occurs mainly at locations where impurity chemicals can concentrate due to the local superheat, mainly at tube supports and at the configurational and sludge crevices at the top of tubesheets, as shown in Figure B.7.19.[1] Figure B.7.20[35] shows a schematic view of the complexity and chemistry of these regions of concentration as well the chemicals that typically concentrate and lead to SCC. With time, chemicals accumulate in the heat transfer crevices to produce solids and saturated solutions owing to the superheat. Further, as local transport is stifled by the formation of solids, a steam phase develops. The main intimation here is the complexity of chemical, electrochemical, and physical conditions. Such an array provides many different conditions that can produce corrosion and stress corrosion cracking.

SCC on the OD occurs where the superheat is the greatest, and this is mainly on the inlet or hot leg side with the variation of intensity shown in Figure B.7.21a[36] according to distance from the inlet of the hot side. An indication of the magnitude of concentrations of chemicals in these crevices is given in Figure B.7.21b.[37]

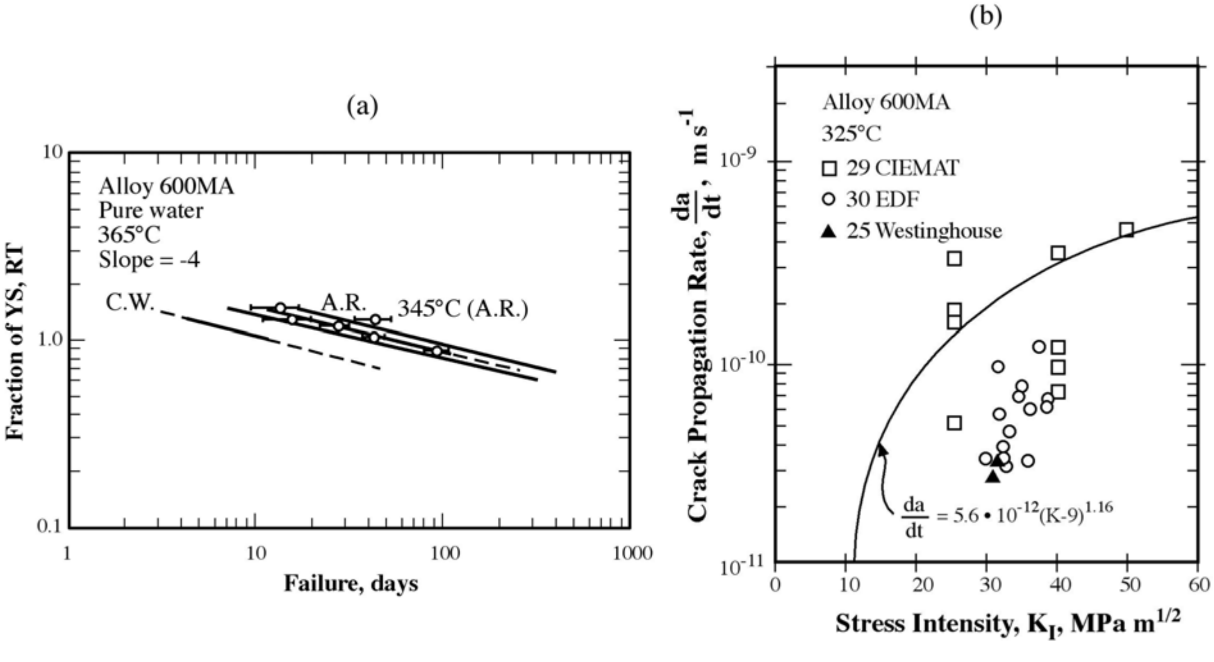

Figure B.7.18 (a) Fraction of RT yield stress vs. time-to-failure for Alloy 600MA at 365°C in pure water. Stress exponent about -4. Yield point stresses in the range of 323 to 386 MPa. From Bandy and van Rooyen.[33] (b) Crack propagation rate vs. stress intensity for Alloy 600MA at 325°C. From Scott.[34]

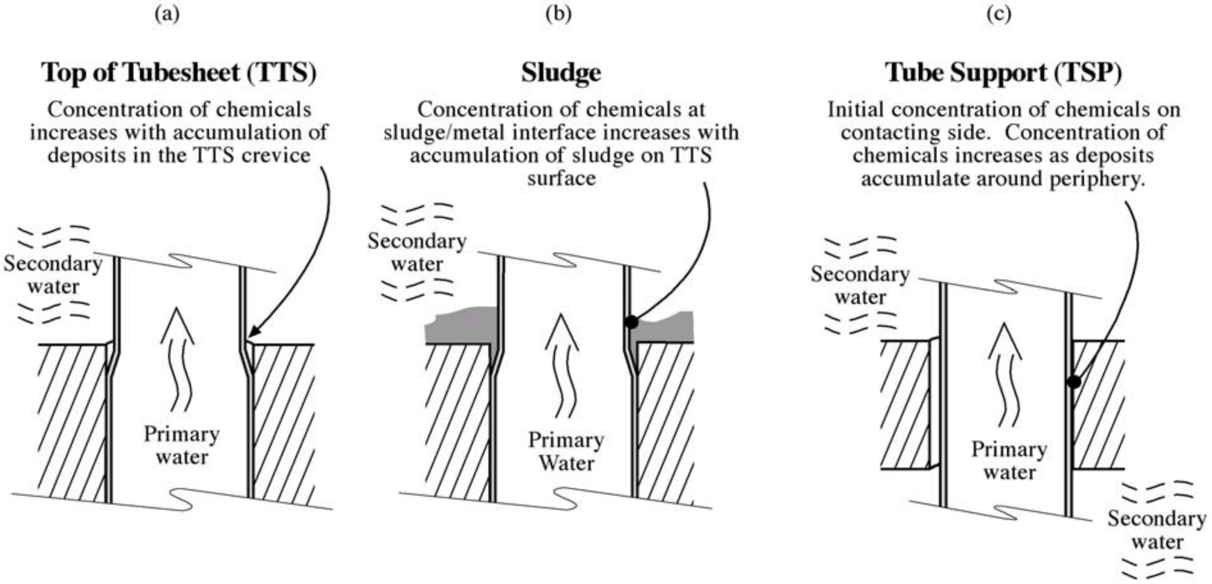

Figure B.7.19 Geometries that produce heat transfer crevices involving tubing in steam generators: (a) top of the tubesheet crevice; (b) sludge at the top of the tubesheet; (c) tube support. From Staehle and Gorman.[1]

2. Surface chemistry--ODSCC is chemistry driven

Some indication of the complexity of the chemistries on the surfaces of tubes is shown in Figure B.7.22, taken from the work of Cattant et al.,[38] where the residual chemistry on the surface of a tube at a tube support region has been analyzed both inside the crevice and outside on the freespan adjacent to the crevice. Figure B.7.23[38] shows the ratio of species inside the crevice to outside on the freespan, indicating that the concentrations, species, and enrichments vary.

3. The bulk chemistry

While the chemistries inside the heat transfer crevices provide a variety of possibly corrosive environments, the bulk environment provides important bounding chemistries affecting corrosion:

a. Low hydrogen--The hydrogen concentration on the secondary side is in the range of 1 ppb due to the boiling action removing gases. This low concentration of hydrogen, following the Nernst equation, leads to raising the open circuit potential on the order of 200-250 mV above that on the primary side where there is not boiling and hydrogen is deliberately added at about 3 ppm. A 200-250 mV increase could be sufficient to take the secondary side out of the range of LPSCC.

b. Hydrazine (affects potential)--N_2H_4 is added to the secondary side in concentrations of about 5-100 ppb in order to reduce the oxygen concentration in the recirculating water to <5 ppb. It is also believed by some that additions of N_2H_4 lower the tendency for corrosion to occur in heat transfer crevices. It may also lower the corrosion potential due to the relatively low equilibrium potential for the N_2/N_2H_4 equilibrium. The overall combined effect of low hydrogen and the N_2H_4 on potential is not clear.

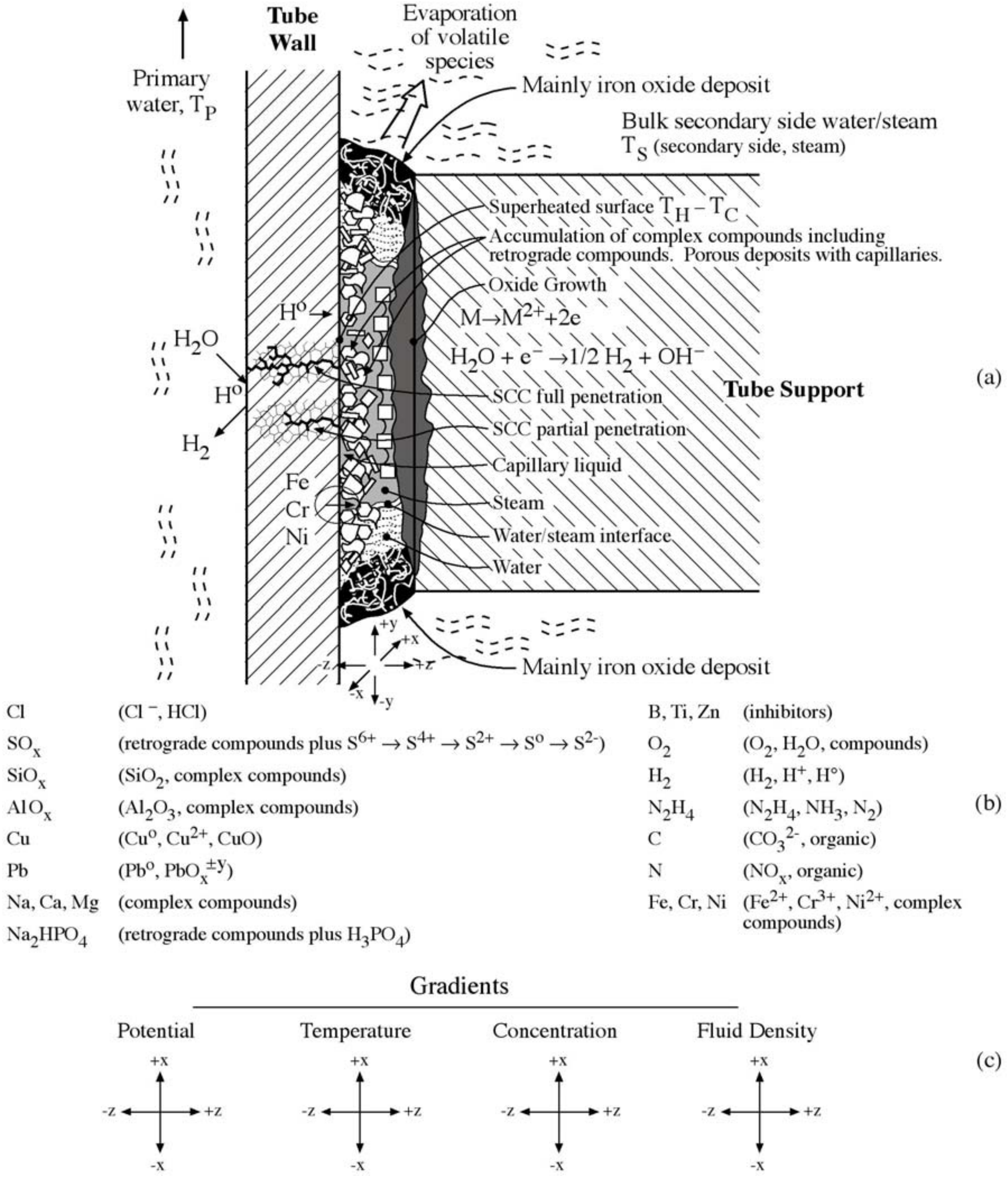

Cl	(Cl^-, HCl)	B, Ti, Zn	(inhibitors)
SO_x	(retrograde compounds plus $S^{6+} \rightarrow S^{4+} \rightarrow S^{2+} \rightarrow S^o \rightarrow S^{2-}$)	O_2	(O_2, H_2O, compounds)
SiO_x	(SiO_2, complex compounds)	H_2	(H_2, H^+, H^o)
AlO_x	(Al_2O_3, complex compounds)	N_2H_4	(N_2H_4, NH_3, N_2)
Cu	(Cu^o, Cu^{2+}, CuO)	C	(CO_3^{2-}, organic)
Pb	(Pb^o, $PbO_x^{\pm y}$)	N	(NO_x, organic)
Na, Ca, Mg	(complex compounds)	Fe, Cr, Ni	(Fe^{2+}, Cr^{3+}, Ni^{2+}, complex compounds)
Na_2HPO_4	(retrograde compounds plus H_3PO_4)		

Figure B.7.20 Schematic view of heat transfer crevice at a tube support. (a) Geometry. (b) Chemicals that accumulate and transform. (c) Types of gradients inside the heat transfer crevice. From Staehle.[35]

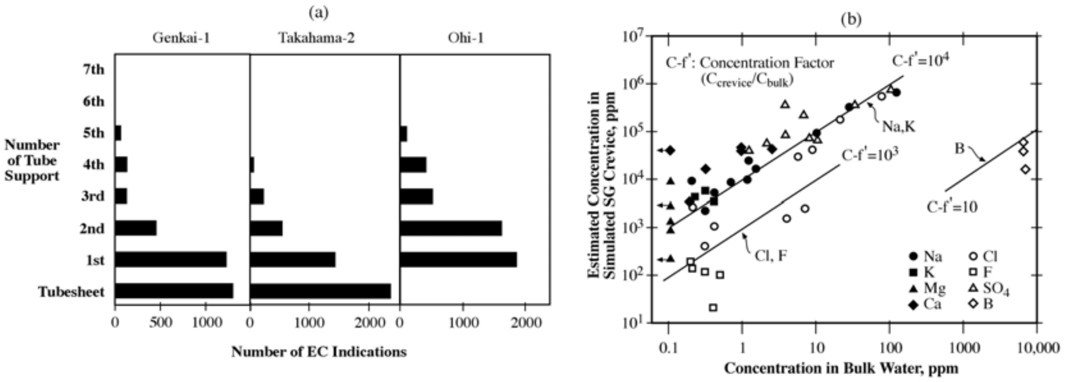

Figure B.7.21 (a) Number of indications at successive tube support locations for three plants using Alloy 600MA after about 12 to 15 years service. From Takamatsu et al.[36] (b) Estimated concentration of species in a simulated SG crevice vs. concentration in the bulk water. Various concentration factors shown. From Takamatsu et al.[37]

c. Hydrazine (a reductant)-- N_2H_4 produces a second effect as it combines with sulfate impurities reducing them to lower valence and ultimately to sulfides. Sulfides are well known to accelerate the entry of hydrogen and to reduce passivity.[39,40,41]

Thus, there are two important environmental influences that affect the occurrence of corrosion on the secondary side. One is the concentration of chemistry inside heat transfer crevices and the other involves the combined effects of low hydrogen and high hydrazine as they interact with the bulk and the crevice chemicals.

4. Steam phase

Figure B.7.20 suggests that, in addition to the complexity of chemistry, there is also a steam phase in heat transfer crevices. Such local steam conditions and the associated two phase interface have been shown to accelerate SCC in Alloy 600 as reviewed by Staehle and Gorman.[1]

5. Acidic and alkaline chemistries

Aside from the LPSCC on the primary side as discussed in Section 2.2 and the possibility of its occurring on the secondary side, both acidic and alkaline environments have been investigated as being possibly related to the SCC that has occurred in the secondary side. The overall view of AcSCC and AkSCC for Alloy 600MA is shown in Figure B.7.9a as well as in Figure B.7.10a.

Figures B.7.24a[42] and 24b[43] show the effect of electrochemical potential on SCC in alkaline environments specifically for Alloys 600MA, 600TT and 690TT. Here, it is clear that the three alloys sustain AkSCC in the same range of potential with Alloys 600TT and 690TT being more resistant. Staehle and Gorman[1] discuss AkSCC and its dependencies extensively.

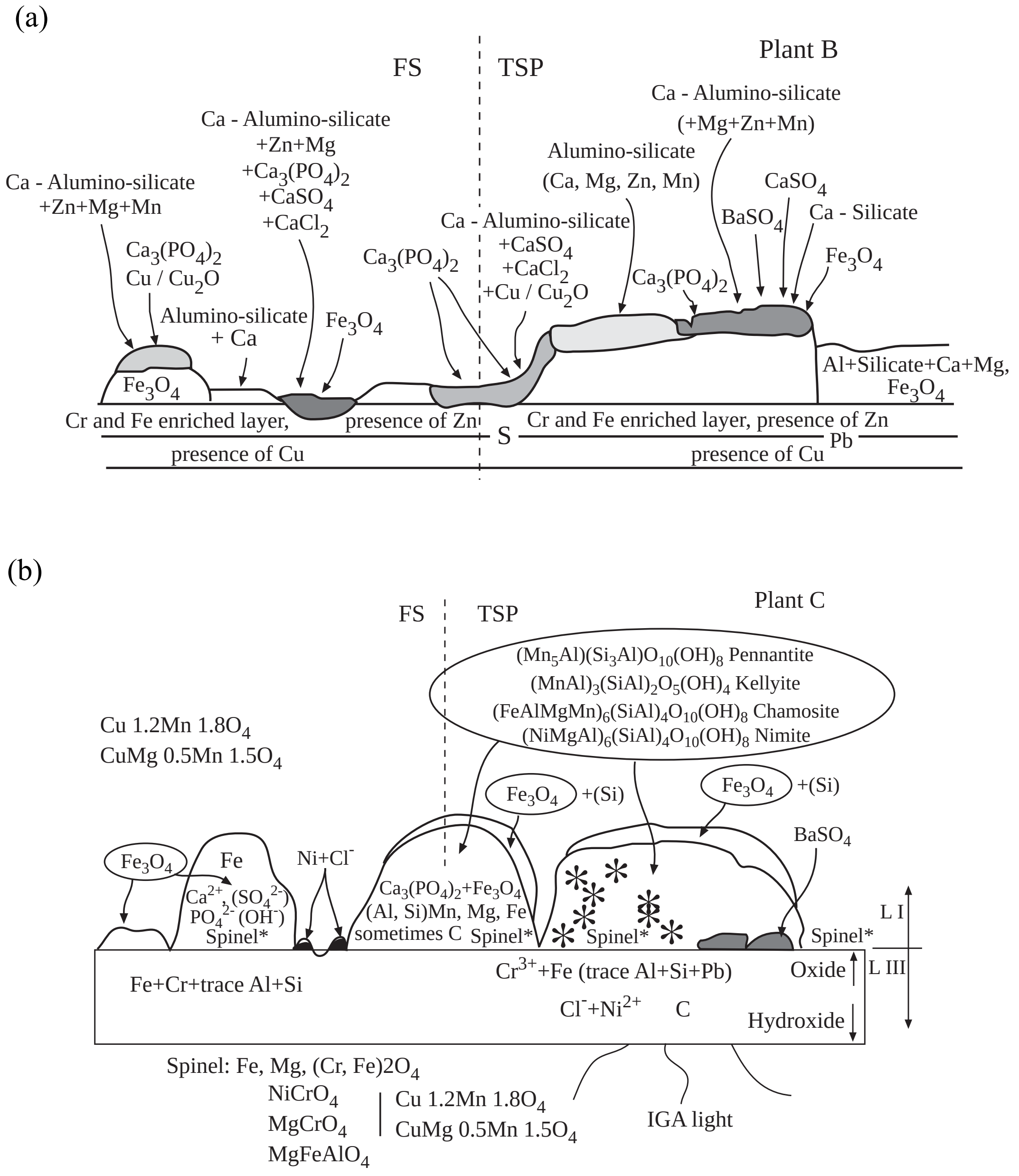

Figure B.7.22 (a) Schematic view of OD tubesheet from a TSP showing adjacent regions from inside the TSP and outside on the free surface. The condenser was brass and the water chemistry was morpholine AVT. (b) Schematic view of OD tube surface from TSP 2 showing adjacent regions inside the TSP and outside on the free surface. The condenser was titanium and the water conditioning was NH_3 AVT. The tube was examined after 79,900 hours. From Cattant et al.[38]

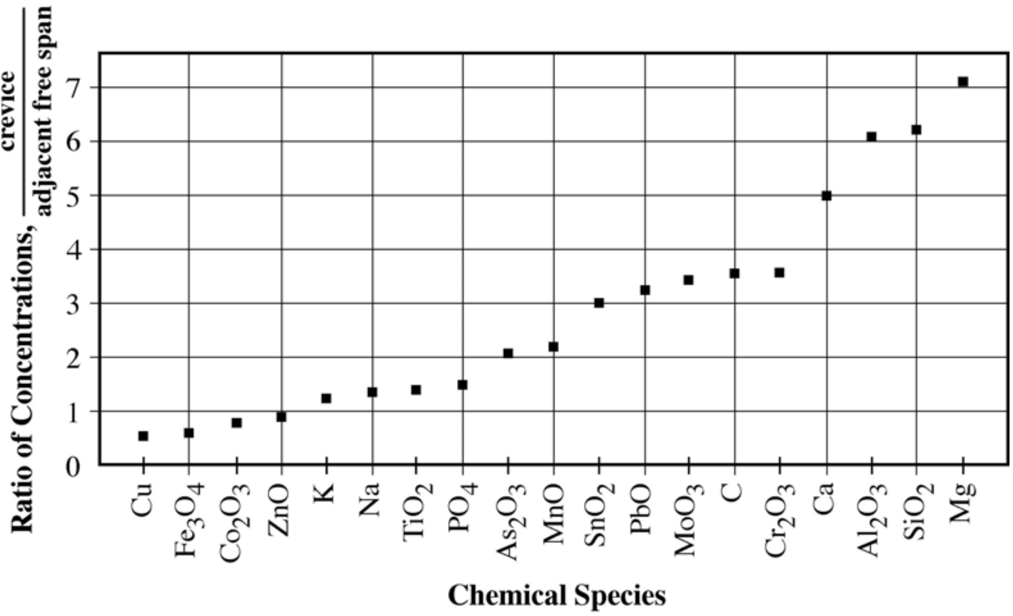

Figure B.7.23 Ratio of concentrations of elemental species in deposits from occluded heat transfer crevices vs. those from adjacent free-span surfaces. Species given in ascending order of ratio. Data from 340 pulled tubes. From Cattant et al.[38]

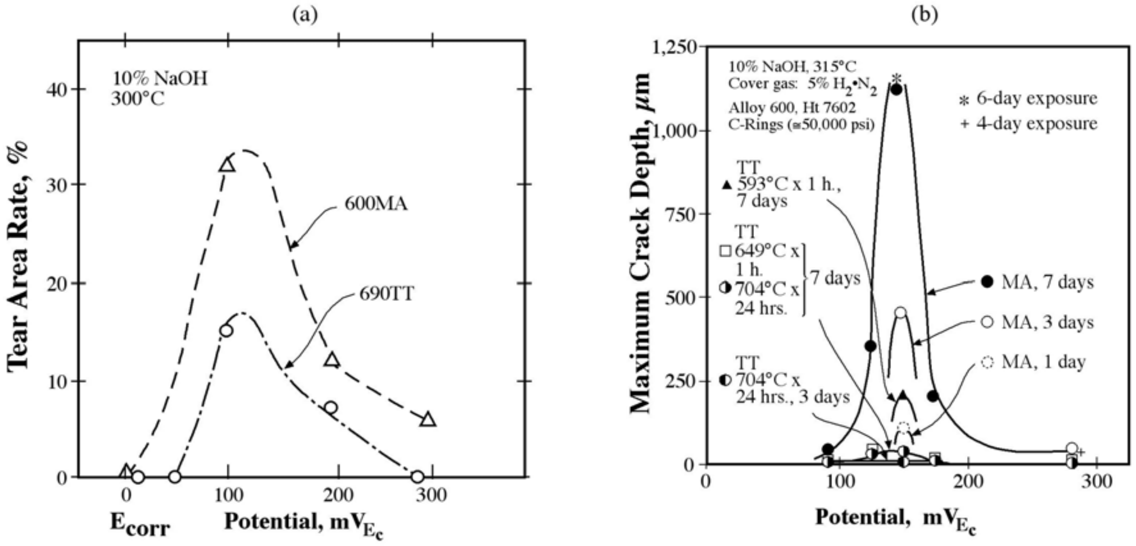

Figure B.7.24 Dependence of AkSCC on applied potential above the deaerated open circuit potential. (a) Tear area rate (%) for Alloy 600MA and Alloy 690TT at 300ºC as a function of potential in a 10% NaOH solution. From Suzuki.[42] (b) Maximum crack depth vs. potential for Alloy 600 exposed in 10% NaOH at 315°C for mill-annealed and various thermal treatments. From Pessall.[43]

Figures B.7.25 and 26 provide insights into AcSCC for Alloys 600MA, 600TT and 690TT and conform also to the patterns noted in Figures B.7.9 and 10. Figure B.7.25[44] shows that the intensity of AcSCC, when exposed to sulfate anions, decreases with increasing pH, and as expected, continues into the slightly alkaline region for both Alloys 600MA and 600TT.

Figure B.7.26[49] shows the effect of potential on the AcSCC of Alloys 600MA and 690TT also exposed to sulfate anions. Here, the potentials are achieved by adding cupric oxide and by changing the hydrogen concentration. Note in Figure B.7.26c, simply adding copper does not produce significant SCC relative to the CuO. This Figure shows that Alloy 690TT sustains AcSCC but not at normal open circuit potentials; whereas, Alloy 600MA sustains AcSCC regardless of the potentials, although there is an acceleration at pH 4+ at higher potentials.

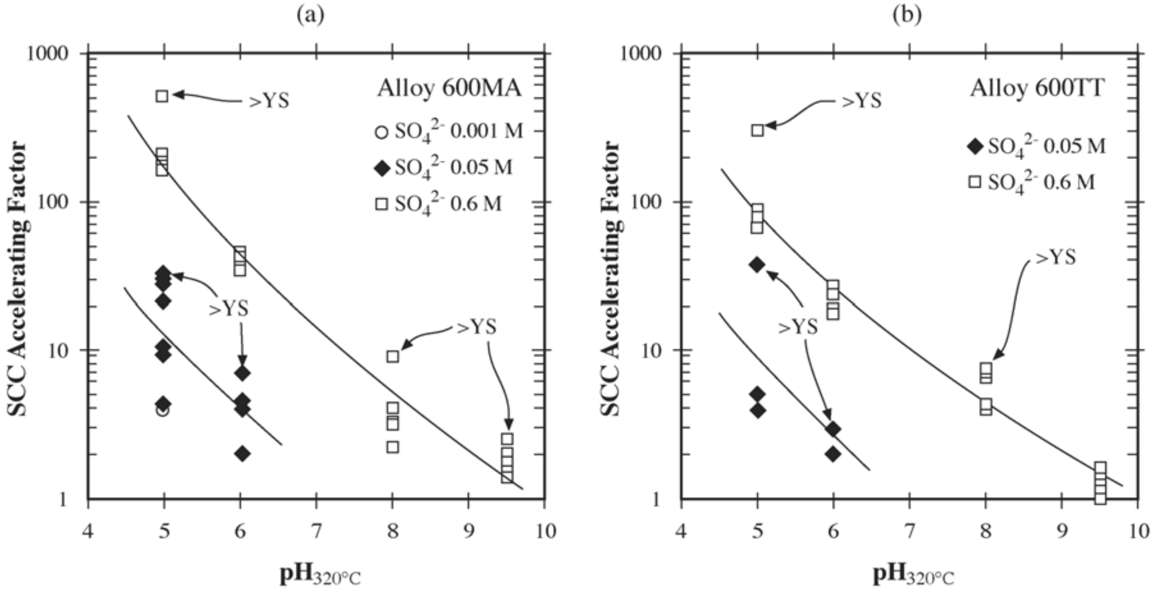

Figure B.7.25 SCC accelerating factor vs. pH with different concentrations of SO_4^{2-} and with different stresses for (a) Alloy 600MA and (b) Alloy 600TT. Accelerating factor taken from rate of crack initiation at 0.001M ($pH_{320°C}$ = 5) being the reference. >YS refers to "two legs touching" condition of the branches of the C-ring; below this stress, specimens were stressed at 0.8 YS and 1.0 YS. From deBouvier et al.[44]

6. Lead chemistries, PbSCC

PbSCC has had varying importance over time. It was first identified as important in the 1965 paper of Copson and Dean[45] and was suggested then as the reason for the SCC observed by Coriou. In this first paper, SCC due to Pb was said to be characteristically TGSCC; since most of the subsequent field observations of SCC exhibited IGSCC, Pb was not considered important, and ODSCC was mainly attributed to AkSCC and to AcSCC.

However, due to the review of Sarver[46] of old work of Copson, it became clear that PbSCC of Alloy 600MA was predominantly IGSCC; whereas, PbSCC of Alloy 600TT, SR, and SS was predominantly TGSCC. This evolution is described by Staehle.[47] Also important are the results from Bruemmer and Thomas,[48] who have shown that as much as 7w/o of Pb occurs in the tips of some SCC taken from SGs. Further, Pb has been observed to concentrate on heat transfer surfaces in many examinations of pulled tubes even where no accidental intrusions of Pb have occurred.

While the proof is not substantial, it is a reasonable speculation that much of the IGSCC on the secondary side, especially after the early concerns about AkSCC and AkIGC, could have been due to Pb.

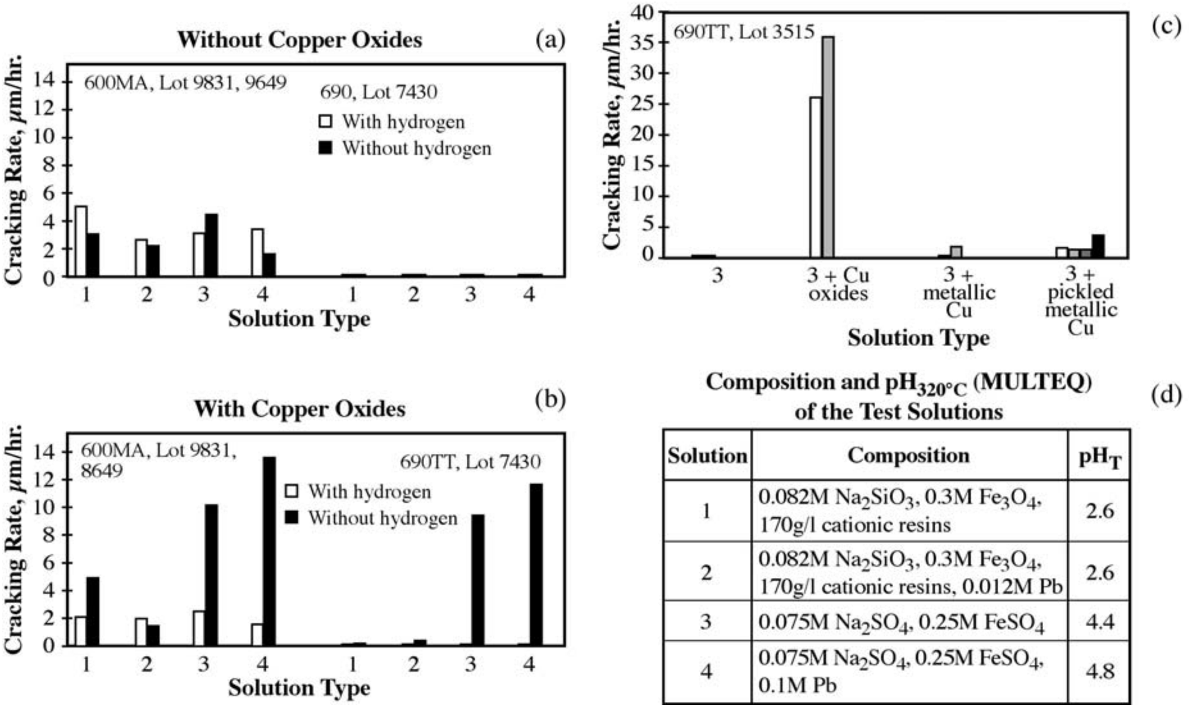

Composition and $pH_{320°C}$ (MULTEQ) of the Test Solutions

Solution	Composition	pH_T
1	0.082M Na_2SiO_3, 0.3M Fe_3O_4, 170g/l cationic resins	2.6
2	0.082M Na_2SiO_3, 0.3M Fe_3O_4, 170g/l cationic resins, 0.012M Pb	2.6
3	0.075M Na_2SO_4, 0.25M $FeSO_4$	4.4
4	0.075M Na_2SO_4, 0.25M $FeSO_4$, 0.1M Pb	4.8

Figure B.7.26 (a) Cracking rates for Alloys 600MA and 690TT in acidic solutions without copper oxides with and without 5% H_2 added to argon cover gas in capsules at 320°C. (b) Cracking rates for Alloys 600MA and 690TT in acidic solutions with copper oxides with and without 5% H_2 added to argon cover gas in capsules at 320°C. (c) Cracking rates obtained for Alloy 690TT with solution #3 at 320°C. (d) Compositions of environments. From Pierson and Laire.[49]

The occurrences of PbSCC over the range of pH are shown in Figures B.7.27, 28, and 29. Figure 27[51,52] shows the four alloys in an alkaline solution with and without the presence of Pb. The Pb substantially accelerates SCC especially for Alloys 800 and 690TT. At lower pH, which is characteristic of AVT environments, Wright and Mirzai[50] have summarized the results from various authors as a function of Pb concentration as shown in Figure B.7.28. SCC occurs in Alloy 600MA as a function of Pb readily at 1 ppm. However, PbSCC does not seem to occur in Alloy 690TT in this AVT environment. At lower pH in chloride, PbSCC occurs in both Alloys 600MA and 690TT; however, the rate of SCC in Alloy 690TT is lower. At this lower pH of 4.5 and at 300 ppm Pb, as $PbCl_2$, the Alloy 690 also sustains SCC and corrodes generally.

7. Low valence sulfur chemistries

Low valences of sulfur-containing anions are important because they can greatly accelerate SCC at least in the limited work performed to date in alkaline solutions and because these ions can be produced by the reduction of sulfate ions with hydrazine. Further, from studies at lower temperatures, the lower valence sulfur ions greatly accelerate general corrosion. In particular, the low valence sulfur species accelerate the AkSCC of Alloy 690.

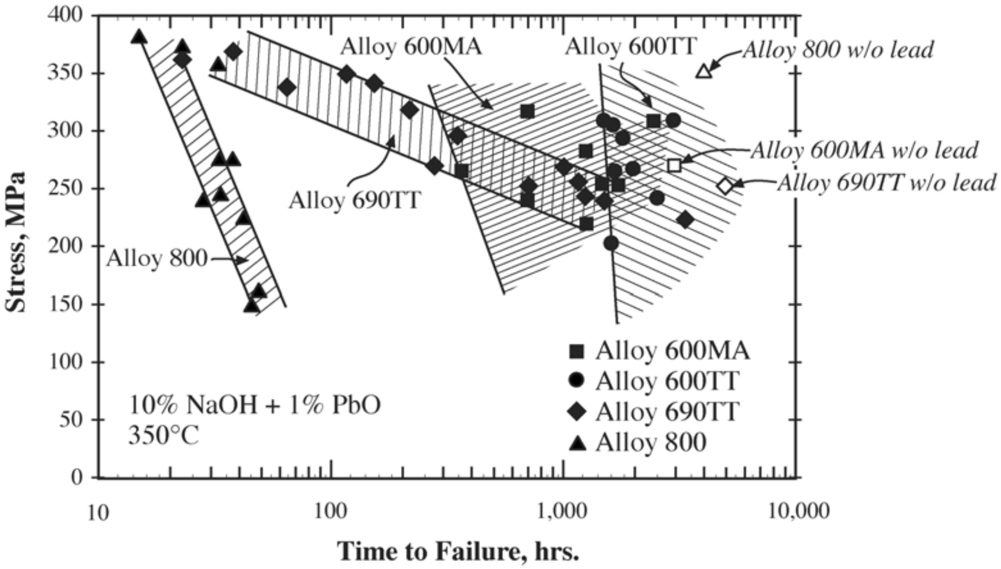

Figure B.7.27 Stress vs. time-to-failure of Alloys 600MA and 600TT (two tubes), 690TT (four tubes), and 800 (two tubes) in 10% NaOH + 1% PbO at 350º C. From Vaillant et al.[51] and Rocher et al.[52]

Table B.7.3 compares concentrated alkaline solutions with various additions of CuO, PbO, $S_2O_3^{2-}$, and $NaSO_4$+$FeSO_4$.

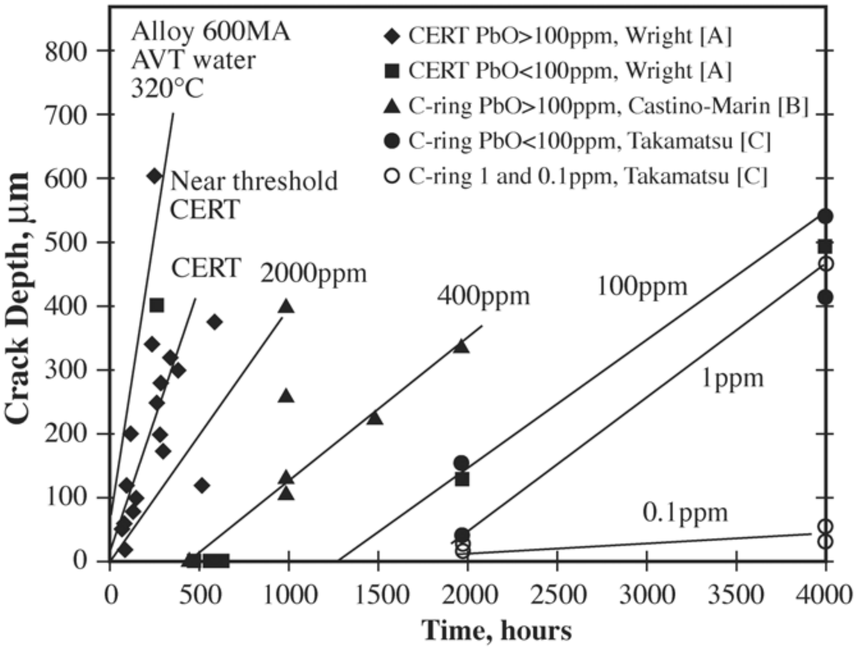

Figure B.7.28 Crack depth vs. time data for Alloy 600MA in AVT water at 320°C with various concentrations of PbO. From Wright and Mirzai,[50] with data from [A] Wright,[53] [B] Castano-Marin et al.[54] [C] and Takamatsu et al.[55]

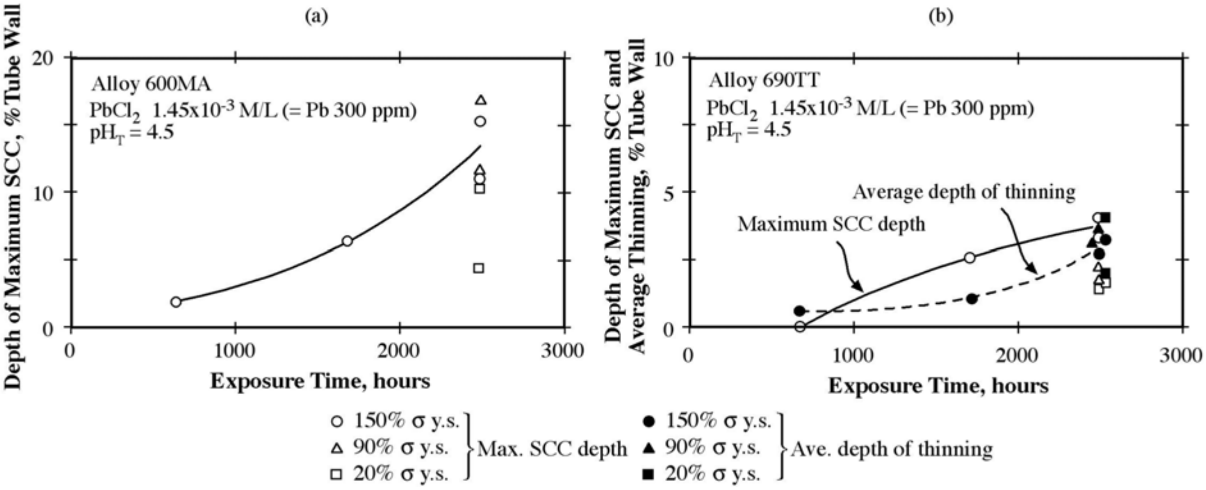

Figure B.7.29 Depth vs. time for PbSCC at $pH_{340°C}$ 4.5 in which various stresses were applied for 2500 hour exposure in water where $O_2 < 5$ ppb and Pb was added as $PbCl_2$. From Sakai et al.[56] (a) Alloy 600MA at 1.45 x 10^{-3} M/L of $PbCl_2$. (b) Alloy 690TT at 1.45 x 10^{-3} M/L of $PbCl_2$. Maximum SCC depth plus average depth of GC.

Table B.7.3 Results from Visual Examination of Specimens Exposed* to Alkaline Solutions at 350°C with Added Species (cracked samples/tested samples). From Briceno and Castano.[57]

Material	10% NaOH	10% NaOH + 0.1M CuO	10% NaOH + 0.1 M PbO	50% NaOH + 5% $Na_2S_2O_3$	0.75% M Na_2SO_4 + 0.25% M $FeSO_4$	0.75% M Na_2SO_4 + 0.25% M $FeSO_4$
Alloy 800 7-73243	3/3	3/3	4/4	4/4	4/4	0/4 (3/4)**
Alloy 800SP 81373	15/15	15/15	15/15	15/15	15/15	11/15 (15/15)**
Alloy 690TT WF816T	0/15	0/15	15/15	14/14	0/15	1/15
Alloy 690TT 764408	0/15	0/15	15/15	15/15	0/15	0/15
Alloy 600MA 1450	8/9	0/9 (2/9)**	0/9 (3/9)**	2/9	6/9 (8/9)**	9/9

* 500 hours exposure; C-ring specimens; 2% strain.

** Visual examination after bending the samples.

Table B.7.4 Results of Cathodic Polarization Scans in 50% NaOH with 5% Additions at 316°C. From King.[58]

5% Addition	Alloy 600		Alloy 690	
	Worst Case	Observations	Worst Case	Observations
Na_2CO_3	No difference*	General attack	No difference*	Slight g.b. intrusions
Na_2S	TT ring	Heavy general attack	MA C-ring	TGSCC
NaHS	No difference	Heavy general attack	MA C-ring	TGSCC
$Na_2S_2O_3$	No difference	Heavy general attack	MA C-ring	TGSCC
Na_2SO_4	No difference	Slight general attack	MA C-ring	Slight g.b. intrusions

* No difference indicates no substantial difference between ring or C-ring specimens for mill-annealed and thermally-treated condition.

MA - Heat treatment not defined

TT - Mill annealed plus 704°C /16 hrs

TGSCC - Transgranular stress corrosion cracks

Table B.7.4 compares the behavior of Alloys 600MA and 690MA with a cathodic dynamic polarization, which was applied during testing in solutions where low valence sulfur, carbonate, and sulfate were added separately. Here, Alloy 690MA sustained the most intense SCC; in the low valence sulfur, little SCC for Alloy 690MA was observed with either carbonate or sulfate additions to the alkaline base solution. In these experiments, no SCC was observed in Alloy 600, but extensive GC was observed in the presence of low valence sulfur.

There is little other relevant work on lower valence sulfur except for studies at room temperature as discussed by Staehle and Gorman.[1]

3.0 Alloy 600TT

Alloy 600TT was developed based on the work of Blanchet et al.[32] who showed that sensitization would substantially reduce LPSCC. Their results are shown in Table B.7.2. These data were the basis for the development of the TT treatment.

In general Alloy 600TT is somewhat more resistant to SCC than Alloy 690TT. Typical data from testing Alloy 600TT in various environments are as follows:

1. Primary water as LPSCC

Figure B.7.30 shows results from about 6.5 years of testing in an operating plant from the work of Cattant et al.[26] Here, the extent of LPSCC penetration as measured by eddy current seems at least five times faster for Alloy 600MA than for Alloy 600TT.

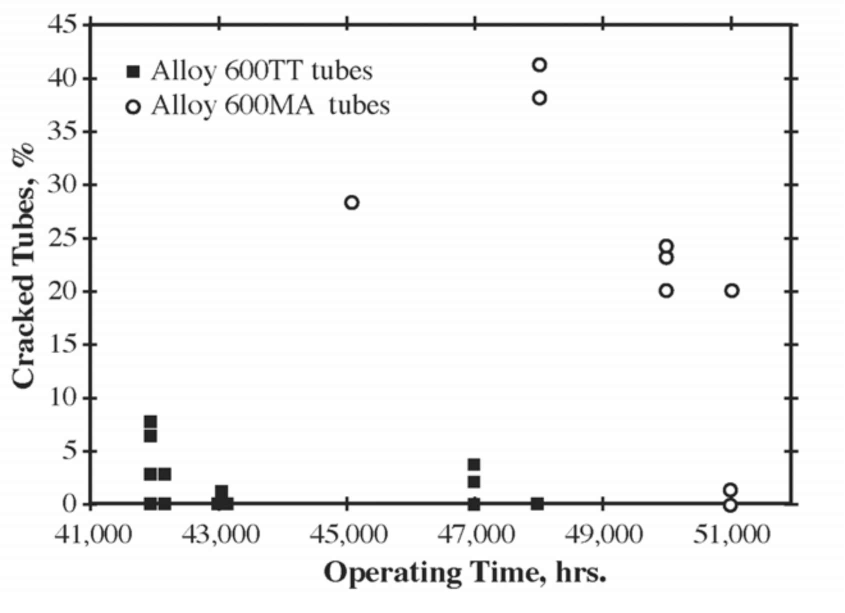

Figure B.7.30 Percent of tubes cracked in primary water vs. operating time for Alloy 600TT and MA tubes. LPSCC located at sludge pile level. Results from eddy current testing. From Cattant et al.[26]

In addition to this work directly from operating plants, Figure B.7.31 from the work of Jacko[59] shows that Alloy 600TT is improved relative to Alloy 600MA in about the same proportions as the results in Figure B.7.30. Here, Alloy 690 exhibits no LPSCC.

2. Alkaline as AkSCC

In alkaline solutions the intensity of AkSCC in Alloy 600TT is less than Alloy 600MA as shown in Figures B.7.10b and 10d. Figure B.7.32[7] shows that the plateau crack velocity of Alloy 600TT is a 5-10 times less than for Alloy 600MA in 4 and 100 g/l NaOH solutions; and Figure B.7.25 shows that the peak rate of SCC for the TT type of heat treatment is about 10 to 100 less than the MA heat treatment in a 10%NaOH solution.

3. Acidic as AcSCC

Depending on the data, Alloy 600TT exhibits improvements compared to Alloy 600MA. Figure B.7.33[61] shows significant improvements over a range of slightly acidic pH in sulfate solutions; whereas, Figure B.7.24 does not exhibit such improvements.

4. Lead

The work of Miglin and Sarver,[60] which covered a broad range of pH with Pb additions, showed that Alloy 600TT was generally, but not substantially, improved over Alloy 600MA.

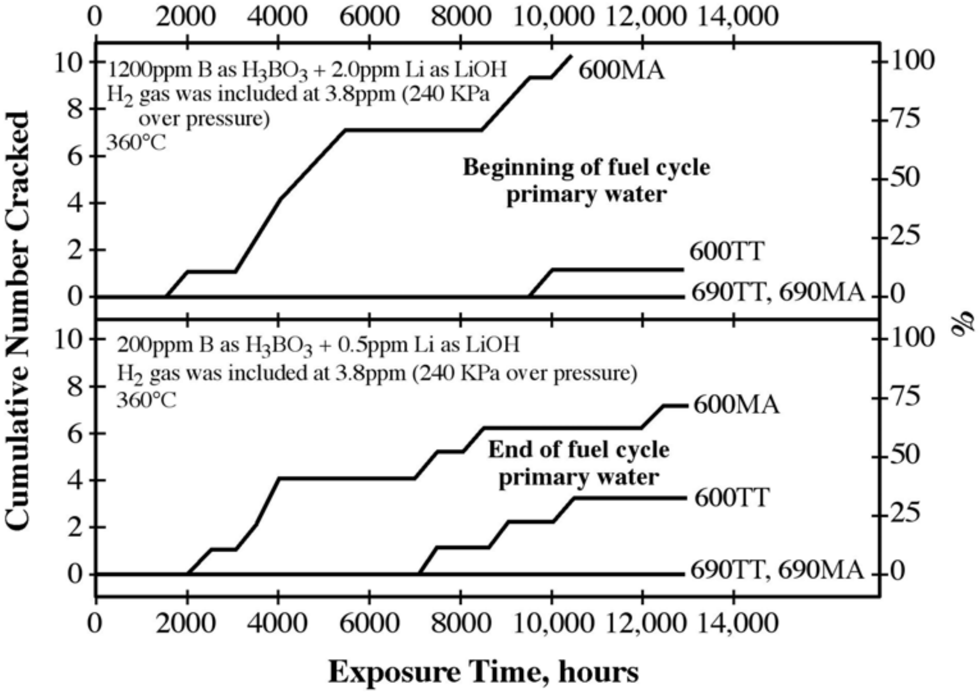

Figure B.7.31 Cumulative number of Alloy 600 and 690 specimens exposed for 13,000 hours in chemistries typical of the (a) beginning of life and (b) end of life for a fuel cycle. From Jacko.[59]

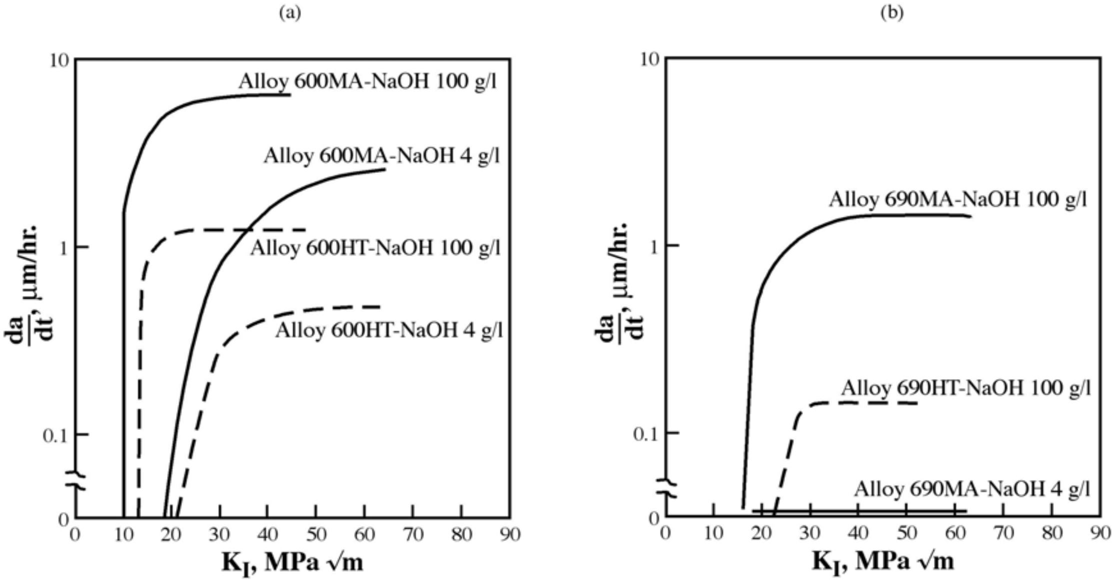

Figure B.7.32 da/dt vs. K for Alloys 600 (a) and 690 (b) exposed to various concentrations of NaOH at 350°C with a WOL type specimen. HT corresponds to 700°C for 16 h. From Berge and Donati.[7]

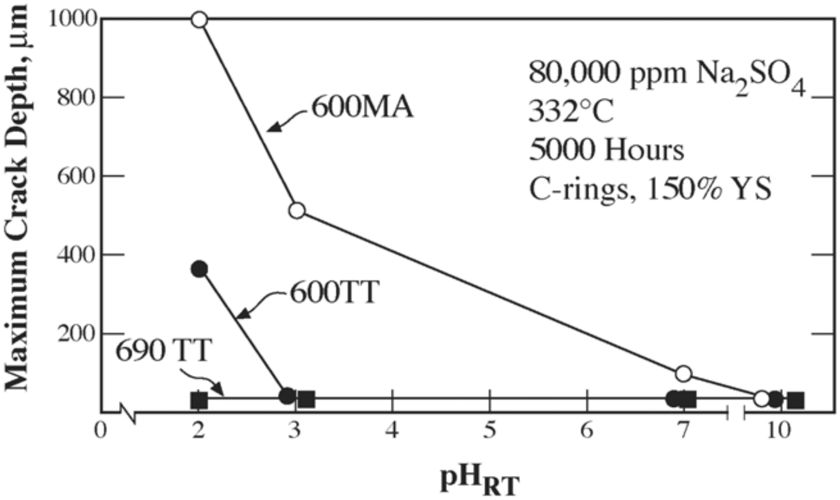

Figure B.7.33 Maximum crack depth vs. room temperature pH for Alloy 600MA, Alloy 600TT, and Alloy 690TT exposed in acidic sulfate solutions at 332°C for 5000 hours as C-rings stressed to 150% of the yield strength. From Smith et al.[61]

Figure B.7.27 shows that Alloy 600TT is improved relative to Alloy 600MA possibly by a factor of five in time-to-failure, but there are no significant differences in the stress threshold.

In AVT environments, as shown in Figure B.7.34,[55] Alloy 600TT is improved, compared to Alloy 600MA, and does not support SCC at such low concentrations of Pb. However, Alloy 600TT is not significantly better at higher concentrations.

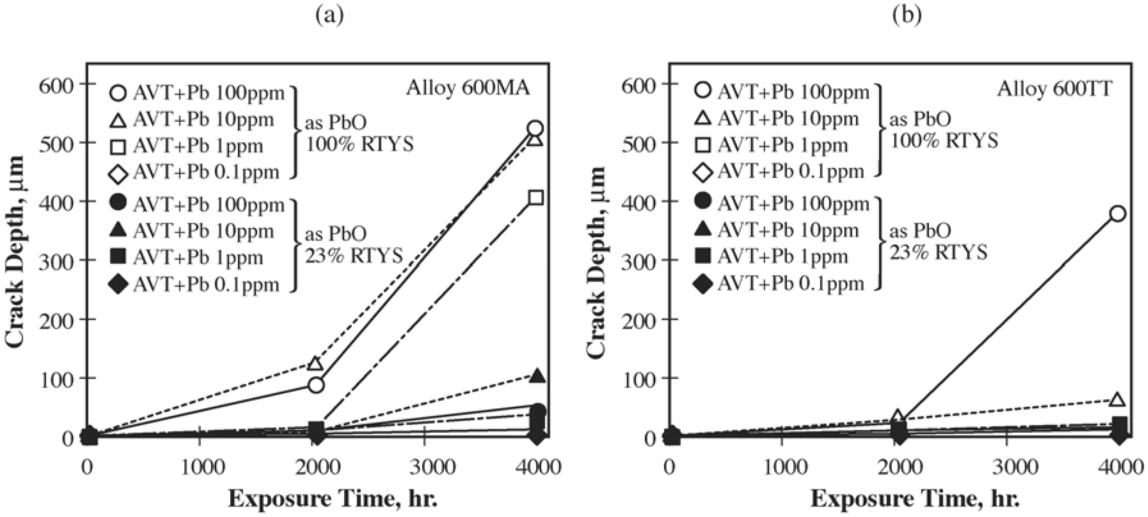

Figure B.7.34 Crack depth vs. time for various concentrations of Pb at two stresses and for Alloys 600MA and 600TT in deaerated AVT water containing 0.26 ppm NH_3+0.1ppm N_2H_4. From Takamatsu et al.[55]

5. Sulfur

There appear to be no data for the SCC of Alloy 600TT in solutions which contain low valence sulfur.

4.0 Alloy 690 TT

As it became clear that Alloy 600 was not adequate for the initially intended 40 year license period, work had begun, at least by 1970, to develop an improved alloy as reported by Copson et al.[62] and Flint and Weldon.[63] This work involved evaluating alloys in three environments: highly oxygenated environments with double U-bend crevices, lead environments, and alkaline environments. Sensitized and non-sensitized alloys were studied, and a relatively large range of iron and chromium additions to a nickel base were evaluated.

Alloy 690TT is now becoming the standard material for use in SG tubing as well as for welding and for thick sections where substantial corrosion resistance, together with compatibility of the thermal expansion coefficient with adjacent low alloy steel components, is required, as shown in Figure B.7.5.

From these early tests, the highly oxygenated solutions were not particularly useful from the point of view of PWR applications, except for the non-defined conditions inside double crevices. However, the testing in the Pb-containing solutions proved to be of great interest in later years as shown in Figure B.7.35.[46]

Figure B.7.35 shows the combined effects of iron and nickel both on the SCC and scaling of alloys exposed to high temperature water containing Pb. Both figures show the locations of the Alloy 690 composition. These results showed that Alloy 690 composition is close to a scaling condition (severe general corrosion) and to SCC in Pb environments. Regardless, the Alloy 690 composition seemed to be an optimum as shown in Figure B.7.35, and the testing in the Pb-containing solutions foresaw, unintentionally, the importance of Pb on the secondary side. In the following years development of these high chromium alloys continued and intensified in the late 1970s and early 1980s.

1. Primary water as LPSCC

The improvement of Alloy 690TT over Alloy 600MA, as well as over Alloy 600TT, is shown in Figure B.7.31 where laboratory testing was carried out for about 13,000 hours at 360°C.

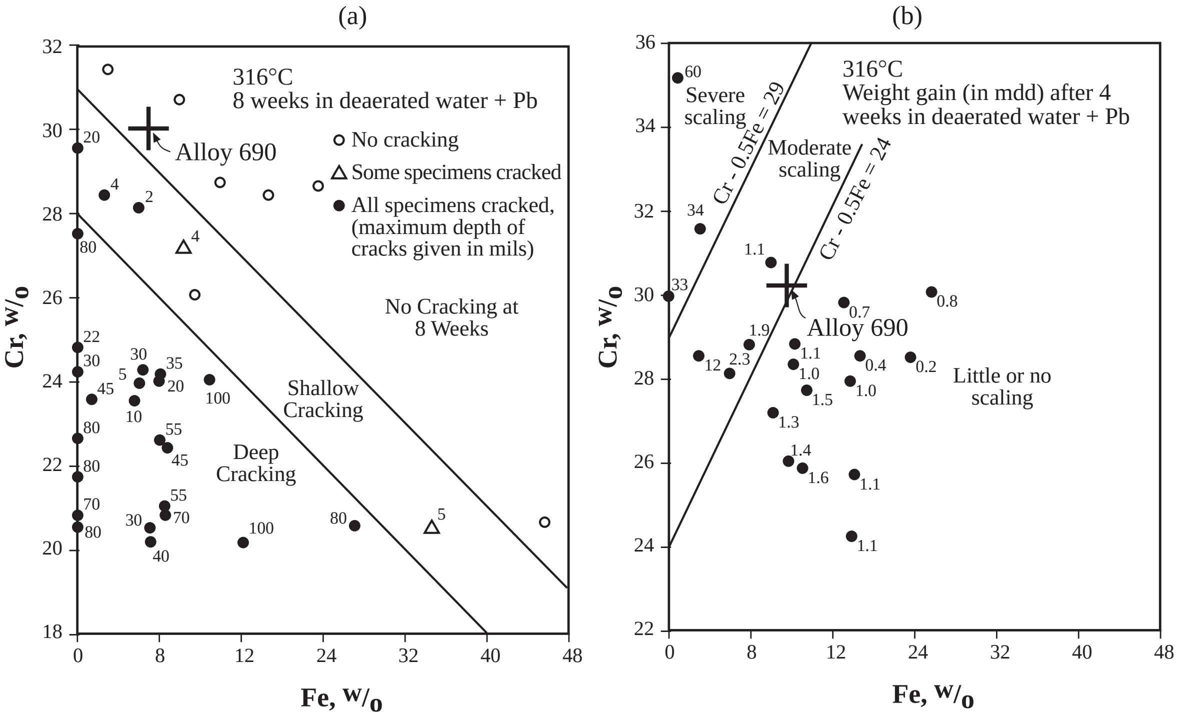

Figure B.7.35 (a) Maximum depth of SCC of Ni-Cr-Fe alloys after 8 weeks in deaerated water plus Pb at 316°C. (b) Weight gain of Ni-Cr-Fe alloys after 4 weeks in deaerated water plus Pb. From Sarver et al.[46]

2. Alkaline as AkSCC

Figure B.7.32 for crack growth rate vs. stress intensity shows that the plateau velocity for Alloy 690 is a factor of 10-100 less than for Alloy 600MA depending on the concentration of NaOH.

The overall mapping of SCC for the three alloys of 600MA, 600TT, and 690TT in Figure B.7.10 shows that Alloy 690TT is improved and the threshold of pH for the onset of AkSCC is higher.

3. Acidic as AcSCC

Figure B.7.26 shows that Alloy 690TT at open circuit in sulfate solutions does not sustain AcSCC. This is similar to the pattern for Figure B.7.10. However, with Figure B.7.26 it appears that Alloy 690TT does sustain significant AcSCC, but at potentials that may exceed the normal open circuit range depending on what potentials are actually present in crevices and that results from the very low hydrogen on the secondary side.

4. Lead as PbSCC

The extensive work of Miglin and Sarver, which is discussed by Staehle and Gorman[1] and by Staehle,[35] shows that Alloy 690 is improved, in terms of resistance to PbSCC, over both Alloy 600MA and Alloy 600TT until pH 9.9 is reached, at which point the SCC of Alloy 690TT is significant, especially in steam (implying easy vapor phase transport of Pb). Figure B.7.27 reflects this greatly increased sensitivity of Alloy 690 in alkaline solutions.

While Figure B.7.26 shows that sulfates seem to inhibit PbSCC of Alloy 690TT in acidic solutions, Figure B.7.29b shows the Pb as $PbCl_2$ promotes PbSCC, although at a rate about 1/5 that for Alloy 600MA.

5. Sulfur as S^{y-}SCC

Tables B.7.3 and 4 show that the presence of low valence sulfur either as a –2 (sulfide) or +2 (thiosulfate) accelerates S^{y-}SCC for Alloy 690TT relative to Alloy 600MA.

5.0 Alloy 800

Figure B.7.4 from Coriou et al.[13] based on the general trends of his observations, suggests that the composition of Alloy 800 as shown in Figure B.7.2 and Table B.7.1 would resist SCC in both pure water and chloride-containing water, although Copson and Cheng's[6] work in Figure B.7.3 suggests that Alloy 800 is within the domain of chloride SCC. Such SCC of commercial grade Alloy 800 in chloride solutions was also observed by Staehle et al.[64] for commercially available materials at the time.

Mainly based on the work of Coriou plus internal work, Siemens chose a controlled version of Alloy 800 for their steam generators, and this alloy has exhibited excellent in-service performance.

1. Primary water as LPSCC

The dependence of LPSCC on nickel concentration was reported by Coriou et al.[65] They showed that the nickel concentration of Alloy 800 was below the Ni concentration that would permit

LPSCC. Later Nagano et al.[66] showed that Alloy 800 was equivalent to Alloy 690 as shown in Figure B.7.36.

Since the first observation of Coriou in his schematic assessment in Figure B.7.4, Alloy 800 has remained resistant to LPSCC.

2. Alkaline as AkSCC

Alloy 800 does not generally perform well in alkaline solutions. Figure B.7.37 from Nagano et al.[67] and Figure B.7.38 from Wilson et al.[68] is consistent with this trend. In Figure B.7.37, at 20% Cr and Ni near the composition of Alloy 800, significant AkSCC occurs. Further in Figure B.7.38, the stress threshold for AkSCC is not much different from Alloy 600MA in the alkaline solution.

The fact that Alloy 800 has given such good performance in operating plants suggests that alkalinity has not been significant in the crevices.

3. Acidic as AcSCC

Alloy 800 is more resistant to AcSCC than Alloys 600MA and 600TT as shown in Figure B.7.39.[44]

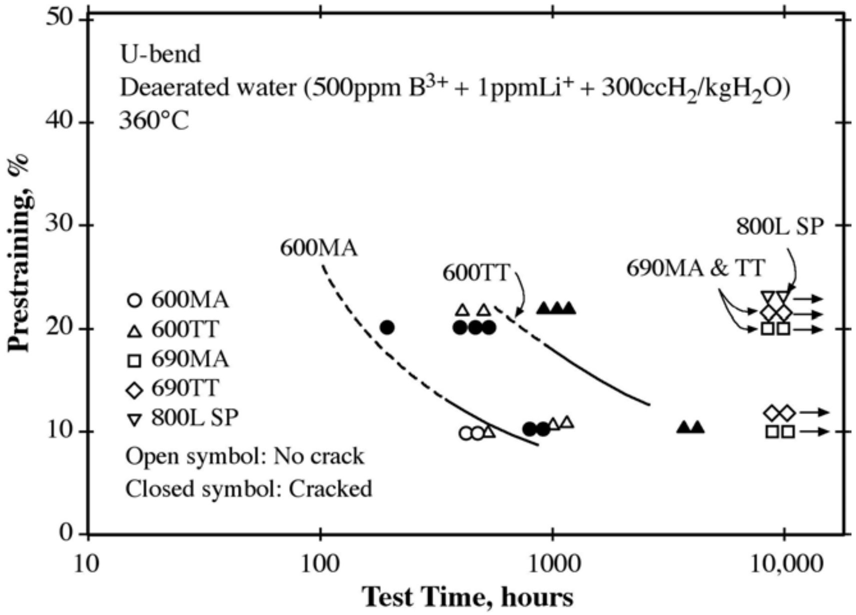

Figure B.7.36 Prestraining percent vs. test time for Alloys 600, 690, and 800 exposed at 360˚C in deaerated water. From Nagano et al.[66]

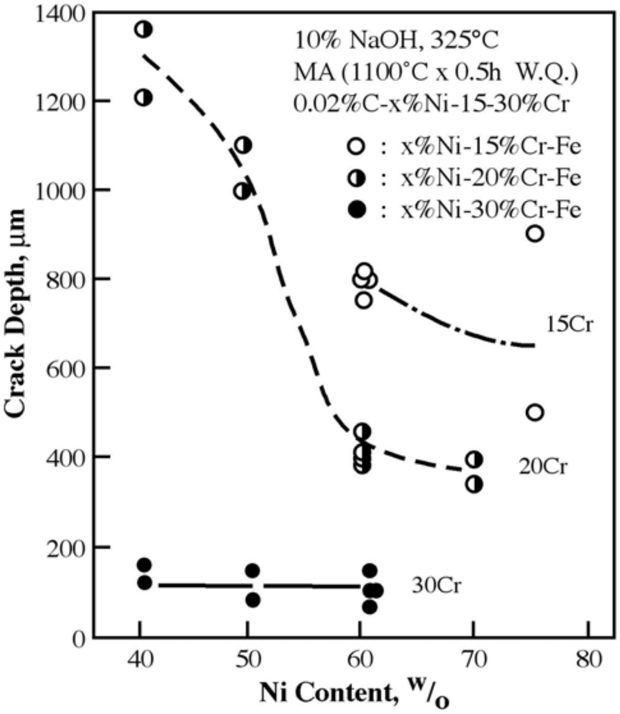

Figure B.7.37 Crack depth vs. Ni concentration for Ni-Cr-Fe alloys + 0.02%C exposed in a deaerated 10% NaOH solution at 325°C for 200 hours as single U-bends. Specimens mill annealed. From Nagano et al.[67]

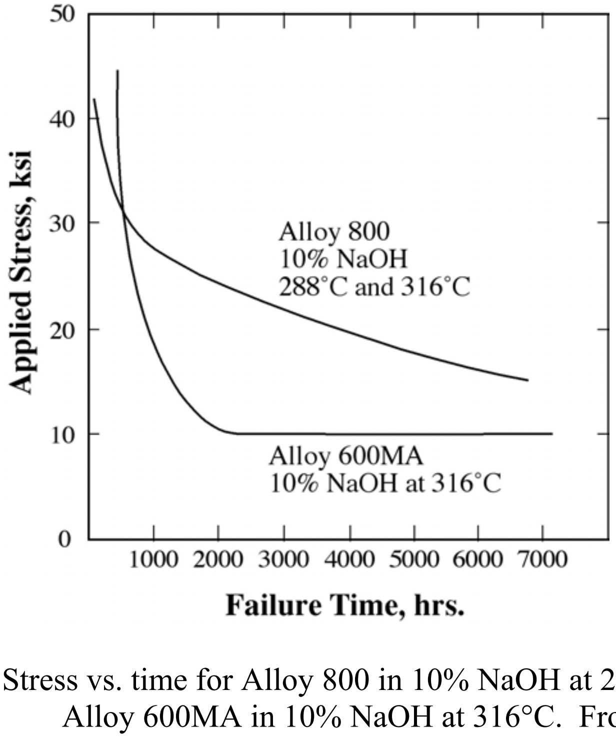

Figure B.7.38 Stress vs. time for Alloy 800 in 10% NaOH at 288 and 316°C, and for Alloy 600MA in 10% NaOH at 316°C. From Wilson et al.[68]

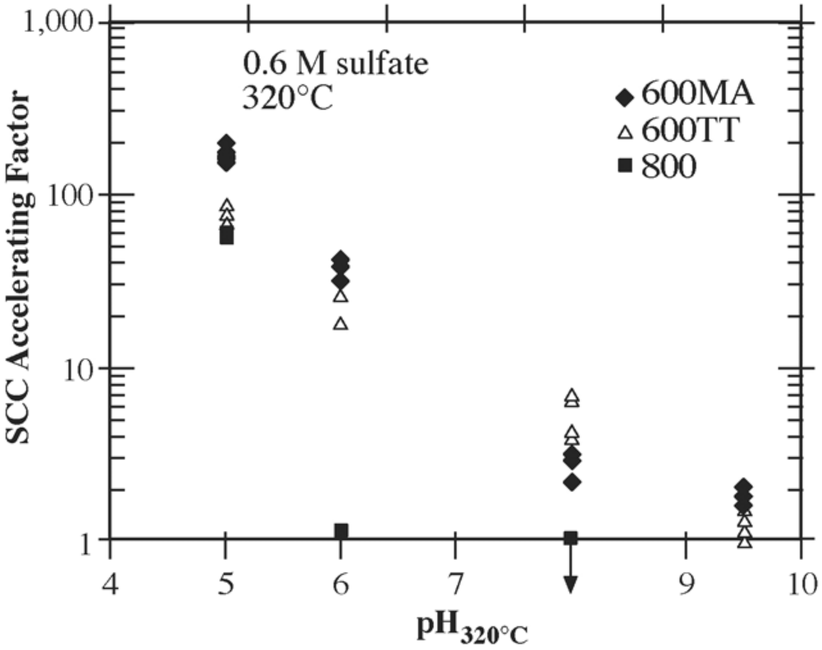

Figure B.7.39 SCC accelerating factor vs. pH for three alloys in 0.6M sulfate environments at 320°C. Accelerating factor taken from the rate of crack initiation at 0.001M ($pH_{320°C}$ =5) being the reference. 150% YS refers to the "two legs touching" condition of the branches of the C-ring; below this stress, specimens were stressed at 0.8 YS and 1.0 YS.
From deBouvier et al.[44]

4. Lead

Alloy 800 seems to be the least resistant of the Alloys 600MA, 600TT, 690TT and 800 in alkaline solutions containing Pb as shown in Figure B.7.27. Despite the relative trends, more recent electrochemical studies by Y. Lu of AECL have shown the standard SG Alloy 800 is generally resistant to PbSCC in alkaline solutions.[69]

5. Sulfur

Table B.7.3 shows that Alloy 800 is similarly prone to SCC in S^{y-}SCC (alkaline base) as Alloy 690 in alkaline solutions. There appear to be no other data for other ranges of pH for any of the alloys.

6.0 Conclusions

1. The early choice of Alloy 600MA for tubing in PWR steam generators together with drilled hole tube supports, less pure secondary water chemistry, and relatively high residual stresses produced extensive failures of tubing leading to the eventual replacement of many steam

generators tubed with Alloy 600MA. This choice of Alloy 600MA was based on a set of untested assumptions.

2. A set of mitigations has reduced, for the present, the rate of SCC on the primary and secondary sides of SG tubes associated with Alloy 600MA. These mitigations have included:

    - Using better alloys including Alloy 600TT, Alloy 690TT, and Alloy 800.
    - Using line contact tube supports and changing the materials of the tube supports to stainless steel.
    - Improving the secondary water chemistry.
    - Reducing residual stresses.
    - Improved methods of inspection.

3. The potential for secondary-side corrosion problems still exist:

    - Pb and S impurities.
    - Acidic crevices, especially with chloride.
    - Longer time and significant accumulation of impurities in line contact tube supports.
    - Denting and increased stresses at the top of the tubesheet.
    - Possible large releases of sequestered lead resulting from subtle changes in water chemistry, perhaps due to a still further increase in purity of the boiler water.
    - Nucleation of SCC at locations of dings, dents, and scratches.

7.0 Acknowledgements

It is a pleasure to acknowledge Jeffrey Gorman of Dominion Engineering, Robin Jones of EPRI, Yucheng Lu of AECL, Al McIlree of EPRI, Peter Scott of Framatome, and Robert Tapping of AECL for their help in preparing this report. Also, I appreciate the many who contributed to the Staehle and Gorman[1] reference. In my office I appreciate, as usual, the work of Julie Daugherty and John Ilg.

8.0 References

---

[1] R.W. Staehle and J.A. Gorman, “Quantitative Assessment of Submodes of Stress Corrosion Cracking on the Secondary Side of Steam Generator Tubing in Pressurized Water Reactors,” *Corrosion*, Part 1 Vol. 59 No. 11 November 2003, Part 2 Vol. 60 No. 1 January 2004, Part 3 Vol. 60 No. 2 February 2004, NACE, Houston, Texas.

[2] The Shippingport Pressurized Water Reactor, prepared for the USAEC, Addison-Wesley Publishing Company, Inc., Reading, Massachusetts, 1958.

[3] W.F. Brindley, L.R. Scharfstein, and M.A. Golik, “Chloride Stress Corrosion Testing of Type 347 Stainless Steel Steam Generator Tubing,” Bettis Technical Review: Reactor Chemistry and Plant Materials, Vol. 1, No. 3, WAPD-BT-3, 1957.

[4] L.R. Scharfstein and W. Brindley, “Chloride Stress Corrosion Cracking of Austenitic Stainless Steel – Effect of Temperature and pH,” *Corrosion Vol. 60*, NACE, Houston, Texas, 1958.

[5] J.W. Pugh and J.D. Nisbet, “A Study of the Iron Chromium Nickel Ternary System,” *Journal of Metals Vol. 188,* 1950, p. 269.

[6] H.R. Copson and C.F. Cheng, “Some Case Histories of Stress Corrosion Cracking of Austenitic Stainless Steels Associated with Chlorides,” *Corrosion Vol. 13,* 1957, p. 397.

[7] Ph. Berge and J.R. Donati, “Materials Requirements for Pressurized Water Reactor Steam Generator Tubing,” *Nuclear Technology Vol. 55*, 1981, p. 88.

[8] ASM Specialty Handbook, Stainless Steels, J.R. Davis, ed., ASM International, Materials Park, 1994.

[9] Guidelines for PWR Steam Generator Tubing Specifications and Repair; Volume 1: Specification for Alloy 600 Steam Generator Tubing; NP-6743, EPRI, Palo Alto, 1991.

[10] J.A. Gorman, Guidelines for PWR Steam Generator Tubing Specifications and Repair, Volume 2, Revision 1: Guidelines for Procurement of Alloy 690 Steam Generator Tubing; TR-016743-V2R1, EPRI, Palo Alto, 1999.

[11] B. Stellwag, N. Wieling, and L. Stieding, “Corrosion Resistance of SG Tubing Materials Alloy 800 and Alloy 690 – A Comparative Study,” Proceedings of the Second International Symposium on Environmental Degradation of Materials in Nuclear Power Systems – Water Reactors, J.T.A. Roberts, J.R. Weeks, and G.J. Theus, chair., American Nuclear Society, Chicago, 1986, p. 301.

[12] H. Coriou, L. Grall, V. Le Gall, and S. Vettier, “Corrosion Fissurante Sous Contrainte De L’Inconel D’American Nuclear Society L’eau à Haute Température,” Third Colloque De Mêtallurgue, North Holland Publishing Company, Amsterdam, 1960, p. 161.

---

[13] H. Coriou, L. Grall, P. Olivier, and H. Willermoz, "Influence of Carbon and Nickel Content on Stress Corrosion Cracking of Austenitic Stainless Alloys in Pure or Chlorinated Water at 350°C," Fundamental Aspects of Stress Corrosion Cracking; NACE-1, R.W. Staehle, A.J.Forty, and D. van Rooyen, eds., NACE, Houston, 1969, p. 352.

[14] B.L. Dow, Jr., Steam Generator Progress Report, Revision 14; TE-106365-R14, EPRI, Palo Alto, 1999.

[15] P.M. Scott and P. Combrade, "On the Mechanisms of Secondary Side PWR Steam Generator Tube Cracking," Proceedings of the Eighth International Symposium on Environmental Degradation of Materials in Nuclear Power Systems -Water Reactors, A.R. McIlree, chair., American Nuclear Society, Chicago, 1997.

[16] P. Combrade, O. Cayla, M. Foucault, D. Vancon, A. Gelpi, and G. Slama, "About the Role of Surface Films on Alloy 600 Corrosion in High Temperature Deaerated Environments," Proceedings of the Third International Symposium on Environmental Degradation of Materials in Nuclear Power Systems – Water Reactors, G.J. Theus and J.R. Weeks, eds., TMS, Warrendale, Pennsylvania, 1988.

[17] P. Combrade, "The Role of Surface Films on the Control of Alloy 600 Corrosion in PWR Reactors – No Results, a Few Comments, a Lot of Questions," Proceedings: Specialist Meeting on Environmental Degradation of Alloy 600; TR-104898, R.G. Ballinger, A.R. McIlree, and J.P.N. Paine, eds., EPRI, Palo Alto, 1994.

[18] I. Ohsaki, K. Onishi, Y. Ohkubo, T. Hattori, and S. Tokunaga, "Study of the Improvement of Steam Generator Tubing and Tube Support Plate Materials," 2nd International Steam Generator and Heat Exchange Conference, D.E. Anderson, ed., Canadian Nuclear Society, Toronto, 1994, p. 8.93.

[19] S. Tsujikawa and S. Yashima, "Results of Steam Generator Tubing Reliability Test," 2nd International Steam Generator and Heat Exchange Conference, D.E. Anderson, ed., Canadian Nuclear Society, Toronto, 1994, p. 6.73.

[20] R. Varrin Jr., Characterization of PWR Steam Generator Deposits; TR-106048, EPRI, Palo Alto, 1996.

[21] Proceedings of the 1987 Workshop on the Mechanism of Primary H_2O IGSCC; NP-5987-SP, G. Economy, R.J. Jacko, J.A. Begley, and F.W. Pement, eds., EPRI, Palo Alto, 1987.

[22] D.S. Morton, S.A. Attanasio, and G. A. Young, "Primary Water SCC Understanding and Characterization Through Fundamental Testing in the Vicinity of the Nickel/Nickel Oxide Phase Transition," Proceedings of the Tenth International Symposium on Environmental Degradation of Materials in Nuclear Power Systems - Water Reactors, P. Ford, G. Was, and L. Nelson, eds., NACE, Houston, Texas, 2002.

---

[23] T. Yonezawa and K. Onimura, “Effect of Chemical Compositions and Microstructure on the Stress Corrosion Cracking Resistance of Nickel Base Alloys in High Temperature Water,” International Conference on Evaluation of Materials Performance in Severe Environments; EVALMAT ’89, The Iron and Steel Institute of Japan, 1989, p. 235.

[24] H. Nagano and H. Kajimura, “Clarification of Stress Corrosion Cracking Mechanism on Nickel Base Alloys in Steam Generators for their Long Lifetime Assurance,” Proceedings of the Seventh International Symposium on Environmental Degradation of Materials in Nuclear Power Systems – Water Reactors, TMS, Warrendale, Pennsylvania, 1995.

[25] K. Norring, J. Engstrom, and P. Norberg, “Intergranular Stress Corrosion Cracking in Steam Generator Tubing. Testing of Alloy 690 and Alloy 600 Tubes,” Proceedings of the Third International Symposium on Environmental Degradation of Materials in Nuclear Power Systems – Water Reactors, G.J. Theus and J.R. Weeks, eds., The Metallurgical Society, Warrendale, Pennsylvania, 1988, p.587.

[26] F. Cattant, D. Garriga-Majo, F. de Keroulas, P. Todeschini, and J.C. Van Duysen, “Effectiveness of 700°C Thermal Treatment on Primary Water Stress Corrosion Sensitivity of Alloy 600 Steam Generator Tubes: Laboratory Tests and In Field Experience,” Proceedings of the Fifth International Symposium on Environmental Degradation of Materials in Nuclear Power Systems -Water Reactors, D. Cubicciotti, chair., American Nuclear Society, La Grange Park, Illinois, 1992, p. 901.

[27] G.L. Webb, “Environmental Degradation of Alloy 600 and Welded Filler Metal EN 82 in an Elevated Temperature Aqueous Environment,” Proceedings of the Sixth International Symposium on Environmental Degradation of Materials in Nuclear Power Systems-Water Reactors, R.E. Gold and E.P. Simonen, eds., TMS, Warrendale, Pennsylvania, 1993, p. 687.

[28] T.B. Cassagne, P. Combrade, M.A. Foucault, and A. Gelpi, “The Influence of Mechanical and Environmental Parameters on the Crack Growth Behavior of Alloy 600 in PWR Primary Water,” 12th Scandinavian Corrosion Congress & Eurocorr ‘92, P.J. Tunturi, ed., Corrosion Society of Finland, Helsinki, 1992, p. 55.

[29] J.M. Gras, “Stress Corrosion Cracking of Steam Generator Tubing Materials Review and Assessment,” Parkins Symposium on Fundamental Aspects of Stress Corrosion Cracking,”S.M. Bruemmer, E.I. Meletis, R.H. Jones, W.W. Gerberich, F.P. Ford and R.W. Staehle, eds., TMS, Warrendale, 1992, p. 411.

[30] P. Saint-Paul and G. Zacharie, La Corrosion Sous Contrainte de L’Alliage 600 Dans L’eau, EDF/DER/EMA No. D 729A, Electricite de France, Paris, 1990.

[31] D. Garriga-Majo, J.M. Gras, Y. Rouillon, F. Vaillant, J.C. Van Duysen, and G. Zacharie, “Prediction of the Stress Corrosion Cracking Resistance of Alloy 600 in Pure/Primary Water,” Life Prediction of Corrodible Structures, R.N. Parkins, ed., NACE, Houston, 1994, p. 1104.

---

[32] H. Blanchet, H. Coriou, L. Grall, C. Mahieu, C. Otter, and G. Turleur, “Historical Review of the Principal Research Concerning the Phenomena of Cracking of Nickel Base Austenitic Alloys,” Stress Corrosion Cracking and Hydrogen Embrittlement of Iron Base Alloys, NACE-5, R.W. Staehle, J. Hochmann, R.D. McCright, and J.E. Slater, eds., NACE, Houston, 1977, p. 1149.

[33] R. Bandy and D. van Rooyen, Tests with Inconel 600 to Obtain Quantitative Stress Corrosion Cracking Data for Evaluating Service Performance; BNL-NUREG-31814, U.S. Nuclear Regulatory Commission, Washington, 1983.

[34] P.M. Scott, “Prediction of Alloy 600 Component Failures in PWR Systems,” Proceedings of Corrosion ’96: Part 1: Life Prediction of Structures Subject to Environmental Degradation,” P.L. Andresen and R.N. Parkins, chair., NACE, Houston, 1996, p. 135.

[35] R.W. Staehle, Bases for Predicting the Earliest Penetrations Due to SCC for Alloy 600 on the Secondary Side of PWR Steam Generators; NUREG-CR-6737, U.S. Nuclear Regulatory Commission, Washington, 2001.

[36] H. Takamatsu, T. Kitera, and K. Arioka, “Corrosion Experience with the Secondary Side of Steam Generators in Japan,” Control of Corrosion on the Secondary Side of Steam Generators, R.W. Staehle, J.A. Gorman, and A.R. McIlree, eds., NACE, Houston, 1996, p. 113.

[37] H. Takamatsu, K. Matsueda, E. Kadokami, K. Arioka, T. Tsuruta, S. Okamoto, and T. Ueno, “Evaluation of SG Crevice Environment by Directly Sampled Method Using an On-Site Autoclave Facility,” Proceedings of the Fifth International Symposium on Environmental Degradation of Materials in Nuclear Power Systems - Water Reactors, D. Cubicciotti, chair, American Nuclear Society, Chicago, Illinois, 1992, p. 752.

[38] F. Cattant, M. Dupin, B. Sala, and A. Gelpi, “Analyses of Deposits and Underlying Surfaces on the Secondary Side of Pulled Out Tubes From a French Plant,” Contribution of Materials Investigation to the Resolution of Problems Encountered in Pressurized Water Reactors; Proceedings of the International Symposium: Fontevraud III, F. de Keroulas, chair., French Nuclear Energy Society, Paris, 1994, p. 469.

[39] Z. Fang and R.W. Staehle, “The Effect of Valence of Sulfur on the Passivation of Alloys 600 and 690 at 25˚ and 95˚C,” presented at Corrosion ’98, Paper No. 272, NACE, Houston, TX, 1998.

[40] J. Daret, T. Cassagne, Y. Lefevre, and T.Q. Tran, “Evidence for the Reduction of Sulfates under Representative SG Secondary Side Conditions, and for the Role of Reduced Sulfates on Alloy 600 Tubing Degradation,” Proceedings of the Ninth International Conference on Environmental Degradation of Materials in Nuclear Power Systems – Water Reactors, S.M. Bruemmer, F.P. Ford, and G.S. Was, eds.,TMS, Warrendale, Pennsylvania, 1999, p. 567.

---

[41] O. de Bouvier, E-M Pavageau, F. Vaillant, and D. Vermeeren, "Influence of High Reducing Conditions on IGA/SCC of Alloy 600 in Neutral Sulfate Environments," presented at the 11th International Conference on Environmental Degradation of Materials in Nuclear Power Systems – Water Reactors, Chair, L. Nelson, August 10-14, 2003. Stevenson, Washington, ANS, La Grange Park, Illinois.

[42] S. Suzuki, "IGA Resistance of TT Alloy 690 and Concentration Behavior of Broached Egg Crate Tube Support Configuration," Proceedings of the Fifth International Symposium on Environmental Degradation of Materials in Nuclear Power Systems -Water Reactors, D.Cubicciotti, chair., American Nuclear Society, Chicago, Illinois, 1992, p. 752.

[43] N. Pessall, "Prediction of Stress Corrosion Cracking in 10% Caustic Soda Solutions at 315°C (600°F)," *Corrosion Science Vol. 20,* 1980, p. 225.

[44] O. deBouvier, B. Prieux, F. Vaillant, M. Bouchacourt, and P. Lemaire, "Nickel Alloy Stress Corrosion Cracking in Neutral and Lightly Alkaline Sulfate Environments," Proceedings of the Ninth International Conference on Environmental Degradation of Materials in Nuclear Power Systems – Water Reactors, S.M. Bruemmer, F.P. Ford, and G.S. Was, eds., TMS, Warrendale, Pennsylvania, 1999, p. 695.

[45] H.R. Copson and S.W. Dean, "Effect of Contaminants on Resistance to Stress Corrosion Cracking of Ni-Cr Alloy 600 in Pressurized Water," *Corrosion Vol. 21,* 1965, p. 1.

[46] J.M. Sarver, "IGSCC of Nickel Alloys in Lead Contaminated High Purity Water," EPRI Workshop on Intergranular Corrosion and Primary Water Stress Corrosion Cracking Mechanisms; NP-5971, EPRI, Palo Alto, 1987, p. C11/1.

[47] R.W. Staehle, "Assessment of and Proposal for a Mechanistic Interpretation of the SCC of High Nickel Alloys in Lead-Containing Environments," presented at the 11th International Conference on Environmental Degradation of Materials in Nuclear Power Systems – Water Reactors, Chair, L. Nelson, August 10-14, 2003. Stevenson, Washington, ANS, La Grange Park, Illinois.

[48] S.M. Bruemmer and L.E. Thomas, "Insights into Stress Corrosion Cracking Mechanisms from High-Resolution Measurements of Crack-Tip Structures and Compositions," presented at The 2nd International Conference on Environment-Induced Cracking of Metals: EICM-2, Banff, Canada, September 19-23, 2004.

[49] E. Pierson and C. Laire, "The Influence of Copper on the SCC of Alloy 600 and Alloy 690 Steam Generator Tubes," Contribution of Materials Investigation to the Resolution of Problems Encountered in Pressurized Water Reactors; Proceedings of the International Symposium: Fontevraud IV, F. de Keroulas, chair., French Nuclear Energy Society, Paris, 1998, p. 381.

[50] M.D. Wright and M. Mirzai, "Lead-Induced SCC Propagation Rates in Alloy 600," Proceedings of the Ninth International Conference on Environmental Degradation of Materials in

---

Nuclear Power Systems -Water Reactors, S.M. Bruemmer, F.P. Ford, and G.S. Was, eds., TMS, Warrendale, Pennsylvania, 1999, p. 657.

[51] F. Vaillant, D. Buisine, B. Prieux, D. Gomez Briceno, and L. Castano, “Influence of Lead on the Secondary Side Cracking of Alloys 600, 690 and 800,” Eurocorr’96; Session 1X: Nuclear Corrosion and Protection; Extended Abstracts, F. de Keroulas, chair., Centre Francais de L’Anticorrosion Societe de Chimie Industrielle, Nice, 1996, p. 13-1.

[52] A. Rocher, F. Cattant, D. Buisine, B. Prieux, and M. Helie, “Effect of Lead on the OD Degradation of Steam Generator Tubes,” Contribution of Materials Investigation to the Resolution of Problems Encountered in Pressurized Water Reactors; Proceedings of the International Symposium: Fontevraud III, F. de Keroulas, chair., French Nuclear Energy Society, Paris, 1994, p. 537.

[53] M.D. Wright, “Establishing Thresholds for Lead Induced Cracking of Steam Generator Tube Alloys,” Water Chemistry of Nuclear Reactor Systems 7, T. Swan, chair., British Nuclear Energy Society, London, 1996, p. 435.

[54] M.L. Castano-Marin, D. Gomez-Briceno, and F. Hernandez-Arroyo, “Influence of Lead Contamination on the Stress Corrosion Resistance of Nickel Alloys,” Proceedings of the Sixth International Symposium on Environmental Degradation of Materials in Nuclear Power Systems-Water Reactors, R.E. Gold and E.P. Simonen, eds., TMS, Warrendale, Pennsylvania, 1993, p. 189.

[55] H. Takamatsu, B.P. Miglin, P.A. Sherburne, and K. Aoki, “Study on Lead-induced Stress Corrosion Cracking of Steam Generator Tubing under AVT Water Chemistry Conditions,” Proceedings of the Eighth International Symposium on Environmental Degradation of Materials in Nuclear Power Systems -Water Reactors, A.R. McIlree, chair., American Nuclear Society, La Grange Park, 1997, p. 216.

[56] T. Sakai, T. Senjuh, K. Aoki, T. Shigemitsu , and Y. Kishi, “Lead-induced Stress Corrosion Cracking of Alloy 600 and 690 in High Temperature Water,” Proceedings of the Fifth International Symposium on Environmental Degradation of Materials in Nuclear Power Systems -Water Reactors, D. Cubicciotti, chair., American Nuclear Society, La Grange Park, Illinois, 1992, p. 764.

[57] D. G. Briceno and L. Castano, “Inconel 690TT and Incoloy 800 in S, Cu and Pb Environments,” EPRI Workshop on Steam Generator Secondary Side IGA/SCC, Reston, Virginia, 1991.

[58] Courtesy of P. King, Babcock and Wilcox, Alliance, Ohio, September, 2001. Private communication.

[59] R.J. Jacko, “Stress Corrosion Testing of Candidate Steam Generator Materials,” Proceedings: Workshop on Thermally Treated Alloy 690 Tubes for Nuclear Steam Generators; NP-4665S SR,

---

C.E. Shoemaker, ed., EPRI, Palo Alto, 1986, p. 15/1.

[60] B.P. Miglin and J.M. Sarver, Investigation of Lead as a Cause of Stress Corrosion Cracking at Support Plate Intersections; NP-7367-S, EPRI, Palo Alto, 1991.

[61] K. Smith, A. Klein, P. Saint-Paul, and J. Blanchet, "Inconel 690; A Material with Improved Corrosion Resistance for PWR Steam Generator Tubes," Proceedings of the Second International Symposium on Environmental Degradation of Materials in Nuclear Power Systems – Water Reactors, J.T.A. Roberts, J.R. Weeks, and G.J. Theus, chair., American Nuclear Society, Chicago, 1986, p. 319.

[62] H.R. Copson, D. van Rooyen, and A.R. McIlree, "Stress Corrosion Behavior of Ni-Cr-Fe Alloys in High Temperature Aqueous Solutions," 5th International Congress on Metallic Corrosion, NACE, Tokyo, 1972, p. 376.

[63] G.N. Flint and B.A. Weldon, "Some Investigations into the Stress Corrosion Behaviour of Fe-Ni-Cr Alloys in High Temperature Water," Direction des Etudes et Recherches, EDF, Ermenonville, France, March 13-17, 1972.

[64] R.W. Staehle, J.J. Royuela, T.L. Raredon, E. Serrate, C.R. Morin, and R.V. Farrar, "Effect of Alloy Composition on Stress Corrosion Cracking of Fe-Cr-Ni Base Alloys," *Corrosion Vol. 26*, NACE, Houston, Texas, 1970.

[65] H. Coriou, L. Grall, and M. Pelras, "Studies of the Corrosion Resistance of Chromium Nickel Iron Austenitic Alloys with a View to Their Application in the Nuclear Field," 3rd International Congress in Metal Corrosion, M. Kolotyrkin, ed., Swets and Zeitlinger, Amsterdam, 1969, p. 303.

[66] H. Nagano, K. Yamanaka, K. Kobayashi, and M. Inoue, "Development and Manufacturing System of Alloy 690 Tubing for PWR Steam Generators," The Sumitomo Search, No. 40, 1989.

[67] H. Nagano, K. Yamanaka, T. Minami, M. Inoue, T. Yonezawa, K. Onimura, N. Sasaguri, and T. Kusakabe, "Effect of Alloying Elements and Heat Treatment on the Corrosion Resistance of Alloy 690," Proceedings: Workshop on Thermally Treated Alloy 690 Tubes for NuclearSteam Generators; NP-4665S SR, C.E. Shoemaker, ed., EPRI, Palo Alto, 1986, p. 10/1.

[68] I.L.W. Wilson, F.W. Pement, R.G. Aspden, and R.T. Begley, "Caustic Stress Corrosion Behavior of Fe-Ni-Cr Nuclear Steam Generator Tubing Alloys," *Nuclear Technology Vol. 31,* 1975, p. 70.

[69] Courtesy of Y. Lu, AECL, Chalk River, Ontario, March, 2005. Private communication.

B.8 Stress Corrosion Cracking of Carbon and Low Alloy Steels

Introduction

This topical paper covers stress corrosion cracking of carbon and low alloy steel components and their associated weldments. These ductile structural materials are used as pressure boundary materials in pressure vessels and piping in the RCS, ECCS, secondary water and service water systems of LWRs. Stress corrosion cracking is part of a spectrum of failure mechanisms, including strain–induced cracking (SIC) [1] and corrosion fatigue. This topical paper includes SIC. The topics of corrosion fatigue and stress corrosion cracking of higher strength steels used as bolting, for instance, are discussed in other topical reports.

The reasons for the use of carbon and low alloy steels in LWRs are their combination of relatively low cost, good mechanical properties in thick sections and good weldability. In components of the RCS, such as the pressure vessel, pressurizer and some piping, the carbon and low alloy steels are clad on the inside wetted surface with corrosion resistant materials such as austenitic stainless steels or nickel-base alloys. Thicker pads of alloy 182 have also been welded directly onto the pressure vessel steel in order to act as attachment points for internal structures; the higher yield strength of alloy 182, the thicker section and its known SCC susceptibility raise special concerns for these areas. In these cases it is possible that stress corrosion cracking or thermal fatigue of the austenitic alloy can occur such that the crack tip propagates to the interface between the austenitic and ferritic alloys. The practical questions are therefore; “Will this crack propagate further into the underlying low alloy pressure vessel steel under constant load conditions?”, and ”What is the crack propagation rate vs. stress intensity factor (V/K) disposition relationship relevant to the material, stress and environment conditions?” In cases where the ferritic steels are not clad, the relevant question is “Will a stress corrosion crack initiate (at, for instance, a pit), coalesce with nearby microcracks to form a primary crack, and then propagate to a significant depth?”

In general the resistance of the ferritic materials to transgranular stress corrosion cracking in LWR circuits has been very good, but isolated incidences have occurred. In order to understand the details of these observations, the mechanism of cracking and the associated corrosion system dependencies are discussed in order to (a) put this plant experience in the context of the conjoint conditions of environment, material and stress required to initiate and sustain cracking and (b) to define the predictive capabilities that are necessary in order to identify future areas of concern.

Mechanistic Understanding and Corrosion System Dependencies Governing Stress Corrosion Cracking of Carbon and Low Alloy Steels in LWRs

For a high-aspect ratio crack to advance in aqueous environments it is necessary that a mechanism exists to accelerate and focus the degradation at the strained crack tip. This degradation is generally related to localized oxidation processes at the crack tip, although historically there have been arguments that the degradation may be primarily associated with the production of hydrogen at the crack tip (which is, in turn, related to the crack tip corrosion rate) and its subsequent interaction with the microscopic deformation processes taking place there. There is a further factor, however, and that is that the crack sides must be protected by a film (oxide, salt, etc). If this latter criterion is not met then the incipient crack will degrade to a blunt notch [2-6]. Such requirements for a mechanically driven "electrochemical knife" [2] greatly limit the environmental conditions under which severe susceptibility is possible, and they provide a predictive capability for identifying the potential / pH regions where danger situations may occur in practice. For instance, cracking of carbon and low alloy steels in lower temperature aqueous environments (i.e. below 150°C) that might be representative of LWR service water or ECCS systems under faulted water chemistry conditions, is confined to potential / pH regions where a soluble species ($Fe^{2+,}$ $HFeO_2^-$) can form when a protective magnetite, mixed oxide or salt film in hydroxide, nitrate, carbonate /bicarbonate or phosphate containing solutions is ruptured. A relatively concentrated anionic solution is required for subsequent crack propagation to be significant under these conditions, thereby requiring precursor conditions of, for instance, crevice corrosion or localized boiling to create these high anionic activities. Thus the fact that there are these limiting criteria, indicate why transgranular stress corrosion cracking of carbon and low alloy steels in lower temperature LWR components are relatively rare. However, it should be noted that, in recent years, SCC has been observed in dilute solutions of molybdates and nitrites and in oxygenated water where the metal is cold worked in the 15-20% range or higher, and the temperature is in the range of 90-150°F and higher. As discussed below in relation to service experience, such failures have been observed in tertiary systems of nuclear plants.

In higher temperature PWR primary circuits, the oxide is protective magnetite (Fe_3O_4) but, as will be discussed below, the kinetics of crack propagation at static load of the carbon and low alloy steels under these low potential conditions will generally be low and of little practical importance. Under relatively high purity "normal water chemistry", (oxidizing), BWR water conditions the surface oxide at low temperature is unprotective, and any incipient crack degrades to a non-propagating pit [5]. However at temperatures above approximately 150^0C a highly protective, duplex oxide film of magnetite/haemetite forms and allows the existence of a sharp crack, the propagation of which will depend on a variety of material, stress and environment conditions discussed below.

A considerable amount of attention has been focused internationally on the mechanism and kinetics of crack propagation in the carbon and low alloy steels used in, especially BWR, systems under at-power temperature and coolant chemistry conditions. Unfortunately there is a wide scatter in the stress corrosion crack propagation rate data (Figure B.8.1) [7,8], which poses a practical problem to the design or operational engineer requiring a specific life prediction or crack disposition algorithm (i.e. crack propagation rate (V) vs stress intensity factor (K) relationship) which is technically sound and relevant to his particular plant.

The reason for the scatter in the stress corrosion data in Figure B.8.1 is associated with the fact that the crack propagation rate is controlled by interactions between various system parameters that are not always well defined or controlled in the plant or laboratory experiments. These factors include:

- Stress intensity and mode of stressing e.g., constant load, constant displacement, loading rate, periodic unloading etc.
- Test temperature
- MnS inclusion morphology and dispersion with respect to the crack plane
- Dissolved oxygen content (or, more accurately, corrosion potential as controlled by the coolant flow rate, alloy surface composition, dissolved hydrogen in the coolant, and oxidants such as oxygen, hydrogen peroxide, cupric cations, etc.)
- Solution flow rate past the crack mouth (or, more specifically, the extent to which hydrodynamic conditions permit flushing out of the internal crack environment)
- Solution conductivity (or, more accurately, anionic activity)
- Extent of crack tip constraint, i.e. plane stress vs plane strain
- Yield stress of the material
- Testing time (and sequence of loading changes made during the test)

As a result there has evolved in the testing community a set of "quality control" criteria that can be applied to a given data set to assess their relevance to the conditions in operating Light Water Reactors. [8]

Coincident with these quality control actions, there has been a considerable international effort [7, 9-13] to develop a quantitative understanding of the mechanism of cracking, with the purpose of providing a sound basis for predicting and managing the cracking under the diverse corrosion system parameters listed above.

The hypothesis that has been most widely accepted for crack propagation in the carbon and low alloy steel /LWR water systems is the slip–oxidation mechanism. This mechanism relates crack advance to the enhanced oxidation rate that occurs at the crack tip when the thermodynamically stable and protective oxide film is ruptured by a strain increment in the underlying metal matrix. Once the protective oxide is ruptured, the crack will rapidly advance into the metal but will, within a matter of milliseconds, begin to slow down as the thermodynamically stable and protective oxide reforms at the crack tip. Continued crack advance depends, therefore, on a maintaining a strain rate in the low alloy steel in the vicinity of the crack tip that will allow repeated rupture of the oxide film.

Thus the crack propagation rate, V, is governed by a relationship of the general form;

$$V = A\,(d\varepsilon/dt)_{ct}^{\,n} \qquad (1)$$

where the parameters A and n are related to the dissolution and passivation kinetics at the strained crack tip [11], and $(d\varepsilon/dt)_{ct}$ is the crack tip strain rate, which may be formulated in terms of "engineering parameters such as stress, stress intensity, stress amplitude, loading frequency, etc. [11,12].

Both the dissolution and passivation kinetics on a bare low alloy steel surface depend critically on potential and the anionic activity in the crack tip environment [9,11,14] and these kinetics are bounded asymptotically by two limiting conditions associated [15] with the maintenance of either <20 ppb or >0.5 ppm S^{2-}. (Note that earlier investigations focussed primarily on the deleterious effect of sulfur-rich anions; more recent investigations indicate that chloride anions will also affect the crack propagation rate). This, in turn, leads to a predicted range in V vs.$(d\varepsilon/dt)_{ct}$ responses which are bounded by the "high" and "low" sulfur lines;

$$\text{“High Sulfur”} \qquad V = 2.25 \times 10^{-3}\,(d\varepsilon/dt)_{ct}^{\;0.35} \qquad mm.s^{-1} \tag{2}$$

$$\text{“Low Sulfur”} \qquad V = 10^{-1}\,(d\varepsilon/dt)_{ct}^{\;1.0} \qquad mm.s^{-1} \tag{3}$$

As can be seen in Figure B.8.2 the theoretical bounding crack propagation rates described by Eq. 2 are not maintainable at the lower $(d\varepsilon/dt)_{ct}$ values, which are pertinent to creep rates under constant load or displacement conditions. The divergence from the maximum theoretical rates depends on the dissolved oxygen content and flow rate of the water. One reason for these divergences relates to the origin of the dissolved sulfur and other anions at the crack tip which can control the crack tip oxidation rate. As illustrated schematically in Figure B.8.3, the crack tip concentration of anions that originated in the bulk environment will be governed by the anionic concentration in the bulk environment and the mass transport mechanisms governed by convection, Fickian (i.e. concentration gradient) and potential gradient considerations within the crack. However, the concentration of sulfur-rich anions will be controlled not only by these specific mass transport mechanisms, but also by the rate of introduction of dissolvable MnS precipitates to the crack tip solution as the advancing crack tip exposes them to the crack tip solution. Thus it is predicted and observed that the crack propagation rate will be a sensitive function of, for example, the corrosion potential (Figure B.8.4), flow rate of the water past the crack mouth, the bulk anion concentration and, finally, the MnS size, shape and distribution. If the crack propagation rate falls below a critical value, such that a dissolved sulfur activity >0.5ppm S^{2-} cannot be maintained, then crack arrest may well occur in high purity water (i.e. no other anionic purities present).

The achievement and maintenance of crack propagation rates associated with the "high sulfur" rates depends not only on the maintenance of a high crack tip sulfur activity but also on the maintenance of a sustainable crack tip strain rate. The conjoint engineering system conditions that will achieve all these criteria will be met by combinations of;

- High sulfur content steels, mainly in the form of MnS inclusions
- High corrosion potentials
- Stagnant or low flow rate water
- Highly impure water conditions, primarily chloride
- Unconstrained plane stress crack tip conditions

It is interesting therefore to note that the extremely high propagation rates that have been recorded by some laboratories [17-21] where combinations of the above system criteria have been met, are in agreement with the predicted "high-sulfur" rates (Figure B.8.1).

$$V = 9.6 \times 10^{-8} K^{1.4} \quad \text{mm.s}^{-1} \tag{4}$$

with K in units of MPa√m

These combinations of conditions do not exist generally in operating LWRs. For PWRs (and for the majority of the pressure vessel of BWRs on hydrogen water chemistry or Noblechem^{TM}) the low corrosion potential effectively preclude stress corrosion crack growth at rates that could be of any engineering significance. Under conditions more symptomatic of BWRs operating under "normal water chemistry" the crack propagation rates are generally lie below the "low sulfur" line; i.e.

$$V = 3.29 \times 10^{-14} K^{4} \quad \text{mm.s}^{-1} \tag{5}$$

with K in units of MPa√m

The comparisons between observation and theory in this case are shown in Figure B.8.5 for an older data base [9] where a variety of loading conditions have been applied, and in Figure B.8.6 [8] for a constant load data set from one laboratory [21-23] that has been screened for data quality. In these cases it is seen that, in general, the "low sulfur" line bounds the data sets, except at high stress intensity factors (a point that is addressed later).

It should be emphasized that the "low sulfur" propagation rates defined by Eq. 5 are limiting values and the reason for this is that, in addition to maintaining a given dissolved sulfur activity at the crack tip, it is also necessary to maintain the crack tip strain rate. As discussed elsewhere [11, 12, 24-26], the formulation of the crack tip strain rate in terms of engineering parameters (stress intensity, yield stress, etc) has been the source of much international debate, which is still not finally resolved. However certain ruling concepts are understood and accepted, and it is expected that, under constant load or displacement conditions, the crack tip strain rate will decrease according to a logarithmic creep relation of the general form;

$$(d\varepsilon/dt)_{ct} = B.(C\sigma^{m}).\ t^{-1} \tag{6}$$

where σ is the tensile stress

Thus, there are two phenomena that indicate that the stress corrosion cracks may arrest under certain system conditions; the first is due to the lack of maintenance of a critical dissolved sulfur content at the crack tip, referred to earlier, and the second is the lack of maintenance of the crack tip strain rate under constant load. In fact [26-28], crack arrest is frequently observed (Figure B.8.7) [26] and, as analyzed by Laepple [28], the deceleration rate approximates the predicted t^{-1} rate in high purity BWR environments

Taking into account that there is an observed and understood tendency for crack arrest under closely controlled water chemistry purity (with no significant transients) and constant load conditions, the engineering judgment [29-32] is that, for disposition purposes, the crack propagation under full power operations is given by;

$$V = 2x10^{-8} \quad mm.s^{-1} \qquad (7)$$

up to a stress intensity factor of 55 MPa√m . Above this K_1 level, but also below it (Figure B.8.8) in the case of either water chemistry transients or slight load variations, the low sulfur line of Eq. 5 is considered more appropriate.

It should be emphasized that, although crack arrest is both predicted and observed, this may be counteracted by other material/environment/stressing factors and, thereby, may challenge the appropriateness of the disposition relations in Eq. s 5 and 7 when the strict water chemistry and loading caveats associated with these equations are violated [32]. Such factors may be categorized as those that increase the effective crack tip strain rate and/or markedly increase the crack tip anionic impurity concentration. Examples of the former factor include;

- Enhanced crack tip plasticity due to a loss of plastic constraint. This concern is illustrated in Figures B.8.6 and 8 by the increase in crack propagation at stress intensity values beyond that where plane strain constraint to the crack tip plasticity is largely overcome. For usual laboratory specimens this is limit is defined as K values > 55 MPa√m. [22,23,26]. In large section pressure vessel components it is unlikely that this plane strain related criterion would be exceeded, but it may be a factor to be considered in thin section components.

- Further factors that may increase the effective crack tip plasticity and hence maintain the crack propagation rates beyond those defined by Equations 5 and 7 are major increases in yield strength or hardness and/or in the degree of dynamic strain aging. The former effect has long been noted in the field of stress corrosion. As indicated in Figure B.8.9, the hardness effect on cracking susceptibility under constant load in oxygenated water is relatively minor over the hardness range associated with LWR pressure vessel steels, but a significant increase in susceptibility is observed should the heat treatment be such as to produce a (hard) martensitic microstructure [33].

- The effect of discontinuous yielding at a crack tip, which effectively increases the crack tip strain rate, and thereby the stress corrosion susceptibility, has been demonstrated in a variety of other cracking systems. The possibility of dynamic strain aging (DSA) having such an accelerating effect on the cracking of low alloy steels in LWR systems has been demonstrated by a number of investigators [33-38]. This opens up the question of the definition of allowable compositional limits for the low alloy steel, (mainly aluminum and nitrogen), and the resultant temperature ranges where the increase in cracking susceptibility is most marked.

This latter aspect is of particular importance with respect to evaluating the susceptibility of, for example, feedwater piping which may operate in the temperature range 220-250^{0}C rather than at 288^{0}C where the majority of investigations have been focused. The cracking susceptibility can maximize in this lower temperature region under cyclic, monotonically increasing strain as well as static loading conditions; historically this peak in the susceptibility has been attributed to a balance between the expected thermal activation of the corrosion processes fundamental to the crack propagation mechanism, and the changes in corrosion potential with temperature, especially at dissolved oxygen contents in the water less than 400ppb. This added contribution due to DSA is not yet fully evaluated

- Transient loading condition. It has long been recognized that small repeated transients in loading (eg "ripple loading") can accelerate crack propagation due to the Bauschinger effect that leads to enhanced plasticity at the crack tip. This is illustrated in Figure B.8.10 for laboratory tests involving high R (ratio of minimum stress intensity to maximum stress intensity) loading [33]

As emphasized earlier, the crack tip chemistry is of vital importance in defining the cracking susceptibility, and this impacts on the required degree of water purity control during steady state operation, and the control of the magnitude and duration of water chemistry transients. Of particular importance is the extent of chloride transients since, as illustrated in Figure B.8.11, chloride transients, in marked comparison with sulfate transients, may give extremely high sustainable crack growth rates approaching the theoretical maximum values defined by Eq. 4; it should be noted that although the chloride transient (to 49 ppb) illustrated in Figure B.8. 11 would be excessive for current BWR operating conditions and would have triggered an orderly plant shut down action, lower level transients (to10 ppb) also lead to significantly increased crack propagation rates [32].

Service History

In the 1970's there were numerous occurrences of *intergranular* stress corrosion cracking of low alloy NiCrMoV steels in steam turbine wheels and, to a lesser extent turbine rotors. The specific cracking locations were primarily regions of high stress (due to wheel shrink-on and centrifugal stresses) and creviced regions such as keyways or blade attachment where stress localization and contaminant concentration was possible. Initially these cracking incidents were primarily in fossil fired plant in low pressure stages where steam condensation was possible, but since the mid to late 1970s cracking has been noted in lower temperature PWR and BWR driven turbines. These incidents have been widely reported and discussed [39-42]. It is significant, however, that many of the mechanisms-based concepts discussed above are of relevance. For instance, the narrow potential range for cracking associated with caustic cracking and the aggravating role vis à vis cracking susceptibility of contaminants such as chloride, sulfide (from lubricant), the presence of dissolved oxygen or other oxidants (e.g. Cu^{2+}), increased surface hardness due to abusive reaming of keyways and, finally, high yield strength associated with the bainitic or martensitic structures. Thus these earlier experiences act as an historical guide to understanding service failures in the systems of interest in this topical report that occurred in the late 1970s and early 1980s.

The accumulated operating experience and performance of the ductile carbon and low alloy steels in the majority of LWR systems has been very good worldwide and this is likely to continue. The reason for this optimistic statement is that the primary system in PWRs operates at low corrosion potentials, and the same observation applies to the vast majority of BWRs (in the US) that are currently operating under hydrogen water chemistry and/or noble metal addition (e.g."NobleChem^{TM}") conditions; these factors ensure that there is a considerable margin in corrosion potential (see Figure B.8.4) before transgranular cracking would be expected.

There is cause for concern, however, in the PWR secondary systems for although they also operate at low corrosion potential (which is very strictly applied because of concerns that a more oxidizing potential will aggravate corrosion problems with alloy 600 tube bundles), there is a higher risk of oxidizing corrosion potentials in the event of persistent leaks at interfaces with the environment, particularly in the condenser. There are also concerns for BWRs not consistently on hydrogen water chemistry, since cracking may be possible under more oxidizing conditions, especially if there are other aggravating factors. Indeed there have been two relatively major classes of cracking incidents of unclad carbon or low alloy steel components in operating LWRs that illustrate these concerns; cracking of carbon steel BWR feedwater piping due to strain-induced cracking, and cracking of PWR steam generator girth welds due primarily to water chemistry transients. These are discussed below in order to lay the basis for the next section that evaluates the potential erosion of margins due to evolving fabrication (or repair) and operational practices.

Strain-Induced Cracking of Steam, Feedwater and Condensate Piping

The cracking of steam, feedwater and condensate piping systems due to strain-induced stress corrosion has been extensively analyzed [1, 43-45] for German BWRs where these components have been fabricated with relatively fine-grained, higher-strength steels (WB 35, WB36) that allow the use of thinner walled piping without stress relief treatment of the welds. The features that aggravated the cracking susceptibility in these incidents were;

- *Dynamic straining* associated with, for instance, reactor start-up or thermal stratification during low feedwater flow or hot standby conditions. Such operations lead to a wide range of applied strain rates [46] that may be as high as 10^{-4} s^{-1}, and would be expected to increase the crack propagation rate (see Figure B.8.2).
- *High local stress* at or above the high temperature yield stress, thereby giving a lack of plastic constraint at the incipient crack tip, and consequently an anomalous increase in crack propagation rate (see Figures B.8.6 and 8) due to the effective increase in crack tip strain rate. Such high local stresses were attributed in the

failure analyses to weld defects (e.g. misalignment of weld edges, presence of root notches, etc), piping fit-up stresses and, in some cases inadequate pipe support at elbows. The combination of this high stress adjacent to the weld and the high applied strain rate led to a distribution of multiple cracks around the circumference of the pipe that was no longer confined by the asymmetric azimuthal distribution of weld residual stresses. These cracks propagated on separate planes and did not interlink, thereby potentially alleviating concerns about "leak before break" safety analyses that would be raised for a fully circumferential crack propagating evenly through the pipe wall.

- *Oxidizing* conditions, in conjunction with intermediate temperatures and potential anionic impurities. The affected piping generally operates in the temperature region 220^0C -250^0C where, as discussed earlier, the cracking susceptibility is at a maximum. Moreover, cracking was often observed in stagnant steam lines where. the dissolved oxygen concentration may be in excess of 100ppb well in excess of the 30ppb quoted to be the "threshold" value above which strain-induced cracking is to be expected in these steels at 250^0C [47]; note that, as with the majority of EAC phenomena, the quotation of a firm "threshold" parameter (stress/strain rate, corrosion potential, anionic activity, temperature, etc.) is open to discussion, since the value defined will depend on the other relevant corrosion system parameters. This conjunction of environmental factors was further aggravated by the fact that during reactor shut-down stagnant water was sometimes left exposed to air in horizontal portions of piping; pitting and general corrosion occurred under these low temperature conditions, and these pits were observed to act as crack initiators during subsequent power operation conditions.

Stress Corrosion Cracking of Steam Generator Girth Welds

Very similar aggravating factors have been observed in transgranular cracking incidents in Model 44 and 51 designs of Westinghouse steam generators, starting with an isolated occurrence in Europe which was followed in 1982 with a well analyzed cracking incident at the Indian Point-3 PWR after approximately three effective full–power years. This cracking occurred at the upper shell to cone girth weld and was extensive with over a hundred circumferential cracks propagating to a maximum of 25mm. The cracking was attributed primarily to stress corrosion cracking with a component due to fatigue [48]. Similar incidents were subsequently observed at other US and European PWRs plants [49].

As with the case with the strain–induced cracking cases discussed above for the higher strength steels in German BWRs, the cracking in the PWR steam generator manufactured with lower strength SA 302 grade B weldments and SA 533 grade B plate steels, was aggravated by the fact that the weld was subjected to significant dynamic thermal stresses, in this case due to the fact that the incoming feedwater at 204-227^0C was impacting on the hotter steam generator shell before mixing with the steam generator recirculating water. Moreover in the affected plants this particular weld was the final closure weld, with a localized stress relief being applied; subsequent hardness measurements indicated that this stress relief had not been fully effective. Finally, with respect to the stress/strain rate conditions, there had been extensive weld repairs applied at Indian Point-3, an operation which has been widely associated with premature cracking in, for instance, nickel base alloys in PWR primary components due to the attendant weld residual stresses.

Start-up operations in many of the cracking cases for this component involved the introduction of auxiliary feedwater from the condensate storage tank (CST) into the steam generator; unfortunately this water was aerated, since a nitrogen blanket was not applied to the CST. This deleterious oxidizing condition (Figure B.8.4) was exacerbated by the presence of Cu^{2+} associated with corrosion of the brass condenser tubes. Such oxidizing conditions promoted pitting, which, in turn acted as initiation sites for the stress corrosion cracks and poor chemistry control may also have increased the crack propagation rate.

Thus the unusual circumstances behind the cracking in these incidents were the conjoint presence of oxidizing secondary water conditions, high residual stress with a component of dynamic straining and a strong indication of high hardness due to inadequate stress relief.

Stress Corrosion Cracking in Tertiary Systems

Certain tertiary systems, which are fabricated of carbon steel such as the component cooling water system, have sustained SCC in the range of 90-150°F within times in the range of 5-10 years. Such SCC has perforated the walls especially at the higher range of temperature. These systems sustain such SCC in normal aerated chemistry with various inhibitive additives, within their nominal concentrations, such as molybdate and nitrite. Such SCC occurs where residual stresses are high due to fabrication, i.e. elbows, or at welds.

Observations of SCC in carbon steel in oxygenated water in this low range of temperature have been observed at least in six plants. However, these systems are not extensively inspected. Also, there are possibly ten different water chemistry treatment programs among the world utilities. There may be some interaction with MIC in some cases, but SCC can occur without the MIC and MIC does not always occur.

Other Cases

There have been other reported incidences of environmentally-assisted-cracking of carbon and low alloy steel in, especially, BWRs. The most significant of these have been cracks at nozzles associated with mixing of lower temperature water with hot water in a vessel, i.e., thermal fatigue cracks in BWR reactor vessel feedwater nozzles and control rod drive return line nozzles [50-54]. Although a component of SIC or stress corrosion cracking might be appropriate, it is apparent that the dominating degradation mechanism in these cases was corrosion fatigue, and discussion of these incidents is given in the fatigue topical report.

Other potential cracking incidents have been reported but have been either isolated in occurrence or inadequately analyzed to allow a positive attribution to stress corrosion cracking. For instance, a through-wall crack developed in the low alloy steel wall of an early BWR (Garigliano) secondary steam generator channel head. The crack appeared to have grown due to SCC and was attributed to the presence of cracks in the Alloy 400 type cladding (Alloy 190 weld metal) that acted as initiating sites for the SCC in the base material, combined with high residual stresses due to an ineffective post weld heat treatment and, possibly, to an unusually high dissolved oxygen content in this unique BWR design.

In addition, a few flaw indications have been detected in vessel base materials by UT performed for baseline or in-service inspections, e.g., due to laminations or inclusions in the steel plates or forgings. The base material flaws have rarely if ever required repair. There appear to be no reported cases of service-induced growth of flaws present in the base plates or forgings. Finally, significant numbers of cracks have developed in the cladding of BWR reactor vessel heads. In some cases, the cracks have penetrated short distances into the low alloy steel base material. This cracking has required significant inspection and analysis to demonstrate the continued safe condition of the affected parts. In a few cases it has been concluded that the cladding cracks may have penetrated into the base material as the result of service, but it appears more likely that such ***penetration occurred during fabrication.***

Concerns Associated with Lack of Predictive Knowledge in Conjunction with Changing Operational Practices

There is no question that our capability to predict the changes in stress corrosion or strain-induced cracking of carbon and low alloy steels in LWRs due to the effects of materials, environment and stressing modes has significantly improved over the last 20 years. Prior to that time we would not have been able to quantitatively rationalize the cracking response of safety related components and thereby define appropriate remedial actions beyond qualitative judgments to “reduce stress”, improve chemistry control”, etc. Consequently we under stand in some quantitative detail the reasons why it is relatively hard to initiate and propagate stress corrosion cracks in carbon and low alloy steels in LWRs operating under good water chemistry control. We also understand many of the “upset” operating conditions that might give cracking, and these are generally met for the few instances where cracking in the plant has been observed.

However the bar is rising as reactors (in the US) apply for license renewal, power uprate, extended fuel cycles (and therefore increased inspection periods) and, possibly, limited load following. All of these changes potentially increase the danger of undetected stress corrosion degradation. Items of concern that need research attention in order to reduce that risk for stress corrosion (and strain-induced cracking) of carbon and low alloy steels include:.

- A quantification of the sequential actions of pit formation, microcrack initiation and coalescence, followed by “short” and then “long” crack propagation. This sequence is well recognized in carbon and low alloy steels and has been quantified for gas pipelines. Such quantification has not been conducted for the nuclear systems. It is known that cracks may accelerate or arrest during this sequence; the quantification of this is inherent to the prediction of cracking of unclad ferritic piping

- The propagation rates are, in general, reasonably well understood; There are, however, some system parameters that can affect these rates, but which are insufficiently characterized at this time. Until this is done, the industry is open to unforeseen incidents. Prime examples include;

    - Ripple loading. As indicated in Figure B.8.10, ripple loading can significantly increase the crack propagation rate above the current disposition value, but we do not know the full extent (in terms of amplitude and periodicity) of these effects.

    - Dynamic strain aging. This is also a recognized effect, but insufficiently characterized. This has a direct impact on the definition of the maximum temperature for cracking degradation and on the compositional specifications for the steel. This latter aspect is of particular importance since steel manufacturers globally are modifying steel compositions (and in particular Al and N contents) in order to improve toughness together with higher yield stress. It imperative that such mechanical property driven changes also account for potential changes to the EAC resistance.

    - Heat affected zone (HAZ) anomalies. IGSCC in the weld HAZ is well recognized in austenitic alloys for a variety of material and local stress/strain reasons. There is not a similar understanding of the potential increases in crack propagation rate in the HAZ of carbon and low-alloy steels.

    - IGSCC of Carbon and Low Alloy Steels. IGSCC of higher strength bainitic steels used in steam turbines is a recognized phenomenon. The incidence of IGSCC in carbon and low alloy steels in the LWR system has not, however, been widely observed, leaving the possibility that there may be unrecognized and potentially kinetically faster degradation modes under very specific operating and material conditions. There has been a recent isolated incidence of such cracking in a CANDU feeder elbow [55] that was associated with higher than normal hardness and residual stress associated with cold bending; flow assisted corrosion was also observed at the (assumed) crack initiation site. Moreover laboratory information [56] indicates that IGSCC is possible in higher hardness HAZs at temperatures < 265^{o}C. It is necessary, therefore, to evaluate this degradation mode with respect to the relevant system variables, with some attention to potential synergisms with flow assisted corrosion and the associated hydrogen production.

References

[1] J. Hickling, D. Blind, "Strain-induced corrosion cracking of low-alloy steels in LWR systems – Case histories and identification of conditions leading to susceptibility", Nuclear Engineering and Design, 91, pp. 305-330, (1986).

[2] T.R.Beck Corrosion, 30, 408,1974

[3] T.P Hoar "Theory of Stress Corrosion Cracking" Ericiera, Portugal, March 1971, p106, Pub. NATO, Brussels, Ed. J.C.Scully

[4] R.N.Parkins "Stress Corrosion Cracking" in "Environment – Induced Cracking of Metals", Kohler Oct 2-7 1988 pp 1-19, Ed R.P.Gangloff & M.B.Ives. Pub NACE

[5] F.P.Ford in "BWR Environmental Cracking Margins for Carbon Steel Piping" General Electric Report NEDC24625, January 1979

[6] F.P. Ford, "Stress-Corrosion Cracking", chapter in "Corrosion Processes" (Ed. RN Parkins), (Pub. Applied Science Publishers, 1982). ISBN 0-85334-147-8.

[7] F.P. Ford, "Status of Research on Environmentally-Assisted Cracking in LWR Pressure Vessel Steels". Proc. of ASME/PVP Conference, San Diego, CA, June 28-July 2, 1987 (Ed. R. Rungta), ASME PVP119, pp. 43-62.

[8] J. Hickling: "Evaluation of acceptance criteria for data on environmentally.assisted cracking in Light Water Reactors" SKI Report 94:14 from September 1994

[9] F.P. Ford, "Environmentally Assisted Cracking of Low Alloy Steels" EPRI/report NP7473L, January 1992, EPRI Contract C102-1.

[10] P.M. Scott, "A Review of Environmental Effects on Pressure Vessel Integrity," Proc.of Third International Symposium on Environmental Degradation of Materials in Nuclear Power Systems/Water Reactors, Traverse City (August 1987).

[11] F.P. Ford, D.F. Taylor, P.L. Andresen and R.G. Ballinger: "Corrosion-Assisted Cracking of Stainless and Low-Alloy Steels in LWR Environments" EPRI Contract RP2006-6, Report NP5064M, (February 1987).

[12] F.P. Ford, Trans ASME J.of Pressure Vessel Tech. 110, 2, 113-128, (1989).

[13] F.P. Ford, P.L.Andresen, D.Weinstein, S.Ranganath and R.Pathania "Stress Corrosion Cracking of Low Alloy Steels in High Temperature Water "Proceedings of 5th International Environmental Degradation of Materials in Nuclear Power Systems, Monterey, August 1991, p. 561-569.

[14] P. Combrade "Prediction of Environmental Crack Growth in Nuclear Power Plant Components" . Final Report of EPRI Contact RP2006-1 and RP2006-8.

[15] L.Young, P.L.Andresen, " Crack Tip Microsampling and Growth Rate Measurements in a 0.01%S Low Alloy Steel", Proceedings of 7th International Environmental Degradation of Materials in Nuclear Power Systems, Breckenridge, August 1995, p.1193-1204.

[16] R.C. Cowan, et.al. "The ICCGR Interlaboratory Round Robin on Slow Strain Rate SCC of PWR Forging", From Proc.of Second International Atomic Energy Agency Specialists Meeting on Subcritical Crack Growth, Sendai Japan, NUREG CP-0067 (May 15-17, 1985) pp. 181-197.

[17] K. Kussmaul, et. al., Int. J. Pressure Vessels and Piping 25, pp. 111-138 (1986).

[18] M.O. Speidel and R. Magdowski, Intl. J. Pressure Vessels & Piping 34, 119-142, (1988).

[19] E. Tenckhoff, M. Erve, E. Lenz and G. Vazoukis: Nuclear Eng.& Design 119, 371-378, 1990.

[20] K. Matocha, V. Hluchan, J. Wozniak, I. Jiricek and J. Vosta "Environmentally-Assisted Cracking of Steam Generator Pressure Vessel Steel in High Temperature Water". Proc. Of Third International Atomic Energy Agency Specialists Meeting on Subcritical Crack Growth, Moscow, USSR, (May 1990).

[21] K. Kussmaul & B. Iskluth:"Environmentally assisted crack growth in a low alloy boiler steel in high temperature water containing oxygen" Nucl. Eng. & Design, 119, (1990), 415-430

[22] K. Kussmaul, D. Blind & V. Läpple:"New observations on the crack growth of low alloy nuclear grade ferritic steels under constant active load in oxygenated high-temperature water" Nuclear Eng. and Design, 168 (1997) 53-75.

[23] V. Läpple, D. Blind & P. Deimel: "Stand der Forschung zum korrosionsgestützte Rißwachstum niedriglegierter ferritischer Stähle in sauerstoffhaltigem Hochtemperaturwasser" VGB-Konferenz "Chemie im Kraftwerk 1996", October, 1996.

[24] R.N. Parkins, G.P. Marsh and J.T. Evans: "Strain Rate Effects in Environment Sensitive Fracture", Proceedings of EPRI Conference on "Predictive Methods for Assessing Corrosion Damage to BWR Piping and PWR Steam Generators", Mt. Fuji, Japan, May/June 1978. Eds. H. Okada and R. Staehle. Pub. NACE (1982).

[25] T Shoji "Progress in Mechanistic Understanding of BWR SCC and Implication to predictions of SCC Growth Behaviour in Plants", . Proceedings of Eleventh International Conference on Environmental Degradation in Nuclear Power Systems – Water Reactors. Skamania Lodge August 5-9, 2003. Eds. G.Was, L. Nelson Published by American Nuclear Society.

[26] J.Heldt, H-P Seifert " The Stress Corrosion Cracking of Reactor Pressure Vessel Steel under BWR Conditions" Proceedings of 9th Environmental Degradation of Materials in Nuclear Power Systems Conference. Newport Beach 1999 pp 901-910

[27] D. Weinstein, et al.:"Stress Corrosion Cracking in low alloy steels, Interim Technical Report" GE Nuclear Energy Report on EPRI Contract.No. RP C102-4, dated February 1994

[28] V. Laepple: "Einfluß von Probengeometrie und Belastungsart auf das Bedingungen. korrosionsgestützte Rißwachstum niedriglegierter ferritischer Stähle unter SWR-Zusatzauftrag: Auswertung des EPRI-Forschungsberichtes RPC 102-4 und Vergleich mit Korrosionsergebnissen der MPA Stuttgart" MPA/VGB Forschungsvorhaben 3.1.2.5; MPA Auftrags Nr 944 703 700 February 1997.

[29] R.Pathania et al "Stress Corrosion Cracking in Low Alloy Steels" EPRI Report RPC 102-4, EPRI Palo Alto CA USA February, 1994

[30] "BWR Vessel and Internals Project; Evaluation of Stress Corrosion Cracking in Low Alloy Steel Vessel Materials in the BWR Environment (BWRVIP-60)" , March 1999. Submission from EPRI - BWRVIP to USNRC.

[31] F.P.Ford, R.M.Horn, J.Hickling, R.Pathania, G.Bruemmer, “Stress Corrosion of Low Alloy Steels under BWR Conditions; Assessment of Crack Growth Rate Algorithms”, Proceedings of 9th Environmental Degradation of Materials in Nuclear Power Systems Conference. Newport Beach 1999, pp.855-869

[32] J.Hickling, H-P. Seifert, S Ritter “Research and Service Experience with Environmentally Assisted Cracking of Liw Alloy Steel” , Power Plant Chemistry7(1) pp.4-15, 2005

[33] H.P.Seifert and S. Ritter “New Observations of the SCC Crack Growth Behaviors of Low-Alloy RPV Steels under BWR/NWC Conditions”, Proceedings of 11th Environmental Degradation Conference. Stevenson August 2003, pp 341-350

[34] H.Hanninen et al, “Effects of Dynamic Strain Aging on Environment-Assisted Cracking of Low Alloy Pressure Vessel and Piping Steels” Proceedings of10th Environmental Degradation of Materials in Nuclear Power Systems Conference. Lake Tahoe,August 2001, pp 341-350

[35] H.D.Solomon, R.DeLair , E.Tolksdorf , “LCF Crack Initiation in WB 36 in High Temperature Water”, Proceedings of 9th Environmental Degradation of Materials in Nuclear Power Systems Conference. Newport Beach 1999, pp. 865-874

[36] J.Hickling, “Strain Induced Cracking of Low Alloy Steels under BWR Conditions; are there still open issues”, Proceedings of 10th Environmental Degradation of Materials in Nuclear Power Systems Conference. Lake Tahoe, August 2001.

[37] J.D. Atkinson, J.Yi “The Role of Dynamic Strain Aging in the Environment Assisted Cracking Observed in Pressure Vessel Steels” Fatigue,Fracture Eng.Mater. Struct. Vol 20,pp1-12,1997

[38] H.D.Solomon, R.E.DeLair “The Influence of Dynamic Strain Aging on the Low Cycle Fatigue Behaviour of Low Alloy and Carbon Steels in High Temperature Water“, Proceedings of 10th Environmental Degradation of Materials in Nuclear Power Systems Conference. Lake Tahoe, August 2001.

[39] Hodge J.M., Mogford I.L. UK Experience of Stress Corrosion Cracking in Steam Turbine Discs). Proceedings of Inst. Mech Eng. Vol.193, No.11, 93 1979.

[40] Lyle F.F., Burghard H.C. Materials Perf. Vol.21, 11, pp35-44, Nov. 1982

[41] M.O.Speidel “Stress Corrosion Cracking of Steam Turbine Steels” Proceedings of 2nd Environmental Degradation of Materials in Nuclear Power Systems Conference.Monterey, September, 1985 pp 267-275.

[42] F.F.Lyle, A.McMinn , G.R.Leverant “Low Pressure Steam Turbine Disc Cracking – an Update” Proceedings of Inst. Mech Eng. Vol.199, pp 59-67, 1985.

[43] H.P.Seifert, S Ritter, J. Hickling “ Environmentally-Assisted Cracking of Low Alloy RPV and Piping Steels under LWR Conditions”, ”, Proceedings of 11th Environmental Degradation of Materials in Nuclear Power Systems Conference. Stevenson August 2003, pp 73-89.

[44] E.Lenz, N.Weiling Nucl.Eng. Design Vol.9 pp331-344, 1986

[45] H.P Seifert, S. Ritter, J. Heldt “ Strain-Induced Corrosion Cracking of Low Alloy RPV Steels under BWR Conditions”, “, Proceedings of 10th Environmental Degradation of Materials in Nuclear Power Systems Conference. Lake Tahoe, August 2001.

[46] F.P.Ford, S.Ranganath, D.Weinstein “Environmentally-Assisted Cracking Fatigue Crack Initiation in Low Alloy Steels – A Review of the Literture and the ASME Code Requirements” EPRI TR-102765, EPRI Palo Alto CA USA 1993.

[47] T.Aria et al, Paper 140 NACE Corrosion Conference 1998.

[48] W.J.Bamford, G.V.Rao, J.L.Houtman “Investigation of Service –Induced Degradation of Steam Generator Shell Materials” Proceedings of 5th Environmental Degradation of Materials in Nuclear Power Systems Conference.Monterey, August,1992.

[49] NRC Information Notice No. 90-04, "Cracking of the upper shell to transition cone girth welds in steam generators", (1990).

[50] R. Snaider, BWR Feedwater Nozzle and Control Rod Drive Return Line Nozzle Cracking: Resolution of Generic Technical Activity A-10 (Technical Report), NUREG-0619-REV-1, Nov. 1980.

[51] B. M. Gordon and G. M. Gordon, "Corrosion in Boiling Water Reactors," Metals Handbook, Volume 13, Corrosion, p927-937, ASM International, 1987.

[52] B. M. Gordon, D. E. Delwiche, and G. M. Gordon, "Service Experience of BWR Pressure Vessels," Performance and Evaluation of Light Water Reactor Pressure Vessels, PVP-Vol. 119, p9-17, ASME, 1987.

[53] N. G. Cofie, et al., Evaluation of Stress Corrosion Crack Growth in Low Alloy Steel Vessel Materials in the BWR Environment (BWRVIP-60), EPRI TR-108709, March 1999.

[54] R. Snaider, BWR Feedwater Nozzle and Control Rod Drive Return Line Nozzle Cracking: Resolution of Generic Technical Activity A-10 (Technical Report), NUREG-0619-REV-1, Nov. 1980.

[55] A Celovsky et al. “S-08; Investigation and Repair of a Cracked Feeder at Point Lepreau GS” CANDU Maintenance Conference., 2000

[56] Nakayama G., Akashi M “Effects of Test Temperature and Hardness of Material on the Intergranular Stress Corrosion Cracking Behavior of Carbon Steel in a Simulated BWR Environment”. Proceedings of 8th Environmental Degradation of Materials in Nuclear Power Systems Conference.Amelia Island, August 1997, pp947-952.

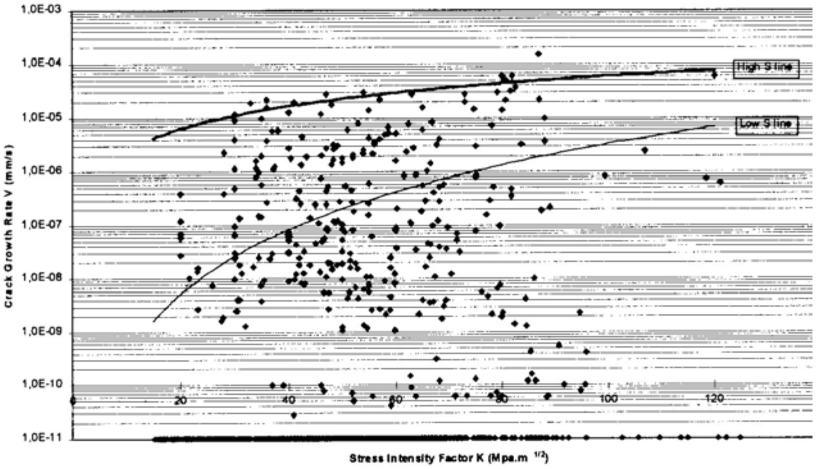

Figure B.8.1 Crack propagation rate vs. stress intensity factor data for low alloy steels in "BWR" water at 288^{0}C (8). Note that there must be a sound technical basis for the choice of the indicated disposition relationships.

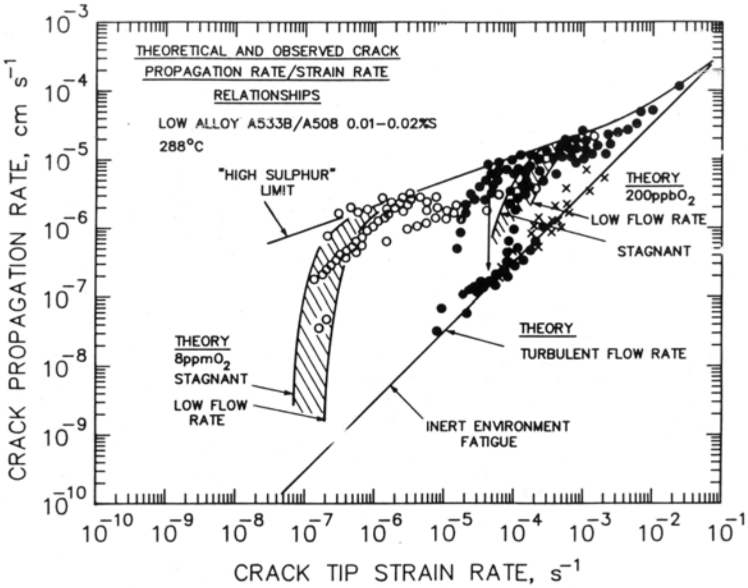

Figure B.8.2 Observed and theoretical crack propagation rate / crack tip strain rate relations for low alloy steel in 288^{o}C water at various corrosion potentials (9,12). The strain rate values are pertinent to tests conducted under corrosion fatigue (at the higher end), slowly increasing applied strain, and constant load creep (at the lower end).

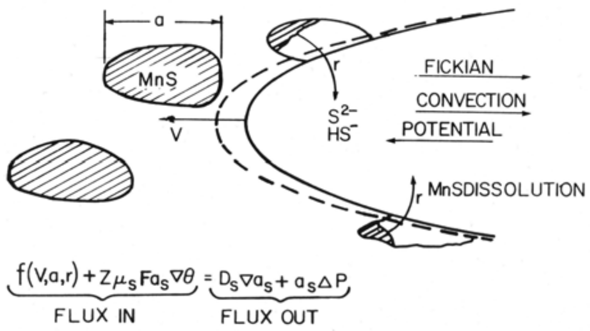

Figure B.8.3 Schematic of crack tip illustrating the relationship between the MnS precipitate morphology and the advancing crack tip, and the various mass transport phenomena that will control the anionic activity at the crack tip

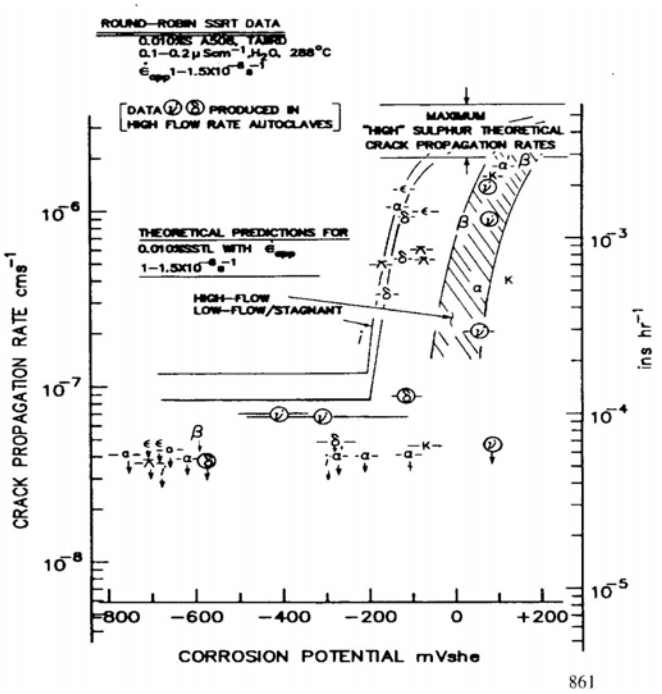

Figure B.8.4 Observed (16) and theoretical (9) dependency of the average stress corrosion crack propagation rate on corrosion potential for 0.010% sulfur A508 steel strained at 1-1.5 x 10 $^{-6}$ s.$^{-1}$ in 288^{o}C water with conductivity of 0.02µS. cm $^{-1}$

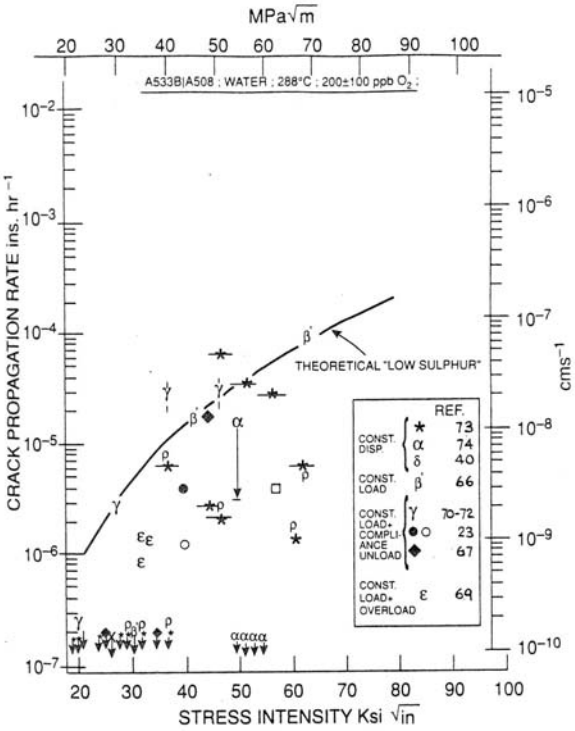

Figure B.8.5 Theoretical "low–sulfur" crack propagation rate vs. stress intensity relationship (Eq. 5) compared with selected laboratory data obtained in 288°C water containing 200 ppb oxygen, and stressed under constant load, constant displacement or constant load with periodic cycling conditions (9)

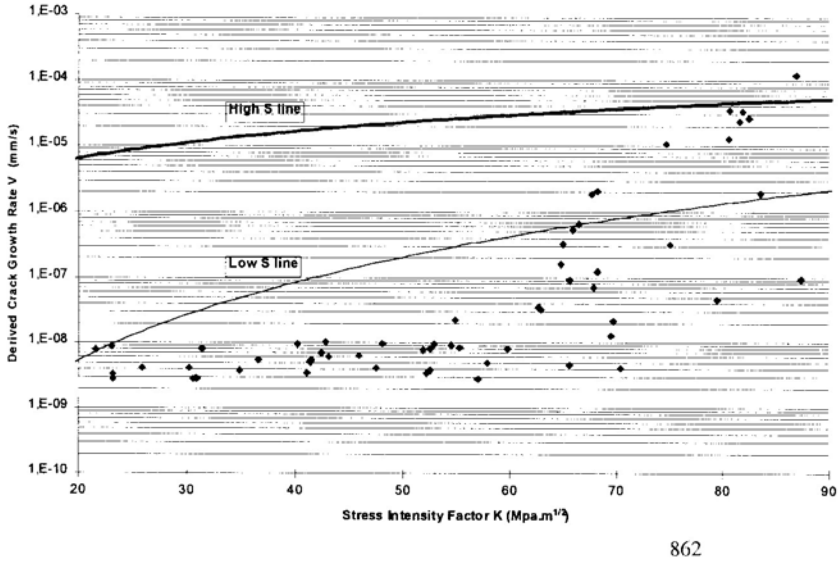

Figure B.8.6 Observed (21-23) crack propagation rates, screened for quality (8), obtained under constant load for low alloy steels in 240°C water with 0.4 or 8.0 ppm oxygen. These data are compared with the theoretical relationship in Eq. 5.

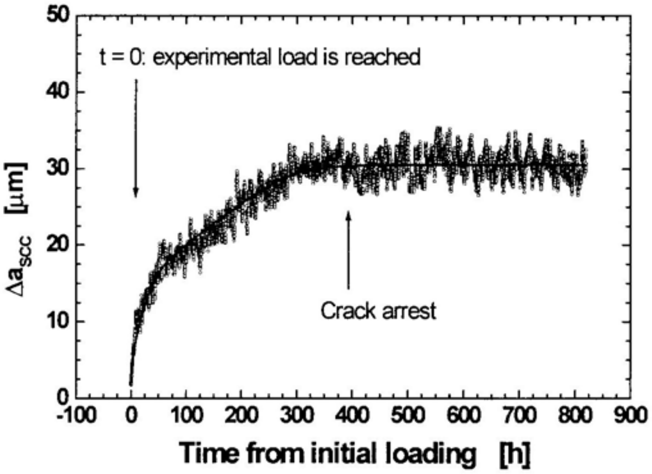

Figure B.8.7 Crack length as a function of time for a low alloy steel specimen under constant load in BWR coolant (26)

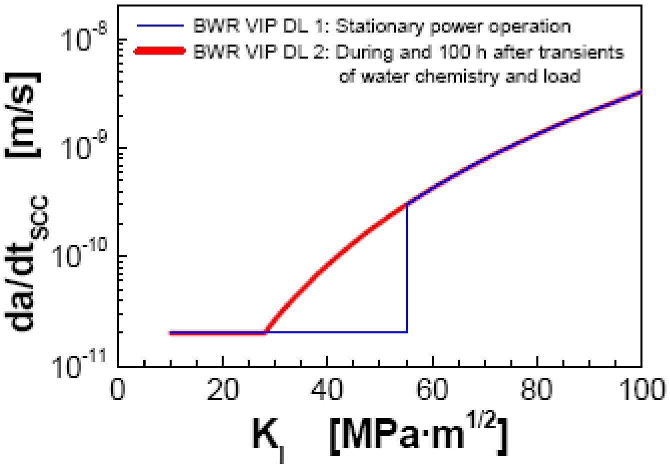

Figure B.8.8 Propagation rate vs stress intensity relationships for low alloy steels in BWR environments proposed by industry for disposition of cracks under stationary power operation (Eq. 7), and during the 100 hours after limited water chemistry and load transients (Eq. 5)

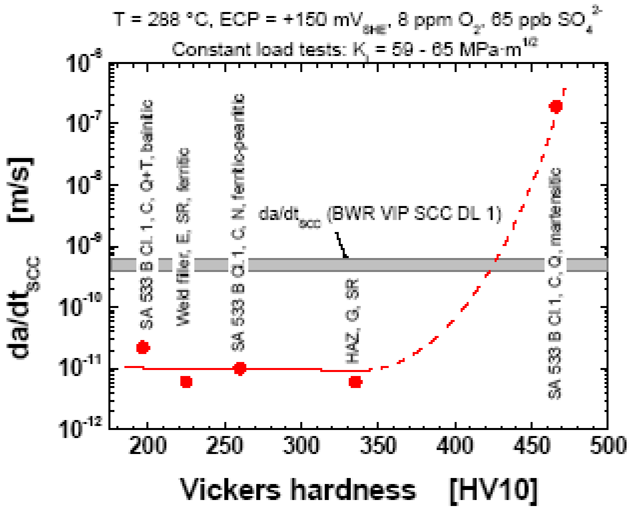

Figure B.8.9 Effect of hardness on the crack propagation rate for various low alloy steel weldments, plate,etc. in 8 ppm oxygenated water at 288^{o}C in comparison with the disposition propagation rate defined by Eq. 5 (33)

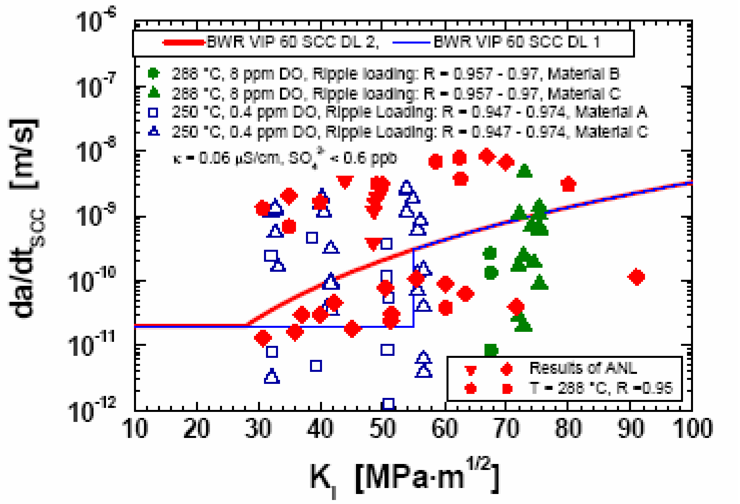

Figure B.8.10 Effect of ripple loading (R>0.95) on the crack propagation rates for various low alloy steels in high purity, oxygenated water, indicating the possibility of exceeding the disposition propagation rates in Eq. s 5 and 7 depending on the specifics of material condition. (33)

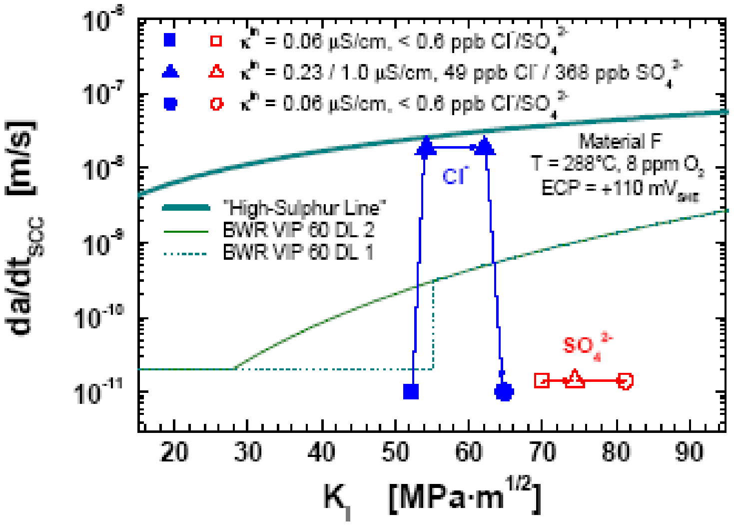

Figure B.8.11 Effect of chloride and sulphate on the crack propagation rate of a low alloy steel in 8ppm oxygenated water at 288^{0}C, (33)

B.9 Environmental Degradation of High Strength Materials

Introduction

Many high strength materials are used in PWRs and BWRs for bolts, studs and springs. Typical uses of high strength, martensitic, low alloy steels are for the closure studs and nuts of pressure vessels and manway cover plates, pump casings and support assemblies, valve bonnets and packing glands. They are also used for bolts and tie rods in PWR secondary water in steam generators. High strength stainless steels and nickel base alloys are deployed in many components in the primary coolant circuits of both PWRs and BWRs. Examples include valve stems, internal bolting and springs in main coolant pumps and valves, control rod drive assemblies, core internals, fuel hold down springs, etc.

Failures of internal bolts and springs can give rise to loose parts and loss of essential function of the component concerned. External bolts and studs are clearly critical to maintaining the integrity of the principal pressure boundary. From the very beginning of exploitation of PWRs and BWRs for power production, small but significant numbers of failures of high strength materials have occurred in service. They have usually been attributed to stress corrosion cracking (SCC) or hydrogen embrittlement (HE). A few have also been attributed to corrosion fatigue and in the specific case of low alloy steels used for external bolting in the primary circuit, also to boric acid corrosion by primary water leaks and steam cutting. Recurring themes in the case of high strength low alloy and stainless steels have been the initial unsuitability of the heat treatment and hardness of the as-installed component, or in some cases after thermal aging leading to unacceptable hardness, and the presence of inappropriate lubricants to facilitate assembly. For the nickel base alloys, attention has also been focused on the suitability of the initial heat treatment to obtain the desired mechanical properties but here the in-service problems encountered have been more analogous to those of nickel base alloys in general, particularly in PWR primary water service.

Nickel base alloys

Alloys X750 and 718 are nickel base alloys that are age hardened to precipitate the strengthening phases γ' and/or γ''. Their chemical compositions are given in Table B.9.1. Bolts in alloy X750 can have yield strengths of 115-140 ksi (790-965 MPa) while Alloy 718 can be hardened to higher strengths, for example 170-180 ksi (1170-1240 MPa) for bolts and even over 200 ksi (1380 MPa) for springs dependent on the level of cold work applied before age hardening (1). Many more components fabricated from alloy X750 have experienced intergranular stress corrosion cracking (IGSCC) in service in both PWRs and BWRs while only a very limited number of similar failures of alloy 718 have been observed in PWR service (1,2).

Improvements have been made to alloy X750 for PWR primary water service by increasing the solution annealing temperature to 1950-2100°F (1060-1150°C) and with it the resultant grain size, and by the adoption of a single step aging heat treatment at

1300°F (704°C) for 20 hours. Although the main goal of the aging heat treatment is to precipitate the strengthening phase γ', $Ni_3(Ti, Al)$, an added advantage of these particular heat treatment conditions for PWR primary water service is a fine, dense $M_{23}C_6$ carbide distribution at grain boundaries (3). In addition, great attention is now paid to keeping the design stresses, including those at stress concentrations, at least below the proportional limit. Surface condition of components is also known to influence the risk of IGSCC, in particular cold work and residual stress. Moreover, the atmosphere used during the aging heat treatment alloy of X750 was found to have a profound influence on initiation times for IGSCC in PWR primary water (3). This was due to oxidation of surface layers that had to be removed by machining after heat treatment in order to ensure optimum performance in service. The combination of all these improvements has seemingly stopped the previously generic failures of alloy X750 control rod drive split pins, for example, with operating periods presently exceeding 100,000hours without failure.

Alloy 718 is a normally highly reliable high strength alloy for use in PWR primary water although a few failures in PWR service are known (1,2). Some studies in the literature have implicated the formation during thermal aging of δ phase, the thermodynamically most stable form of the strengthening phases γ'', as having an aggravating influence on subsequent IGSCC susceptibility (4). Others have not observed a major effect of δ phase on product performance (2). Indeed, δ phase is a necessary feature to avoid excessive grain growth during solution treatment prior to aging (2). By contrast, intergranular oxidation of the surface during product rolling and heat treatment can have a severe adverse influence on IGSCC initiation in PWR primary water. For optimum IGSCC resistance in plant, it is essential to remove the layer affected by the furnace atmosphere, as observed previously for alloy X750.

Stainless steels

The most commonly used high strength bolting material in PWR primary circuits is cold worked Type 316 stainless steels with strength levels, depending on component diameter, up to 100 ksi (700 MPa), which requires typically 10 to 20% cold work. Even cold worked Type 304 (not L grade) may be used in PWR primary water although the practical extent of its use is not for the moment clear. With the exception of heavily neutron irradiated core baffle bolts there have been no known failures in service.

Where higher strength levels are required for components such as bolts, springs and valve stems, materials such as A286 precipitation hardened austenitic stainless steel, A410 and similar martensitic stainless steels and 17-4PH precipitation hardened martensitic stainless steel are used (Table B.9.1). Over the years, small numbers of such components have cracked in service usually attributed to stress corrosion or hydrogen embrittlement.

A286, an austenitic, precipitation hardened, stainless steel is strengthened by γ', $Ni_3(Ti,Al)$, formed during aging at 1330°F (720°C). Its use is favored where the expansion coefficient relative to other austenitic stainless steels is an important design factor. Unfortunately, it is susceptible to IGSCC in PWR primary water when loaded at or above the room temperature yield stress, typically 100 ksi (700 MPa) (5-10). Cold work prior to aging in combination with the lower of two commonly used solution annealing temperatures of 900 and 980°C has a particularly adverse effect on IGSCC resistance (8). Hot heading of bolts, which can create a heat-affected zone between the head and shank, is another known adverse factor. Nevertheless, even if these metallurgical factors are optimized, immunity from cracking cannot be assured unless the stresses are maintained below the room temperature yield stress, which necessitates strictly controlled bolt-loading procedures. There is also strong circumstantial evidence that superimposed fatigue stresses can lower the mean threshold stress for IGSCC even further. Finally, the role of impurities, including oxygen introduced during plant shut down and possibly consumed only slowly in confined crevices, in helping crack initiation is clear from all the evidence available. Once initiated, cracks grow relatively easily even in well-controlled PWR primary water (7).

Components such as valve stems, bolts and tie rods requiring rather high strength combined with good corrosion resistance in PWR primary circuit water have been typically fabricated from martensitic stainless steels, particularly Type 410 and 17-4 PH. A significant number of failures of martensitic stainless steels such as Type 410, for example, have occurred (11). In most cases, the affected components have usually entered service in an overly hard condition due to tempering at too low a temperature but no in-service aging seems to have been involved in these cases, the materials proving susceptible to stress corrosion cracking / hydrogen embrittlement in PWR primary water in the as-fabricated condition. A high tempering temperature above 1100°F (600°C) is preferred to avoid hydrogen embrittlement susceptibility. An additional problem has been caused by pitting/crevice corrosion of Type 410 and similar martensitic stainless steels in contact with graphite containing materials in the packing glands of valves, sometimes leading to valve stem seizure. The preferred replacement material has often been 17-4 PH with its higher chromium and molybdenum content conferring better resistance to crevice corrosion.

A significant number of service failures of 17-4 PH precipitation hardening stainless steel have also occurred in PWR primary water (11-14). Initially, intergranular cracking by stress corrosion / hydrogen embrittlement was associated with the lowest temperature aging heat treatment at 900°F (480°C) designated H900. This gives a minimum Vickers hardness value of 435HV well in excess of the limit of 350HV commonly observed to limit the risk of hydrogen embrittlement. The H1100 (593°C) aging heat treatment was subsequently widely adopted and normally yields a hardness value below 350HV. Nevertheless, a small number of failures, due either to brittle fracture or stress corrosion / hydrogen embrittlement, have continued to occur. The origin of these failures appears to be thermal aging in service.

Two main thermal aging mechanisms of martensitic stainless steels are recognized. The first "reversible temper embrittlement" is related to the diffusion of phosphorus (and arsenic, antimony and tin) to grain boundaries at aging temperatures generally above 750°F (400°C) and can occur in both Type 410 and 17-4 PH stainless steels. The grain boundaries are consequently embrittled and are particularly susceptible to intergranular hydrogen embrittlement but no general increase in hardness is observed. It can be reversed by heat treating around 1100°F (600°C) and avoided by reducing the phosphorus content and by small (1%) alloying additions of molybdenum.

The second thermal aging embrittlement mechanism is relevant only to precipitation hardened stainless steels such as of 17-4 PH. It arises from an intra-granular decomposition of the martensitic matrix into two phases, α which is rich in iron, and α' which is chromium rich. Further hardening arises from additional precipitation of the copper rich ε phase. A generalized increase in hardness is observed with corresponding increases in strength and ductile / brittle transition temperature and loss of fracture toughness. This hardening cannot be reversed without re-solution annealing. French studies have shown that this aging mechanism can occur in 17-4 PH steels on time scales relevant to the design lives of PWRs at temperatures exceeding 485°F (250°C) and quantitative models for component assessment have been developed (12,13). Mechanical fractures occur by cleavage although those involving corrosion can also be intergranular. Both types of failure have been associated with hardness values after in-service aging significantly exceeding 350HV. Corrosion related failures have also been aggravated by impurities coming from valve packing gland materials.

Low alloy martensitic steels

High strength martensitic and maraging steels are used in many external fastener applications in nuclear power reactors and a significant number of failures of this class of component have occurred (15). Most have been described as corrosion related failures. The problems encountered with external bolting have affected both support bolting and pressure boundary fasteners. Support bolting, in particular, can be affected by severe localized corrosion at interfaces with concrete where water may accumulate and protective plating or a polymeric coating system is often necessary.

Cracking of low alloy (AISI 4340 and 4140) and maraging steel support bolting has been attributed mainly to hydrogen embrittlement. Steels with ultra high yield strengths greater than 140 ksi (1000 MPa) have failed due to a combination of too high applied stresses and humid or wet environments collecting around the bases of components. Steels with lower yield strengths have also failed due to poor heat treatment or material variability. Consequent on these failures, a review of environmental cracking properties of high strength steels exposed to water or salt water at low temperatures was carried out and regulatory guidelines based on this information were published in the USA (16). Acceptability of high strength bolting was based on a lower bound approach to K_{ISCC} as a function of yield strength. This fracture mechanics based approach may have some attractions for defining a quality assurance procedure and for defect assessment. However, hydrogen cracks can start from free surfaces, usually in crevices, and consequently it is advisable also to have an upper hound strength limit (normally defined by a hardness level acceptance criterion such as <350HV) to avoid this type of cracking.

The second category of bolt failures is concerned with the integrity of the primary pressure boundary at locations such as the flanges of manway covers, pump casings and valves. Most of these incidents have been caused by boric acid corrosion or steam cutting (erosion-corrosion) due to PWR primary water seal leaks. A small number of failures among this category of bolts have, however, been associated with stress corrosion cracking / hydrogen embrittlement rather than wastage (16). The ferritic bolting steels involved were not out of specification but had been in contact with molybdenum disulfide lubricants. It has been postulated that the lubricant dissociated on contact with hot water to yield hydrogen sulfide, which is a severe hydrogen embrittling agent for ferritic steels. Consequently sulfide containing lubricants are no longer permitted. More generally, the main remedy for this category of high strength bolting failures is to avoid leaks at flanges seals by improved gasket design.

References

[1] A. R. McIlree, "Degradation of high strength austenitic alloys X-750, 718 and A286 in nuclear power systems", Proceedings of 1^{st} Int. Symposium on Environmental Degradation of Materials in Nuclear Power Systems - Water Reactors, Myrtle Beach, NACE 1984, pp. 838-849.

[2] P. M. Scott, "Stress corrosion cracking in Pressurized Water Reactors - Interpretation, modeling and remedies", Corrosion, Vol 56(8), 2000, pp. 771-782.

[3] M. Foucault, C. Benhamou, "Influence of surface condition on the susceptibility of Alloy X-750 to crack initiation in PWR primary water", Proceedings of 6th International Symposium on Environmental Degradation of Materials in Nuclear Power Systems – Water Reactors, San Diego, CA, The Metallurgical Society 1993, pp. 791-797.

[4] M. T. Miglin, J. V. Monter, C. S. Wade, J. K. Tien, J. L. Nelson, "Stress corrosion cracking of chemistry and heat treat variants of Alloy 718, Part 1: Stress corrosion test results", Proceedings of 6th International Symposium on Environmental Degradation of Materials in Nuclear Power Systems – Water Reactors, San Diego, CA, The Metallurgical Society 1993, pp. 815-818.

[5] G. O. Haynor, R. S. Piascik, D. E. Killian, K. E. Moore, "Babcock & Wilcox experience with Alloy A-286 reactor pressure vessel internal bolting", Proceedings of Fontevraud I, SFEN 1985, pp. 93-101.

[6] P. J. Plante, J. P. Mieding, "Degradation of reactor coolant pump impellor-to-shaft bolting in a PWR", Proceedings of 4th International Symposium on Environmental Degradation of Materials in Nuclear Reactor Systems- Water Reactors, Jekyll Island, Georgia, NACE 1990, pp. 11-45 to 11-55.

[7] US NRC Information Notice, "Stress corrosion cracking of reactor coolant pump bolts" 90 – 68 (1990) and supplement 1 (1994).

[8] R. S. Piascik, J. V. Monter, G. J. Theus, M. E. Scott, "Stress corrosion cracking of Alloy A-286 bolt material in simulated PWR reactor environment", Proceedings of the Second International Symposium on Environmental Degradation of Materials in Nuclear Reactor Systems- Water Reactors, Monterey CA, American Nuclear Society 1986, pp. 18-25.

[9] I. Wilson, T. Mager, "Stress corrosion of age hardenable NiFeCr alloys", Corrosion, Vol 42(6), 1986, pp. 352-360.

[10] J. B. Hall, S. Fyfitch, K. E. Moore, "Laboratory and operating experience with Alloy A286 and Alloy X750 RV internals bolting stress corrosion cracking", Proceedings of 11th International Conference on Environmental Degradation of

Materials in Nuclear Power Systems – Water Reactors, Stevenson, Washington, American Nuclear Society 2003, pp. 208-215.

[11] US NRC Information Notice, "Valve stem corrosion failures", 85-59, 1985.

[12] J. M. Boursier, D. Buisine, M. Fronteau, Y. Meyzaud, D. Michel, Y. Rouillon, B. Yrieix, "Vieillissement en service des aciers inoxydables", Proceedings of Fontevraud IV, SFEN 1998, pp. 1123-1134.

[13] B. Yrieix, M. Guttmann, "Aging between 300 and 450°C of wrought martensitic 13-17 wt% Cr stainless steels", Materials Science and Technology, Vol 9(2), 1993, pp. 125-134.

[14] H. Xu, S. Fyfitch, "Aging embrittlement modeling of Type 17-4PH at LWR temperature", Proceedings of the 10th International Conference on Environmental Degradation of Materials in Nuclear Power Systems – Water Reactors, August 3 to 9, 2001, Lake Tahoe, CA, NACE International 2001

[15] C. J. Czajkowski, "Corrosion and stress corrosion cracking of bolting materials in light water reactors", Proceedings of 1st Int. Symposium on Environmental Degradation of Materials in Nuclear Power Systems - Water Reactors, Myrtle Beach, NACE 1984, pp. 192-208.

[16] A. Goldberg, M. C. Juhas, "Lower bound KIscc values of bolting materials – a literature study", NUREG Report CR 2467, 1982.

Table B.9.1 Compositions of Some Common High Strength Nickel Base Alloys and Stainless Steels

	Alloy X750	**Alloy 718**	**A-286**	**17-4PH**
Nickel	>70.0	50-55	24-27	3.0-5.0
Chromium	14-17	17-21	12-15	15-17.5
Iron	5-9	Bal.	Bal.	Bal.
Titanium	2.25-2.75	0.65-1.15	1.55-2.0	
Aluminum	0.4-1.0	0.2-0.8	≤0.35	
Niobium plus Tantalum	0.7-1.2	4.75-5.50		0.15-0.45
Molybdenum		2.8-3.3	1.00-1.50	
Carbon	≤0.08	≤0.08	≤0.08	≤0.07
Manganese	≤1.0	≤0.35	≤2.0	≤1.0
Sulfur	≤0.010	≤0.010	≤0.030	≤0.030
Phosphorus			≤0.040	≤0.040
Silicon	≤0.5	≤0.35	≤1.0	
Copper	≤0.5	≤0.30		3.0-5.0
Vanadium			0.10-0.50	

B.10 BWR Water Chemistry Guidelines

Introduction

The 2004 revision of the BWR Water Chemistry Guidelines continues to focus on intergranular stress corrosion cracking (IGSCC), which can limit the service life of susceptible materials and components in BWR water environments. In addition, the guidelines place increased emphasis on fuel performance concerns, in view of the increasing incidence of fuel failures since the last revision in 2000. Many plants have adopted noble metal chemical application (NMCA) in the past four years, and this document addresses the resultant issues with IGSCC mitigation, fuel performance and radiation fields.

This document provides proactive water chemistry recommendations for BWRs during all modes of operation. It summarizes the technical bases for all water chemistry alternatives and provides guidance on the development of plant-specific chemistry programs. The guidelines recommend tightening some limits, relaxing others, and implementing more cost-effective monitoring, which will improve protection against materials and fuel problems and also reduce the risks of loss of output from chemistry transients.

Background

The first edition of these guidelines focused on impurity control to reduce stress corrosion cracking and fuel degradation. Consideration of hydrogen water chemistry to reduce electrochemical potential was added subsequently, and noble metal chemical addition was considered in the latest revision, including the effects on radiation buildup. With fuel heat rates increasing, and examples of corrosion induced fuel failures in recent years, fuel/water chemistry interactions are now a central theme in the latest edition.

The BWR Water Chemistry Guidelines Committee and the Mitigation Committee of the BWR Vessel and Internals Program (BWRVIP) issued this document to provide proactive water chemistry guidance for mitigating IGSCC, maintaining fuel integrity, and controlling radiation fields. The BWR Fuels Focus Group of the Fuel Reliability Program has been closely involved in the development of this document to address the increased industry concern about fuel performance issues. It updates the *BWR Water Chemistry Guidelines - 2000*, providing an enhanced methodology for establishing site-specific BWR water chemistry control programs.

A committee of industry experts collaborated to review the available field and laboratory data on BWR water chemistry controls and their impact on plant operation, corrosion mechanisms, fuel performance and radiation fields. The committee included utility specialists, Nuclear Steam Supply System (NSSS) vendors and fuel vendor representatives, Institute of Nuclear Power Operation (INPO) representatives, consultants, and EPRI staff. The committee identified a range of water chemistry regimes from which utility personnel can select their site-specific program.

Key Points and Technical Issues

The content of this document is summarized below, with major changes from the 2000 revision noted:

Management Issues: Section 1. A recent policy of the U.S. nuclear industry commits each nuclear utility to adopting the responsibilities and processes on the management of materials aging issues described in *"NEI 03-08: Guideline for the Management of Materials Issues."* Section 1 of the BWR Water Chemistry Guidelines specifies which portions of the document are *"Mandatory," "Needed,"* or *"Good Practices,"* using the classification described in NEI 03-08.

Intergranular Stress Corrosion Cracking: Section 2 discusses the technical basis for water chemistry control of IGSCC. This Section has been updated with the latest information on the effects of impurities such as sulfate and chloride on crack growth rate and covers a wider range of electrochemical potential (ECP). The strong effect of copper ions on the effectiveness of hydrogen water chemistry (HWC) is detailed. The overall goal of demonstrating the effectiveness of mitigating IGSCC of piping and reactor internals using HWC and NMCA is discussed in detail, including the *Guidelines'* relationship to inspection relief programs contained in BWRVIP-62 and BWRVIP-75.

Some of the previous IGSCC concerns in BWRs have largely been resolved by replacing the impacted materials with more IGSCC-resistant materials or by performing simple repairs. However, there is a limit to what can be achieved by replacement and repair. For example, repair/replacement of internals below the core is expensive and could lead to premature shutdown and decommissioning in the worst cases. An aggressive mitigation strategy will reduce the probability of escalating repair costs.

For many BWRs, the best-available initial strategy is likely to be to adopt HWC-M (1.0-2.0 ppm hydrogen in feedwater) to protect components in the lower core region as soon as possible. This provides mitigation to plant components thought to be the most difficult to repair. Plant data should be used to optimize the hydrogen feed rates. For other BWRs, HWC-M may not be economically feasible and the implementation of NMCA will provide the IGSCC mitigation solution.

All utilities not currently using HWC-M or NMCA are recommended to conduct an updated economic analysis. If the analysis indicates that HWC-M or NMCA is cost-beneficial, it is recommended that they implement HWC-M or NMCA to protect components in the lower core and lower plenum region. However, additional fuel technical issues need to be assessed with NMCA implementation. NMCA has several benefits compared to HWC-M such as reduced hydrogen injection rate, operation with NWC dose rates, decreased personnel exposure during operation, elimination of increased localized shielding requirements and increased mitigation of components in the upper shroud annulus. On the other hand, HWC-M offers several benefits compared to NMCA such as no outage time for the "classical" NMCA application, no "crack flanking" concerns and no potential fuel crudding and corrosion issues.

Radiation Field Effects: Section 3. The discussion of the effects of NMCA and zinc injection on radiation fields has been updated with the most recent plant data. The discussion on control of feedwater iron has been strengthened, with the recognition that iron increases fuel crud formation and decreases the efficiency of zinc. The “desired range” recommendations for feedwater iron have been specified as 0.1 – 1.5 ppb for HWC and NMCA plants, and 0.5 – 1.5 ppb for normal water chemistry plants.

The technologies available to mitigate IGSCC via BWR water chemistry control can significantly affect both operating and shutdown dose rates. The injection of hydrogen into the feedwater at levels required for mitigation increases the main steam line radiation level by a factor of 5X and requires either increased shielding or changed operation modes or both. In addition, operation with feedwater hydrogen injection results in increased shutdown dose rates due to increased ^{60}Co uptake into the oxides formed under reducing conditions. Mitigation of the increased shutdown dose rates can be accomplished with feedwater zinc injection.

The NMCA method uses low feedwater hydrogen addition rates and operating dose rates are increased by only 10% or less. To mitigate the increased shutdown dose rates due to increased uptake of ^{60}Co into corrosion films, the reactor water ratio of soluble ^{60}Co to soluble Zn must be kept below 2.0×10^{-5} µCi/ml/ppb. Due to the nature of the restructuring of the corrosion films during initial operation during the first post NMCA cycle the resulting shutdown dose rates can be kept very low if this ratio is established early in the first post-NMCA cycle. For this reason, some plants may need to increase feedwater zinc concentrations. Increased zinc may also be desirable for a period following a chemical decontamination. However, because of fuel performance concerns, it is best to limit the average feedwater zinc concentration value (below 0.6 ppb for HWC and 0.4 ppb for NMCA plants) while establishing and maintaining this ratio.
Feedwater iron input is also an important parameter to control shutdown radiation dose rates. A long-term goal of less than 1 ppb input is recommended with a minimum value of either 0.1 ppb or 0.5 ppb. Establishing this goal will make establishing the ^{60}Co(s)/ Zn(s) ratio much easier when limiting feedwater zinc levels as suggested above.

Flow Accelerated Corrosion (FAC): Section 4. Flow-accelerated corrosion (also called flow-assisted corrosion and, misleadingly, erosion/corrosion) causes wall thinning of carbon steel piping, vessels, and components. The wall thinning is caused by an increased rate of dissolution of the normally protective oxide layer, (e.g., magnetite), that forms on the surface of carbon and low alloy steel when exposed to high velocity water or wet steam. The oxide layer reforms and the process continues. The problem is widespread in all types of conventional and nuclear power plants. Wall thinning rates as high as ~120 mpy (3 mm/year) have been observed. If the thinning is not detected in time, the reduced wall cannot withstand the internal pressure and other applied loads. The result can be either a leak or complete rupture.

The rate of wall loss (wear rate) of a given component is affected by the alloy composition, the pH at operating conditions, the liquid phase dissolved oxygen concentration, fluid bulk velocity, component geometry and upstream influences, fluid temperature and steam quality.

The effect of NMCA on the corrosion behavior of carbon steel in 550°F (288 °C) water containing various amounts of oxygen and hydrogen was examined and the data confirm that there is no adverse effect of NMCA on FAC. At low oxygen concentrations and a reducing environment, noble metal treatment of carbon steel surfaces raised the corrosion potential to values closer to the hydrogen/water reversible potential, suggesting that FAC of wetted carbon steel components will be reduced under these conditions.

Overall, due to the catalytic nature of noble metals, plants that undergo NMCA are able to inject lower amounts of hydrogen while still achieving SCC mitigation of the reactor vessel and internals (wetted regions). Plants with low HWC have higher reactor water oxygen contents when compared to moderate HWC plants. Typical reactor water oxygen levels with low HWC/NMCA plants have often been in the region of 30 to 80 ppb whereas under moderate HWC conditions, the reactor water oxygen is often less than 2 ppb. Consequently, there is less suppression of radiolysis and a higher oxygen concentration in steam. In those regions of the steam cycle where moderate HWC causes an increase in FAC, there will be less of an increase with NMCA-HWC.

Control of Chemistry for Fuel Integrity Concerns. Section 5 discusses water chemistry impacts on fuel integrity, and now includes a discussion of corrosion-related fuel failures. The need for control of feedwater zinc, iron and copper is discussed. Based on fuel integrity issues, quarterly average maxima for feedwater zinc of 0.6 ppb for HWC plants and 0.4 ppb for NMCA plants are recommended. A feedwater copper limit of <0.1 ppb is highly desirable for all plants. Given the industry trend of increasing fuel duty and the possibility of further chemistry modifications for plant system material protection, reducing the feedwater iron to <1.0 ppb should be considered at all plants.

Largely through improvement of cladding nodular corrosion resistance and vigilant utility efforts in maintaining good water purity, no industry-wide events relating to cladding corrosion fuel failure, with the exception of an isolated case, was reported throughout the decade of 1990-2000. However, the industry has experienced rapid changes in fuel designs and the water chemistry environment over the past decade. Higher efficiency fuel designs and operational procedures have been introduced to meet the needs for higher discharge burn-up, longer cycle lengths, and improved cycle economics. Increasing fuel duty can increase rates of deposition of crud and hideout of harmful chemical species if present. Water chemistry conditions that were acceptable in the 1990s may no longer provide adequate margin for maintaining fuel reliability. Thus, the rapid changes in fuel and chemistry have created highly challenging conditions for the industry to maintain the high fuel integrity achieved during the 1990s.

This Section reviews fuel cladding corrosion observations and assess the potential role of water chemistry and possible mitigation measures. The current state of knowledge of the effects of chemistry additives, hydrogen, zinc, NMCA, and impurities, such as Fe, Cu, electro-hydraulic control (EHC) fluid, etc., on fuel crud deposition and Zircaloy cladding corrosion is critically reviewed based on fuel surveillance results, fuel operation experiences, and simulation tests. Finally, recommendations on water chemistry conditions are provided with the aim of mitigating the future occurrence of fuel failures due to accelerated cladding corrosion.

Minimizing tenacious crud formation and preventing intrusion of potentially harmful chemical impurities are two key chemistry considerations to improve fuel operational margin and prevent fuel cladding corrosion-related issues. Each plant must optimize their reactor chemistry programs to maximize fuel performance and minimize the risks to reactor integrity and personnel dose

BWR Water Chemistry Control: Section 6. Recognizing the increasing urgency of corrective actions with increasing impurity concentrations, the following rationale was used for establishing water chemistry control parameters, recommended operating limits, and recommended monitoring frequencies:

- Ingress of impurities into the RCS should be kept to a practical and achievable minimum.

- The oxidizing power of the reactor water should be maintained below a value at which both laboratory and specific reactor experience demonstrate that sensitized austenitic stainless steels and nickel-based alloys do not exhibit significant rates of IGSCC.

- Action levels should be based on quantitative information about the effects of the chemistry variables on the corrosion behavior of RCS materials, fuel performance and radiation field buildup. In the absence of quantitative data, achievable action level values should be specified.

- Action Levels and responses to exceeding Action Levels can vary with the approach to chemistry control, i.e., normal water chemistry (NWC), hydrogen water chemistry (HWC), or HWC following noble metal chemical application (NMCA).

- Recommended control, diagnostic and confirmatory parameters should be reliably measurable at the levels specified using currently available equipment and procedures.

- Monitoring frequencies should be established with the recognition that utility resources should be devoted to high-priority work.

This section comprises the recommendations for water chemistry control and diagnostic parameters, for start up, operation and shutdown. These now include separate tables for hydrogen water chemistry, HWC/ NMCA and normal water chemistry. The Action Level tables now address the possibility that IGSCC may be reduced with continued operation if the Action Levels are exceeded.

Recommended Goals for Water Chemistry Optimization: Section 7. This is a new section containing recommended goals for water chemistry optimization. These are "good practice" recommendations for targets that plants may use in optimizing water chemistry that balances the conflicting requirements of materials, fuel and radiation control. Significant time and expense may be required to meet these targets; thus efforts to achieve these goals should be considered in the context of the overall strategic plan for the plant.

Data Monitoring and Evaluation: Section 8. This Section discusses recommended chemistry surveillance. Recommendations from the 2000 revision of the *Guidelines* were reviewed. In support of the utilities' need to reduce O&M costs, recommended surveillance and monitoring frequencies were reduced when such could be done without significant adverse impact on plant chemistry.

Appendix A discusses the effects of impurity transients on crack growth rates. It has been considerably enhanced, including two tables of documented BWR transients that have occurred during operation and shutdown, possible water chemistry responses to transients plus examples of decision trees for evaluating actions to minimize the detrimental effects on IGSCC.

Appendix B covers auxiliary systems.

Appendix C is new. It addresses calculations that may be made to correct the measured conductivity for the presence of ionic species that are benign toward system integrity.

Appendix D is a new appendix covering ultrasonic fuel cleaning.

Appendix E updates the appendix on the BWRVIA model in the 2000 revision.

REFERENCES

[1] BWR Water Chemistry Guidelines, 2004 Revision. EPRI Report 1008192
[2] Robin L. Jones, “Mitigating Corrosion Problems in LWRs via Chemistry Changes,” Power Plant Chemistry, November 2004, pp663-669
[3] Robert. L. Cowan, “Modern BWR Chemistry Operating Strategies”, International Conference on Water Chemistry of Nuclear Reactor Systems, San Francisco, October 2004

B.11 PWR Primary Water Chemistry Guidelines

Introduction

The fifth revision of the PWR Primary Water Chemistry Guidelines, published in 2003, describes an effective, state-of-the-art program from which a utility can develop an optimized program for their plant. The philosophy embodied in this document has generic applicability, but can be adapted to the particular conditions of the utility and the site. The detailed guidelines presented in Volume 1 on operating chemistry and in Volume 2 on startup and shutdown chemistry comprise a program that should serve as a model for the development of site-specific chemistry plans.

Ensuring continued integrity of RCS materials of construction and fuel cladding and maintaining the industry trend toward reduced radiation fields requires continued optimization of reactor coolant chemistry. Optimization of coolant chemistry to meet site-specific demands becomes increasingly important in light of material corrosion concerns in steam generator and reactor vessel penetrations, the movement toward extended fuel cycles, higher duty cores, increasingly stringent dose rate control, decreased refueling outage duration, and reduced operating costs. This document is the sixth in a series of industry guidelines on PWR primary water chemistry. Like each of the others in the series, it provides a template for development of a plant-specific water chemistry program.

Background

Historically, the guidelines focused on radiation field control while maintaining fuel and materials integrity. Thus a trend of gradual increase in recommended pH levels can be seen in successive revisions. With some plants increasing fuel duty, more attention is now been paid to water chemistry/fuel interactions, particularly crud deposition. Increasing pH is also beneficial in controlling crud buildup. The guidelines have always considered the small effects of chemistry on initiation of stress corrosion cracking of nickel-based alloys. Although chemistry effects are minor, ne exception has been zinc injection, where a delay in crack initiation has been observed in laboratory tests. Recent crack growth data have also been considered, but again the influence of chemistry was found to be minor. The latest data shows a potential benefit from increasing hydrogen during operation, and this will be addressed in future editions, as will the possibility of mitigating low temperature crack propagation by adjusting shutdown procedures.

The *Guidelines* were prepared by a committee of experienced industry personnel through an effort sponsored by EPRI. Participation was obtained from chemistry, materials, steam generator, and fuels experts to ensure the Guidelines present chemistry parameters that are optimum for each set of operating and material conditions. Each EPRI-member utility operating a PWR participated in generation or review of these *Guidelines*. Therefore, this document serves as an industry consensus for PWR primary water chemistry control. In essence, it is a report from industry specialists to the utilities documenting an optimized water chemistry program.

Key Points and Technical Issues

The content of the 2003 revision is summarized below, with major changes from the previous revision noted:

Volume 1

Relative to Rev. 4 of these *Guidelines*, the major changes in Volume 1 of this document are as follows:

Management Responsibilities: Section 1. The U.S. nuclear industry established a framework for improving the reliability of steam generators, described in *"NEI 97-06: Steam Generator Program Guidelines"* Section 1 of the PWR Primary Water Chemistry Guidelines specifies which portions of Volume 1 *are* required in a "strategic water chemistry plan" to meet the intent of NEI 97-06. Volume 2 of these *Guidelines* addresses aspects of startup and shutdown chemistry practices which are not believed to impact SG tube integrity. Therefore, utilities need not meet the intent of Volume 2 to be in compliance with the NEI Initiative.

Technical Basis for Coolant Chemistry Control: Section 2 has been updated to include recent field experiences, laboratory test results and related investigations. Some of the key changes in Section 2 include:

- The quantitative discussion of the influence of water chemistry on primary water stress corrosion cracking (PWSCC) was updated to reflect recent data and a revised statistical evaluation of relevant test data. This evaluation indicates that use of the higher lithium levels required for constant elevated pH_T regimes (e.g., pH_T of 7.1 - 7.3 constant vs. earlier pH_T 6.9 constant or modified pH_T 6.9 regimes) results in little or no penalty in the characteristic time to PWSCC, and that any chemistry effect will be much smaller than the influence of material composition, stress or temperature. This conclusion is supported by plant experience where no significant effects of higher pH regimes have been observed at French, Swedish and U.S. plants that are experiencing PWSCC at low levels and have increased pH_T from 6.9 or 7.0 to 7.1 or higher. The discussion regarding the effects of hydrogen on PWSCC was revised to reflect recently published information that shows that the hydrogen concentration associated with the highest crack growth rate varies as a function of temperature.

- A brief discussion was added of recent test results regarding low temperature crack propagation (LTCP) in thick parts made from nickel-base alloys X-750, 82, 52, and 690, and how this cracking mode is affected by hydrogen levels in low temperature water.

- The discussion regarding the use of zinc in the field as an additive to mitigate PWSCC was updated. The discussion regarding use of zinc to reduce shutdown dose rates was updated to reflect the continuing encouraging results from both domestic and foreign plants. Even low levels of zinc added continuously are resulting in significant dose rate reductions in U.S. and German plants over multiple cycles. Approximately 20 PWRs are currently injecting zinc, mainly to control radiation fields, but plants using higher zinc concentrations are starting to see a reduction in PWSCC in steam generator tubing.

- An expanded discussion was included of the benefits of constant high pH regimes with regard to crud management, fuel deposits, and radiation dose rate. This discussion applies to all plants, but is especially relevant to plants with high duty cores where risks of fuel deposits and associated problems such as axial offset anomaly (AOA), or under-deposit clad corrosion failures are a concern.

- The review of the influence of the effects of primary water chemistry on corrosion of fuel cladding and on core performance was updated. The discussion emphasizes the importance of crud to corrosion of cladding, and discusses how increasing core duty increases the potential for crud deposition, cladding corrosion, and occurrence of axial offset anomaly (AOA). The review of fuel issues takes into account substantial industry experience with lithium concentrations up to 3.5 ppm, and use of lithium over 3.5 ppm for short periods of time. The review also reflects increased experience with use of zinc additions to the primary coolant, but indicates that use of zinc still demands successful completion of a field demonstration program for high duty cores. The review updates the evaluation of the effects of high silica on fuel performance, and indicates that increasing amounts of experience with silica levels of up to 3 ppm and even higher have been accumulated with no adverse effects.

Power Operation Chemistry Control Recommendations: Section 3 was revised to provide increased emphasis on the desirability of using a constant elevated pH_T (such as constant pH_T between 7.1 and 7.3) at all plants, but especially those with high duty cores, and to provide guidance with regard to making a transition to a constant elevated pH_T regime. Constant elevated pH_T has been shown to provide benefits in crud management, fuel deposits, AOA, and shutdown dose rates. The guidance also reflects the two potential concerns regarding high pH_T regimes that need to be considered: possible effects of higher lithium (e.g., over 3.5 ppm) on fuel cladding corrosion, and possible effects of higher lithium or pH on PWSCC. With regard to the effects of lithium on fuel, it was agreed to raise the level at which consideration of a fuel vendor review is indicated as being appropriate from 2.2 ppm to 3.5 ppm. Table 3-4, "Reactor Coolant System Power Operation Diagnostic Parameters (Reactor Critical)," was revised to add zinc as a diagnostic parameter. This reflects the Committee decision to recommend that all plants consider the use of zinc for its demonstrated dose reduction benefits.

Methodology for Plant-Specific Optimization: Section 4 was updated to reflect lessons learned from its use since it was first published in Revision 4. This mainly involved revising Table 4-1, “Chemistry Control Program Approaches,” to reflect the latest assessments of the positive and negative impacts of various options.

Appendix A “Calculation of pH_T and Data Evaluation methodology,” was modified to incorporate first order ionic strength corrections to 25°C values of pH and conductivity relevant to the spent fuel pool, and to include a discussion of thermodynamically predicted pressure and temperature effects on pH that are produced by the strong dependence of the ionization product of water on these variables.

Appendix B "Chemistry Control of Supporting Systems," was thoroughly reviewed and many corrections and improvements were incorporated. The changes made included additions to the descriptions of plant experiences, and some minor changes to the chemistry monitoring tables for the volume control tank, boric acid storage tanks, refueling water storage tank, and spent fuel cooling and cleanup system. Sulfate was added as a diagnostic parameter for the reactor water storage tank and for the spent fuel pool water.

Appendix C "Status of Enriched Boric Acid (EBA) Application," was updated to reflect industry experience of the past few years.

Appendix D "AOA and Ultrasonic Fuel Cleaning," that describes EPRI ultrasonic fuel cleaning technology and field experience demonstrating its promising role in ameliorating AOA and reducing dose rates was added.

Appendix E "Oxygen and Hydrogen Behavior in PWR Primary Circuits," was revised to incorporate a few minor improvements.

A new **Appendix F**, "Sampling Considerations for Monitoring RCS Corrosion Products," was added. It provides a description of typical PWR RCS letdown sampling systems and considerations, and includes descriptions of modern, high temperature, RCS hot leg particulate corrosion product sampling systems that can be used to provide improved monitoring of RCS particulates that are derived by re-entrainment of activated core deposits.

A new **Appendix G**, "Reactor Coolant Radionuclides," was added as an aid to chemistry staff and laboratory personnel for dealing with radionuclides and the potential significance of their trends during transient evolutions as well as trends from cycle to cycle.

A new **Appendix H**, "Definition of High Duty Core," was added to provide guidance with regard to the use and meaning of the high duty core index (HDCI) parameter, which is considered when evaluating effects of chemistry on fuel performance in cores with elevated local assembly steaming or core-wide subcooled nucleate boiling, as discussed in Section 2.4. The HDCI was defined and statistically tested against available cores that produced elevated steaming and/or AOA by the Robust Fuel Program specifically for this revision of the *Guidelines*.

Guidance in both Volume 1 and Volume 2 with respect to oxygen control in pressurizers was revised to reflect the interim guidance issued on August 31, 2001 by the Steam Generator Management Program. In addition, the guidance was expanded to cover control of oxygen during shutdowns, as well as during startups as addressed by the interim guidance.

Volume 2

This second volume of the PWR Primary Water Chemistry Guidelines focuses on startup and shutdown chemistry. As noted for the previous revision, the decision to cover startup and shutdown chemistry in a separate volume was made for two main reasons: (1) the increasingly large amount of information regarding shutdown and startup chemistry contained in the Guidelines warrants a separate volume, and (2) locating the startup and shutdown information in a separate volume separates it from the NEI Steam Generator Initiative requirements of Volume 1. This Volume 2 contains no specific requirements (with limited exceptions identified in Tables 4-2 and 4-3) which must be met by utilities to be in compliance with the NEI 97-06 Initiative.

The combined shutdown and startup chemistry coverage in this Volume 2 was updated from that in Revision 4 of the Guidelines to reflect new information and experience gained since issuance of that revision. Volume 2 continues to provide: (1) technical discussions regarding plant experiences with different types of shutdown and startup chemistries; and (2) tables of demonstrated options, together with their perceived benefits and possible negative impacts, for refueling and mid-cycle outages. Section 2 is modified to include the substantially new information since Revision 4 on the nature of fuel deposits and their role in activity transport for plants operating high duty cores. Sections 3 and 4 contain industry guidance for shutdown and startup, respectively, together with accompanying discussion and technical support.

Relative to Revision 4 (March 1999) of these Guidelines, the major changes made to Volume 2 are as follows:

1. Descriptions of the morphology and properties of the newly discovered fuel crud constituents bonaccordite and zirconium oxide were added to Section 2, as well as a discussion of how their largely insoluble nature affects shutdown chemistry strategies.

2. Discussions were added and expanded of methods for monitoring and controlling hydrogen and oxygen concentrations in the pressurizer during shutdowns and startups.

3. Discussion was expanded regarding the use of acid reducing conditions during mid-cycle outages in a manner that might reduce AOA in high duty cores.

4. Plant experience was described that shows strong benefits from using the maximum practical RCS cleanup flow during shutdowns. This experience indicates that modifying system designs to increase the maximum cleanup flow rate can be beneficial.

5. Discussion was expanded of the need and methods to maintain oxidizing conditions in the reactor water through flood-up in order to minimize activity release during that operation.

6. Oxygen control strategies (including hydrogen degassing on shutdown and oxygen removal on startup) appropriate to plants that maintain a two-phase pressurizer are offered that are consistent with material integrity goals for pressurizer materials.

7. A variety of experiences were described regarding use or non-use of reactor coolant pumps during shutdown, including when adding hydrogen peroxide.

8. A discussion was added regarding the benefits of using higher cross-linked resins.

9. Many changes were made to the startup and shutdown tables in Sections 3 and 4. These tables present the various options that are available, and their possible benefits and negative impacts. The changes reflect the experience gained since the last revision, including

the topics noted above, and also reflect concerns that the industry must develop methods appropriate to PWR materials, temperature and stress intensities to assess the possibility of low temperature crack propagation (LTCP) in nickel-base alloys.

10. A new Appendix was added that details an example of the decision logic that chemists may find useful when deciding what options are consistent with cycle chemistry goals when faced with unplanned mid-cycle outages whose duration may not be known precisely at the point in time of shutting down the reactor.

References

[1] PWR Primary Water Chemistry Guidelines, Revision 5. EPRI Report 1002884 (2003)
[2] Robin L. Jones, "Mitigating Corrosion Problems in LWRs via Chemistry Changes," Power Plant Chemistry, November 2004, pp663-669
[3] Keith Fruzzetti, "A Review of EPRI PWR Water Chemistry Guidelines," International Conference on Water Chemistry of Nuclear Reactor Systems, San Francisco, October 2004

B.12 PWR Secondary Water Chemistry Guidelines

Introduction

The sixth revision of the PWR Secondary Water Chemistry Guidelines, published in 2004, describes an effective, state-of-the-art program from which a utility can develop an optimized program for their plant. Previous revisions of these Guidelines have identified a detailed water chemistry program that was deemed to be consistent with the then current understanding of research and field information. Each revision, however, has recognized the impact of these *Guidelines* on plant operation and has noted that utilities should optimize their program based on a plant-specific evaluation prior to implementation. To assist in such plant-specific evaluations, Revisions 4 and 5, issued in 1996 and 2000, respectively, provided an increased depth of detail regarding the corrosion mechanisms affecting steam generators and the balance of plant, and provided additional guidance on how to integrate these and other concerns into the plant-specific optimization process. Revision 6 retains the format of Revisions 4 and 5, and adds to the detailed information contained in these revisions.

Background

The main thrust of the secondary guidelines has always focused on controlling intergranular stress corrosion cracking of steam generator tubing. Successive revisions have tightened impurity limits, and have added recommendations to control sludge build-up using amines and crevice corrosion through molar ratio control. Future additions will probably consider the use of polyacrylic dispersants to minimize sludge deposition.

A committee of industry experts—including utility specialists, nuclear steam supply system vendor representatives, Institute of Nuclear Power Operations representatives, consultants, and EPRI staff—collaborated in reviewing the available data on secondary water chemistry and secondary cycle corrosion. From these data, the committee generated water chemistry guidelines that should be adopted at all PWR nuclear plants. Recognizing that each nuclear plant owner has a unique set of design, operating, and corporate concerns, the guidelines committee developed a methodology for plant-specific optimization.

This sixth revision of the *PWR Secondary Water Chemistry Guidelines*, endorsed by the utility executives of the EPRI Steam Generator Management Project, represents another step in maintaining proactive chemistry programs to limit or control steam generator degradation, with consideration given to corporate resources and plant-specific design/operating concerns.

Key Points and Technical Issues

Revision 6 of the *PWR Secondary Water Chemistry Guidelines*—which provides recommendations for PWR secondary systems of all manufacture and design—includes the following chapters:

Chapter 1 identifies Management Responsibilities. It also describes which elements of the *Guidelines* are mandatory and "shall" requirements under NEI 03-08, Guideline for the

Management of Materials Issues, (consistent with NEI 97-06) and which are recommendations. The only mandatory requirement is to have a Strategic Water Chemistry Plan. “Shall” requirements include the Action Level 1, 2 and 3 control parameters and responses and the hold parameters in the control tables of Chapters 5 and 6, including both values and monitoring frequencies for these parameters. The balance of the guidance elements provided in the *Guidelines* are recommendations.

Chapter 2 presents a compilation of corrosion data for steam generator tubing and, to a lesser extent, balance-of-plant materials. It is not intended to relate operational bulk water chemistry to the corrosion phenomena, which is covered in Chapter 3. The corrosion data presented in Chapter 2 serve as the technical bases for each of the specific parameters and programs detailed in the balance of the document. Chapter 2 was revised to reflect recent research results regarding specific impurity effects on IGA/SCC, the effects of hydrazine on flow accelerated corrosion, and regarding the effects of amines on secondary side deposition processes.

Chapter 3 discusses the role of the concentration processes in the various locations of the steam generator and the chemistry “tools” available for modifying the resulting chemistry within these concentrating regions. It briefly identifies the supporting aspects of and the considerations for adopting these chemistry regimes. It refers the reader to more detailed documents for application of the chemistry strategies. The treatment of deposit control practices was significantly modified in Chapter 3 to reflect current practices and currently available methods. Chapter 3 also contains an expanded discussion on thermal performance issues, and new sections on the loss of hydrazine scenario and startup oxidant control.

Chapter 4 presents a detailed methodology for performing the plant-specific optimization that can be used to develop a modified chemistry program that satisfies site-specific concerns. Chapter 4 also presents example startup and operating chemistry parameters and limits that can be used as a starting point for site-specific evaluations. The main discussion of integrated exposure was relocated from Appendix A to Chapters 4 and 7, and the discussion was revised to reflect its removal as a diagnostic parameter from Chapters 5 and 6. Chapter 4 was also revised to include a list of items that should be covered in strategic water chemistry plans.

Chapters 5 and 6 present water chemistry programs for recirculating steam generators (RSGs) and once-through steam generators (OTSGs), respectively. These are the chapters most frequently referred to by chemistry personnel. The tables contained within these chapters provide boundaries of the envelope within which plant-specific optimization should occur.

Chapter 5 was revised to incorporate additional guidance regarding control of wet layup during short outages. The condition to which plants should go to as part of an Action Level 3 response was changed to “<5% power” from “hot or cold shutdown.” The control tables for RSGs in Chapter 5 were thoroughly reviewed and edited. Some of the more significant changes to the tables were:

- Inclusion of Action Level 2 and 3 actions for loss of hydrazine.

- Addition of a requirement that plants reduce power to below 5% power if sodium, chloride or sulfate exceed 250 ppb, or if they exceed 50 ppb for more than 100 hours, while between 5% and 30% power.

- Reduction in the blowdown impurity level for sodium at the 30% power hold from 20 to 10 ppb, and addition of an explicit recommendation that plants achieve sodium, chloride and sulfate blowdown concentrations below their respective Action Level 1 concentrations prior to exceeding 30% power.

- Additional guidance was added such that plants are no longer required to go to Action Level 3 as long as the impurity concentrations remain below Action Level 2 values.

- Deletion of integrated exposure as a diagnostic parameter, and inclusion of lead and integrated corrosion product transport as diagnostic parameters.

- Addition of a footnote to allow reduced frequency for sampling for copper for plants that are copper free or have confirmed low levels of copper transport (<20 ppt).

Chapter 6 was revised to incorporate additional guidance regarding control of wet layup during short outages. The Action Level 3 response was modified to indicate that there may be some circumstances under which plant shutdown may not be necessary, and to provide an initial two-hour period with impurities over the Action Level 3 limit (but less than 20 ppb) before shutdown is required. Some of the main changes to the OTSG control tables in Chapter 6 were:

- Inclusion of Action Level 2 and 3 actions for loss of hydrazine.

- Deletion of integrated exposure as a diagnostic parameter, and inclusion of integrated corrosion product transport as diagnostic parameters.

- Addition of guidance indicating that monitoring moisture separator drain concentrations of sodium and chloride is the preferred method to monitor these species, as opposed to monitoring them directly in the feedwater.

- Addition of a footnote to allow reduced frequency for sampling for copper for plants that are copper free or have confirmed low levels of copper transport (<20 ppt).

- Addition of a clarifying note indicating that silica limits are provided to protect the turbines and not the steam generators, and therefore do not fall under the purview of NEI 97-06.

Chapter 7 provides information on data collection, evaluation, and management. This chapter covers use of *EPRI chemWORKS*™ modules for evaluating plant data and predicting high-temperature chemistry environments throughout the cycle. Chapter 7 was revised to delete tables detailing sampling data requirements, to add more guidance regarding hideout returns, species to analyze in deposits, and integrated exposure evaluations, and to add a new section regarding effectiveness assessments. A discussion of lead sampling and additional recommendations on corrosion product transport sampling was also added.

Appendix A provides detailed guidance with regard to use of the integrated exposure concept, for example ppb*days. This appendix was created to demonstrate how some plants use integrated exposure in practice. Three plant documents (or summaries of plant documents) are presented, which describe different methodologies for use of integrated exposure.

Appendix B provides a review of PWR steam chemistry considerations. Steam chemistry is controlled in power plants to prevent or control deposition of impurities on turbine blades, to minimize erosion of turbine blades and to control general and localized corrosion of turbine blades and discs, cross over piping and extraction lines. In well-operated nuclear plants, the major consideration for steam chemistry control is the environmentally assisted cracking of turbine blade/disc attachments and FAC of piping in two-phase regions of the BOP. The latter consideration is addressed through pH control by organic amines and/or ammonia based AVT.
This revision of the *Guidelines* continues the approach of helping utilities maintain a proactive chemistry program to limit or control steam generator degradation while taking into consideration limits on corporate resources and plant-specific design/operating concerns.

It is recognized that a specific program applicable to all plants cannot be defined due to differences in design, experience, management structure, and operating philosophy. However, the goal is to maximize the availability and operating life of major components such as the steam generator and the turbine. To meet this goal, an effective corporate policy and water chemistry control program are essential and should be based upon the following:

- A recognition of the long-term benefits of, and need for, avoiding or minimizing corrosion degradation of major components.

- Clear and unequivocal management support for operating procedures designed to avoid this degradation.

- Adequate resources of staff, equipment, funds, and organization to implement an effective chemistry control policy.

- An evaluation of the basis for each chemistry parameter, action level and specification, as well as those of similar guidelines.

- Management agreement at all levels, prior to implementing the program, on the actions to be taken in response to off-normal water chemistry and the methods for resolution of conflicts, and unusual conditions not covered by the guidelines.

- Continuing review of plant and industry experience and research and revisions to the program, as appropriate.

- A recognition that alternate water chemistry regimes, if used, should not be a substitute for continued vigilance in adherence to the guidelines.

References

[1] PWR Secondary Water Chemistry Guidelines, Revision 6, EPRI Report 1008224 (2004)
[2] Robin L. Jones, "Mitigating Corrosion Problems in LWRs via Chemistry Changes," Power Plant Chemistry, November 2004, pp663-669
[3] Keith Fruzzetti, "A Review of EPRI PWR Water Chemistry Guidelines," International Conference on Water Chemistry of Nuclear Reactor Systems, San Francisco, October 2004

B.13 Degradation of Fracture Resistance: Low Temperature Crack Propagation (LTCP) in Nickel-Base Alloys

This topical paper provides a summary of the information currently available on a form of fracture resistance degradation called Low Temperature Crack Propagation (LTCP). LTCP is a form of hydrogen embrittlement which has not yet been identified in commercial nuclear reactors but which causes severe degradation of the fracture resistance of certain nickel-base alloys in laboratory tests performed under specific test conditions.

The laboratory test results indicate that the fracture resistance of alloys 600 and 690 in low-temperature water is lower than the fracture toughness (test in air), but that the difference is relatively small[1]. Therefore LTCP is not considered to be an important degradation mechanism for alloys 600 and 690. However, alloys X-750, 182/82, and 152/52 (in order of decreasing susceptibility) all suffer substantial degradation of fracture resistance in laboratory tests in hydrogenated water when the following conditions are met:

- The test temperature is less than 150°C;
- The dissolved hydrogen concentration in the environment is between 150 and 0 cm^3 H_2/Kg H_20 for alloy X-750 and between 150 and 10 cm^3 H_2/Kg H_20 for alloys 182/82 and 152/52[*];
- Properly-oriented sharp cracks (e.g., fatigue cracks or certain welding defects) are present that are open to the hydrogenated environment;
- The sustained stress intensity factor is higher than the equivalent critical stress intensity factor for LTCP determined from fracture testing, and;
- The stress intensity ramp rate (loading rate) is slow.

Mills et al.[1,2,3,4,5,6,7,8], Lenartova[9], and Symons[10] have done studies on Ni-based alloys in low-temperature environments. A recent (2004) report by Brown and Mills[5] provides a thorough summary of some of these studies for alloys 82H, 52, and 690. A comparison of load-displacement curves for as-welded alloy 82H specimens is shown in Figure B.13.1[5]. For non-precharged specimens (**Figure B.13.1**(a)), the material response changes from ductile in 338°C hydrogenated water (similar to air) to brittle (intergranular) in 54°C hydrogenated water. The degree of embrittlement and the intergranular nature of cracking observed in 54°C water can be reproduced in specimens pre-charged in high-pressure hydrogen and then tested in air (Figure B.13.1(b)). This implies that the degradation is due to hydrogen-induced intergranular cracking. The presence of hydrogen at the crack tip, regardless of its source, reduces fracture resistance mostly by reducing grain boundary cohesion and promoting planar slip[7]. The combination of hydrogen-precharging and testing in hydrogenated water (54°C water with 150 cm^3 H_2/Kg H_20) results in additional degradation of fracture resistance (Figure B.13.1(b)). Presumably, hydrogen

---

[*] It is not known whether or not LTCP can occur at dissolved hydrogen concentrations below 10 cm^3 H_2/Kg H_20 for alloys 182/82 and 152/52 -- no tests have yet been performed at lower hydrogen concentrations.

from the water further increases the hydrogen concentration ahead of the crack and reduces the loss of pre-charged hydrogen from the crack tip region[7]. The type of intergranular cracking associated with LTCP in the case of 82H welds is believed to be caused by hydrogen trapping by fine niobium and titanium-rich carbonitrides at grain boundaries[6].

In 54°C water with 150 cm^3 H_2/Kg H_20 at an average pH of 10.2, the LTCP fracture resistance was an order of magnitude lower than the elastic-plastic fracture toughness, J_{IC}, (test in air) for alloys 82H, and 52, and 5 times lower for alloy 690[8]. The LTCP tearing resistance (test in environment) was two orders of magnitude lower than the tearing modulus (test in air) for alloys 82H, and 52[8]. The tearing modulus is a measure of the tearing resistance after J_C is exceeded. However, the tensile properties of the alloys were unaffected by the environment, except for the total elongation of the weld materials[8]. For all alloys considered, LTCP fracture resistance and LTCP tearing resistance generally increase with increasing water temperature and decreasing hydrogen concentration – these effects are illustrated for alloy 52 in **Figure B.13.2**. The LTCP fracture resistance is also recovered at high rates of stress intensity factor increase (loading rates), presumably because there is insufficient time to embrittle grain boundaries ahead of the crack.

LTCP does not initiate at as-machined notches, but has been shown to initiate at sharp natural weld defects[5]. Testing showed that weld root defects and fatigue pre-cracks exhibit similar LTCP responses[5]. Mills et al. were not able to conclude (from the results of cooldown testing of alloy 82H under constant displacement[5]) whether or not residual stress contributes to LTCP. Given these results, residual stress cannot be eliminated as a contributor to LTCP, to date.

An EPRI study confirmed the Mills et al. test results for alloy 82H[11]. In rising-load tests at a temperature of 54°C in pH 10 water with 150 cm^3 H_2/Kg H_20, the LTCP fracture resistance of alloy 82H was an order of magnitude lower than the fracture toughness. Alloy 182 was also investigated in this study and its LTCP fracture resistance was also an order of magnitude lower than the fracture toughness under similar test conditions. Reducing the concentration of hydrogen to 100 cm^3 H_2/Kg H_20, and testing at pH 7 in simulated primary water, did not alter the magnitude of the difference between the LTCP fracture resistance and the fracture toughness in alloy 182. A current EPRI study is investigating the effects of chemical conditions closer to those typical during shutdown as well as the effects on LTCP in alloy 182 of using stress corrosion cracking (SCC) to produce the starter cracks instead of fatigue. The current test conditions are 30 or 10 cm^3 H_2/Kg H_20 water at 54°C, pH of 4.5, and an extension rate of 10^{-6} in. s^{-1}. The preliminary results for the tests with fatigue pre-cracks indicate that alloy 182 still exhibits a factor of 5 difference between the LTCP fracture resistance and the fracture toughness in 30 cm^3 H_2/Kg H_20 water (compared to air) and a factor of 4 difference in 10 cm^3 H_2/Kg H_20 water. In order to determine if there is a critical hydrogen concentration in the water under which LTCP does not occur, further fracture resistance testing on alloy 182 is planned, first in non-hydrogenated water (i.e., 0 cm^3 H_2/Kg H_20), and then at other hydrogen concentrations below 10 cm^3 H_2/Kg H_20, if necessary. Reducing the pH from 7 to 4.5 does not seem to affect LTCP susceptibility significantly. No results are available yet for the planned tests with SCC as starter cracks.

Alloy X-750 is a precipitation-hardened high-strength nickel-base alloy used for bolts and springs in PWR service. Several studies related to LTCP have been performed on this alloy by Mills et al.[2] and by Symons[10]. X-750 is highly susceptible to LTCP below 150°C in pre-cracked specimens, especially in earlier heat treatments (AH and BH), with growth rates as high as 7 mm/min[2]. It appears that phosphorous and sulfur at grain boundaries act as hydrogen traps and increase the LTCP susceptibility[2]. The grain boundary carbides were shown to control the embrittlement of this alloy[10]. Some testing performed by Mills et al. in argon-sparged water[2], which corresponds to a non-hydrogenated water environment, shows that K_{Pmax} (stress intensity at maximum load) obtained during a rising load test is lower in non-hydrogenated water than in air for X-750[2]. These observations suggest that the corrosion-generated hydrogen at the crack tip is sufficient to cause embrittlement for alloy X-750 in non-hydrogenated water.

The critical source of hydrogen source for LTCP appears to be the environmental hydrogen, as the hydrogen has to diffuse only for a very short distance to get to the highly strained region ahead of the crack tip (**Figure B.13.3**) and therefore the hydrogen concentrations required to embrittle the crack tip in a water environment are very low (probably on the order of a few ppm)[5,10]. By contrast, in precharged specimens tested in air, hydrogen levels at the crack tip approach zero. The critical cracking location moves inboard toward the peak hydrostatic stress location where strains are much lower (**Figure B.13.3**); hence, higher local hydrogen concentrations are needed to embrittle grain boundaries. The hydrogen previously diffused in the metal from operation can be an additional hydrogen source for LTCP; but it is not identified as sufficient on its own, as the hydrogen concentrations in the bulk of the metal resulting from operation are low compared to the concentration required to embrittle hydrogen-precharged specimens.

EPRI has begun an assessment of whether or not the conditions necessary for the occurrence of LTCP exist in PWRs[12]. The necessary conditions for LTCP are material susceptibility, low temperature, hydrogen concentration, sharp cracks, sustained stress/strain level, and low strain rate. The hydrogen and temperature conditions that cause LTCP can be present in some PWRs depending on plant and shutdown practices[13,14], but do not appear to be present in PWR startups[15]. The sharps cracks that cause LTCP to initiate can potentially be present in the form of SCC cracks[16,17] or lack-of-fusion defects in alloys 82/182[18] and particularly in alloys 52/152, which exhibit weldability problems[19]. Some stress analyses for components like reactors vessel nozzles have been performed for critical PWR shutdown conditions. Preliminary results suggest that actual stress intensity factors in PWR components are lower than the equivalent critical stress intensity factor for LTCP for detectable crack sizes, but high enough to raise some concern. Therefore additional analyses are necessary, including some repaired components cases and using stress redistribution with crack growth for the stress intensity factors calculation. Finally, the strain rates during shutdown appear to be low enough that there is sufficient time for hydrogen to embrittle the region ahead of the crack.

Additional work is required to determine unequivocally whether or not LTCP of nickel-alloy components can occur under PWR primary system service conditions. Nevertheless, several interim conclusions can be reached at this point:

- First, because LTCP only occurs at temperatures below 150°C, it is not an issue either during normal power operation or during those stages of plant cool-down and start-up when the temperature of the primary coolant is above 150°C.

- Second, LTCP is unlikely to occur during either the stages of plant shut-down when the system is depressurized and hydrogen peroxide has been added or those stages of plant start-up when the temperature is below 150°C, because the primary coolant is not hydrogenated during these periods and the calculated hydrogen concentrations resulting from previously diffused hydrogen in the material are low compared to the concentration required to embrittle hydrogen-precharged specimens.

- Third, although most of the conditions required for LTCP are (or, potentially, could be) satisfied during the stages of cool-down when the coolant is hydrogenated and the temperature is below 150°C, additional stress analyses are required to determine whether or not the mechanical requirements for LTCP identified in the laboratory tests are likely to be met in any nickel-alloy components.

Finally, additional laboratory tests and plant impact assessments should be considered to determine whether stopping hydrogenation of the primary coolant at an earlier stage of plant cool-down would be an effective and acceptable countermeasure to LTCP.

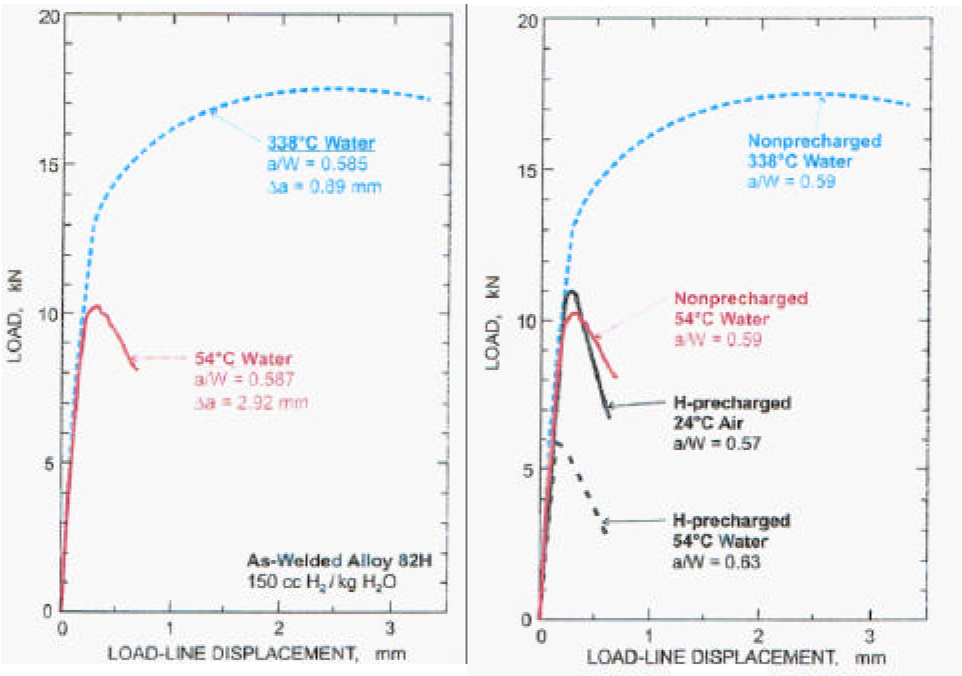

(a) (b)

Figure B.13.1 Load-displacement curves for as-welded 82H[5]

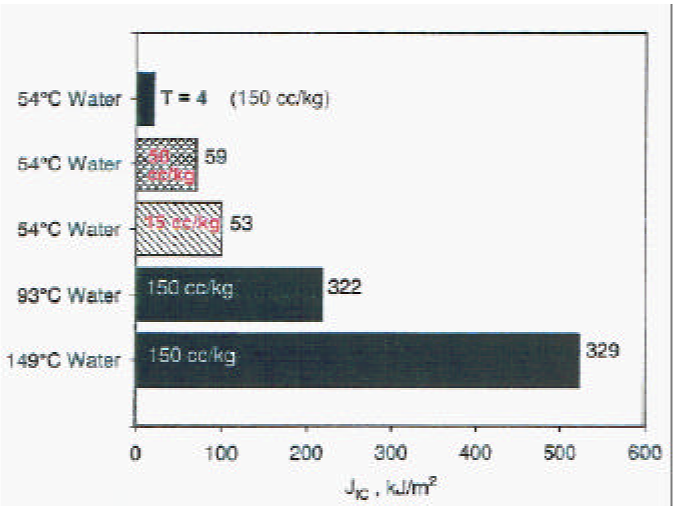

Figure B.13.2 LTCP fracture resistance (in water) of alloy 52 welds (values of LTCP tearing resistance are provided beyond each bar)[1,5]

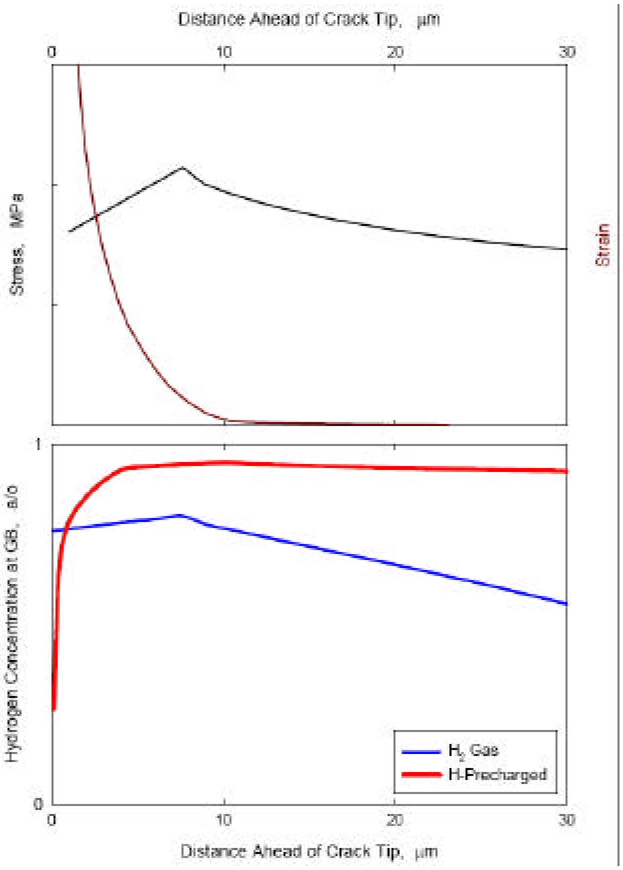

Figure B.13.3 Stress, strain and hydrogen concentration at grain boundaries for either specimens in environmental hydrogen (H_2 gas) or hydrogen precharged specimens (H-precharged), as a function of distance ahead of the crack tip[5]

References

[1] W.J. Mills and C.M. Brown, *Fracture Behavior of Nickel-Based Alloys in Water*, Ninth International Conference on Environmental Degradation of Materials in Nuclear Power Systems - Water Reactors, TMS, 1999, pp. 167-174.

[2] W.J. Mills, M.R. Lebo, and J.J. Kearns, *Hydrogen Embrittlement, Grain Boundary Segregation, and Stress Corrosion Cracking of Alloy X-750 in Low- and High-Temperature Water*, Metallurgical and Materials Transactions A, Vol. 30A, 1999, pp. 1579-1596.

[3] C.M. Brown and W.J. Mills, *Fracture Toughness of Alloy 690 and EN52 Welds in Air and Water*, Metallurgical and Materials Transactions A, Vol. 33A, 2002, pp. 1725-1735.

[4] W.J. Mills and C.M. Brown, *Fracture Toughness of Alloy 600 and an EN82H Weld in Air and Water*, Metallurgical and Materials Transactions A, Vol. 32A, 2001, pp. 1161-1174.

[5] W.J. Mills and C.M. Brown, *Low Temperature Crack Propagation Behavior of Alloy 82H Welds, Alloy 52 Welds and Alloy 690*, Report B-T-3549, 2004.

[6] W. J. Mills, C. M. Brown and M. G. Burke, *Effects of Microstructure on Low Temperature Cracking Behavior of EN82H Welds*, Tenth International Conference on Environmental Degradation of Materials in Nuclear Power Systems - Waters Reactors, NACE, 1999 (CD-ROM).

[7] W.J. Mills and C.M. Brown, *Fracture Toughness of Alloy 600 and EN82H Weld in Air and Water*, Report B-T-3264, 1999.

[8] C.M. Brown and W.J. Mills, *Effect of Water on Mechanical Properties and Stress Corrosion Behavior of Alloy 600, Alloy 690, EN82H Welds, and EN52 Welds*, Corrosion, Vol. 55, No. 2, pp.173-186 (1999).

[9] I. Lenartova, *Fragilisation par l'Hydrogène et Corrosion Sous Contrainte d'Alliages de Nickel et d'un Acier Inoxidable Utilisés dans les Generateurs de Vapeur: Influence de la Composition Chimique et de la Microstructure (English translation: Hydrogen Embrittlement of Nickel Base Alloys and a Stainless Steel Used in Steam Generators: Influence of Chemical Composition and Microstructure)*, PhD Thesis, Ecole Centrale de Paris, 1996.

[10] D.M. Symons, *A Comparison of Internal Hydrogen Embrittlement and Hydrogen Environment Embrittlement of X-750*, Engineering Fracture Mechanics, Vol. 68, 2001, pp. 751-771.

[11] *Materials Reliability Program: Low-Temperature Cracking of Nickel-Based Alloys and Weld Metals (MRP-108)*, EPRI, Palo Alto, CA and U.S. Department of Energy, Washington, D.C.: 2004. 1009400.

---

[12] A.G. Demma and A.R. McIlree, *White Paper on Low Temperature Crack Propagation,* EPRI White Paper, November 2004.

[13] *PWR Shutdown Chemistry Practices*, EPRI, Palo Alto, CA: 1998. Report TR-109569.

[14] *Proceedings of the June 2004 EPRI PWR Primary Shutdown Workshop*, EPRI, Palo Alto, CA: 2004, 1011106.

[15] *Analysis Report on 1999-2001 Field Experience with Elevated, Constant pH*, EPRI, Palo Alto, CA: 2001, 1003153.

[16] *Materials Reliability Program: Reactor Vessel Closure head Penetration Safety Assessment for U.S. PWR Plants (MRP-110)*, EPRI, Palo Alto, CA: 2004. 1009807.

[17] *Materials Reliability Program: Welding Residual and Operating Stresses in PWR Plant Alloy 182 Butt Welds (MRP-106),* EPRI, Palo Alto, CA: 2003. 1009378.

[18] *Materials Reliability Program: Evaluation of the Effect of Weld Repairs on Dissimilar Metal Butt Welds (MRP-114),* EPRI, Palo Alto, CA: 2004. 1009559.

[19] *Materials Reliability Program: Resistance to Primary Water Stress Corrosion Cracking of Alloys 690, 52, and 152 in Pressurized Water Reactors (MRP-111),* EPRI, Palo Alto, CA: 2004. 1009801.

B. 14 Fatigue

Fatigue life evaluation (S-N approach)

High-cycle fatigue

The most 'classical' fatigue-related degradation mechanism is high-cycle (HC) fatigue. HC fatigue involves a high number of cycles at a relatively low stress amplitude (typically below the material's yield strength but above the fatigue endurance limit of the material) [i]. The crack initiation phase is dominant here, since crack growth is usually fairly rapid. High cycle fatigue may be:

Mechanical in nature, i.e. vibration or pressure pulsation, or due to flow-induced vibration (FIV). FIV can induce HC fatigue in otherwise normally passive components merely through interaction of flow adjacent to the component or within the system, establishing a cyclic stress response in the component. Power uprates are of some concern here, as an increase in flow may change the acoustical characteristics of the system and excite a HC mode where a resonant frequency is achieved.

Thermally induced due to mixing of cold and hot fluids, where local instabilities of mixing lead to low-amplitude thermal stresses at the component surface exposed to the fluid.

Due to combinations of thermal and high cycle mechanical loads, such as might occur on pump shafts in the thermal barrier region.

Low-cycle fatigue

Low cycle fatigue is due to relatively high stress range cycling where the number of cycles is less than about 10^4 to 10^5. To induce cracking at this number of cycles requires that the stress/strain range causes plastic strains that exceed the yield strength of the material. Cycling thus causes local plasticity leading to more rapid material fatigue degradation. In reactor coolant system components, the cumulative combined effects of reactor coolant system pressure and temperature changes are considered in the component design analysis. The stress or, more correctly, strain cycling that contributes to low cycle fatigue is generally due to the combined effects of pressure, piping moments and local thermal stresses that result during reactor operation. The latter are usually highest in connection with transients (such as plant start-up/shut-down or hot stand-by). Particular attention must be paid to the possibility of locally high component stresses (e.g. from notch effects at welds or from piping restraints), even though nominal system design criteria are met.

---

[i] One of the recent concerns for fatigue cracking is "Giga Cycle" fatigue, which may take place beyond the 10^6 cycles usually used to define fatigue endurance guidelines. There are several observations showing a change in the mechanism of crack initiation. In Giga Cycle fatigue, cracks initiate inside the material, not from a surface, as commonly observed in normal HC fatigue Also, there is almost no data on environmental effects for Giga Cycle fatigue, which may be related, for example, to the failure of socket welds.

The major difference between high and low cycle fatigue is that, for low cycle fatigue, it is the crack growth rate which dominates component life, since crack initiation can occur after relatively few loading cycles. Fatigue crack propagation is discussed separately in Section II.

Thermal fatigue

Thermal fatigue is due to the cyclic stresses that result from changing temperature conditions in a component or in the piping attached to the component. Thermal fatigue may involve a relatively low number of cycles at a higher strain (e.g., plant operational cycles or injection of cold water into a hot nozzle) or due to a high number of cycles at low stress amplitude (e.g. local leakage effects or cyclic stratification). Although such issues have been known (and intensively studied) for many years, fatigue damage sometimes still occurs (see Section 6) when unexpected thermal loading is encountered, e.g. due to thermal stratification arising from incomplete mixing of water streams at different temperatures, which has led to significant incidents (e.g. at feedwater nozzles).

Environmental fatigue

Environmental fatigue concerns the reduction in fatigue "life" in reactor water environments compared to "room temperature air" and is also known as corrosion fatigue. It involves two primary aspects: the effects of a reactor water environment on the overall fatigue life of reactor components (i.e. both crack initiation and crack growth), and the potential accelerated growth of an identified or assumed crack-like defect due to cyclic loading in high-temperature water environments. Important examples of the effects on overall life for carbon and low-alloy steels (C&LAS) and for stainless steels (SS) are to be found in [1] & [2]. Reference [3] contains extensive discussion of corrosion fatigue crack growth for C&LAS, while the workshop presentations in [4] give a good overview of what is known here for SS and nickel-base alloys.

With regard to the evaluation of fatigue for component aging management, consideration of the effects of a particular environment on the overall fatigue life is usually more relevant (see Section 5). A key finding is that environmental fatigue often results in the disappearance of the high-cycle fatigue endurance limits that can be measured for the same alloy in air. Environmental acceleration of fatigue crack growth is also important, however, in dispositioning detected/postulated flaws in a component so as to permit continued operation.

It should be noted that confusion often arises through the (unrecognized) use of different definitions for fatigue crack initiation in terms of flaw size. In laboratory studies of low-cycle corrosion fatigue at constant strain amplitude, initiation is usually taken to correspond to a certain load drop (typically 25%) during testing. However this already corresponds to a relatively deep crack, and recent studies [5] confirm that incipient flaws form much earlier during cycling, although they may often not continue to grow. In the field, "initiation" is usually more arbitrarily defined as the crack length/depth that can reliably be detected during non-destructive component examination.

Fatigue crack initiation and crack growth rates are governed by a number of material, structural and environmental factors, such as stress (or, more fundamentally, strain) range, temperature, ECP (usually categorized only approximately as dissolved oxygen content), mean stress, loading frequency (although strain rate and wave form are more fundamental parameters), surface roughness and number of cycles. A factor that has often been left out of consideration to date is degree of coolant purity, which is surprising given the attention paid to this key environmental variable in studies of SCC field behavior. Some data is now available showing just how important this can be, at least for low-alloy steel in oxygenated BWR environments [6].

In the field, cracks typically initiate at local geometric stress concentrations, such as welds, notches, other surface defects, and structural discontinuities. The presence of pits in the surface of many alloys is often presumed to decrease corrosion fatigue life, since they can act as stress concentrators and potential fatigue crack initiation sites. In fact, however, pitting may often reflect environmentally assisted enhancement of fatigue cracking more indirectly (by indicating the local presence of an aggressive medium at the metal surface [7]) rather than being a fundamental stage in the corrosion fatigue process.

The major factor that has not received adequate consideration in laboratory investigations of environmental fatigue is undoubtedly flow rate. For C&LAS, the high flow rates typical of reactor operation are known to be very beneficial in reducing corrosion fatigue effects (with regard to both the initiation and growth of cracks). For stainless steels, the picture is more complex and experimental work in this area is still ongoing [8, 9, 10].

Fatigue crack propagation (da/dN vs. DK approach)

As has been described above, fatigue life evaluation is based mostly upon S-N curves, but several modes of fatigue crack propagation should also be taken into account in proactive materials aging management. Fatigue crack propagation can be caused by mechanical or thermal fatigue loading, and environmental fatigue effects may contribute to crack growth in both cases. The crack growth characteristics are interpreted in terms of da/dN vs. ?K, taking account of the stress ratio R and the frequency of loading. Such curves are, of course, dependent upon both materials and the environment.

If environmental effects are present, the flow rate of the medium also affects the crack propagation rate and, in general, a higher flow rate results in a lower crack growth rate for pressure vessel steels in PWR environments. In the case of low alloy steels, local crack tip chemistry can be modified by dissolution of MnS inclusions, thus acidifying the crack tip environment and resulting in higher growth rates for high sulfur materials. Up to now, no systematic crack propagation testing in terms of flow rate effects has been done on austenitic alloys under PWR conditions.

Extensive research on fatigue crack propagation has been done for many years by members of the international cooperative group on cyclic crack growth (ICCGR, former name of the current ICG-EAC group). The outcome has been largely taken into account in ASME Section XI rules for flaw evaluation, although some aspects (e.g. with regard to rules for components exposed to NWC in BWR plants) are still a subject of debate. For PWR environments, in particular, da/dN vs. ?K curves have been developed based upon a more mechanistic approach, i.e., time domain analysis.

One important issue, which was pointed out already in the 1970's, is the effect of ripple loading on crack growth rate, when the environmental effects associated with simultaneous stress corrosion cracking have to be considered. Such synergy of effects must be taken into account in the PMDA program. E.g., low-alloy steels, which have a rather high resistance to SCC in LWR environments, showed crack growth at a stress ratio of 0.98 and high frequency, even in pure water at 85C.

Crack propagation caused by thermal stress is another important area. Many field incidences of cracking are associated with initiation from local thermal stresses due exposure to water streams of different temperatures. However, these thermal stresses cause mostly very shallow cracks, because the temperature changes due to such water mixing are surface phenomena. However, such shallow cracks may start to propagate by other structural loads (including the effects of weld residual stress).

Significant reduction in the fatigue life of stainless steels has been observed in PWRs, but there is currently no mechanistic interpretation of these phenomena. Fatigue crack growth behavior in PWRs has been observed with mainly marginal enhancement, but it may be important to examine a possible impact on accelerated crack growth in PWR components due to this mechanism and studies are ongoing.

Synergistic effects of microstructural changes by aging at operating temperature and environmental effects can be a potential issue associated with license renewal. One example of such synergy involves dynamic strain aging and environmental fatigue crack propagation. Thermal aging of duplex SS, hydrogen entry into structural materials and irradiation can be other important microstructural changes with aging.

ASME Code rules on fatigue

Design against fatigue damage is based primarily on the fatigue curves in Section III, Appendix I (e.g., Figures I-9.1 and I-9.2) of the ASME Code. These curves indicate the number of stress cycles at a given amplitude of cyclic stress that is required to reach a so-called usage factor of 1.0. The fatigue curves are based on test data taken in air at room temperature, but reduced by a factor of 2 on stress range or 20 on cycles to failure (whichever is most conservative) to account for scatter of data, size effects, roughness, and non-laboratory environments. For carbon and low-alloy steel materials, the most adverse conditions of mean stress are used to correct the test data prior to applying these factors. The exact interpretation of the extent to which so-called "moderate service environments" were already taken into consideration when the ASME Code rules were drafted continues to be a major source of contention (see, e.g., reference [11]). Despite many years of development [12,13], more appropriate treatment of reactor water effects by the application of a so-called environmental fatigue multiplier (F_{en} factor) has not (yet?) found favor in the US within the ASME Code, although it is being applied on a plant-specific basis in the context of license renewal applications [14]. Such approaches are already used in Japan, however, [15] and incorporate specific consideration of key factors such as strain rate, temperature, oxygen content and (for C&LAS) sulfur content of the material.

The ASME Code includes analytical approaches and criteria for determining usage factors for Class 1 components. For Class 1 code components, the cumulative usage factor must be shown to be less than 1.0 for the component life. However, a fatigue usage factor of unity does not imply actual crack initiation both because of the safety factors applied to the stress amplitude or number of allowed cycles for the Code fatigue curves and because of the often conservative nature of the design-basis loads that have been assumed. Fatigue monitoring of real components can be valuable to reveal margins in this context. The assumed load pairs present a particular challenge in evaluating environmental fatigue, where realistic strain rates are a key consideration [16]

The crack growth that follows fatigue crack initiation can be predicted if the crack can be characterized and if the cyclic stress field is known. Procedures for performing crack growth analyses are contained in Section XI of the ASME Code. Again, the consideration given to environmental effects has sometimes been controversial and the present disposition lines do not necessarily reflect the current state of knowledge [6]. Significant progress has been made, however, for the specific case of LAS in PWR reactor water through the introduction of Code Case N-643 [17], which is currently undergoing further refinement. Work is ongoing to develop analogous cases for SS in PWR environments and for all classes of material in BWR reactor coolant.

Service experience of fatigue

Mitigation of fatigue damage for existing components is accomplished by reducing the magnitude of the applied loads or thermal conditions or reducing the number of cycles of loading. For thermal transients, reduction in the rate of temperature change for extreme temperature cycles can be effective (although it should noted that this can also increase any environmental component of damage, if present). However, the normal operating cycles are not generally the source of significant fatigue damage in nuclear plants. The observed fatigue cracking in service has mostly been due to high cycle fatigue as a result of conditions not anticipated at the time of original plant design. Some instances of (very) low-cycle fatigue cracking (with a significant environmental contribution) have also been reported, mainly in Germany [7].

Major areas of plant where fatigue failures and leakage have occurred are as follows:

RCS Piping

A number of fatigue issues have been identified, as described below.

The major occurrence of leakage has been due to mechanical vibration-induced cracking of small attached lines (primarily socket welded instrument lines). Power uprate has contributed to a number of recent incidences.

Thermal fatigue has also caused cracking in normal flowing lines where relatively colder water is injected into flowing RCS lines.

Thermal fatigue has also occurred in a number of normally stagnant branch lines attached to flowing RCS lines. The source has been thermal stratification/cycling due to valve in-leakage in up-horizontal running safety injection line configurations and swirl-penetration thermal cycling in down-horizontal drain/excess letdown lines. This is being addressed by the MRP Fatigue ITG and new guidelines are to be issued in mid-2005.

Although no occurrences of leakage have been identified, an issue related to surge line stratification was identified in 1988. The issue was resolved by analysis; however, the computed usage factors were quite high. Environmental fatigue effects are potentially significant for these lines.

Other potentially susceptible locations include PWR charging nozzles and BWR RHR tees, where significant thermal transients can occur in some plants.

Reactor Pressure Vessels

The effects of fatigue are adequately managed by adherence to the plant design basis, where thermal transients were considered in the original plant designs. The notable exception was BWR feedwater nozzles and control rod drive nozzles, where the effects of cold water injection caused cracking early in the life of some plants. Mitigating actions and continued monitoring have been implemented and have proved to be effective.

Pressurizers

There have been no known fatigue failures in pressurizers. However, recent considerations of cold water insurge to pressurizers have been identified that may be a contributing factor to leakage that has been observed in pressurizer heater sleeve welds. The pressurizer spray nozzle is also affected by some significant thermal transients. Pressurizer surge nozzles can be affected by thermal stratification conditions in the surge line.

Steam generator shell, tubes, and internals

Steam generator feedwater nozzles have exhibited cracking as a result of thermal stratification and cycling, but high oxygen content of the feedwater for low-power conditions may have also increased environmental effects. Girth weld cracking of the steam generator shells and cracking at feedwater nozzle blend radii have also been observed, where both hot/cold water thermal fatigue and an environmental contribution were identified.

RPV internals components

The major issue identified has been that due to flow induced vibration of BWR steam dryers following power uprates. This has led to cracking of the vessel-attached support brackets at several plants.

Areas for further research

Although fatigue is not perceived to be an issue of safety consequence based on the studies reported in [18], the combined effects of adverse loadings and environments may lead to more cracking in the future than has been observed in the past. In addition, the effects of power uprate have increased the occurrences of flow induced vibration failures and related damage to component supports. Thus, research in the following areas is recommended:

Develop a better understanding of the relationship between laboratory environmental testing and actual reactor water conditions. The conditions in laboratory testing are often significantly different than those observed in actual flowing reactor water (flow rate is a key variable deserving closer attention here)[ii].. In addition, material conditioning between the extremes of actual cyclic conditions may be beneficial in reducing environmental effects. Although this has been primarily identified as a License Renewal issue, the laboratory effects are real and indicate that the fatigue resistance in a water environment is not as good as was originally thought.

Understand better the extent to which laboratory test data (usually on small specimens) can really be transferred to complex component geometries.

Investigate high cycle fatigue effects due to hot and cold water mixing. Several incidences of cracking in France have led to EdF embarking on major research programs in this area.

Improve methods for predicting and quantifying flow-induced vibration and acoustic loadings. A number of cases have been identified that have resulted in component wear and failure. Giga Cycle fatigue at very small amplitudes is one of the issues for further investigation here (including environmental effects).

Past attention to fatigue issues has related primarily to pressure-retaining components. Additional, more detailed, evaluations are probably needed to determine flow-induced fatigue effects and safety consequences for reactor internals (and possibly other support components).

Consider whether random loading spectra (which may be more typical of some plant components) are properly represented in the fatigue testing database.

Synergistic effects of various forms of material degradation, such as thermal aging, on fatigue need to be studied, with special emphasis on the effect of ripple loading together with time dependent (SCC) crack growth.

[ii] Most of the experimental work on flow rate effects has been done in BWR environments, where effects of flow rate on fatigue life are very complicated. Sometimes higher flow rate seems to be beneficial and sometime harmful, depending upon materials, DO and corrosion potential. Flow rate affects the thickness of the surface boundary layer, supply rate of oxidants to the surface, removal of corrosion products from surfaces, flush out of cracks and, clearly, local water chemistry. Some experimental data obtained in the EFT program in Japan revealed such complicated effects of flow on fatigue life. More details in Japanese at

http://www.jnes.go.jp/katsudou/seika/2003/pdf_kikaku/04kizai-0006.pdf

References

1 NUREG/CR-6583 (ANL-97/18), "Effects of LWR Coolant Environments on Fatigue Design Curves of Carbon and Low-Alloy Steels," March 1998.

2 NUREG/CR-5704 (ANL-98/31), "Effects of LWR Coolant Environments on Fatigue Design Curves of Austenitic Stainless Steels," April 1999.

3 H.P. SEIFERT, S. RITTER, J. HICKLING, "Environmentally-Assisted Cracking of Low-Alloy RPV and Piping Steels under LWR Conditions", *Proc. 11th Int. Conf. on Environ-mental Degradation of Materials in Nuclear Power Systems – Water Reactors*, 2003, CD-ROM, ANS/TMS/NACE, Skamania Lodge, Stevenson, WA, USA, August 10 – 14, 2003.

4 Materials Reliability Program: Second International Conference on Fatigue of Reactor Components (MRP-84), EPRI, Palo Alto, CA, and Organisation for Economic Co-Operation and Growth (OECD/NEA/CSNI/R (2003) 2), and the U.S. NRC: 2003. 1003536.

5 H.D. SOLOMON, R.E. DELAIR & E. TOLKSDORF, Proc. 9th Int. Symp. on Env. Deg. of Materials in Nuclear Power Systems –Water Reactors, Pub. TMS, 2000, pp. 865 – 872.

6 J. HICKLING, H.P. SEIFERT & S. RITTER, "Research and Service Experience with Environmentally Assisted Cracking of Low Alloy Steel", PPChem 2005 7(1) pp. 04-12.

7 J. HICKLING, "Strain-Induced Corrosion Cracking of Low-Alloy Steels under BWR Conditions: Are There Still Open Issues?", Proc. 10th Int. Conf. on Environmental Degradation of Materials in Nuclear Power Systems – Water Reactors, Pub. NACE, 2002.

8 A. Hirano et al., "Effects of Water Flow Rate on Fatigue Life of Carbon Steel in Simulated LWR Environment Under Low Strain Rate Conditions", Journal of Pressure Vessel Technology, Vol. 125, (2003), pp. 52-58.

9 A. Hirano et al., "Effects of Water Flow Rate on Fatigue Life of Carbon and Stainless Steels in Simulated LWR Environment", PVP-Vol. 480, ASME, (2004), pp. 109-119A.

10 R. Kilian et al., "Environmental fatigue testing of stainless steel pipe bends in flowing, simulated primary water at 240 °C", 3rd International EPRI Conference on Fatigue of Reactor Components, Seville, Spain, Oct. 2004 (proceedings to be published by MRP).

11 Welding Research Council, Inc. Bulletin 487, "PVRC's Position on Environmental Effects on Fatigue Life in LWR Applications," W. Alan Van Der Sluys, December 2003.

12 "An Environmental Factor Approach to Account for Reactor Water Effects in Light Water Reactor Pressure Vessel and Piping Fatigue Evaluations," TR-105759, EPRI, Palo Alto, CA, December 1995.

13 H.S. MEHTA, "An Update on the Consideration of Reactor Water Effects in Code Fatigue Initiation Evaluations for Pressure Vessels and Piping," PVP-Volume 410-2, pp. 45-51, American Society of Mechanical Engineers, 2000.

14 Materials Reliability Program Guidelines for Addressing Fatigue Environmental Effects in a License Renewal Application (MRP-47), EPRI, Palo Alto, CA, U.S. Department of Energy, Washington, D.C.: 2001. 1003083.

15 "Guidelines for Environmental Fatigue Evaluation for LWR Component," Thermal and Nuclear Power Engineering Society (TENPES), June 2002 (Translated into English in November 2002).

16 S. RANGANATH & J. HICKLING, "Development of a possible bounding corrosion fatigue crack growth relationship for low alloy steel pressure vessel materials in BWR environments", 3rd International EPRI Conference on Fatigue of Reactor Components, Seville, Spain, Oct. 2004 (proceedings to be published by MRP).

17 ASME Code Case-643, "Fatigue Crack Growth Rate Curves for Ferritic Steels in PWR Water Environment," May, 2000.

18 NUREG/CR-6674 (PNNL-13227), "Fatigue Analysis of Components for 60-Year Plant Life," June 2000.

B.15 Predicting Failures Which Have Not Yet Been Observed— Microprocess Sequence Approach (MPSA)

1. Background

The purpose of this topical report is to describe an approach to predicting corrosion failures that have not yet been observed but could occur after long times, such as those associated with LWRs that are re-licensed. This approach is in the category of "*pro-active*" prediction, where possibly future failures are intentionally sought out, and the credibility for producing failures is assessed. This approach also challenges conventional assumptions about the cause and nature of corrosion failures. In the past, failures have occurred first; and the nuclear materials community, then, has responded usually with excellent work aimed at explaining the observations. This is "*re-active*" research. We are concerned here, rather, with the mechanics of "*pro-active*" prediction.

This discussion deals with predicting corrosion processes in LWRs, although the approaches described here would apply broadly to other industries. This discussion is also mainly concerned with stress corrosion cracking (SCC) and corrosion fatigue (CF), as they are connected; and, some aspects of flow-assisted corrosion (FAC) are included. These are the most likely modes of corrosion to produce serious failures. Other topics of accelerated damage include wear at anti-vibration bars (AVB), but these are not discussed here, although such modes are within the scope of this approach.

An essential assumption of this discussion is that very long times until failure are not related to a monotonic progression of SCC processes. Rather, the long times are most likely associated with other factors that produce specific local conditions that "open the gate" for SCC or other rapid processes. These preliminary processes occur over a "precursor period." Schematically, such cases are shown in Figure B.15.B.15.1. Case I corresponds to SCC, starting upon initial exposure to an environmental condition that produces SCC, as described in Section 2.1; Case I corresponds to failure processes (e.g. to LPSCC) that initiate as soon as the surfaces are exposed to primary water at operating temperature. Case II corresponds to SCC that starts after necessary conditions for initiation are achieved in relatively short times (e.g. half to 20 years), for which there are already examples as described in Section 2.2.

The approach described here for predicting failures, which have not yet occurred, is the "Microprocess Sequence Approach" (MPSA). This approach utilizes sets of elements from the environments and materials where these elements can be identified, and quantified, and connected sequentially or in parallel, to provide a scenario leading to the initiation of failure. The overall procedure is described in Figure 38 of Section 5.0.

What is actually being predicted here is not the course of the SCC itself but rather the time to arrive at the conditions for SCC to start, as shown for shorter cases in Case II and much longer times in Case III of Figure B.15.1. It is assumed here that existing correlations, (e.g. from Staehle and Gorman,[i]) for the occurrence of SCC will be activated once the precursor period has produced the necessary conditions for SCC to initiate.

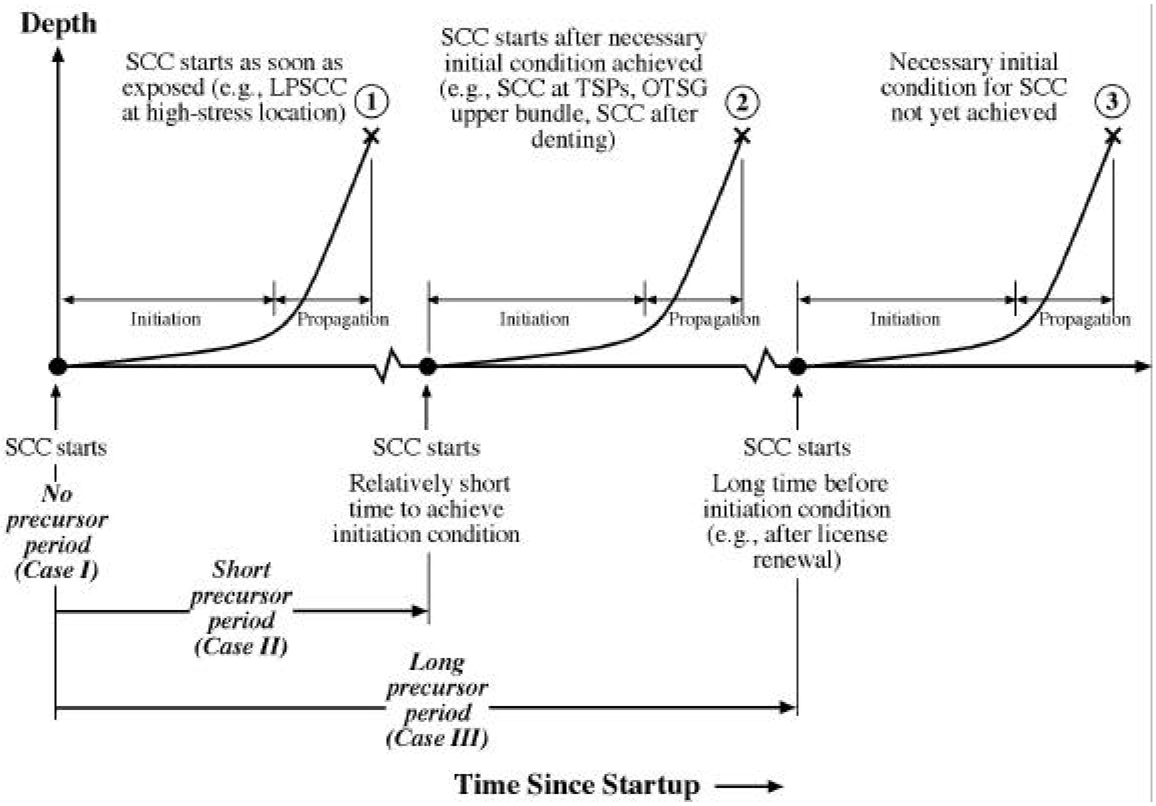

Figure B.15.1 Schematic view of three cases for the time-dependence of SCC. Initiation and propagation times assumed to be the same. The three cases are differentiated by the length of the precursor periods.

Such longer times should be compared with the range of time over which re-licensing is expected to occur as shown in Figure B.15.2. Relative to the schedule for re-licensing, it appears that instances of SCC in the nuclear industry have occurred in essentially three stages as suggested in Figure B.15.3. In Stage I, failures occurred in the early use of stainless steel tubes and then in Alloy 600 tubes. These failures were extensive. In Stage II, the present stage, SCC is occurring in the laboratory for Alloy 690TT and in the non-decorated grain boundaries of stainless steel. This present discussion about prediction applies to a Stage III, where a pro-active approach is required and where future failures are assessed by the reasonableness of scenarios as described in Section 5.0 and Figure 38. In this Stage III, a relatively long time is consumed by the precursor period in which conditions for the occurrence of SCC must first develop before SCC can start, as shown for Case III in Figure B.15.1.

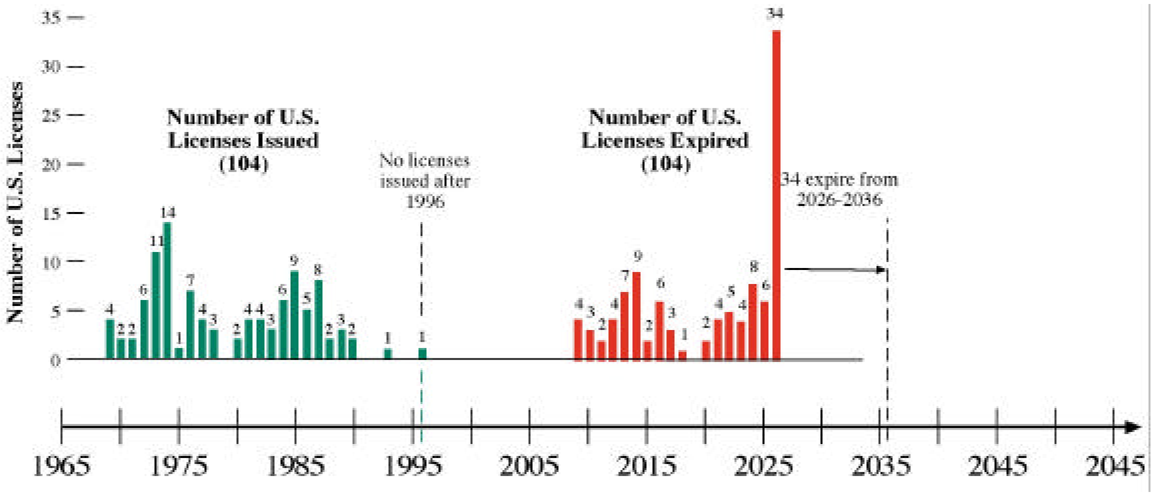

Figure B.15.2 Number of U.S. licenses issued and expired vs. time compared with a 20-year life extension after a presumed re-licensing.

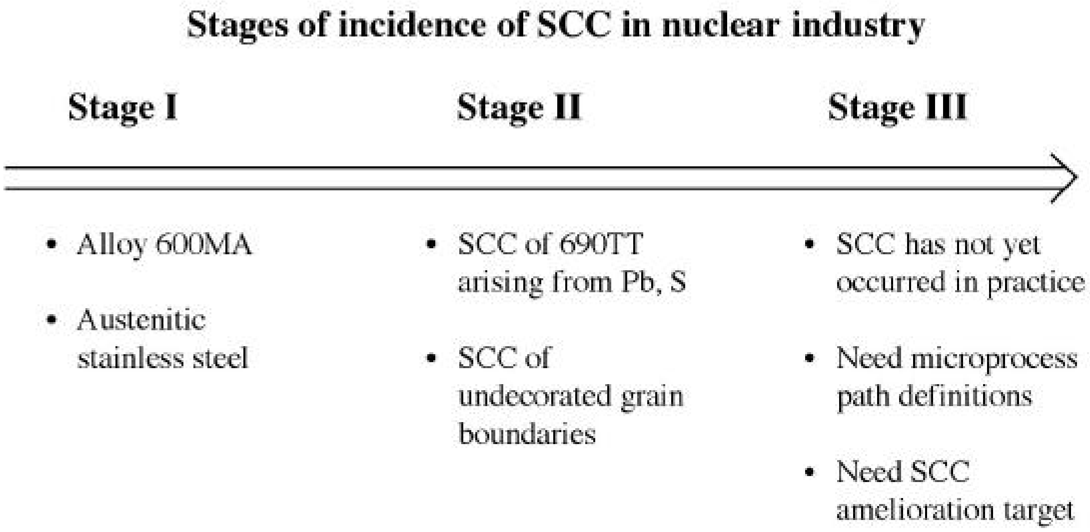

Figure B.15.3 Schematic illustration of the stages of SCC occurrences over time in the LWR industry.

The theme of this report is illustrated in Figure B.15.1 for Case III. Here, the conditions that are necessary for SCC to occur have not yet fully developed during the initial licensing period. The central question, then, is: what are the processes that could produce the necessary conditions to activate the SCC at this later time? Our assertion here is that predicting SCC/CF that has not yet occurred, i.e. *pro-active* prediction, can be approached credibly by using information and understandings that are already available and linking them in sensible ways to predict the time required for completion of the precursor period, of Figure B.15.1 Case III, before the SCC can start. The challenge, then, is to identify this information and explore out understandings. Such an approach is described in Sections 3.0 and 4.0.

There are, presently, no serious predictive methods for SCC that are not based on extrapolating from already existing failures. Current methods include:

- Accelerated testing and carrying forward the data, usually the mean value, with experimentally determined dependencies such as the activation energy (e.g. Q=40kcal) or the stress exponent (e.g. n=4). This is more or less how performance is predicted at the present.

- Developing correlation equations and choosing limits for scatter (e.g. three sigma) for design, i.e. safety factors.

- Enclosing scattered data with an enveloping curve and assuming that the envelope gives a conservative value.

- Taking a Bayesian statistical approach where successive failures on a cumulative distribution give progressively more confidence to the shape factor and its extrapolation.

- Using probabilistic fracture mechanics where the probability of occurrence of critically sized defects and the probabilistic evaluation of the critical stress intensity provide the basis for the probability of future failures.[ii,iii,iv,v,vi]

- Applying a "fitness for service" approach where defects are assessed at some time during service, (e.g. an inspection period), and then assessing whether these defects can lead to potential failures.

- Using the Corrosion Based Design Approach (CBDA), as described by Staehle,[vii] involving the ten segments of environmental definition, material definition, mode definition, superposition, failure definition, statistical definition, accelerated testing, prediction, monitoring and inspection, and feedback.

- Using the "Locations for Analysis" (LA_i) approach as described by Staehle,[vii] where obvious locations containing multiple stressors of relatively intense values occur together.

- Using physically based statistics for predicting the "First Failure" as described by Staehle.[viii,ix] Here, each of the statistical parameters is modeled using existing data for the seven primary variables as shown in Figure B.15.4.[i,ix,xxxvii] The final distribution then, includes the three, now physically dependent, statistical parameters with their respective dependencies.

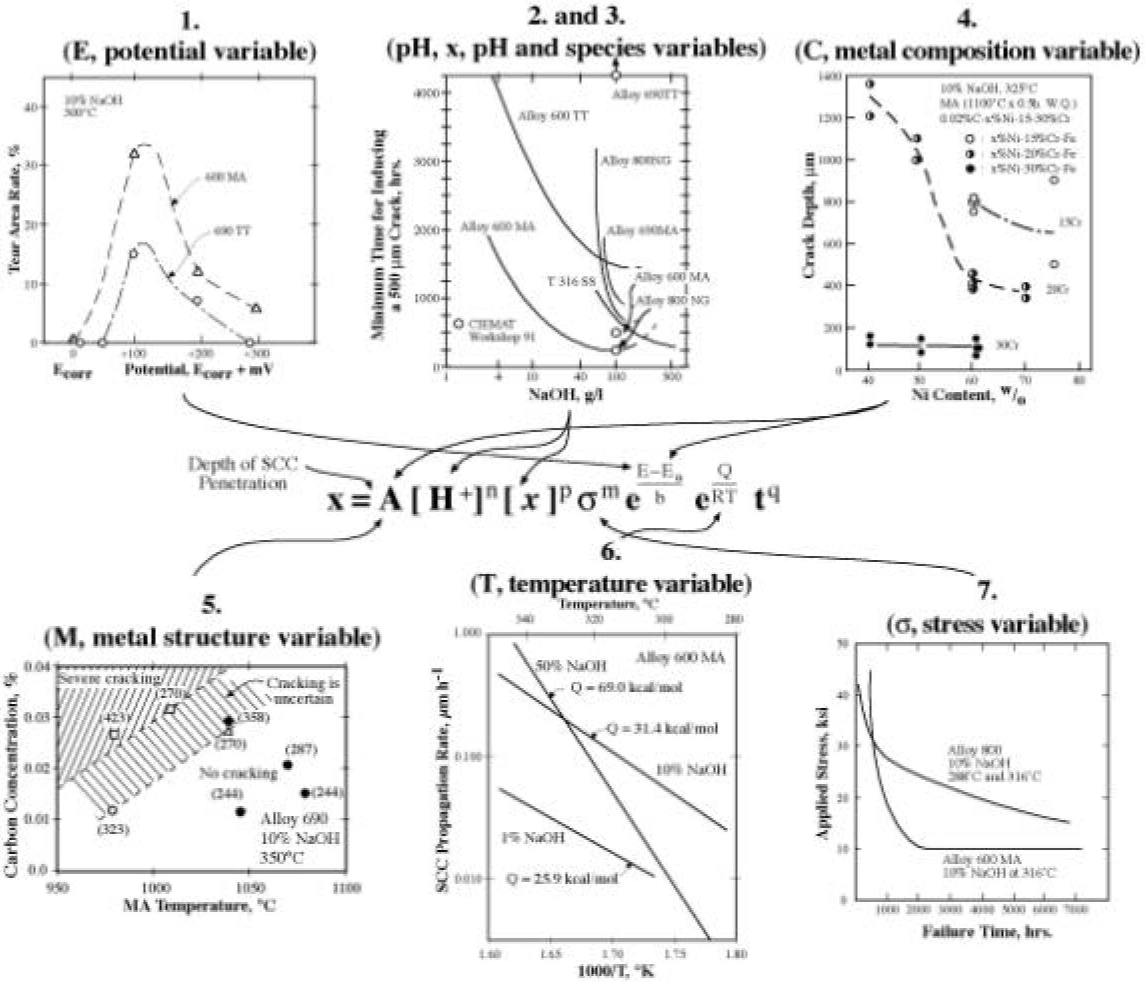

Figure B.15.4 Examples of dependencies on the seven primary variables for SCC as they apply to a correlation equation that might be used to model the statistical parameters for a statistical distribution. These examples are taken from data, which describe SCC in alkaline solutions. These data are discussed by Staehle and Gorman.[i]

A practical question here, is how can failures that have not yet occurred be found? The essence of the approach in this report, the "Microprocess Sequence Approach (MPSA)" for predicting the precursor conditions that must coalesce before SCC occurs, as indicated in Figure B.15.1, consists of six steps as follows:

- The influences on materials can be divided into six domains and their respective microprocesses. The breakdown of the domains is somewhat arbitrary, but practical and convenient choices are: global environment, bulk environment, outside surface, protective surface layer, inside metal surface, and bulk metal. These domains, with examples of possible microprocesses, are identified in Figure B.15.5. These domains are discussed in Sections 3.0 and 4.0.

- Identify the modes of failure of interest, (e.g. SCC, CF, FAC), and develop information bases for their dependencies of occurrence, as described in Section 6.0. These define targets for scenarios, as described in Section 5.0, which involve practical aggregations of domains and their microprocesses.

- Identify the "microprocesses" of these domains that could affect the modes of failure. These microprocesses, as they apply for the six domains, are described in Section 4.0; and examples are shown in Figure B.15.5.

- Develop likely scenarios as suggested in Figure B.15.6 and Section 5.0, which connect microprocesses of the six domains, and which have a high likelihood for leading to failure. These scenarios would constitute the precursor period as identified in Figure B.15.1 for Cases II and III.

- Quantify possibly critical microprocesses in terms of their dependence on the variables that lead to critical conditions for SCC to occur at the end of the precursor period.

- Develop critical experiments to assess whether the proposed scenarios and their component microprocesses are credible.

Predicting SCC in LWRs in the past has been hindered by overly restrictive and often poorly informed assumptions on the microprocesses such as:

- SCC occurs only in the presence of "specific ions."

- SCC does not occur either in pure environments or in pure materials; i.e. SCC of Alloy 600 in pure deoxygenated water is not credible.

- Boiling $MgCl_2$ is a suitable environment to assess the dependence of SCC on alloy composition.

- Pure water cannot produce SCC of sensitized stainless steel.

- Water chemistry used for fossil boilers should be adequate for nuclear boilers.

- Tube support crevices will not accentuate any chemistry that could lead to SCC.

- There is not sufficient Pb in feed water to produce PbSCC even if it is concentrated.

- SCC due to Pb in Alloy 600MA is transgranular.

- Stainless steel without sensitization will not sustain SCC.

- The high purity of water in secondary OTSG water will not produce deposits on superheated upper bundle surfaces.

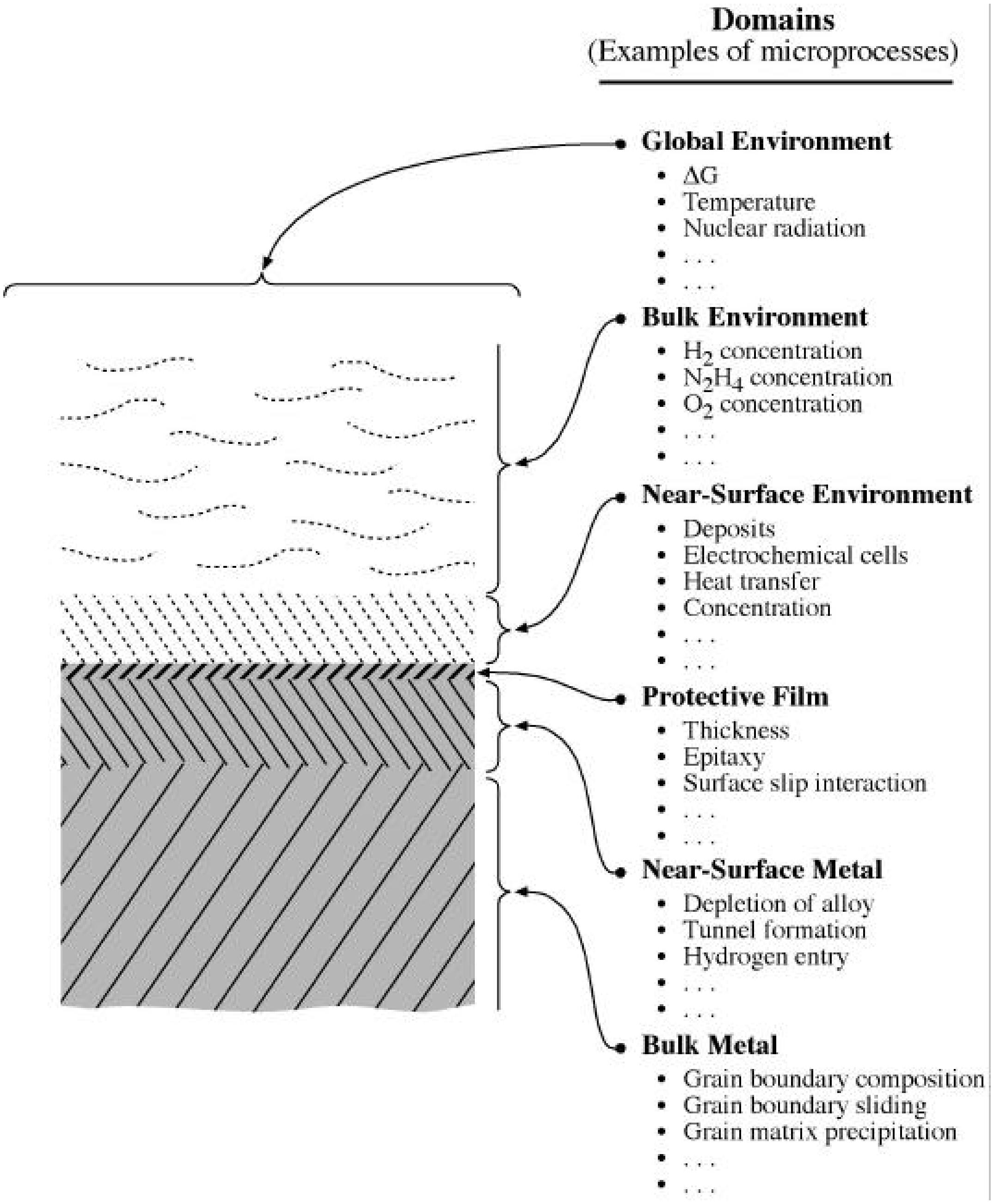

Figure B.15.5 Schematic view of six domains for quantifying microprocesses relating to the continuum from a global environment through to the bulk metal. Examples of microprocesses indicated.

There are more such assumptions. Rarely have engineers recognized and thought critically to question and test such assumptions. Similar assumptions may still hinder our capacity to predict performance. In Section 2.0, examples of failures, which have occurred and are already known, and which follow this microprocess route are considered and provide examples of important aspects of the MPSA approach. Section 3.0 describes domains and their inherent icroprocesses; Section 4.0 describes physical details of microprocesses and their implications; Section 5.0 describes how scenarios are developed and applied; Section 6.0 describes the failure target (e.g. start of SCC after the precursor produces necessary conditions) for the development of scenarios; finally, in Section 7.0 some predictions for future and not yet observed damage are developed based on the procedures described in this report.

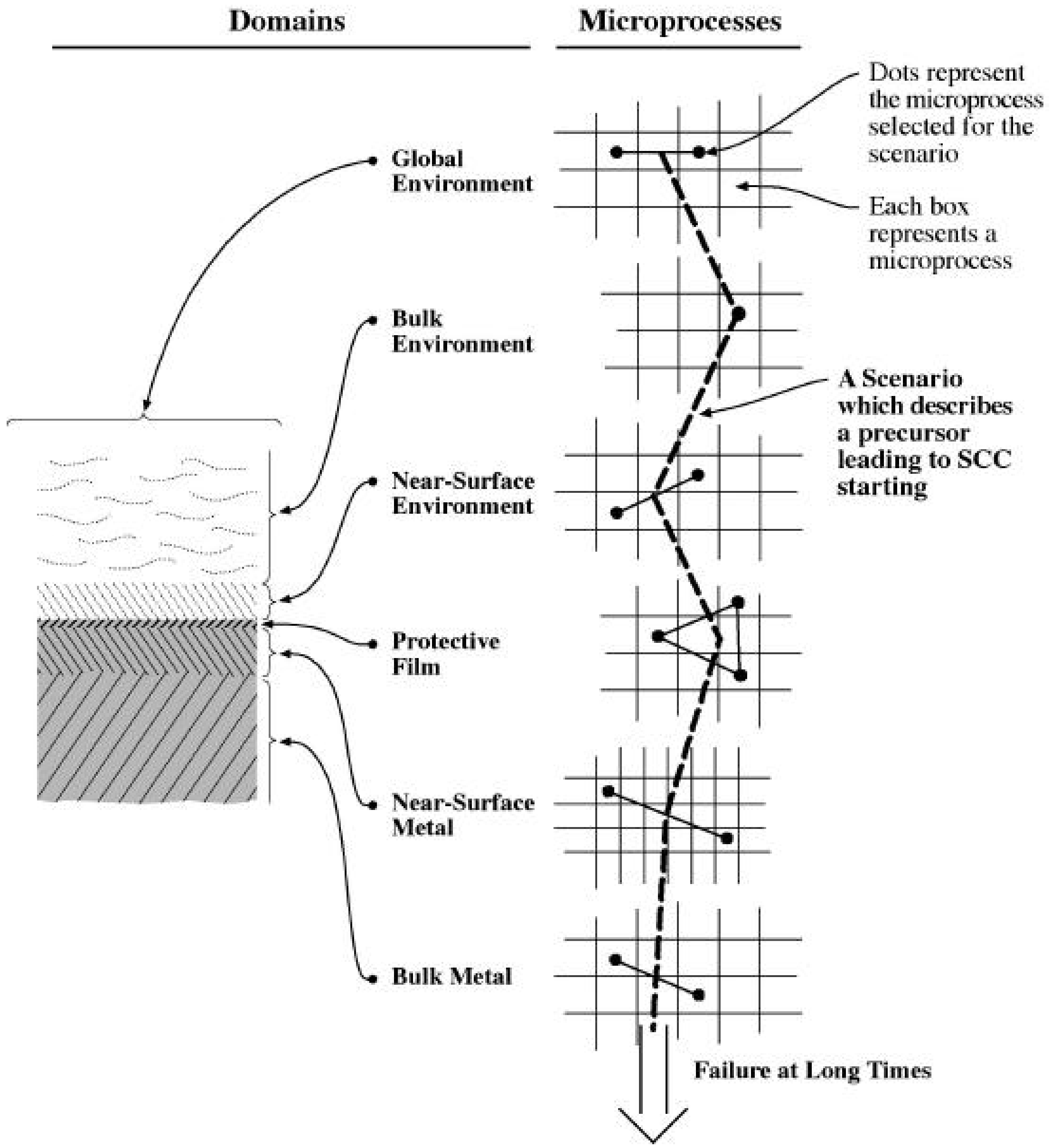

Figure B.15.6 Schematic view of a scenario that might be developed, which links microprocesses in successive domains as the scenario would apply to the precursor stage of Figure B.15.1.

2. Examples of Past Sequential Failures

The purpose of this section is to describe examples of failures that correspond to Cases I and II of Figure B.15.1. These failures provide insights to how failures with longer precursor times might evolve. Section 2.1 describes failures that begin when the plant starts and where the time-to-penetration is associated with the evolution of the SCC or FAC itself with no need to develop pre-conditions over time. This corresponds to Case I of Figure B.15.1. Section 2.2 corresponds to Case II of Figure B.15.1 where a relatively short (e.g. half to 20 years) precursor period precedes the evolution of the SCC itself.

2.1 Failures without time-dependent pre-conditions, no precursors, Case I

SCC on the primary side, LPSCC--no precursor

On the primary side of steam generator tubes there are no crevices, and the chemistry is generally constant with time. The major stressors are residual stresses and temperature; thus, any SCC that occurs does not depend on accumulation processes in a precursor period. The highest residual stresses are initially present either at small diameter U-bends or at roll transitions at the top of the tubesheet; Figure B.15.7a[x] shows data for the temperature dependence of LPSCC in the small diameter U-bends of SGs. The earliest failures at the highest temperature, about 306°C, occurred after 20-30 months. Figure B.15.7b[xi] shows a cumulative distribution function (cdf) in Weibull coordinates for the LPSCC in US and French plants. Here, the values of *q* (characteristic space parameter in the Weibull distribution) are in the range of 10 to 41 EFPY and the values of *b* (slope or "shape factor" in the Weibull distribution) are in the range of 1.36 to 4.93 (noting that these data were analyzed with a two parameter Weibull fit). Such data suggest that the first failures occur in the range of about 0.1 of the mean. The data of Figure B.15.7, taken together and recognizing the differences in temperature, indicate that early LPSCC can occur in about a year. Details of dependencies of LPSCC are described by Staehle and Gorman.[i]

Local cold work on the secondary side, Case I--no precursor

Figure B.15.8 describes a situation in which relatively deep scratches, which were present at the start of the operation, produced local cold work that initiated extensive SCC. Staehle and Gorman[i] have summarized numerous such instances. Such SCC has penetrated the full thickness of the tubes five years after the start of operation and was found on the surfaces of the cold leg of the secondary side. Hundreds of SCC events per inch occurred on some of the scratches. The fact that such SCC initiated and propagated on the free span of the cold side attests to the severity of the initial cold work.

Figure B.15.8 shows first in (a)[xii] and then (b)[xii] the location of the failures. Figure B.15.8c[xii] shows details of the scratch in plan view, and Figure B.15.8d[xii] shows the scratch in cross section with the SCC emanating. Figures 8e[xiii] and 8f[xiv,xv] show the accelerative effects of cold work, which supports the conclusion that local cold work started the cracks nucleating early. The scratches here seem to be deeper than ordinary scratches from processing.

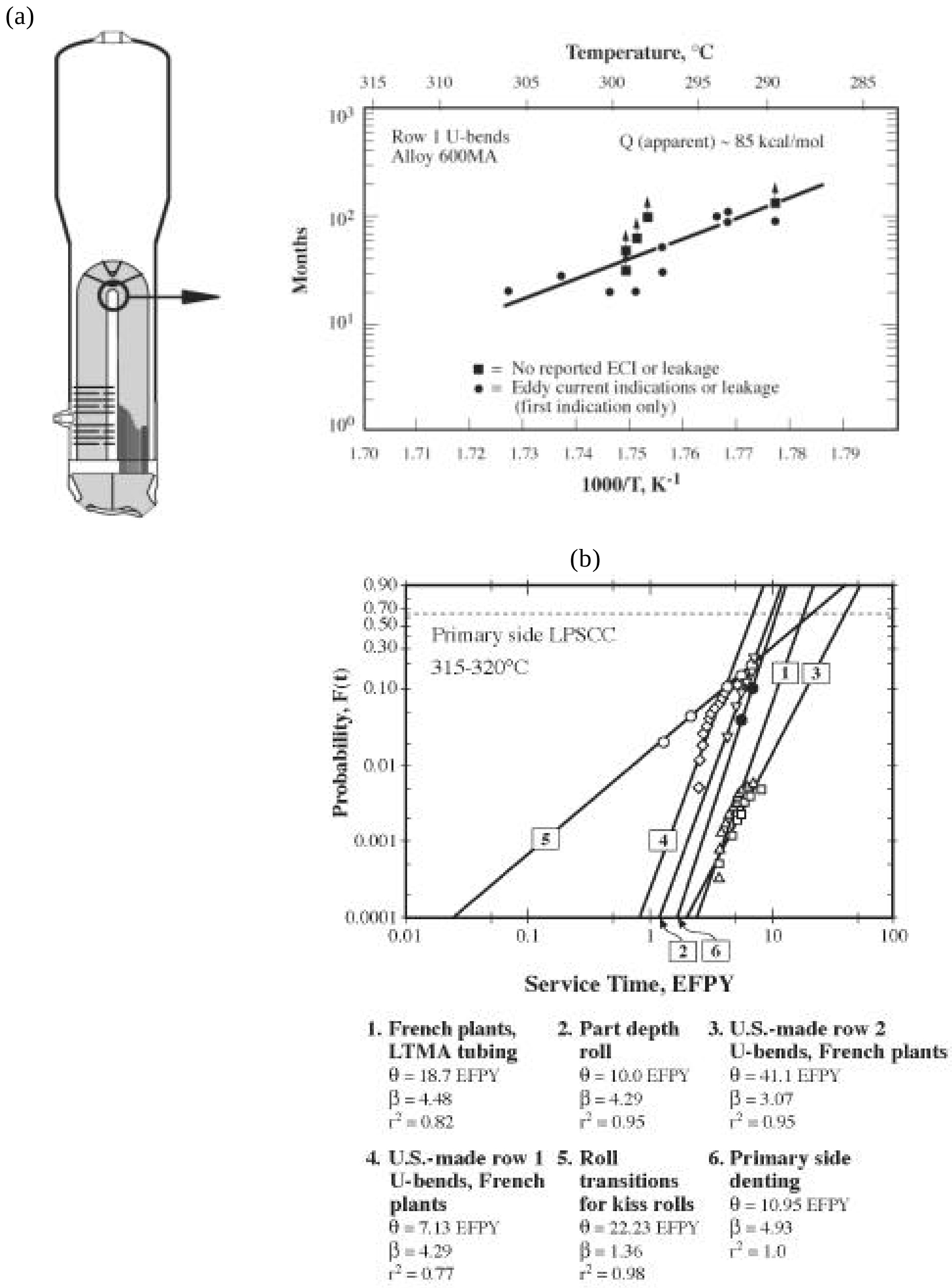

Figure B.15.7 (a) Time-to-failure for Row 1 U-bends of PWR steam generators on the primary side. From Begley et al.[x] (b) Probability vs. service time (EFPY) for the LPSCC occurring on the primary side of tubes from operating SGs in PWRs. Temperatures in the range of 315 to 320° C. From Staehle et al.[xi]

Figure B.15.8 also shows a scenario starting with M-1 ("M" identifies a "microprocess") through M-4, i.e. from the scratch through the cold work to the SCC, as accelerated by cold work and the SCC propagating as it moves beyond the cold work. However, here, this SCC certainly began at the start of life of the plant. The scratches accelerated the initiation. The relatively long time for perforation, compared with Figure B.15.7, results from the lower cold leg temperatures.

Flow assisted corrosion (FAC) at Mihama—no precursor

Figure B.15.9 shows a failed pipe in a section from Mihama 3 at the orifice between the #4 low pressure heater and the deaerator operating at approximately 142°C. The pipe was 560mm in diameter and the wall was 10mm thick. The flow rate of water was 22m/s at a pressure of 0.93MPa and a pH of 8.6-9.3. The failure occurred after 185,700 hours of operation. The failure resulted from flow-assisted corrosion (FAC) at a location where there had been no inspections. The resulting failure killed five people and injured four others.

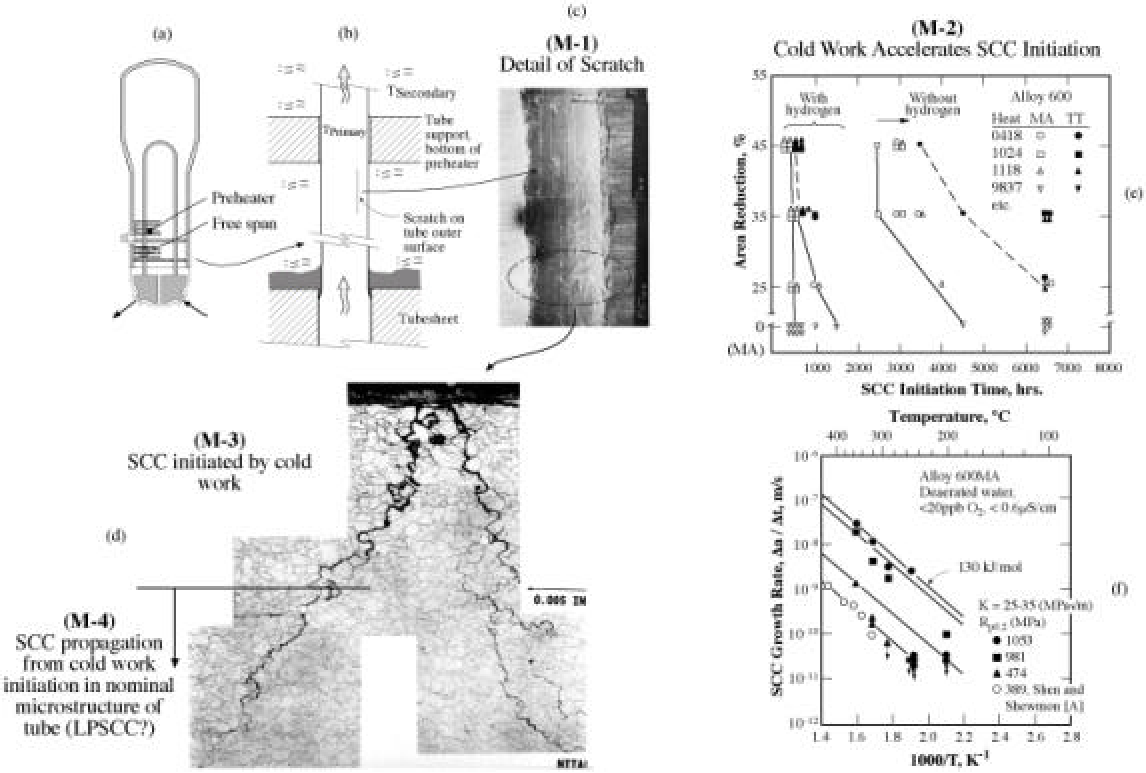

Figure B.15.8 SCC at free-span cold leg at McGuire-2 in an Alloy 600MA tube. (a) General location of scratch and SCC. (b) Schematic view of location of SCC. (c) Detail of scratch with SEM. (d) Cross section of SCC. From Eaker.[xii] (e) Area reduction vs. SCC initiation time for Alloy 600 for several heats in environments with and without hydrogen.[xiii] (f) SCC growth rate vs. 1000/T for Alloy 600MA with various yield strengths achieved by cold work. From Speidel and Magdowski,[xiv] with data from [A] Shen and Shewmon.[xv]

The pipe was a thin wall large diameter pipe with high velocity water flowing at 22m/s. The FAC involved in this accident most certainly started at the initial operation and did not involve any precursor period according to Case I of Figure B.15.1. Although the FAC proceeded at a relatively slow rate, no inspections were performed and no analysis of an acceptable operating period had been performed.

Stress corrosion cracking in sensitized and non-sensitized stainless steels in BWR applications – no precursor

Figure B.15.10 shows three examples of data for SCC in stainless steels, which are used in BWR applications. These include sensitized Type 304, non-sensitized Type 304, and stabilized Types 321 and 347. Numerous instances of SCC in non-sensitized stainless steel have occurred.[xvi,xvii,xviii,xix] In these cases, the local environment and condition of material do not change, although low temperature sensitization could aggravate the susceptibility to SCC.

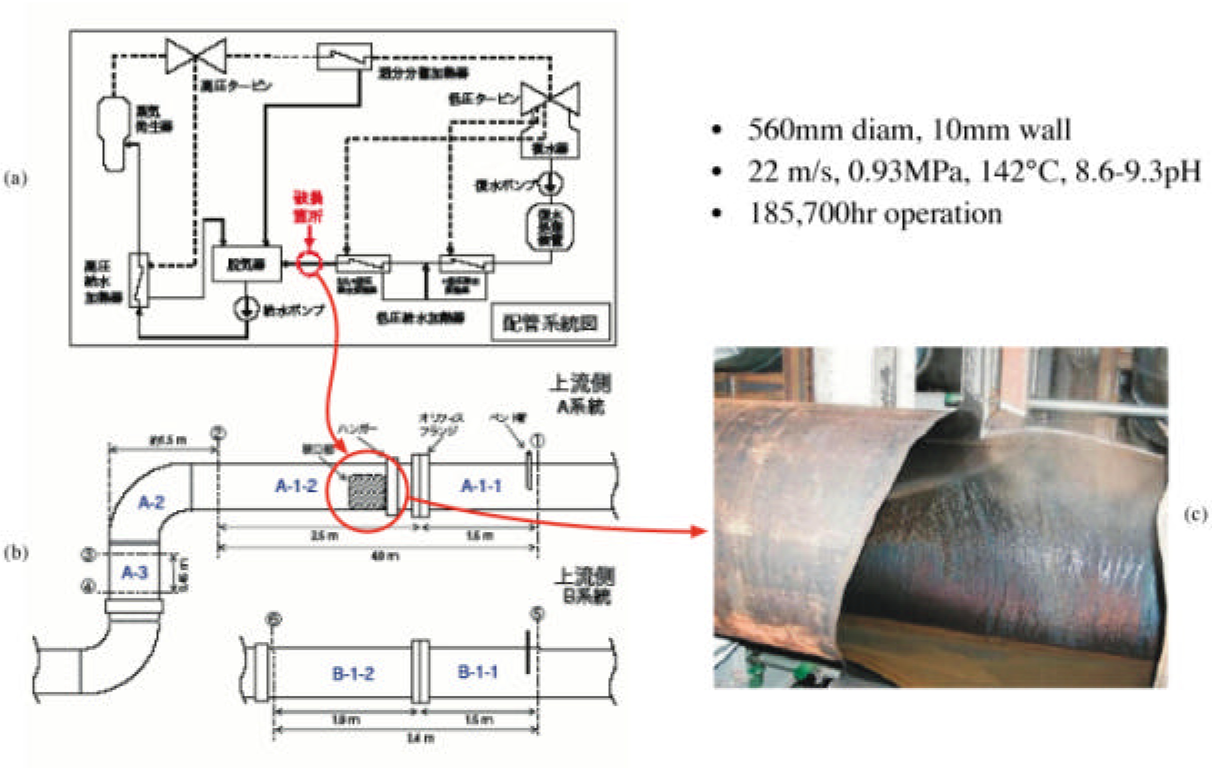

- 560mm diam, 10mm wall
- 22 m/s, 0.93MPa, 142°C, 8.6-9.3pH
- 185,700hr operation

Figure B.15.9 (a) and (b) Locations of failure. (c) Failure of pipe.

Figure B.15.10a[xx] shows the probability of cracking vs. time for SCC of 2” and 4” stainless steel piping that was sensitized at welds and exposed to BWR conditions. Here, the probabilistic nature of the ultimate failures is clear, although the initiation most likely started with the beginning of operation of the plants.

Figure B.15.10b, from work by Angeliu et al.,[xxi] compares sensitized and non-sensitized Type 304 stainless steel in BWR environments vs. the corrosion potential and shows that the crack growth rates for both heat treatments are not significantly different. The crack growth rate for the cold worked materials is increased.

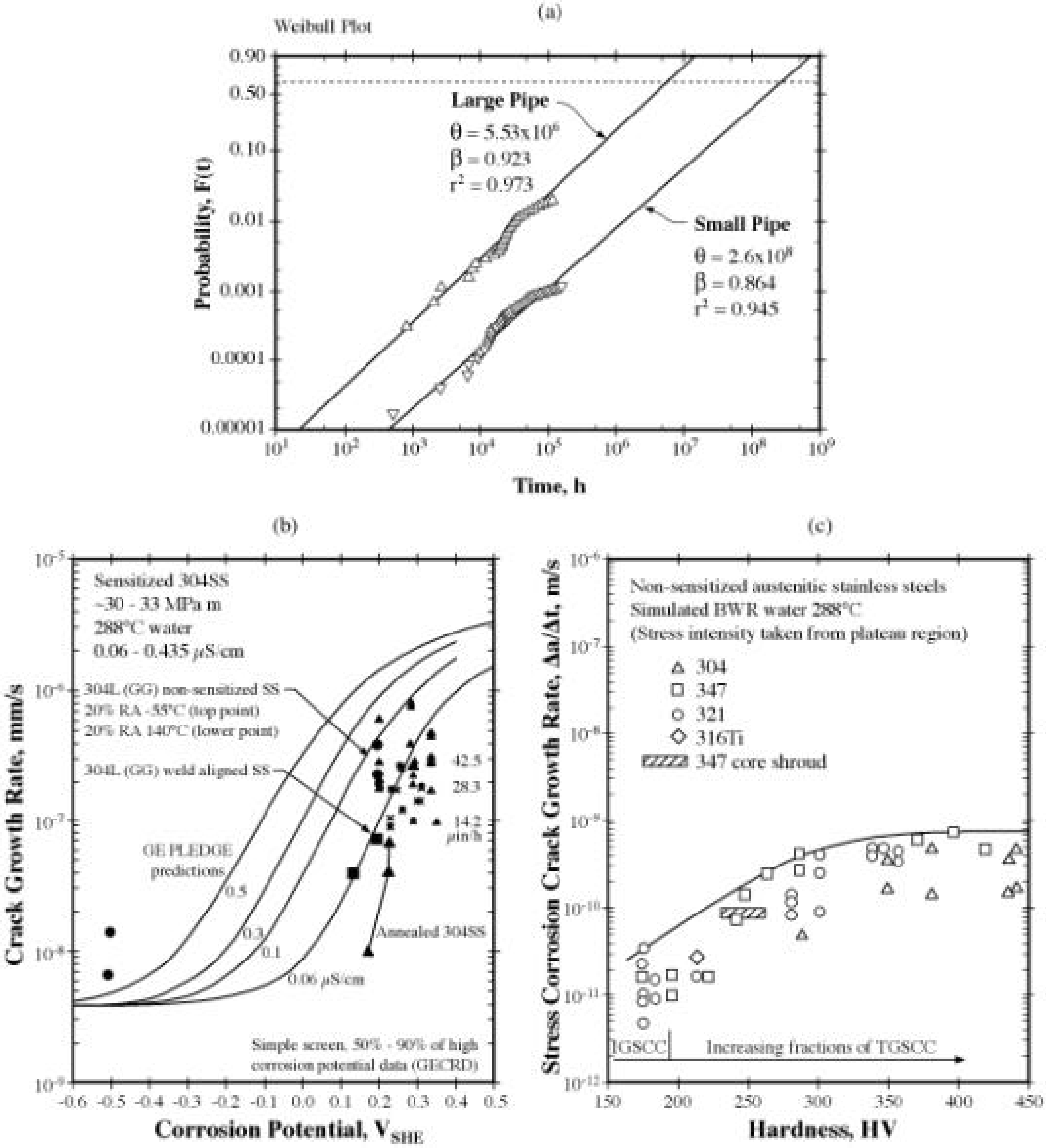

Figure B.15.10 SCC of stainless steels exposed to normal BWR water chemistry. (a) Probability vs. time for the failure of Type 304 stainless steels in two different pipe diameters in operating plants as shown in Weibull coordinates. Failures or indications have occurred at the smooth inside surfaces associated with welds. From Eason and Shusto.[xx] (b) Crack growth rate vs. corrosion potential for stainless steels in sensitized and non-sensitized Type 304 stainless steel. Specimens of non-sensitized stainless steel are cold worked. From Angeliu et al.[xxi] (c) Crack growth rate vs. hardness for non-sensitized stainless steels. From Speidel and Magdowski.[xxii]

Figure B.15.10c, from work by Speidel and Magdowski,[xxii] compares Type 304 with stabilized stainless steels and with a core shroud as a function of hardness. Here, the trend in Figure B.15.10b is corroborated and extended.

2.2 Failures with significant but relatively short precursor times, Case II.

In this section, examples of failures are described where the SCC is preceded by a precursor step, as shown in Case II of Figure B15.1. These examples suggest how such precursors might arise and proceed.

ODSCC at tubesheets and tube supports--precursor

Figure B.15.11 shows successive steps (M-X) leading to SCC on the outside diameter of SG tubes in heated crevices. The precursor steps involve at least the following:

a. Build-up of deposits in crevice (M-1).

b. Concentration of chemicals in heat transfer crevices (M-2).

c. Further concentration and chemical reactions inside the crevices (M-3).

Then, the resulting SCC, as shown at (M-4), can initiate. This precursor process is not lengthy, but the overall process is nonetheless a Class II process with a precursor preceding the initiation of SCC.

Denting associated with tubesheets and tube supports--precursor

Figure B.15.12 shows an integrated view of the denting processes as they may occur at tube supports or at the top of the tubesheet and as related to previous experimental work of Pickering et al.[xxiii] and Pilling and Bedworth.[xxiv] The precursor steps for denting are much like the ODSCC in Section 2.2-1. The precursor steps involve at least the following:

a. Build-up of deposit in crevice (M-1).

b. Concentration of chemicals in the heat transfer crevices (M-2).

c. Corrosion products expand, according to the predictions of Pilling and Bedworth,[xxiv] as the carbon steel of the tube supports corrodes. These corrosion products produce stresses (M-3), as measured by Pickering et al.,[xxiii] in the tube wall and cause it to collapse (M-4).

The straining of the tube, after the corrosion products expand, produces SCC from both inside and outside of the tubes (M-5). Such SCC has not been observed associated with denting at the top of the tubesheet, but such a result is imminent as described in Section 7.0. From the analysis of Staehle and Gorman,[i] based on extensive work in the literature, it appears that the growth of the oxide was particularly influenced by the presence of chloride and copper in the secondary environment. Thus, improving the integrity of the condensers and changing the condenser materials from copper-base alloys to titanium were the main avenues for mitigation.

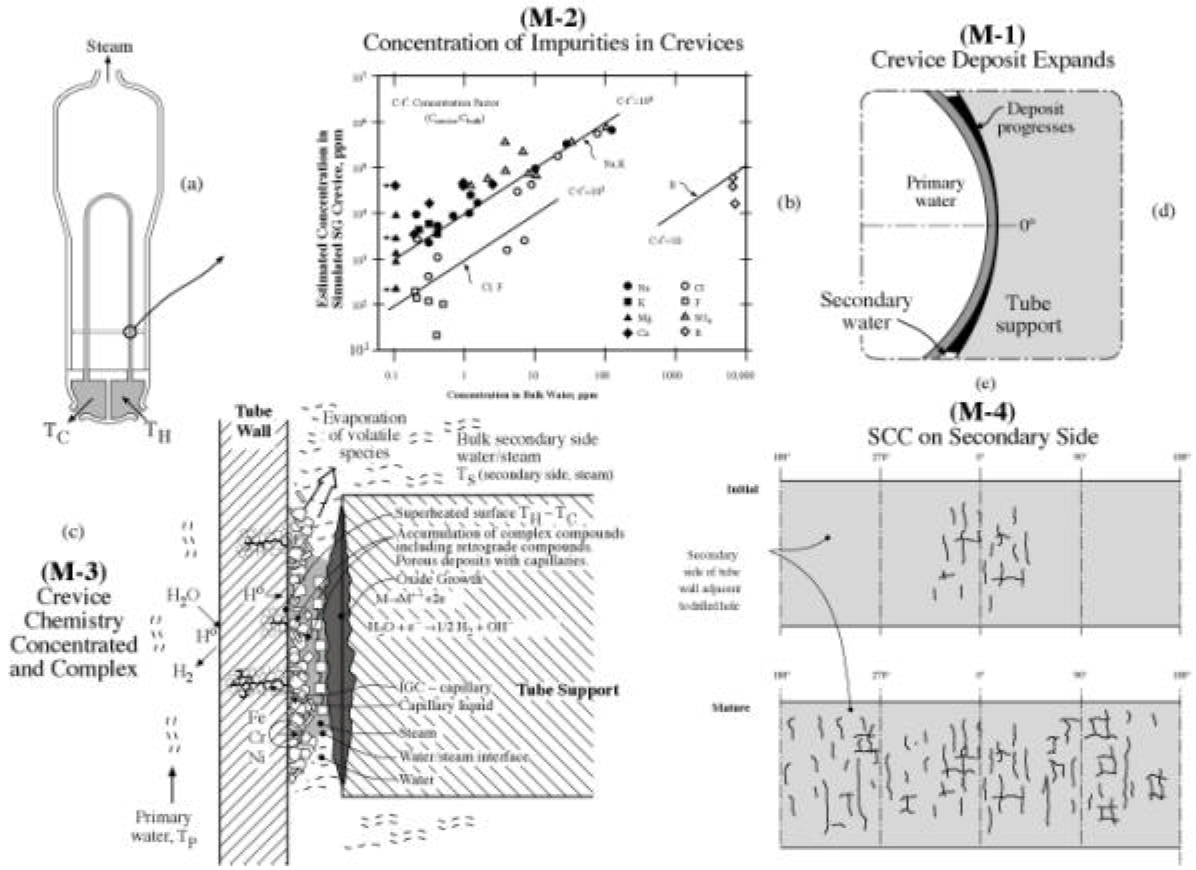

Figure B.15.11 Steps involved in the SCC on the OD of a tube associated with a drilled hole geometry of an Alloy 600-tubed steam generator.

SCC in OTSG upper bundle--precursor

SCC has occurred in the upper bundles of SGs where the steam is progressively superheated. While this SCC appears to be mostly focused at scratches, SCC and IGC occur outside these scratches to a lesser extent. The tube material is Alloy 600SR (stress relieved). Figure B.15.13a[xxv] shows the composition of various parts of the surface and SCC. It appears that the design of these OTSG units assumed that the water would be so pure that such accumulations of chemicals would not occur and would certainly not damage the tubes. The SCC was quite extensive in the superheated region. Figure B.15.13b[xxvi] shows the tubes plugged vs. time. Significant tube plugging started after 12 years in 1986. The precursor step is comprised mainly of the accumulation of chemicals on the surfaces until a sufficient amount of chemicals is present. The precursor period appears to have been about 10-12 years.

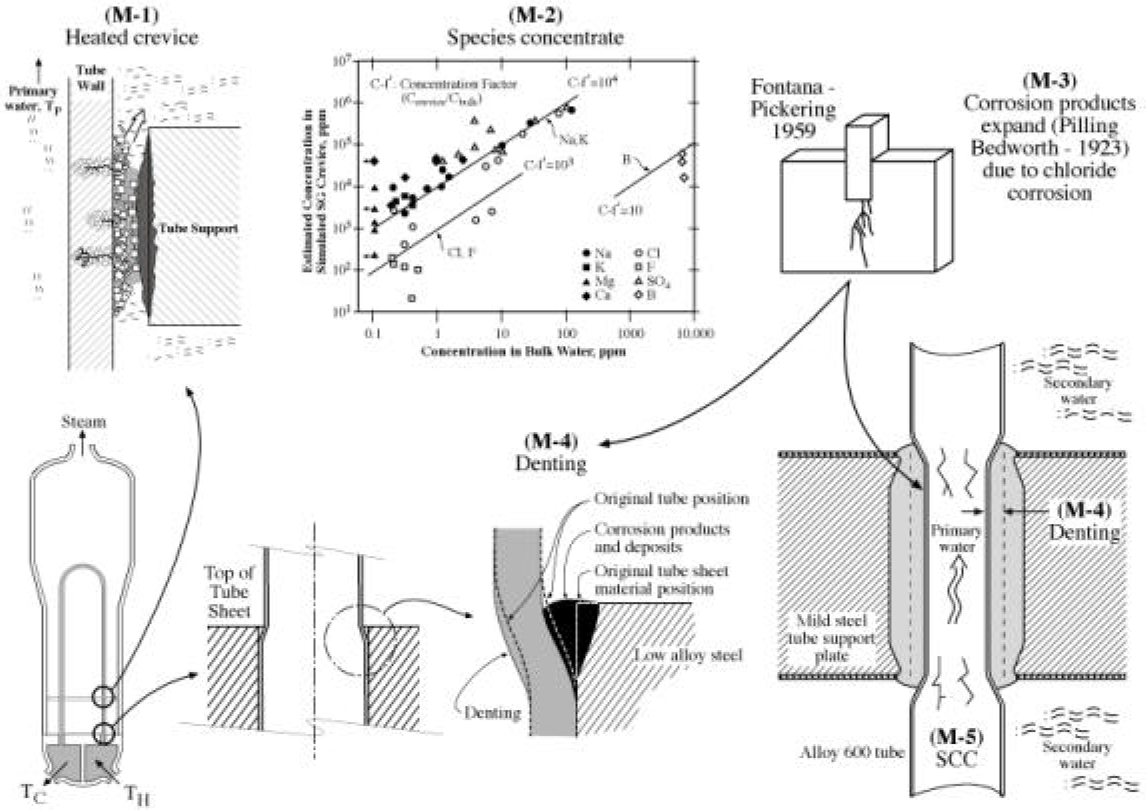

Figure B.15.12 Steps in the development of denting at both tube supports and at the top of the tubesheet. The straining is shown at the tube supports to have produced SCC starting from both inside and outside surfaces.[xxiii,xxiv]

Fuel failures in BWR plants--precursor

Fuel failures in BWR plants seem to be occurring as the heat flux increases with increasing demands for high outputs. The failure is not SCC, but rather a corrosion perforation. However, the precursor process is useful to analyze here. The precursor steps, as summarized in Figure B.15.14, are mainly:

a. High, and increasing, heat flux (M-1).

b. Impurities that participate in forming deposits with higher heat transfer resistance (M-1).

c. Increase in corrosion rate and formation of thicker oxide with higher heat transfer resistance (M-2).
d. Deposition of impurities and growth of oxide produces higher surface temperatures that accelerate perforation of cladding (M-3).

e. The cladding then perforates (M-4) as illustrated in Figure B.15.14d. This process occurs within a fuel cycle and is therefore a several year process.

Davis Besse--precursor

In the case of the Davis Besse failure, as shown in Figure B.15.15, LPSCC was part of the precursor, rather than the terminal part, and an extensive volume of corrosion ensued after an SCC-incited leak occurred in a control rod drive nozzle. The precursor elements were:

a. High residual stresses due to welding (M-1).

b. LPSCC in the Alloy 600MA nozzle (M-2).

c. Perforation of the Alloy 600MA permits borated water to exit and produce both a high velocity and corrosive solution (M-3).

The corrosion rate of the steel is about 2” per year and consumes a volume of steel that is the thickness of the head and about 6” in diameter. The precursor time, i.e. the time for the LPSCC to perforate the wall of the nozzle, was about 18 years, which is comparative to the rate for SG tubes when the differences in thicknesses are accounted for.

3. Structure of Domains and Microprocesses – Approach to Quantifying Precursors of Case III

3.1 Introduction

The purpose of this section is to describe the structure and application of “domains” and “microprocesses,” as used in developing scenarios that are part of the precursor events that precede initiating SCC as shown in Figures 1, 5 and 6. This discussion is the essence of the approach to quantifying precursors for Case III. Figures 16 through 21 describe each of the domains, which are identified in Figures 5 and 6, together with examples of relevant microprocesses.

Again, the purpose of this report is to propose an approach to predicting failure processes, mostly SCC, that have not yet been observed. In order to develop such a prediction, a rational intellectual structure and some assumptions are necessary. The intellectual structure is discussed in this section in terms of the domains and microprocesses. The principal assumptions and features of this intellectual structure are:

- Predicting failures, which have not yet occurred, is mostly related to long term changes in the domains and microprocesses, which are precursors, as described in Figure B.15.1 and Figure B.15.6, and which enable SCC to initiate and propagate at later times.

- Some new mode of SCC is not reasonably expected. It is more likely that the development of the precursors will permit some existing failure process to occur rather than some totally new one.

- The development of precursor conditions depends on the progression of microprocesses in various domains, as shown in Figure B.15.5, which may act conjointly or individually.

- The choices of specific domains and microprocesses must be based upon experience, and an awareness of the wide varieties of microprocesses that can be important.

- The idea of microprocesses focuses on specific processes that occur within the domains and have been shown to be critical processes in the nucleation, initiation, and growth of SCC. Further, these microprocesses are often capable of being quantified by known procedures of analysis.

- Finally, the domains and microprocesses can be linked to a scenario for the development of critical conditions for the initiation and propagation of SCC or a similarly aggressive process. Several scenarios could be envisioned as options for precursors. Section 7.0 provides suggestions for failure processes that might be predicted with the MPSA approach.

3.2 The “domains”

The “domains” in this discussion are shown in Figure B.15.5. These domains provide an intellectual framework for identifying explicitly the sequence of events and for organizing the microprocesses.

A sample scenario that might constitute a precursor to SCC could be the following:

a. Microprocess #1 (M-1): A line-contact crevice slowly accumulates deposit.

b. Microprocess #2 (M-2): The deposit gradually hardens.

c. Microprocess #3 (M-3): Even dilute species in the bulk water.

d. Microprocess #4 (M-4): Metallurgical ripening over time increases slip coplanarity leading to sharper slip steps and greater local forces at internal barriers.

These first four steps constitute a precursor as shown in Figure B.15.1, and may require many years.

e. SCC initiates when the environment in the crevice interacts with a metallurgical slip of greater coplanarity in the metal substrate.

Starting from the overall schematic view in Figure B.15.5, where the adjacent domains are identified and shown adjacent to a schematic cross-section of a metal in an aqueous solution, the respective domains are described in Figures 16-21. These domains, as identified in the Figures, start from the global domain to the bulk metal according to the order in Figure B.15

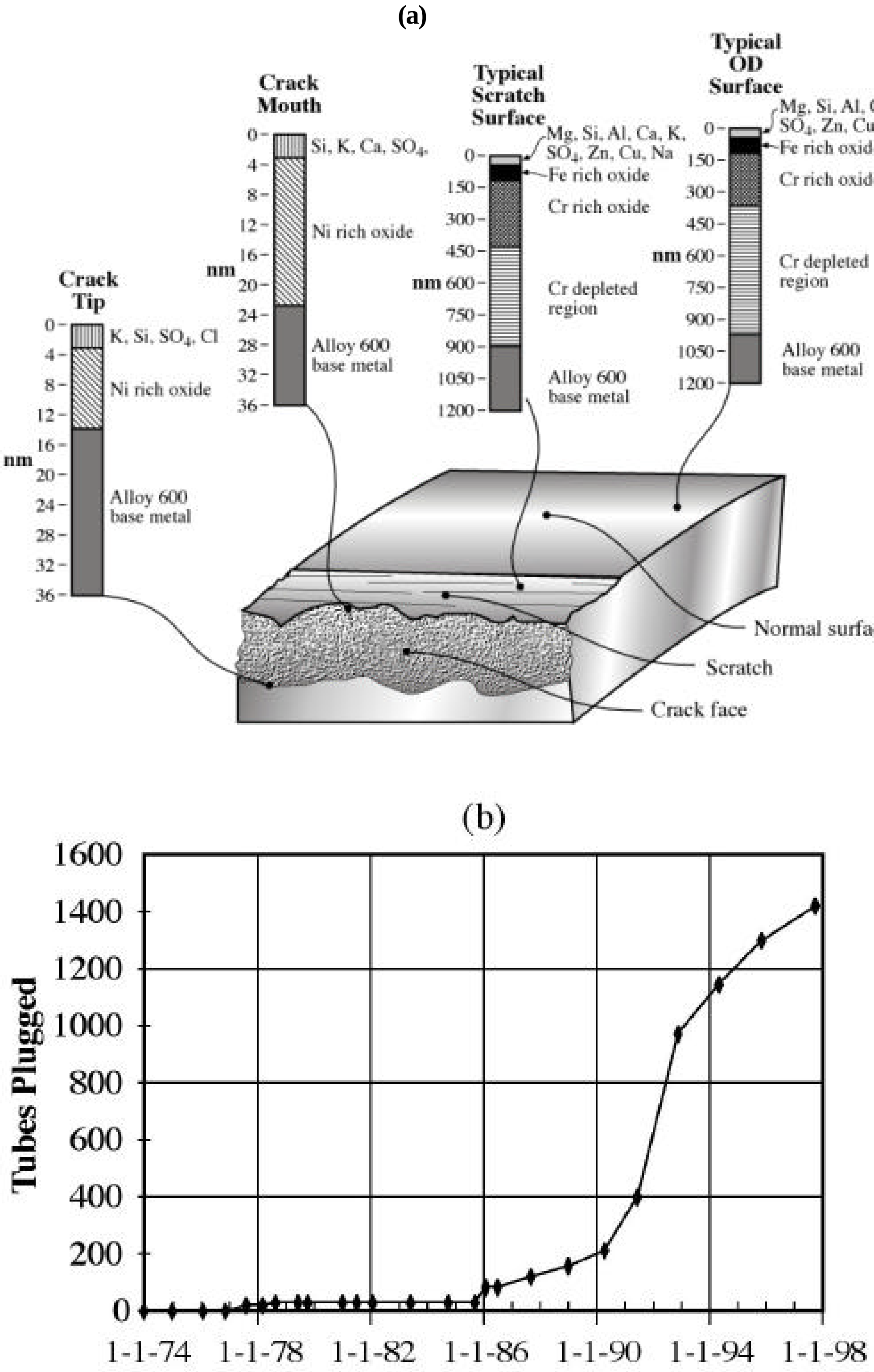

Figure B.15.13 (a) Compositions of surfaces of tubes at four locations in the upper bundle of Oconee Nuclear Station. Outside surfaces and inside SCC and IGC as determined by Auger spectroscopy. From Rochester.[xxv]
(b) Tubes plugged vs. time for Oconee-1B. From Rochester and Eaker.[xxvi]

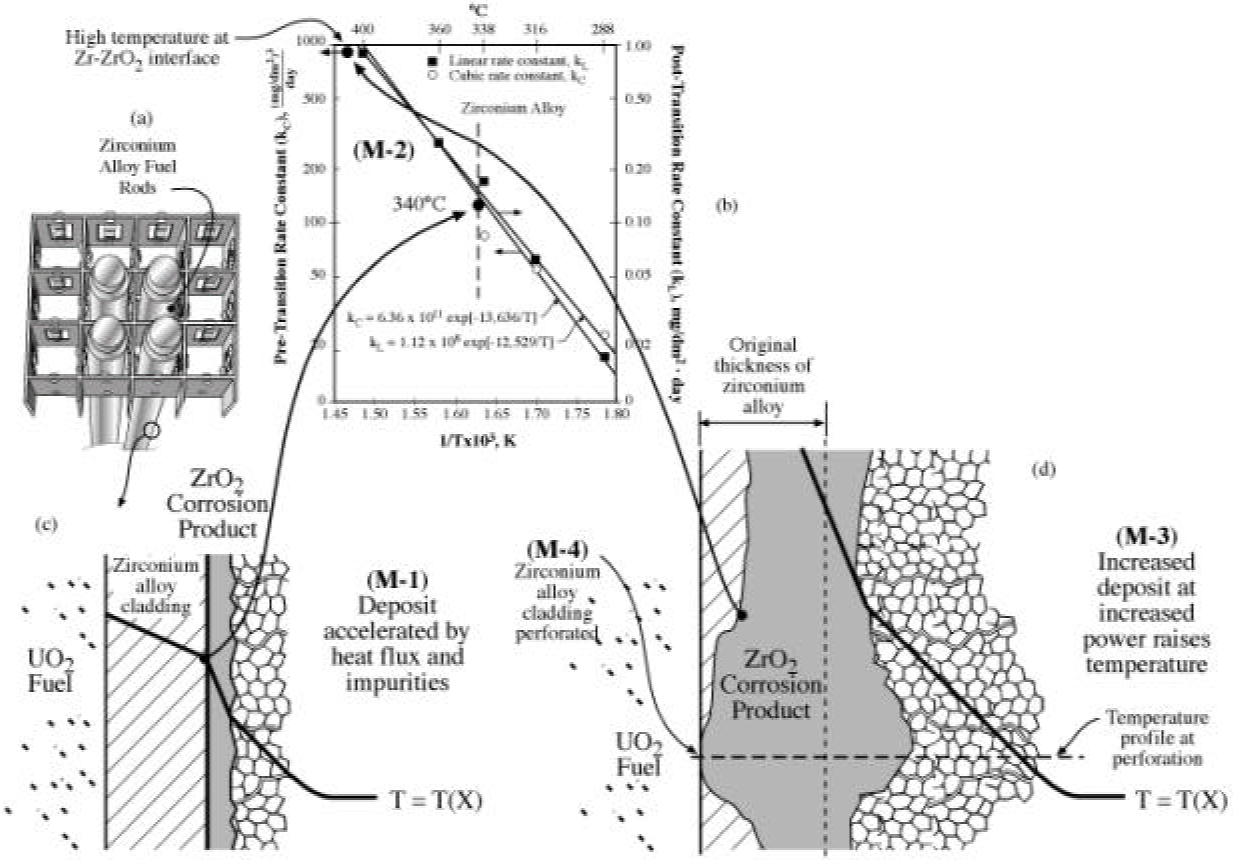

Figure B.15.14 Stepwise process for the perforation of fuel that results first from deposits, the formation of which is accelerated by high heat flux (M-1), then by accelerated corrosion (M-2), then by progressively higher surface temperatures (M-3), thereby increasing the corrosion rate, and ultimately failure (M-4).

Each of the domains consist of the "microprocesses" that are shown at the left, and some examples of nominal effects are identified at the right. These microprocesses are the elements, which contribute to the precursor, that would be quantified.

The "Global Domain" is shown in Figure B.15.16. The Global Domain is intended to include microprocesses that apply to all the domains, (e.g. temperature, neutron flux). The Global Domain also includes the free energy change, ΔG, as the environment reacts with the metal to produce reaction products.

The "Bulk Environment Domain" is shown in Figure B.15.17. The Bulk Environment Domain refers to the primary water, the secondary water, steam, tertiary water, ambient inside the containment or outside, and similar fluids to which components and materials are exposed.

The "Near-Surface Environment Domain" is shown in Figure B.15.18. The Near-Surface Environment Domain consists mainly of deposits, flow gradients, MIC pustules, and electrochemical cells. Such a domain has been a main part of the crevice deposits on the secondary side in heat transfer crevices or the accumulation of sludge at the bottom of SGs.

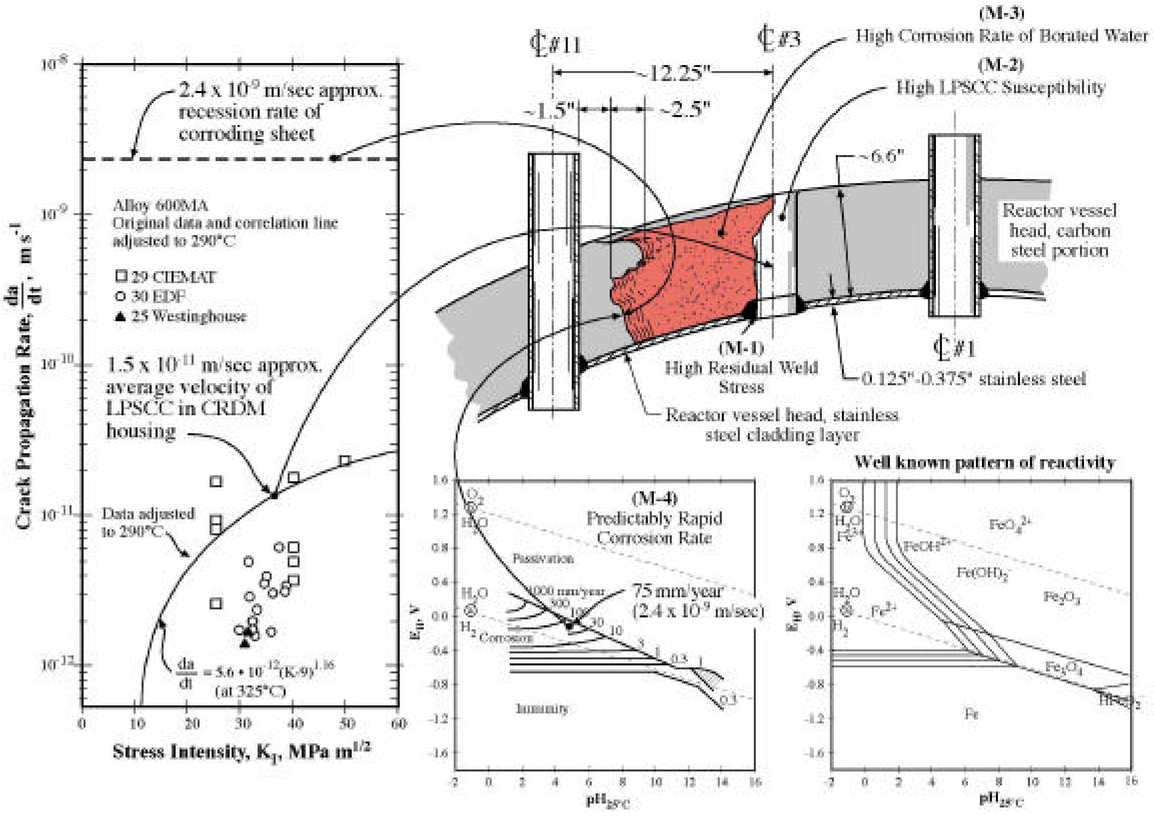

Figure B.15.15 Stepwise process leading to the failure at Davis-Besse. Here, LPSCC was part of the precursor, and rapid general corrosion was the propagation process. The LPSCC started with the high residual stresses from welding and the already well-known susceptibility of the Alloy 600MA.

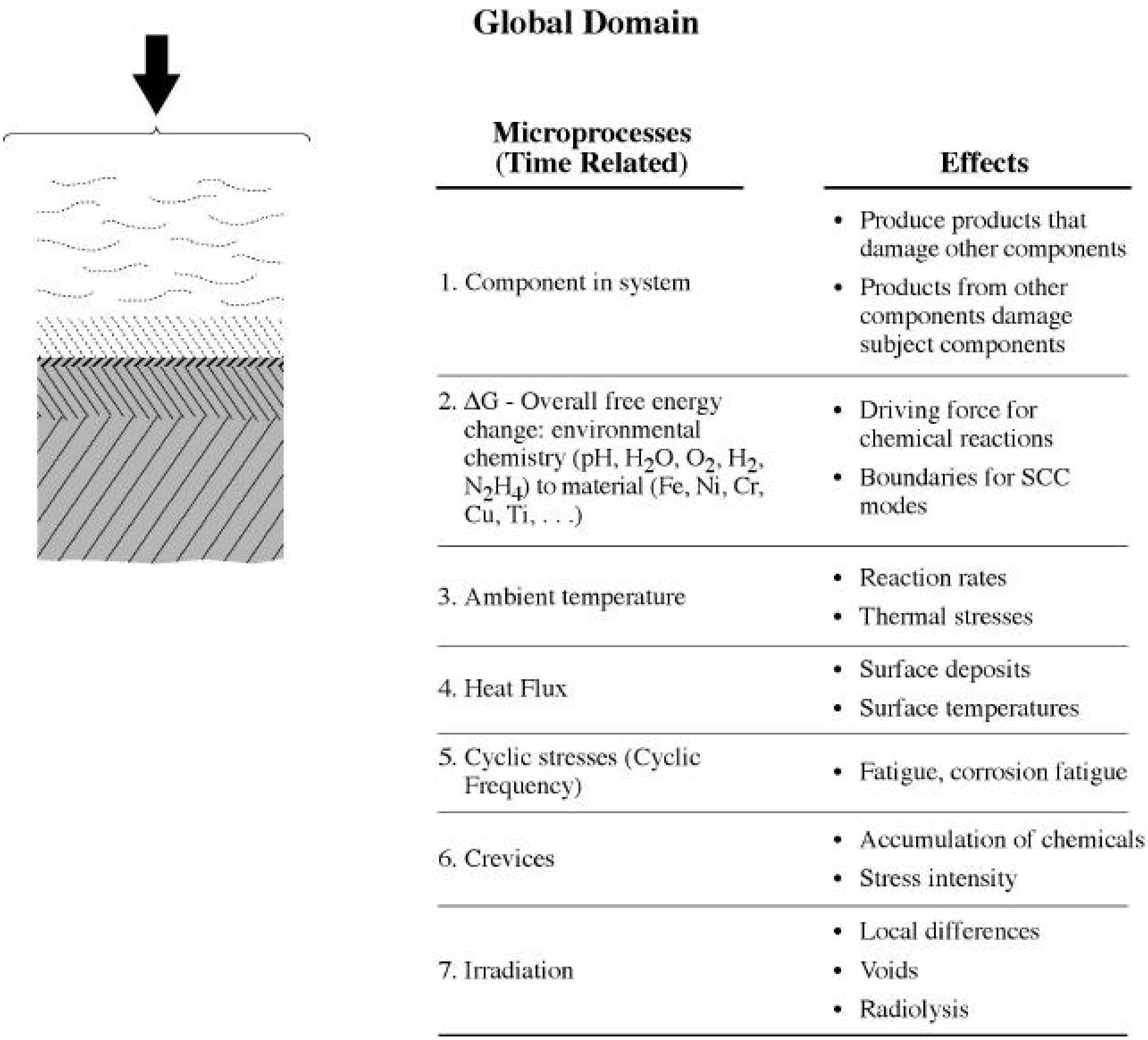

Global Domain

Microprocesses (Time Related)	Effects
1. Component in system	• Produce products that damage other components • Products from other components damage subject components
2. ΔG - Overall free energy change: environmental chemistry (pH, H_2O, O_2, H_2, N_2H_4) to material (Fe, Ni, Cr, Cu, Ti, . . .)	• Driving force for chemical reactions • Boundaries for SCC modes
3. Ambient temperature	• Reaction rates • Thermal stresses
4. Heat Flux	• Surface deposits • Surface temperatures
5. Cyclic stresses (Cyclic Frequency)	• Fatigue, corrosion fatigue
6. Crevices	• Accumulation of chemicals • Stress intensity
7. Irradiation	• Local differences • Voids • Radiolysis

Figure B.15.16 Microprocesses and their effects in the Global Domain.

The "Protective Film Domain," which is shown in Figure B.15.19, includes what is sometimes called the "passive film." However, there are other deposits that form as part of the protection, (e.g. carbonates), and are not part of the chemistry of the metal substrate. In the protective film, the electrochemical catalytic processes are affected as the defect structure of the protective film changes – such defect structures are changed by Pb, Cl^-, S^{2-} and others. Because this film is usually epitaxially attached to the surface, the protective film also affects both stresses in the substrate and the nucleation of dislocations at the surface. This film changes with time in its geometry and chemistry.

Bulk Environment Domain

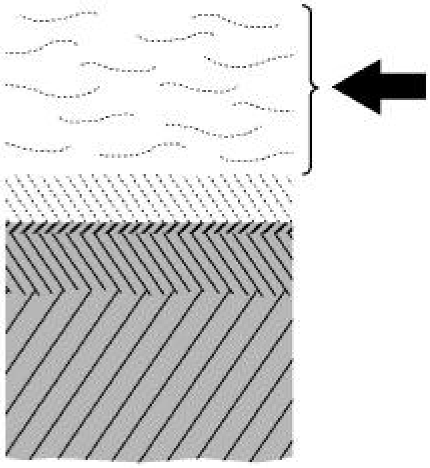

Microprocesses (Time Related)	Effects
1. Flow	• Transports chemical and suspended solids • Influence rates of surface reactions • Low flow / high flow deposits solids • FAC
2. Boiling	• Deposit solids
3. Transport to or from other components	• Cu^{2+}, HS^-
4. Chemical composition • O_2, H_2, N_2H_4 impurities (Pb, Cl^-, SO_4), pH inhibitors, suspended solids	• Electrochemical state • Corrosion reactions • Raise E with low H_2
5. Homogenous chemical reactions	• Reduce $SO_4^= \rightarrow HS^-$ with N_2H_4
6. Radiolysis and radiolytic synthesis	• $H_2O \rightarrow O_2 + H_2$ • $N_2 + H_2O \rightarrow HNO_3$ • $O_2 + N_2H_4 \rightarrow H_2O$
7. Multiple oxygen incidents	• Corrosion • SCC

Figure B.15.17 Microprocesses and their effects in the Bulk Environment Domain

The "Near-Surface Domain on the Metal Side," which is shown in Figure B.15.20, is the region in which near-surface processes occur such as slip dissolution, tunnel penetration, enrichment/depletion of species, solubilization of species that enter grain boundaries, and precipitation of vacancies.

Near-Surface Domain (Environment Side)

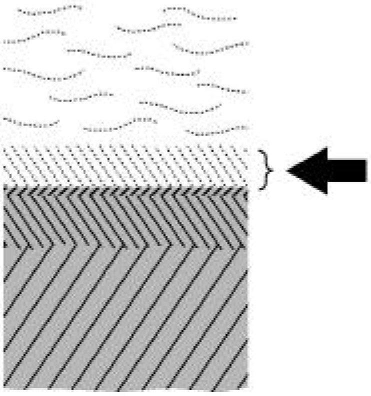

Microprocesses (Time Related)	Effects
1. Deposits	• Corrosion cells • Heat transfer resistance • Galvanic processes
2. Heat flux	• Concentrate chemicals • Raise surface temperatures
3. Sequestering, crevices	• Concentrate chemicals
4. FAC	• Remove material • Produce hydrogen • Inhibit initiation of SCC
5. MIC	• Act at temperatures below 100°C • Acidic and other corrosive environments

Figure B.15.18 Microprocesses and their effects in the Near-Surface Environment Domain

Protective Film Domain

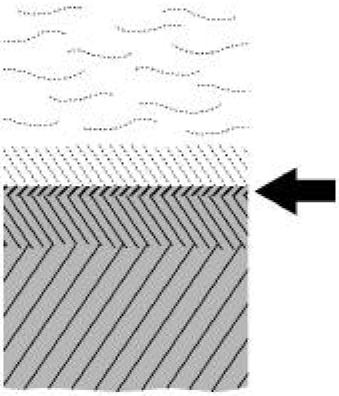

Microprocesses (Time Related)	Effects
1. Thickness	• Surface stress • Heat transfer
2. Composition (environment contribution, alloy contribution, defect structure, xtal/amorphous)	• Conductivity • Pit nucleation • SCC initiation
3. Stresses (average, metal interface)	• Film degradation
4. Kinetics (repassivation, dissolution, growth)	• Local penetration • Slip dissolution
5. Slip interactions	• Slip height • Step distribution • Dislocation nucleation

Figure B.15.19 Microprocesses and their effects in the Protective Film Domain

Near Surface Domain (Metal Side)

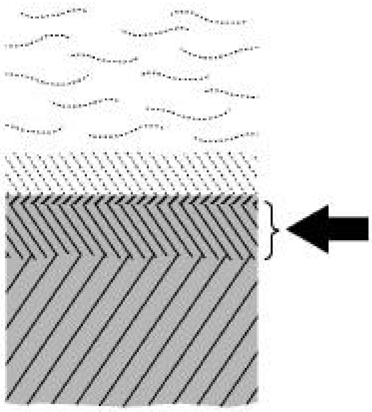

Microprocesses (Time Related)	Effects
1. Enrichment/depletion	• Brittle layer • Catalysis • Change chemistry into SCC mode • Galvanic • Voids
2. Hydrogen entry	• SCC
3. Surface slip	• SCC initiation
4. Grain boundary (composition, diffusion)	• IGC • G.B. diffusion
5. Irradiation-induced voids	• Stresses, distortion
6. Slip dissolution	• SCC initiation
7. Tunnels	• SCC initiation
8. General dissolution	• Surface recession
9. Pits, IG corrosion, electrochemical cells	• Penetration • CF initiation
10. SCC initiation	• Accelerate
11. FAC	• Recession • Remove SCC initiation • Hydrogen production
12. Abuse (dings, dents, machining, grinding)	• SCC initiation

Figure B.15.20 Microprocesses and their effects in the Near-Surface Metal Domain

The “Bulk Metal Domain,” which is shown in Figure B.15.21, is, in a sense, the “semi-infinite region” of the metal, which, on a gross scale, is homogeneous but on a microscopic—and micro-process scale—is quite heterogeneous. These local heterogeneities provide paths or influences that affect the development and propagation of corrosion damage.

The six domains of Figures 16 through 21, as summarized in Figure B.15.5, are shown with associated small boxes in Figure B.15.6, each of which represents a microprocess. When a “scenario” is constructed as in Figure B.15.6, these boxes are connected, as they would be naturally. Such a scenario constitutes a precursor as shown in Figures 1 and 6 that identifies the relevant microprocesses, which need to be quantified and validated in order to reach the conditions necessary for SCC to initiate. In this quantification, some kind of time dependence needs to be developed in order to predict when the resulting precursor can lead to the start of SCC.

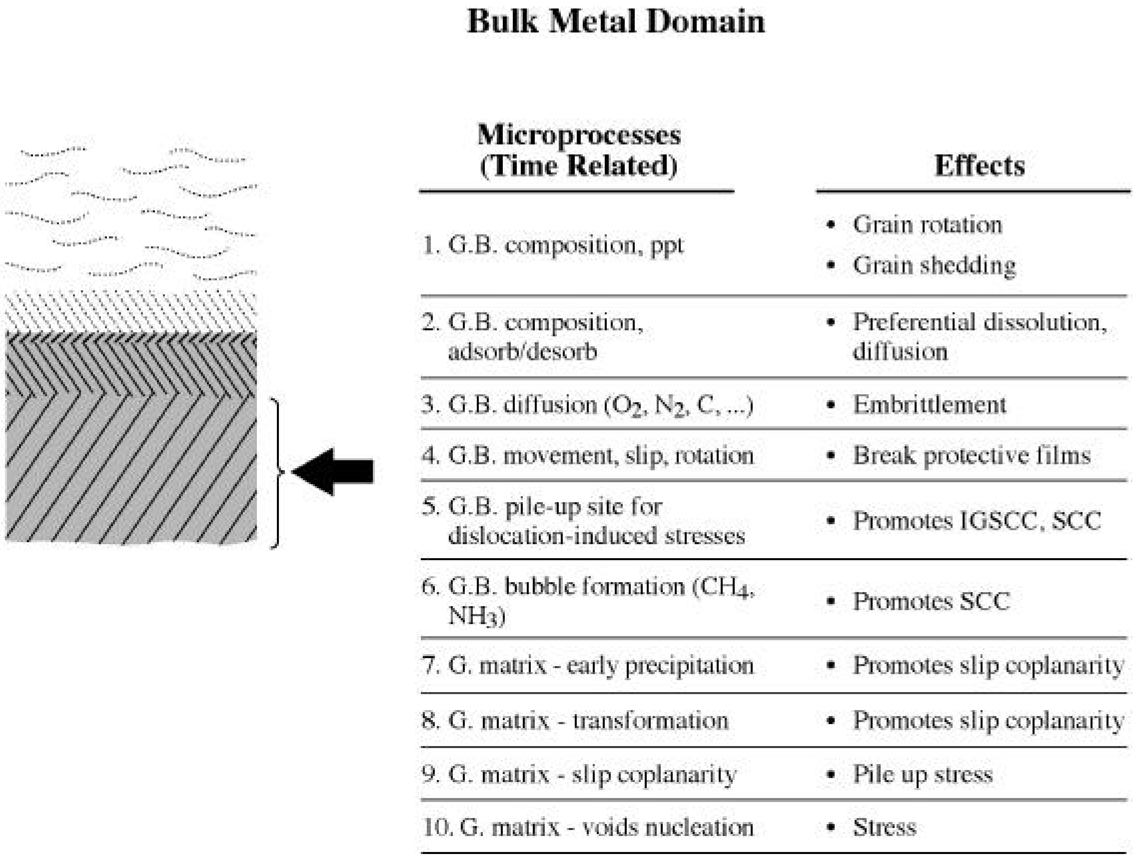

Bulk Metal Domain

Microprocesses (Time Related)	Effects
1. G.B. composition, ppt	• Grain rotation • Grain shedding
2. G.B. composition, adsorb/desorb	• Preferential dissolution, diffusion
3. G.B. diffusion (O_2, N_2, C, ...)	• Embrittlement
4. G.B. movement, slip, rotation	• Break protective films
5. G.B. pile-up site for dislocation-induced stresses	• Promotes IGSCC, SCC
6. G.B. bubble formation (CH_4, NH_3)	• Promotes SCC
7. G. matrix - early precipitation	• Promotes slip coplanarity
8. G. matrix - transformation	• Promotes slip coplanarity
9. G. matrix - slip coplanarity	• Pile up stress
10. G. matrix - voids nucleation	• Stress

Figure B.15.21 Microprocesses and their effects in the Bulk Metal Domain

4. Examples and properties of microprocesses

The purpose of this section is to describe examples of microprocesses, which are part of the six domains. This description is not comprehensive but illustrative; there are probably 50-100 really significant microprocesses that might be identified.

As shown in Figures 11-16, each domain contains a particular array of microprocesses, which are significant to the occurrence of corrosion damage. Many of these microprocesses are already known to participate in corrosion processes under various conditions of temperature, stress, environmental chemistry, and material chemistry.

The emphasis here is upon microprocesses that require some time to develop their roles in accelerating or intensifying future and aggressive corrosion; and during these early processes of development there is no support for SCC or other accelerated processes until certain necessary conditions conglomerate. Once some critical array of microprocesses develops, SCC can then initiate and propagate.

The "microprocesses" are the elements that are identified, quantified, and connected in scenarios to develop the characteristics of the precursor regimes as follows:

Identification

Identifying the microprocess in a domain, as in Figure B.15.6, is largely a matter of expert experience. Some of these microprocesses are well known and some maybe not. To identify further clues to microprocesses that are not obvious, it may be necessary to look into the physical and organic chemistry of homogenous materials and the surface chemistry of their interfaces in aqueous solutions. Other microprocesses might be identified from metal physics. "Identification" is a matter of making microprocesses explicit.

Quantification

Quantification of microprocesses provides bases for the dependencies that determine the duration of the precursor period. Such dependencies include considerations of growth rates, diffusion, rates of transformation, rates of accumulation, and rates of production. These can usually be approached with conventional knowledge of such processes as they respond to the temperatures and chemistries of LWRs. Developing the rates of microprocesses contributes to an overall model of a time-dependent precursor. From this model, the duration of the precursor can be calculated.

Connection into scenarios

Constructing a scenario, as in Figure B.15.6, involves essentially developing the features of the precursor. There may be several equally attractive scenarios. A scenario is shown schematically in Figure B.15.6, including selected microprocesses. Figure B.15.6 suggests that there may be several important microprocesses in some domains. A fully identified and connected scenario, as in Figure B.15.6, then, is a precursor to the occurrence of starting SCC or some similarly rapid process of penetration.

Note that FAC is probably not compatible with the development of these microprocesses since it starts from the beginning of operation, unless there is a change in velocity, pH, potential, inhibitors, or alloys that would activate the flow acceleration at some later time. However, FAC generally proceeds at a rate that is similar to the low end of SCC; and FAC might be initiated at a later time as a result of changes in chemistry (changes in oxygen or pH), temperature, and flow. This sequence is not so much a precursor as a later and influential (although unwise) change in operation.

4.1 Global Domain

A schematic view of the Global Domain is shown in Figure B15.16. In Section 4.1 three examples of microprocesses are discussed, and a more extensive set is suggested in Figure B.15.16. Each of these examples is typical of important effects that could change the conditions for onset of SCC. Further, they are associated with the kinds of times that are involved with precursors that could lead to SCC at long times.

Mode diagrams, ΔG

One example of a microprocess here is the free energy difference between the environment and the material. This is usually identified by a diagram of potential vs. pH as shown in Figure B.15.22, and much of the necessary data are available in handbooks containing thermodynamic data. Here, the Ni-H_2O diagram is shown with some of the Fe equilibria. Superimposed on this diagram are the locations of the major submodes of SCC. This diagram represents the global domain where the lines in the diagram indicate equilibria for the metal and environment that react to produce chemical products. The application of this diagram and the incorporation of submodes of SCC have been described by Staehle and Gorman.[i] Such a global microprocess as the difference in free energy of metal and water, is important to virtually all of the scenarios.

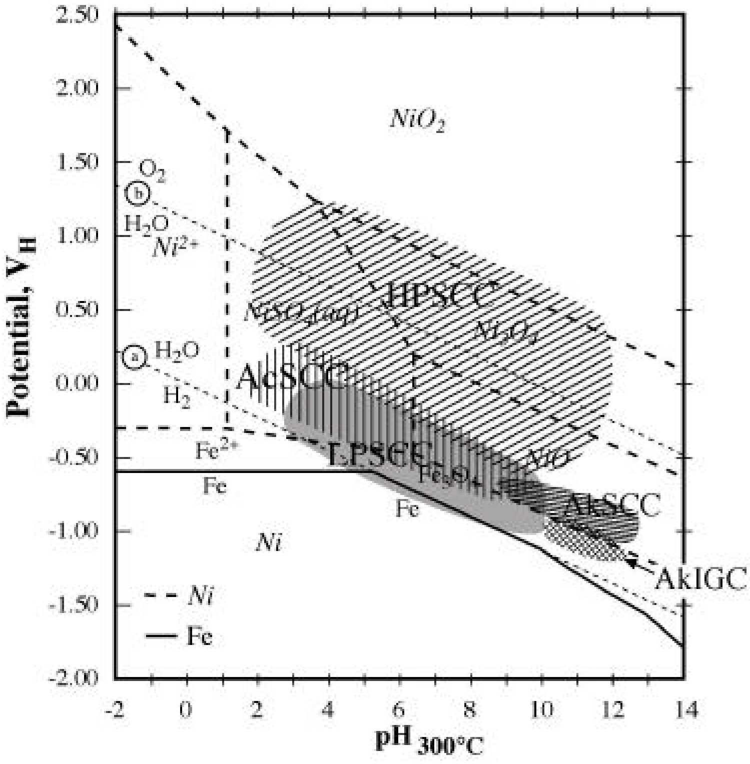

Figure B.15.22 Electrochemical potential vs. pH at 300°C for Ni in H_2O with important equilibria shown. Locations for AkSCC, LPSCC, AcSCC, and HPSCC of Alloy 600MA shown. From Staehle and Gorman.[i]

Neutron flux, void formation

Neutrons, as they react with Ni isotopes, produce helium atoms. These helium atoms coalesce to produce voids. Such voids are shown in Figure B.15.23[xxvii] in baffle bolts. These voids, as they coalesce, lead to strains that cause stresses and distortions.

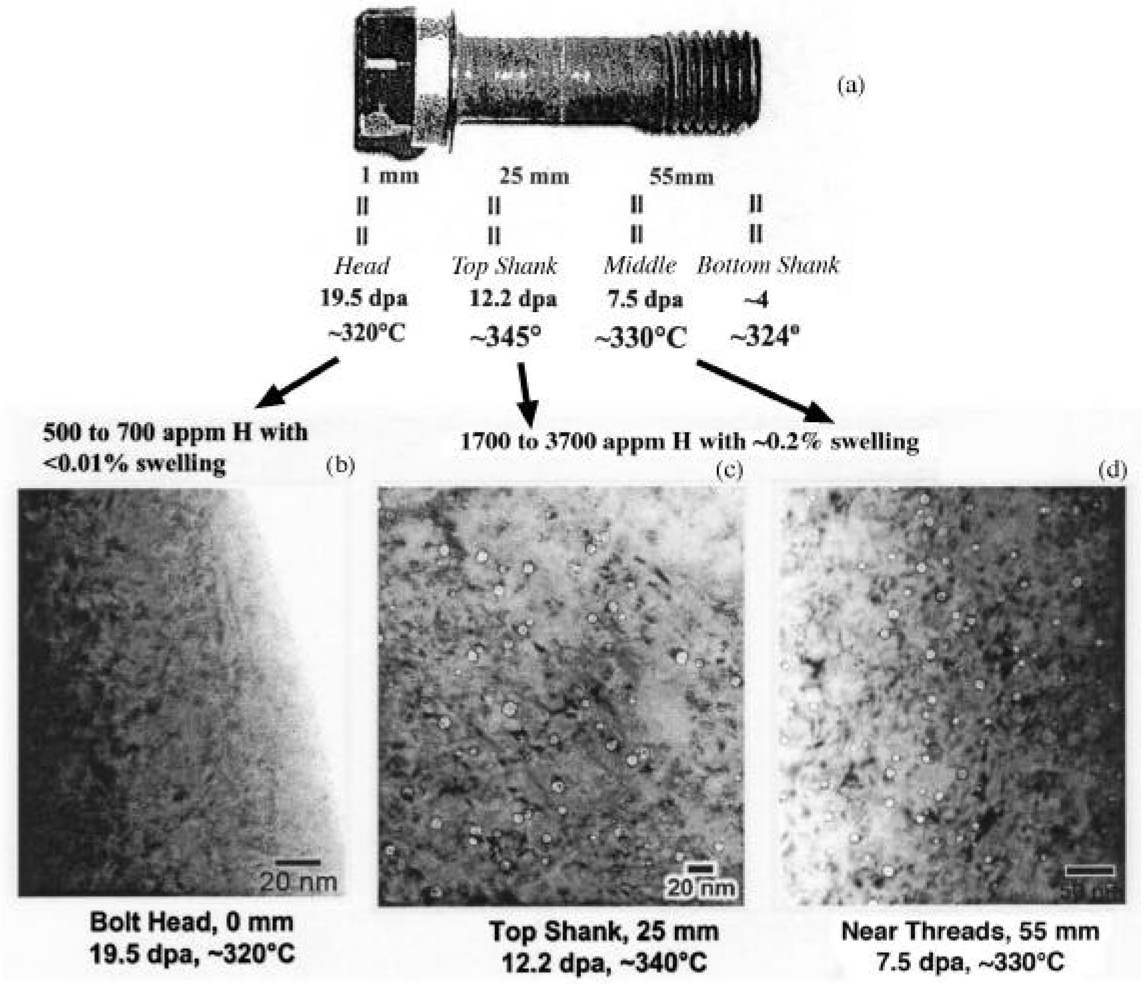

Figure B.15.23 Bolt connecting former and baffle from Tihange-1 PWR shown in terms of neutron dose giving concentration of He and swelling at locations along a bolt. From Garner et al.[xxvii]

Neutron flux, change composition of grain boundaries

A third example of a microprocess in the global domain is neutron flux, as it leads to changes of chemistry at grain boundaries. Figure B.15.24[xxviii], from the work of Bruemmer, shows such a change of Cr in stainless steel after up to 13.3 dose per atom. These alterations affect the reactivity of the grain boundaries as well as changing the mechanical properties and diffusivity of environmental species such as oxygen.

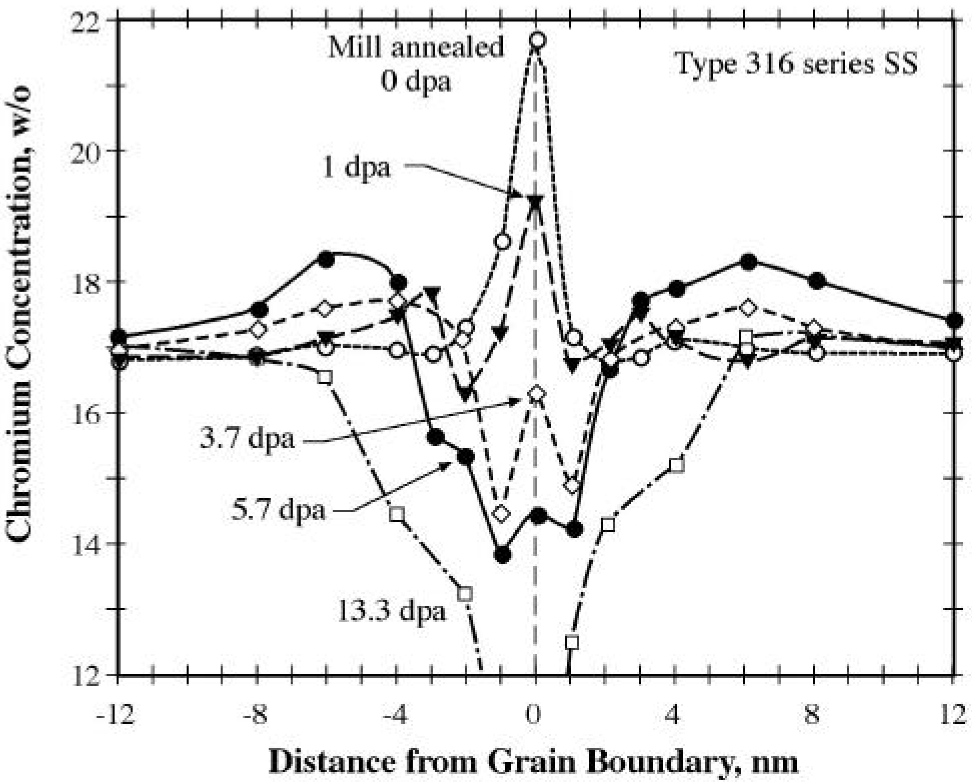

Figure B.15.24 Concentration of Cr across a grain boundary of mill-annealed Type 316 stainless steel as a function of dose up to 13.3 dpa. From Bruemmer.[xxviii]

4.2 Bulk Environment Domain

A schematic view of the Bulk Environment Domain is shown in Figure B.15.17, where several microprocesses are identified. This section gives two examples of such microprocesses.

Hydrazine (N_2H_4) reduces sulfate to sulfide

Hydrazine (N_2H_4) is added to the secondary side in order to reduce the concentration of oxygen that is assumed to promote SCC in crevices. As an aside, it is not clear that such an effect is important; and second, the very low hydrogen on the secondary side raises the potential, regardless. Whether hydrazine significantly counters this effect of low hydrogen is not clear.

Work by Daret, et al.[xxix] shows that the occurrence of sulfide produces SCC in Alloy 600MA, as shown in Figure B.15.25; further, this work is linked to the reduction of sulfate in secondary systems by hydrazine as shown in the reactions of Figure B.15.25. Work by Sakai et al.,[xxx] Sala et al.,[xxxi] Allmon et al.,[xxxii] and de Bouvier et al.[xxxiii] have shown clearly that N_2H_4 reduces SO_4^{2-} to S^{2-}.

Chloride inhibits dissolution

The rate of dissolution of high nickel alloys is very much affected by the anion as shown from work of Cullen in Figure B.15.26a[xxxiv]. Here, the dissolution of these alloys over a pH range from 1-6 is shown for several ratios of chloride and sulfate including the 100% compositions of each. These data show that the 100% chloride solution corrodes Alloy 600 about two orders of magnitude less than the 100% sulfate. In support of this trend, Figure B.15.26b[xxxv] from Choi and Was, shows that the aspect ratio of pitting follows the same pattern. As the chloride-to-sulfate ratio increases, the pits become sharper, which is expected in view of the inhibitive effect of Cl^- as suggested in Figure B.15.26c from Staehle.[xxxvi]

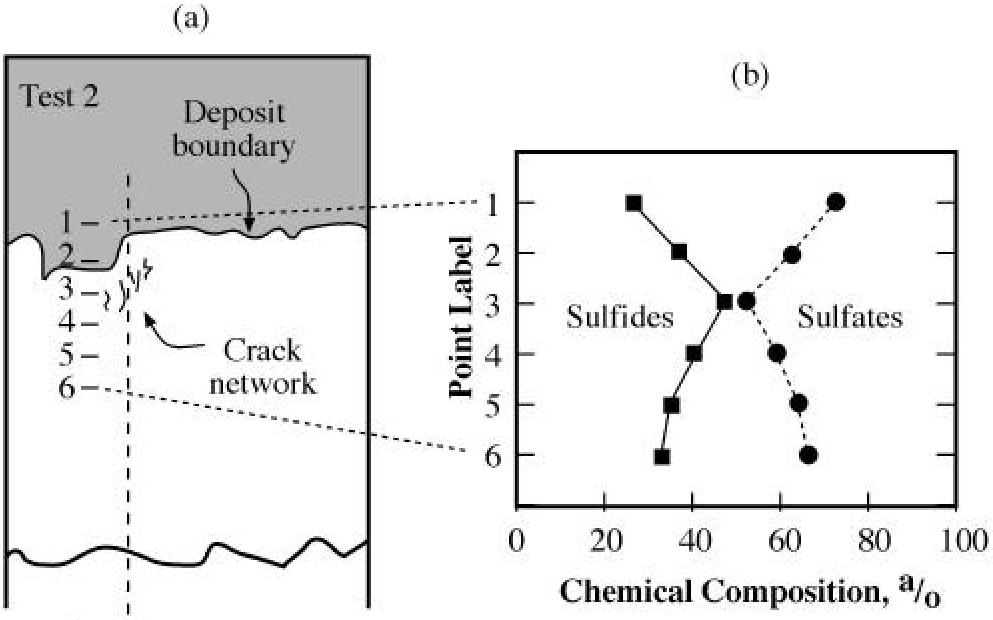

Sulfate is reduced to S^{2-} by hydrazine

$$2(SO_4)^{2-} + 18H^+ + 12e^- \rightarrow 2(HS^-) + 8H_2O$$

Hydrazine is oxidized

$$3(N_2H_4) + 12OH^- \rightarrow 3N_2 + 12H_2O + 12e^-$$

Figure B.15.25 Results from model boiler experiments with primary temperature in range of 330 to 350°C and secondary side temperatures in the range of 290 to 295°C with AVT chemistry. Sodium sulfate was added at 0.5 mg/kg in makeup water, and hydrazine was in the range of 10-50 µg/kg. Dissolved oxygen less than 1 µg/kg. (a) Location of SCC, boundary of deposit, and locations of analysis for sulfates and sulfides (1-6) for Alloy 600MA. (b) Atomic percent of sulfates and sulfides vs. distance from the boundary of the deposit into the metal and through the SCC zone. From Daret et al.[xxix]

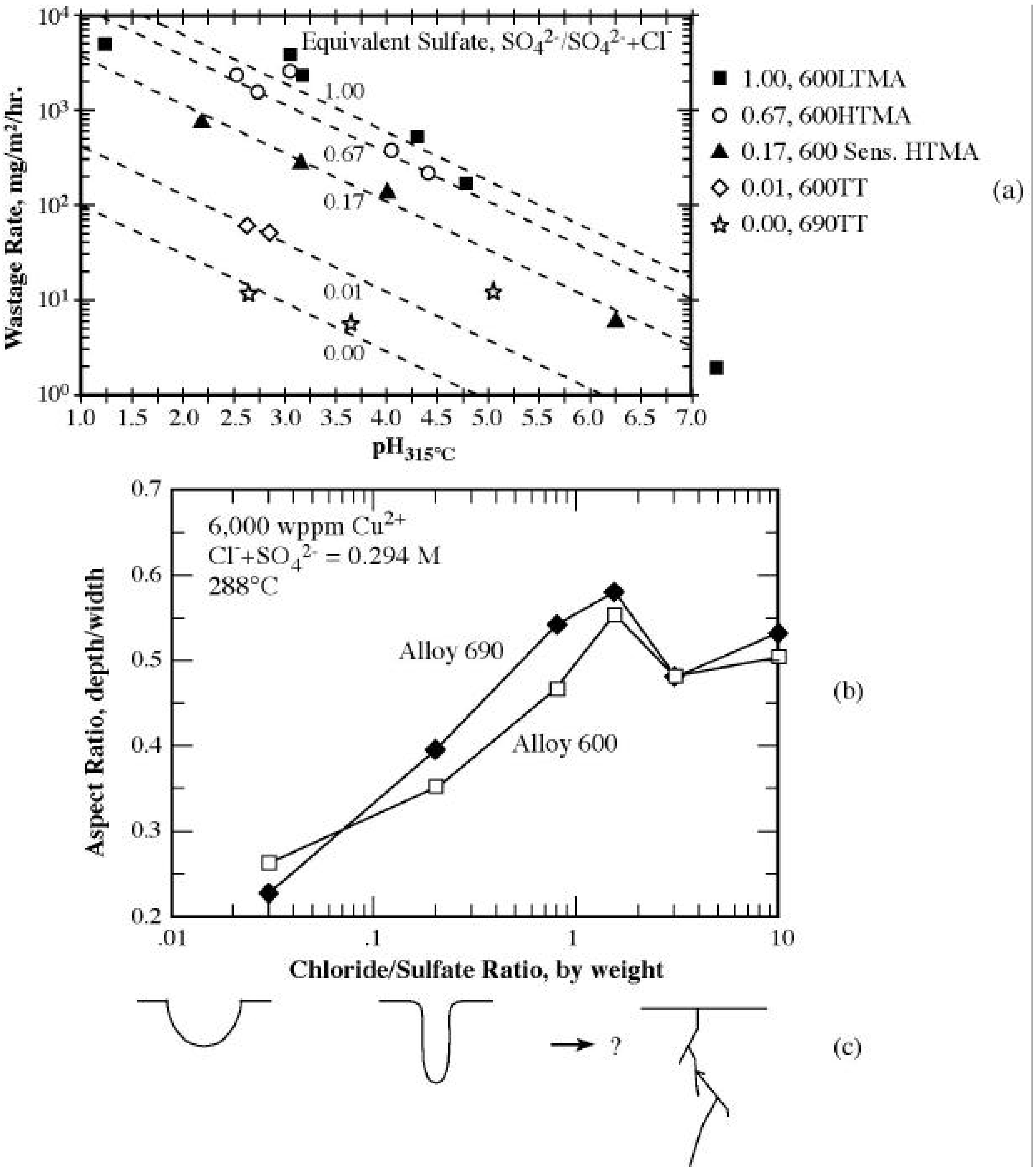

Figure B.15.26 (a) Wastage rate vs. pH for retort tests using Alloys 600 and 690 in various heat treatments in concentrated acidified sulfate and chloride solutions at a test temperature of 315°C. From Cullen.[xxxiv] (b) Aspect ratio for pits vs. Cl^-/SO_4^{2-} ratio for Alloys 600 and 690 exposed in 6000 wppm Cu^{2+} at 288°C for $Cl^-+SO_4^{2-}$ = 0.294M. From Choi and Was.[xxxv] (c) Schematic view of implications of increasing acuity. From Staehle.[xxxvi]

4.3 Near-Surface Environment Domain

A schematic view of the Near-Surface Environment Domain is shown in Figure B.15.18 as a part of the overall array of domains in Figure B.15.5. Examples from this domain are the following:

Heat transfer crevice

While the heat transfer crevice has been changed in the new generation of SGs, from the comprehensive envelopment of drilled holes, the occurrence of conditions for concentrating impurities persists as deposits continue to accumulate in line-contact geometries, although the possibly resulting concentrations of species in these geometries have not been studied. Figures 27a, b, c[xxxvii] show the nature of the chemical crevice in its complexity of chemistry, phases and gradients. Figures 27d and e[i] show a schematic view of accumulation of deposits at egg crate line-contact crevices. These near-surface environments are substantially different from bulk environments in concentrations as well as in ratios of elements. Further, their chemistry changes in time. Such concentrating capacities of these crevices enable concentrating Pb, (e.g. from the ppt range to the low percentage range), at the metal-environment surfaces. It is likely that the line-contact accumulations will produce different chemistries from the drilled holes in view of the differences of geometry as these affect the concentration of species.

Accumulation of deposits and cells

Deposits accumulate with time due to superheat at the surfaces of tubes at tube supports and at the top of the tubesheet, as shown in Figures 28a, b, c,[i] at the bottom of steam generators. Such accumulations vary with locations. These deposits lead to the formation of electrochemical cells.

Deposit expansion and forces

Aside from the chemical and electrochemical aspects of deposits, as well as their heat transfer resistance; deposits also produce large forces in constrained geometries. Figure B.15.29, from the work of Pickering et al.,[xxiii] shows a stainless steel specimen that was exposed in the non-stressed conditions with a stainless steel insert. The corrosion products that accumulated in the crevice between the specimen and the insert produced stresses, which caused SCC to start at the bottom of the crevice. After this SCC had propagated some distance, the insert was removed as part of the experimental program, and the corrosion products in the propagating SCC exerted sufficient force to cause the SCC to continue. These forces are produced by the larger specific volume of the oxide compared with the metal as reported in 1923 by Pilling and Bedworth.[xxiv]

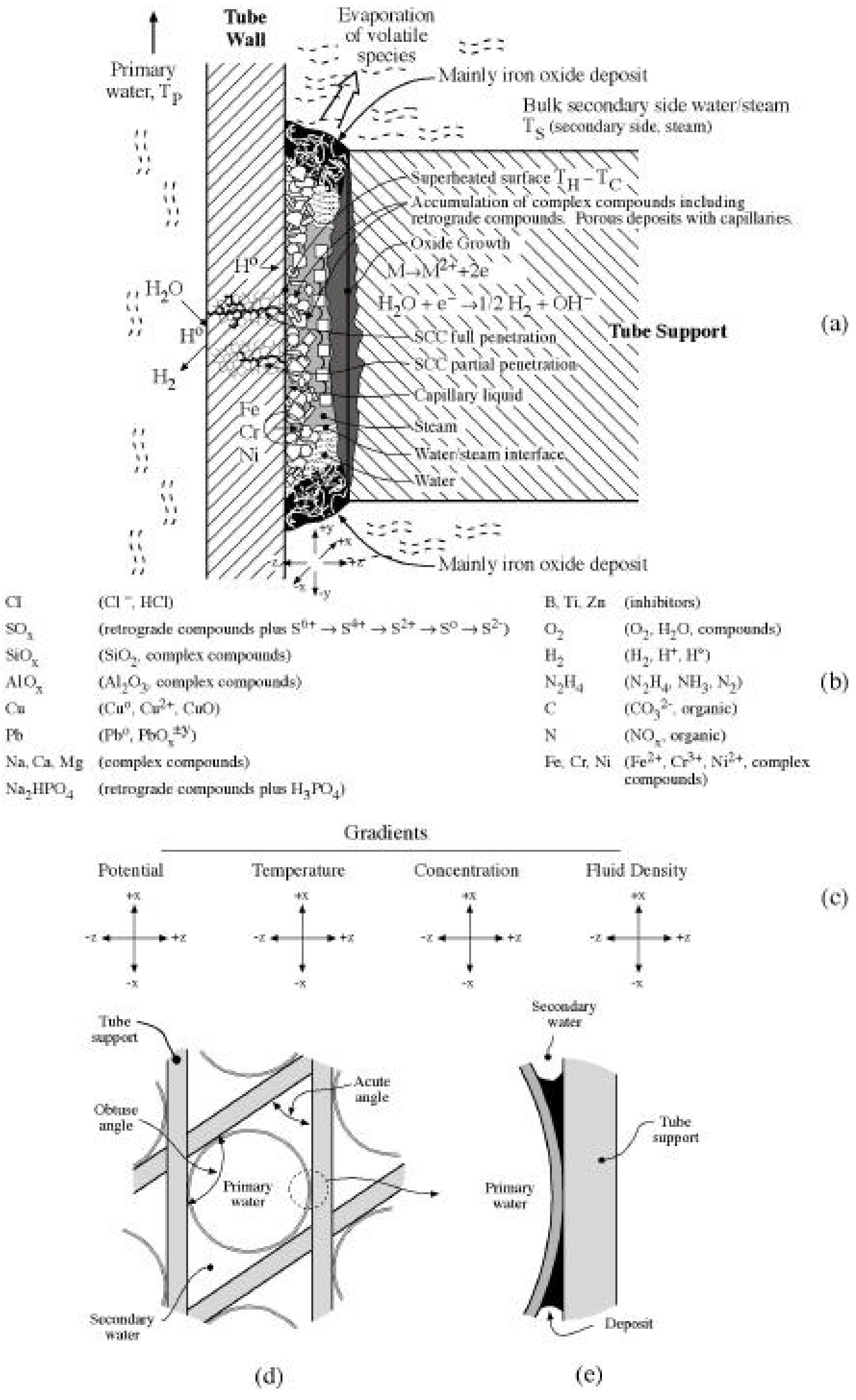

Cl	(Cl^-, HCl)	B, Ti, Zn	(inhibitors)
SO_x	(retrograde compounds plus $S^{6+} \rightarrow S^{4+} \rightarrow S^{2+} \rightarrow S^o \rightarrow S^{2-}$)	O_2	(O_2, H_2O, compounds)
SiO_x	(SiO_2, complex compounds)	H_2	(H_2, H^+, H^o)
AlO_x	(Al_2O_3, complex compounds)	N_2H_4	(N_2H_4, NH_3, N_2)
Cu	(Cu^o, Cu^{2+}, CuO)	C	(CO_3^{2-}, organic)
Pb	(Pb^o, $PbO_x^{\pm y}$)	N	(NO_x, organic)
Na, Ca, Mg	(complex compounds)	Fe, Cr, Ni	(Fe^{2+}, Cr^{3+}, Ni^{2+}, complex compounds)
Na_2HPO_4	(retrograde compounds plus H_3PO_4)		

Figure B.15.27 Schematic view of heat transfer crevice at a tube support. (a) Geometry. (b) Chemicals that accumulate and transform. (c) Types of gradients inside the heat transfer crevice. From Staehle.[xxxvii] (d) Egg crate design of tube support and (e) schematic view of accumulation of deposits in line-contact geometry, based on direct observations. From Staehle and Gorman.[i]

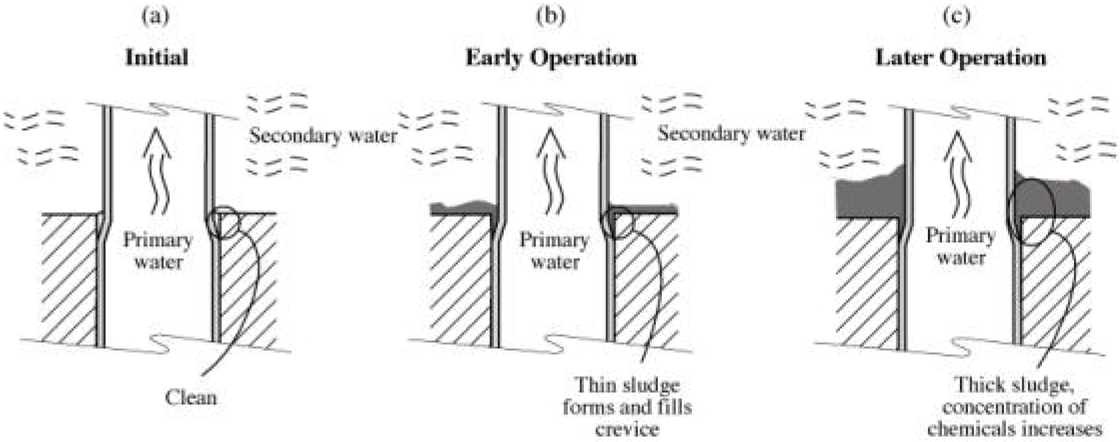

Figure B.15.28 Accumulation of deposits on top of the tubesheet with time. From Staehle and Gorman.[i]

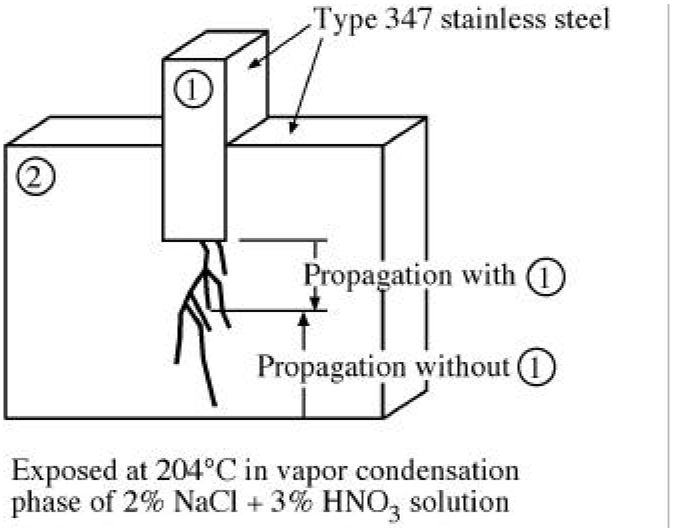

Figure B.15.29 Demonstration of forces produced by corrosion products. Stainless steel block and insert exposed at 204°C in vapor condensation of 2% NaCl+3%HNO_3 solution; no applied stress. SCC propagates with corrosion product forces between block and insert. Insert removed and cracks propagate due only to corrosion products in initial cracks. From Pilling and Bedworth.[xxiv]

4.4 Protective Film Domain

Properties of protective films dominate much of the corrosion behavior of metals. Further, this film interacts with slip processes in the metal and through its normal epitaxial connection to the metal, produces stresses in the substrate. Also, the defect concentration in the film catalytically affects oxidation and reduction reactions. The relative position of the protective film in the domains is shown in Figure B.15.5, and examples of important related microprocesses are shown in Figure B.15.19.

Epitaxial film growth

Epitaxial protective films grow with time according to various rate laws and following influences of alloy, pH, and potential. Figure B.15.30[xxxviii] shows the effect of potential and alloy composition on the thickness of protective films on iron base alloys. These films affect the catalytic influence on electrochemical reactions and the overall rate at which the alloy dissolves, as it is controlled by the properties of these films.

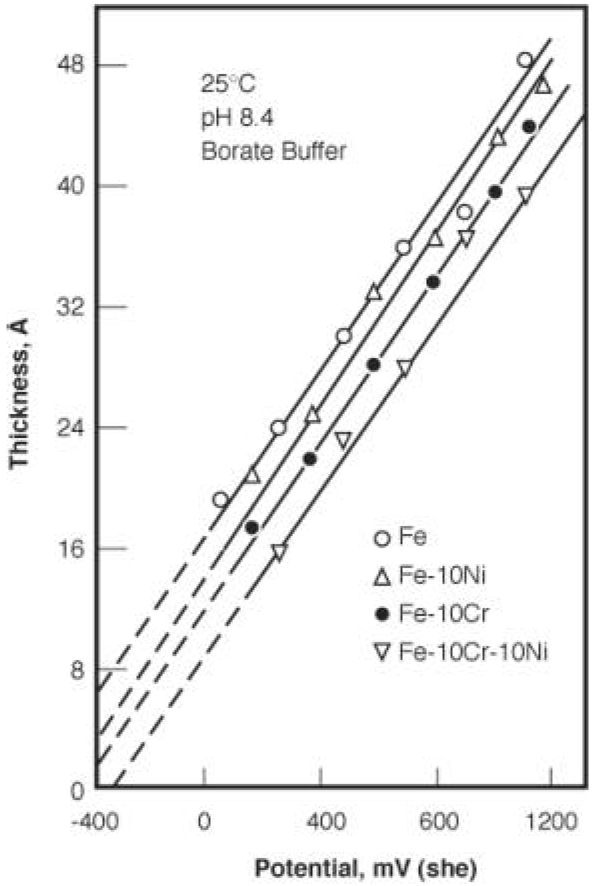

Figure B.15.30 Film thickness vs. electrochemical potential for Fe, Fe-10Ni, Fe-10Cr, and Fe-10Ni-10Cr alloys after one hour of polarization at 25°C measured in a pH 8.4 borate buffer solution. From Goswami and Staehle.[xxxviii]

Slip as affected by protective films

Figure B.15.31[xxxix] shows the effect of epitaxial films on the single slip of a nickel single crystal. The protective film increases the work hardening, therefore inhibiting slope, on the surface as shown by the work of Latanision and Staehle; whereas, the absence of the protective film permits the non-inhibited single slip. In the former, the slip steps are dispersed and finely divided; whereas, for the non-filmed surface, the slip is coarse and sharp. The presence of such films, then, affects the mechanical properties.

Brittle film rupture

Figure B.15.32[xl,xliii] illustrates the process by which SCC proceeds as related to the formation of a brittle reaction product on the surface. Such a brittle surface might develop from the formation of an epitaxial reaction product such as is assumed for copper alloys in ammoniacal solutions. The periodic breaking of such a brittle film has been often suggested as the means of propagation of some SCC. The rate of crack propagation, then, is related to the growth rate of the brittle film.

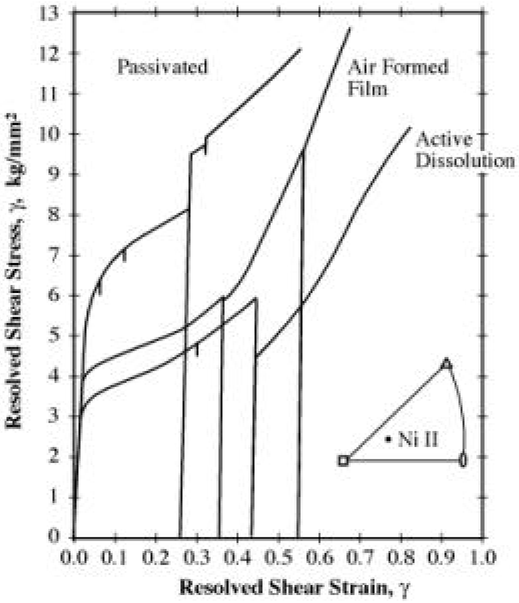

Figure B.15.31 Flow curves illustrating the effect of interruptions in tensile tests under active and passive conditions. About 3-4 *m*m were removed from the crystal surface before deformation under dissolution conditions at a steady state current density of approximately 4 mA/cm^2. From Latanision and Staehle.[xxxix]

4.5 Near-Surface Metal Domain

Enrichment and depletion

As some alloys dissolve, the atoms may dissolve as "alloy atoms," so that they appear to be essentially the same atom, although of different chemistries.[xli] Alternatively, in an alloy, especially where one atom is more electrochemically active than the other, (e.g. Cr in a Ni base or Zn in a Cu base), preferential loss of the more active Cr or Zn is expected, especially in the ranges of pH where the active species are also relatively soluble and in ranges of potential above the solution potentials for the more active species. Figure B.15.33a[xli] shows data from Staehle based on work of Rockel; and Figure B.15.33b[xlii] shows data from Lumsden and Stocker. Figure B.15.33 shows that the surfaces of materials change with time from the original composition of the alloy due to the loss of Cr. Such a change affects the electrochemistry and the mechanical properties of the surface. These depletions and enrichments change the chemical composition of the surface, and thereby change the catalytic and mechanical properties of the near surface—sometimes producing a brittle layer similar to the one described in connection with Figure B.15.32.

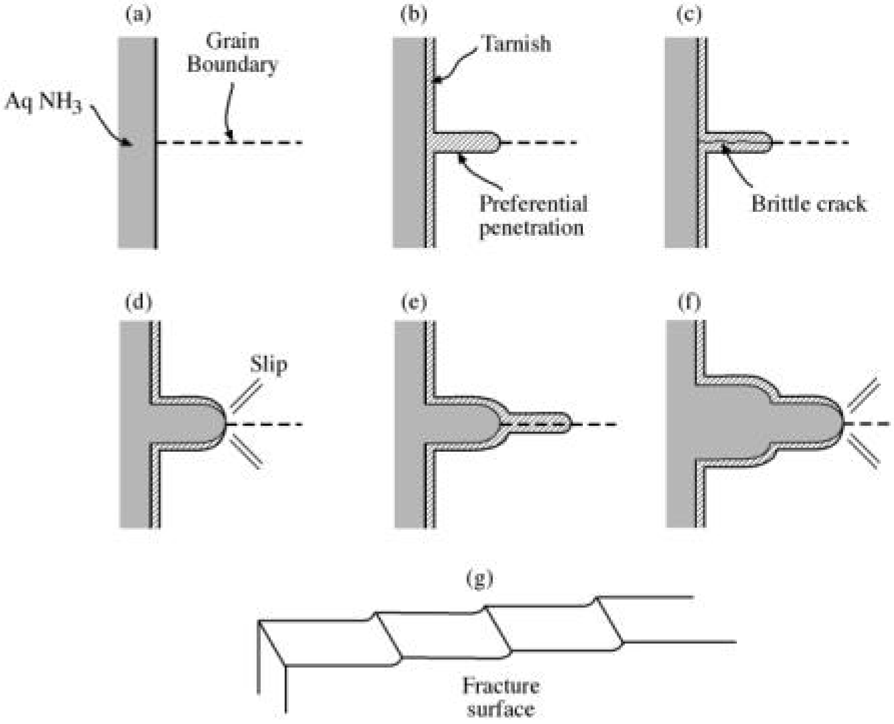

Figure B.15.32 Formation of brittle film on surface followed by successive breaking thereby producing SCC. From Pugh et al.[xl] and Forty and Humble.[xliii]

Preferential dissolution of phases

In the same environment, the phases in a multiphase structure may dissolve differently. These differences depend on the pH and potential of the dominating environments. Figure B.15.34[xliv] shows that the relative dissolution of pearlite, Fe_3C and α-Fe, depends on the pH and potential as well as species. Four modes of dissolution are observed: general dissolution independent of the phase, preferential dissolution of the α-Fe, preferential dissolution of the Fe_3C, and preferential dissolution of the interface between the Fe_3C and α-Fe. Each of these modes could affect initiation and propagation of SCC.

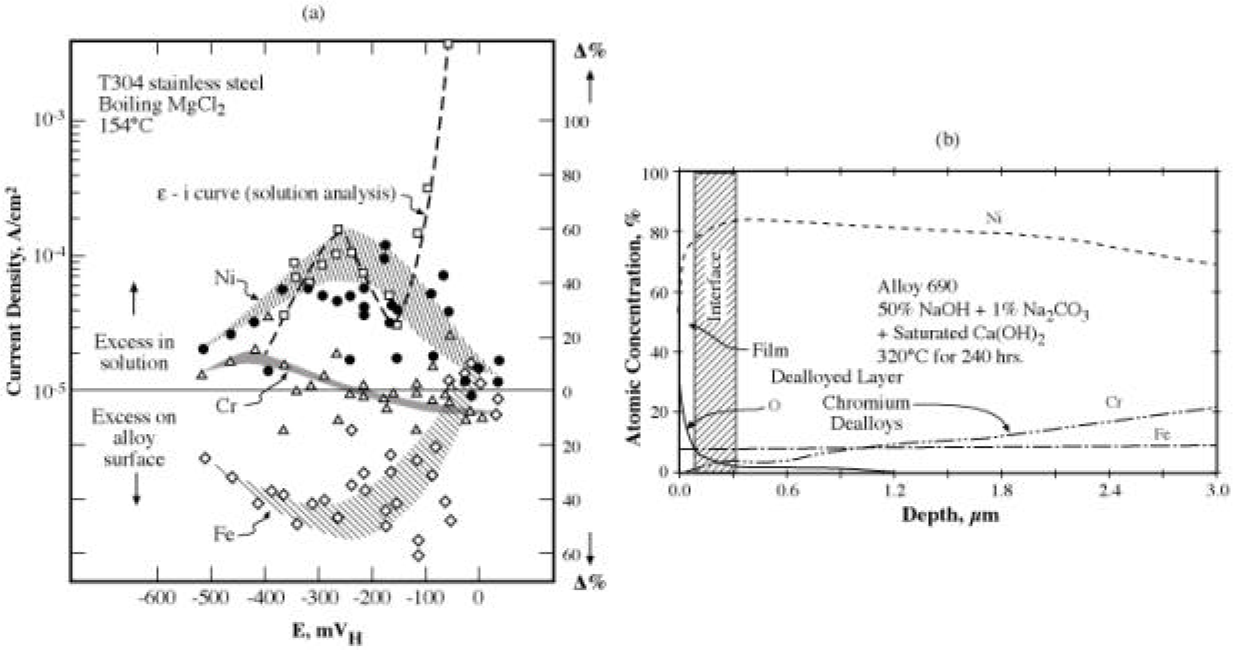

Figure B.15.33 (a) Surface enrichment/impoverishment, ?, of Fe, Cr and Ni on Type 304 steel in MgCl$_2$ at 154°C as a function of applied potential. From Staehle.[xli] (b) Composition profile of Alloy 690 after exposure to 50% NaOH+1%Na$_2$CO$_3$+saturated Ca(OH)$_2$ at 320°C for 240 h from depth analysis using Auger spectroscopy. From Lumsden and Stocker.[xlii]

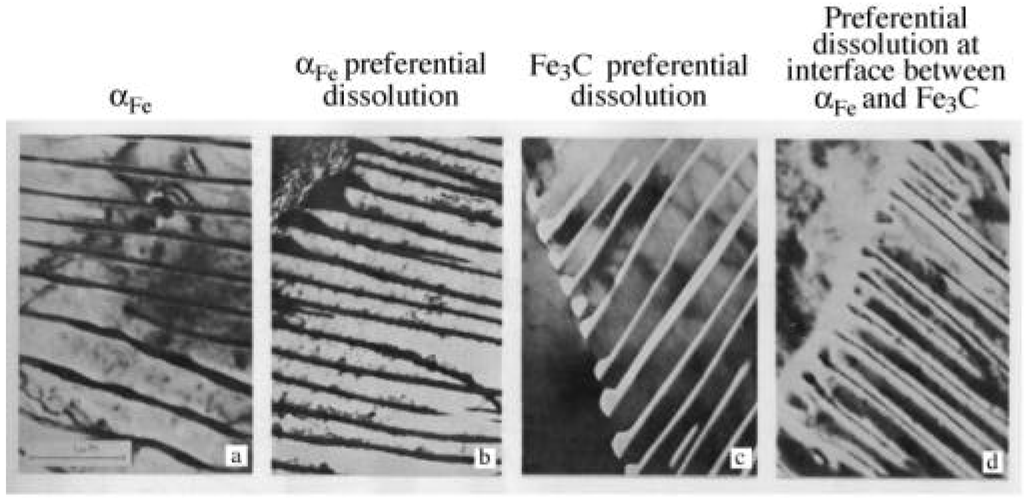

Fe-0.45 $^{w}/_{o}$ C as forged pearlitic structure

pH4 at -290 mV$_H$
10 min.
0.1N NaOH +
0.1M KHC$_8$H$_4$O$_4$

pH4 at +10 mV$_H$
60 min.
HCl

pH4 at -250 mV$_H$
10 min.
Acetic acid

Figure B.15.34 TEM micrographs of pearlite (1045 steel) foils exposed to various pH and potentials and species showing preferential dissolution of three types. From Payer and Staehle.[xliv]

Slip trenches and tunnels

When dislocations move and intersect a passive surface, the passive film is broken; a transient dissolution event occurs, the metal initially dissolves, and then repassivates. Such events are shown in Figure B.15.35a.[xlv,xlvi] In Figure B.15.35a, a thin foil has been exposed to a corrosive environment and stressed, after which it was examined in a transmission electron microscope. The image shows that parallel dissolution events have occurred within a single grain and that dissolution has occurred on both sides of the foil as shown by parallel dissolution traces. In this case, such parallel dissolution traces occur on intersecting slip planes. Figure B.15.35b[xlvii] shows, by examining an oxide film, which was removed from the surface, that tunnels can emanate from the slip trenches observed in Figure B.15.35a. Conditions that support the transient dissolution of Figure B.15.35 depend on pH, potential and species in the environment. It is likely that environments that support transgranular SCC also support both the trenches and the tunnels of Figure B.15.35.

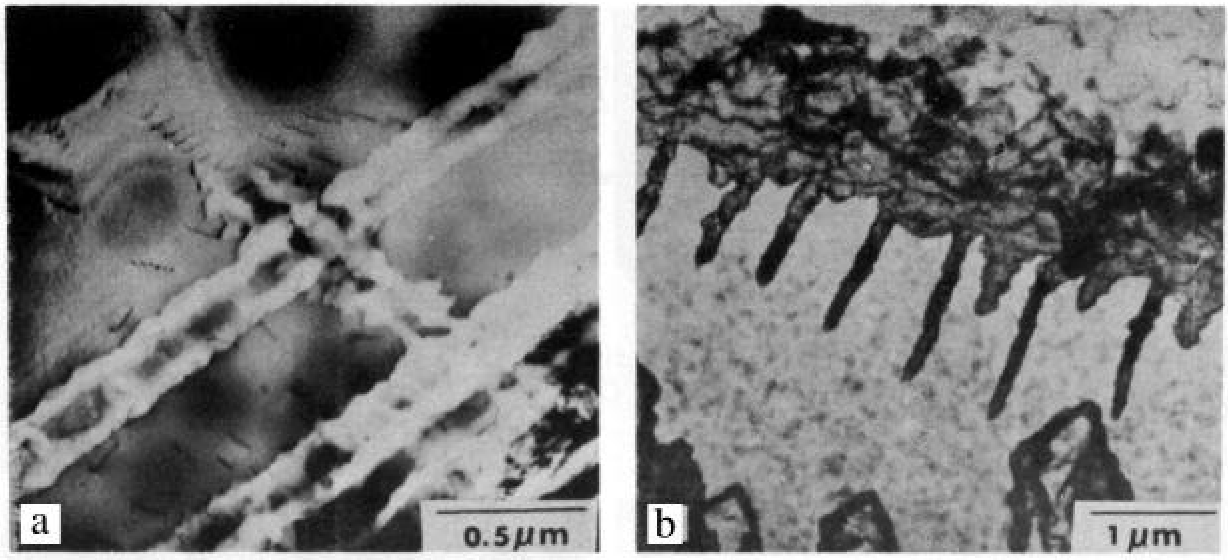

Figure B.15.35 Two similar modes of corrosion at surfaces, which is associated with moving dislocations breaking the surface and protective film. (a) TEM image of thin Fe-Cr-Ni alloy foil stressed in a corrosive medium at RT and then examined in the TEM. Parallel thinned regions indicate preferential dissolution at both sides of the foil. Two slip systems are identified. From work of Smith[xlv] and Davis.[xlvi] (b) An oxide film removed from the surface of stainless steel after exposure in a stressed condition to a corrosive environment. The thick region corresponds to the slip dissolution trenches shown in (a) and the protrusions are "tunnels" that have penetrated from the base of the dissolution trench. From Long.[xlvii]

4.6 Bulk metal domain

Stacking fault energy

Much of stress corrosion cracking and corrosion fatigue depend critically on the movement and relative coplanarity of movement of dislocations as they react to local stresses. There are two main patterns of dislocation movement that affect corrosion processes, as well as other aspects of deformation or fracture that are not considered here. Slip is important to SCC as it relates to breaking protective films, either during the slip process as shown in Figure B.15.35, or as the pile-up of dislocations at internal barriers intensifies local stresses at grain boundaries that interact with a corrosive environment.

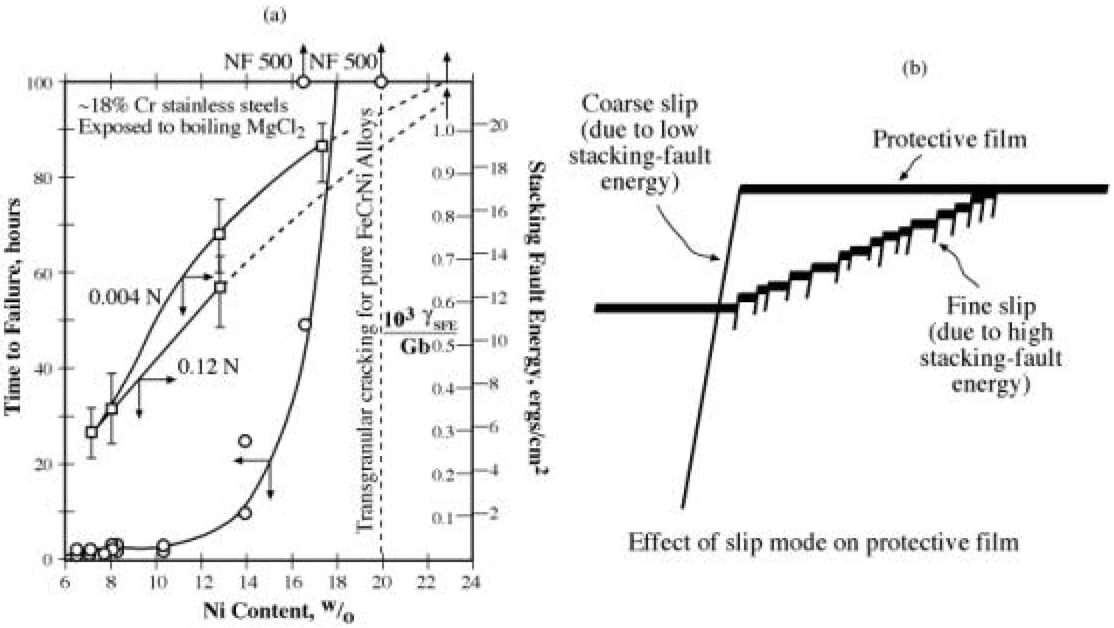

Figure B.15.36 (a) Time-to-failure for 18%Cr stainless steels exposed to boiling $MgCl_2$ compared with stacking fault energies for the same materials. (b) Nature of slip as affected by relatively high and low stacking fault energies.

Both roles, single slip and cross slip, of dislocation movement are related to whether the slip remains generally on single slip planes to intensify local stresses and the sharpness of slip step at the surface or can cross slip to relieve the intensification of local stresses as well as producing distributed slip at the surfaces. Dislocations can be generally constrained to remain on single slip planes once nucleated. On the other hand, the dislocations might “cross slip” out of the single plane and thereby relieve the local pile-up stresses. These two tendencies depend on the “stacking fault energy.” A high stacking fault energy stimulates cross slip, and a low stacking fault energy stimulates single slip. Thus, a high stacking fault energy would mitigate against SCC related to internal barriers; whereas, a low stacking fault energy would promote SCC. Figure B.15.36 shows how the stacking fault energy relates to SCC and to the nature of surface slip.

Composition of grain boundaries

The composition of grain boundaries is affected in two ways and according to somewhat different dimensional scales as shown in Figure B.15.37. Figure B.15.37a[vii] refers to the formation of precipitates, such as chromium carbide, in stainless steel. The dimensions here are on the order of μm. Three conditions obtain in this case. First, the precipitate forms with a concentration of the metal typically greater than in the metal matrix. In the case of stainless steels, the compound is in the range of $Cr_{22}C_7$ or Cr_7C_3. This high concentration of chromium renders the alloy corrosion resistant in neutral solutions; but, in alkaline solutions the chromium is quite soluble relative to iron. Adjacent to the precipitate is a depleted zone from which the chromium has been taken to form the Cr_xC_y compound. Such a zone, when depleted of chromium, is more prone to corrosion in neutral to acidic solutions but is more resistant to alkaline solutions. In addition, there is usually a narrow zone at the interface between the precipitate and the depleted zone where impurities are concentrated. Such interfaces have rarely been studied; but results, such as those in Figure B.15.34d, suggest that they could be prone to preferential corrosion depending on what species have been attracted or reflected during the formation of pearlite. Figure B.15.37c[vii] shows the relative polarization rates for alloys across the range of alloy compositions.

In Figure B.15.37b,[vii] the case of adsorption and desorption of species is shown for impurities and for alloying species. For the case of impurities, concentrations at the grain boundaries have been observed to be up to 10^6 greater than in the grain matrix. The dimensions of these highly concentrated regions are in the range of nm. Such concentrations, although narrow, provide a reactive path for corrosion. Figure B.15.37d shows the effect of such adsorption on the cracking behavior of Ni with sulfur segregated at the grain boundary.[xlviii,xlix]

Much of the preferential IGC and IGSCC is related to cases where such changes in concentration occur at grain boundaries as shown in Figure B.15.37.

5. Development of Scenarios

Developing a scenario is the essential process of predicting failures that occur after long times as shown in Figure B.15.1. A schematic illustration of developing a scenario is shown in Figure B.15.6. The scenario begins with the start of a power plant or from a suitable reference time, and identifies the components in the precursor as shown in Figure B.15.6. The components of the scenario are taken from the domains and their microprocesses, as described in Sections 3.0 and 4.0. Quantifying the microprocesses provides a basis for estimating the time before an SCC process can start. The times consumed by the developing microprocesses depend on the kinetic process that occur in the range of operating conditions of the plant. Further, it is likely that some of the microprocesses occur in sequence, thereby requiring the completion of one before the onset of the next. Finally, at the end of the precursor stage, the chemistry and configuration must lead to a viable SCC or other damage process.

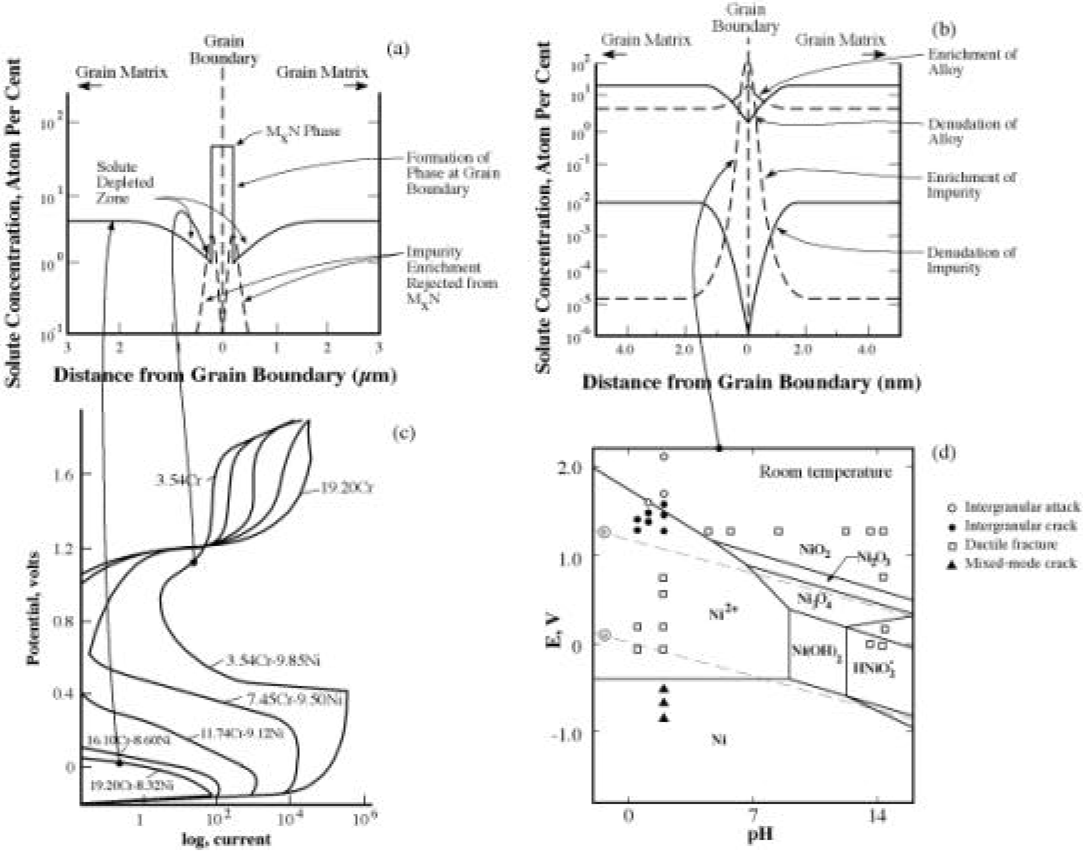

Figure B.15.37 (a) Distribution of species at grain boundary for the case of precipitation. (b) Distribution for the case of adsorption. (c) Polarization behavior in sulfuric acid at RT for alloys across the grain boundaries. From Staehle.[vii] (d) Cracking behavior for a Ni-base alloy with sulfur segregation as a function of pH and potential. From Chaung et al.[xlviii,xlix]

Selecting the domains and microprocesses, as shown schematically in Figure B.15.6, requires expert experience. More than a single scenario would probably be considered.

Figure B.15.38 shows the overall process for selecting a scenario, evaluating the important rates upon which the length of the precursor stage is based, and applying the result to the starting point for the SCC.

6. Target

The goal of developing scenarios is to identify conditions under which SCC or some other important damage process will start according to the pattern of Figure B.15.1, Case III. For such a target to be achieved, the target itself needs to be identified. One might be LPSCC or PbSCC as shown in Figure B.15.22. However, there may be others. There is a task, then, of quantifying possible targets, which embody conditions initiating SCC, some of which have not occurred in the past but can reasonably be identified for possibly occurring in the future.

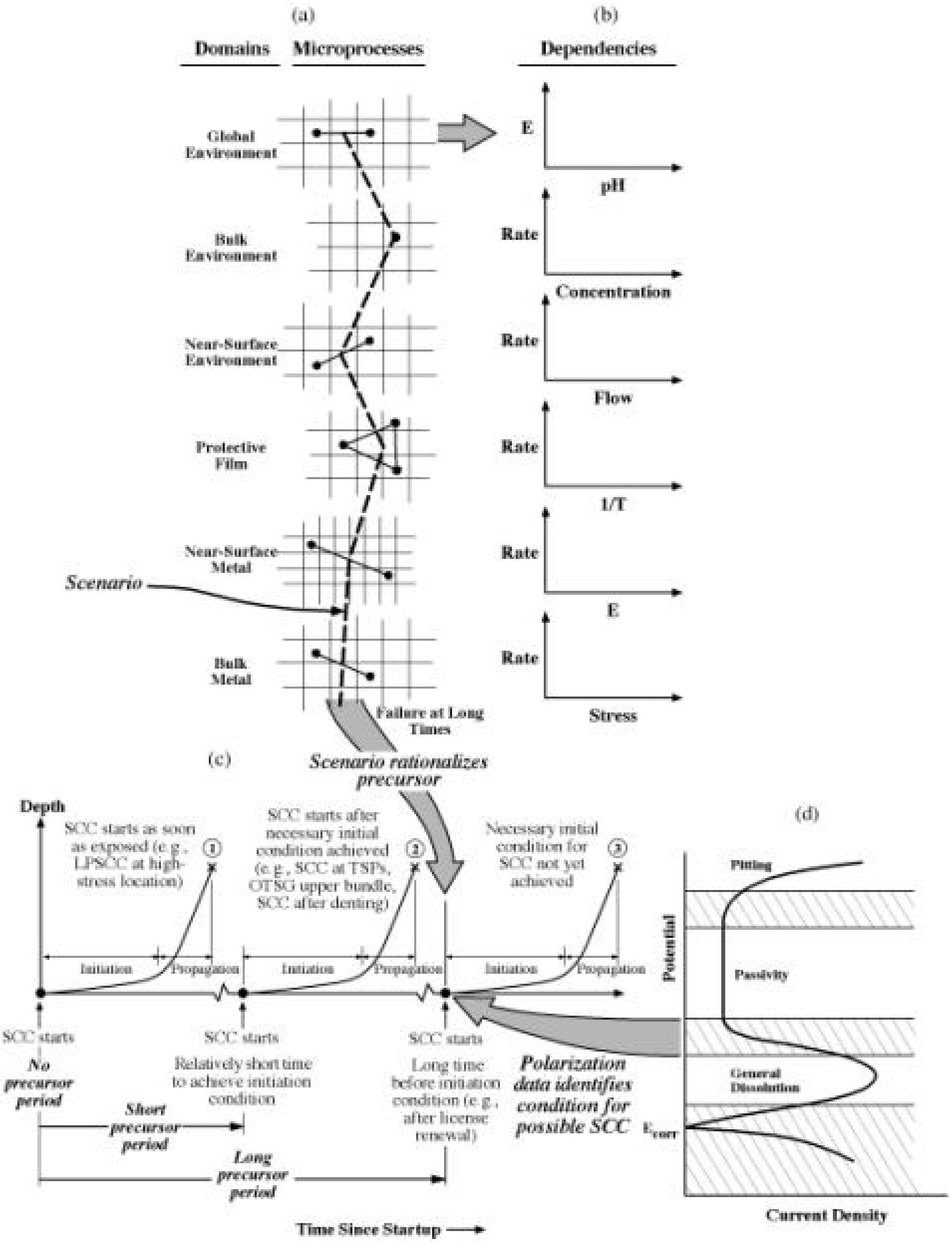

Figure B.15.38 Schematic view of overall process of prediction. (a) Scenario including microprocesses from various domains; scenario connects microprocesses from various domains. (b) Hypothetical rates associated with microprocesses to be used for estimating length of precursor period. (c) Three cases for SCC with precursor times identified. (d) Possible location of target for SCC initiate.

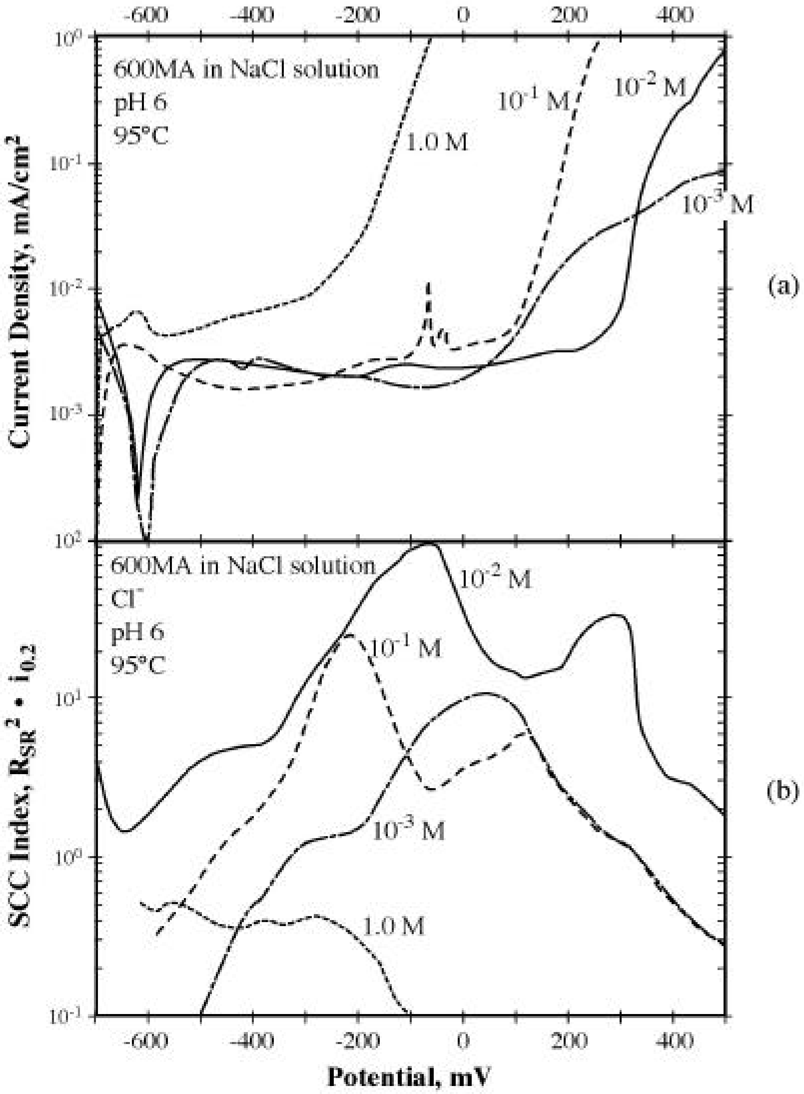

Figure B.15.39 Current density and SCC parameter vs. potential for Alloy 600MA in NaCl solutions at pH 6 and 95°C for concentrations from 10^{-3} to 1.0 M. From Staehle and Fang.[1]

Where some SCC is suspected to occur, but for which no information is available, there are several survey approaches that can be used and have been successful in the past. Figure B.15.39 suggests that locations for the initiation of SCC often occur at potentials near regions of kinetic instability. Such regions can be evaluated using electrochemical methods, either by identifying regions of transition such as in Figure B.15.38d, or regions where there are large differences between slow and fast scans. Figure B.15.39 shows polarization curves for Alloy 600MA in 95°C NaCl solutions. Figure B.15.39b shows a SCC parameter, which has been developed by Staehle and Fang[1] vs. potential. This parameter is based on the differences in currents between fast and slow potentiodynamic scans. Peaks in Figure B.15.39b identify potentials where SCC is likely.

Another approach for identifying regions of possible SCC has involved CERT tests that are conducted as functions of potential. Such data are shown in Figure B.15.40 from experiments by Parkins[li] and others.

There are other well-known methods for identifying targets of the scenarios suggested in Figures 6 and 38. The principal point here is that surveying possible future targets for scenarios is an important part of prediction. Such approaches can rely on the fact that the boundaries and domains of SCC are generally orderly, as suggested by Figure B.15.41, which shows the zone of SCC for stainless steel in acid chlorides at room temperature from the work of Morin and Staehle.[lii,lvii]

7. Predictions

Using the approach described in Sections 3.0 and 4.0 and Figures 1, 6, and 38 some predictions are possible, and examples of these are described in this section.

Transport of low valence sulfur to turbine

Figure B.15.42 shows a sequence of events involving the microprocesses described in Sections 3.0 and 4.0. The essence of prediction as shown in Figure B.15.42 is the following:

a. Sulfate impurities are reduced in steam generators by hydrazine to a low valence sulfur species (M-1) such as HS^-.

b. The low valence sulfur species is transported (M-2) to the turbine.

c. This low valence sulfur species deposits (M-3) on surfaces of the turbine where the materials are generally high strength alloys.

d. High strength alloys are prone to SCC and failure occurs after sufficient accumulation of the low valence sulfur species (M-4).

Such a possible sequence of events can be evaluated by:

a. Analyzing surfaces in turbines.

b. Evaluating the SCC behavior of turbine alloys in such environments as are found on surfaces.

LPSCC of Alloy 690 occurs as chromium is depleted from the surface

Figure B.15.43 shows a sequence of events whereby Alloy 690TT can sustain LPSCC as follows:

a. Chromium dissolves preferentially in the environment at moderately alkaline pH as shown in (M-1).

b. The surface, as it is depleted, (M-2), becomes an alloy like Alloy 600, as at (M-3), and sustains LPSCC as shown in (M-4).

This sequence implies that the LPSCC will propagate as rapidly as the chromium is depleted from the surface. This surface eventually becomes the crack tip; the tip of the crack then advances as rapidly as the chromium is preferentially dissolved. Such a possible sequence can be evaluated with ATEM and by evaluating the pH of solutions inside advancing SCC.

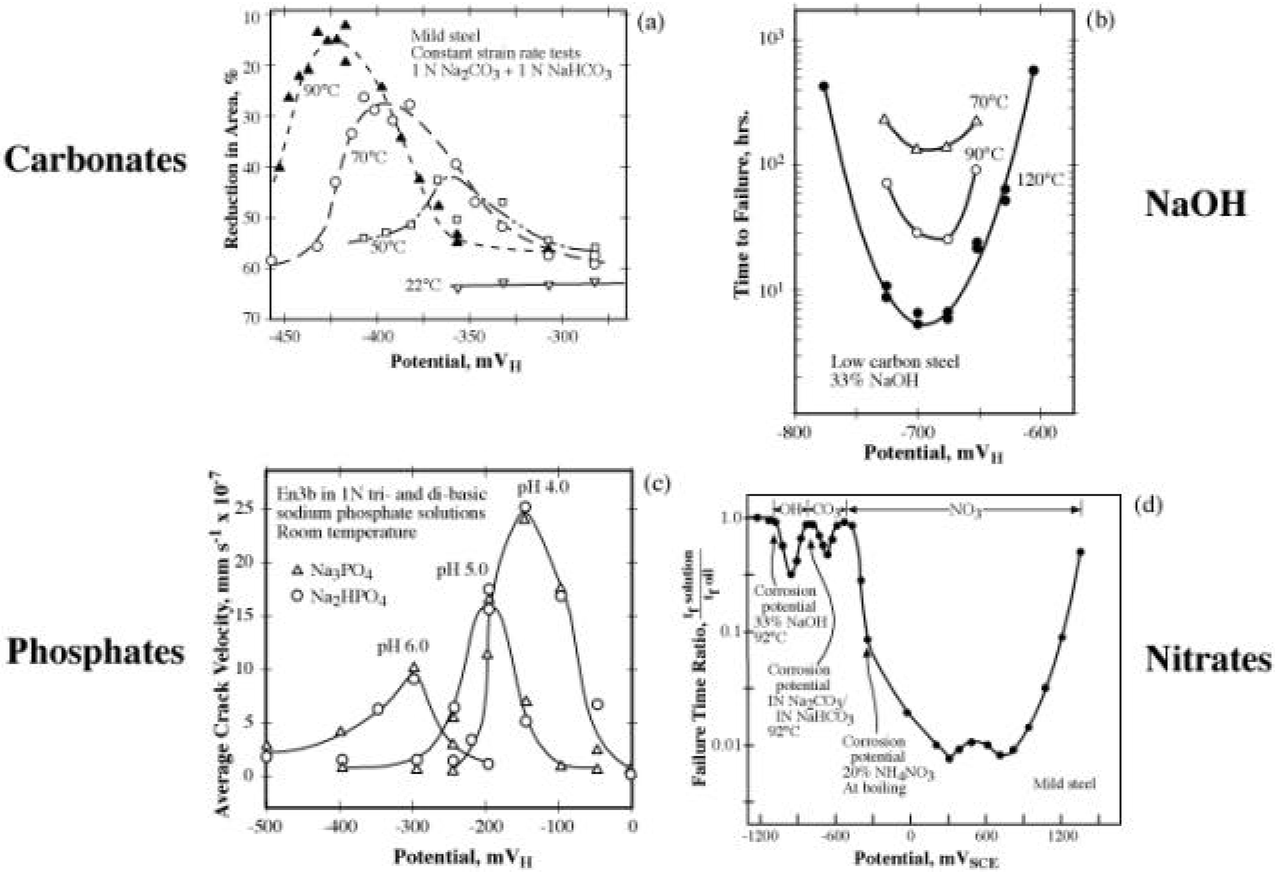

Figure B.15.40 (a) Reduction in area vs. potential for mild steel exposed to carbonate-bicarbonate solutions at various temperatures and tested in CERT. From Sutcliffe et al.[liii] (b) Time-to-failure vs. potential for three temperatures for a low carbon steel in 33% NaOH. From Singh[liv] reporting on Bohnenkamp.[lv] (c) Average crack velocities vs. potential for (plain carbon steel) En3b (w/o C 0.12, Si 0.05, Mn 0.81, S 0.029, P 0.008) steel in Na_3PO_4 and Na_2HPO_4 tested at RT function of pH. From Holroyd.[lvi] (d) Ratio of time-to-failure in solution to time-to-failure in oil vs. potential for NaOH, Na_2CO_3 + $NaHCO_3$ and $NaNO_3$ solutions. From Parkins.[li]

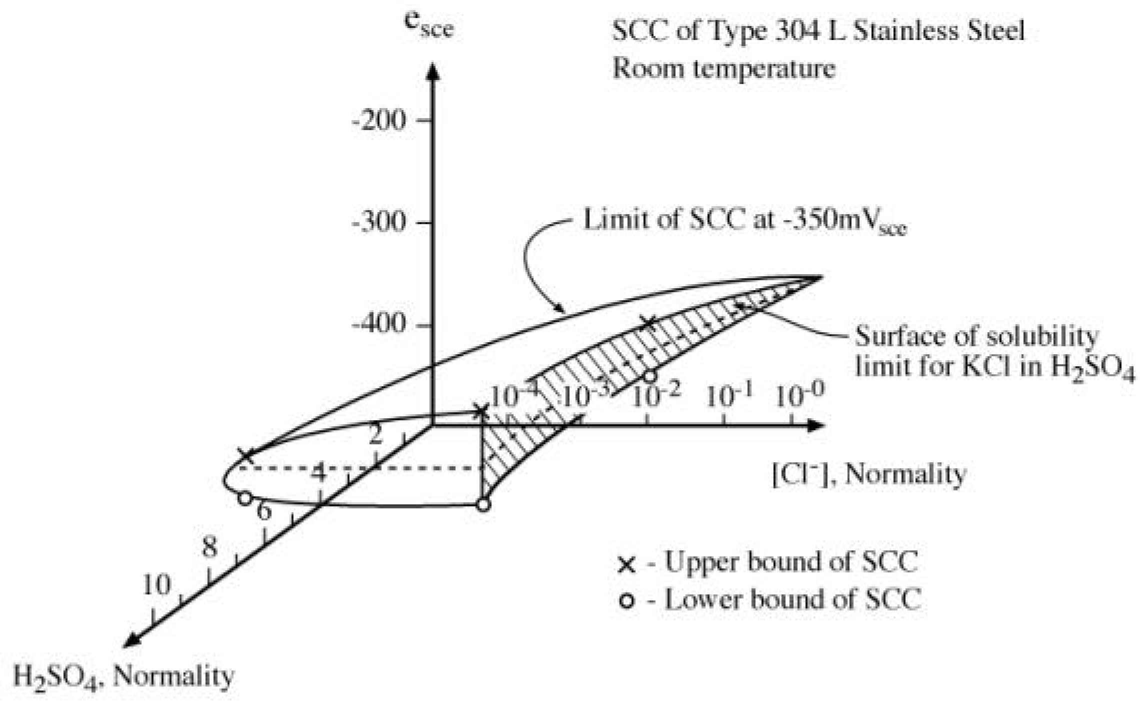

Figure B.15.41 Zone for the occurrence of SCC in stainless steels as a function of potential, H_2SO_4, and KCl at room temperature. From Morin[lvii] and used by Staehle.[lii]

PbSCC occurs as Pb is released from sequestering compounds

One of the major unknowns in the performance of SGs is why massive PbSCC is not occurring despite the relatively large amount of Pb present in crevices and also known to be present in some SCC that have been examined. Further, PbSCC has been shown to produce SCC at relatively low concentrations of Pb. It also appears that PbSCC occurs readily in Alloy 690TT.

Thus, understanding why PbSCC does not occur when the threshold for concentration is so low and the PbSCC is so rapid, is an important question. The answer to why PbSCC does not occur seems related to the fact that the activity of Pb is lowered by the formation of Pb-containing compounds. Such compounds could include silicates, phosphates, sulfates, carbonates, or chlorides separately or as multiple component compounds.

Since the compounds that form in crevices are in some equilibrium with the species in the bulk water, reducing such species might raise the activity of the Pb making it available for producing PbSCC.

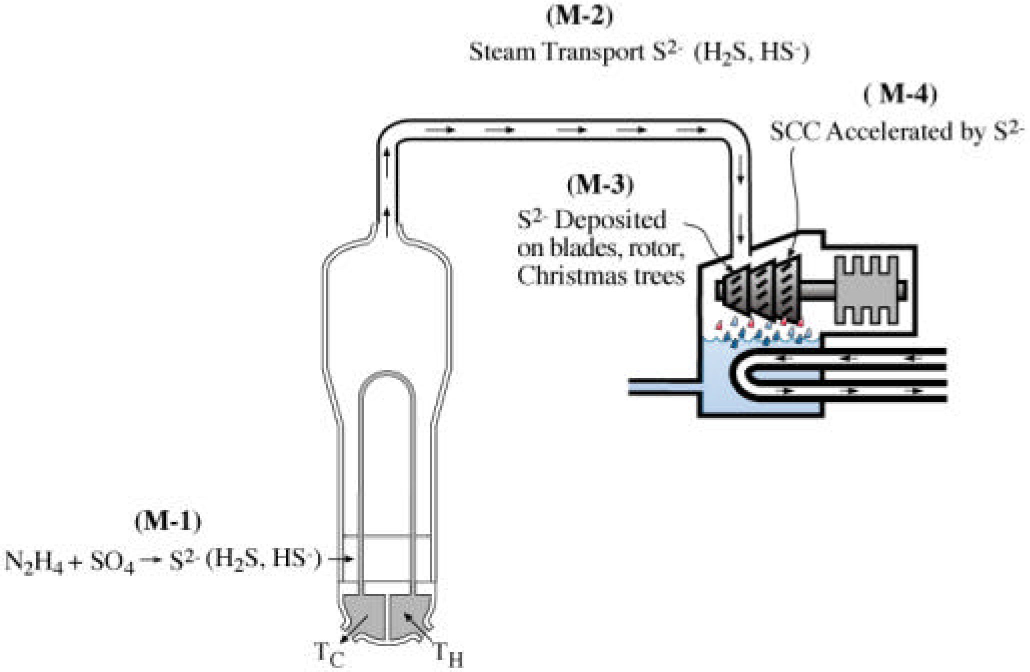

Figure B.15.42 Reduction of SO_4^{2-} by N_2H_4 in the SG and transport of reduced sulfur to the surfaces of the turbine where accelerated SCC is possible especially in view of high strength alloys from which the blades and rotors are constructed.

Figure B.15.44 shows a sequence of events associated with raising the activity of Pb by reducing the available compound-forming species.

a. Heat transfer crevices concentrate chemicals from feed water (M-1).

b. Lead enters heat transfer crevices (M-2).

c. A deposit forms containing Pb (M-3).

d. Pb concentrates on the hot surface as is observed from direct analysis (M-3).

e. Increasing the Pb activity is known to increase the intensity of PbSCC (M-4).

f. The activity of Pb will increase when the activity of compound forming species in the bulk water decreases (M-5).

Thus, it is likely that PbSCC will occur if the secondary water is further purified.

Such a process as described in Figure B.15.44 can be assessed by determining what compounds and chemical processes are immobilizing the Pb. Such work has not yet been undertaken but is important to predicting the course of PbSCC.

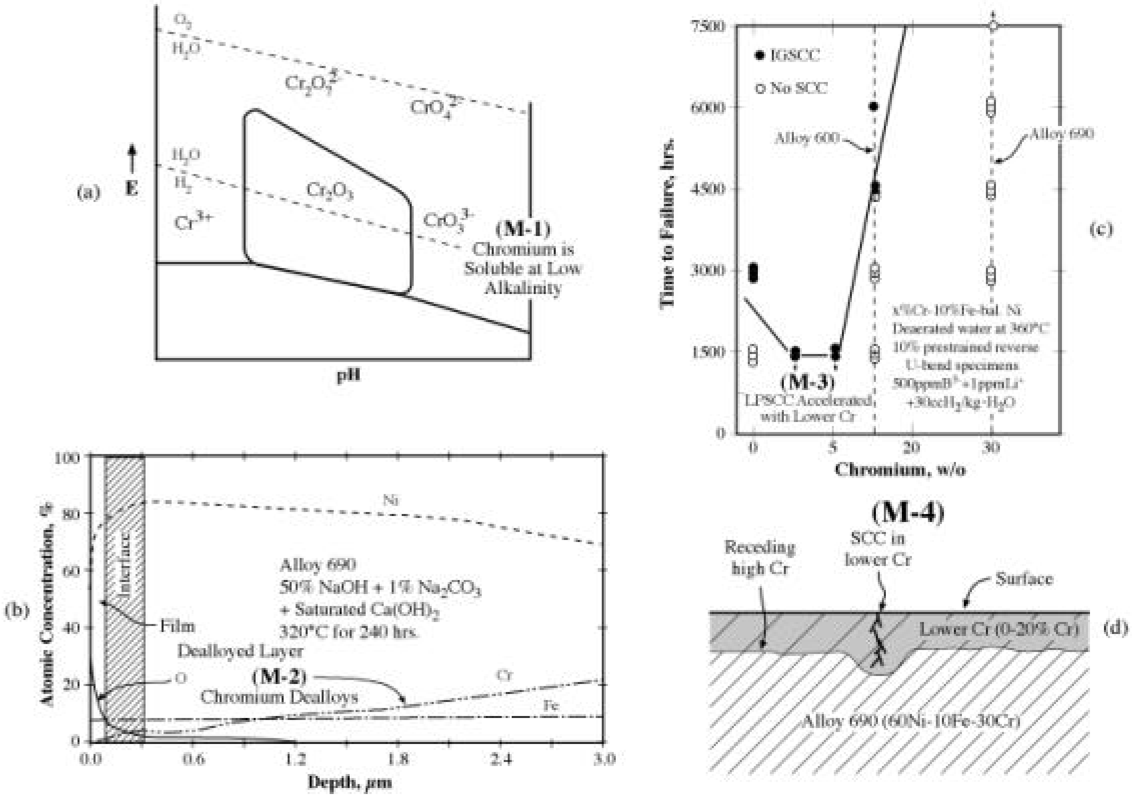

Figure B.15.43 The Cr of Alloy 690 is soluble in mildly alkaline solution and dissolves to give a lower Cr surface and is more prone to LPSCC.

SCC of low alloy steels in FAC type environments

SCC is known to occur episodically in low alloy steels when exposed to FAC type environments as well as to other environments. The episodic nature of the SCC suggests that the high velocity of coolant is, in fact, removing the initiating events, and only initiating events whose velocities that exceed the recession rate of the FAC can actually become growing SCC. Such a pattern suggests that lowering the FAC rate may increase susceptibility to SCC according to the following sequence as shown in Figure B.15.45.

a. The rate of recession of a surface is greater than the rate of penetration of SCC initiation (M-1), (M-2).

b. The initial material is replaced with one having a lower rate of FAC; however, the rate of recession is less than the penetration rate during initiation. (M-3)

c. The rate of initiation now exceeds the rate of recession (M-4).

At this point SCC can initiate and propagate.

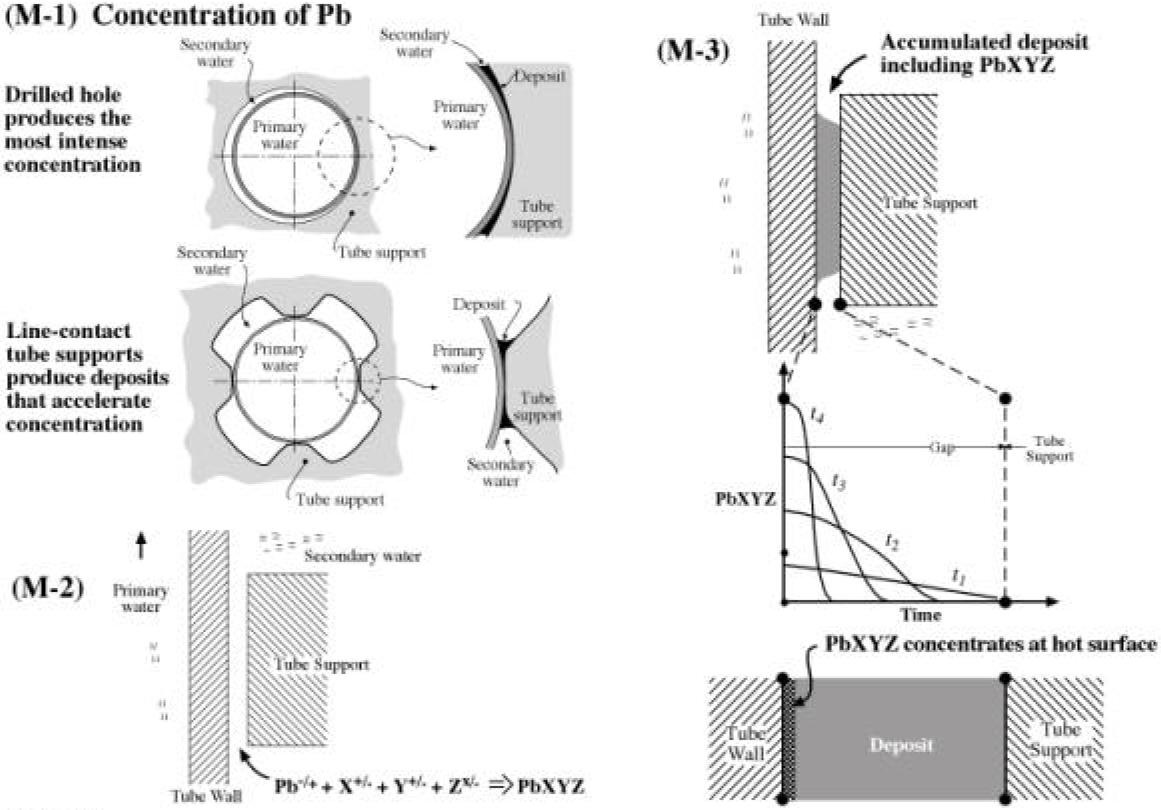

(M-4)

PbSCC increases when Pb activity $[a_{Pb}]$ increases at metal surface $[a_{Pb,\,s}]$

1. **Pb activity increases when activity of compound-forming species decreases**

   e.g., $[a_{Pb,\,s}] \uparrow$ when $[a_{X,\,s}], [a_{Y,\,s}], [a_{Z,\,s}] \downarrow$

2. **Activity of compound-forming species decreases on metal surface when these activities decrease in the bulk solution**

   e.g., $[a_{X,\,s}] \downarrow$ when $[a_{X,\,B}] \downarrow$

(M-5)

PbSCC increases when activity of compound-formers (X,Y,Z) decreases in bulk

Figure B.15.44 Pb is concentrated in heat transfer crevices and accumulates at the surface. Initially, Pb is immobilized by forming compounds. When the activity of these insolubilizing species is reduced, Pb is released and PbSCC occurs.

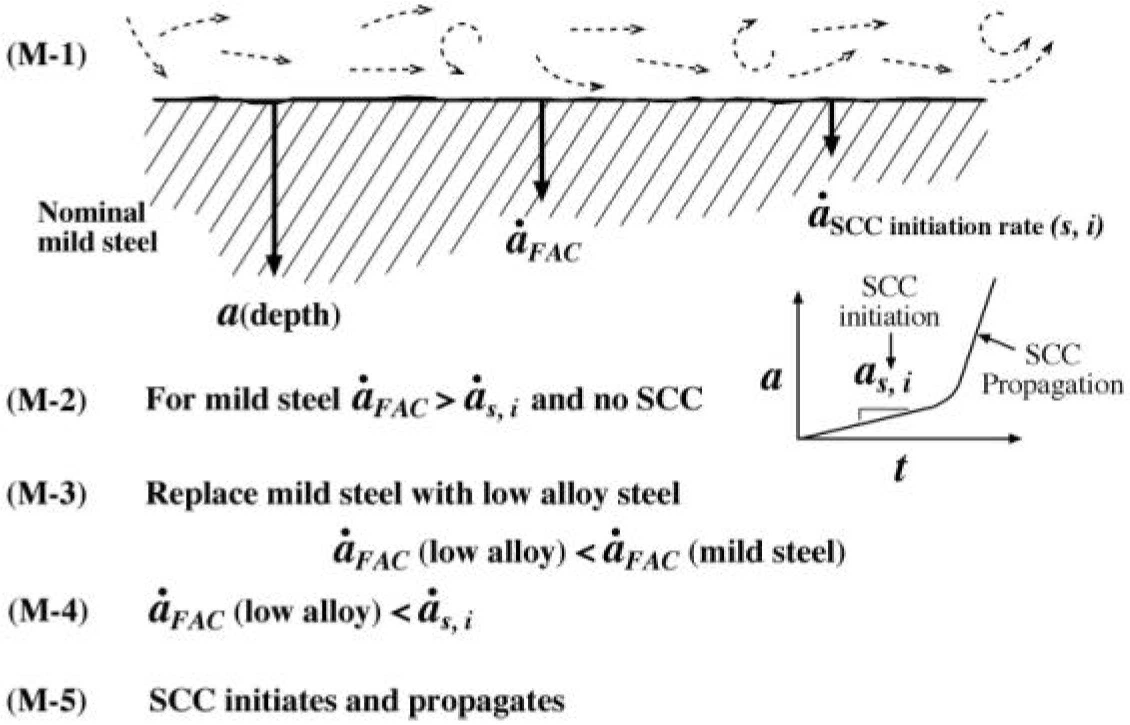

Figure B.15.45 Sequence of events for reduction in rate of FAC and then permitting the SCC initiation process to accelerate and perforate.

8. Conclusions

1. In order to assure reliability for long time performance, it is necessary to develop a method for predicting corrosion failures that have not yet occurred. Such a method involves the Micro-process Sequence Approach (MPSA).

2. The essence of predicting corrosion failures at long times is recognizing that such processes as SCC will not proceed monotonically from the beginning of operation to a failure many tens of years later. Rather, the occurrence of failures after long times most likely results from a multi-step analysis. First, there are some processes that develop conditions that are favorable to the later occurrence of SCC. The first steps are "precursors." Second, once the necessary conditions for SCC coalesce, then the SCC proceeds according to processes that produce failures in times between a month and ten years.

3. Thus, the long times which are necessary for failures to occur depend mainly on the times for precursors to develop.

4. Quantifying the precursor step can be approached by identifying microprocesses that require some time for maturing to produce the conditions necessary for SCC. In general, there might be multiple microprocesses acting in series or in parallel or both.

5. Organizing the microprocesses into a precursor stage is most effectively accomplished by recognizing that there are six domains that influence conditions for initiating SCC after some long time: global, bulk environment, near surface environment, protective film, near surface metal, and bulk metal. Within each of these domains are microprocesses that are already known.

6. The quantitative development of a precursor scenario involves selecting a sequence of microprocesses that become logical constituents of a scenario. Multiple scenarios might be developed. Once such scenarios are identified, the time required for conditions to occur for SCC to initiate can be calculated. Such hypotheses can then be tested experimentally.

7. In addition to developing scenarios for precursors, it is necessary to identify what conditions must be met for SCC to occur. An array of such specific conditions can be assessed using various survey methods already well known.

8. The total time for failure to occur, then, involves the time for the precursor step to produce conditions necessary for SCC and the time for the SCC, once initiated, to propagate to failure.

9. Acknowledgements

The development of the ideas in this paper is based on many discussions with my colleagues in the corrosion community. Among these are Masatsune Akashi, Peter Andresen, Sam Armijo, Allen Baum, Ted Beck, John Bockris, Floyd Brown, Steve Bruemmer, H.E. Chaung, Pierre Combrade, John Congleton, Jacques Daret, Jim Davis, David Douglass, Zhi Fang, (the late) Mars Fontana, Bob Frankenthal, Rick Gangloff, Jack Gilman, Jeff Gorman, Mac Hall, John Hirth, (the late) Sam Hoar, Bill Hocking, Xiangchun Jiang, Rob Kelly, Jerry Kruger, Ronald Latanision, Bill Lindsay, Mike Long, Jesse Lumsden, Al McIlree, Charlie McMahon, Bruce Miglin, Peter Millett, Joe Muscara, Roger Newman, (the late) Peter Paine, (the late) Redvers Parkins, Joe Payer, Neal Pessall, Howard Pickering, (the late) Marcel Pourbaix, Neville Pugh, Bob Rapp, Peter Rhodes, Norio Sato, Steve Sawochka, Peter Scott, John C. Scully, John R. Scully, Masahiro Seo, Bill Shack, Toshio Shibata, Tetsuo Shoji, Karl Sieradski, Ed Simonen, Susan Smialowska, Tom Smith, Bill Smyrl, Markus Speidel, Narasi Sridhar, Norm Stoloff, Peter Swann, Bob Tapping, Larry Thomas, Gary Was, Jack Westbrook, Bert Westwood, Mike Wright, and many others.

I particularly appreciate the stimulation by Dr. Joe Muscara of the NRC to think about the subject in this report through his persistently advocating a pro-active approach to predicting corrosion processes. I also appreciate the support of both Dr. Joe Muscara and Dr. Bill Shack of ANL for my research into predicting early SCC failures in steam generators.

I appreciate also the stimulating discussions of my colleagues in the PMDA group. Again, I thank Joe Muscara for bringing this project into being and for assembling such a group of outstanding colleagues.

Also, I greatly appreciate the careful reviews of this manuscript by Robert Tapping, William Shack, and Jack Westbrook.

Finally, as always, I thank my office staff who individually and as a group exhibit such high standards of professionalism in their attention to details and their refusal to compromise on lesser quality work. Specifically, I appreciate Julie Daugherty who prepared the manuscript in its final form and who resolved the many questions associated with sometimes inscrutable details; I also appreciate the talent and diligence that John Ilg brings to the preparation of my graphics. Marcia Parrish-Siggelkow and Erin Kate Rediger also assisted.

10. References

---

[i] R.W. Staehle and J.A. Gorman, "Quantitative Assessment of Submodes of Stress Corrosion Cracking on the Secondary Side of Steam Generator Tubing in Pressurized Water Reactors," *Corrosion*, Part 1 Vol. 59 No. 11 November 2003, Part 2 Vol. 60 No. 1 January 2004, Part 3 Vol. 60 No. 2 February 2004, NACE, Houston, Texas.

[ii] D.O. Harris, E.Y. Lim, and D.D. Dedhia, "Probability of pipe fracture in the primary coolant loop of a PWR plant," NUREG/CR-2189, Vol. 5, U.S. Nuclear Regulatory Commission, Washington, August, 1981.

[iii] D.O. Harris, D.D. Dedhia and S.C. Lu, "Theoretical and User's Manual for PC-PRAISE: A Probabilistic Fracture Mechanics Computer Code for Piping Reliability Analysis," NUREG/CR-5864, U.S. Nuclear Regulatory Commission, Washington, 1992.

[iv] J.W. Provan, Probabilistic Fracture Mechanics and Reliability, Dordrecht, Boston, Massachusetts, 1987.

[v] T.L. Dickson, R.D. Cheverton, J.W. Bryson, B.R. Bass, D.K.M. Shum, and J.A. Keeney, "Pressurized Thermal Shock Probabilistic Fracture Mechanics Sensitivity Analysis for Yankee Rowe Reactor Pressure Vessel," NUREG/CR-5782, U.S. Nuclear Regulatory Commission, Washington, 2004.

[vi] J.M. Bloom and J.C. Ekvall, Probabilistic Fracture Mechanics and Fatigue Methods: Applications for Structural Design and Maintenance – A Symposium, ASTM Committee E-9 on Fatigue; ASTM Committee E-24 on Fracture Testing, STP 798, American Society for Testing and Materials, Philadelphia, Pennsylvania, 1983.

[vii] R.W. Staehle, "Lifetime Prediction of Materials in Environments," Uhlig's Corrosion Handbook, 2nd edition, Ed. R.W. Revie, John Wiley and Sons, New York, 2000, pp. 27-84.

[viii] R.W. Staehle, "Approach to Predicting SCC on the Secondary Side of Steam Generators," presented at Fontevraud 5, Contribution of Materials Investigation to the Resolution of Problems Encountered in Pressurized Water Reactors, SFEN, Paris, September 23-27, 2002.

[ix] R.W. Staehle, "Predicting the First Failure," presented at Corrosion 2003, San Diego, March 16-20, NACE, Houston, Texas, 2003.

---

[x] R.T. Begley, A.W. Klein, and R.E. Gold, "Investigation of ID Stress Corrosion Cracking in Field and Laboratory Programs," Contribution of Materials Investigation to the Resolution of Problems Encountered in PWR Plants: International Symposium, French Nuclear Energy Society, Paris, 1985, p. 217.

[xi] R.W. Staehle, J.A. Gorman, K.D. Stavropoulos, and C.S. Welty, Jr., "Application of Statistical Distributions to Characterizing and Predicting Corrosion of Tubing in Steam Generators of Pressurized Water Reactors" Life Prediction of Corrodible Structures, R.N. Parkins, ed., NACE, Houston, 1994, p. 1374.

[xii] Courtesy of R. Eaker of Duke Power, Charlotte, North Carolina. Private communication.

[xiii] G. P. Airey, Optimization of Metallurgical Variables to Improve Corrosion Resistance on Inconel Alloy 600; NP-3051, EPRI, Palo Alto, 1983.

[xiv] M.O. Speidel and R. Magdowski, "Stress Corrosion Crack Growth of Cold Worked Nickel Base Alloy 600," International Conference on Corrosion-Deformation Interactions; CDI '92, Electricite de France, Paris, 1992, p. 107.

[xv] C.H. Shen and P.G. Shewmon, "A Mechanism for Hydrogen-Induced Intergranular Stress Corrosion Cracking in Alloy 600," *Metallurgical Transactions Vol. 21A*, 1990, p. 1261.

[xvi] H.M. Chung, "Formation of Microcavities in BWR Core Shroud Welds," Proceedings of the Tenth International Conference on Environmental Degradation of Materials in Nuclear Power Systems – Water Reactors, P. Ford, G. Was, and L. Nelson, eds., NACE, Houston, Texas, 2002.

[xvii] A. Kimura, "Dependence of Susceptibility to IGSCC on the Location of HAZ of Welded SUS304 Core Shroud for BWR," Proceedings of the Tenth International Conference on Environmental Degradation of Materials in Nuclear Power Systems – Water Reactors, P. Ford, G. Was, and L. Nelson, eds., NACE, Houston, Texas, 2002.

[xviii] J. Hickling, P.L. Andresen, R.M. Horn, and H. Hoffmann, "Characteristics of Crack Propagation Through SCC Under BWR Conditions in Stainless Steels Stabilized with Titanium or Niobium," Proceedings of the Ninth International Conference on Environmental Degradation of Materials in Nuclear Power Systems – Water Reactors, S.M. Bruemmer, F.P. Ford, and G.S. Was, eds.,TMS, Warrendale, Pennsylvania, 1999, p. 299-308.

[xix] K. Matocha and J. Wozniak, "Stress Corrosion Cracking Initiation in Austenitic Stainless Steel in High Temperature Water," Proceedings of the Ninth International Conference on Environmental Degradation of Materials in Nuclear Power Systems – Water Reactors, S.M. Bruemmer, F.P. Ford, and G.S. Was, eds.,TMS, Warrendale, Pennsylvania, 1999, p. 383-388.

[xx] E.D. Eason and L.M. Shusto, Analysis of Cracking in Small Diameter BWR Piping, EPRI NP 4394, Electric Power Research Institute, Palo Alto, 1986.

[xxi] T.M. Angeliu, P.L. Andresen, E. Hall, J.A. Sutliff, S. Sitzman, and R.M. Horn, "Intergranular Stress Corrosion Cracking of Unsensitized Stainless Steels in BWR Environments," Proceedings of the Ninth International Conference on Environmental Degradation of Materials in Nuclear Power Systems – Water Reactors, S.M. Bruemmer, F.P. Ford, and G.S. Was, eds.,TMS, Warrendale, Pennsylvania, 1999, p. 567.

[xxii] M.O. Speidel and R. Magdowski, "Stress Corrosion Cracking of Stabilized Austenitic Stainless Steels in Various Types of Nuclear Power Plants," Proceedings of the Ninth International Conference on Environmental Degradation of Materials in Nuclear Power Systems – Water Reactors, S.M. Bruemmer, F.P. Ford, and G.S. Was, eds.,TMS, Warrendale, Pennsylvania, 1999, p. 567.

[xxiii] H.W. Pickering, F.H. Beck, and M.G. Fontana, "Wedging Action of Solid Corrosion Product During Stress Corrosion of Austenitic Stainless Steels," *Corrosion Vol. 18*, NACE, Houston, Texas, 1962, p. 230-239.

[xxiv] N.B. Pilling and R.E. Bedworth, "The Oxidation of Metals at High Temperatures," *Metals Vol. 29*, 1923, p. 529-582.

[xxv] D.P. Rochester, "Laboratory Investigation of Free-Span Axial Corrosion in Oconee Nuclear Station's Once Through Steam Generators," Water Chemistry of Nuclear Reactor Systems 8, British Nuclear Energy Society, London, 2000, p. 1.

[xxvi] D.P. Rochester and R.W. Eaker, "Laboratory Examination Results from Oconee Nuclear Station Once Through Steam Generator Tubes," Proceedings of the Ninth International Conference on Environmental Degradation of Materials in Nuclear Power Systems -Water Reactors, S.M. Bruemmer, F.P. Ford, and G.S. Was, eds. TMS, Warrendale, Pennsylvania, 1999, p. 639.

[xxvii] F.A. Garner, L.R. Greenwood, and D.L. Harrod, "Potential High Fluence Response of Pressure Vessel Internals Constructed from Austenitic Stainless Steels," Proceedings of the Sixth International Conference on Environmental Degradation of Materials in Nuclear Power Systems – Water Reactors, R.E. Gold and E.P. Simonen, eds., TMS, Warrendale, Pennsylvania, 1993.

[xxviii] S.M. Bruemmer, "New Issues Concerning Radiation-Induced Material Changes and Irradiation-Assisted Stress Corrosion Cracking in Ligh-Water Reactors," Proceedings of the Tenth International Conference on Environmental Degradation of Materials in Nuclear Power Systems – Water Reactors, P. Ford, G. Was, and L. Nelson, eds., NACE, Houston, Texas, 2002.

[xxix] J. Daret, T. Cassagne, Y. Lefevre, and T.Q. Tran, "Evidence for the Reduction of Sulfates under Representative SG Secondary Side Conditions, and for the Role of Reduced Sulfates on Alloy 600 Tubing Degradation," Proceedings of the Ninth International Conference on Environmental Degradation of Materials in Nuclear Power Systems – Water Reactors, S.M. Bruemmer, F.P. Ford, and G.S. Was, eds., TMS, Warrendale, Pennsylvania, 1999, p. 567.

[xxx] T. Sakai, S. Okabayashi, K. Aoki, K. Matsumoto, F. Nakayasu, and Y. Kishi, "Effect of Reduced Sulfur on High Temperature Aqueous Corrosion for Alloy 600," Proceedings of the Fourth International Symposium on Environmental Degradation of Materials in Nuclear Power Systems - Water Reactors, D. Cubicciotti, ed., NACE, Houston, 1990, p. 12/37.

[xxxi] B. Sala, P. Combrade, R. Erre, R. Benoit, and M. Le Calvar, "Chemistry of Sulfur in High Temperature Water Reduction of Sulfates," Proceedings of the Fifth International Symposium on Environmental Degradation of Materials in Nuclear Power Systems - Water Reactors, D. Cubicciotti, chair., American Nuclear Society, Chicago, 1992, p. 39.

[xxxii] W.E. Allmon, P.L. Daniel, and S.J. Potterton, "Conditions for the Chemical Reduction of Sulfates in an Aqueous Environment," Proceedings: Workshop on the Role of Sulfur Species on the Secondary-Side Degradation of Alloy 600 and Related Alloys; NP-6710-SD, U.E. Gustafsson, ed., EPRI, Palo Alto, 1990, p. 10/1.

[xxxiii] O. de Bouvier, E.-M. Pavageau, F. Vaillant, and D. Vermeeren, "Influence of High Reducing Conditions on IGA/SCC of Alloy 600 in Neutral Sulfate Environments," from the 11th International Conference on Environmental Degradation of Materials in Nuclear Power Systems – Water Reactors; August 1-14, Stevenson, Washington, 2003.

[xxxiv] W.H. Cullen, "Review of IGA, IGSCC and Wastage of Alloys 600 and 690 in High Temperature Acidified Solutions," Control of Corrosion on the Secondary Side of Steam Generators, R.W. Staehle, J.A. Gorman, and A.R. McIlree, eds. NACE, Houston, 1996, p. 273.

[xxxv] D. Choi and G.S. Was, "Pit Growth in Alloy 600/690 Steam Generator Tubes in Simulated Concentrated Environments (Cu^{2+}, Cl^- and SO_4^{2-})," *Corrosion Vol. 46*, 1990, p. 100.

[xxxvi] R.W. Staehle, "Occurrence of Modes and Submodes of SCC," Control of Corrosion on the Secondary Side of Steam Generators, R.W. Staehle, J.A. Gorman, and A.R. McIlree, eds., NACE, Houston, 1996, p. 135.

[xxxvii] R.W. Staehle, "Bases for Predicting the Earliest Penetrations Due to SCC for Alloy 600 on the Secondary Side of PWR Steam Generators," NUREG-CR-6737, U.S. Nuclear Regulatory Commission, Washington, 2001.

[xxxviii] F.N. Goswami and R.W. Staehle, "Growth Kinetics of Passive Films on Fe, Fe-Ni, Fe-Cr, Fe-Cr-Ni Alloys, *Electrochimica Acta 16*, 1971, pp. 1895-1907.

[xxxix] R.M. Latanision and R.W. Staehle, "Plastic Deformation of Electrochemically Polarized Nickel Single Crystals," *Acta Metallurgica 17*, March, 1969, pp. 307-319.

[xl] E.N. Pugh, J.V. Craig, and A.J. Sedriks, "The Stress-Corrosion Cracking of Copper, Silver, and Gold Alloys," in *Proceedings of Conference Fundamental Aspects of Stress Corrosion Cracking*, September 11-15, 1967, NACE-1, Houston: National Association of Corrosion Engineers, 1969, p. 118.

[xli] R.W. Staehle, "Stress Corrosion Cracking of the Fe-Cr-Ni Alloy System," NATO Science Committee Research Evaluation Conference, from The Theory of Stress Corrosion Cracking in Alloys, edited by J.C. Scully, 1971.

[xlii] J.B. Lumsden and P.J. Stocker, "Inhibition of IGA in Nickel Base Alloys in Caustic Solutions," *Corrosion '88*, Paper 252, NACE, Houston, Texas, March 21-25, 1988.

[xliii] A.J. Forty and P. Humble, *Phil.Mag.,* 8, 247 (1963).

[xliv] J.H. Payer and R.W. Staehle, "Dissolution Behavior of Carbides in Aqueous Environments," Localized Corrosion, NACE-3, Eds. R.W. Staehle, B.F. Brown, J. Kurger and A. Agrawal, NACE, Houston, Texas, 1974, conference held at Williamsburg, Virginia, December 6-10, 1971, NACE, Houston, 1974, pp. 482-501.

[xlv] T. Smith, "Relationship of Defect Structure to the Corrosion Behavior of Some Austenitic Stainless Steels," M.S. Thesis, The Ohio State University, 1965.

[xlvi] J.A. Davis, "Local Dissolution Phenomena Occurring on Iron-Chromium-Nickel Alloys: An Electron Microscopic Study," Ph.D. Dissertation, The Ohio State University, 1968.

[xlvii] M. Long, "The Polarization Behavior of Iron-Nickel-Chromium Alloys in Caustic Solutions," M.S. Thesis, The Ohio State University, 1973.

[xlviii] H.E. Chaung, Z. Szklarska-Smialowska, and R.W. Staehle, "The Effects of Heat Treatment on Surface Segregation in Inconel 600," *Scripta Metallurgica Vol. 13,* 1979.

[xlix] H.E. Chaung, J.B. Lumsden and R.W. Staehle, "Effect of Segregated Sulfur on the Stress Corrosion Susceptibility of Nickel," *Metallurgical Transactions 10A*, 1979.

[l] R.W. Staehle and Z. Fang, "SCC of Alloys 600 and 690 in the Mid-Range of pH," presented at the International Symposium Fontevraud IV, *Contribution of Materials Investigation to the Resolution of Problems Encountered in Pressurized Water Reactors,* held September 14-18, 1998.

[li] R.N. Parkins, F. Mazza, J.J. Royuela, and J.C. Scully, "Stress Corrosion Test Methods," *British Corrosion Journal, Vol. 7*, 1972, p. 154.

[lii] R.W. Staehle, "Development and Application of Corrosion Mode Diagrams," Parkins Symposium on Stress Corrosion Cracking, Eds. S.M. Bruemmer, E.I. Meletis, R.H. Jones, W.W. Gerberich, F.P. Ford, and R.W. Staehle, conference held in Cincinnati, Ohio, October 21-24, 1991, TMS (The Minerals, Metals and Materials Society), Warrendale, Pennsylvania, 1992. pp. 447-491.

[liii] J.M. Sutcliffe, R.R. Fessler, W.K. Boyd, and R.N. Parkins, "Stress Corrosion Cracking of Carbon Steel in Carbonate Solutions," *Corrosion, Vol. 28*, 1978, p. 313.

[liv] V.K. Singh, "Stress Corrosion Cracking of Low-Carbon and Low-Alloy Steels," *Steel India, Vol. 11*, 1988, p. 53.

[lv] K. Bohnenkamp, "Caustic Cracking of Mild Steel," Fundamental Aspects of Stress Corrosion Cracking: NACE-1, R.W. Staehle, A.J. Forty, and D. van Rooyen, eds., NACE, Houston, Texas, 1969, p. 374.

[lvi] N.J.H. Holroyd, "Environmental Aspects of Stress Corrosion Cracking of Ferritic Steels," Ph.D. Thesis, University of Newcastle-upon-Tyne, 1977.

[lvii] C.R. Morin, "Potential Dependent Stress Corrosion Cracking of Type 304-L Stainless Steel in H_2SO_4 + KCl at 25°C," Thesis presented in partial fulfillment of the requirement for degree of Master of Science, The Ohio State University, 1972.

B. 16 Microbiologically Influenced Corrosion (MIC)

Introduction

The objective of this topical discussion is to describe the subject of Microbiologically Influenced Corrosion (MIC) as applied to LWRs.

"Microbiologically Influenced Corrosion (MIC)" refers to corrosion that results from the presence and activities of microorganisms. MIC can result from microbial processes that produce corrosive environments such as organic acids or lower valence sulfur. The modes of corrosion, which can result from microbiologically produced local environments, include general corrosion (GC), pitting (PIT), crevice corrosion, de-alloying, galvanic corrosion, intergranular corrosion (IGC), stress corrosion cracking (SCC), and corrosion fatigue (CF).

Generally, the environments produced in the process of MIC are of three types:

- Formation of colonies, which are sometimes of substantial size, within which additional transformations beyond the initial metabolic processes can occur. Such colonies also have some of the features of "crevices" with the additional feature of dynamic changes of internal chemistry.
- Reactions between microorganisms and nutrients, e.g. nitrite oxidized to nitrate, or sulfuric acid/reduced sulfate compounds generated by sulfate-reducing bacteria, with a change in the corrosion modes thereby enabled.
- Corrosion directly on metal surfaces.

The term "microorganisms" includes bacteria and fungi. Both produce metabolic products that are acidic, as well as other byproducts. The range of temperatures for vitality or growth and metabolic activity of the two are different, with the latter having a lower temperature tolerance limit than bacteria. Bacteria and fungi also differ with respect to the ranges of optimal growth in the sense that fungi and bacteria can survive different ranges and sets of unfavorable conditions. The intensity of MIC and the associated products of the microorganisms depend mainly on the following influences:

- Temperature, with there being a narrow optimum temperature for growth of each species of organisms.
- Water is necessary to the metabolic processes of all microorganisms. Bacteria require liquid (e.g. a thin surface film of liquid on which a biofilm can grow) for growth, but fungi can grow at relative humidity of 60% or higher.
- Oxygen is the electron acceptor for aerobic organisms, but anaerobes can use a variety of other terminal electron acceptors, e.g., SO_4^{2-}, NO3, Fe(III), Mn(IV), Cr(VI).

- Nutrients including carbon, sulfur, phosphorous, nitrogen, are required. Such nutrients must include the capacity for electron exchange involving oxidation and reduction reactions. In some cases where nutrient availability is limited, secondary metabolic byproducts may be involved in the overall microbiological process and sustain the corrosion.

- Flowing, especially slowly flowing, environments tend to favor the growth of microbes by providing a ready supply of nutrients (in particular, periodically flushed systems). Stagnant areas adjacent to flowing areas are particularly susceptible to MIC (e.g, dead legs in piping).

- Microorganisms can grow in natural and processed waters including marine, potable, distilled, and fresh.

- Some species, e.g. boric acid, are toxic to microbes in high concentrations.

General Features of Microorganisms Relative to MIC

The following general properties concerning microorganisms as applied to nuclear applications are taken from Pope:[1]

- Individual microorganisms are small (from less than two-tenths to several hundred micrometers (µm) in length by up to two or three µm in width) a quality which allows them to penetrate crevices, etc., easily. Bacterial and fungal colonies can grow to macroscopic proportions.

- Bacteria may be motile, capable of migrating to more favorable conditions or away from less favorable conditions, e.g., toward food sources or away from toxic materials.

- Bacteria have specific receptors for certain chemicals, which allow them to seek out higher concentrations of those substances, which may represent food sources. Nutrients, especially organic nutrients, are generally in short supply in most aquatic environments; but surfaces, including metals, adsorb these materials, creating areas of relative plenty. Organisms able to find and establish themselves at these sites will have a distinct advantage in such environments.

- Microorganisms can withstand a wide range of temperatures (at least -10 to 99°C), pH (about 0 - 10.5) and oxygen concentrations (0 to almost 100% atmospheres).

- Microorganisms grow in colonies, which help to cross-feed individuals and makes survival more likely under adverse conditions.

- Microorganisms can reproduce very quickly if field conditions are particularly favorable

- Individual cells can be widely and quickly dispersed by wind and water, animals, aircraft, etc., and thus the potential for some of the cells in the population to reach more favorable environments is good.

- Many can quickly adapt to use a wide variety of different nutrient sources. For example, *Pseudomonas fluorescens* can use well over 100 different compounds as sole sources of carbon and energy including sugars, lipids, alcohols, phenols, organic acids, etc.

- Many form extracellular polysaccharide materials (capsules or slime layers). The resulting slimes are sticky and trap organisms and debris (food), resist the penetration of some toxicants (e.g., biocides) or other materials (corrosion inhibitors) and hold the cells between the source of the nutrients (the bulk fluid) and the surface toward which these materials are diffusing.

- Many bacteria and fungi produce spores, which are very resistant to temperature (some even resist boiling for over 1 hour), acids, alcohols, disinfectants, drying, freezing, and many other adverse conditions. Spores may remain viable for hundreds of years and germinate on finding favorable conditions. In the natural environment, there is a difference between survival and growth. Microorganisms can withstand long periods of starvation and desiccation. If conditions are alternating wet and dry, microorganisms may survive dry periods but will grow only during the wet periods.

- Microorganisms are resistant to many chemicals (antibiotics, disinfectants, etc.) by virtue of their ability to degrade them or by being impenetrable to them (due to slime, cell wall or cell membrane characteristics). Resistance may be easily acquired by mutation or acquisition of a plasmid (essentially by naturally-occurring genetic exchange between cells, i.e., genetic engineering in the wild).

Applications to LWRs

MIC occurs in light water plants in two general locations. One is on outside surfaces where there are moisture and the other requirements, **animal droppings**, of microorganism growth. The second occurs inside in low temperatures components mainly where water is flowing slowly or periodically flushed; both situations provide a good supply of nutrients. Truly stagnant systems with no replenishment of nutrients (e.g. not exposed to air) are not favorable for significant MIC activity. Chemicals that are common in LWR waters can affect the growth of microorganisms. MIC has been found in a wide range of systems, from fire protection and service water systems to ECC storage systems and spent fuel pools.

1. Temperature and pH

Hyperthermophiles can grow up to a temperature of 110C. Bacteria can grow over the pH range from 0 to about 10.5, in effect the entire spectrum of pH found in LWR systems.

2. Boric acid

The acute boron toxicity level for bacteria is between 8-340 mg/l. Bacteria have a low sensitivity to boron. Metabolism of boric acid is thermodynamically unfavorable. There are no known bio-transformations of borate.

3. Hydrazine

Hydrazine sulfate at 1mM is an inhibitor for bacterial utilization of amino acids. However, some growth was observed. Hydrazine can be metabolized to nitrogen gas by some nitrifying bacteria or reduced to ammonia by nitrogenase isolated from a nitrogen-fixing bacterium. Only concentrations below 1 mg/liter were completely degraded. Higher concentrations were inhibitory. The acute toxicity of hydrazine in water was 0.019 mg/liter at 20C for *Pseudomonas putida*. Hydrazine is genotoxic in bacteria, and yeast. Reference: International Programme on Chemical Safety website

In summary, some bacterial growth has been observed in dilute aqueous solutions of hydrazine.

Acknowledgements

RLT and RWS acknowledge the contributions and assistance of Dr. Brenda Little of Stennis Space Center and Dr. Peter Angel of AECL.

References

[1] D. Pope, "A Study of Microbiologically Influenced Corrosion in Nuclear Power Plants and a Practical Guide for Countermeasures," Electric Power Research Institute Report NP-4582, May 1986.

[2] In Vitro Determination of Ruminal Protein Degradation Using Freeze-Stored Ruminal Microorganisms ND Luchini, GA Broderick and DK Combs J Animal Science 1996 74:2488-249

B. 17 Flow-Accelerated Corrosion

Background

Flow-accelerated corrosion (FAC, sometimes termed flow-assisted corrosion) is a degradation mechanism affecting metallic materials that do not form tightly adherent passive surface films when the materials are exposed to fluid flow environments in power reactor systems, and thermal power plants. In reactor coolant/heat transfer systems where materials are exposed to flowing water this degradation mechanism typically affects only carbon steels and copper alloys. Sometimes the FAC is results in sufficient wall loss that catastrophic piping failure occurs (Figure B.17.1), although more frequently leakage is the consequence, without rupture. It is important to note the distinction between FAC and erosion corrosion (EC). FAC is an electrochemical corrosion process dependent on pH, temperature, electrochemical potential and fluid mass transfer (velocity and turbulence). FAC is a flow-accelerated increase in the corrosion rate of a material; the increase in corrosion rate, which can be very large, can be simplistically thought of as a flow-induced increase in mass transfer of dissolving and reacting (corrosive) species at a high flow or highly turbulent location. Under low flow conditions, the corrosion rate of carbon steel is an electrochemically-coupled reaction and is a function of the rate of dissolution of the substrate (Fe for carbon steels) and the oxide formed by reaction of some of the dissolved iron with water and water-borne oxidants, and the rate of formation of a surface oxide. Under FAC conditions the rate of Fe/ iron oxide dissolution exceeds the rate of formation of the oxide that would be expected under low flow conditions. This coupled oxidation/dissolution reaction is best described as an electrochemical process, determined by the concentration of electrochemically active species at the metal-fluid interface, in particular those controlling the pH and oxidants.

Erosion corrosion is properly described as the abrasive or cavitation-induced (mechanical) removal of surface material. The abrasive material is typically entrained in a fluid flow, for instance sand entrainment in water intake flows, and both FAC and EC may occur simultaneously, depending on the flow conditions. Typically, power plant cooling and heat transfer systems do not contain abrasive materials in quantities sufficient to cause EC. Under very high flow conditions, best described as water jetting or steam jetting, the abrasive wear or cutting of the material can take place without abrasive materials being present. Typical examples are steam cutting/wear in condenser inlets and the use of high pressure (typically 5000 to 10 000 psi) water lances to cut concrete. It should be noted that the term “erosion-corrosion” has been frequently used as a synonym for FAC, which can be confusing and is incorrect.

Factors Influencing Material Susceptibility

There are several factors affecting susceptibility to FAC:

- pH
- Temperature
- Water chemistry
- Material properties (alloy content)
- Mass transfer (flow, turbulence, steam quality)

For carbon steels, the pH should be controlled in the range 7 to 10, preferably between 9 and 10 (room temperature pH) to minimize corrosion in water. For copper alloys the pH should be between 7 and 9; thus in mixed metal systems pH control is a compromise between corrosion of carbon steels and copper alloys, and pH is typically in the range 8.8 to 9.4. Most nuclear plants have now switched to all-ferrous piping systems, primarily to protect steam generators from degradation, and thus there is little concern for corrosion of copper alloys. In all-ferrous systems the pH is typically maintained >9.4, often as high as 9.8 to 10.0. Note that in two-phase systems, such as in steam generators, it is the liquid phase pH that is important, and pH control agents should be chosen such that preferential partitioning to the steam phase does not occur, or does not lower the liquid phase pH below an acceptable level. So-called "alternative amines" have been used to ensure that such partitioning is limited and thus the high temperature pH of the liquid phase remains in an acceptable range.

Water temperature significantly affects FAC, with the maximum FAC rates occurring, all else being equal, at about 130°C in single-phase flow, and at about 180°C in two-phase flow. Thus the feedwater systems are at significant risk of FAC, and these systems are typically inspected on a routine basis to ensure that wall thinning is monitored. FAC in these systems can result in wall loss rates of >10 mm/year in unfavourable situations, and in a few cases has resulted in deaths as a consequence of pipe rupture when the wall thickness decreased sufficiently that mechanical failure occurred. Typically FAC rates decrease at temperatures on either side of the peak temperature, all other factors being equal, but given that FAC is often very localized because of mass transfer effects, the rate may still be sufficient to result in wall thinning and piping failure in thin-walled pipes.

Water chemistry is an important variable for FAC. The conditions leading to increased FAC rates are reducing chemistry (low electrochemical potential) and low dissolved iron concentrations in the water. Steam generators are an example of how FAC can occur under the highly reducing conditions that are typically used to protect the SG tube bundle. In several instances (Bruce NGS and Gravelines, for example) carbon steel support plates have disintegrated as a consequence of FAC, where it was concluded that a significant factor was the use of high hydrazine concentrations (>100 to 200 ppb). The sensitivity of FAC to low dissolved iron concentrations is a consequence of the dependence of FAC on the solubility of iron, and to the local potential. In fundamental terms this dependence relates to the liquid layer at the steel surface, which becomes more difficult to measure and predict in two-phase flows. In feedwater systems this iron solubility dependence is most obvious in systems such as the moisture separator reheater drain lines, where steam has been condensed and relatively iron-free water is flowing. Many cases of FAC have occurred in such lines. Note also the use of alternative amines to ensure appropriate high temperature pH in two-phase flows (see Secondary Water Chemistry Topical Report) also mitigates these effects of iron concentration and potential on FAC.

Material properties have a significant impact on FAC rates, and typically the plant operator has no control over this unless replacement of piping is an option. The most important alloy variable affecting FAC is chromium (Cr) content of the alloy. Although copper and molybdenum content have also been suggested to have beneficial effects, the effects are typically small and not clearly related to plant experience. It is generally regarded that in single phase piping subject to FAC, a

Cr content >0.1 wt.% is recommended. Plant and laboratory data suggest that Cr contents below about 0.04 wt.% are insufficient to provide any useful protection against FAC, and concentrations above 0.05 to 0.08 wt.% are necessary to show significant improvement. Many experts now recommend a Cr content >0.2 wt.% to provide optimal resistance. The beneficial effect of Cr on FAC is thought to be related to the formation of a Cr-rich oxide at the oxide-metal interface, and that this oxide confers resistance to FAC. In two-phase flows, which are typically very much higher velocity than single phase flows, it is probably expedient to use Cr-Mo steels or, preferably, stainless steels. Many feedwater system components are now fabricated from these materials to minimize FAC degradation.

Mass transfer effects relate to areas where locally high turbulence is created, usually by geometric factors. Elbows, bends, orifices, valves, etc., all cause local turbulence which significantly increases FAC rates in or immediately downstream of the component. This turbulence increases the FAC rate by increasing the transport of dissolving iron away from the surface and, by increasing mechanical stresses on the oxides formed at the site of the corrosion, which can be significant under very high velocities.

Typical Occurrences of FAC in Power Plants

Most of the FAC degradation in power plants has occurred in feedwater, extraction steam, and drains systems. However, there have been observations of FAC in steam generators and in primary side piping in CANDU power plants. In these systems, FAC has been found in most parts of the system, and is often associated with areas of high mass transfer, such as downstream of welds and valves, reducers, orifices, and in elbows and tees. The SG FAC has been typically found in two-phase flow areas, including upper support plates, steam separators and blowdown piping. In the CANDU heat transport system (310°C, velocity 15 to 18 m/s), the FAC has occurred at bends in carbon steel outlet feeder piping. The FAC rates there are much lower than in the feedwater and SG systems, but still can impact the integrity of the thin-wall feeder piping.

In condensers, steam impact erosion has occurred on the outer tube bundle where the steam inlets are located, a FAC-related degradation phenomenon similar to that found in turbines, and has been resolved using stainless steels in this area and changes to the flow. On the water side of condensers made with copper alloy tubing, in particular Admiralty Brass, significant FAC and erosion occurs, usually resulting in tube leakage and the need to replace the condensers after about 15 years or so.

Inspection and Remediation Strategies

The most effective inspection strategy for FAC of feedwater systems is to employ EPRI's CHECWORKS code to predict locations most susceptible to FAC. Without use of this code, or its equivalent, it is difficult to predict and prioritize the many locations that could suffer FAC. Usually the Cr content of the steel is unknown, so it is not possible to restrict inspections to only one train of a given system, regarding it as a "lead" train. It is generally known that all high mass transfer areas are susceptible to FAC, but some may degrade at much slower rates than others, depending on hydraulic and chemistry conditions, –and thus an inspection prioritization plan is needed. Note that the recent Mihama-3 pipe failure (see Figure B.17.1), caused by FAC, was in a line predicted by CHECWORKS to be at risk, but never inspected.

For steam generators, visual inspection for internal secondary side carbon steel components is usually necessary; this inspection, based on in-service experience so far, can be limited to upper support plates and separators.

The most effective remediation strategies are to replace all degraded material with stainless steel, or with Cr-Mo material if the post-weld heat treatment requirements are feasible. Typically as feedwater system carbon steel components have failed, replacements have been with FAC-resistant material. For new systems, analysis of the system can identify locations at risk of FAC and these are fabricated from austenitic stainless steels (Qinshan CANDU plants, for example). Some plants have essentially all-stainless steel feedwater systems (KWU Konvoi plants, for example). All new SGs have stainless steel support plates and other internals susceptible to FAC. For condensers, most plants have now replaced any copper-alloy condensers with Ti-tubed units (seawater cooling), with appropriate baffles to prevent inlet steam erosion of the outer row Ti tubing, or with stainless steel units (seawater and freshwater cooling).

Remediation by chemistry modification has limited application given that most plants now employ an effective feedwater chemistry control designed to minimize FAC and other degradation mechanisms. For SGs with carbon steel secondary side internals, reducing hydrazine to <100 ppb is recommended.

Life Management Issues

Current industrial practice is to routinely inspect for FAC-induced wall thinning, usually using a predictive tool such as CHECWORKS in order to minimize the number of critical locations, as well as to generate a database of at-risk locations, the inspection history, and the wall thinning rate. Where piping failures occur, replacement of a failed component should be with a more-resistant material. It is cost-effective to reduce inspection by replacing carbon steel with stainless steel in at-risk areas. Chemistry control should be monitored to ensure that it is compatible with reduced FAC risk; operation of feedwater systems at very low dissolved oxygen (<5 ppb), for instance, can place the system at increased risk compared to slightly higher oxygen (5 to 10 ppb).

Figure B.17.1 Failed steam line at Mihama-3.

References

[1] B. Chexal et al, "Flow-Accelerated Corrosion in Power Plants", EPRI Report TR-06611-R1, 2001

[2] "Erosion/Corrosion in Nuclear Plant Steam Piping: Causes and Inspection Program Guidelines", EPRI Report NP-3944, 1985

[3] I.S.Woolsey, "Erosion-Corrosion in PWR Secondary Circuits", CEGB Report TPRD/L/3114/R67, 1987

B.18 Topical Report on Boric Acid Corrosion (BAC)

Understanding of BAC prior to the 2002 Davis Besse Incident

Corrosion of carbon and low-alloy steel (C&LAS) components by leaking borated water has posed significant maintenance problems for many PWR plants[1]. Two incidents illustrate the potential importance of this problem. In 1980, leakage from the gaskets of two reactor coolant pumps at one plant resulted in severe corrosion to seven coolant pump flange studs. The diameter of the worst-case stud was reduced from its original 3.5 inches (89 mm) to 1.0-1.5 inches (25-38 mm). This represents a reduction to less than 20% of the original stud cross-sectional area. In 1986, leakage from a valve body-to-bonnet gasket at another plant resulted in corrosion that extended two-thirds of the way through the wall thickness of a low-alloy steel nozzle in the main coolant piping system.

Subsequent to these and other significant events, the NRC issued Generic Letter 88-05 [1], requiring operators of PWR-type power plants to develop and implement a plan to ensure that there is an extremely low probability of abnormal leakage, rapidly propagating failure, or gross rupture as a result of boric acid corrosion (BAC) of primary coolant loop components.

EPRI efforts to provide assistance to utilities in addressing the requirements of NRC GL 88-05 and BAC issues in general have centered around the *Boric Acid Corrosion Guidebook*, originally published in 1995 and updated in 2001 [2], which summarized the extent of the BAC problem as recognized at the respective times, as well as compiling and assessing data from previously performed BAC test programs.

Background

Borated water is used in the primary systems of PWR plants to control reactivity during normal plant operation and refueling and under potential accident conditions. This is accomplished by adding boric acid to the primary side water. In some cases, boric acid is also injected into the secondary side of PWR plants at low concentrations to reduce the potential for corrosion of Alloy 600 steam generator tubing at crevice locations.

In general, there is little concern with general corrosion inside the primary and secondary systems since the concentrations of boric acid and oxygen in these systems are low, and corrosion rates are typically less than 0.001 inches per year (in/yr) (0.025 mm/yr). Although C&LAS are not normally exposed directly to PWR primary water, the use of high-alloy materials in contact with the coolant is for reasons of chemistry (including radiation protection) and cleanliness, rather than the avoidance of C&LAS corrosion. In fact, LAS is sometimes exposed as a result of a "half-nozzle" repair to component penetrations and this has been deemed acceptable by the U.S. regulator from a corrosion standpoint [3].

Exceptions to this generally good experience for materials in intended direct contact with PWR operating media include 1) stress corrosion cracking of some stainless steel pipes containing stagnant, high-concentration boric acid solutions, 2) cracking of stainless steel cladding in some components that leads to galvanically driven stress corrosion cracking (SCC) of the low-alloy steel base materials, and 3) primary water stress corrosion cracking of Alloy 600 nozzle penetrations and welds (considered in a separate topical report).

If borated water leaks from primary and secondary systems through gasketed joints, valve packing, mechanical seals, etc., significant corrosion problems can develop. Specifically, the water can become oxygenated and the boric acid can concentrate as the water boils off or evaporates. These factors can increase the corrosion rate of exposed carbon steel to several inches per year.

The reported plant incidents prior to 2002 ranged in severity from minor corrosion of parts, which can be accepted without evaluation or repair, to major incidents involving plant shutdowns and significant loss of material on major components (see Fig. B.18.1).

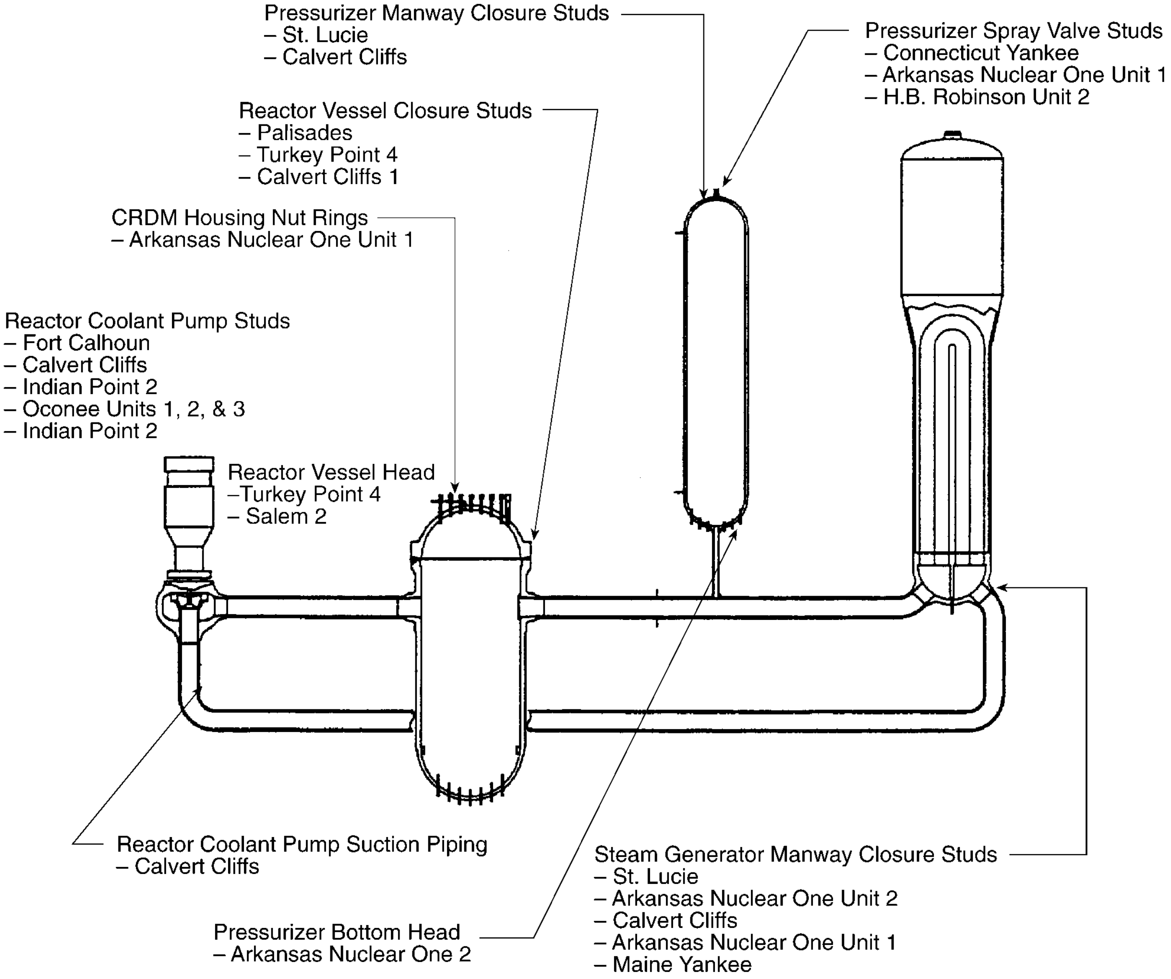

Figure B.18.1 Locations of boric acid corrosion experienced in primary loop [2]

Reference 1 required that utilities develop and implement programs to identify leaks and take corrective action to prevent recurrence. All plants have developed programs that respond to this generic letter. Fig. B.18.2 gives some information on the identified sources of leakage.

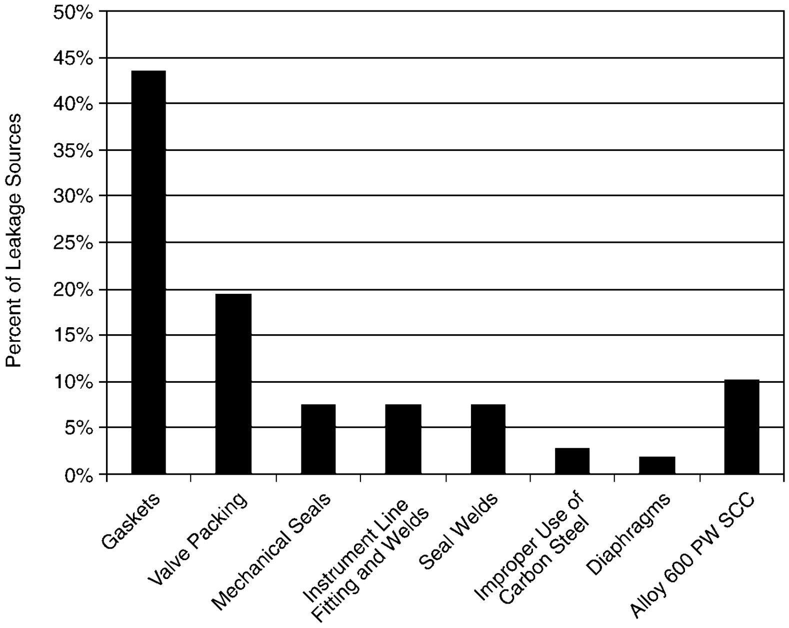

Figure B.18.2 Distribution of reported leakage incidents (US prior to 2002) by source [2]

Main type of boric acid corrosion observed

Overall, the mode of corrosion of greatest concern due to leakage of borated water is uniform corrosion, often referred to by plant engineers as "wastage", of C&LAS. Boric acid in water can result in an aggressive environment that uniformly attacks the surface of the metal. Although boric acid is considered a "weak" acid when compared to acids such as hydrochloric or nitric acid, boric acid in water will still increase the concentration of hydrogen ions (H) and lead to a drop in pH. In reality, the process of surface attack is further accelerated by what amounts to miniature galvanic cells, whereby small areas of the metal surface behave cathodically or anodically due to slight changes in the alloy composition (for example, higher chromium or nickel in steel), surface imperfections or defects, or surface strain. In addition, the corrosion product itself may be cathodic to the surrounding base metal. The anodic/cathodic areas on the metal surface can shift with time, resulting in an essentially uniform rate of attack over the entire metal surface. One of the reasons that the rate of attack of the unprotected, exposed steel can be so great is that the exposed area of the cathodic surfaces often exceeds that of the anodic material.

Surfaces which are corroded generally often exhibit some increase in texture as a result of small differences in the rate at which different areas of the surface are attacked. It is sometimes difficult to detect general corrosion of a surface because there is no clear reference point for assessing the amount of material loss, particularly if the rust is continually solubilized by, or entrained into, the fluid stream.

General corrosion is usually the easiest form of corrosion to predict using experimental data. However, as with all modes of corrosion, the rate can be affected significantly by factors that were not included in the experiments used as the basis for the predictions. Some of these factors are discussed in the following paragraphs.

Effect of Impurities on General Corrosion

When impurities are present in the metal, they may act as the source of local anodes/cathodes and thus accelerate corrosion. If impurities are present in the corrosive medium, they can have a variety of effects on the corrosion rate. Impurities may act to increase the conductivity of the aqueous solution, thereby often increasing corrosion rates, and can also cause increased corrosion rates by affecting or destroying the protective layer of hematite (rust) or other metal oxide that builds up on the exposed surface of the metal, helping to protect it from further damage. In other cases, impurities in the fluid stream can actually help retard corrosion by acting as inhibitors. In any event, the effect of impurities is generally complex and non-linear and must be determined through experiments designed to simulate the actual metal/environment combination.

Effects of Oxygen and pH on General corrosion

The corrosion of most steels which are soluble in acids depends on pH similar to the pattern shown in Figure B.18.3. In the middle pH range of 4 to 10, the corrosion rate is generally controlled by the rate of diffusion of oxygen to the surface and the insolubility of oxides in oxidizing systems, which increases with increasing electrochemical potential. At lower pH, the uniform corrosion rate increases owing to the progressive increase of oxide solubility in acidic solutions and the increased availability of hydrogen ions for reduction in the cathodic areas. At intermediate pH values, both the rate itself, and the extent to which corrosion becomes non-uniform, are still affected by the concentration of dissolved oxygen (the other main cathodic reactant).

Effect of Temperature on Wastage

In most cases of corrosion in acids, corrosion rates increase with increasing temperature and high enough temperatures also boil the water away, leaving more concentrated acid and thus even higher corrosion rates. However the concentration of dissolved oxygen in the water decreases with increasing temperature, so that the situation is more complex with a weak acid such as that resulting from leakage of primary water. Furthermore, as the temperature continues to increase, the water may be boiled off completely, leaving dry boric acid crystals that are not very corrosive at all.

Effect of Flow Velocity on Wastage

In many of the field reports, general corrosion is accelerated by the impingement of borated water, or steam with boric acid carryover, onto hot metal surfaces. This impingement has the dual effect of removing protective corrosion films from the surface of the metal and replenishing the corrodent with fresh, oxygenated acid. Both of these factors can markedly increase the corrosion rate.

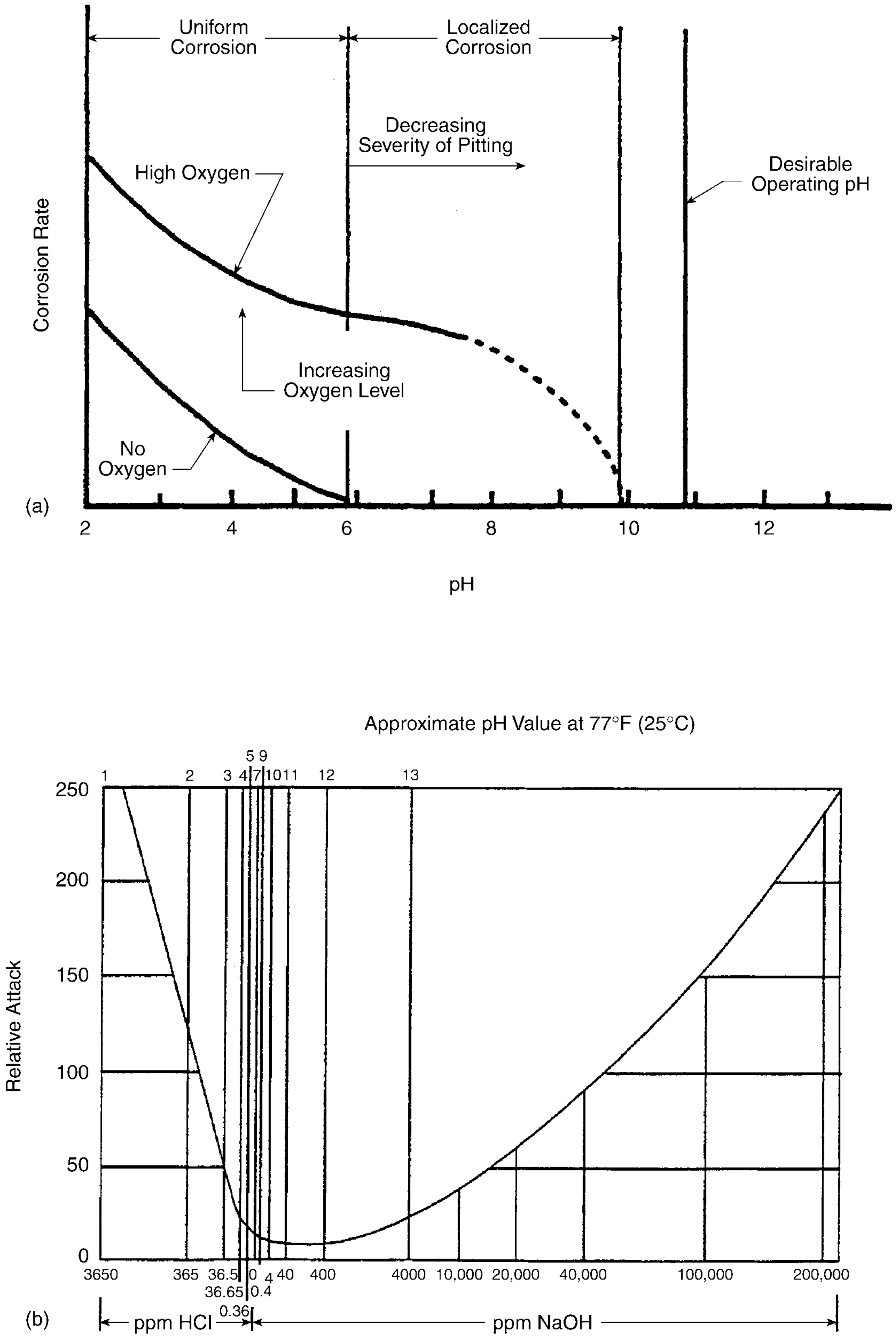

Figure B.18.3 Summary of oxygen and pH effects on general corrosion of iron [4]

Secondary Types of Boric Acid Corrosion

In addition to general corrosion (the predominant type of boric acid corrosion), there have been isolated reports of other types of corrosion, such as galvanic corrosion, crevice corrosion, pitting, intergranular attack, and stress corrosion cracking.

Galvanic Corrosion

A practical example of such a condition in an aerated, borated water environment in a PWR plant would be a weld between a low-alloy steel pipe and a stainless steel pipe. The stainless steel is the more noble material, and the low-alloy steel is the more active material. Field experience and laboratory test results both indicate that a galvanic couple between carbon steel and stainless steel can accelerate the local corrosion rate in the carbon steel, typically by about 1.5 times. Therefore, the galvanic effect for BAC can be significant, but is not usually overwhelming and will depend upon pH, boric acid concentration and dissolved oxygen level. It is not expected to be a major factor in deaerated primary water of nominal composition. [3]

Crevice Corrosion

Environmental conditions in a crevice can be significantly different than on adjacent bare metal surfaces. Under many conditions, the environment in the crevice can be more aggressive than outside the crevice, and accelerated local corrosion can take place. Typical crevice locations on the outside surfaces of PWR pressure boundary parts include bolts, washers, and gaskets. Crevice corrosion has not generally been reported to be a significant practical problem in borated water environments on the outside surfaces of PWR components. However, this may not always be the case if the part or component includes crevices.

Both galvanic and crevice effects can become significant in the case of C&LAS exposed to boric acid via a crack or other such defect in a stainless steel or nickel base cladding.

Pitting

Pitting has not generally been reported to be a significant problem in borated water environments on the outside surfaces of PWR components, probably because the conditions under which it might be expected (see Fig. B.18.3) involve higher pH values than would normally be expected for BAC and because boric acid is a buffer that does not support local acidification within an incipient pit.

Intergranular Corrosion

Intergranular corrosion is localized attack along the grain boundaries of a metal or alloy and is most common with stainless steels or nickel-base alloys that are generally resistant to BAC. There are no reports of intergranular corrosion being a significant contributing factor to problems associated with C&LAS corrosion due to leakage of borated water.

Stress Corrosion Cracking

Stress corrosion cracking in the presence of borated water leakage has been reported to be a problem only in the case of highly loaded steam generator manway studs that have been coated with lubricants containing sulfur and is not thought to be associated with boric acid itself. The most celebrated case occurred at Maine Yankee where 6 of 16 studs were found to have failed after disassembly, and 5 more were found to be cracked. The stress corrosion cracking in this case was attributed to interaction between the leaking borated water, leak sealant, and sulfur-containing thread lubricant. This experience identified the need to minimize the use of sulfur-containing compounds around pressure boundary parts.

Summary of Corrosion Rates for Various Situations

Figure B.18.4 summarizes the results for all of the corrosion tests reported in reference 2 and points out the main areas of interest. Briefly summarizing the key points:

Corrosion rates for immersion in deaerated, dilute boric acid solutions are usually quite low regardless of temperature. Moderate corrosion rates, between 0.02 and 0.05 in/yr (0.5 and 1.3 mm/yr), have typically been measured[a] during immersion in deaerated, concentrated boric acid solutions.

For cases involving immersion in aerated borated water, corrosion rates are in the range of 0.001–0.01 in/yr (0.025–0.25 mm/yr) for low concentrations at room temperature and increase to a maximum of 1–10 in/yr (25–254 mm/yr) for high concentrations at 200–220°F (93–104°C).

The main problem regarding borated water dripping on hot metal surfaces is that the solution can concentrate as the water boils off and the boiling can lower the local metal temperature to the boiling point (212–230°F [100–110°C]) of the concentrated boric acid solution, thus avoiding dry-out. Therefore, the typical situation is to have concentrated boric acid at around 212–220°F (100–104°C), which is the point of the maximum corrosion rate. However, if the metal surfaces are hot and the leakage rate sufficiently low, the water evaporates rapidly, leaving dry boric acid crystals that cause essentially no corrosion. Lower corrosion rates are expected when the surfaces onto which the borated water is dripping are below the boiling point of the borated water.

If borated steam impinges on hot metal surfaces, the corrosion rates can be very high as a result of the combination of high concentration, local metal temperatures near the boiling point of the borated water, and some mechanical effects due to the flow impingement. This condition can be highly damaging as evidenced by several cases involving rapid stud corrosion.

Laboratory results suggest that borated water leaking from a PWSCC-type crack should not cause corrosion deep in the annular clearance gap to the vessel shell since there is little oxygen at this location. However, tests with upward-pointing nozzles suggest that corrosion rates

---

[a] Note, however, that ongoing work referred to later in this topical paper appears to suggest that these values can be exceeded under certain circumstances.

exceeding 1 in/yr (25 mm/yr) are possible. It is not yet clear if these test data are directly relevant to CRDM penetrations in the RPV head.

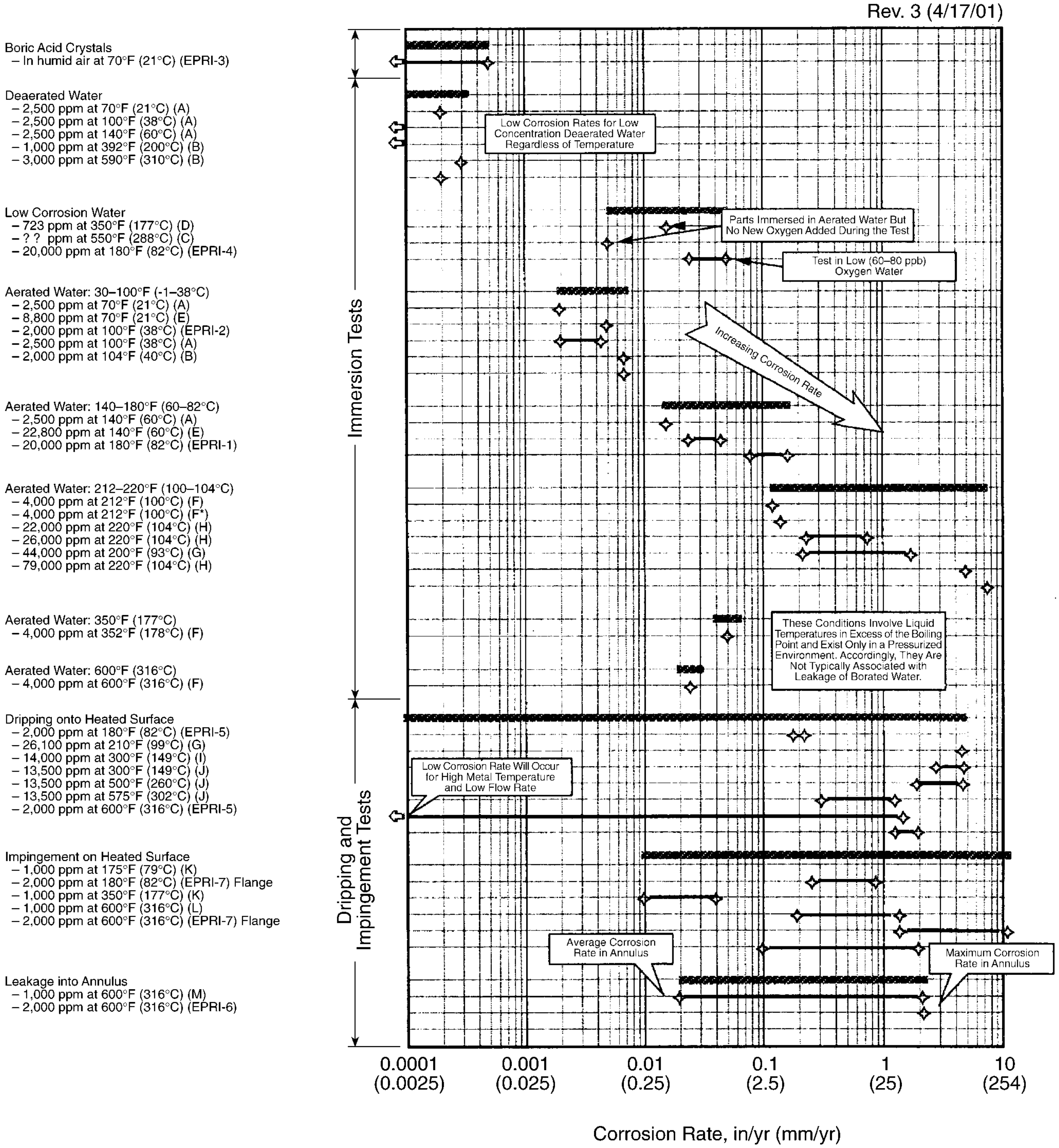

Figure B.18.4 Summary of corrosion tests on BAC of C&LAS prior to 2002 [2]

BAC management programs at US PWRs

The first level of protection against boric acid corrosion should be to prevent leaks from occurring in the first place. If there is no leakage, there will be no boric acid corrosion.

Detecting and preventing leakage

The requirements of the Code of Federal Regulation, the NRC, and the ASME Boiler and Pressure Vessel Code are remarkably similar as they apply to leakage from reactor coolant systems. The common themes in these requirements are:

- Closures should be designed to have a low risk of leakage.
- Closure designs and materials should be such that there is a low risk of rupture or abnormally high leakage.
- Closures should be fabricated and assembled to have a low risk of leakage.
- Inspection programs should be developed and implemented to find leakage and to determine other areas where the leakage could have flowed or accumulated.
- Corrective action should be implemented to correct situations where leakage has occurred.

The NRC is prepared to grant relief from the ASME Code requirements to remove insulation during the final VT-2 inspections of insulated flanges. However, several reasonable concessions have to be made to obtain the relief.

In most cases, the technical means for reducing leakage are not difficult. However, developing an effective program for reducing leakage risk from the many possible sources requires concerted effort by both plant management and staff. A major key to cost effective leakage reduction is to start with state-of-the-art procedures and materials that are capable of developing high-integrity joints and then train craft personnel to follow the procedures and identify adverse conditions [5]. EPRI sponsors a Fluid Sealing Technology Working Group where utilities meet on a regular basis to review the results of relevant research, discuss plant-specific leakage problems, obtain complementary information on current areas of research from sealing technology vendors, and establish priorities for further leakage reduction activities.

A more problematic source of leakage is through-wall cracks which can develop under certain circumstances in reactor components themselves. For example, there have been many reported cases of leakage of primary water from primary water stress corrosion cracks (PWSCC) in Alloy 600 nozzles attached to pressure boundary parts by partial penetration J-groove welds [6,7]. Another major source of leakage of primary coolant above the RPV has been transgranular SCC in stainless steel canopy welds [8].

Preventing Degradation If Leaks Occur

The consequences of leakage in both joint fasteners themselves and adjacent components can often be reduced by replacing the carbon steel or low-alloy steel parts with more corrosion-resistant materials or diverting any leakage to areas where it will not cause damage (e.g., by installing protective shrouds).

The primary emphasis should always be on preventing leakage from occurring in the first place and then stopping leaks when they are found by retightening joints, injecting sealants, and other similar procedures. In some cases, however, it may be necessary to continue operating a plant with leakage and/or continuing degradation. A prime reason is that leakage may be discovered during plant operation, and it may be desirable to defer maintenance until the next scheduled refueling outage so that the repairs will not result in a power decrease or plant shutdown. In other cases, it may be desirable to defer repairs for problems discovered during a refueling outage due to a lack of parts, or for other reasons. In either case, a justification for continued operation (JCO) with the leakage and/or degradation must be prepared and reference [2] describes a recommended methodology for this. The level of effort in developing the JCO will depend upon the criticality of the affected parts. Preparation of a JCO for operation with a small leaking valve in an isolable line requires significantly less effort than a JCO for continued operation with a leaking reactor coolant pump flange gasket.

Condition monitoring

A key factor in a successful boric acid corrosion management program is sound condition monitoring. This includes both equipment condition assessment and leakage detection. Information on equipment condition can lead to improvements that can reduce the potential for leakage. For example, potentially detrimental effects of smooth flanges, gouged flanges, out-of-flat flanges, misalignment, damaged valve stems, damaged or corroded bolts, etc., can be rectified and, thereby, reduce the potential for leakage. Similarly, low levels of plant leakage and a good leakage detection system can improve the ability to detect leaks early enough to take corrective action before more drastic measures are required. Enhanced monitoring for leakage may be advisable under certain circumstances and various systems are now available for this purpose [9].

Ongoing BAC activities following the 2002 Davis Besse incident

Background

Between November 2000 and April 2001, leaks were discovered from reactor vessel top head penetrations at Arkansas Nuclear One-1 and Oconee 1,2: and 3. The leaks were discovered by visual inspections of the heads, which showed small amounts of boric acid crystal deposits ("popcorn" – see Fig. B.18.5) that were determined to have come from the annulus between the nozzles and the vessel head. The CRDM nozzle leaks were traced to predominantly axial PWSCC cracks in the Alloy 600 material of the head penetrations.

In August 2001, the NRC issued Bulletin 2001-01 requesting that PWR licensees provide information related to the structural integrity of the RPV head penetration nozzles, including the extent of nozzle leakage and cracking found. In response to this NRC bulletin, PWR licensees performed bare metal visual inspections of the RPV head looking for boric acid deposits adjacent to RPV head penetrations. An extensive safety analysis was also carried out to demonstrate that structural integrity was maintained, even with leaking CRDM penetrations [10]. The extent and way in which head penetrations of PWR vessels are inspected to detect boric acid leakage have also now been refined and details of current practices are contained in [11].

Figure B.18.5 Typical appearance of boric acid deposits (without wastage) at a leaking Alloy 600 CRDM penetration in a RPV head

In March 2002, in conjunction with an earlier inspection regime, the Davis-Besse (D-B) plant discovered evidence of significant wastage of the low alloy steel head contiguous to CRDM nozzle #3 (see Figs. B.18.6 & 7) and much less substantial wastage adjacent to other CRDM nozzles. The extent of the corrosion at nozzle #3 was completely unanticipated given the results of previous head inspections there and at other plants which had shown small volumes of leakage from a few nozzles, but little evidence of corrosion of the low-alloy steel head.

Figure B.18.6 Cavity in RPV head at D-B after removal of CRDM nozzle #3

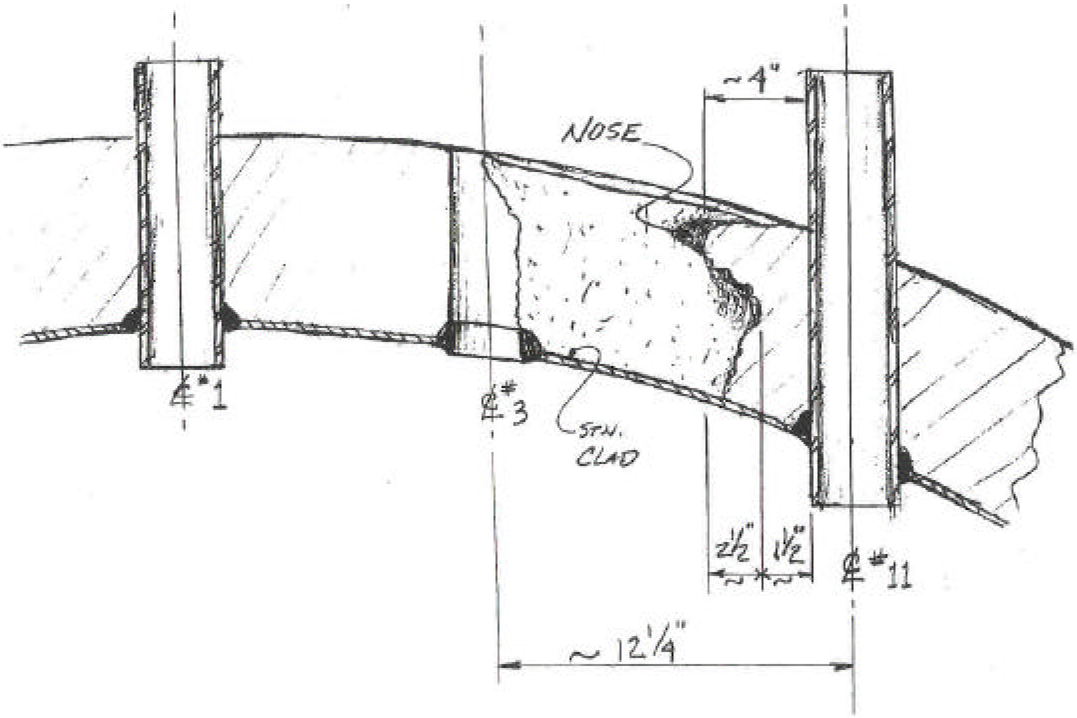

Figure B.18.7 Sketch of D-B RPV head degradation between nozzles 3 and 11

In response to the findings at D-B, the NRC issued Bulletin 2002-01 focusing on the integrity of the reactor coolant pressure boundary including the reactor pressure vessel head and the extent to which inspections have been undertaken to identify corrosion of the RPV head.

Analysis carried out to understand the severe BAC in the D-B RPV head

Reference 2 is a relatively comprehensive source document with regard to managing boric acid corrosion issues at PWR stations. Care is needed, however, in interpreting its content with regard to the way in which PWR primary coolant might attack the LAS of the vessel head if it leaks from a through-wall SCC crack in an adjacent Alloy 600 penetration tube. At the point in time where a tight, highly-branched, intergranular crack in the Alloy 600 material (or indendritic crack in the J-groove weld) first intersects the outer surface of the high-alloy material, the leakage rate will be extremely low, irrespective of the annulus geometry (i.e. interference fit or radial gap). Thus the pressure drop to saturated vapor pressure will occur within the stress corrosion crack itself and the environment immediately above the J-weld is likely to be hydrogenated, superheated steam. As the leakage rate into the annulus from SCC of the high-alloy material increases, boiling (and possible concentration) of primary water will occur within the annulus itself, i.e. external to the crack or cracks. The exact location of the boiling transition and the extent of concentration near the liquid/vapor interface will be a complex function of the crack and annulus geometries.

In considering the composition of the liquid formed with regard to its propensity to initiate OD SCC of the CRDM penetration, the MRP Expert Panel on PWSCC considered that it would most likely to be buffered to a pH close to that of normal PWR primary water [12] as a result of precipitation of various boron compounds (including iron metaborate arising from corrosion of the LAS). It was agreed that back diffusion of oxygen into the crevice environment could be disregarded for a number of reasons (steam counterflow, hydrogen concentration, etc.), even without taking into account the gettering effect of corrosion at the LAS crevice wall. This scenario would appear to describe the situation at most leaking CRDM nozzles (including those at D-B apart from #3), where little or no wastage corrosion of the RPV head material has been observed.

To account for the development of the cavity found at D-B adjacent to leaking nozzle #3, a large number of potential BAC mechanisms (and their complex interaction over time) have been postulated [13], as illustrated by the preliminary analysis shown in Figs. B.18.8 and 9.

The initial industry model ("top-down" corrosion – see Appendix C of reference [14]) concentrated on the formation of a pool of highly concentrated boric acid on the top of the RPV head adjacent to nozzle #3 due to the ready supply of boric acid (from pre-existing deposits on the head) and local cooling of the metal so as to maintain an acidic pool of aerated liquid, despite the high temperature of the rest of the head. Independent thermohydraulic analyses confirmed that such a scenario is indeed viable, once the leakage rate of primary water through a cracked nozzle is sufficiently high, although some of the assumptions made in the calculations (e.g. with regard to the effective cross-sectional area of the PWSCC cracks in the nozzle material) require experimental verification. However, it was considered likely that flow and impingement effects adjacent to the liquid exiting the SCC cracks might also be involved. Furthermore, a possible role of LAS corrosion in "molten" boric acid within the deposits was recognized.

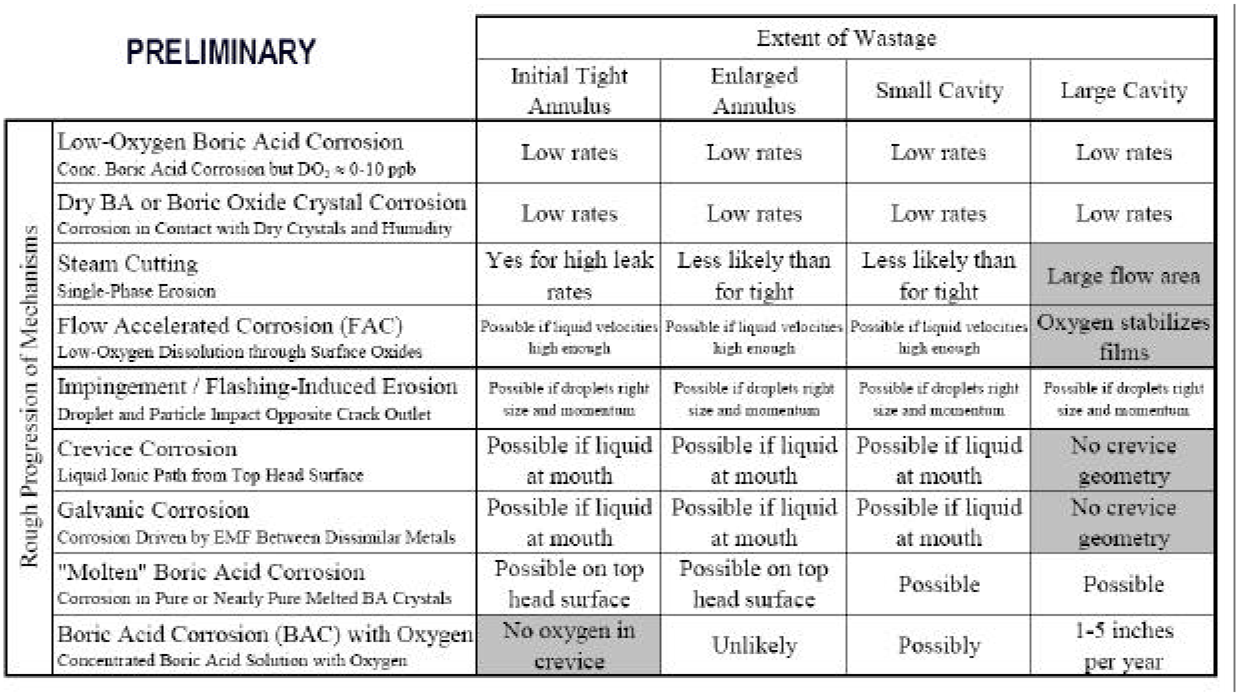

PRELIMINARY

Rough Progression of Mechanisms	Extent of Wastage			
	Initial Tight Annulus	Enlarged Annulus	Small Cavity	Large Cavity
Low-Oxygen Boric Acid Corrosion Conc. Boric Acid Corrosion but $DO_2 \approx 0\text{-}10$ ppb	Low rates	Low rates	Low rates	Low rates
Dry BA or Boric Oxide Crystal Corrosion Corrosion in Contact with Dry Crystals and Humidity	Low rates	Low rates	Low rates	Low rates
Steam Cutting Single-Phase Erosion	Yes for high leak rates	Less likely than for tight	Less likely than for tight	Large flow area
Flow Accelerated Corrosion (FAC) Low-Oxygen Dissolution through Surface Oxides	Possible if liquid velocities high enough	Possible if liquid velocities high enough	Possible if liquid velocities high enough	Oxygen stabilizes films
Impingement / Flashing-Induced Erosion Droplet and Particle Impact Opposite Crack Outlet	Possible if droplets right size and momentum	Possible if droplets right size and momentum	Possible if droplets right size and momentum	Possible if droplets right size and momentum
Crevice Corrosion Liquid Ionic Path from Top Head Surface	Possible if liquid at mouth	Possible if liquid at mouth	Possible if liquid at mouth	No crevice geometry
Galvanic Corrosion Corrosion Driven by EMF Between Dissimilar Metals	Possible if liquid at mouth	Possible if liquid at mouth	Possible if liquid at mouth	No crevice geometry
"Molten" Boric Acid Corrosion Corrosion in Pure or Nearly Pure Melted BA Crystals	Possible on top head surface	Possible on top head surface	Possible	Possible
Boric Acid Corrosion (BAC) with Oxygen Concentrated Boric Acid Solution with Oxygen	No oxygen in crevice	Unlikely	Possibly	1-5 inches per year

Figure B.18.8 Preliminary analysis of possible BAC mechanisms to cause D-B cavity [13]

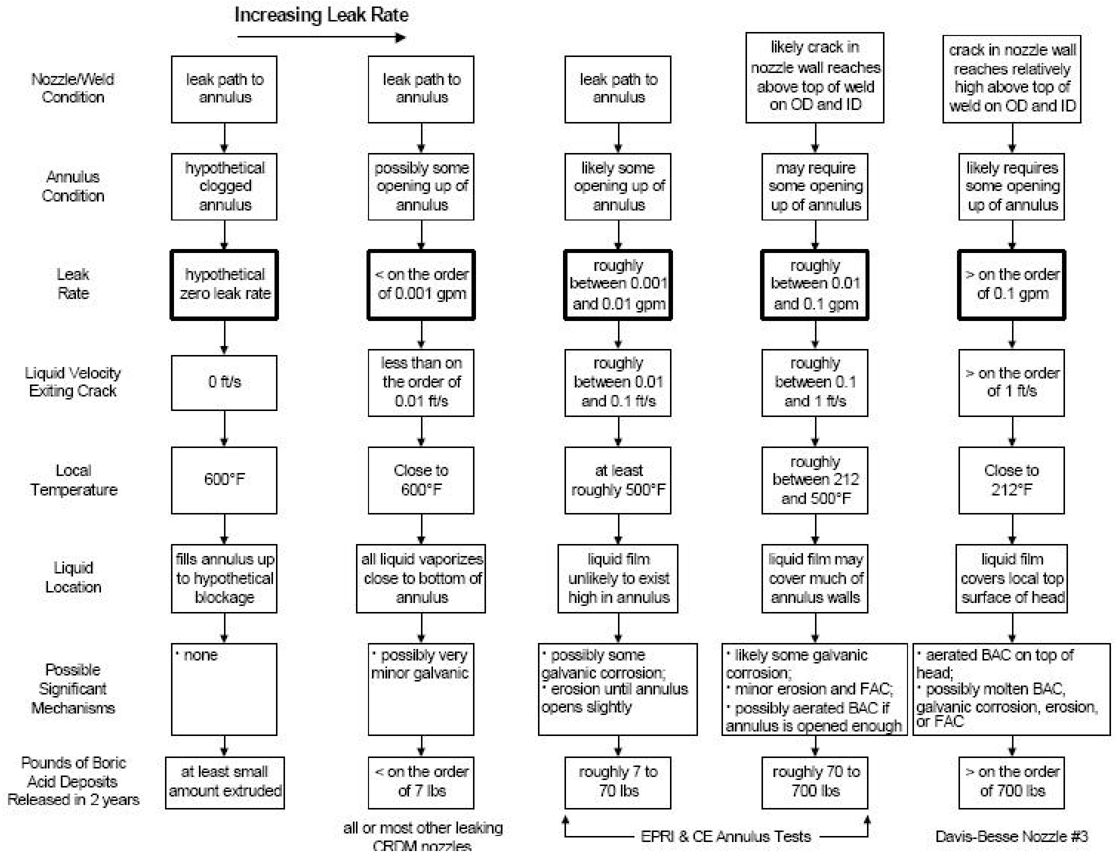

Figure B.18.9 Postulated progression of degradation with leak rate as main parameter[13]

Additional experimental work on BAC following the D-B incident

- Both the US PWR industry and NRC Research have initiated major programs on BAC since 2002, the results of which have yet to be fully reported. The EPRI-managed program is structured to
    - improve understanding of the progression of boric acid wastage at RPV head penetrations,
    - identify the influence of plant specific parameters on wastage, and
    - support development of required inspection intervals for PWR plants with various penetration designs.

It consists of 4 main tasks, as shown schematically in Fig. B.18.10, culminating in an instrumented, full-scale RPV head penetration mock-up test (due to start in 2005):

Task 1: Corrosion tests in stagnant and low flowing (<0.005 gpm) primary water, simulating early stages of CRDM penetration degradation. [15]

Task 2: Corrosion tests in flowing primary water, with measurement of real time corrosion rate and ECP under laminar and impact flow. [16]

Task 3: Testing focused on a matrix of laboratory immersion corrosion, autoclave chemistry, and electrochemical polarization curve tests for concentrated boric acid and wetted molten boric acid environments. [15]

Task 4: Full-scale mockup tests for CRDM nozzles (planned examination of synergies considering the detailed results from Tasks 1, 2, and 3).

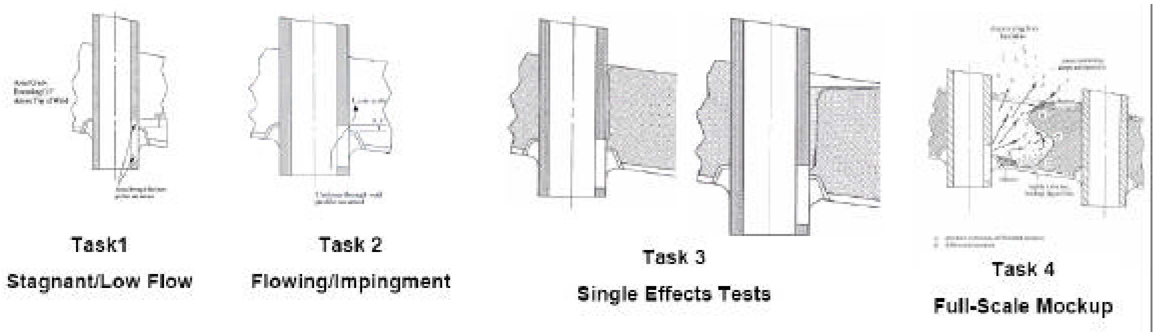
Task1
Stagnant/Low Flow
Task 2
Flowing/Impingment
Task 3
Single Effects Tests
Task 4
Full-Scale Mockup

Figure B.18.10 Schematic of additional industry BAC testing program started in 2003

At the time of writing (March 2005), some initial results from Task 3 have been publicly reported [17] with the following preliminary conclusions:

- Corrosion rates up to about 6 inches/yr were observed for the laboratory conditions tested.
- Corrosion was significantly slowed by the presence of lithium, with the effect being most apparent at high temperatures.
- Corrosion was greatest at intermediate temperatures and boric acid concentrations (50%, versus 1% or 90%).
- For high boric acid concentrations, no large reduction in corrosion rate due to deaeration was observed for the laboratory conditions tested
- pH measurements will be used to verify that this is due to low pH.
- Corrosion rates under deoxygenated conditions were about half to two-thirds of the rate under the corresponding oxygenated conditions.
- No significant acceleration was noted due to galvanic coupling or crevices.

The NRC experimental program at ANL has been completed and preliminary results, together with a survey of BAC plant experience and some analysis of the most likely scenario at D-B, are given in reference [18]. The authors conclude that "the galvanic difference between A533 Grade B steel, Alloy 600, and 308 stainless steel is not significant enough to consider galvanic corrosion as a strong contributor to the overall boric acid corrosion process". In addition, the NRC test program has found that the corrosion rate of A533 Grade B steel in contact with molten salts of the H-B-O system at 150°C to 170°C can be as great as that of A533 Grade B steel in contact with an aqueous, aerated solution of boric acid at temperatures near the boiling point, although the MRP test program suggests that this situation may not be applicable to operating plants [17].

Finally, it should be mentioned that a full-scale destructive examination of the D-B RPV head cavity has now been carried out. These results were recently reported [19].

Improvements to plant BAC management programs

Subsequent to the D-B incident, considerable attention has been paid to the way in which monitoring for BAC leakage is actually being carried out at operating plants [20] and revised "best practice" guidance is currently being put into effect within the industry [21].

References

1 "Boric Acid Corrosion of Carbon Steel Reactor Pressure Boundary Components in PWR Plants", NRC Generic Letter 88-05, March 17, 1988.

2 *Boric Acid Corrosion Guidebook, Revision 1*: "Managing Boric Acid Corrosion Issues at PWR Power Stations", EPRI, Palo Alto, CA: 2001. 1000975.

3 "Low-Alloy Steel Component Corrosion Analysis supporting Small Diameter Alloy 600/690 Nozzle Repair/Replacement Programs", NRC SER on CE NPSD 1198-P from Feb. 2002.

4 "*Handbook of Corrosion Engineering*". McGraw-Hill, 1999.

5 "Establishing an Effective Leak Management Program". EPRI, Palo Alto, CA: December 2000. TR-114761.

6 " PWSCC of Alloy 600 Materials in PWR Primary System Penetrations". EPRI, Palo Alto, CA: July 1994. TR-103696.

7 " PWSCC of Alloy 600 Type Materials in Non-Steam Generator Tubing Applications - Survey Report Through June 2002 Part 1 PWSCC in Components Other than CRDM/CEDM Penetrations" (MRP-87), EPRI, Palo Alto, CA: 2002. 1007832.

8 C. M. Pezze, I. L. W. Wilson, "Transgranular Stress Corrosion Cracking of 304 Stainless Steel Canopy Seal Welds in PWR Systems." *Proceedings of the Fourth International Symposium on Environmental Degradation of Materials in Nuclear Power Systems–Water Reactors*, Jekyll Island, GA (August 6–10, 1989) pp. 4-164–4-179.

9 "Survey of On-Line PWR Coolant Leak Detection Technologies" (MRP-94), EPRI, Palo Alto, CA: 2003. 1009062.

10 "Reactor Vessel Closure Head Penetration Safety Assessment for US PWR Plants" (MRP-110), Epri, Palo Alto, CA : 2004. 1009807.

11 "Materials Reliability Program Inspection Plan for Reactor Vessel Closure Head Penetrations in U.S. PWR Plants" (MRP-117), Epri, Palo Alto, CA: 2004. 1007830.

12 " Crack Growth Rates for Evaluating Primary Water Stress Corrosion Cracking (PWSCC) of Thick-Wall Alloy 600 Materials" (MRP-55, Rev. 1), EPRI, Palo Alto, CA: 2002. 1006695.

13 G. White, C. Marks, and S. Hunt, "Technical Assessment of Davis-Besse Degradation", NRC ADAMS Accession No. ML021420150, May 5, 2002.

14 "PWR Reactor Pressure Vessel (RPV) Upper Head Penetrations Inspection Plan, Revision 1" (MRP-75), EPRI, Palo Alto, CA: 2002. 1007337.

15 A. McIlree et al., "MRP Boric Acid Corrosion Testing, Tasks 1 & 3", EPRI/MRP Alloy 600 PWSCC Workshop", Tamaya Resort, New Mexico, March 2005.

16 J. Pongpuak et al., "Corrosion of Reactor Pressure Vessel Steel by an Impinging Jet of PWR Coolant: Status Report on an EPRI/MRP Experimental Study", EPRI/MRP Alloy 600 PWSCC Workshop", Tamaya Resort, New Mexico, March 2005.

17 EPRI/MRP Boric Acid Corrosion (BAC) Testing Program: Immersion Test Results, NRC/ANL/MRP meeting, Argonne, IL, January 2005.

18 S. Crane & W. Cullen, "Survey of Boric Acid Corrosion Events" (Rev. 9), Materials Engineering Branch, Office of Regulatory Research, US NRC; ADAMS Accession No. ML0430002740, October 22, 2004.

19 S. Fyfitch, "Boric Acid Corrosion of the Davis-Besse Reactor Pressure Vessel Head", EPRI/MRP Alloy 600 PWSCC Workshop", Tamaya Resort, New Mexico, March 2005.

20 "Materials Reliability Program: EPRI Boric Acid Corrosion Workshop", July 25-26 2002 (MRP-77), EPRI, Palo Alto: 2002. 1007336.

21 T. Satyan Sharma, "WCAP-15988, Revision 1: Generic Guidance for an Effective Boric Acid Corrosion Control Program for Pressurized Water Reactors", EPRI/MRP Alloy 600 PWSCC Workshop", Tamaya Resort, New Mexico, March 2005.

B. 19 Variability in the Corrosion of Materials in LWR Environments

Introduction

Regardless of the mode or intensity of corrosion, failures in identical components exposed to identical conditions in the same or different plants do not occur simultaneously. There is always a “first failure” in a set of identical components; and, when failures can occur, the first failure is followed by others. This first failure is frequently, and erroneously, attributed to a “bad heat” or to some carelessness in manufacturing or operation. As failures of the same mode accumulate, it is common to accept the inevitable trend, rather than having accepted the inevitability of subsequent failure at the earliest failure. Sometimes, the first failure may occur several orders of magnitude in time earlier than the mean value as determined by later testing or much later failures in the field.

The objective of this discussion is to describe the reality of the nature and scope of variability in the occurrence of corrosion damage in operating LWR plants as well as in the laboratory testing that is intended to elucidate the nature of such failures in applications. A further objective here is to alert regulators, designers, and operators to the inevitability of the statistical nature of corrosion failures.

Statistical Distributions

Variability in the corrosion of materials has been described by Staehle and co-workers in several references [1-6]. In order to discuss the variability in corrosion of materials, a brief review of the statistical methodology and terminology is useful. For the purposes of this discussion, the statistical methodology is described in terms of the Weibull distribution [7-9]. Of the several distributions, which are available for correlating failure data, the Weibull distribution usually fits failure phenomena the best. However, there are several useful distributions that are widely used as described in texts by Nelson and others [10-13] The background of applying statistical distributions to corrosion is described by Staehle[1] and by Shibata [14].

The principal relationships used to describe the distribution of data in the Weibull framework are shown in Equations 1-8

where:

$$f(t) = \left[\frac{b}{(q - t_o)^b}\right](t - t_o)^{b-1} \exp\left[-\left(\frac{t - t_o}{q - t_o}\right)^b\right], t > t_o \tag{1}$$

$$F(t) = P\{t' \leq t\} = \int_0^t f(t)dt \tag{2}$$

$$F(t) = 1 - \exp\left[-\left(\frac{t - t_o}{q - t_o}\right)^b\right] \tag{3}$$

$$\ln\left[\ln\left(\frac{1}{1 - F(t)}\right)\right] = b\left[\ln(t - t_o) - \ln(q - t_o)\right] \tag{4}$$

$$R(t) = P\{t' > t\} = \int_t^{\infty} f(t)dt = 1 - F(t) = \exp\left[-\left(\frac{t - t_o}{q - t_o}\right)^b\right] \tag{5}$$

$$h(t) = \frac{f(t)}{1 - F(t)} \tag{6}$$

$$h(t) = \left(\frac{b}{q - t_o}\right)\left(\frac{t - t_o}{q - t_o}\right)^{b-1} = \frac{b}{(q - t_o)^b}(t - t_o)^{b-1} \tag{7}$$

$$F_T(t) = 1 - [1 - F_1(t)][1 - F_2(t)] \bullet\bullet\bullet [1 - F_n(t)] \tag{8}$$

where:

t = Time
t_o = Location parameter, sometimes called, erroneously, the “initiation time.”
q = Scale parameter or the Weibull characteristic which is evaluated at $t = q$ where the probability is 0.632.
b = Shape parameter or often called the “Weibull slope” as is evident from the linearized version in Eqn. (4). b is also called the “dispersion.”
$f(t)$ = Probability density function, pdf.
$F(t)$ = Cumulative distribution function, cdf, also the probability of failure in time.
$F_T(t)$ = Total probability including the ith element.
$F_i(t)$ = Probability for the ith element.
$R(t)$ = Reliability
$R_T(t)$ = Total reliability
$R_i(t)$ = Reliability of ith element
$h(t)$ = Hazard function

Until about ten years ago, it was common to evaluate only the scale parameter, q, and the shape factor, b, owing to the difficulty of evaluating the three parameters including the location parameter, t_o; further, it was mistakenly thought that a phenomenon that started at the beginning of component life would have a t_o=0. Now, with a number of good computer programs [15], all three parameters are customarily evaluated giving a “three parameter fit” of the data rather than a “two parameter fit.”

Eqn. (1) and Figure B.19.1a show the “probability density function (pdf),” which gives the probability of occurrence, $f(t)$, (of corrosion failure in this discussion) in the interval dt. This is a familiar form, and in normal statistics the pdf gives the widely recognized “bell shaped curve.”

Of more use is the “cumulative distribution function (cdf),” which gives the cumulative failures or probability of failure, $F(t)$ vs. time. $F(t)$ vs. time is obtained by integrating the pdf from zero to “t” as shown in Eqn. (2) and Figure B.19.1b. The result of this integration is Eqn. (3); and Eqn. (3) is usually linearized for the Weibull distribution as Eqn. (4) by taking the natural log of both sides twice. The result is a relationship of the form, y=mx+b, where the shape parameter, b, is the slope. This shape parameter is often called the “dispersion” since it describes how broadly the data are distributed. The probability of failure, $F(t)$, which is the probability of failure at time, t, is 1-$R(t)$, where $R(t)$ is the “reliability” or the probability that the components will not fail by time, t. $R(t)$ is given in Eqn. (5).

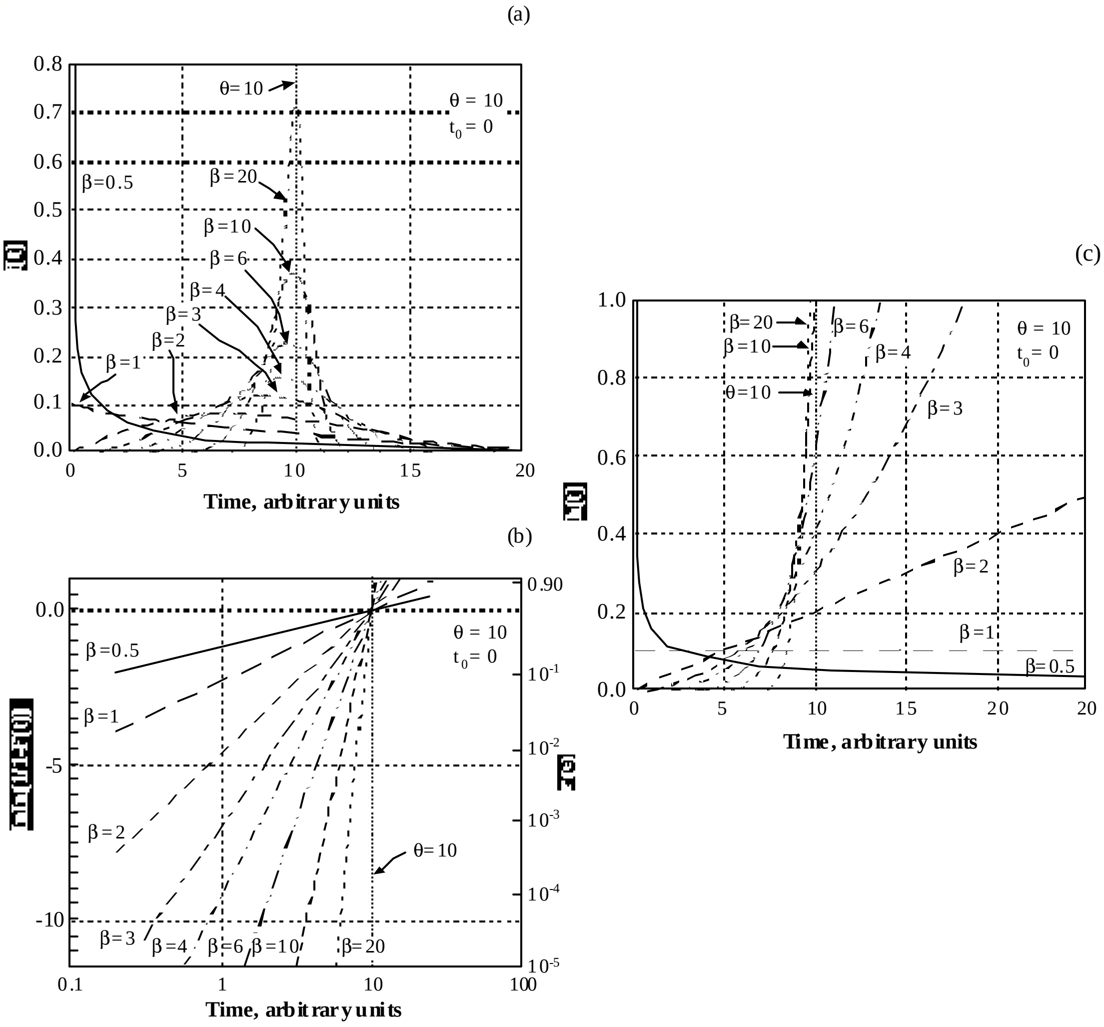

Figure B.19.1 (a) $f(t)$ vs. time for constant q. (b) $F(t)$ vs. time for constant q. (c) $h(t)$ vs. time for constant q. From Staehle [3]

Finally, another useful relationship is the "hazard function (hf)," $h(t)$, which is the probability of failure of components that have not yet failed. The hazard function is given in Eqn. (6) and Figure B.19.1c. The hazard function has the interesting property that, when $b=1$, the probability of failure is independent of time as is evident in Eqn. (7) and is shown in Figure B.19.1c. A shape factor of $b=1$ is commonly observed in field failures, thereby indicating that the probability of failure for components, which have not yet failed, is independent of time.

Often, failures of components result from multiple modes of failure as has been common in the tubes of steam generators, which are described by Staehle and Gorman.[i] Thus, the total probability of failure can be evaluated using Eqn. (8). Here, the separate $F_i(t)$ are evaluated for multiple modes of failure and then inserted into Eqn. (8) where the total probability of failure, $F_T(t)$, is evaluated. Eqn. (8) assumes that the multiple failure modes do not interact.

Interpretation of Distributions

Figure B.19.2 shows the commonly used cumulative distribution from the Weibull distribution shown in Figure B.19.1b. Figure B.19.2a shows the probability of failure vs. time for two values of the shape parameter, *b*, where *b*=1.0 and *b* =4.0; these values, as well as the range between them, are commonly observed in failures that occur in nuclear applications.

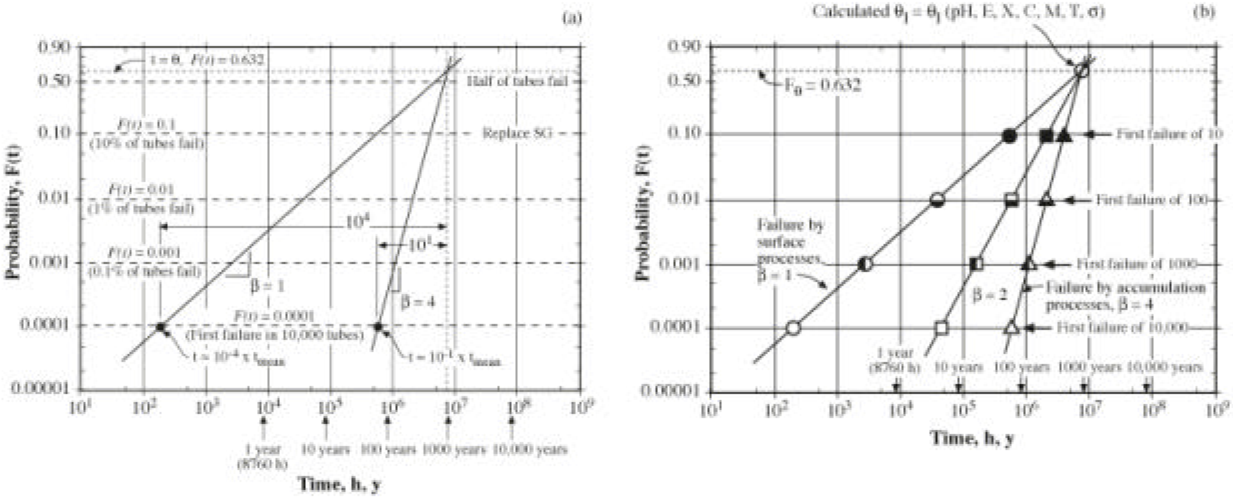

Figure B.19.2 (a) Cumulative distribution function with two values of b shown together with relationship between the failure time at F(t)=0.0001 and the mean failure time.. (b) Schematic view of probability vs. time for a calculated *q* and three options for slopes within the range of engineering experience. Locations of the earliest failures noted for various populations according to three values of *b*. From Staehle [3]

Figure B.19.2a shows how the cumulative distribution is commonly used and interpreted:

- The ordinate is the probability, *F(t)*, of failure and the abscissa is time-to-failure, usually in seconds, hours, or years. Sometimes, in nuclear applications, the time is given as EFPH (equivalent full power hours).

- The ordinate is shown for the range of 0.00001 (1/100,000) to 0.90. This range applies to the failure or plugging of tubes in steam generators. Commonly, there are about 4000 tubes in a single steam generator, and, with up to four steam generators, there may be 12,000 to 16,000 tubes total. The failure or plugging of one tube in 10,000 is a failure probability of 0.0001.

- A horizontal dotted line is shown at *F(t)*=0.632 which is the value of *F(t)*when *q* =*t*. This "Weibull" characteristic is nearly the same as the mean value where *F(t)*=0.5. The location of *F(t)*=0.5 is also shown.

- Two straight lines are shown for slopes of *b*=1.0 and *b*=4.0 with both lines having the same time for *F(t)*=0.632.

- Also shown are dotted horizontal lines for *F(t)*=0.1, 0.01, 0.001, and 0.0001 or, respectively 10%, 1%, 0.1% and 0.01% failures as these horizontal lines intersect the lines for b=1.0 and b=4.0. Black dots are shown at 0.01% failures indicating a point for the first failure of one tube in a population of 10,000 tubes.

- Also, at *F(t)*=0.0001 (0.01%) probability there are notes that the first failure or tube plugging in 10,000 is some fraction of the mean. Thus, for b=1.0 the first failure in 10,000 tubes occurs at about 10^{-4} of the mean time-to-failure; whereas, at b =4.0 the first failure at *F(t)* =0.0001 occurs at about 10^{-1} of the mean time-to-failure.

- Note also that Figure B.19.2, as well as Figure B.19.1b, emphasizes early failures or tube plugging as the scale is expanded at low probabilities. Other types of distributions emphasize failures in the high range.

- Data points are placed on the plot in terms of the fraction of the total failed or plugged at a given time; i.e. the first tube failed in 10,000 would be plotted as 0.0001 at the time of failure. After 100 tubes fail, this would be plotted as 0.01 after failures of the first 100 are observed.

Figure B.19.2b shows the same information as in Figure B.19.2a in more detail for three values of b and shows the times-to-failure of the first failure for various populations from 10 to 10,000.

With respect to the performance of steam generators, it is common that an SG is considered failed when about 10% of the tubes have been pluged. On Figure B.19.2, this is a probability of 10% or 0.1.

Plotting the occurrence of failures on such plots is described in detail by Abernethy [13]. There are several computer programs for preparing such plots [15].

Applications of Distributions

The application of a cumulative distribution of the type shown in Figures B.19.1b and 2 by incorporating actual data is described stepwise in Figure B.19.3 with plots of Figures B.19.3a, b, c. Figure B.19.3 also shows how the accumulating data are used to reach conclusions of future performance in terms of progressively more refined projections based on progressively improved values of the shape factor, b. As data are successively accumulated, it becomes possible to predict when some critical fraction of failures can occur, e.g. 10% of tubes in an SG.

Figure B.19.3a shows a black dot where the first failure of 10,000 tubes is plotted. This first failure is shown to occur at about 5 time units (hours, years) and is plotted at a probability of 0.0001 or one tube of 10,000. At this point, straight lines are drawn through this point using values of b= 1.0 and 10.0 which include a reasonable range of expected shape factors or dispersions of data.

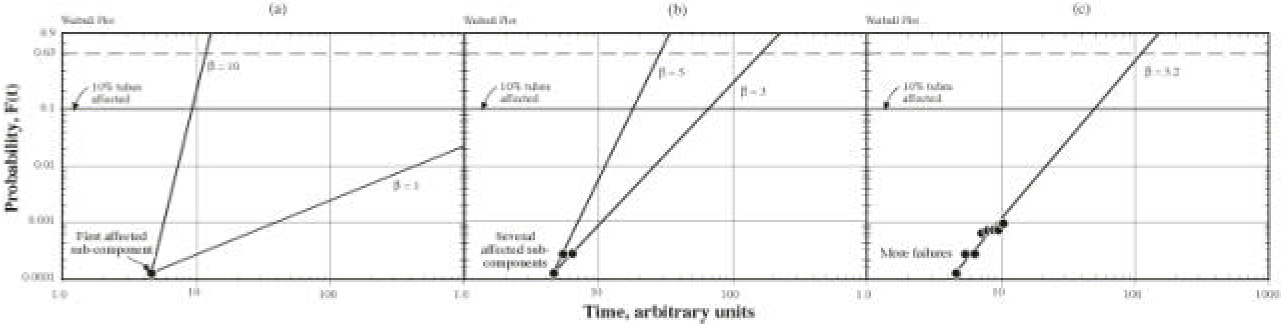

Figure B.19.3 (a), (b), (c) Schematic Weibull plots for cdfs and the evolution of failure points together with expected slopes for prediction. From Staehle.[3]

With only one point, more precision is not possible. With these values of b= 1.0 and 10.0, failure of the SG (e.g. 10% of tubes failed) might occur as early as 10 units or as late as about 10,000 units of time. Further precision is not possible with a single first point.

After more failures occur, the range of slopes can be estimated more precisely as suggested in Figure B.19.3b. Here, a range of b=3.0 to b=5.0 is suggested showing that the SG failure point for 10% or 0.1 of the tubes failed might occur between 20 to 70 time units.

As more early failures occur, as shown in Figure B.19.3c, an even more precise value of b can be estimated, which is shown as a b=3.2. Now the time for 10% failure of tubes can be estimated to be about 50 time units. This is a basis for a nuclear utility to take action to purchase a new steam generator at some time (e.g. 3-4 years) before SG failure is predicted to occur. In the meantime more data points would be accumulated at successive inspections.

Note that each point plotted gives the total number of failures to time, t, divided by the population, giving the fraction failed in a given time. As shown in Abernethy [13], there are some adjustments to the data used in plotting to take account of sample size, but these are not useful to discuss here.

Weibull Distributions for Corrosion Failures in LWRs.

Cumulative corrosion failures of various components in LWRs have been dealt with using cumulative distributions and procedures as described for Figures B.19.1b, 2, and 3 [16-19]. This section describes some typical examples from operating systems and laboratory experiments.

Corrosion failures in welds from BWR pipes are plotted in Figure B.19.4 based on data from Eason and Shusto [18]. Figure B.19.4 shows the probability of failure of welds in 2” and 4” pipes in BWR applications vs. time. In both cases the b is about unity or a little less. It is interesting that about 100,000 welds are included in the 2” group and 10,000 welds in the 4” group. The fact that so many welds from different plants follow consistent Weibull behavior indicates the usefulness of the Weibull correlation and the coherence of the data.

Figure B.19.5 from Bjornqvist and Gorman [20] show data from the failures of SG tubes in Ringhals-4 PWR. Such data are taken at successive shutdowns using various NDE methods including eddy current. These data show seven different modes of failure; and the failure data from the seven modes are combined using Eqn. (8) to produce an "aggregate all mechanisms." This aggregate probability can then be extrapolated to 10% failure in order to define when new SGs should be purchased. This method and such plots have been widely used for estimating the time when steam generators should be replaced and thereby defining when such SGs should be purchased.

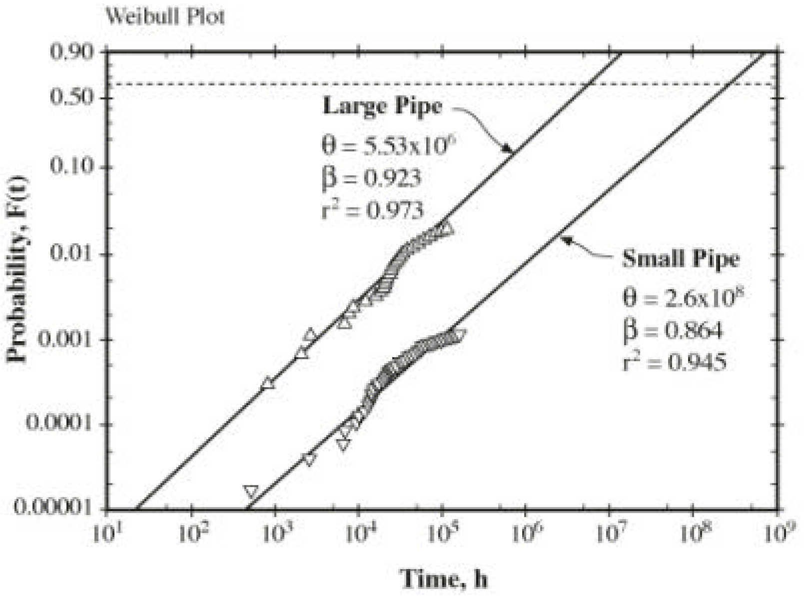

Figure B.19.4 Probability vs. time since startup for SCC failure of welded stainless steel pipes from piping used in boiling water nuclear reactors (BWR). "Large pipe" refers to 4-inch diameter. "Small pipe" refers to 2-inch diameter. Adapted from Eason and Shusto.[18]

In addition to pipes and SG tubes, the failures of bolts, as affected by nuclear radiation, have been analyzed by Scott as shown in Figure B.19.6 [19]. Again, this correlation shows good agreement with the Weibull distribution, noting the values of r^2, and shows clearly the dependence on neutron dose. The displacements of the Weibull correlations for different locations of formers seems related to the differential thermal expansion effects on bolt loads at these locations.

The SCC of Zircaloy-2 exposed to iodine gas as a function of stress was investigated by Shimada and Nagai, as shown in Figure B.19.7, [17] where the data are summarized in a Weibull format. Here the value of the space parameter q decreases with stress as does the location parameter, t_o. The shape parameter, b, is unusually high and increases, as expected, with increasing stress. These experiments are relevant to the effect of iodine, which is released during fission, on the integrity of fuel cladding.

Figures B.19.4 through B.19.7 show four different applications of Weibull cdfs to LWR applications, e.g. piping, SG tubes, bolts and fuel cladding. Clearly, the Weibull correlation is useful and permits carrying forward trends as shown in Figure B.19.3. There are many more examples, especially in Staehle,[1] as well as in private and non-published sources.

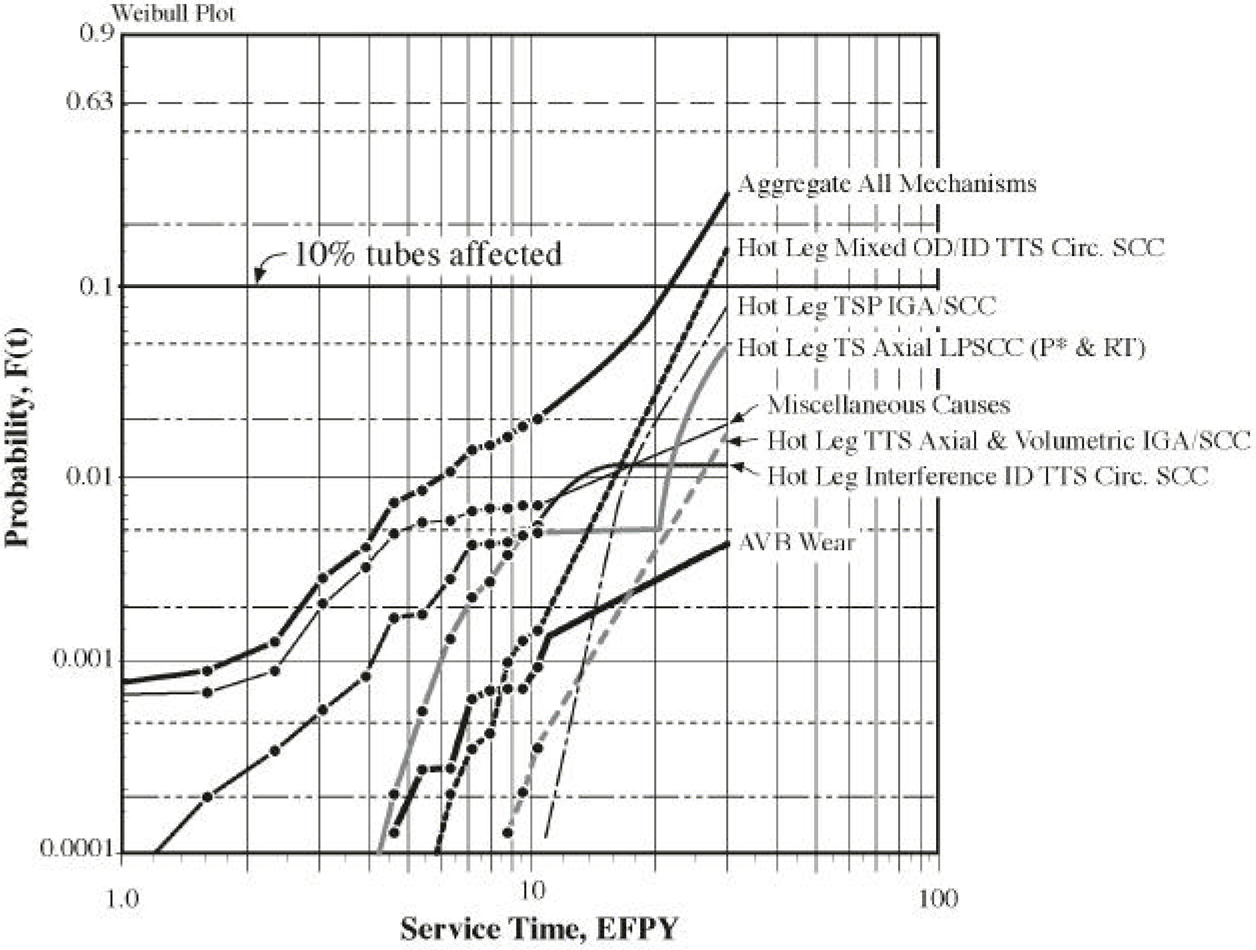

Figure B.19.5 Probability vs. equivalent full power years (EFPY) for failures of tubing from a set of SGs in the Ringhals 4 PWR. Designations: TTS = "top of tube sheet." TS = "tubesheet." Circ. SCC = "circumferential SCC." P* = special location where SCC is not serious. RT = "roll transition." AVB = "antivibration bars".[20]

Background for Random Occurrences of Corrosion Failures

It would seem that experiments could be carried out with such care that there would be no variability in the results. This is a frequent aspiration of both design and materials engineers. However such an aspiration cannot be achieved even from the most careful work. Corrosion, and particularly SCC, involve multiple events in their evolution as illustrated in Figure B.19.8. Here, the sequence of events from the earliest stage of initiation to final fast fracture is shown to include nine segments. Within each of these are micro-options that affect the courses of initiation and propagation. With such an array of macro and micro options, single deterministic times-to-failure for a corrosion process, e.g. SCC, are not possible even under the best of circumstances.

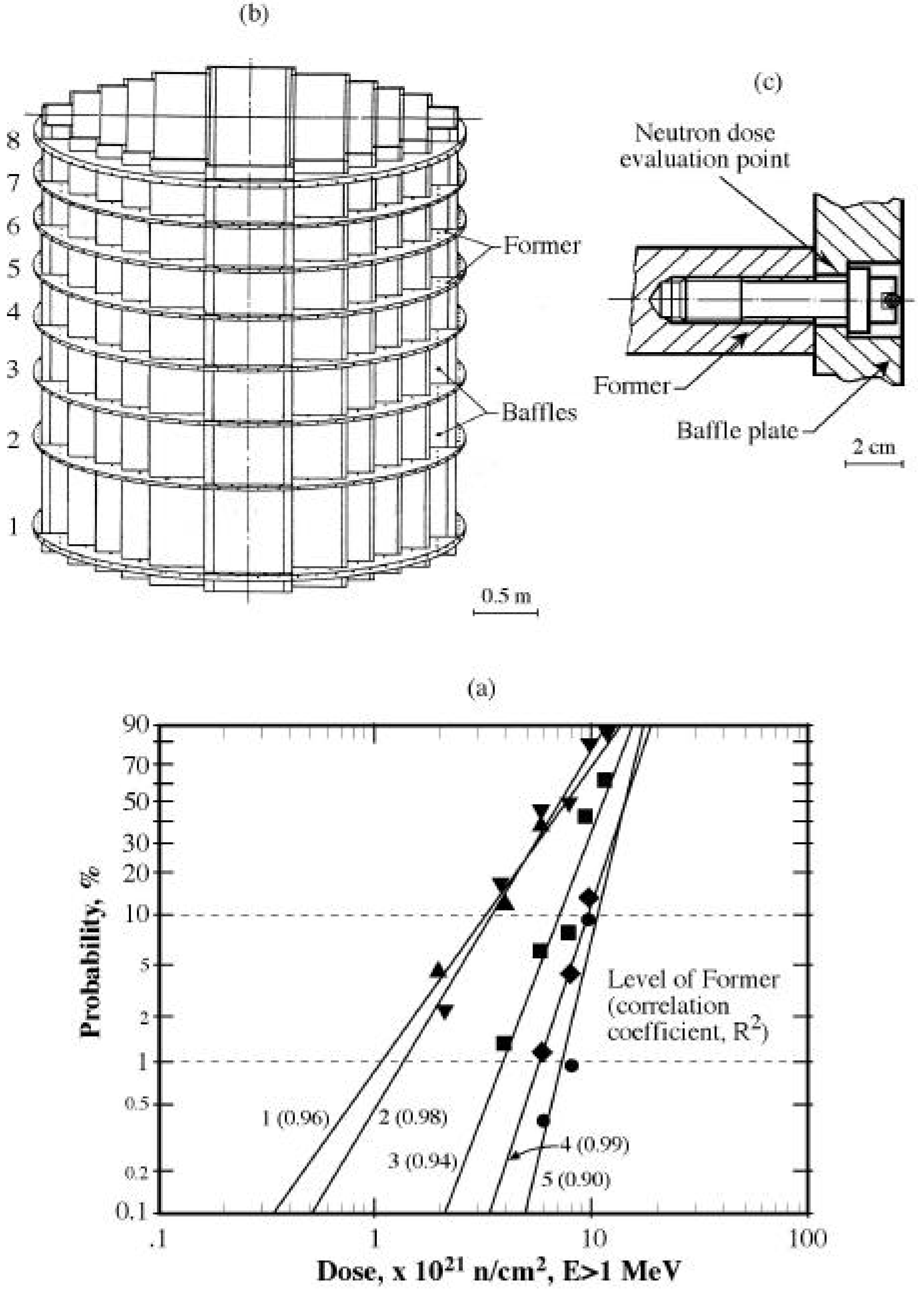

Figure B.19.6 (a) Probability of defective bolts at the joints between the formers and baffles vs. neutron dose based on data for all inspections for Bugey-2 plant. (b) Arrangement of formers and baffles. (c) View of bolts and location of neutron dose used for (a). Adapted from Scott et al.[ii]

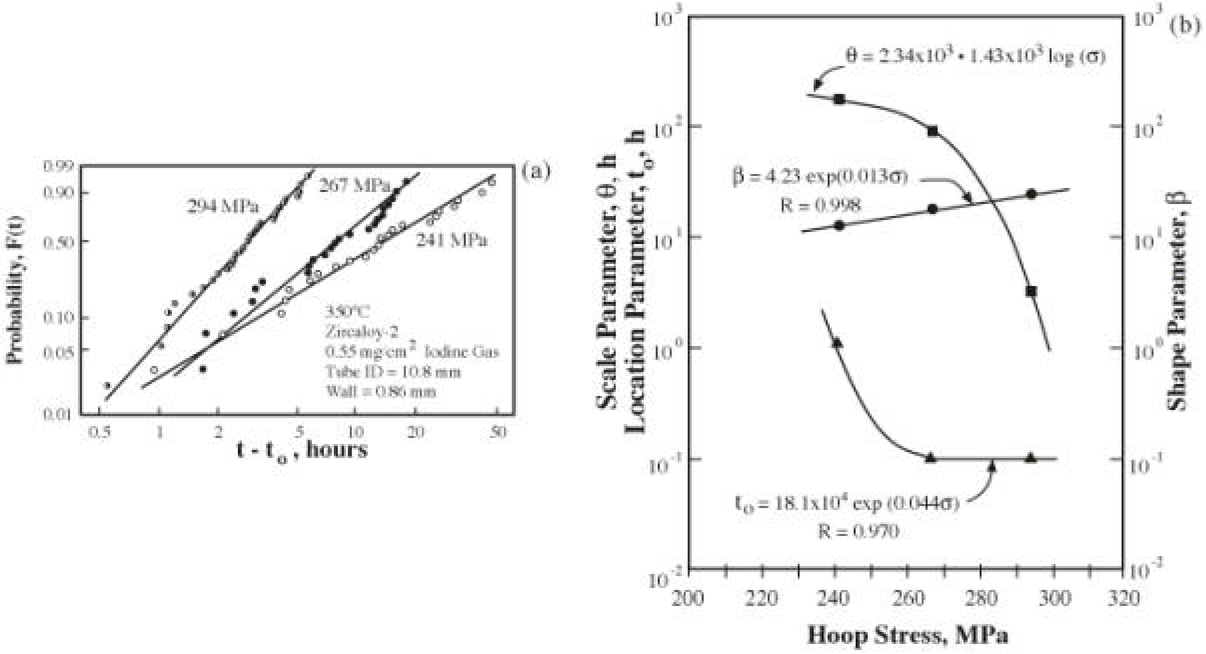

Figure B.19. 7 (a) Probability vs. time-to-failure for Zircaloy 2 fuel cladding material exposed at 350°C to iodine gas. (b) Weibull parameters vs. hoop stress. Adapted from Shimada and Nagai.[17] Calculated dependencies by Fang and Staehle.**Error! Bookmark not defined.**

The discussion of Figure B.19.8 concentrates generally on the metallurgical aspects of the variability. In addition, another kind of variability is related to environments as illustrated by Figure B.19.9a,[iii] which shows schematically aspects of environments in heated crevices at tube supports on the secondary side of SGs. Here, dilute chemicals are concentrated by the local heat transfer conditions, and the resulting environments are variable as implied by the distribution of chemicals inside the heat transfer crevice, which is shown in Figure B.19.9b.[iv]

Figures B.19.8 and 9 show some of the reasons for the variability of the time-to-failure shown in Figure B.19.5.

The large variability of corrosion data in general and in SCC in particular is not so widely appreciated; but such variability exists and is sometimes extensive. Scott, in his Speller Lecture [19] reported results from his study of failure indications of SG tubes. Figure B.19.10 shows results from his study of tubes with NDE indications (not necessarily plugged) from both primary and secondary sides of two different SGs after relatively long times; 40,000 hours for the primary side and 75,000 hours for the secondary side. Figure B.19.10a for the primary side shows 41 vertical bars that correspond to 41 separate heats that were used to produce tubes for the same SG. These heats all manufactured by the same company, are arranged in order of the dates of melting At the top of each bar is the number of tubes that were used in the respective SG from the respective heat. The height of each bar indicates the percentage of tubes in that heat with NDE indications. All the tubes were exposed to the same secondary or same primary environments in the applicable steam generator.

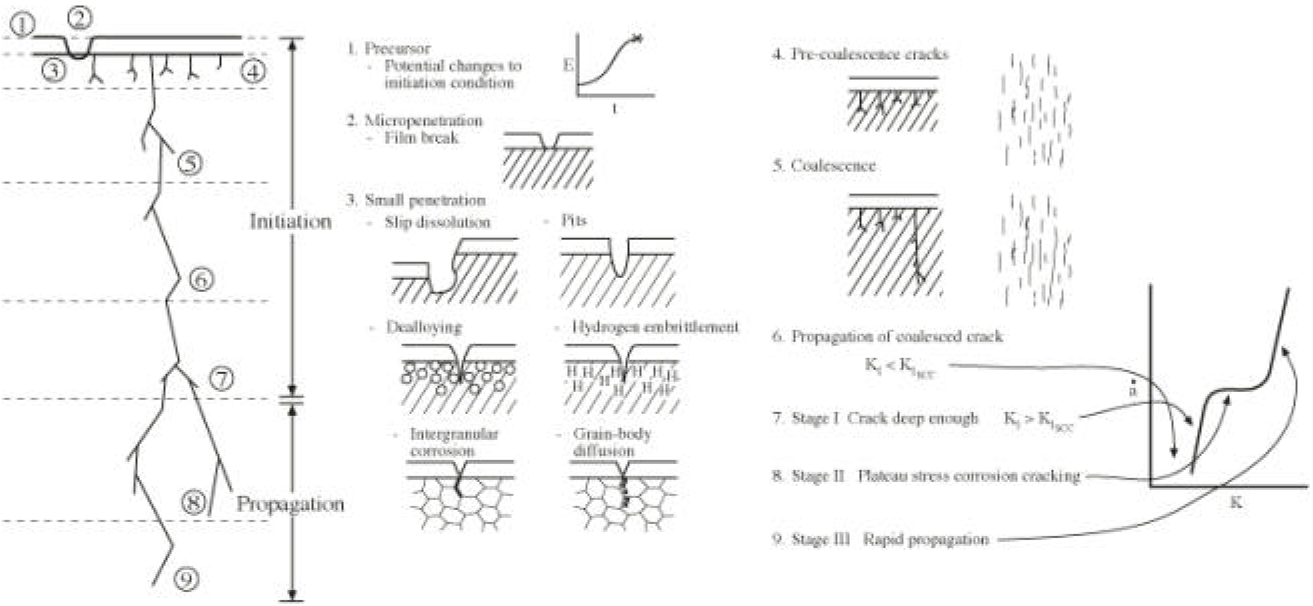

Figure B.19.8 Nine sequential segments of SCC. Practical transition from initiation to propagation shown. Protective film adjusts to the environment. From Staehle.[3]

Despite all the factors that were constant for the heats in Figure B.19.10a, the fraction of the tubes, which failed on the primary side, varied from zero to 41%. A similar pattern occurs on the secondary side after 75,000 hours. Note that these data for the primary and secondary sides were taken from different SGs.

Supposing that one of the heats with a high failure rate, as identified in Figure B.19.10, was chosen for an experimental program; then, it would be concluded that a high failure rate is characteristic—and vice versa. In fact, nearly all the experimental programs have used heats that were known to be very susceptible. One can only conclude that there is large variability in the failure rate of SG tubes despite the best efforts to assure similar conditions—such a pattern can be expected for all materials. The patterns of Figure B.19.10 indicate that attention that should be given to selecting a suitable array of materials with which to conduct tests.

Similar implications, to those in Figure B.19.10 from Scott, have been shown by Jiang and Staehle [24] from evaluating the SCC of stainless steels in boiling $MgCl_2$; and the results are shown in Figure B.19.11. Data are shown for the time-to-failure for specimens exposed over a ranges of temperatures, Figure B.19.11a, and ranges of stresses, Figure B.19.11b. The data for effects of temperatures in Figure B.19.11a includes experiments by 23 different investigations and for stress in Figure B.19.11b from 40 different investigations. Figures B.19.11c and 11d show the range activation energies from the data of Figure B.19.11a; Figures B.19.11e and 11f show the ranges of stress exponents from the data in Figure B.19.11b.

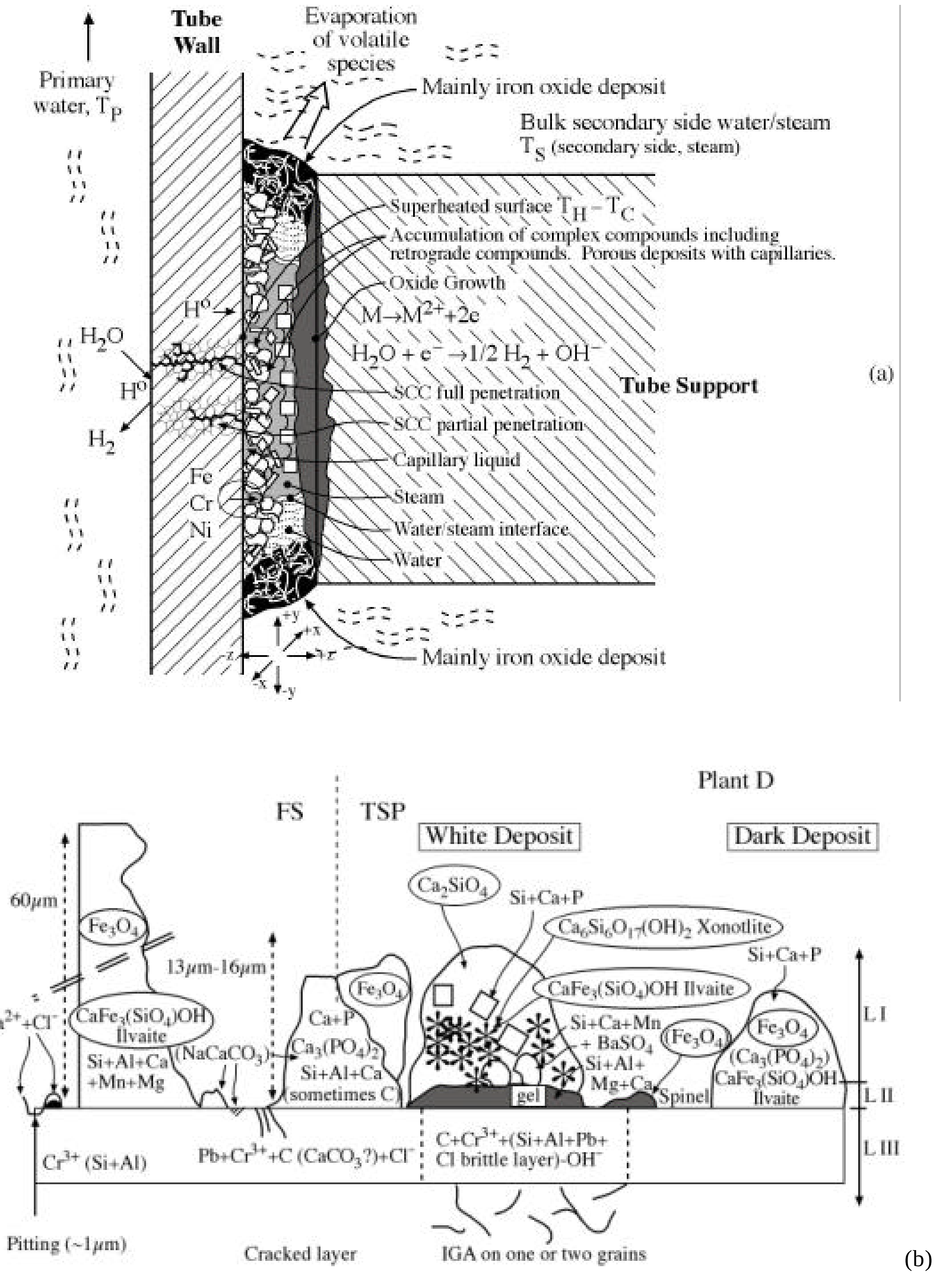

Figure B.19.9 (a) Schematic view of chemical conditions inside a heat transfer crevice on the secondary side of PWR SGs. From Staehle [22]
(b) Schematic view of an OD tube surface inside the tube support and outside on the free surface. The condenser was titanium and the water conditioning was NH_3. The tube was examined after 81,900 hours. From Cattant et al. [23]

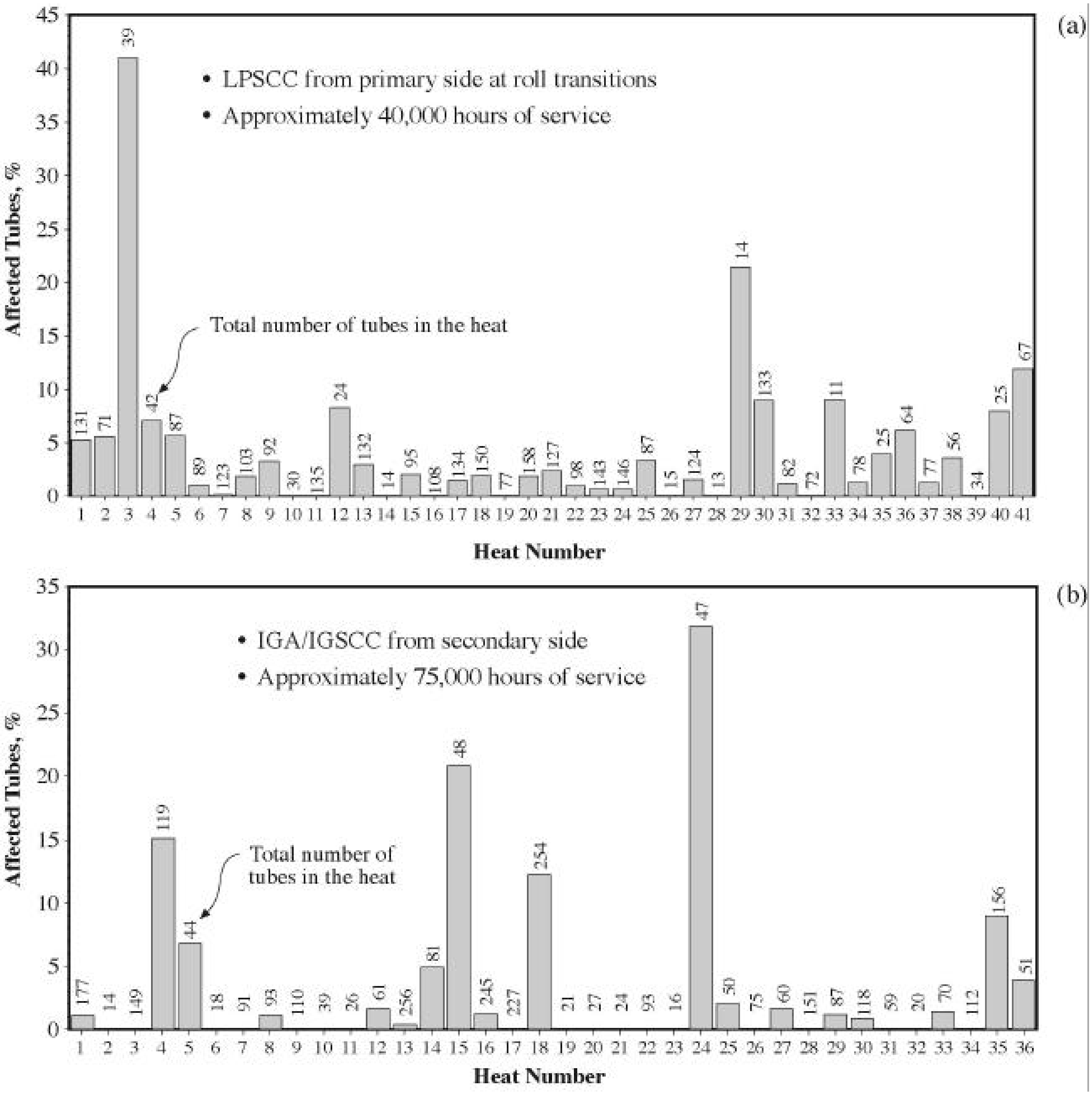

Figure B.19.10 (a) Percent of tubes affected by LPSCC (i.e. with NDE indications) from the primary side of a PWR steam generator vs. heat number determined at roll transitions after approximately 40,000 hours of service. Primary surface temperature at this location is about 310°C. Environment is primary water as identified in Figure 4. (b) Percent of tubes affected by IGA and IGSCC (i.e. with NDE indications) vs. heat number from the secondary side of a PWR steam generator in heat transfer crevices after approximately 75,000 hours of service. From Scott.[19]

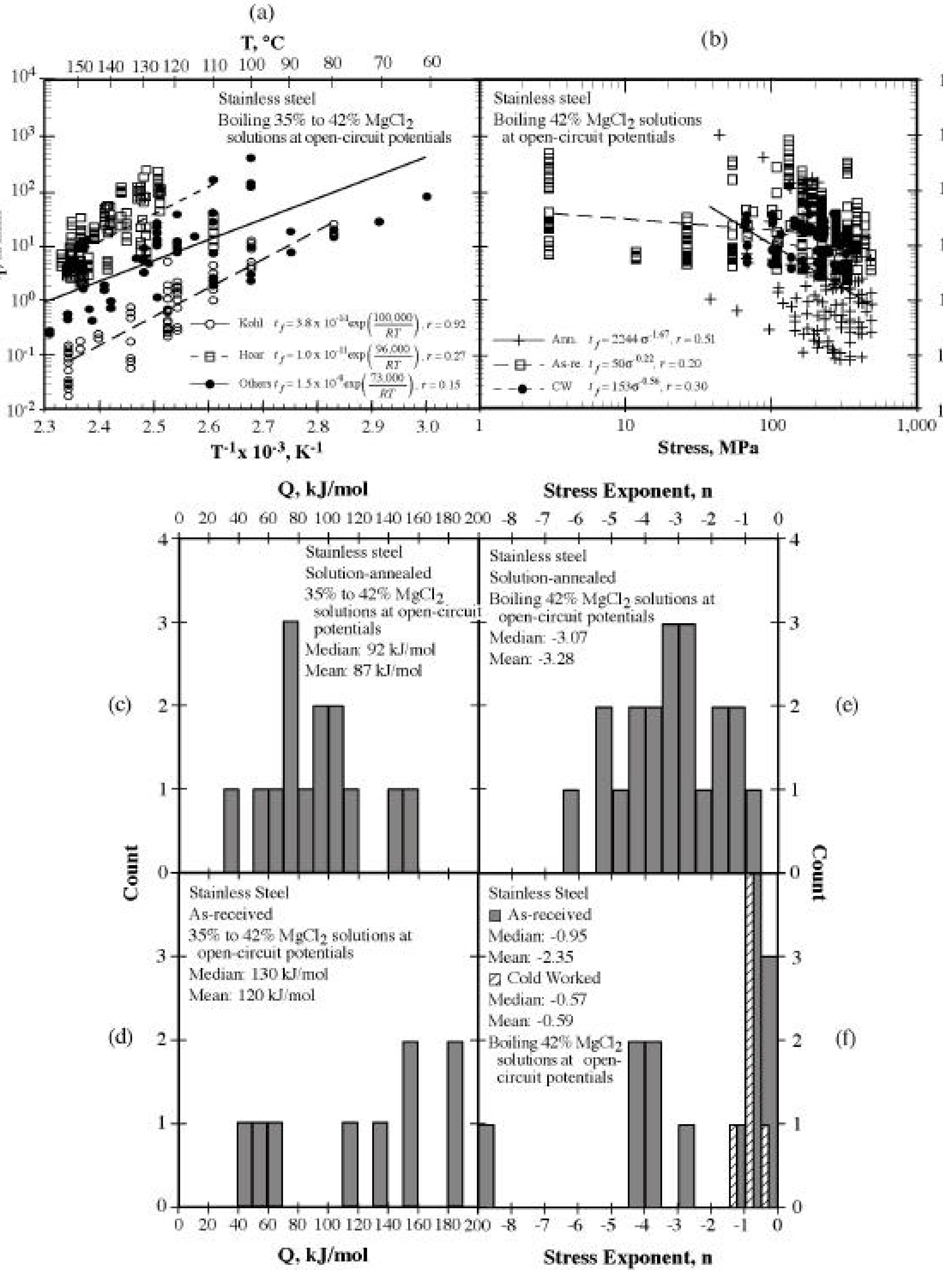

Figure B.19.11 Time-to-failure vs. temperature (a) vs. stress (b) for stainless steel in boiling $MgCl_2$. The units of time-to-failure have been normalized by a cross-sectional area of specimens used by different investigators. (c), (d), (e), and (f) show the array of activation energies and stress exponents from the various studies which were analyzed. From Jiang and Staehle.[24]

The data of Figure B.19.11 are equivalent to using different manufacturers where the materials are exposed, as components, to essentially the same environments. These data are prototypic of corrosion in crevices, such as in Figure B.19.9, where the solutions are concentrated by heat transfer. It is likely that the boiling $MgCl_2$ environments, even those used in multiple laboratories, are more uniform than the environments that occur in heat transfer crevices. The data in Figure B.19.11 exhibit ranges of failure times of about 10^4. The implications here are similar to those of Scott in Figure B.19.10.

Implications of the variability in SCC of SGs are shown in Figure B.19.12, from Staehle and Gorman [16] where they plot the replacements of SGs vs. time. These did not all fail at the same time despite their general similarity of design--again, an indication of the variability of the corrosion phenomena that produce failures.

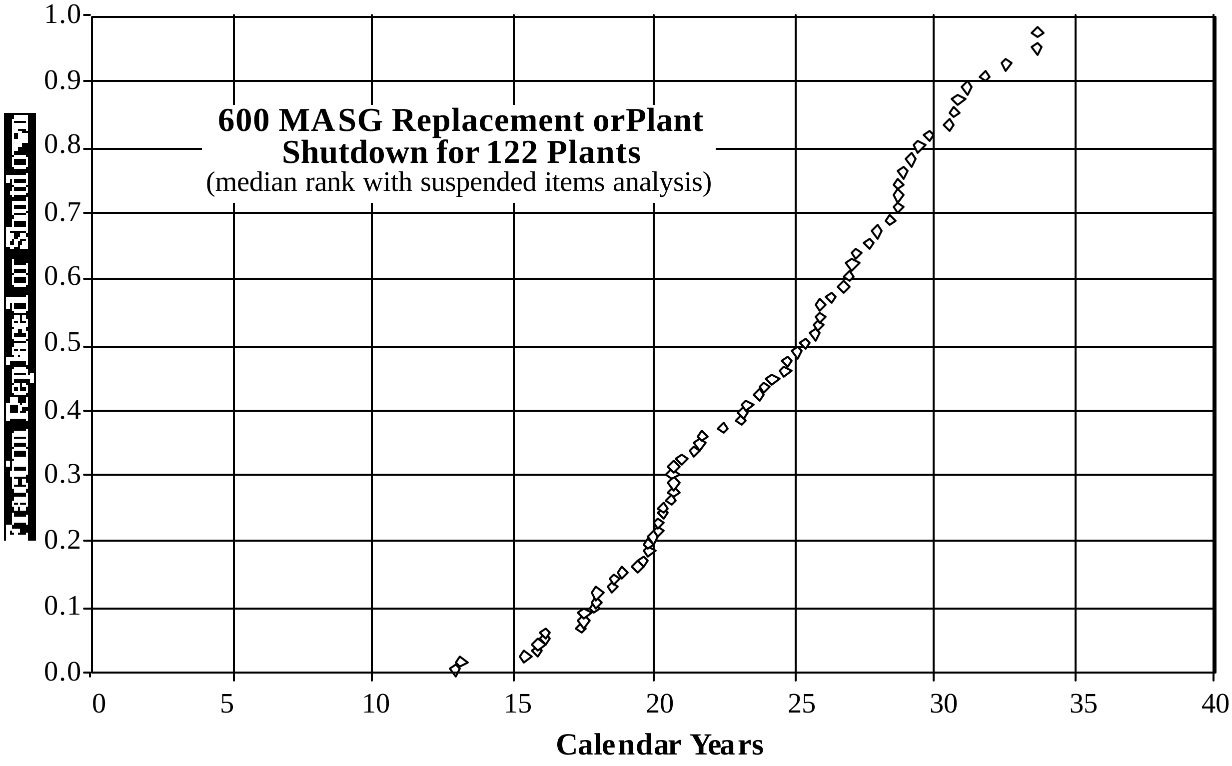

Figure B.19.12 Fraction of replaced or shutdown steam generators vs. calendar years for 600MA plants in the world. From Staehle and Gorman.[16]

Finally, a further contributor to the variability of corrosion that produced the results shown in Figure B.19.12 was the variety of modes of failures and the multiple locations where corrosion failures occurred as shown in Figure B.19.13 [16]. Thus, in addition to the variability in a single SCC, which is implied in Figure B.19.8, there is further variability in corrosion failures owing to multiple modes of failure and multiple locations of failures. . Multiple failures are dealt with as shown in Figure 5 and through the use of Eqn. (8).

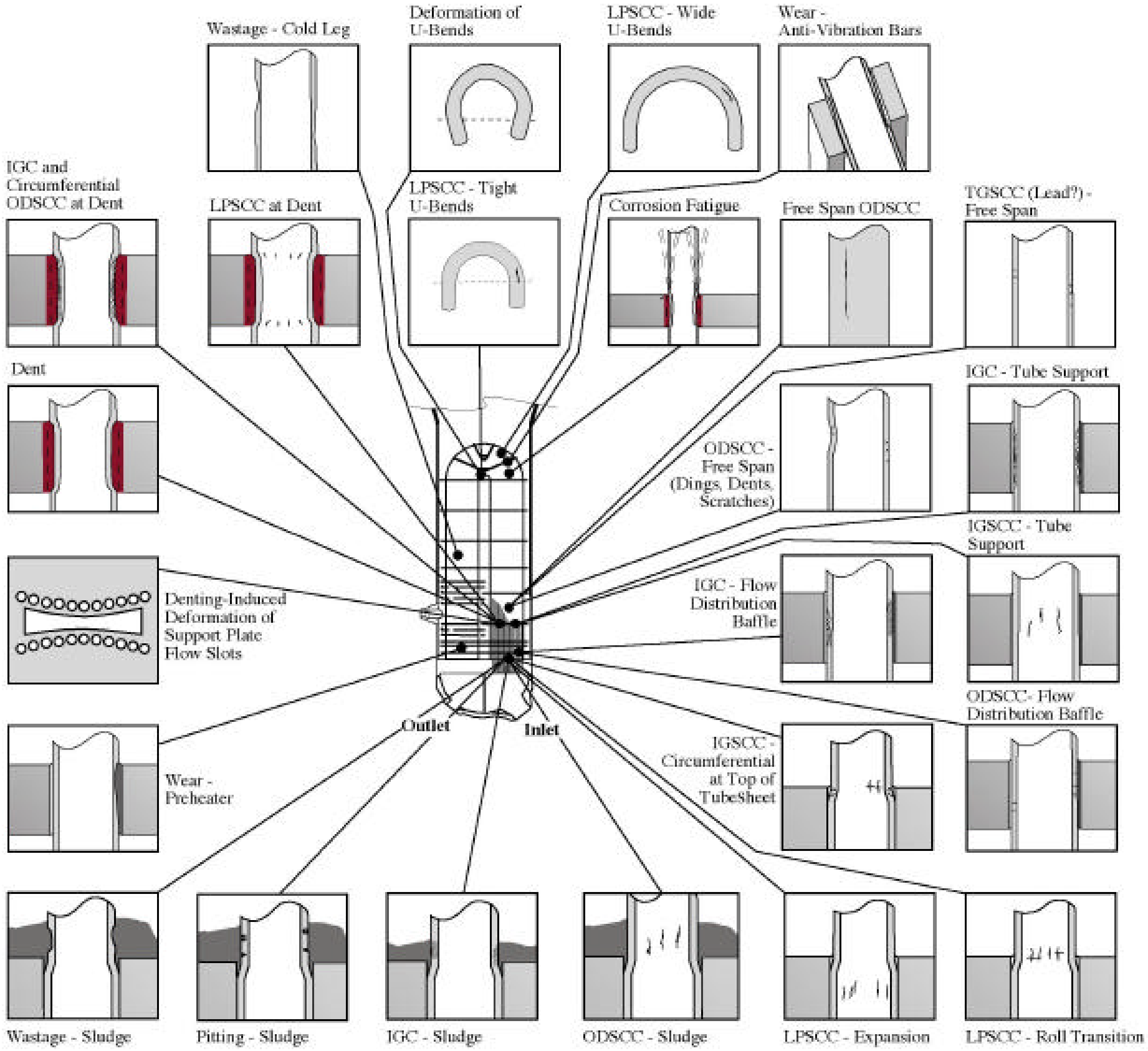

Figure B.19.13 Array of modes of failure at various locations (mode-location cases) that have occurred in recirculating steam generators. From Staehle and Gorman.[16]

The Physical Meaning of Statistical Parameters

The statistical correlations as illustrated in Eqns. (1) through (8) and in Figures B.19.1, 2, 3, 4, 5, 6, and 7 are nominally pure correlations without having been derived from physical experience; although Weibull developed his distribution based on his interest in modeling the failures of ball bearings [7]. Nonetheless, in the paper by Staehle [25] it was shown that statistical parameters could be extrapolated and interpolated using activation energies and stress exponents.

In a detailed analysis by Staehle [1], it was shown that the statistical parameters could be correlated according to generally regular dependencies on temperatures, stresses, and concentrations. For example, Figure B.19.14 shows two separate cumulative distributions in Figures B.19.14a and 14b for SCC of Type 304 stainless steel tested at 288°C in high purity oxygenated water. One study was conducted by Clark and Gordon [26] in the United States and the other was conducted by Akashi and Ohtomo[27] in Japan. The dependence of statistical parameters on stress is compared in Figure 14c. The results are quite similar for the dependencies of q, b, and t_o. Such regular dependencies were found by Staehle[1] for other alloys in various environments and for the variables of temperature, stress, and concentration of solutions. Such regular dependencies suggest that statistical distributions could be extrapolated over ranges of temperature, stress, and concentration as well as over other variables that control corrosion such as pH, potential, alloy composition, and alloy structure as has been described by Staehle.[6]

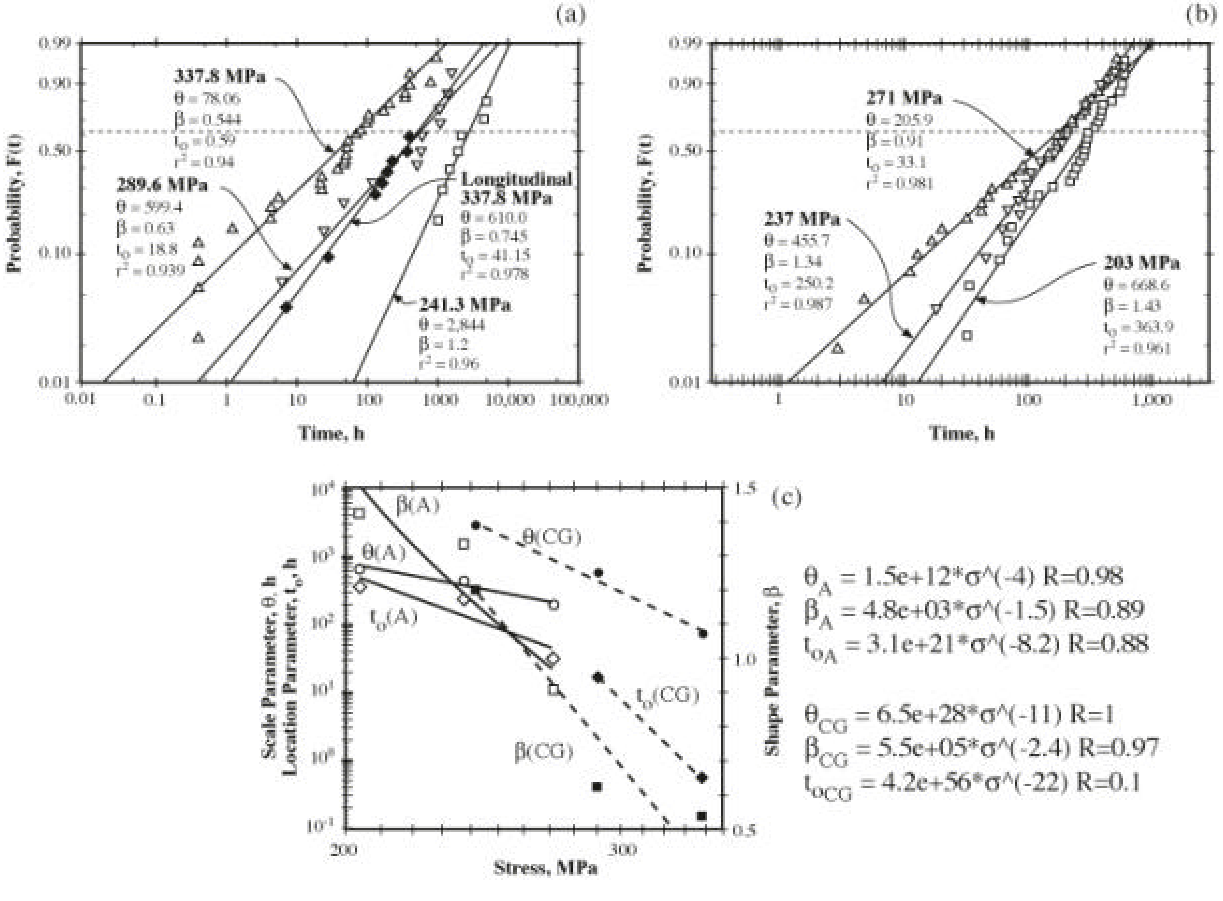

Figure B.19.14 a) Probability vs. time for sensitized Type 304 stainless steel tested at 288°C in high purity oxygenated water. Adapted from Clarke and Gordon.[26] (b) Probability vs. time for sensitized Type 304 stainless steel tested at 288°C in high purity oxygenated water. Adapted from Akashi and Ohtomo.[27] (c) Weibull parameters vs. stress from both the Clarke and Gordon (CG) (dotted lines) and Akashi (A) (solid lines) distributions.

From the analyses by Staehle,[1,6] it appears that the values of b in many cases are directly related to physical conditions. Figure B.19.15 shows a cdf and hf for the cases where b=1.0 and 4.0, together with schematic illustrations of their physical significance. As shown in Figures B.19.1b and 2, the slope of the $F(t)$ vs. time for b=1.0 is lower than that for b=4.0 which means that the first failure occurs at a much shorter time relative to the mean for b=4.0 than for b=1.0. In Figure B.19.15b the hf is independent of time for b=1.0 whereas, the hf increases sharply around the value of q for b=4.0.

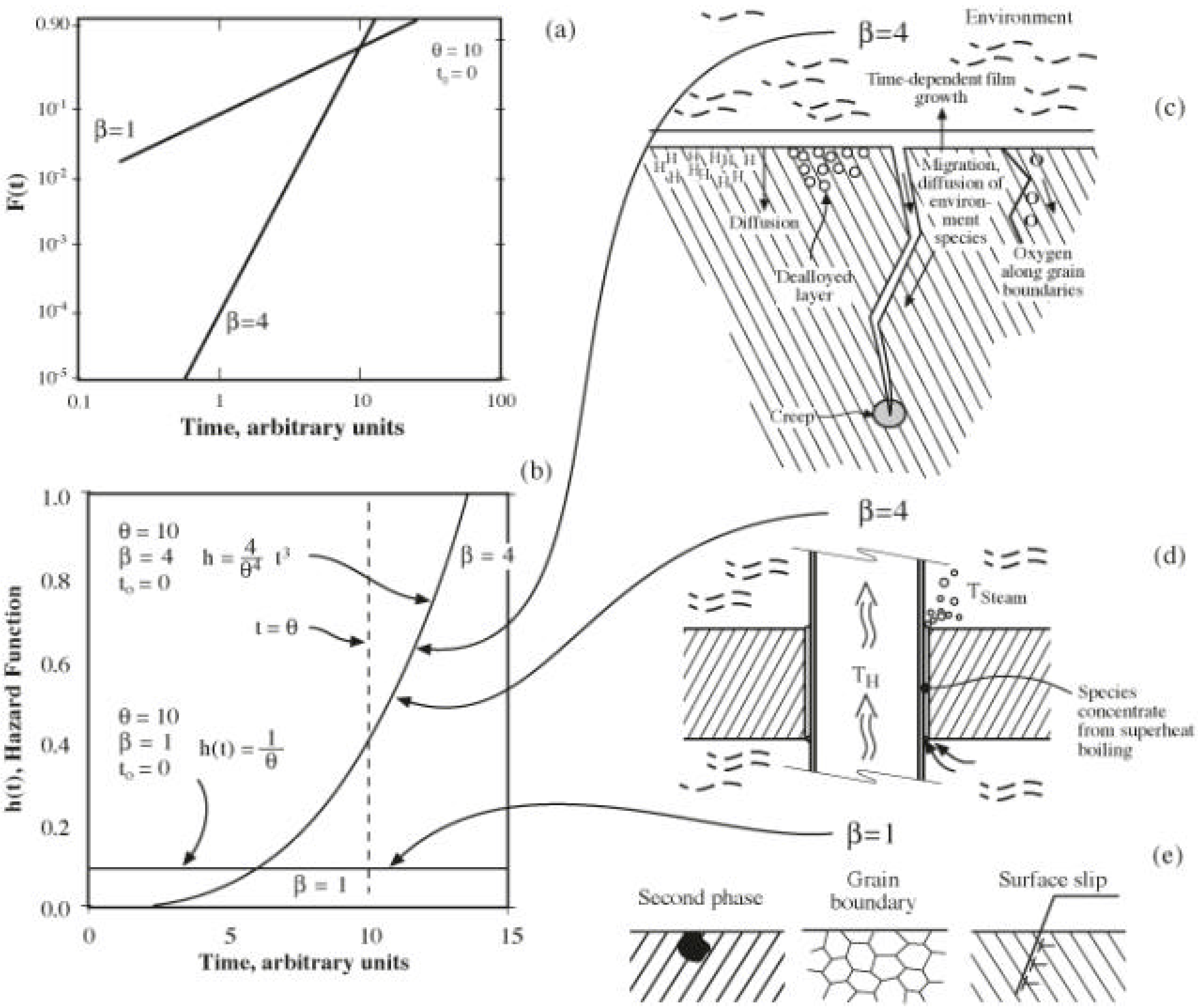

Figure B.19.15 a) cdf for b=1 and b=4 vs. time. (b) hf vs. time for b=1 and b=4 cases at q=10 and t_o=0. (c) Possible contributions in the metal substrate, for a growing SCC, to the accumulation case for b=4. (d) Possible contributions to the accumulation case b=4 from a superheated tube support geometry. (e) Possible contributions to the b=1 case from surface processes. From Staehle.[3]

A reasonable interpretation of the tendencies in Figure B.19.15b is suggested in the schematic illustrations of Figures B.19.15c, 15d, and 15e. It has been well known that lower values of *b* e.g. a *b*=1.0 are related to surface processes and the initiation stages of pitting and SCC. Such morphologies for surface reactions are illustrated in Figure 15e. On the other hand, the relatively rapid rise in the hf for *b*=4.0 after an initial quiescence suggests that some time or pre-condition is required before SCC can occur; but, when the necessary conditions are present, SCC can proceed relatively rapidly. Such pre-conditions may be associated with critical early diffusive or migration processes as illustrated in Figure 15c or geometrical conditions, which present an impeded diffusion path, as illustrated in Figure 15d.

The validity of the implication in Figure 15b, as related to the comparison between the initiation stage of Figure 15e and the propagation of Figure 15c, is shown in Figure B.19.16 from work by Shibata and Takeyama.[28] Here, the *b* for initiation is consistently unity; whereas, that for propagation increases with applied stress following the trend with stress in Figure B.19.7.

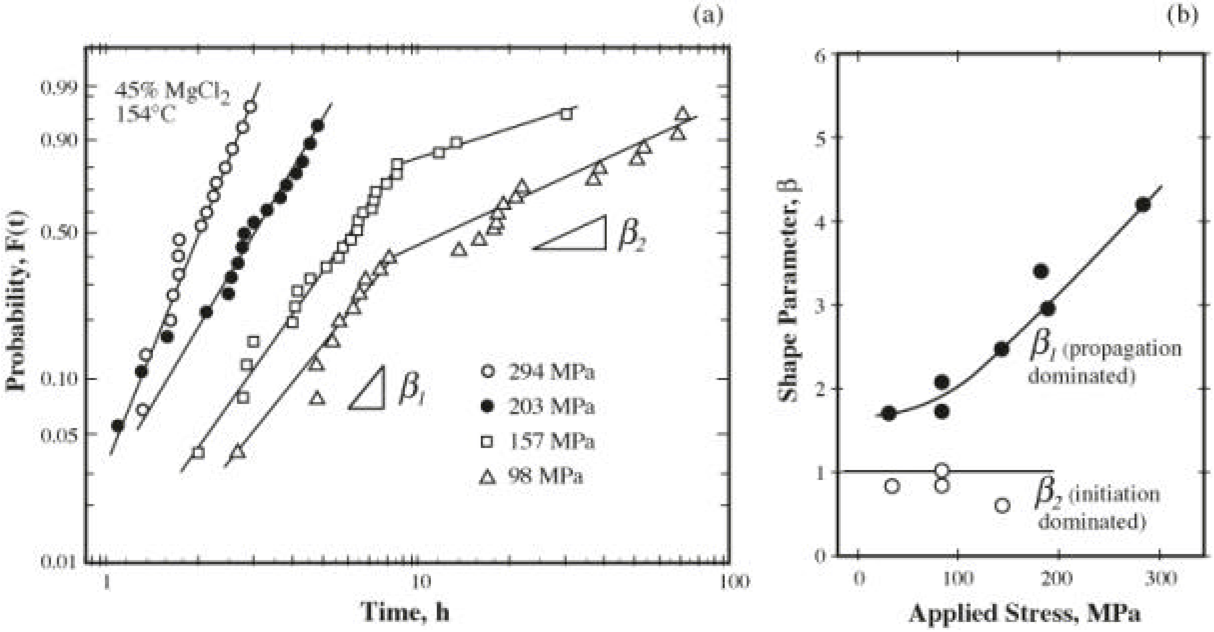

Figure B.19.16 (a) Probability vs. time for Type 304 stainless steel exposed to boiling $MgCl_2$ at 154°C at various stresses. (b) Values of *b* for upper and lower segments vs. stress from (a). From Shibata and Takeyama.[28]

Accelerated Testing and Pitfalls

Testing is often accelerated in order to predict the occurrence of performance in the future. Thus, one could hope that successful performance after some length of time could be predicted by short term testing that is accelerated along vectors of temperature, stress, solution concentration, or some other variable.

It is common to conduct accelerated testing to determine some mean time-to-failure that can predict the mean time-to-failure at longer operating times at conditions that are less severe. An acceleration of about 100 may be about the best to expect. However, such testing is usually conducted to predict mean times-to-failure notwithstanding the implications of Figures 1, 2, and 3 as well as Figures 4, 5, 6, and 7.

In general, the real problem of prediction is not predicting the mean time-to-failure since, by the time 50% have failed, the application has long since failed. What needs to be predicted is the first failure or the first 0.1% of failures. While it would be convenient to assume that the acceleration for the mean time is the same as that for 0.1%, such an assumption cannot be justified *a priori*. For the data from an accelerated test to apply at the 0.1% or 0.001 probability would require that the expected values of b for failures in the field would be the same as the b for failures in tests.

Figure B.19.17 shows schematically a typical plot of field failures with b=1.0 and a schematic plot of hypothetical (but typical as in Figure B.19.4) data from an accelerated test with b=5.0. Here, while the mean value of the accelerated test is about 100 times less than that of the field failures (and thereby being a good acceleration), there is no acceleration at a 0.001 probability. The value of b=5.0 is chosen for this schematic since b is generally increased as the stressors are increased and as the material chemistries are more homogeneous.

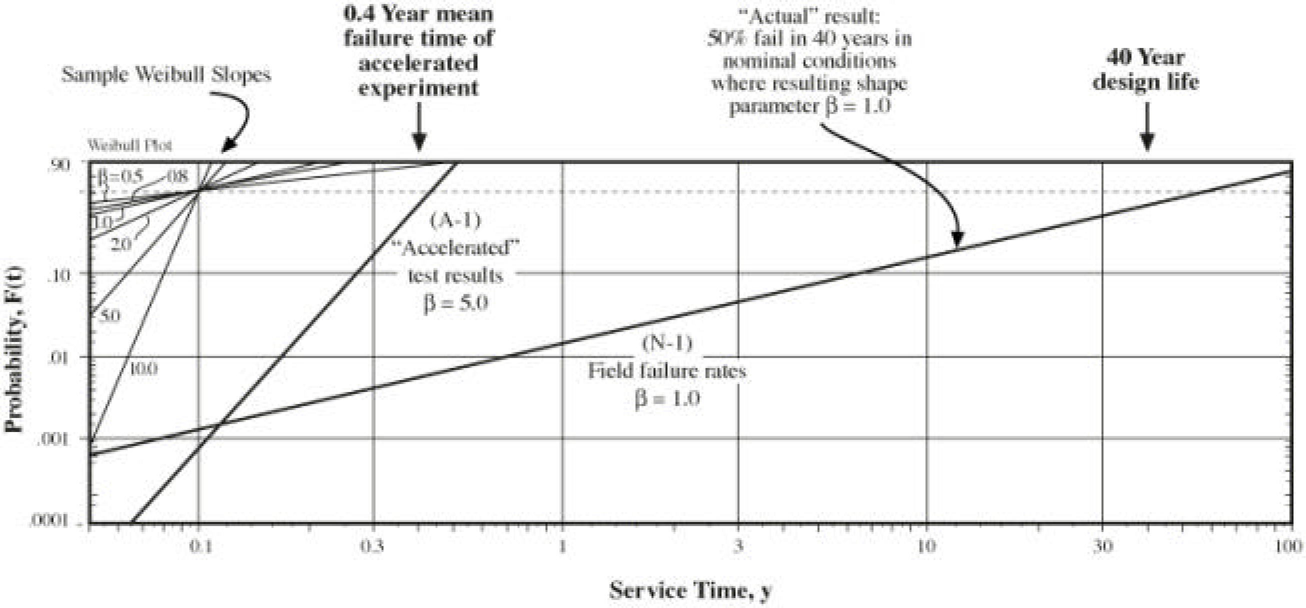

Figure B.19.17 Schematic plot of probability of failure vs. time for field data and accelerated tests based on Weibull coordinates. N-1 corresponds to assumed field results; A-1 corresponds to assumed accelerated testing. From Staehle.[3]

Figure B.19.17 shows that "accelerated testing" may not provide acceleration for the early failures, and such a result cannot be assumed without directly measuring the statistical parameters in the accelerated testing.

Conclusions

1. Corrosion data in the field and in laboratory testing are statistically distributed under the best of circumstances. There are no bases for assuming that even well conducted testing or well-controlled field performance will produce failures at identical times.

2. In choosing materials for testing, it is necessary to chose multiple sources that are typical of applications since a choice of a single heat could misrepresent either the mean, the most rapid or the least rapid rates of corrosion.

3. The occurrences of early failures are not likely to result from "bad heats" or carelessness, but are more likely to be the early failures in a regular distribution of failures.

4. Accelerated testing must consider whether the quantity to be predicted is the mean or early failures, e.g. 0.001 probability. For predicting a 0.001 probability, the values of b ?for the accelerated test must be relevant to the application.

Acknowledgements

I am indebted to my hard working staff for helping with the preparation of this paper; especially Julie L. Daugherty, Marcia Parrish-Siggelkow, and John Ilg. For the work in this paper, I relied on past collaborations with Jeffrey Gorman of Dominion Engineering and Robert Abernethy of Weibull Risk & Uncertainty Analysis. I appreciate also the timely help from Peter Scott of Framatome and Robert Tapping of AECL. Finally, I appreciate the intellectually challenging discussions with my colleagues in the PMDA group.

References

[1] R.W. Staehle, "Bases for Predicting the Earliest Penetrations Due to SCC for Alloy 600 on the Secondary Side of PWR Steam Generators;" NUREG/CR-6737, ANL-01/20, RWS-151, U.S. Nuclear Regulatory Commission, Washington, D.C., September, 2001.

[2] R.W. Staehle, "Bases for Predicting the Earliest Failures Due to Stress Corrosion Cracking." Chemistry and Electrochemistry of Corrosion and Stress Corrosion Cracking: A Symposium Honoring the Contributions of R. W. Staehle, Ed. Russell Jones, TMS (The Minerals, Metals and Materials Society,) Warrendale, Pennsylvania, 2001, pp. K1-K92.

[3[R.W. Staehle, "Predicting the First Failure," presented at Corrosion 2003, San Diego, March 16-20, NACE, Houston, Texas, 2003.

[4] J.A. Gorman, R.W. Staehle, K.D. Stavropoulos, "Statistical Analysis of Steam Generator Tube Degradation," EPRI Report NP-7493, Research Project S405-9, September, 1991.

[5] M. Bruemmer, E.I. Meletis, R.H. Jones, W.W. Gerberich, E.P. Ford, and R.W. Staehle, Eds., Parkins Symposium on Fundamental Aspects of Stress Corrosion Cracking, TMS (The Minerals, Metals and Materials Society), Warrendale, Pennsylvania, 1992.

[6] R.W. Staehle, “Approach to Predicting SCC on the Secondary Side of Steam Generators,” presented at Fontevraud 5, Contribution of Materials Investigation to the Resolution of Problems Encountered in Pressurized Water Reactors, SFEN, Paris, September 23-27, 2002.

[7] W. Weibull, “A Statistical Distribution Function of Wide Applicability,” Journal of Applied Mechanics 10, 1951, p. 293.

[8] E.J. Gumbel, “Statistical Theory of Extreme Values and Some Practical Applications,” Applied Mathematics 33, U.S. Dept. of Commerce, National Bureau of Standards, Washington, 1954, p. 1.

[9] E.J. Gumbel, Statistics of Extremes, Columbia University Press, New York, 1958.

[10] W. Nelson, “Weibull Prediction of a Future Number of Failures,” Quality and Reliability Engineering International 16, 2000, p. 23.

[11] K.T. Chang, “Analysis of the Weibull Distribution Function,” Journal of Applied Mechanics 49, 1982, p. 450.

[12] R.K. Reeves and D.W. Hoeppner, “A Weibull Analysis of Center Cracked Panel Crack Growth Data of a 0.40/0.50 Carbon Steel,” Engineering Fracture Mechanics 10, 1978, p. 571.

[13] R.B. Abernethy, The New Weibull Handbook; Fourth Edition, R.B. Abernethy Publisher, North Palm Beach, Florida, 2000.

[14] T. Shibata, “1996 W.R. Whitney Award Lecture: Statistical and Stochastic Approaches to Localized Corrosion,” Corrosion 37, 11, 1996, p. 813.

[15] WINSMITH (TM) Weibull 3.0U.

[16] R.W. Staehle and J.A. Gorman, “Quantitative Assessment of Submodes of Stress Corrosion Cracking on the Secondary Side of Steam Generator Tubing in Pressurized Water Reactors,” *Corrosion*, Part 1 Vol. 59 No. 11 November 2003, Part 2 Vol. 60 No. 1 January 2004, Part 3 Vol. 60 No. 2 February 2004, NACE, Houston, Texas.

[17] S. Shimada and N. Nagai, “Variation of Initiation Time for Stress Corrosion Cracking in Zircaloy-2 Cladding Tube,” Reliability Engineering 9, 1984, p. 19.

[18] E.D. Eason and L.M. Shusto, Analysis of Cracking in Small Diameter BWR Piping, EPRI NP 4394, Electric Power Research Institute, Palo Alto, 1986.

[19] P.M. Scott, “2000 F.N. Speller Award Lecture: Stress Corrosion Cracking in Pressurized Water Reactors – Interpretation, Modeling, and Remedies,” Corrosion Vol. 56, 2000, p. 771.

[20] Unpublished data provided by L. Bjornkvist of Vattenfall and J. Gorman of Dominion Engineering.

[21] P.M. Scott, M-C. Meunier, D. Deydier, S. Silvestre, and A. Trenty, “An Analysis of Baffle/Former Bolt Cracking in French PWRs,” Environmentally Assisted Cracking: Predictive Methods for Risk Assessment and Evaluation of Materials, Equipment and Structures, ASTM 1401, R.D. Kane, Ed., American Society for Testing and Materials, West Conshohocken, PA, 2000.

[22] R.W. Staehle, “Lifetime Prediction of Materials in Environments,” Uhlig’s Corrosion Handbook; 2nd Edition, R.W. Revie, ed., John Wiley and Sons, New York, 2000, p. 27.

[23] F. Cattant, M. Dupin, B. Sala, and A. Gelpi, “Analyses of Deposits and Underlying Surfaces on the Secondary Side of Pulled Out Tubes From a French Plant,” Contribution of Materials Investigation to the Resolution of Problems Encountered in Pressurized Water Reactors; Proceedings of the International Symposium: Fontevraud III, F. de Keroulas, chair., French Nuclear Energy Society, Paris, 1994, p. 469.

[24] X.C. Jiang and R.W. Staehle, “Effects of Potential and Stress on Stress Corrosion Cracking of Austenitic Stainless Steels in Concentrated Chloride Solutions,” Corrosion Journal Vol. 53, No. 8, August, 1997, pp. 631 - 643.

[25] R.W. Staehle, J.A. Gorman, K.D. Stavropoulos, and C.S. Welty, Jr., “Application of Statistical Distributions to Characterizing and Predicting Corrosion of Tubing in Steam Generators of Pressurized Water Reactors,” Presented at the 3rd International Relations Committee Symposium, Life Prediction of Corrodible Structures, Cambridge, UK, NACE, Houston, Texas, 1991.

[26] W.L. Clarke and G.M. Gordon, “Investigation of Stress Corrosion Cracking Susceptibility of Fe-Ni-Cr Alloys in Nuclear Reactor Waste Environments,” Corrosion Vol. 29, 1973, p. 1.

[27] M. Akashi and A. Ohtomo, “Evaluation of the Factor of Improvement for the Intergranular Stress Corrosion Cracking Life of Sensitized Stainless Alloys in High-Temperature, High-Purity Water Environment,” Journal of the Society of Materials Science of Japan Vol. 36, 1987, p. 59.

[28] T. Shibata and T. Takeyama, “Probability Distribution of Failure Times of Stress Corrosion Cracking of 17Cr-11Ni Stainless Steel,” Tetsu-To-Hagane Vol. 66, 1980, p. 693.